Acta Chimica Hungarica

VOLUME 120, NUMBERS 1, SEPTEMBER 1985

NOTICE TO AUTHORS

Acta Chimica publishes original papers on all aspects of chemistry in English. Before preparing a manuscript for submission to this journal authors are advised to consult recent issues.

Form of manuscript

Manuscripts, tables and illustrations should be submitted in triplicate. Manuscripts should be typewritten double spaced (25 lines, 50 characters per line including spaces). The *title page* should include (1) the title of the paper, (2) the full names of the author(s) in the sequence to be published; apply an asterisk to designate the name of the author to whom correspondence should be addressed, (3) name and address of the institution where the work was done. If the paper is part of a series, reference to the previous communication must be given as a footnote.

Abstract

A summary is printed at the head of each paper. This should not exceed 200 words and should state briefly the principal results and major conclusions of the work. It should be suitable for use by abstracting services.

ACTA
CHIMICA
HUNGARICA

VOLUME 120

CONTENTS

1

CALCULATION OF ACTIVATION ENERGIES AND TRANSITION STATE GEOMETRIES FOR HYDROGEN ABSTRACTION REACTIONS BY SEMIEMPIRICAL METHODS

Imre Bálint[1], Márta Révész[1]*, Miklós I. Bán[1], Ferenc Márta[2]** and
Tibor Bérces[2]

*([1]József Attila University, H-6701 Szeged, P.O.B. 105, [2]Hungarian Academy of Sciences,
Central Research Institute for Chemistry, H-1525 Budapest, P.O.Box 17)*

Kinetic parameters for hydrogen atom abstraction reactions by methyl radicals for methane, ethane, propane and isobutane were studied with the semi-empirical BSBL and MINDO/3 methods. Transition state geometries (bond lengths and bond angles) and heights of the potential barriers were determined and the trend found in the series of reactions studied was discussed.

Introduction

It is possible in principle to calculate by quantum mechanics the expected value of any physical quantity with arbitrary accuracy [1], however, because of various theoretical and practical problems experienced, only calculation results obtained for the smallest systems can be regarded as satisfactory. The large number of two-electron integrals to be computed and the rapidly increasing dimension of the configuration space when regarding also electron correlations, frustrates the calculations of higher sophistication. This is especially valid for calculations of potential energy surfaces of adiabatic (and even more of diabatic) type although such calculations are of fundamental importance from the viewpoint of chemical reactions. These circumstances account for the development and use of highly simplified conventional and quantum chemical semiempirical methods, i.e. for the use of empirical parameters.

Moreover, one has to be satisfied generally with the investigation of the most important domains (extrema, local minima, saddle-points, reaction paths, etc.) of the reaction surface instead of calculating the whole potential surface.

---

* Present address: Research Lab. for Inorg. Chem. HASc., H-1502 Budapest, P.O.B. 132
** To whom correspondence should be addressed

1*

*Acta Chim. Hung. 120, 1985
Akadémiai Kiadó, Budapest*

The aim and methods of investigations

Hydrogen transfer reactions between alkyl radicals and alkanes have been investigated by the BSBL and MINDO/3 methods.

The semiempirical BSBL method [2] based on classical theory is an improved version of the BEBO method [3] and can be used for calculating

Reaction: $\dot{C}H_3 + CH_4 \rightleftharpoons CH_4 + \dot{C}H_3$

Model:

Reaction: $\dot{C}H_3 + CH_3CH_3 \rightleftharpoons CH_4 + \dot{C}H_2CH_3$

Model:

Reaction: $\dot{C}H_3 + (CH_3)_2CH_2 \rightleftharpoons CH_4 + \dot{C}H(CH_3)_2$

Model:

Reaction: $\dot{C}H_3 + (CH_3)_3CH \rightleftharpoons CH_4 + (CH_3)_3\dot{C}$
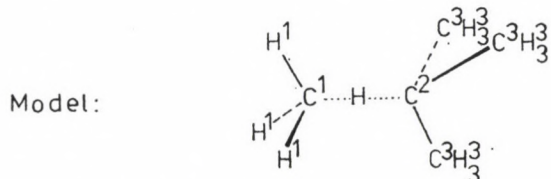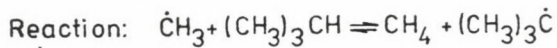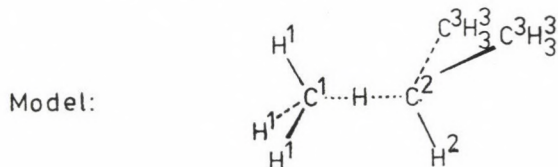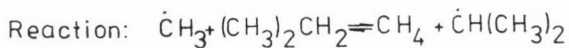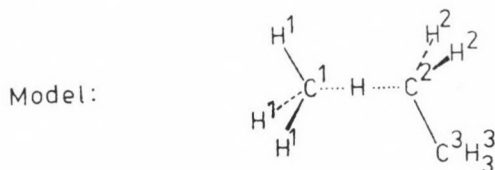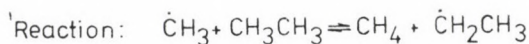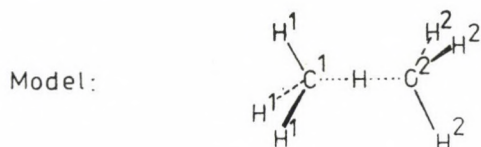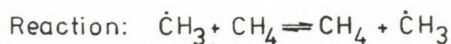
Model:

Fig. 1. Transition state models

Table IA

The energy (kJ/mol) and geometry (distances in pm and angles in degree)
of isolated molecules $\dot{C}H_3$ and CH_4

Property	BSBL	MINDO/3
R° (C^1—H^1) in $\dot{C}H_3$ radical	107.9[a]	109.0
Angle H^1—C^1—H^1 in $\dot{C}H_3$	planar[a]	116.65
R° (C^1—H^1) in CH_4 molecule	109.3[a]	110.2
Angle H^1—C^1—H^1 in CH_4	tetrahedral[a]	109.48
E° ($\dot{C}H_3$)		—16349.85
E° (CH_4)		—17978.86
E° ($\dot{C}H_3$) + E° (CH_4)		—34328.71
ΔE° [b]	0[a]	0

[a] Experimental equilibrium value
[b] $\Delta E^\circ = E^\circ$ ($C^1H^1_4$) + E° ($\dot{C}^2H^2_3$) — E° ($\dot{C}^1H^1_3$) — E° ($C^2H^2_4$)

Table IIA

The energy (kJ/mol) and geometry (distances in pm and angles in degree)
of isolated molecules $\dot{C}_2H_5$ and C_2H_6

Property	BSBL	MINDO/3
R° (C^2—H^2) in $\dot{C}_2H_5$ radical		109.8
R° (C^3—H^3) in $\dot{C}_2H_5$		111.7[a]
R° (C^2—C^3) in $\dot{C}_2H_5$		142.5
Angle H^2—C^2—H^2 in $\dot{C}_2H_5$		109.40
Angle H^3—C^3—H^3 in $\dot{C}_2H_5$		104.43
Angle C^2—C^3—H^3 in $\dot{C}_2H_5$		113.61[a]
Angle C^3—C^2—H^2 in $\dot{C}_2H_5$		120.80
R° (C^2—H^2) in C_2H_6 molecule	109.3[b]	111.1
R° (C^2—C^3) in C_2H_6	153.4[b]	147.7
Angle H^2—C^2—H^2 in C_2H_6		105.56
Angle C^2—C^3—H^3 in C_2H_6		113.14
E° ($\dot{C}_2H_5$)		—31532.90
E° (CH_4)		—17978.86
E° (CH_4) + E° ($\dot{C}_2H_5$)		—49511.76
E° (C_2H_6)		—33137.25
E° ($\dot{C}H_3$)		—16349.85
E° ($\dot{C}H_3$) + E° (C_2H_6)		—49487.10
$\Delta E^{\circ c}$	—25.12[b]	—24.66

[a] Mean value
[b] Experimental equilibrium value
[c] $\Delta E^\circ = E^\circ$ (CH_4) + E° ($\dot{C}_2H_5$) — E° ($\dot{C}H_3$) — E° (C_2H_6)

Table IIIA

The energy (kJ/mol) *and geometry (distances in* pm *and angles in degree)*
of isolated molecules $(CH_3)_2\dot{C}H$ *and* C_3H_8

Property	BSBL	MINDO/3
R° (C^2—H^2) in $\dot{C}_3H_7$ radical		110.9
R° (C^3—H^3) in $\dot{C}_3H_7$		111.5
R° (C^2—C^3) in $\dot{C}_3H_7$		144.1
Angle H^3—C^3—H^3 in $\dot{C}_3H_7$		105.13
Angle C^2—C^3—H^3 in $\dot{C}_3H_7$		113.52
Angle C^3—C^2—H^2 in $\dot{C}_3H_7$		115.58
Angle C^3—C^2—C^3 in $\dot{C}_3H_7$		128.68
R° (C^2—H^2) in C_3H_8 molecule		112.2
R° (C^3—H^3) in C_3H_8	109.3[a]	111.2
R° (C^2—C^3) in C_3H_8	154[a]	149.5
Angle H^3—C^3—H^3 in C_3H_8		105.42[b]
Angle H^2—C^2—H^2 in C_3H_8		102.17
Angle C^2—C^3—H^3 in C_3H_8		113.25[b]
Angle C^3—C^2—H^2 in C_3H_8		108.19
Angle C^3—C^2—C^3 in C_3H_8		120.44
E° ($\dot{C}_3H_7$)		−46702.83
E° (CH_4)		−17978.86
E° (CH_4) + E° ($\dot{C}_3H_7$)		−64681.69
E° (C_3H_8)		−48266.77
E° ($\dot{C}H_3$)		−16349.85
E° ($\dot{C}H_3$) + E° (C_3H_8)		−64616.62
$\Delta E^{\circ c}$	−41.87[a]	−65.08

[a] Experimental equilibrium value
[b] Mean value
[c] ΔE° (CH_4) + E° ($\dot{C}_3H_7$) − E° ($\dot{C}H_3$) − E° (C_3H_8)

the energy of the system ABC in the atom transfer reaction

$$A + B : C \rightarrow ABC \rightarrow A : B + C$$

along a collinear reaction path of minimum energy leading from reactants
to products. The BSBL method is suitable for providing the reaction profile,
the height of the potential barrier with an error of 5—8 kJ · mol^{-1} and for
estimating reliably the bond lengths and force constants of the activated
complex.

Among the quantum chemical semiempirical methods, MINDO/3 [4],
[5] seems to be the most serviceable and useful to calculate the same reaction

Table IVA

*The energy (kJ/mol) and geometry (distances in pm and angles in degree)
of isolated molecules* $(CH_3)_3\dot{C}$ *and* $(CH_3)_3CH$

Property	BSBL	MINDO/3
R° (C^3-H^3) in $i\text{-}\dot{C}_4H_9$ radical		111.4[a]
R° (C^2-C^3) in $i\text{-}\dot{C}_4H_9$		146.9
Angle $H^3-C^3-H^3$ in $i\text{-}\dot{C}_4H_9$		105.91[a]
Angle $C^2-C^3-H^3$ in $i\text{-}\dot{C}_4H_9$		112.90
Angle $C^3-C^2-C^3$ in $i\text{-}\dot{C}_4H_9$		119.92
R° (C^2-H^2) in $i\text{-}C_4H_{10}$ molecule		113.2
R° (C^3-H^3) in $i\text{-}C_4H_{10}$	109.3[b]	111.2[a]
R° (C^2-C^3) in $i\text{-}C_4H_{10}$	154[b]	151.6
Angle $H^3-C^3-H^3$		105.34[a]
Angle $C^2-C^3-H^3$		113.04[a]
Angle $C^3-C^2-H^2$		104.26
Angle $C^3-C^2-C^3$		114.14
E° ($i\text{-}\dot{C}_4H_9$)		−61835.11
E° (CH_4)		−17978.86
E° (CH_4) + E° ($i\text{-}\dot{C}_4H_9$)		−79813.98
E° ($i\text{-}C_4H_{10}$)		−63361.76
E° ($\dot{C}H_3$)		−16349.85
E° ($\dot{C}H_3$) + E° ($i\text{-}C_4H_{10}$)		−79711.61
$\Delta E^{\circ c}$	−47.73[b]	−102.37

[a] Mean values
[b] Experimental equilibrium value
[c] $\Delta E^\circ = E^\circ (CH_4) + E^\circ (i\text{-}\dot{C}_4H_9) - E^\circ (\dot{C}H_3) - E^\circ (i\text{-}C_4H_{10})$

Table IB

*The energy (kJ/mol) and geometry (distances in pm and angles in degree)
of the activated complex for* $\dot{C}H_3 + CH_4 \rightarrow CH_4 + \dot{C}H_3$

Property	BSBL	MINDO/3
$R_{AB}^{\neq} = R_{BC}^{\neq} (= R^{\neq} (C^1-H) \ R^{\neq} (H-C^2))$	128.7	125.6
Angle$^{\neq}$ C^1-H-C^2	180[a]	180
$R^{\neq}$ (C^1-H^1)	109.3[b]	110.1
Angle$^{\neq}$ $H^1-C^1-H^1$	tetrahedral[b]	110.9
Angle$^{\neq}$ H^1-C^1-H	tetrahedral[b]	108
$V^{\neq c}$ $\qquad x$	61.7	43.4

[a] Assumed value
[b] Assumed to be the same as the equilibrium value in CH_4
[c] Barrier height: $V^{\neq} = E^{\neq} (H_3C-H-CH_3) - E^\circ(\dot{C}H_3) - E^\circ (CH_4)$

Table IIB

The energy (kJ/mol) *and geometry (distances in* pm *and angles in degree)*
of the activated complex for $\dot{C}H_3 + C_2H_6 \rightarrow CH_4 + \dot{C}_2H_5$

Property	BSBL	MINDO/3
$R^{\neq}_{AB}$ ($=R^{\neq}$ (C^1-H))	135.0	145.3
$R^{\neq}_{BC}$ ($=R^{\neq}$ (C^2-H))	123.3	117.8
Angle$^{\neq}$ C^1-H-C^2	180[a]	179.9
$R^{\neq}$ (C^1-H^1)	109.3[b]	110.3[d]
$R^{\neq}$ (C^2-H^2)	109.3[c]	110.8[d]
$R^{\neq}$ (C^3-H^3)	109.3[c]	111.5[d]
$R^{\neq}$ (C^2-C^3)	153.4[c]	145.2
Angle$^{\neq}$ $H^1-C^1-H^1$	tetrahedral[b]	110.1[d]
Angle$^{\neq}$ $H^2-C^2-H^2$	tetrahedral[b]	108.7
Angle$^{\neq}$ $H^3-C^3-H^3$	tetrahedral[b]	105.2[d]
Angle$^{\neq}$ H^1-C^1-H	tetrahedral[b]	108.9[d]
Angle$^{\neq}$ H^2-C^2-H	tetrahedral[b]	99.0[d]
Angle$^{\neq}$ $H-C^2-C^3$	tetrahedral[b]	114.3
Angle$^{\neq}$ $C^2-C^3-H^3$	tetrahedral[b]	113.4[d]
$V^{\neq e}$	47.0	28.3

[a] Assumed
[b] Assumed to be the same as in CH_4
[c] Assumed to be the same as in C_2H_6
[d] Mean value
[e] Barrier height: $V^{\neq} = E^{\neq}$ $(H_3C-H-C_2H_5) - E^{\circ}$ $(\dot{C}H_3) - E^{\circ}$ (C_2H_6)

Table IIIB

The energy (kJ/mol) *and geometry (distances in* pm *and angles in degree)*
of the activated complex for $\dot{C}H_3 + C_3H_8 \rightarrow CH_4 + (CH_3)_2 \dot{C}H$

Property	BSBL	MINDO/3
$R^{\neq}_{AB}$ ($=R^{\neq}$ (C^1-H))	138.9	143.8
$R^{\neq}_{BC}$ ($=R^{\neq}$ (C^2-H))	120.6	120.1
Angle$^{\neq}$ C^1-H-C^2	180[a]	179.9
$R^{\neq}$ (C^1-H^1)	109.3[b]	110.4[d]
$R^{\neq}$ (C^2-H^2)	109.3[c]	111.8
$R^{\neq}$ (C^3-H^3)	109.3[c]	111.4[d]
$R^{\neq}$ (C^2-C^3)	154[c]	147.1[d]
Angle$^{\neq}$ $H^1-C^1-H^1$	tetrahedral[b]	108.9[d]
Angle$^{\neq}$ $H^3-C^3-H^3$	tetrahedral[b]	105.1[d]
Angle$^{\neq}$ H^1-C^1-H	tetrahedral[b]	110.0[d]
Angle$^{\neq}$ H^2-C^2-H	tetrahedral[b]	95.3[d]
Angle$^{\neq}$ $H-C^2-C^3$	tetrahedral[b]	106.4[d]
Angle$^{\neq}$ $C^2-C^3-H^3$	tetrahedral[b]	113.5[d]
Angle$^{\neq}$ $C^3-C^2-C^3$	tetrahedral[b]	123.4
$V^{\neq e}$	42.9	20.8

[a] Assumed
[b] Assumed to be the same as in CH_4
[c] Assumed to be the same as in C_3H_8
[d] Mean value
[e] Barrier height: $V^{\neq} = E^{\neq}$ $(H_3C-H-CH(CH_3)_2) - E^{\circ}$ $(\dot{C}H_3) - E^{\circ}$ (C_3H_8)

parameters and many more characteristic data. The potential energy obtained by MINDO/3 is a function of all the nuclear ("internal") coordinates and depends on the charge distribution providing the lowest energy at a given nuclear configuration, therefore, it is suitable for calculating a number of physical quantities (e.g. equilibrium nuclear configurations, force constants, charge distributions, etc.) in various regions of the potential surface. Thus it is obvious that the critical comparison and complementary testing of results obtained by the two different methods is expected to be very useful.

Results and Discussion

Reactions of methyl radicals with methane, ethane, propane and iso-butane were investigated:

(1) $$\dot{C}H_3 + CH_4 \rightarrow CH_4 + \dot{C}H_3$$

(2) $$\dot{C}H_3 + C_2H_6 \rightarrow CH_4 + \dot{C}_2H_5$$

(3) $$\dot{C}H_3 + C_3H_8 \rightarrow CH_4 + (CH_3)_2\dot{C}H$$

(4) $$\dot{C}H_3 + (CH_3)_3CH \rightarrow CH_4 + (CH_3)_3\dot{C}$$
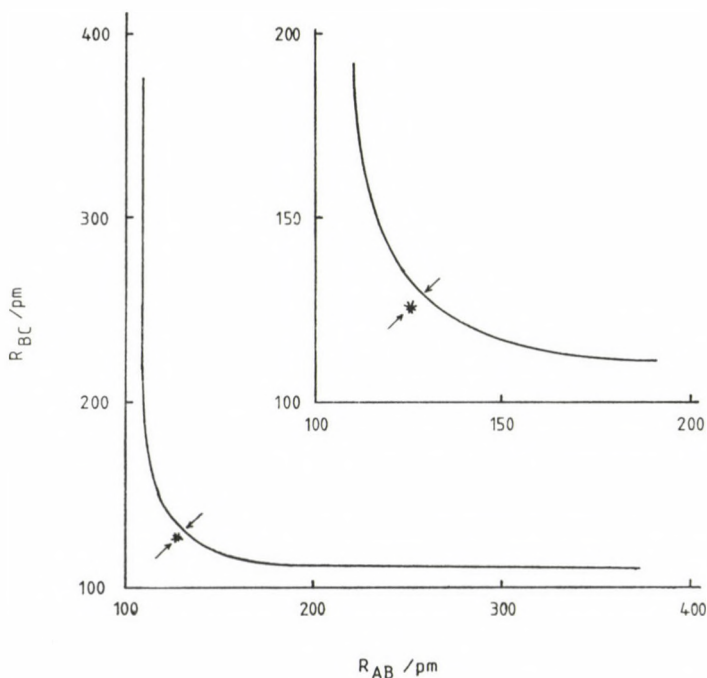
Fig. 2. The BSBL minimum energy path for $\dot{C}H_3 + CH_4 \rightleftharpoons CH_4 + \dot{C}H_3$; location of saddle point from BSBL ($\rightarrow$) and MINDO/3 ($\rightarrow *$) calculations
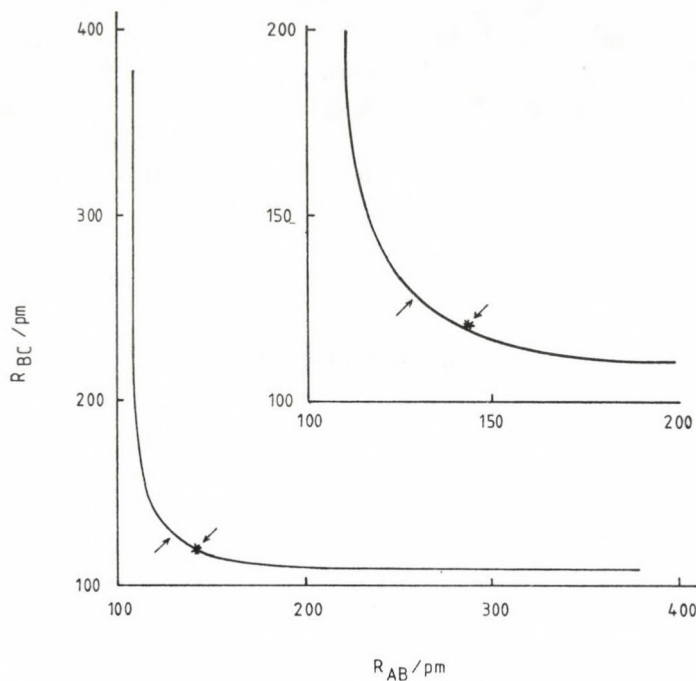
Fig. 3. The BSBL minimum energy path for $\dot{C}H_3 + C_2H_6 \rightleftharpoons CH_4 + \dot{C}_2H_5$; location of saddle point from BSBL ($\rightarrow$) and MINDO/3 ($\rightarrow$*) calculations
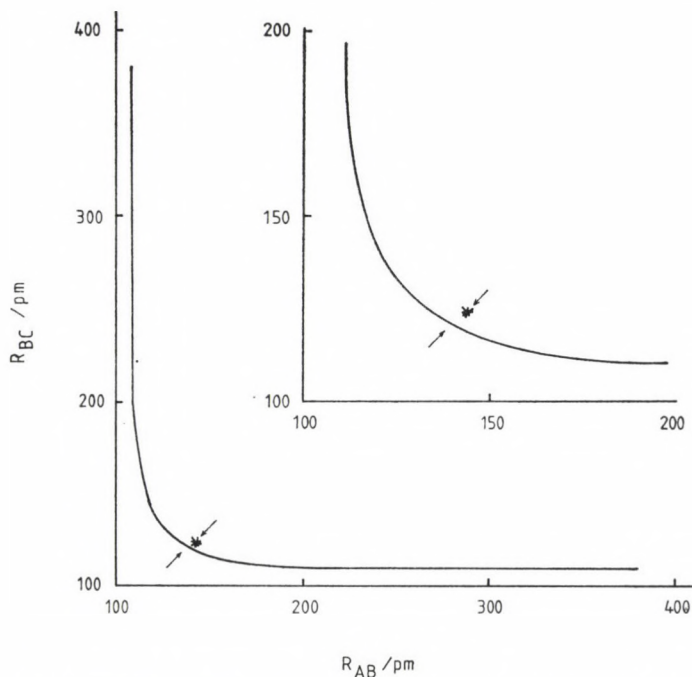
Fig. 4. The BSBL minimum energy path for $\dot{C}H_3 + C_3H_8 \rightleftharpoons CH_4 + (CH_3)_2\dot{C}H$; location of saddle point from BSBL ($\rightarrow$) and MINDO/3 ($\rightarrow$*) calculations
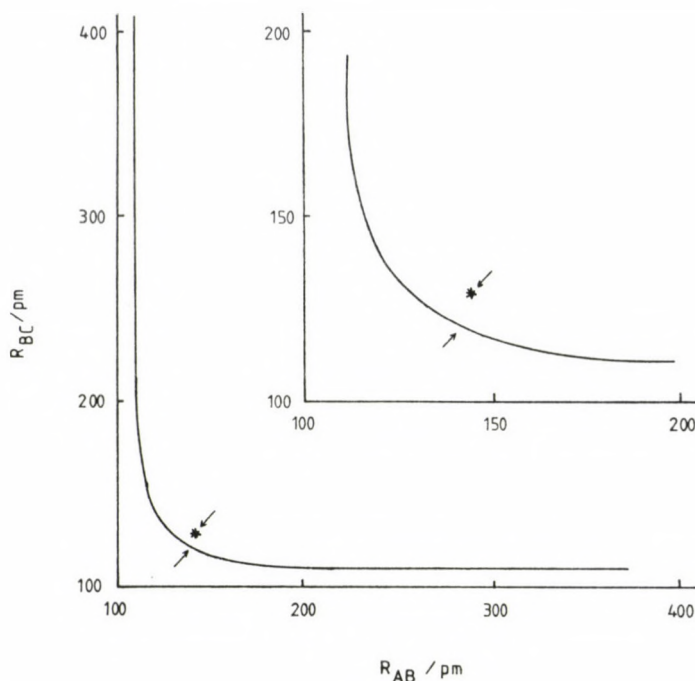
Fig. 5. The BSBL minimum energy path for $\dot{C}H_3 + (CH_3)_3CH \rightleftharpoons CH_4 + (CH_3)_3\dot{C}$; location of saddle point from BSBL ($\rightarrow$) and MINDO/3 ($\rightarrow$*) calculations

The transition state models are displayed in Fig. 1. In the sequence $CH_3 + CH_4$, $CH_3 + C_2H_6$, $CH_3 + C_3H_8$ and $CH_3 + C_4H_{10}$ the first reaction is thermoneutral and the remaining ones are gradually more and more exothermic.

Calculated energies and geometries for isolated reactant and product molecules are given in Tables IA—IVA. The agreement of calculated MINDO/3 results with experimental values is satisfactory where comparison can be made. The only exception is the energetics of methyl attack on isobutane. For this reaction the MINDO/3 calculations predict a reaction energy considerably more exothermic than expected.

The most important results of calculation, i.e. the kinetic properties for hydrogen abstraction reactions by methyl radicals, are given in Tables IB— IVB. Furthermore, some of the kinetic results of primary importance are summarized in Table V. Thus, given are the deviations from the equilibrium values of the bond length in the transition state as well as barrier heights. The appropriate experimental activation energy is included for comparison in the Table.

Finally, in Fig. 2—5. the BSBL reaction paths (minimum energy paths) and BSBL transition states are presented. Indicated are also the locations of saddle points as determined by the MINDO/3 procedure.

Table IVB

*The energy (kJ/mol) and geometry (distances in pm and angles in degree)
of the activated complex for* $\dot{C}H_3 + (CH_3)_3CH \rightarrow CH_4 + (CH_3)_3\dot{C}$

Property	BSBL
$R_{AB}^{\neq} (=R^{\neq} (C^1—H))$	140.9
$R_{BC}^{\neq} (=R^{\neq} (C^2—H))$	119.6
Angle$^{\neq}$ $C^1—H—C^2$	180[a]
$R^{\neq} (C^1—H^1)$	109.3[b]
$R^{\neq} (C^3—H^3)$	109.3[c]
$R^{\neq} (C^2—C^3)$	154[c]
Angle$^{\neq}$ $H^1—C^1—H^1$	tetrahedral[b]
Angle$^{\neq}$ $H^3—C^3—H^3$	tetrahedral[b]
Angle$^{\neq}$ $H^1—C^1—H$	tetrahedral[b]
Angle$^{\neq}$ $H—C^2—C^3$	tetrahedral[b]
Angle$^{\neq}$ $C^2—C^3—H^3$	tetrahedral[b]
Angle$^{\neq}$ $C^3—C^2—C^3$	tetrahedral[b]
$V^{\neq}$[d]	39.0

[a] Assumed
[b] Assumed to be the same as in CH_4
[c] Assumed to be the same as in $(CH_3)_3CH$
[d] Barrier height: $V^{\neq} = E^{\neq} (H_3C—H—C(CH_3)_3) — E^{\circ} (\dot{C}H_3) — E^{\circ} (i\text{-}C_4H_{10})$

Table V

Calculated and experimental activation energies for $A + BC \rightarrow AB + C$
type atom transfer reactions of the methyl radical

Property	$\dot{C}H_3 + H—CH_3$ BSBL	MINDO	$\dot{C}H_3 + H—C_2H_5$ BSBL	MINDO	$\dot{C}H_3 H—C_3H_7$ BSBL	MINDO	$\dot{C}H_3 + H—C_4H_9$ BSBL	MINDO
$R_{AB}^{\neq} — R_{AB}^{\circ}$	19.4	15.4	25.7	35.1	29.6	33.6	31.6	—
$R_{BC}^{\neq} — R_{BC}^{\circ}$	19.4	15.4	14.0	6.7	11.3	7.9	10.3	—
$V^{\neq}$	61.7	43.4	47.0	28.3	42.9	20.8	39.0	—
E_A	59.9		48.1		48.6		39.8	

$R_{AB}^{\neq} — R_{AB}^{\circ}$: Lengthening in pm of the splitting bond in the transition state
$R_{BC}^{\neq} — R_{BC}^{\circ}$: Lengthening in pm of the forming bond in the transition state
$V^{\neq}$: Height of the potential barrier in kJ
E_A: Experimental activation energy in kJ/mol

Both the BSBL and the MINDO/3 results indicate that the saddle point is shifted towards the reactant state as the exothermicity increases in the series. This observation is in agreement with the conclusion derived in a recent study of the location of the saddle point in a series of related reactions where it is found that in order of increasing exothermicity the potential barrier

is shifted to an earlier position along the reaction coordinate [6]. Similar correlations were suggested formerly by Hammond [7] as well as by Mok and Polanyi [8].

In accordance with the results of similar studies, the BSBL results predict the decrease of the height of the potential barrier with increasing exothermicity in the series of homologous methyl radical reactions. The calculations carried out by using the MINDO/3 method and the direct localisation technique described in Ref. [9—11] verify the same trend. Although the MINDO/3 values are lower than the experimental ones they show the decrease of the height of the potential barrier with increasing exothermicity.

REFERENCES

[1] Schaefer III, H. F.: Chem. Brit., **11**, 227 (1975)
[2] Bérces, T., Dombi, J.: Int. J. Chem. Kinet., **8**, 123, 183 (1980)
[3] Johnston, H. S.: "Gas Phase Reaction Rate Theory", The Ronald Press Co., New York 1966
[4] Bingham, R. C., Dewar, M. J. S., Lo, D. H.: J. Amer. Chem. Soc., **97**, 1285, 1294, 1302, 1311 (1975)
[5] Dewar, M. J. S.: Chem. Brit., **11**, 97 (1975)
[6] Bérces, T., László, B., Márta, F.: Acta Chim. Acad. Sci. Hung. **109**, 363 (1982)
[7] Hammond, G. S.: J. Amer. Chem. Soc., **77**, 334 (1955)
[8] Mok, M. H., Polanyi, J. C.: J. Chem. Phys., **51**, 1451 (1969)
[9] Bálint, I., Bán, M. I.: Interntl. J. of Quantum Chem., **24**, 161 (1983)
[10] Bálint, I., Bán, M.: Therret. Chim. Acta, **63**, 255 (1983)
[11] Bálint, I., Bán, M. I.: Interntl. J. Quantum Chem., **25**, 667 (1984)

MOLECULAR REARRANGEMENTS, XVIII*

PHOTOLYSIS OF *N*-ALKYL-ARYLAMINES**

Morsy M. ALY, Mahmoud Zarif A. BADR***, Attiat M. FAHMY and
Safaa A. MAHGOUB

(Chemistry Department, Faculty of Science, Assiut University, Assiut, Egypt. A. R. E.)

The direct photolysis of *N*-benzyl-*N*-methyl-aniline in isopropanol at 25 °C for 15 hours in air gives benzaldehyde, toluene, bibenzyl, *N*-methylaniline and a mixture of *o*- and *p*-benzyl-*N*-methylaniline.

Analogous products are also obtained from the photolysis of *N*-α- or -β-phenethyl-*N*-methyl-aniline in addition to *trans*-2,3-diphenylbutene-2 and 9,10-dimethyl-phenanthrene.

The results are interpreted in terms of an intramolecular free radical mechanism starting by homolysis of the *N*-aralkyl bond into *N*-methyl-anilino and aralkyl free radicals that subsequently contribute to the formation of the identified products.

Rearrangement of *N*-alkyl-aryl amines under the influence of acids or Lewis acid catalysts to give ring-alkylated secondary or primary arylamines through an intermolecular ionic mechanism has long been known as the Hofmann—Martius rearrangement [1—5].

Recently the thermal rearrangement of alkyl-aryl-amines in the absence of any promoter was investigated [6] and it was concluded that the reaction takes place through a free radical mechanism.

Photochemical rearrangements of alkyl-aryl-amines have been little investigated.

It is, however, known that although *N,N*-dimethylaniline is quite stable under ultraviolet light, its hydrochloride salt can be photolysed through an intramolecular charge separated species [7].

The present paper describes the behaviour of some tertiary aryl-alkyl-amines on irradiation with ultraviolet (U.V.) light. The non-sensitized U.V. irradiation of *N*-benzyl-*N*-methylaniline in isopropanol as solvent at room temperature (about 25 °C) for 15 h in the presence of air gives rise to benzaldehyde, toluene and bibenzyl as neutral products, together with *N*-methyl-aniline and a mixture of *o*- and *p*-benzyl-*N*-methylaniline (Scheme 1 and Table I).

$(R = -CH_2-Ph,$
    $-CH_2-CH_2-Ph,$ or
    CH_3
    $|$
    $-CH-Ph)$

+ additional products
(see Table I)
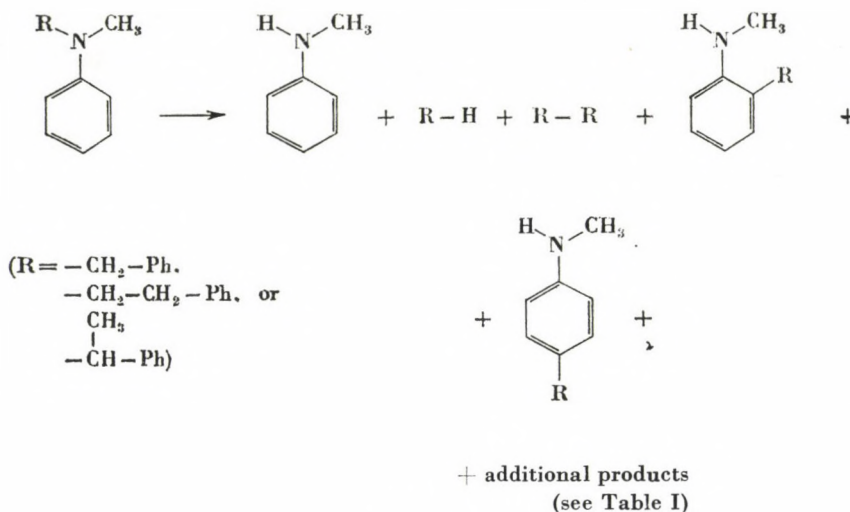
Scheme 1

Photolysis of N-(α-phenethyl)-N-methylaniline in isopropanol gives rise to ethylbenzene, 2,3-diphenylbutane, 2,3-diphenylbutene-2 and 9,10-dimethyl-phenanthrene, together with N-methylaniline and a mixture of o- and p-(α-phenethyl)-N-methylaniline.

Table I

Percentage composition of N-alkyl-arylamine photolysate*

Products	Starting compound and solvent used			
	N-Benzyl N-methyl aniline	N-(β-Phenethyl) N-methylaniline	N-(α-Phenethyl)-N-methyl-aniline	
	Isopropanol	Isopropanol	Isopropanol	Carbon tetra-chloride
Unchanged amine	40.75	5.20	22.90	20.37
Benzaldehyde	34.10	—	—	—
Alkylbenzene	15.60[e]	0.50[t]	2.25[t]	5.65[t]
Dialkyl derivative	0.20	48.50[a]	3.50	1.93
Stilbene derivative	—	—	7.35[b]	39.20[b]
N-Methylaniline	1.34	0.24	0.35	0.13
o-Alkyl-N-methylaniline	7.29	9.52[c]	2.63	2.27
p-Alkyl-N-methylaniline	0.72	30.04[d]	24.12	27.50
9,10-Dimethylphenanthrene	—	—	36.90	2.95

* Irradiation time, 15 h
[a] 1,4-Diphenylbutane : 2,3-diphenylbutane in the ratio 1 : 5
[b] *Trans*-2,3-Diphenylbutene-2
[c] o-(β-phenethyl)-N-methylaniline, no α-isomer was obtained as shown by GLC
[d] p-(β-phenethyl)-N-methylaniline, no α-isomer was obtained as shown by GLC
[e] Toluene
[t] Ethylbenzene

The same products were also obtained when the photolysis was carried out in carbon tetrachloride as a solvent with the exception of an increase of 2,3-diphenylbutene-2 at the expense of 2,3-diphenylbutane.

Photolysis of N-(β-phenethyl)-N-methylaniline in isopropanol gives rise to ethylbenzene, 1,4-diphenylbutane and 2,3-diphenylbutane as neutral products together with N-methylaniline and a mixture of o- and p-(β-phenethyl)--N-methylaniline.

The main feature of these tertiary amine photolyses is the homolysis of the aralkyl-N bond into N-methylanilino and aralkyl free radicals, which subsequently undergo dark reactions contributing to the formation of the identified products. Thus the benzyl free radicals may abstract hydrogen, forming toluene; also, the benzyl radicals undergo oxidation by atmospheric oxygen to give benzaldehyde [8]; they dimerize to bibenzyl, or couple with the mesomeric N-methylanilino free radicals in the o- and p-positions to yield o- and p-benzyl-N-methylanilines, as shown in Scheme 2.

Similarly, the β-phenethyl radicals generated from N-β-phenethyl-N--methylaniline abstract hydrogen to form ethylbenzene; also, they undergo dimerization to 1,4-diphenylbutane, or couple with mesomeric N-methylanilino radicals in the o- or p-positions forming o- and p-(β-phenethyl)-N--methylanilines.
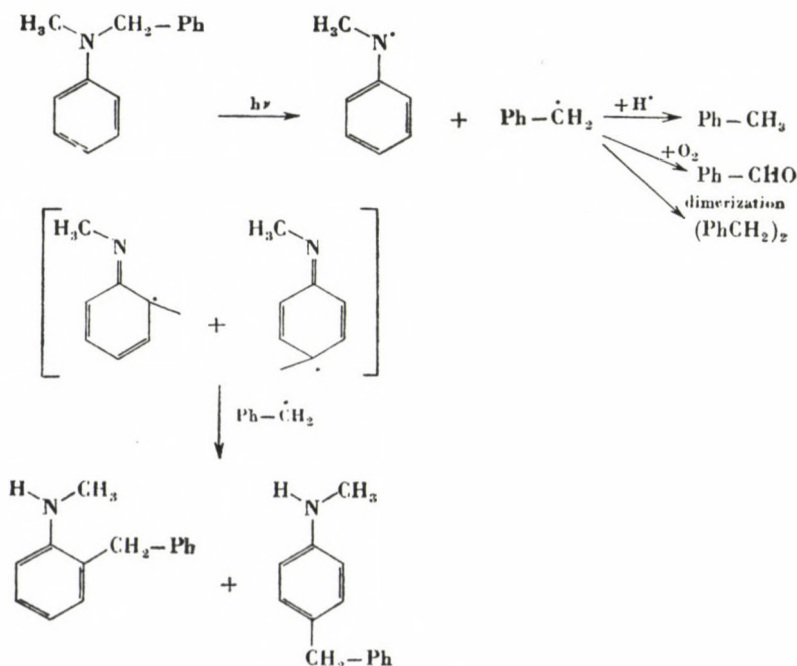
Scheme 2

It may be suggested that β-phenethyl radicals undergo direct rearrangement to their α-isomer prior to their dimerization forming 2,3-diphenylbutane. However, the probability of such a rearrangement (PhCH$_2$ĊH$_2$ → PhĊHCH$_3$), under the present conditions is not easily acceptable [9]. Consequently, the formation of α-phenethyl radicals is best explained as being due to selective H-abstraction of the secondary α-hydrogen rather than the primary β-hydrogen of the ethylbenzene product, since it will give rise to the stabilized α-phenethyl secondary free radical intermediate. Such a long chain of reaction steps curtails the formation of 2,3-diphenylbutene-2 and consequently that of the phenanthrene derivative in the early stages of the reaction, as compared with the case of the photolysis of the α-phenethyl isomer.

Trans-2,3-diphenylbutene-2 is formed from its precursor 2,3-diphenylbutane through dehydrogenation under the influence of the free radicals present in the medium in a manner similar to that described for stilbene formation [10]. However, it may also be assumed to arise via disproportionation of the intermediate benzylic 2,3-diphenylbutyl radical *(a)* (Scheme 3).

The *N*-methylanilino free radical may abstract hydrogen to give *N*-methylaniline, or it may couple with aralkyl radicals in the *o*- or *p*-positions forming the corresponding *o*- or *p*-aralkyl-*N*-methylanilines.

The photo-rearrangement of these tertiary amines seems to be intramolecular in nature, since irradiation of a mixture of *N*-benzyl-*N*-methylaniline and *N*-(α-phenethyl) *p*-toluidine in carbon tetrachloride gives a mixture of 2-(α-phenethyl)-*p*-toluidine, *o*-benzyl-*N*-methylaniline and its *p*-isomer as the amine products, i.e. each amine is seen to undergo rearrangement independently (Table II). No substitution of one alkyl group into the ring of the other compound took place. None of the cross-bred amine products such as
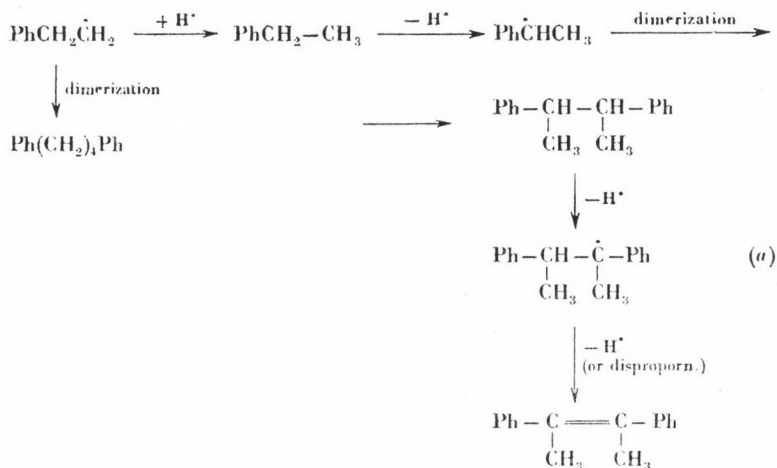
Scheme 3

2-benzyl-*p*-toluidine, *o*- or *p*-(α-phenethyl)-*N*-methylaniline were detected in the photolysate. Hence it can be concluded that the photolysis occurs through homolysis into a free radical pair held together within the solvent cage.

Table II

Amine products obtained from the cross-over photolysis experiment of
N-benzyl-N-methylaniline (0.5 g) and N-(α-phenethyl)-p-toluidine (0.5 g)

	Rf
p-Toluidine	0.48
N-Benzyl-*N*-methylaniline	0.54
N-(α-phenethyl)-*p*-toluidine	0.57
o-benzyl-*N*-methylaniline	0.65
p-benzyl-*N*-methylaniline	0.65
N-Methylaniline	0.37
2-(α-phenethyl)-*p*-toluidine	0.77

The formation of 9,10-dimethylphenanthrene was assumed to take place through the cyclization of *trans*-2,3-diphenylbutene-2 [11] to give the intermediate dihydrophenanthrene derivative that is subsequently dehydrogenated in the presence of atmospheric oxygen or by the action of H-abstracting radicals, as represented in Scheme 4.
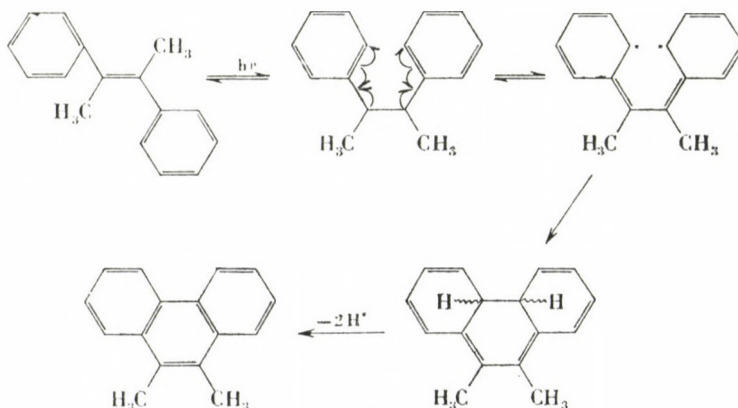
Scheme 4

Photocyclization of 2,3-diphenylbutene-2 to give 9,10-dimethyl-phenanthrene takes place in isopropanol better than in carbon tetrachloride, since isopropanol readily undergoes a process of hydrogen transfer to other molecules forming acetone, which subsequently initiates the photochemical reaction [12].

Experimental

All m.p.'s are uncorrected. Solvents used in the photolyses were of spectrograde quality and used without further purification. The solutions of the amines (1 g) in the solvent used (100 mL) were photolyzed in open-topped pyrex beakers using a Mallinkrodt 150 W mercury discharge lamp at 25 °C for 15 h. The photolysate was separated as indicated in a previous work [6] into amine and neutral products, which were identified by thin layer chromatography (TLC) using glass chromatoplates coated with silica gel G (0.25 mm), and elution with a petroleum ether (40—60 °C) — ether mixture (7:1, v/v). Quantitative analysis was effected by gas-liquid chromatography (GLC) by comparison with the retention times with those of authentic samples, using a Pye-Unicam Gas Chromatograph, "Series 104", equipped with a flame-ionization detector, Model 24, on two columns with different separation characteristics. The glass columns used were 1220×5 mm (4 ft $\times$ 5 mm), packed with 20% SE 30 on Chromsorb W (35—80 mesh), or 10% SE 30 on Celite (60—80 mesh) at 185 °C, using nitrogen as carrier gas. The results are summarized in Table I.

Infrared specra were recorded on a Pye-Unicam IR spectrophotometer, Model SP 200 G. Mass spectra were obtained with a mass spectrophotometer, Model A.E.I.M.S. 902.

Cross-over experiment

A solution of N-benzyl-N-methylaniline (0.5 g) and N-(α-phenethyl)-p-toluidine (0.5 g) in carbon tetrachloride (100 mL) was irradiated for 15 h and the amine components of the photolysate were identified by GLC and TLC by comparison with authentic samples as shown in Table II.

Preparation of the reference compounds

N-Benzyl-N-methylaniline [13]: colourless oil, b.p. 300 °C/760 mm-Hg., n_D^{20} 1.6021; picrate, m.p. 127—8 °C.
N-(α-phenethyl)-N-methylaniline [13]: yellow oil, b.p. 170 °C/760 mm-Hg.
N-(β-Phenethyl)-N-methylaniline [13]: yellow oil, b.p. 180—2 °C/15 mm-Hg.
1,4-Diphenylbutane [14]: colourless oil, b.p. 140—2 °C/15 mm-Hg.
2,3-Diphenylbutane [15]: colourless crystals from ethanol, m.p. 124 °C.
Trans-**2,3-diphenylbutene-2** [16]: colourless crystals from methanol, m.p. 66 °C.
9,10-Dimethylphenanthrene [17]: colourless crystals from acetic acid, m.p. 137 °C.

o- and p-Benzyl-N-methylaniline

Prepared by methylation of the corresponding aminodiphenylmethane by a procedure similar to that described for the preparation of N-methylaniline from aniline [18]; o-isomer, colourless oil, b.p. 148—152 °C/15 mm-Hg; its IR spectrum shows NH stretching vibration at 3351 cm^{-1} and its mass spectrum has a molecular ion at m/e 197. p-Isomer, colourless oil b. p. 150—162 °C/15 mm-Hg; its IR spectrum has NH stretching vibration at 3342 cm^{-1} and it mass spectrum shows a molecular ion at m/e 197. A mixture of o- and p-benzyl-N-methylaniline was also obtained by heating N-benzyl-N-methylaniline (1 g) together with anhydrous aluminium chloride (1 g) in an oil bath at 150 °C for 4 h. The reaction product was decomposed by sodium hydroxide solution, extracted with ether and the ethereal solution evaporated. The residual oil was found by GLC to consist of a mixture of o- and p-benzyl-N-methylaniline in the ratio 1 : 2.5, as compared with the reference samples prepared previously.

o- and p-(α-phenethyl)-N-methylaniline

Prepared as described for o- and p-benzyl-N-methylaniline using o- or p-(α-phenethyl)-aniline [19]; o-isomer, colourless oil, b.p. 153—164 °C/15 mm-Hg; νNH 3352 cm^{-1}, molecular ion at m/e 211; p-isomer, colourless oil, b.p. 152—165 °C/15 mm-Hg, νNH 3344 cm^{-1}, molecular ion at m/e 211.

o- and p-(β-phenethyl)-N-methylaniline

Prepared from N-(β-phenethyl)-N-methylaniline and anhydrous aluminium chloride as described [5b]. The oily product was analysed by GLC. By comparison with the retention

times of the above reference samples it was shown to consist of 34% of unchanged N-(β-
-phenethyl)-N-methylaniline; o- and p-(α-phenethyl)-N-methylaniline; 13.6% and 24.2%,
respectively; o- and p-(β-phenethyl)-N-methylaniline; 11.3% and 16.9% respectively.

REFERENCES

[1] Hofmann, A. W. Martius, C. A.: Ber. Dtsch. Chem. Ges., **4,** 742 (1871); Hofmann, A. W.:
    Ber. Dtsch. Chem. Ges., **7,** 526 (1874)
[2] Hickinbottom, W. J.: J. Chem. Soc., **1932,** 2396; ibid., **1934,** 1700
[3] Ogata, Y., Tabuchi, H., Koshida, K.: Tetrahedron, **20,** 2717 (1964)
[4] Dewar, M. J. S.: Nature, **156,** 784 (1946)
[5] (a) Michael, A.: J. Am. Chem. Soc., **42,** 787 (1920); (b) Beckmann, E., Correns, E.: Ber.
    Dtsch. Chem. Ges., **55,** 852 (1922)
[6] Badr, M. Z. A., Aly, M. M.: Can. J. Chem., **52,** 293 (1974); Osman, A. M., Badr, M. Z. A.,
    Abdel-Rahman, A. E.: Bull. Chem. Soc. Jpn., **49,** 2611 (1976)
[7] Linshitz, H., Grellmann, K. H.: J. Am. Chem. Soc., **86,** 303 (1964); Pac, C., Sakurai, H.:
    Tetrahedron Lett., **1968,** 1865; Ogata, Y., Takagi, K.: J. Org. Chem., **35,** 1642 (1970)
[8] Woodward, A. F., Mesrobian, R. B.: J. Am. Chem. Soc., **75,** 6189 (1953)
[9] Photochemistry, Vol. **8,** Specialist Periodical Reports, The Chemical Society, London,
    p. 319 (1977)
[10] Osman, A. M., Badr, M. Z. A., Aly, M. M., El-Sherief, H. A. H.: J. Appl. Chem. Biotechnol.,
    24, 319 (1974)
[11] Hyser, E. S.: "Free Radical Chain Reactions", p. 38. J. Wiley, New York 1970
[12] Mallory, F. B., Wood, E. S., Gordon, J. T.: J. Am. Chem. Soc., **86,** 3094 (1964)
[13] Gomberg, M., Buchler, C. C.: J. Am. Chem. Soc., **42,** 2059 (1920)
[14] Kuhn, R., Winterstein, A : Helv. Chem. Acta, **11,** 127 (1928)
[15] Conant, J. B., Blatt, A. H.: J. Am. Chem. Soc., **50,** 551 (1928)
[16] Ott, E.: Ber. Dtsch. Chem. Ges., **61,** 2135 (1928)
[17] Meerwein, H.: Justus Liebigs Ann. Chem. **405,** 174 (1917)
[18] Hepp, P.: Ber. Dtsch. Chem. Ges., **10,** 328 (1877)
[19] Hickinbottom, W. J.: J. Chem. Soc., **1934,** 319

β-CHLOROETHYLCARBAMOYL DERIVATIVES OF ENKEPHALIN ANALOGS

Helga Süli-Vargha[1]*, Hedvig Medzihradszky-Schweiger[1],
Katalin DiGleria[2] and Kálmán Medzihradszky[2]

(*[1]Research Group for Peptide Chemistry, Hungarian Academy of Sciences,
H-1088 Budapest, Múzeum krt. 4/B, and [2]Central Research Institute of Chemistry
Hungarian Academy of Sciences, H-1025 Budapest, Pusztaszeri út 57/69.*)

The N^{α}-, N^{ε}- and N^{ω}-β-chloroethylcarbamoyl derivatives of Leu⁵-enkephalin, BOC-Lys-Tyr-Gly-Gly-Phe-Leu-OMe and BOC-Tyr-Gly-Gly-Phe-Leu-NH—NH—CO——CH$_2$—CH$_2$—NH$_2$, respectively, were prepared by reaction of β-chloroethyl isocyanate with the free amino groups. Removal of the *t*-butyloxycarbonyl protecting group led to the β-chloroethylcarbamoyl derivatives of the free peptides. The biological activities of these derivatives were compared with those of Met⁵-enkephalin and H-Lys-Leu⁵--enkephalin methyl ester in the following in vitro tests: guinea pig ileum, mouse vas deferens and the nictitating membrane of the cat.

Chemically reactive synthetic derivatives of peptide hormones and hormone fragments play an important role in studying the mechanism of their biological action. When planning such compounds one must take into consideration that these hormone-derivatives have to recognize their receptors and the groups introduced into the molecules must have suitable reactivity. Highly reactive derivatives will react before reaching their specific receptor, while substituents with low reactivity will not lead to the desired effect.

In the last couple of years many data were reported on the significance of mercapto groups in the organization and functioning of opiate receptors. The described cluster formation of these receptors in the presence of enkephalin is dependent on reactive mercapto groups [1, 2]. It has also been reported that mercapto and disulfide groups are present at the opiate binding site [3, 4]. Moreover, peptidases were found in the brain containing reactive mercapto groups on their active sites [5]. The synthesis of enkephalin derivatives containing substituents reactive toward mercapto groups could significantly contribute to the chemical characterization of the opiate receptor and the degrading enzymes as well.

In order to synthesize reactive derivatives of enkephalin, we introduced into the molecule the N-(β-chloroethyl)carbamoyl group. Amino acids containing this group were shown to have a moderate alkylating activity toward mercapto groups [6]. These derivatives can be readily prepared by means of β-chloroethyl isocyanate from compounds containing free amino groups:

$$R—NH_2 + OCN—CH_2—CH_2—Cl \rightarrow R—NH—CO—NH—CH_2—CH_2—Cl$$
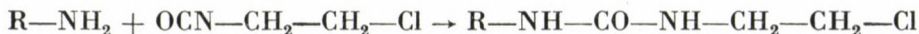
* To whom correspondence should be addressed

An intact N-terminal amino group or a positive charge on the N-terminus is essential for the biological activity of enkephalins [7, 8]. In order to fulfill the requirements mentioned above, an additional amino group had to be introduced into the molecule. This was achieved by two different routes. In the first analog the N-terminus of the peptide was extended by a lysine residue, keeping a free amino group in the α-position, while the ε-function simultaneously served as the reactive site for the addition of β-chloroethyl isocyanate. In the second analog enkephalin hydrazide was prepared and acylated with β-alanine; in this way the NH_2-group of the latter amino acid reacted with the isocyanate.

For the synthesis of the lysine analog H-Tyr-Gly-Gly-Phe-Leu-OMe [9] was acylated with N^α-t-butyloxycarbonyl-N^ϵ-benzyloxycarbonyllysine p-nitrophenyl ester to give the protected hexapeptide I. After removal of the benzyloxycarbonyl group, to the resulting BOC-Lys-Tyr-Gly-Gly-Phe-Leu-OMe (II) β-chloroethyl isocyanate was added, producing BOC-Lys(Q)-Tyr-Gly-Gly-Phe-Leu-OMe (III) (Q = —CO—NH—CH_2—CH_2—Cl). Deprotection with HCl
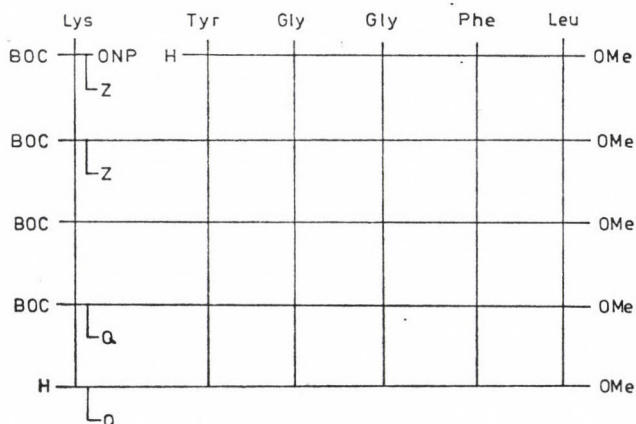
Fig. 1. Synthesis of the lysyl-enkephalin derivative (Q = —CO—NH—CH_2—CH_2—Cl)
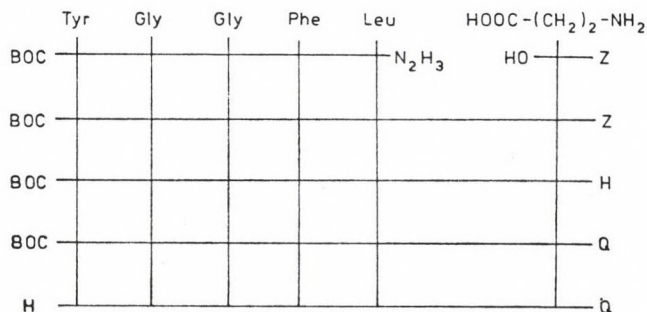
Fig. 2. Synthesis of the β-alanyl-enkephalin derivative (Q = —CO—NH—CH_2—CH_2—Cl)

Table I

Relative biological activities of enkephalin derivatives

	GPI	MVD	CNM
Met⁵-enkephalin	1.0	1.0	1.0
Q-Leu⁵-enkephalin (XI)	0.027	0.009	0.065
H-Lys(Q)-Leu⁵-enkephalin methyl ester (IV)	0.53	0.1	1.24
H-Lys-Leu⁵-enkephalin methyl ester (V)	0.38	0.087	0.26
N^ω-(Q-β-alanyl)-enkephalin hydrazide (X)	0.85	0.75	3.16

in ethyl acetate gave the desired H-Lys(Q)-Tyr-Gly-Gly-Phe-Leu-OMe.HCl (**IV**) (Fig. 1).

In order to obtain comparative biological data, the parent compound, H-Lys-Tyr-Gly-Gly-Phe-Leu-OMe (**V**) was also prepared.

In the synthesis of the β-alanine analog BOC-Tyr-Gly-Gly-Phe-Leu-N_2H_3 (**VI**) was acylated with N-benzyloxycarbonyl-β-alanine in the presence of dicyclohexylcarbodiimide and 1-hydroxybenzotriazole to give BOC-Tyr-Gly--Gly-Phe-Leu-NH—NH—CO—CH_2—CH_2—NH—Z (**VII**). After catalytic hydrogenolysis, BOC-Tyr-Gly-Gly-Phe-Leu-NH—NH—CO—CH_2—CH_2—NH_2 (**VIII**) was treated with β-chloroethyl isocyanate producing BOC-Tyr-Gly-Gly--Phe-Leu-NH—NH—CO—CH_2—CH_2—NH—Q (**IX**). The t-butyloxycarbonyl group was removed by acidolysis to give the free hexapeptide carrying the β-chloroethylcarbamoyl group on the C-terminus (**X**) (Fig. 2).

Finally, as a comparison, the β-chloroethylcarbamoyl derivative of leucine enkephalin (**XI**) was also synthesized and tested for biological activity.

For the biological evaluation some in vitro tests using isolated organs, such as the longitudinal strip of guinea pig ileum (GPI), mouse vas deferens (MVD) and the nictitating membrane of the cat (CNM) were applied. Briefly, compound **IV** proved to be equipotent with methionine enkephalin on CNM, showed half the activity of methionine enkephalin on GPI, and one-tenth of the activity on MVD. These activities are somewhat higher than those of the parent lysyl-enkephalin methyl ester. The β-alanine derivative (compound **X**) has nearly the same activity as shown by methionine enkephalin on GPI and MVD, and was three times more active on CNM (Table I). No sign of irreversibility (alkylation) could be observed under the conditions applied. As expected, Q-Leu⁵-enkephalin did not show significant biological activity in any of the tests used, proving again the importance of the free amino group in the biological activity of enkephalins on one hand, and the lack of any enkephalin-like activity of the Q-group per se, on the other. Details of these measurements were published earlier [10].

The β-chloroethylcarbamoyl derivatives of enkephalin and enkephalin analogs were moderately reactive toward mercapto groups [11].

Experimental

For TLC analysis Merck Silica Gel F_{254} (0.2 mm) sheets were used. Preparative chromatography was performed on Merck Silica Gel 60 (230—400 mesh) in open columns. The retention factors were determined in the following solvent systems (v/v):

S1 Ethyl acetate-pyridine-acetic acid-water = 240 : 20 : 6 : 11
S2 Ethyl acetate-pyridine-acetic acid-water = 120 : 20 : 6 : 11
S3 Ethyl acetate-pyridine-acetic acid-water = 60 : 20 : 6 : 11
S4 Ethyl acetate-methanol = 5 : 1
S5 Butanol-acetic acid-water = 4 : 1 : 1
S6 Ethyl acetate-pyridine-acetic acid-water = 30 : 20 : 6 : 11

BOC-Lys(Z)-Tyr-Gly-Gly-Phe-Leu-OMe (I)

H-Tyr-Gly-Gly-Phe-Leu-OMe acetate (2.52 g; 4 mmol) was dissolved in 25 mL pyridine; 2.1 g (4.2 mmol) BOC-Lys(Z)-ONP was added to the solution which was then allowed to stand 24 h at room temperature. The solvent was evaporated in vacuum and the residue triturated with ether. The resulting powder (I) was chromatographically pure, 3.8 g (88.5%); R_f: 0.78 (S1).
$C_{48}H_{65}N_7O_{12}$ (932.09). Calcd. C 61.58; H 7.03; N 10.52. Found C 61.72; H 6.96; N 10.55%.

BOC-Lys-Tyr-Gly-Gly-Phe-Leu-OMe (II)

Compound I (930 mg; 1 mmol) was dissolved in 20 mL methanol and hydrogenated for 2 h in the presence of 200 mg Pd/C catalyst. The catalyst was filtered off, washed well with methanol, and the filtrate evaporated to give a crude material which was purified on a silica gel column in solvent system S3 to give 620 mg (77.8%) of II; R_f: 0.45 (S3).
$C_{40}H_{59}N_7O_{10}$ (797.96). Calcd. C 60.15; H 7.39; N 12.28. Found C 59.95; H 7.30; N 12.32%.

BOC-Lys(Q)-Tyr-Gly-Gly-Phe-Leu-OMe (III)

BOC-Lys-Tyr-Gly-Gly-Phe-Leu-OMe (120 mg; 0.15 mmol) was dissolved, with stirring, in 2 mL abs. dimethylformamide (DMF) containing 0.014 mL (0.16 mmol) β-chloroethyl isocyanate. The reaction mixture was kept overnight at room temperature, then it was concentrated in vacuum. The residue was purified on silica gel column in solvent system S4. After collecting and evaporating the fractions, the residue was triturated with ether and the resulting white solid was filtered off to obtain 80 mg (50%) of III; R_f: 0.85 (S4) and 0.88 (S2).
$C_{43}H_{63}N_8O_{11}Cl$ (903.9). Calcd. Cl 3.92. Found Cl 4.29%.

H-Lys(Q)-Tyr-Gly-Gly-Phe-Leu-OMe.HCl (IV)

To 80 mg (0.09 mmol) of III there was added 2 mL 2 N HCl/ethyl acetate, at room temperature. After 30 min the reaction mixture was diluted with dry ether, the white precipitate was filtered off and washed on the filter with ether to obtain 140 mg (80%) of IV; R_f: 0.13 (S2) and 0.2 (S4).
$C_{38}H_{56}N_8O_9Cl_2$ (839.82). Calcd. Cl 8.44. Found Cl 8.83%.

H-Lys-Tyr-Gly-Gly-Phe-Leu-OMe.2CH₃COOH (V)

Compound II (800 mg; $\sim$1 mmol) was dissolved in 5 mL trifluoroacetic acid. After 15 min ether was added to the solution and the precipitate was filtered off and washed with ether. The product was dissolved in water and applied onto a column of Amberlite IRA 400 (in acetate cycle) and lyophilized to give 695 mg (85%) of V; R_f: 0.30 (S6).
$C_{39}H_{59}N_7O_{12}$ (817.95). Calcd. C 57.26; H 7.27; N 11.98. Found C 56.97; H 7.00; N 11.62%.

BOC-Tyr-Gly-Gly-Phe-Leu-N$_2$H$_3$ (VI)

BOC-Tyr-Gly-Gly-Phe-Leu-OMe (2 g; 3 mmol) [9] was dissolved in 6 mL DMF and 1.5 mL (30 mmol) 98% hydrazine hydrate was added to the solution. After 24 h half of the solvent was evaporated in vacuum, and 50 mL water was added to the residue. The precipitate was filtered off and washed on the filter with water, cold methanol and, finally, with ether. The crude product was crystallized from a mixture of 15 mL water and 15 mL DMF to give 1.74 g (86.6%) of **VI**; R_f: 0.55 (S2); m.p. 216—218 °C.

C$_{33}$H$_{47}$N$_7$O$_8$ (669.78). Calcd. C 59.12; H 7.02; N 14.63. Found C 60.10; H 6.92; N 15.10%.

BOC-Tyr-Gly-Gly-Phe-Leu-NH—NH—CO—CH$_2$CH$_2$—NH—Z (VII)

Z-β-Ala-OH (557 mg, 2.5 mmol), 420 mg (3 mmol) 1-hydroxybenzotriazole and 1.67 g (2.5 mmol) of **VI** were dissolved in 30 mL dimethylformamide, and the mixture was cooled down to 0 °C. Dicyclohexylcarbodiimide (620 mg; 3 mmol) was added to the stirred solution in small portions. Stirring was continued for 1 h at 0 °C and for 1 h at room temperature. The precipitated dicyclohexylurea was filtered off and the filtrate evaporated. The residue was triturated with ethyl acetate. The resulting white powder was washed well on the filter with sodium hydrogen carbonate and water to give 1.8 g (82.2%) of **VII**. R_f: 0.55 (S1).

C$_{44}$H$_{58}$N$_8$O$_{11}$ (874.99). Calcd. C 60.34; H 6.63; N 12.80. Found C 61.05; H 6.58; N 12.71%.

BOC-Tyr-Gly-Gly-Phe-Leu-NH—NH—CO—CH$_2$CH$_2$—NH$_2$.CH$_3$COOH (VIII)

Compound **VII** (876 mg; 1 mmol) was dissolved in 20 mL 50% acetic acid-methanol and hydrogenated in the presence of 170 mg Pd/C catalyst for 3 h. The product was purified on a silica gel column in solvent system S3 to give 600 mg (75%) of **VIII**; R_f: 0.35 (S3).

C$_{38}$H$_{56}$N$_8$O$_{11}$ (800.92). Calcd. C 56.93; H 6.99; N 13.98. Found C 57.12; H 7.06; N 13.88%.

BOC-Tyr-Gly-Gly-Phe-Leu-NH—NH—CO—CH$_2$CH$_2$—NH—Q (IX)

To a solution of 160 mg (0.2 mmol) of **VIII** in 2 mL DMF, 0.028 mL (0.2 mmol) triethylamine and 0.019 mL (0.22 mmol) of β-chloroethyl isocyanate were added, with stirring. Stirring was continued at room temperature for 3 h, the solvent was then evaporated in vacuum and the residue was triturated with water. The white precipitate was filtered off and washed on the filter with water to give 130 mg (77%) of **IX**; R_f: 0.72 (S4) and 0.63 (S2).

C$_{39}$H$_{56}$N$_9$O$_{10}$Cl (846.40). Calcd. Cl 4.19. Found Cl 4.26%.

H-Tyr-Gly-Gly-Phe-Leu-NH—NH—CO—CH$_2$CH$_2$—NH—Q.HCl (X)

To 170 mg (0.2 mmol) of **IX**, 2 mL 2 N HCl/ethyl acetate was added at room temperature. The reaction mixture was diluted with ether after 30 min. The white precipitate was filtered off and washed on the filter with ether to give 140 mg (90%) of **X**; R_f: 0.6 (S3) and 0.15 (S2).

C$_{34}$H$_{49}$N$_8$O$_8$Cl$_2$ (782.74). Calcd. Cl 9.06. Found Cl 9.72%.

Q-Tyr-Gly-Gly-Phe-Leu-OH (XI)

H-Tyr-Gly-Gly-Phe-Leu-OH (160 mg; 0.3 mmol) was dissolved in 2 mL abs. DMF, with stirring; 0.042 mL (0.3 mmol) triethylamine and 0.028 mL (0.33 mmol) β-chloroethyl isocyanate were added. After 1 h the solvent was evaporated in vacuum, the residue triturated with ether and the precipitate was filtered off. After drying, the white powder was washed with water and dried again over P$_2$O$_5$ in a desiccator to give 160 mg (81%) of **XI**; R_f: 0.4 (S2) and 0.86 (S5).

C$_{31}$H$_{41}$N$_6$O$_8$Cl (661.18). Calcd. Cl 5.36. Found Cl 5.01%.

REFERENCES

[1] Hazum, E., Chang, K.-J., Cuatrecasas, P.: Science, **206**, 1077 (1979)
[2] Hazum, E., Chang, K.-J., Cuatrecasas, P.: Nature, **282**, 626 (1979)
[3] Wilson, H. A., Pasternak, G. W., Snyder, S. H.: Nature, **253**, 448 (1975)
[4] Simon, E. J., Groth, J.: Proc. Natl. Acad. Sci. USA, **72**, 2404 (1975)
[5] Lee, C. M., Arregui, A., Iversen, L. L.: Biochem. Pharmacol., **28**, 553 (1979)
[6] S.-Vargha, H., Medzihradszky-Schweiger, H., Ruff, F., Medzihradszky, K.: Tetrahedon, **39**, 2255 (1983)
[7] Morley, J.: Ann. Rev. Pharmacol. Toxicol., **20**, 81 (1980)
[8] Bajusz, S., Rónai, A., Székely, J., Miglecz, E., Berzétei, I.: FEBS Lett., **110**, 85 (1980)
[9] Medzihradszky-Fölkl, K., Magyar, A., DiGleria, K., Medzihradszky, K.: Acta Chim. Hung. (In the press)
[10] Friedmann, T., Medzihradszky, K., Kovács, A., Kerecsen, L., H. Szécsi, J., DiGleria, K., Knoll, J.: Pol. J. Pharmacol. Pharm., **34**, 53 (1982)
[11] Süli-Vargha, H., DiGleria, K., Medzihradszky-Schweiger, H., Medzihradszky, K.: Proc. 16th Eur. Peptide Symp., 1980, Helsingör, Denmark (Brunfeldt, K., Ed.) p. 547, Copenhagen 1981

DERIVATIZATION OF KETO FATTY ACIDS, VIII

SYNTHESIS OF SUBSTITUTED OXATHIOLANE AND DIOXOLANE

Syed Rafat Husain, Fasih Ahmad* and Mashood Ahmad

(Section of Oils and Fats, Department of Chemistry,
Aligarh Muslim University, Aligarh-202 001, India)

Substituted oxathiolane and dioxolane derivatives have been synthesized from oxo fatty acids. The reaction of 3-mercaptopropan-1,2-diol with 10-oxoundecanoic (1) and 9-oxooctadecanoic (2a) acids affords the corresponding oxathiolanes and dioxolane in good yields. A similar reaction with 2-oxoundecanoic acid does not take place. Mass spectral fragmentation patterns of long-chain oxathiolanes and dioxolane derivatives are detailed.

Many methods have been published in the literature for the synthesis of oxathiolanes [1—3] and dioxolanes [4—6] from oxo compounds. Recent interest developed in the synthesis of oxathiolanes and dioxolanes for various applications, such as antibacterial agents, lubricant additives, rubber substitutes, herbicides and plant growth inhibitors [7]. They have also been found antagonists [6], inhibitors of the secretion of gastric juice [8], as effective as atropine [9], and radioprotectants [10]. As an extension of our studies directed towards the syntheses of heterocycles from oxo fatty acids, we describe here the synthesis of oxathiolane and dioxolane derivatives by the reaction of oxo compounds with 3-mercaptopropan-1,2-diol in the presence of boron trifluoride--etherate (BF_3—Et_2O). The structures of the products were confirmed by spectral data.

Reaction of the penultimate oxo fatty acid, 1 with 3-mercaptopropan-1,2-diol in the presence of acetic acid and BF_3—Et_2O gave three products (1a, b, c) (Scheme 1).

The IR spectrum of product 1a showed the absence of the oxo function (1720 cm^{-1}), suggesting its incorporation into an oxathiolane or dioxolane ring. The spectrum has characteristic bands at 1410 (CH$_2$—S def.); 1240 (C—S wag.); 1160, 1070 (C—O) and 1030 cm^{-1} (acetal ring vibration). The appearance of an additional band at 1750 cm^{-1} (SCOCH$_3$) clearly established that the mercapto group has been converted to the mercaptoacetyl derivative in the course of the reaction. The ^{1}H-NMR spectrum of this compound exhibited characteristic peaks at δ 4.2 m (3×H, 4-methine and 5-methylene pro-

---

* To whom correspondence should be addressed.

$$R-\underset{\underset{O}{\parallel}}{C}-R'$$

1, 2a, 3

$$\downarrow \begin{bmatrix} -SH \\ -OH, \\ -OH \end{bmatrix} \begin{array}{l} AcOH, \\ BF_3-Et_2O \end{array}$$

1, 1a, 1b, 1c   R = $-CH_3$; R' = $-(CH_2)_8COOH$
2a, 2b, 2c   R = $-(CH_2)_8CH_3$; R' = $-(CH_2)_7COOH$
3   R = $-(CH_2)_{15}CH_3$; R' = $-COOH$
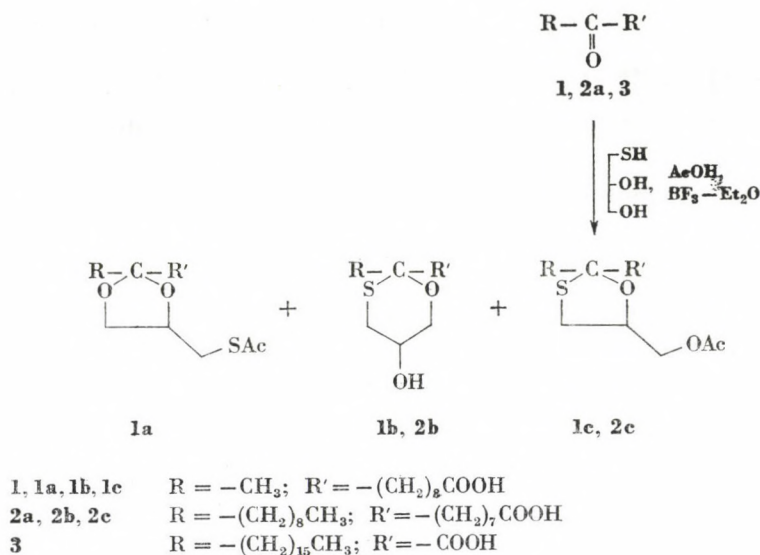
Scheme 1

tons); 3.0 d (2H, CH_2SAc); 2.3 m (4H, methylene protons, α to the ring and carboxyl group); 2.0 s (3H, SCOCH_3); 1.55 s (3H, CH_3—C—). On the basis of these data, **1a** was characterized as 2-methyl-4-[(acetylthio)-methyl]-1,3--dioxolane-2-nonanoic acid.

The IR spectrum of product **1b** displayed bands at 3360 (CHOH) and 1035 cm^{-1} (oxathiane ring vibration) [1]. Its ^{1}H-NMR spectrum showed diagnostic signals at δ 6.0 br, s (1H, CH—OH; disappeared on shaking with D$_2$O); 4.2 m (1H, CH—OH), 3.8 d (2xH, 6-methylene protons); 2.9 d (2xH, 4-methylene protons) along with other usual peaks. The disappearance of the singlet at δ 2.1 for acetate protons indicated that the secondary alcohol is not changed to acetate function. These data supported the product **1b** to be 5-hydroxy-2-methyl-1,3-oxathiane-2-nonanoic acid. The preferential attack [1] of the SH rather than OH function of the reagent on the carbonyl group gives rise to compound **1b** as the major product. The mass spectrum of **1b** (Fig. 1) gave the molecular ion peak at m/z 290 (C$_{14}$H$_{26}$O$_4$S, 1.5) along with other $(M+1)$ and $(M+2)$ peaks. The other structure-revealing peaks were observed at m/z 275 (A, 2.5), 273 (M—OH, 2), 258 (273-CH$_3$, 1), 257 (M-SH, 1.5), 246 (M-C$_2$H$_4$O, 1), 243 (M-CH$_3$S, 2.5), 217 (M-C$_3$H$_5$O$_2$, 3), 201 (M-C$_3$H$_5$O$_3$, 4), 183 (10.5), 133 (B, 76), 115 (B-H$_2$O, 4), 107 (C$_3$H$_7$O$_2$S, 8.5), 75 (B-C$_3$H$_6$O, 10) and 73 (B-C$_2$H$_4$O$_2$, 21.5).

The third product **1c** showed characteristic bands at 1745 (OCOCH$_3$); 1220 (acetate) and 1030 cm^{-1} (oxathiolane ring) in its IR spectrum. ^{1}H-NMR revealed peaks at δ 4.2 br, m (3xH, 5-methine and CH_2OAc protons), 2.9 d (2xH, 4-methylene protons) and 2.2 s (3H, OCOCH_3). The acetate protons

were observed at little more downfield (δ 2.2) than the SCOCH_3 protons (δ 2.0) of product **1b**, which is an additional support to differentiate the products (**1b** and **1c**). Thus compound **1c** was formulated as 2-methyl-5-[(acetoxy)--methyl]-1,3-oxathiolane-2-nonanoic acid. Further support of this structure was obtained by the mass spectrum. It showed (Fig. 2) the molecular ion peak at m/z 332 ($C_{16}H_{28}O_5S$, 1.5); along with the ($M + 1$) peak. The diagnostic peaks observed were at m/z 317 (C, 1.5); 299 (M-SH, 1); 298 (M-SH$_2$, 3); 289 (M-CH$_3$CO, 1); 286 (M-CH$_2$S, 2); 256 (298-CH$_2$CO or C—CH$_3$COOH, 3.5); 225 (256-CH$_2$OH, 1.5); 207 (225-H$_2$O, 2); 175 (D, 2); 133 (D-CH$_2$CO, 5); 125 (159-SH$_2$, 17.5); 117 (175-OCOCH$_2$, 33) and 71 (103-S, 16.5).

Reaction of the internal oxo compound **2a** with 3-mercaptopropan-1,2--diol gave two products **2b, c**. Based on earlier observations, this reaction should have yielded three corresponding products, but owing to its insufficient quantity, one of them could not be isolated. The product **2b** showed IR characteristics almost similar to **1b**. The ¹H-NMR spectrum exhibited the same peaks as that of **1b**, except for the terminal methyl protons at δ 0.88, and six methylene protons (δ 2.3 m) in α-position to the carboxyl group and ring. On the basis of these similar spectral behaviour, **2b** was characterized as 5-hydroxy-2-nonyl-1,3-oxathiane-2-octanoic acid. Its mass spectrum (Fig. 3) showed no molecular ion peak at m/z 388. The characteristic fragment ions noted were at m/z 261 (E, 3); 245 (F, 2.5); 244 (E—H$_2$O, 2); 228 (261-SH or F—OH, 1.5); 216 (E—COOH, 2.5); 212 (245-SH, 2); 201 (261-C$_2$H$_4$O$_2$, 1); 188 (E-C$_3$H$_5$O$_2$, 2); 187 (E-C$_3$H$_6$O$_2$, 1); 185 (E—C$_2$H$_4$OS, 2); 171 (E—C$_3$H$_6$OS, 3.5); 169 (F—C$_2$H$_4$OS, 2); 155 (F—C$_3$H$_6$OS, 4.5); 118 (C$_4$H$_6$O$_2$S, ring, 7.5) and 73 (118-CHS, 38).

The other product, **2c** revealed characteristic signals similar to those of **1c** in its IR and ¹H-NMR spectra, except for the appearance of α methylene protons at δ 2.3 and terminal methyl protons at δ 0.88. The product **2c** was designated as 2-nonyl-5-[(acetoxy)-methyl]-1,3-oxathiolane-2-octanoic acid. Here again the mass spectrum (Fig. 4) did not show the molecular ion peak at m/z 430. The diagnostic peaks observed were at m/z 303 (G, 1.5); 287 (K, 1); 258 (G—COOH, 1.5); 228 (K—OCOCH$_3$, 1); 201 (G—C$_4$H$_6$O$_3$, 1); 187 (G—C$_5$H$_8$O$_3$, 1.5); 185 (K—C$_4$H$_6$O$_3$, 2); 160 (G—(CH$_2$)$_7$COOH, 8.5); 155 (K—C$_5$H$_8$O$_2$S, 6.5); 140 (155—CH$_3$, 5); 117 (160-CH$_3$CO, 3) and 102 (160-OCOCH$_2$, 12.5).

The satisfactory results obtained from the reaction of 3-mercaptopropan--1,2-diol with 10-oxoundecanoic acid (**1**) and 9-oxooctadecanoic acid (**2a**) prompted us to carry out the same reaction with 2-oxooctadecanoic acid (**3**), where the oxo function is in close proximity of the carboxyl group. The reaction of **3** with 3-mercaptopropan-1,2-diol did not take place. The non-reactivity of **3** may be attributed to its peculiar structural feature. The inductive effect caused by the chain and acid carbonyl groups makes the oxo function less reactive. Another factor, steric hindrance, may also play an important role.
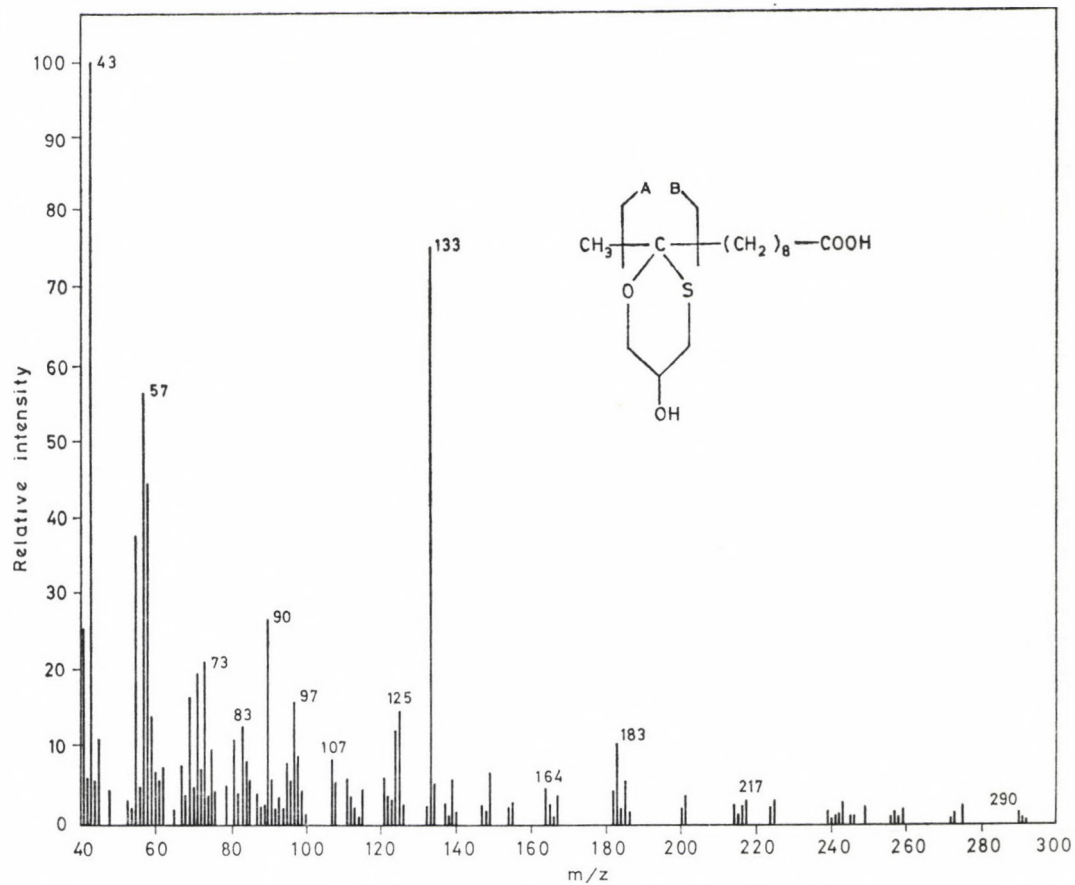
Fig. 1. Mass spectrum of **1b**
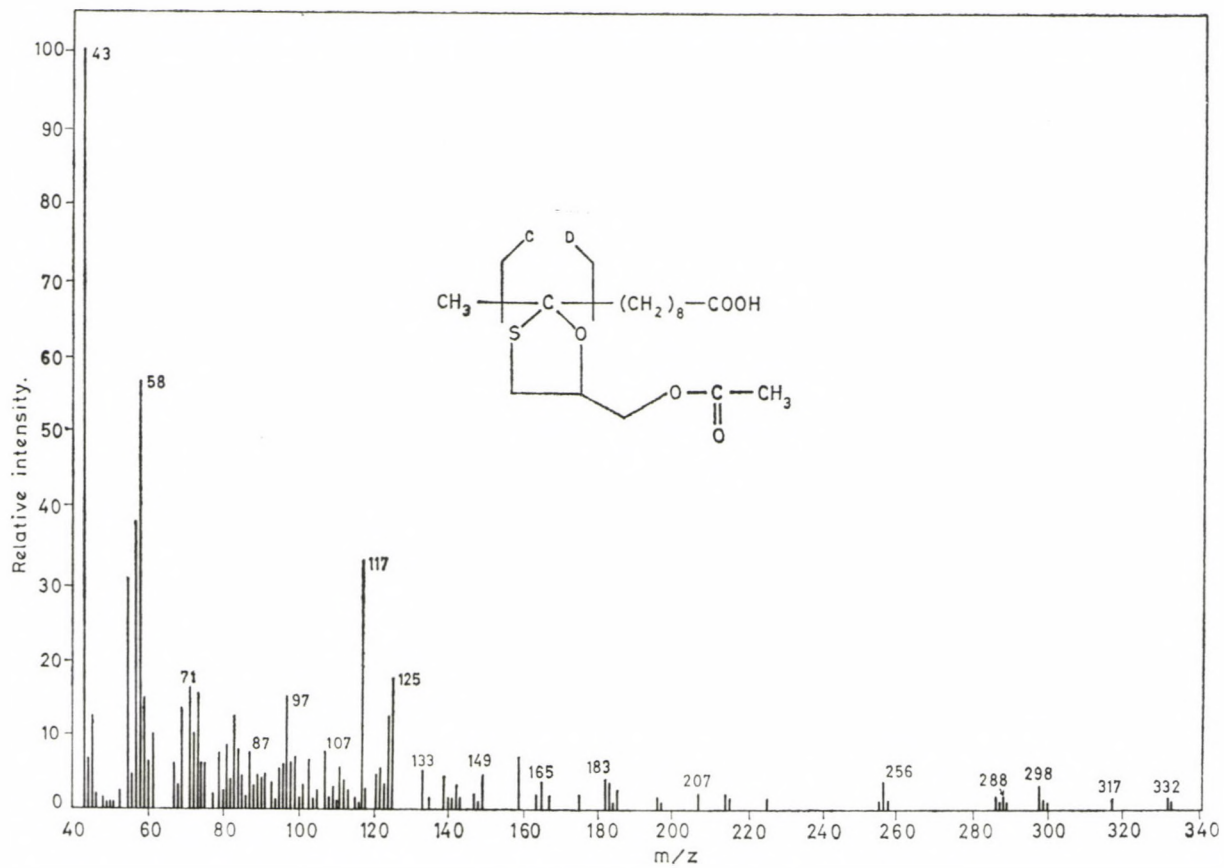
Fig. 2. Mass spectrum of 1c
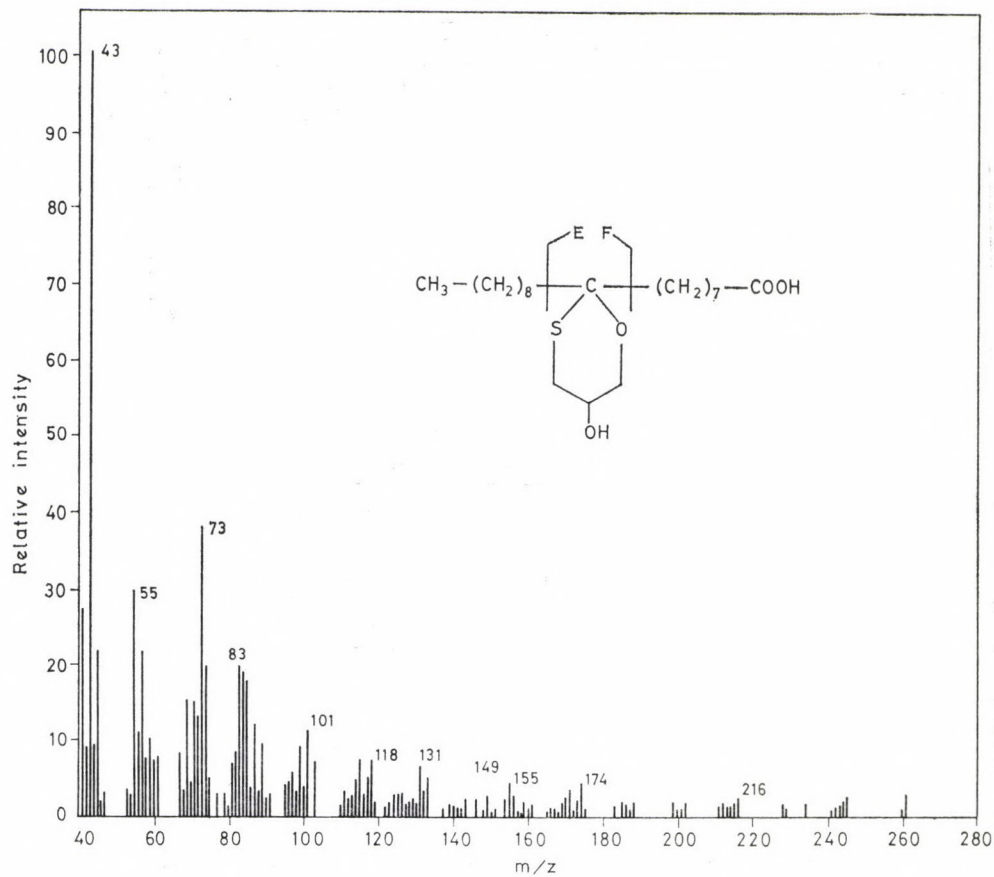
Fig. 3. Mass spectrum of **2b**
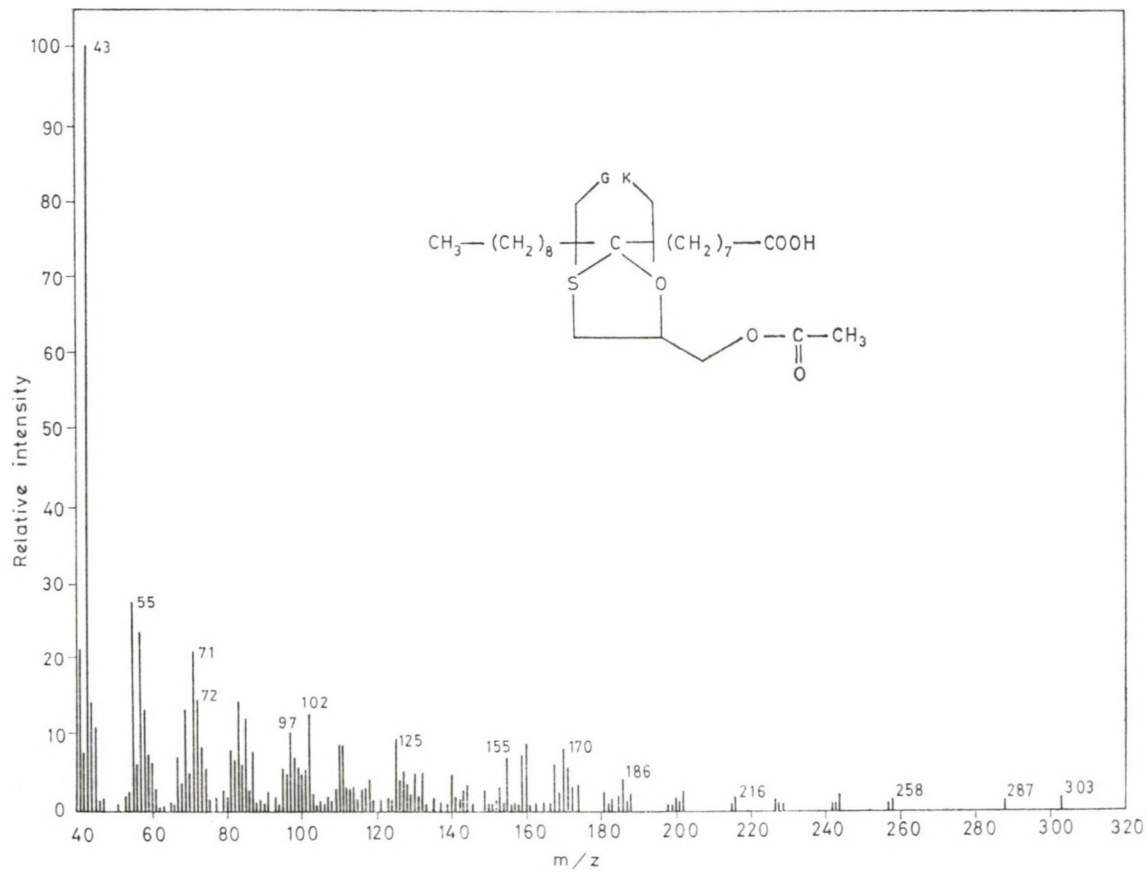
Fig. 4. Mass spectrum of 2c

The formation of BF_3-complex is supposed to be the first step in the synthesis of oxathiolane and dioxolane, which is hindered in this case owing to the close proximity of the carbonyl function.

MS fragmentations of oxathiolanes

A literature survey revealed that few reports are available dealing with the MS of oxathiolanes. Fenselau et al. [15] have studied the MS of steroidal dioxolanes, oxathiolanes and dithiolanes. The MS of steroidal oxathiolane mostly gave $M\text{-}CH_2CH_2S$ as a base peak. Here we report the MS fragmentation of substituted five- and six-membered oxathiolanes (see Figures). From our present investigations we can infer a few generalizations, with some reservations. In all the cases cleavages β to the oxygen of the ring were noted to be prominent. The α cleavage ions can serve to determine the molecular weight of the compounds 2b and 2c, where molecular ion peaks were not observed. In the case of the six-membered oxathiane the loss of H_2O was surprisingly noted.

Experimental

All the experimental procedures are essentially the same as reported in a previous paper [11], except where specified. Infrared (IR) spectra were recorded with a Perkin-Elmer 621 spectrophotometer (liquid film, or in 1% solution in CCl_4). Nuclear magnetic resonance (NMR) spectra were obtained in $CDCl_3$ with a Varian A60 spectrometer. Mass spectra (MS) were measured with a Kratos MS-45 spectrometer with a digital PDPB/1 data interface system. The figures in parentheses denote the source of ion along with the intensity relative to the base peak 100. Accurate mass measurements and metastable transition patterns were not studied. IR and NMR values usually associated with long-chain acids (1710 cm^{-1}; δ 0.88 — terminal methyl protons, 1.2-chain methylene protons, 2.3 — methylene protons α to the carboxylic function) are not specified; only diagnostic values are discussed. The abbreviation PE refers to the mixtures of petroleum ether and ether used in column chromatography.

Preparation of oxo fatty acids
10-Oxoundecanoic acid (1)

The method of preparation of 10-oxoundecanoic acid (m.p. 58 −59 °C) has been reported in a previous paper [11].

9-Oxooctadecanoic acid (2a)

Pure 9-hydroxy-*cis*-12-octadecanoic (isoricinoleic) acid was isolated from *Wrightia tinctoria* seed oil by the Gunstone partition procedure [12]. Hydrogenation of the γ-hydroxy-olefinic acid in the presence of palladium-charcoal in ethyl acetate yielded 9-hydroxyoctadecanoic acid, m.p. 80 −81 °C, which on Jones' oxidation afforded 9-oxooctadecanoic acid (2a), m.p. 79 −80 °C (*lit.* [12] m.p. 79.5 −80°C).
    IR (nujol): 1720 cm^{-1} (chain carbonyl).

2-Oxooctadecanoic acid (3)

The α-bromination of stearic acid in the presence of red phosphorus in dry bromine gave 2-bromooctadecanoic acid, which on refluxing with potassium hydroxide in ethanol yielded 2-hydroxyoctadecanoic acid, m.p. 90 −91 °C (*lit.* [13] m.p. 90.5 °C) and some α,β-

-unsaturated acid. Jones' oxidation of 2-hydroxy-octadecanoic acid afforded 2-oxooctadecanoic acid (*3*), m.p. 74—75 °C (*lit.* [14] m.p. 74.5 °C).

IR (nujol): 1720 cm^{-1} ($-CH_2-CO-COOH$).

Reaction of 3-mercaptopropan-1,2-diol with 1

A solution of 10-oxoundecanoic acid 2 g; 10 mmol) in acetic acid (30 mL) was allowed to react with 3-mercaptopropan-1,2-diol (1.08 g; 10 mmol), using BF_3-Et_2O as catalyst, at 25 °C, according to the procedure of Fieser [3]. TLC monitoring of the reaction mixture showed that the reaction was completed in 20 min. After adding a few drops of methanol to the reaction mixture, it was diluted with water, extracted with ether, washed successively with 5% $NaHCO_3$ and finally with water, and dried.

The evaporation of the solvent left a viscous oil (1.9 g). TLC examination of this oil showed three distinct spots at lower R_f values than the spot of the starting material. The reaction mixture was fractionated on a silica gel (40 g) column. The elution with different mixtures of PE gave the products in the following ratio:

PE (13%): **1a**, 0.4 g (ca. 21%). $C_{16}H_{28}O_5S$ (332.45). Calcd. C 57.80; H 8.48. Found C 57.74; H 8.37%.

PE (29%): **1b**, 0.8 g (ca. 42%). $C_{14}H_{26}O_4S$ (290.41). Calcd. C 57.90; H 9.02. Found C 57.87; H 8.91%.

PE (45%): **1c**, 0.65 g (ca. 34.2%). $C_{16}H_{28}O_5S$ (332.45). Calcd. C 57.80; H 8.48. Found C 57.76; H 8.32%.

Reaction of 3-mercaptopropan-1,2-diol with 2a

Reaction of 3-mercaptopropan-1,2-diol (0.54 g; 5 mmol) with 9-oxooctadecanoic acid (1.61 g; 5 mmol) as described earlier, yielded a viscous oil (1.5 g) showing two distinct and one faint spot on the TLC plate. Silica gel (30 g) column was used to separate the individual components. The product showing a faint spot on TLC could not be isolated because of its insufficient quantity. Chromatographic elution with different ratios of PE mixtures afforded the following two products:

PE (32%): **2b**, 0.8 g (ca. 53.3%). $C_{21}H_{40}O_4S$ (388.60). Calcd. C 64.90; H 10.37. Found: C 64.87; H 10.27%.

PE (48%): **2c**, 0.6 g (ca. 40.0%). $C_{23}H_{42}O_5S$ (430.63). Calcd. C 64.15; H 9.83. Found: C 64.07; H 9.89%.

Reaction of 3-mercaptopropan-1,2-diol with 3

A similar reaction of 2-oxooctadecanoic acid (1.59 g) with 3-mercaptopropan-1,2-diol did not show any change in the R_f value on TLC plate even after a prolonged reaction time. Final work-up regenerated the original 2-oxo acid, as evidenced by co-TLC and spectral behaviour.

*

REFERENCES

[1] Djerassi, C., Gorman, M.: J. Am. Chem. Soc., **75**, 3704 (1953)
[2a] Hauptmann, H.: J. Am. Chem. Soc., **69**, 592 (1947)
[b] Romo, J., Rosenkranz, G., Djerassi, C.: J. Am. Chem. Soc., **73**, 4961 (1951)
[3] Fieser, L. F.: J. Am. Chem. Soc., **76**, 1945 (1954); **75**, 4386 (1953)
[4] Oliveto, E. P., Clayton, T., Hershberg, E. B.: J. Am. Chem. Soc., **75**, 486 (1953)
[5] Vu Moc Thuy, Pierre, M.: Bull. Soc. Chim. Fr., **1979**, 264
[6] Villa, L., Ferri, V., Grana, E.: Farmaco Ed. Sci., **29**, 167 (1974)
[7] Walker, F. H.: Chem. Abstr., **91**, 123731 (1979)
[8] Fr. Demande 2, 146, 962; Chem. Abstr., **79**, 78776 (1973)

[9] Nakanishi, M., Arimura, K., Ao, H.: Chem. Abstr., **78**, 124567 (1973)
[10] Robbe, Y., Fernandez, J. P., Dubief, R., Chapat, J. P., Sentenoc-Roumanou, H., Fotome, M., Laval, J. D.: Eur. J. Med. Chem. Chim. Ther., **17**, 235 (1982)
[11] Nasirullah, Ahmad, F., Osman, S. M., Pimlott, W.: J. Am. Oil Chemists' Soc., **59**, 411 (1982)
[12] Gunstone, F. D.: J. Chem. Soc., **1954**, 1611; **1952**, 1274
[13] Artamonov, P. A.: Zh. Obsch. Khim., **28**, 135 (1958)
[14] Markley, K. S.: Fatty Acids, Part 4, p. 2546, 2nd Ed., Inter-Science Publishers, New York 1967
[15] Fenselau, C., Milewich, L., Robinson, C. H.: J. Org. Chem., **34**, 1374 (1969)

THE FORCE OF AIR BUBBLE DETACHMENT
FROM THE SURFACE OF GRAPHITE/n-ALKANE
FILM IN 1-PROPANOL AQUEOUS SOLUTION

Bronisław JAŃCZUK

*(Department of Physical Chemistry, Institute of Chemistry, UMCS, pl.
Marii Curie-Skłodowskiej 3, 20-031 Lublin, Poland)*

Measurements of the force of air bubble detachment from graphite surface
wetted with *n*-alkane in aqueous propanol solutions were carried out in the concentra-
tion range from 0 to 300 mg · dm^{-3}. Eleven aliphatic hydrocarbons in the homologous
series from hexane to hexadecane were used for the measurements. From the results
obtained it has been found that discrete changes of the detachment force occur at
appropriate film thickness in relation to the length of the *n*-alkane molecule and that
the stability of the system graphite/*n*-alkane film-air bubble-aqueous propanol solu-
tion depends on the thickness and nature of the hydrocarbon film and on propanol
concentration in water.

Introduction

The experimental and theoretical studies of the contact angle in the
system of graphite/*n*-alkane film-air bubble-aqueous solution of polar liquid
[1] have shown that its value depends on the thickness and nature of the film
of a nonpolar liquid on graphite surface and on the concentration of a polar
liquid. Properties of films of nonpolar and polar liquids (e.g. thickness, struc-
ture and film pressures) which are formed on a solid-air and solid-aqueous
solution interfaces, exert an influence not only on the value of contact angle
but also on the value of the adhesion force of an air bubble to the surface of
the solid [2—6]. This adhesion force plays an important role in the flotation
processes [7—9].

The studies carried out by Wójcik [4] suggest that even a small amount
of a polar liquid added to the solid/*n*-alkane film-air bubble-water system
decreases its stability.

A slightly different conclusion on was drawn by Melik—Gajkazjan
[5, 6] from the analysis of the forces acting on the air bubble attached to solid
surface in the presence of nonpolar and surface active liquid. He maintains
that at low concentrations of surface active agents the contact of an air bubble
with solid surface becomes strengthened, but at greater amounts of a polar
liquid in this system it becomes less stable.

Controversial opinions dealing with the influence of polar substances on the adhesion of air bubble to solid surface [4—6] show, that the problem has not been explained sufficiently.

Therefore studies on the influence of the amount and type of a nonpolar liquid and the concentration of a polar substance on the force of a bubble detachment from graphite surface have been undertaken in the system: graphite/n-alkane film-air bubble-aqueous propanol solution.

For these studies eleven aliphatic hydrocarbons were used in the homologous series from hexane to hexadecane and solutions of propanol at the concentration from 0 to 300 mg · dm^{-3} (this concentration is characteristic in the process of foam flotation).

Experimental

Measurements of the force of air bubble detachment from graphite surface wetted with particular n-alkane in aqueous solution of n-propyl alcohol at the given concentration (from 0 to 300 mg · dm^{-3}) were made by the method described elsewhere [10]. In this method the value of detachment force is read under the microscope from the deformation of calibrated quartz rods in the moment of disruption of the system solid-air bubble-liquid. Cylindrical graphite grains 85.68×10^{-5} m in diameter and about 1×10^{-3} m long, wetted in excess with n-alkane tested, were attached to these rods (the preparation of grains and their attachment were described earlier [11]).

The set grain-rod was fixed in the measuring vessel filled with propanol solution at a desired concentration. Then the graphite grain (wetted with n-alkane) was contacted with an air bubble of 40.46×10^{-4} m in diameter, which was pushed out of a capillary by means of a micrometer screw and the detachment force was measured.

The process of contacting and detaching subsequent air bubbles with simultaneous measurement of the detachment force was repeated until a constant value of the force was obtained.

All measurements of the detachment force were made at 293 K ± 0.1 K, and the standard deviation of measurements was ±5 × 10^{-4} mN.

Results and Discussion

From the measurements carried out it appears that with the decrease of n-alkane film thickness on graphite surface for c = const., r_k = const., and R = const. the values of the detachment force are changed. For all the n-alkanes studied the stability of the system graphite/n-alkane film-air bubble-solution initially increased with the increasing number of air bubbles contacted with graphite surface, passing through its maximum, and then it decreased until the value of F_0 becomes constant. The relationship between F_0 and the number of air bubbles is different for the particular hydrocarbons and propanol concentrations in water. It is characteristic that the changes of F_0 in relation to the number of air bubbles are greater at higher propanol concentrations in water, which can be seen in Fig. 1. This figure also shows an example of the detachment force changing in relation to the number of air bubbles detached
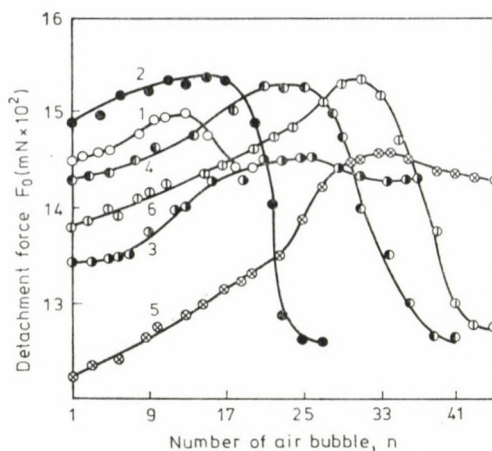
Fig. 1. The detachment force F_0 as a function of the number of air bubbles contacted with the surface of graphite/n-alkane in aqueous propanol solution (Curves 1, 3,5 for 20 mg · dm^{-3} and Curves 2, 4, 6 for 300 mg. dm^{-3}). Curve 1 ,2, for hexane film, 3, 4, for decane film, and 5, 6 for hexadecane film

from graphite surface wetted with hexane (curves 1, 2), decane (curves 3, 4), and with hexadecane (curves 5, 6) in aqueous propanol solutions at concentrations of 20 mg · dm^{-3} (curves 1, 3, 5) and 300 mg · dm^{-3} (curves 2, 4, 6), respectively.

From Fig. 1 it can be seen that the thickness of n-alkane film on graphite surface has a considerable effect on F_0 values.

The effect of propanol concentration in water on F_0 is less distinct in this figure. To show it more clearly the relationship between F_0 and c should be plotted for equal film thickness of the given n-alkane on the solid surface. This, however, is practically impossible to do on the basis of the studies presented. Nevertheless, a certain explanation of this problem can be obtained from Fig. 2. It shows an example of changes of the force of detachment from graphite surface wetted with decane vs. propanol concentration (in the range from 0 to 300 mg · dm^{-3}) for the first air bubble contacted with this surface, $F_{0(1)}$ (see Fig. 1, curve 1), for the air bubble with F_0 max (curve 2) (points corresponding to maximum F_0 value from Fig. 1), and the change of F_0 min (curve 3) (F_0 min — constant values of F_0 (final) — see Fig. 1), respectively. From Fig. 2 it can be seen that $F_{0(1)}$ values (curve 1) and F_0 max (curve 2) increase, whereas F_0 min (curve 3) decreases as a function of propanol concentration in water. The course of curve 3 in Fig. 2 confirms the conclusions drawn by Wójcik [4], and curves 1 and 2 support the observations of Melik—Gajkazjan [5, 6].

To explain both results [4—6] let us consider the change of the parameters determining F_0 value under the influence of a polar and nonpolar liquid in the systems studied.

From the equation derived earlier [12] the detachment force of air bubble from the graphite/n-alkane film in aqueous solution of propanol, may be determined by means of $F_0 = f(\gamma_L, r_k, R, \gamma_{Sf}, \gamma_{SfL}, \pi_e)$. Since in the concentration range from 0 to 300 mg · dm^{-3}, γ_L changes slightly and r_k, and R are constant, hence values of F_0 depend mainly on γ_{Sf}, γ_{SfL} and π_e. If $\gamma_{Sf} \leq \gamma_L$ then according to Fowkes theory [14, 15] $\pi_e \approx 0$ and $F_0 = f(\gamma_{Sf}, \gamma_{SfL})$.

Assuming that, for given n-alkane γ_{Sf} is constant, and $\pi_e \approx 0$, then the change of F_0 vs. c depends upon the change of γ_{SfL} values only. If the concentration of propanol solution is increased adsorption of n-propanol molecules on graphite/n-alkane film-solution interface also increases.

Probably as a result of the adsorption polar interactions arise on these interfaces [14, 16]. These polar interactions change the γ_{SfL} values as a function of the concentration.

Taking into account that on surfaces of high energy hydrophobic solids, the alkane film having a thickness up to 2 statistical monolayers is very stable, it seems that obtained F_0 min values result from such thickness of the films.

When such film is present on the graphite surface irrespective of the solution concentration (up to 300 mg · dm^{-3}) then F_0 min $= f(\gamma_{SfL})$.

According to Wójcik's studies [4], for such thin films decrement in stability of graphite/n-alkane film-air bubble-solution system vs. c value (Fig. 2 — curve 3) appears as a result of polar interactions arising on graphite/n-alkane film-solution interface.

For the films corresponding to the systems in which F_0 max and $F_{0(1)}$ are obtained it could not be assumed that γ_{Sf} as a function of c value is constant. Hence $F_{0(1)} = f(\gamma_{Sf}, \gamma_{SfL})$ and F_0 max $= f(\gamma_{Sf}, \gamma_{SfL})$ and changes of γ_{Sf} and γ_{SfL} as functions of c are such that cause the detachment force increase when the concentration of propanol solution is increased.
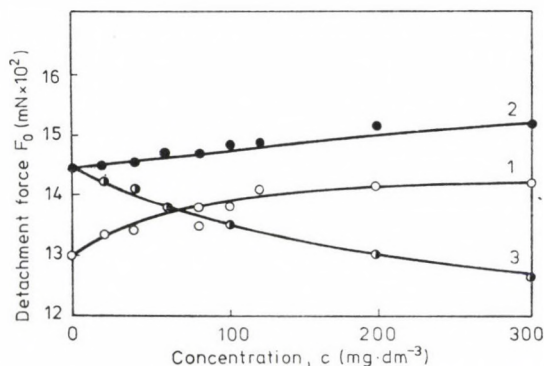
Fig. 2. The effect of propanol concentration on F_0 force of air bubble detachment from graphite surface wetted with n-alkane. Curve 1 — $F_{0(1)}$ values (for the first air bubble measured — Fig. 1), curve 2 — F_0 max values and curve 3 — F_0 min values

Unfortunately, for the systems presented in this paper it is impossible to make a detailed quantitative analysis of the parameters determining the value of the force of air bubble detachment from graphite surface wetted with n-alkane in aqueous propanol solutions, since it is not possible to determine quantitatively the pressure of hydrocarbon film on graphite surface, which depends on the film thickness and kind of hydrocarbon.

The effect of the nature of hydrocarbon on F_0 can be shown only qualitatively on the basis of Fig. 3—5.

These figures represent the changes of the initial values of the detachment force ($F_{0(1)}$) (Fig. 3), F_0 max values (Fig. 4) and F_0 min values (Fig. 5) vs. the number of carbon atoms in a hydrocarbon molecule for two propanol concentrations in water (20 mg $\cdot$ dm^{-3} — curve 1; 300 mg $\cdot$ dm^{-3} — curve 2). From these figures it can be seen that for a thick n-alkane film the stability of the system decreases with the length of the hydrocarbon molecule (Fig. 3), but the changes of F_0 min (Fig. 5) from hexane to hexadecane are small.

It is characteristic that both in Fig. 3 and Fig. 5 no discrete changes of F_0 are observed in relation to the number of carbon atoms in n-alkane, except for F_0 max in Fig. 4. The changes of F_0 max value for all the studied propanol concentrations in water (in Fig. 4 only the concentrations 20 and 300 mg $\cdot$ dm^{-3} are taken into consideration) are not similar to those of maximum values of the force of air bubble detachment from graphite surface wetted with n-alkane in water [17], but they are analogous to the changes of F_0 max in the system Teflon/n-alkane film-air bubble-water [18] and to the changes of zeta potential for the system sulphur/n-alkane film-water and Teflon/n-alkane film-water as a function of the length of the hydrocarbon chain [18, 19]. Discrete changes of the detachment force, wetting contact angle [18, 20] and zeta potential as a function of the number of carbon atoms in n-alkane molecule similarly to the change in their melting temperature are interpreted in the literature [18—22] by differences in the structure of even and odd hydrocarbon molecules. Hence it may be concluded that the initial values ($F_{0(1)}$ — Fig. 1) of the force of air bubble detachment from graphite surface wetted with the given n-alkane in aqueous propanol solution result in such a thickness of the film at which its outermost layer from the graphite surface possesses very similar properties as its bulk phase does, and therefore there is no discrete change in $F_{0(1)}$ results for even and odd hydrocarbons (Fig. 3, curve 1). With decreasing the film thickness caused by contacting and then detaching air bubbles (Fig. 1) we reach the hydrocarbon layers, the properties of which differ from its bulk phase and there are probably some differences in the structure of the even and odd n-alkane film. This would result in the fact that the film of one of them can be "thinned" by air bubbles less easily than of the other, which also may reflect in the discrete changes of F_0 max in relation to the length of the hydrocarbon chain (Fig. 4). The contacting of a great number of air bubbles with
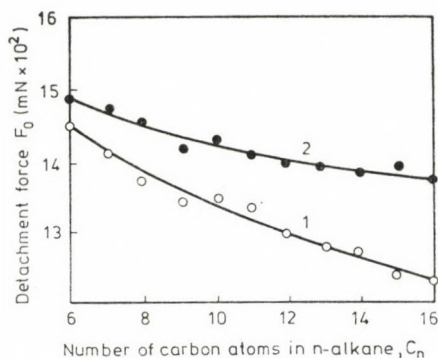
Fig. 3. The effect of *n*-alkane chain length on $F_{0(1)}$ detachment force in the presence of propanol at a concentration of 20 mg · dm^{-3} (curve 1) and 300 mg · dm^{-3} (curve 2)
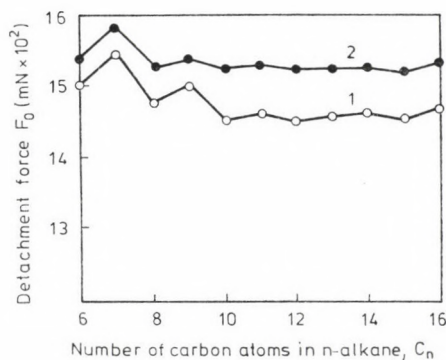
Fig. 4. The effect of *n*-alkane chain length on F_0 max detachment force in the presence of propanol at a concentration of 20 · mg · dm^{-3} (curve 1) and 300 mg · dm^{-3} (curve 2)
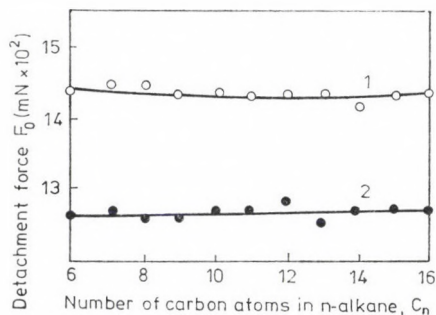
Fig. 5. The effect of *n*-alkane chain length on F_0 min detachment force in the presence of propanol at a concentration of 20 mg · dm^{-3} (curve 1) and 300 mg · dm^{-3} (curve 2)

graphite surface wetted with n-alkane in the solution of n-propanol alcohol
may cause a destruction of a homogeneous structure of the n-alkane film
(the film becomes discontinuous) and in such a case no difference is observed
between the even and odd hydrocarbon film in the effect of the length of the
hydrocarbon chain on the change of the detachment force (F_0 min — Fig. 5).

Conclusions

From the studies presented above it can be concluded that n-alkane
and n-propanol influence the adhesion of air bubbles to graphite surface.
The adhesion depends on the nature and thickness of n-alkane film on graphite
surface, and concentration of aqueous propanol solution. For thin films a
decrease, and for thick films an increase in the values of detachment force
of air bubbles from a graphite surface appears as the concentration of propanol
solution is increased but when this concentration is constant and the thickness
of the n-alkane film is changed, detachment force is varied too. It is very
characteristic that the detachment force in relation to the n-alkane film
thickness has a maximum.

In turn the maximum values of the detachment force as a function of
the number of carbon atoms in the hydrocarbon molecule change stepwise
from even to odd hydrocarbon.

Stepwise changes of the detachment force as a function of the length of
n-alkane molecule are not observed for very "thin" and very "thick" n-alkane
films. Stepwise changes of the maximum detachment force have been explained
suggesting a different structure of even and odd alkane molecules on graphite
surface.

Symbols

c	concentration of aqueous propanol solution
F_0	detachment force of air bubble from the graphite grain
R	air bubble radius
r_k	radius of the air bubble contact plane with graphite grain
γ_L	surface tension of the aqueous propanol solution
γ_{Sf}	surface free energy of graphite covered with hydrocarbon film
γ_{SfL}	interfacial free energy of the graphite/hydrocarbon film-solution
π_e	decrease in surface free energy of the graphite (covered with hydrocarbon film) resulting from the adsorption of propanol and water molecules from aqueous propanol solution.

REFERENCES

[1] Jańczuk, B.: Croat. Chem. Acta (in press)
[2] Zimon, A. D.: Adhesion of Liquid and Wettability, Chem., Moscow 1974 (in Russian)
[3] Krochin, S. J.: In "Physico-Chemical Problems of Nonpolar Collectors Action in Ore an Coal Flotation", p. 12, Nauka, Moscow 1965 (in Russian)
[4] Wójcik, W.: Przem. Chem., **58**, 149 (1979)
[5] Melik-Gajkazjan, W. I.: in "Physico-Chemical Problems of Nonpolar Collectors Action in in Ore an Coal Flotation", p. 22, Nauka, Moscow 1965 (in Russian)

[6] Melik-Gajkazjan, W. I.: Dokl. AN. SSSR, **173,** 4 (1967)

[7] Leja, J.: Surface Chemistry of Froth Flotation, Plenum Press, New York—London 1982

[8] Schuhe, H. J.: Physikalisch-chemische Elementarvorgänge des Flotations prozesses, Deutscher Verlag der Wissenschaften, Berlin 1981

[9] Bogdanov, O. C.: Theory and Technology of Ore Flotation, Nedra, Moscov 1980 (in Russian)

[10] Barcicki, J., Waksmundzki, A., Maruszak, E.: Chem. Stosowana **1,** 99 (1962)

[11] Jańczuk, B.: J. Colloid Interface Sci., **93,** 411 (1983)

[12] Jańczuk, B., Chibowski, E.: J. Colloid Interface Sci., **94,** 570 (1983)

[13] Jańczuk, B.: Przem. Chem., **62,** 174 (1983)

[14] Fowkes, F. M.: Ind. Eng. Chem., **56,** 40 (1964)

[15] Fowkes, F. M.: J. Phys. Chem., **66,** 382 (1962)

[16] Zettlemoyer, A. C.: in "Hydrophobic Surfaces", (Ed. F. M. Fowkes), p. 1, Acad. Press. New York—London 1969

[17] Jańczuk, B.: J. Colloid Interface Sci. (in press)

[18] Chibowski, E., Janczuk, B., Wójcik, W.: in "Physico-Chemical Aspects of Polymer Surfaces" (Ed. K. L. Mittal), Vol. 1, p. 217, Plenum. Press., New York 1983

[19] Chibowski, E.: Przem. Chem., **59,** 525 (1980)

[20] Waksmundzki, A., Janczuk, B.: in "The Crystal Chemistry, Surface Properties and Flotation of Silicate Minerals", XII International Mineral Processing. Congress. Sao Paulo, p. 35 (1977)

[21] Fowkes, F. M.: J. Colloid Interface Sci., **28,** 493 (1968)

[22] Vigdergauz, M. S., Seomkin, V. J.: J. Chromatogr., **158,** 57 (1978)

APPLICATION OF ELECTROPHORETIC TECHNIQUE IN THE STUDY OF MIXED LIGAND COMPLEXES IN SOLUTION

M-NITRILOTRIACETATE-PROLINATE SYSTEMS

Deepa Gupta, Satyendra Singh and Kanhaiya Lal Yadava*

(Electrochemical Laboratories, Department of Chemistry, University of Allahabad, Allahabad-211002, India)

A new method, involving the use of paper electrophoresis is described for the study of the equilibria in mixed ligand complex systems in solution. The technique is based on the movement of a spot of metal ion under an electric field with the complexants added in the background electrolyte at pH 8.5. The concentration of primary ligand (NTA) was kept constant while that of secondary ligand proline was varied. The plots of [proline] against mobility were used to obtained information on the formation of the mixed complex and to calculate its stability constants. The binary equilibria M(II)--proline and M(II)-NTA have also been studied since it is a prerequisite for the investigation of mixed complexes. The stability constants of the metal NTA-prolinate complexes have been found to be 5.95, 5.85, 5.20, 3.96 and 3.90 (log K values) for Cu(II) UO_2(II), Be(II), Co(II) and Mn(II) respectively, at $\mu = 0.1$ and temperature 35 °C

Introduction

Paper electrophoresis was applied to the study of metal complexes in solution, attempts are made to determine the stability constants of the complex species [1, 2]. Recently in this Laboratory a new method has been developed for the study of stepwise complex formation [3, 4, 5, 6], and for the study of mixed complexes [7, 8, 9, 10]. The present work is an extension of the technique and report our observation on the mixed system.

Experimental

Apparatus

Electrophoresis equipment (Systronics model, 604 INDIA) has been used. It has a built-in power supply (A.C.—D.C.) which is directly fed to paper electrophoresis tanks. In most electrophoresis instruments no attention is paid to the control of temperature. The electric current running through the paper strips generates heat which causes evaporation of the background electrolyte leading to serious errors. In order to eliminate it, two hollow metallic plates coated outwardly with thin paper plastics have been used for sandwiching paper strips, and thermostated water (35 °C) is circulated through them. pH measurements were made with an Elico model L_1-10 pH meter using a glass electrode.

* To whom correspondence should be addressed.

Chemicals

Cu(II), UO$_2$(II), Be(II), Co(II) and Mn(II) perchlorates were prepared by precipitating the corresponding carbonates with sodium carbonate from solutions of nitrates, washing the precipitates thoroughly with boiling water and treating with a suitable amount of 1% perchloric acid. The resulting mixture was heated to a boiling on a water bath and then filtered. The metal contents of the filtrates were determined as usual and final concentration was kept at 5.0×10^{-3} *M*.

(2-pyridylazo)-2-naphthol (PAN), 0.1% (*W/V*) in ethanol was used for detecting the Cu(II), UO$_2$(II), Co(II) and Mn(II) ions. And aluminium-ammonium acetate mixture in water was used for detecting the Be(II) ion. A saturated aqueous solution of silver nitrate (0.9) was diluted with acetone to 20 mL. Glucose was detected by spraying with this solution and then with 2% ethanolic sodium hydroxide.

Background electrolyte

Stock solution of 9.0 *M* perchloric acid 2.0 *M* sodium hydroxide and 0.5 *M* proline were prepared from AnalaR (B.D.H., Poole, Great Britain): 0.01 *M* nitrilotriacetic acid was prepared from a sample obtained from E. Merck (Darmstadt, G.F.R.). Each solution was standardized as usual. The background electrolyte in study of binary complexes consists of 0.1 *M* perchloric acid and 1.0×10^{-2} *M* proline (1.0×10^{-3} *M* NTA) while in study of ternary complexes, it consists of 0.1 *M* sodium perchlorate, 1.0×10^{-3} *M* NTA and varying amount of 1.0×10^{-2} *M* proline; it was maintained at pH 8.5 by addition of sodium hydroxide.

General procedure

Binary complexes

Paper strips Whatman No. 1 (30×1 cm) in duplicate are spotted in the middle with metal ions. An extra strip was marked with glucose. The strips are sandwiched between two insulated hollow plates. The plates are mounted in the electrophoresis equipment with the end of paper strips dipping into the tank of the instrument. Each tank is filled with 150 mL of background electrolyte. An hour is allowed for strips to get wet by diffusion with background electrolyte solution. Subsequently, electrophoresis is carried out for 60 minutes under the influence of 200 V potential difference between the two tank solutions. The strips are then removed from the tank, dried and migrated spots are detected with specific reagents. Distance travelled by spots is measured from previous marked points. Duplicate strips always recorded
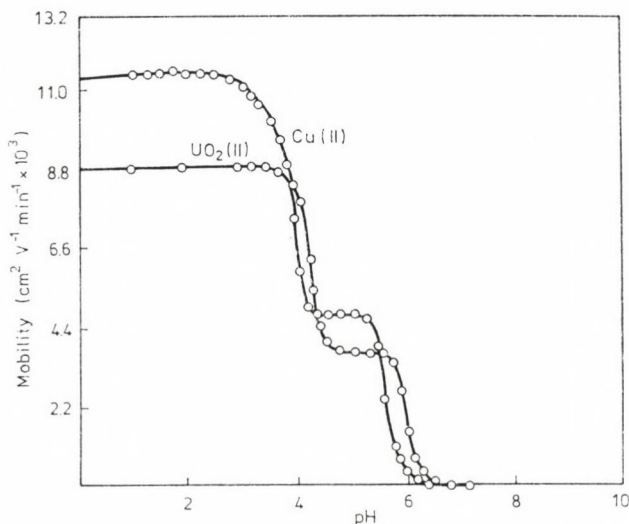
Fig. 1. Mobility curve M(II)-Proline system (temp. 35 °C, ionic strength 0.1)
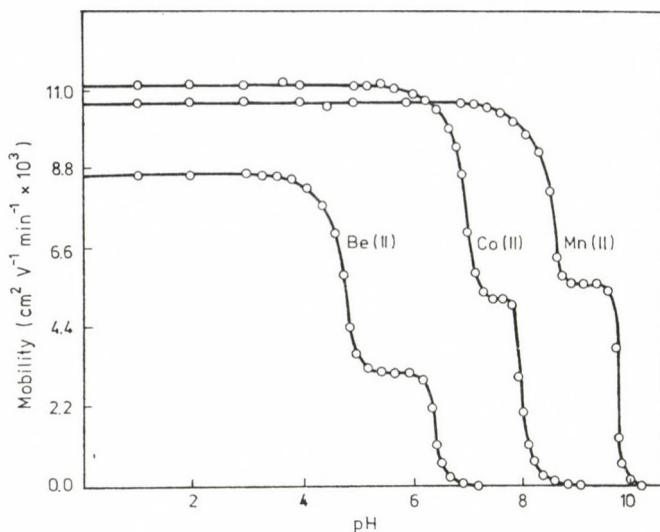
Fig. 2. Mobility curve M(II)-Proline system (temp. 35 °C, ionic strength 0.1)

less than 5% variation in travelled distances. Mean of the two was taken for calculation of mobility. Movement of glucose is used as correction factor for electroosmosis. The electrophoretic migration of metal spot on paper was observed at different pH of background electrolyte. Distance travelled toward the anode are assumed to be negative and those towards the cathode to be positive. The length of unimmersed strips above the tank containing background electrolyte is 26.5 cm, so the potential gradient applied in each experiment is 7.5 V/cm. Dividing the movement by the potential gradient yields the mobility, which is plotted in Figs. 1 and 2.

Ternary complexes

Strips are marked with metal ions in duplicate along with as additional one marked with glucose. After trenching the strips with background electrolyte the electrophoresis was carried out for one hour at the same potential difference as in the case of binary complexes. For subsequent observation, a prolinate solution, maintained at pH 8.5, was added progressively and the ionophoretic mobility recorded. A plot of mobility against log proline was made, which is shown in Figs. 5 and 6.

Results and Discussion

Metal-prolinate binary system

The plot of overall electrophoretic mobility of the metal spot against pH gives a curve with a number of plateaus shown in Figs. 1 and 2. A plateau is obviously an indication of the pH range where the speed is practically constant. This is possible only when a particular complex is overwhelmingly formed. Thus every plateau indicates the formation of a certain complex species. The first one in the beginning corresponds to a region in which metal ions are uncomplexed. It lies in the low pH region where concentration of highly protonated species of proline is obviously maximum, hence it is con-

4

cluded that this protonated species of proline is non-complexing. Beyond this
range, the metal ion spots have progressively decreasing velocity and hence
the complexation of metal ion should be taking place with other ionic species
of proline whose concentration increases progressively with increase of pH.
The figure reveals second plateau in each case with a positive mobility, indicat-
ing the formation of a 1 : 1 complex of cationic nature. Further increase in
pH gives rise to a third plateau with zero mobility in each case which again
indicates formation of electrically neutral 1 : 2 metal complexes. This is
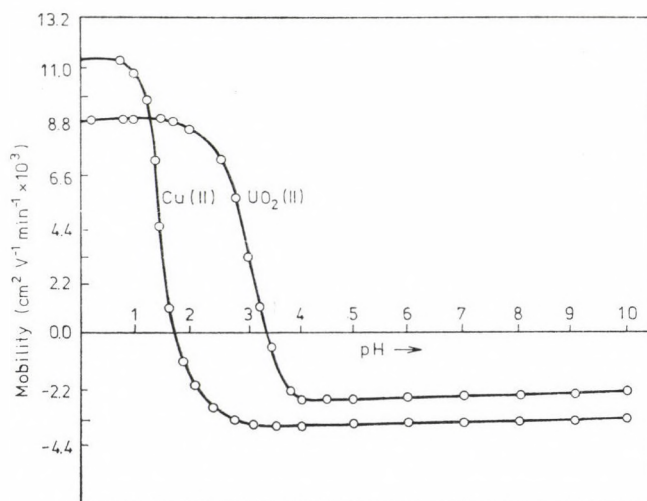
Fig. 3. Mobility curve M(II)-NTA system (temp. 35 °C, ionic strength 0.1)
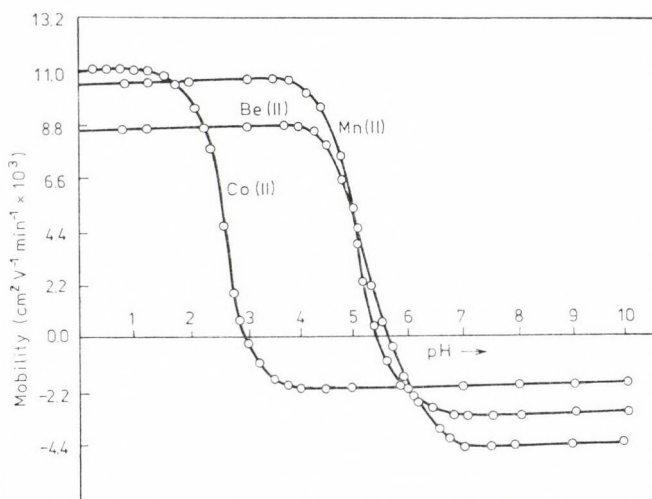
Fig. 4. Mobility curve M(II)-NTA system (temp. 35 °C, ionic strength 0.1)
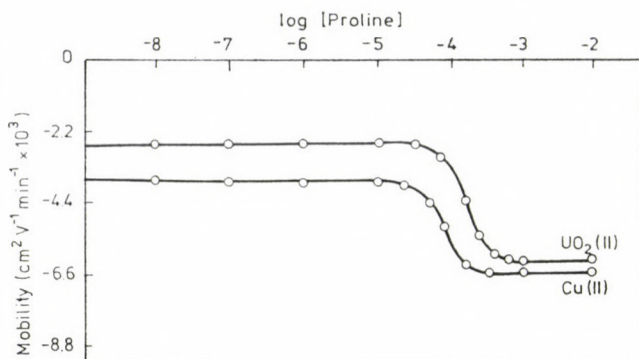
Fig. 5. Mobility curve M-NTA-Proline system (temp. 35 °C, ionic strength 0.1)
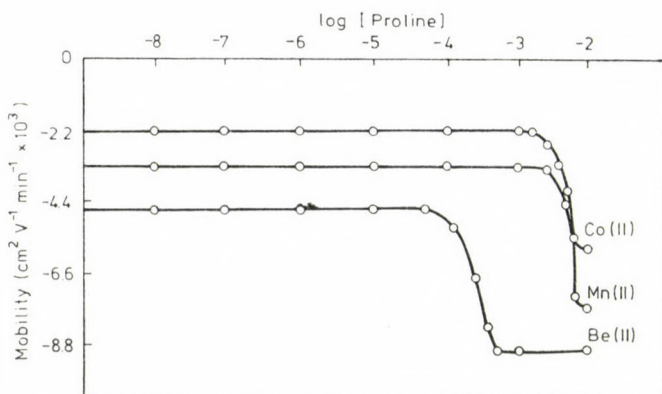
Fig. 6. Mobility curve M-NTA-Proline system (temp. 35 °C, ionic strength 0.1)

possible only when two anionic species of proline combine with one divalent metal ion. The literature also assigns prominent ligating properties to unprotonated anionic species of proline ruling out any such property of zwitterions [11, 12, 13]. Further increase of pH has no effect on the mobility of metal ions.

In view of the above observation the complexation of metal ion with prolinate anion (L) may be represented as

$$M^{2+} + L^- \overset{K_1}{\rightleftharpoons} ML^+$$

$$ML^+ + L^- \overset{K_2}{\rightleftharpoons} ML_2$$
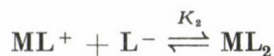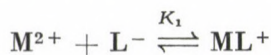
The metal spot of the paper is thus a conglomeration of uncomplexed metal ions, 1 : 1 complex and 1 : 2 complex. For the spot moving under the

4*

influence of electric field, the overall mobility is given by the equation

$$u = \sum_n u_n f_n$$

where u_n and f_n are the mobility and mole fraction of a particular complex species.

This equation is transformed into the following form on taking into consideration different/equilibria:

$$U = \frac{u_0 + u_1 K_1 [L^-] + u_2 K_1 K_2 [L^-]^2}{1 + K_1 [L^-] + K_1 K_2 [L^-]^2}$$

where u_0, u_1 and u_2 are mobilities of uncomplexed metal ions, $1:1$ metal complex and $1:2$ metal complex respectively.

This equation has been used for calculating stability constants of the complex of metal ions with prolinate anion. For calculating first stability constants K_1, the region between the first and second plateau is pertinent. The overall mobility 'U' will be equal to the arithmetic mean of mobility of uncomplexed metal ion, u_0, and that of the first complex u_1 at a pH where $K_1 = 1/[L^-]$ with the help of dissociation constants of proline ($K_1 = 10^{1.90}$, $K_2 = 10^{10.03}$) [14] the concentration of prolinate anion (L) is determined for the pH, from which K_1 can be calculated. The stability constants K_2 of the second complex can be calculated by taking into consideration the region between the second and third plateau of the mobility curve. These calculated values are given in Table I.

Metal-NTA binary systems

The observation on overall mobility of metal spots in presence of NTA at different pH values are represented in Figs. 3 and 4. It is evident from the figure that with all five metal ions two plateaus are obtained. The mobility of the last plateaus lies in the negative region showing the negative charge of complexes. Hence only one NTA anion is assumed to combine with one divalent metal ion to give $1:1$ M-NTA$^-$ complex which is in conformity with other finding [15, 16, 17]. The stability constants of complexes with NTA are calculated in a manner described in the preceding paragraph. The calculated values are given in Table I.

Metal-nitrilotriacetate-proline-ternary systems

The study of this system has been done at pH 8.5. It is observed from the mobility curves of M-proline and M-nitrilotriacetic acid binary systems that binary complexes, M-prolinate and M-nitrilotriacetate are formed at a

Table I

Stability constants of some binary and ternary complexes of Cu(II), UO$_2$(II), Be(II), Co(II), and Mn(II)
(ionic−strength = 1.0); temperature = 35 °C;
NTA anion = N(CH$_2$COO)$_2^{-3}$; prolinate anion = L =
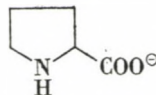
Metal ion	Calculated stability constants				Literature value			
	log K_{ML}^M	log $K_{ML_2}^M$	log K_{M-NTA}^M	log $K'^{M-NTA}_{M-NTA-L}$	log K_{ML}^M	log K_{M-NTA}^M	log $K_{ML_2}^M$	log $K'^{M-NTA}_{M-NTA-L}$
Cu(II)	8.48	6.78	12.74	5.96	8.83 [18] 8.72 [18]	12.94 [20] 13.60 [21] 12.75 [21]	7.57 [18] 7.63 [18]	5.59 [21]
UO$_2$(II)	7.73	6.38	9.77	5.85	—	9.50 [20] 7.88 [21] 9.50 [21]	—	—
Be(II)	7.52	5.98	7.25	5.20	—	7.11 [20]	—	—
Co(II)	4.88	3.78	10.32	3.96	—	10.38 [20] 10.38 [21]	—	3.23 [21]
Mn(II)	3.98	2.13	7.55	3.90	3.34 [18] 3.97 [18] 2.84 [19]	—	2.43 [18] 3.90 [19]	—

Where, $K_{ML}^M = \dfrac{[ML]}{[M][L]}$; $K_{ML_2}^M = \dfrac{[ML_2]}{[ML][L]}$; $K_{M-NTA}^M = \dfrac{[M\text{-}NTA]}{[NTA][M]}$: and $K_{M-NTA-L}^{M-NTA} = \dfrac{[M-NTA-L]}{[M-NTA][L]}$

pH lower than 8.5. Thus it would be proper to study the transformation of M-NTA complex into M-NTA-prolinate complex at pH 8.5 in order to avoid any side interaction.

The plot of mobility against logarithm of concentration of added proline gives curves (Figs. 5 and 6) containing two plateaus, one in the beginning and an other in the end. The mobility in the range of the first plateau corresponds to mobilities of 1 : 1 M-NTA complexes. The mobility in this range is also in agreement with the mobility of 1 : 1 M-NTA complex as evident in the study of the binary M-NTA system. The mobility of the last plateau is more negative than that of the first plateau so it indicates the formation of a more negatively charged complex. Further, the mobility in the last plateau does not tally with the mobility of 1 : 1 and 1 : 2 metal proline complexes (observed in our study of binary M-prolinate system). It is inferred that the last plateau is due to co-ordination of prolinate anion to 1 : 1 M-NTA moiety, resulting in the formation of 1 : 1 : 1 mixed complex (M-NTA-prolinate)

$$M-NTA^- + L^- \overset{K'}{\rightleftharpoons} M-NTA-L^{2-}$$
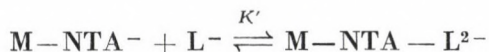
In the present electrophoretic study the transformation of a simple complex into mixed complex taken place, hence the overall mobility is given by

$$U = u_0 \cdot f_{M-NTA} + u_1 \cdot f_{M-NTA-L}$$

where u_0, u_1 and f_{M-NTA} and $f_{M-NTA-L}$ are the mobilities and the mole fraction of M-NTA$^-$ and M-NTA-L^{2-} complexes, respectively. Substituting the mole fractions, the overall mobility is given by equation

$$U = \frac{u_1 + u_1 K'[L^-]}{1 + K'[L^-]}$$

u_0 and u_1 are the mobilities in the regions of the two plateaus of the curve. From the figure the concentration of proline at which the overall mobility is the mean of the mobilities of two plateaus is determined. The concentration of anionic species of proline at pH 8.5 for this proline concentration is calculated; K' is obviously equal to $1/[L^-]$. All the calculated values of K' are given in Table I.

REFERENCES

[1] Jokl, V.: J. Chromatography, **14**, 71 (1964)
[2] Biernat, J.: Rocz. Chem., **38**, 343 (1964)
[3] Singh, R. K. P., Yadava, J. R., Yadava, P. C., Yadava, K. L.: Z. Phys. Chemie, Leipzig, **264**, 3 (1983)
[4] Singh, R. K. P., Sircar, J. K., Yadava, J. R., Yadava, P. C., Yadava, K. L.: Electrochim. Acta, **26**, 395 (1980)
[5] Singh, R. K. P., Sircar, J. K., Khelawan, R., Yadava, K. L.: Chromatographia, **13**, 709 (1980)
[6] Singh, S., Yadava, H. L., Yadava, K. L.: Rev. Chim. Minerale (in press)

[7] Yadava, P. C., Ghose, A. K., Yadava, K. L., Dey, A. K.: J. Chromatog., **9,** 416 (1976)
[8] Yadav, J. R., Sircar, J. K., Yadav, K. L.: Electrochim. Acta, **26,** 391 (1981)
[9] Singh, R. K. P., Yadav, J. R., Yadav, K. L.: J. Electrochem. Soc., **30,** 250 (1981)
[10] Singh, R. K. P., Yadav, K. L.: Trans. SEAST, **16,** 3 (1981)
[11] Li, N. C., Doddy, E.: J. Am. Chem. Soc., **76,** 221 (1954)
[12] Perrin, D. D.: J. Chem. Soc., **1958,** 3125
[13] Kustin, K., Liu, S. T.: J. Chem. Soc. Dalton, **1973,** 278
[14] Martell, A. E., Smith, R. M.: Critical Stability Constants, Vol. **I,** Amino Acids, pp. 6,
     14, 7, 12, 36, 69, 73, 66. Plenum Press. New York and London 1974
[15] Elenkova, N. G., Tsoneva, R. A.: J. Inorg. Nucl. Chem., **35,** 841 (1973)
[16] Rabenstien, D. L., Blakney, G.: Inorg. Chem., **12,** 128 (1973)
[17] Ramanujam, V. V., Rajlakshmi, M., Shivashankar, M.: Ind. J. Chem., **20A,** 531 (1981)
[18] Martell, A. E., Smith, R. M.: Critical Stability Constants. Vol. **I,** Amino Acids, p. 69,
     Plenum Press, New York and London 1974
[19] Perrin, D. D.: Stability Constants of Metal Ion Complexes, Part *B.* Organic Ligands, p.
     311. Pergamon Press, Oxford, IUPAC series No. 22, 1979
[20] Martell, A. E., Smith, R. M.: Critical Stability Constants, Vol. **I,** Amino Acids, p. 139,
     Plenum Press, New York and London 1974
[21] Perrin, D. D.: Stability Constants of Metal Ion Complexes, Part *B.* Organic Ligands, p.
     417, Pergamon Press. Oxford, IUPAC Series No. 22.

INHIBITION OF THE CORROSION OF IRON
IN NITRIC ACID SOLUTION

Awad Ibrahem AHMED, Abd El-Aziz El-Sayed FOUDA*
and Abd El-Monem El-Hosany EL-ASKLANY

(Chemistry Department, Faculty of Science, Mansoura University, Mansoura Egypt)

The use of some phenoxy acetamide derivatives as corrosion inhibitors of iron in 3 N nitric acid was studied by thermometric and weight-loss methods. The two methods gave concordant results. The additives caused a decrease in the maximum reaction temperature and a corresponding reduction in the reaction number (RN). The results indicate that the additives reduce the corrosion rate by way of adsorption through the carbonyl group, while the aromatic nucleus lies flat on the surface of the corroding metal. The inhibitory character of the compounds depends upon the concentration of the inhibitor, as well as its chemical composition.

The corrosion of iron and its alloys and their inhibition by different organic inhibitor in acid solutions has been studied by several authors [1—6]. Kuznetsov et al. [3] have reported that aliphatic amines act as corrosion inhibitors for metallic iron in formic acid solution. Also, thiourea and its derivatives were investigated [4] for their inhibition effects on the corrosion of iron in aerated and deaerated hydrochloric acid. Knikeev et al. [5] and Nemehaninova et al. [6] used some organic nitrogen compounds as corrosion inhibitors or iron in acid solutions.

The methods of comparing the efficiency or inhibition are numerous [7—9]. Recently Aziz and Shams El-Din [10] applied the Mylius thermometric method [11] to study the dissolution of aluminium and zinc in hydrochloric acid and sodium hydroxide solutions. Owing to the technical importance and widespread use of iron, it is necessary to protect iron against corrosion.

The object of this paper is to apply the Mylius thermometric and weight-loss methods to study the dissolution of iron in nitric acid, and throw some light on the mode of adsorption of some phenoxy-acetamide compounds on the iron surface.

Experimental

The phenoxy-acetamide compounds used as corrosion inhibitors in this investigation are:

p-chloro-phenoxy-acetamide; (I) Cl—⟨◯⟩—OCH₂CONH₂

---

* To whom correspondence should be addressed.

p-Methyl-phenoxy-acetamide; (II) CH_3—⟨ ⟩—OCH_2CONH_2

p-Amino-phenoxy-acetamide; (III) NH_2—⟨ ⟩—OCH_2CONH_2

p-Hydroxy-phenoxy-acetamide; (IV) HO—⟨ ⟩—OCH_2CONH_2

Phenoxy-acetamide; (V)   ⟨ ⟩—OCH_2CONH_2
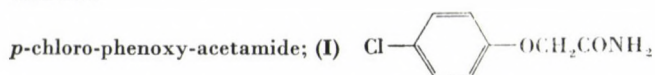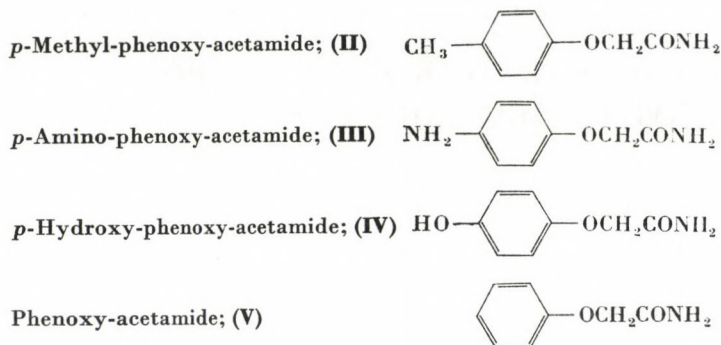
3 N HNO$_3$ was obtained by dilution from concentrated stock solution. The reaction vessel and the procedure for determining the dissolution of iron in corroding media were the same as described elsewhere [11]. Iron test-pieces (with purity > 99.2%) measuring $10 \times 100 \times 5$ mm were used in the thermometric method, and test pieces measuring $20 \times 50 \times 5$ mm were employed in the weight-loss method. Also the iron test-piece surface was degreased with methyl alcohol and etched in a solution of the composition: 1 *conc.* H$_2$SO$_4$: 1 *conc.* HNO$_3$: 2 H$_2$O. Each experiment was carried out with 15 mL of the corrosive solution in the thermometric method and 100 mL of the corrosive solution in the weight-loss method. All experiments started at 25 ± 0.1 °C.

The extent of corrosion inhibition by a certain concentration of a particular additive is evaluated from the percentage reduction in the reaction number RN, viz.

$$\% \text{ Reduction in reaction number RN} = \frac{(RN)_{free} - (RN)_{inh}}{(RN)_{free}} \times 100.$$

where $(RN)_{free}$ and $(RN)_{inh.}$ are the reaction number in absence and in presence of inhibitors respectively. Where reaction number (RN) is defined as:

$$RN = \frac{T_m - T_i}{t} \text{ °C min}^{-1}$$

Where T_m and T_i are the maximum and starting temperatures, respectively, and t is the time in minutes taken to reach T_m.

The loss in weight is:

$$\% \text{ inhibition efficiency} = \frac{W_{free} - W_{inh.}}{W_{free}} \times 100$$

Where W_{free} and $W_{inh.}$ are the loss in weight of the test pieces in absence and in presence of the inhibitors.

Results and Discussion

The dissolution of iron in 3 N nitric acid was accompanied by temperature change. The maximum temperature is 55.2 °C, and is attained within 13 min, corresponding to RN of 2.323 °C/min (curve 1, Fig. 1). To this solution increasing amounts of p-phenoxy-acetamide compounds are added. The effect depends both on the concentration and the type of the additive used. The curves of Fig. 1 show the behaviour in the presence of p-chloro-phenoxy-acetamide. Curves having the same character are obtained with the other materials tested.
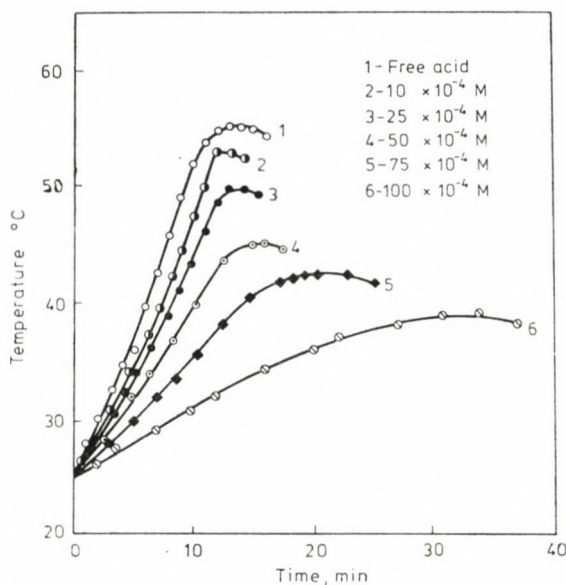
Fig. 1. Temperature-time curves for *p*-chloro-phenoxy-acetamide

In all cases the dissolution of iron in nitric acid solution starts directly as the metal is introduced into the solution. On increasing the concentration of the additive, the time required to reach T_m increases. This indicates that the additives retard the dissolution of iron in 3 N nitric acid, presumably by their adsorption on the surface of the metal. The extent of retardation or inhibition depends on the degree of coverage of the metal with the adsorbate, and the temperature-time curves provide a means of differentiating between weak and strong adsorption [10]. Weak adsorption is noted for all phenoxy-acetamide studied.

The fact that the compounds studied bring about a decrease in RN indicates that they act as inhibitors, and this is substantiated by the decrease

Table I

Efficiency of corrosion inhibition as determined
by percentage reduction in RN

Concentration of additives M	% Reduction				
	I	II	III	IV	V
5×10^{-4}	5.3	2.7	22.5	11.3	1.4
10×10^{-4}	7.4	5.3	26.0	13.9	2.3
25×10^{-4}	18.2	10.5	36.3	24.2	7.5
50×10^{-4}	45.8	26.4	65.6	52.6	16.5
75×10^{-4}	63.0	50.9	83.6	74.2	31.1
100×10^{-4}	81.9	65.6	94.8	86.7	52.2
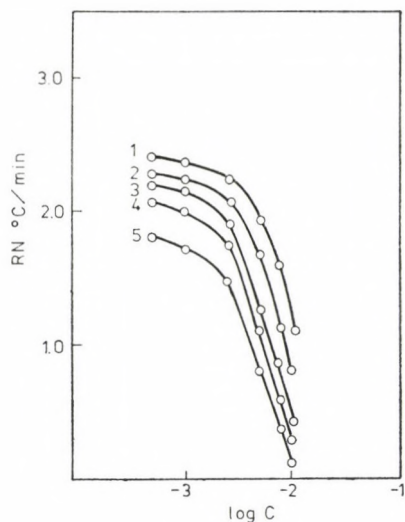
Fig. 2. Variation of RN with the logarithm of concentrations of the additives used. 1-phenoxy-
-acetamide;   2-*p*-methyl-phenoxy-acetamide;   3-*p*-chloro-phenoxy-acetamide;   4-*p*-hydroxy-
-phenoxy-acetamide; 5-*p*-amino-phenoxy-acetamide
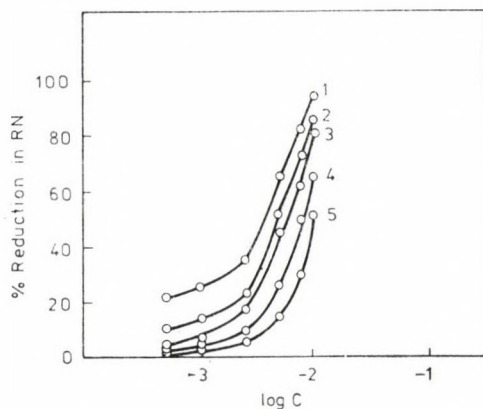
Fig. 3. % Reduction in RN — log *C* curves for all additives used. 1-*p*-amino-phenoxy-aceta-
mide; 2-*p*-hydroxy-phenoxy-acetamide; 3-*p*-chloro-phenoxy-acetamide; 4-*p*-methyl phenoxy-
-acetamide; 5-phenoxy-acetamide

in RN with increase in the concentration of the additive. The results recorded
in Table I reveal that the efficiency of corrosion inhibition as determined from
the percentage reduction in RN varies with both the concentration and the
type of phenoxy-acetamide derivatives.

Figure 2 shows the variation of the decrease in RN as function of log C_{inh}
for iron in nitric acid solution. These are invariably sigmoid in nature, sub-
stantiating the idea that the phenoxy-acetamide reduces the corrosion rate
by way of adsorption. The turn in the curves is rather sharp, suggesting that

it is associated with the formation of a monolayer of the inhibitor on the surface of the corroding metal. The points of inflexion of the RN — log C curves for the additives fall at 25×10^{-4} M. Previously mentioned ideas [12] about the modes of adsorption in the case of aromatic acids apply in the present case. In this case the additives are adsorbed on the surface through their carbonyl group, while the aromatic nucleus might be expected to lie flat on the surface of the metal. The same conclusion can be obtained on plotting the percentage reduction in RN against log C_{inh} (Fig. 3).

The percentage reduction in RN decreases in the order: p-amino-phenoxy--acetamide $>$ p-hydroxy-phenoxy-acetamide $>$ p-chloro-phenoxy-acetamide $>$ p-methyl-phenoxy-acetamide $>$ phenoxy-acetamide. Adsorption of the carbonyl group on the metal surface would depend essentially on its charge density. The magnitude of the latter should depend on the p-substituent which increases the charge density on the carbonyl group. NH_2 is more basic than $OH > Cl > CH_3 >$ unsubstituted compound. Thus, the participation of the polar structure to the ground state of the molecule [13] in p-amino-phenoxy-acetami-de would be larger than in the other derivatives. Accordingly, p-amino--phenoxy-acetamide should exhibit the highest adsorption tendency and hence the largest corrosion inhibitive action. The charge density on the carbonyl of unsubstituted compound is low and hence gives the least corrosion inhibition.

Weight-loss measurements

The effect of phenoxy-acetamide derivatives on the dissolution of iron in 3 N HNO_3 acid solution was also established by the weigh loss method. Fig. 4 represents the weight loss-time curves for p-chlorophenoxy-acetamide. The curves obtained in presence of additives fall below that of the free acid. These curves are straight lines passing from the origin and are characterized by initial increase in weight loss. The linearity of the weight loss with time from the beginning may be interpreted as the breakdown of the oxide film and the start of the attack. Weight loss of iron depends on both the type and the concentration of the additives in the same way as the percentage reduction in RN does. In Table II the additives examined are arranged in the order of

Table II

Efficiency of corrosion inhibition as determined by thermometric and weight-loss techniques at 100×10^{-4} M

Substances	% Reduction in RN	% Inhibition
III	94.8	92.8
IV	86.7	88.5
I	81.9	79.9
II	65.6	63.1
V	52.5	52.9
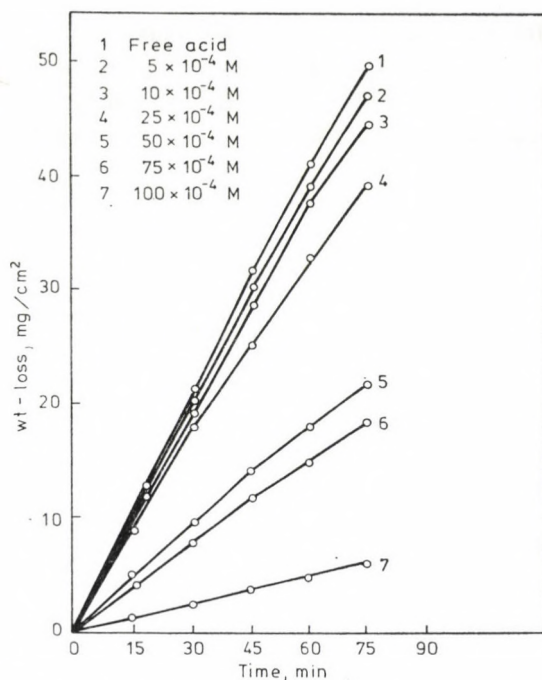
Fig. 4. Weight loss — time curves for *p*-chloro-phenoxy-acetamide

increasing inhibition efficiency. Also Table II shows that the compounds used
follow the same order when arranged according to the percentage reduction
in RN at the same concentration of the inhibitor $(100 \times 10^{-4}\ M)$ and after
60 min from the start.

Thus the same order of inhibitory action is obtained by weight-loss and
thermometric measurements. This indicates the validity of the results obtained
by the two different methods for the use of phenoxy-acetamide derivatives as
corrosion inhibitors of iron in 3 *N* nitric acid solution.

REFERENCES

[1] Krithirasan, N., Tsuru, T. H. S.: Boshohu Gijutsu., **296,** 275 (1980)
[2] Vosta, J., Pelikanj, S. M.: Wekst. Korros., **25,** 750 (1974)
[3] Kuznetsov, V. V., Zelenaya, S. A., Sorokin, V. I.: Issled obl Korroz. Zashch. Met., **11,**
    53 (1971)
[4] Narayan, R., Pillai, K.: Trans. Soc. Advan. Eletrochem. Sci. Technol., **7,** 63 (1972)
[5] Enikeev, E. Kh., Rozenfeld, I. L., Gonik, A. A., Zvezdinskii, K. V., Getmanskii, M. D.
    Nizamov, K. R.: Zashch. Met., **11,** 566 (1975)
[6] Nemehaninova, G. L., Klyuchnikov, N. G.: Inhibitory Korroz. Met, **20,** 117 (1972)
[7] Khalaf-Alla, S. E., Shama El-Din, A. M., Marei, S. A.: Roc. Trav. Chemir, **78,** 513 (1959)
[8] Gatos, H.: J. Electrochem. Soc., **101,** 443 (1954)
[9] Kaesche, H., Gackerman, N. J.: Electrochem. Soc., **105,** 191 (1958)
[10] Aziz, K., Shams El-Din, A. M.: Corros. Sci., **55,** 484 (1965)
[11] Mylius, F.: Z. Metal, **14,** 233 (1922)
[12] Saleh, M. R., Shams El-Din, A. M.: Corros. Sci., **12,** 688 (1972)
[13] Issa, I. M., Elsamahy, A. A., Temerk, Y. M.: Egypt. J. Chem., **13,** 121 (1970)

POTENTIOSTAT WITH AUTOMATIC IR-COMPENSATION

József Farkas[1]*, László Dobos[2] and Pál Kovács[1]

(¹ *Department of Physical Chemistry and Radiology, L. Eötvös University,*
H-1088 Budapest, Puskin u. 11—13 and ² *Department of General and*
Physical Chemistry, A. József University, H-6701 Szeged, Rerrich B. tér 1.)

A potentiostat operating on the principle of current interruption has been designed: it is especially suitable for electrochemical systems where the uncompensated resistance varies with time. The application possibilities of the instrument are illustrated by a series of potentiodynamic measurements.

In electrochemical studies, ohmic voltage drops on the electrolyte resistance between the reference electrode (the end of the Luggin capillary) and the working electrode, as well as on the eventual coating layer resistance cannot be compensated by simple potentiostats. A number of authors dealt with the solution of this problem, these works are summarized in the paper of Britz [1].

Methods used or suggested can be classified into three groups:

1) The ohmic resistance (R_1) is known (or can be determined) and stable in time. In this case on a resistance placed into the conducting circuit of the potentiostat having an identical value (R_1), the same voltage drop, IR_1 is generated as in the electrolyzing cell. On correcting the control signal of the potentiostat with this IR_1 potential, the ohmic voltage drop of the cell can be eliminated (positive, passive feed-back) [2, 3].

2) The a.c. methods utilize the electric properties of the electrolyzing cell; e.g. by superimposing a harmonic signal of small amplitude on the electrolyzing current, it can be achieved that the a.c. signal measurable between the reference and working electrodes depends only on the value of R_1 (the double-layer capacitance behaves as a short-circuit), and on knowing R_1 and I, the IR_1 potential can be generated by which the control of the potentiostat should be modified [4—7].

3) By a periodic interruption of the current of the potentiostat, information may also be obtained from which the IR_1 ohmic voltage drop can be generated [8], thus the control signals can also be modified. The latter two methods are suitable for the automatic compensation of ohmic voltage drop depending on the time and/or potential.

---

* To whom correspondence should be addressed
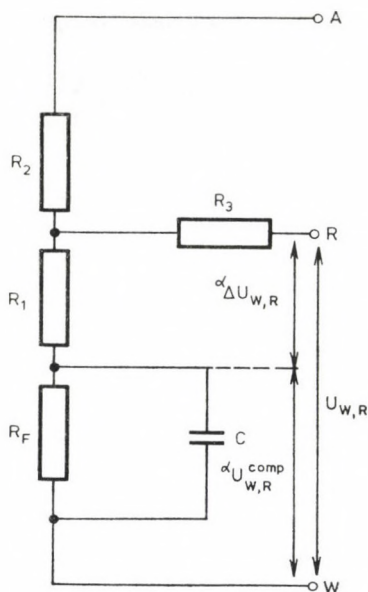
Fig. 1. Schematic equivalent circuit of the electrolyzing cell: W: connection of the working electrode, R: connection of reference electrode, A: connection of conducting electrode, R_F: Faraday impedance, C_F: capacitance of double-layer, R_1: Resistance between the reference electrode (end of the Lugging capillary) and the working electrode, R_2: resistance of the electrolyzing cell, R_3: internal resistance of the reference electrode, $U_{W,R}$: voltage drop between the working and the reference electrodes, $^{\alpha}\Delta U_{W,R}$: voltage drop on resistance R_1, $^{\alpha}\Delta U_{W,R}^{COMP}$ real potential of the working electrode
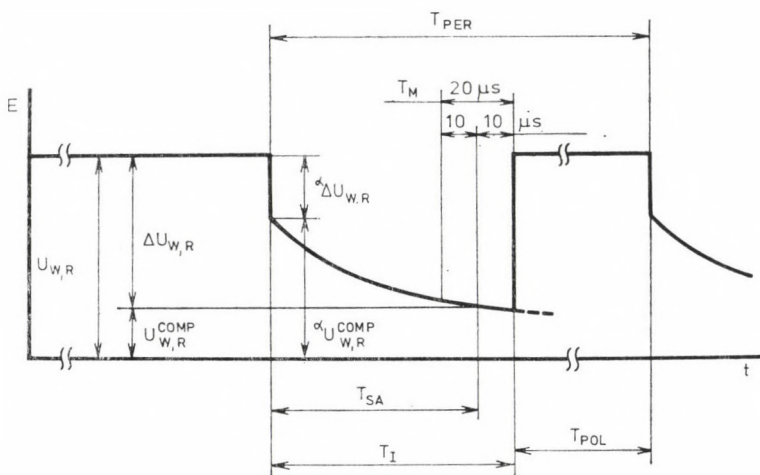
Fig. 2. Time dependence of electrode potential (ε) during operation of the instrument (schematically) $U_{W,R}$, $^{\alpha}\Delta U_{W,R}$, $^{\alpha}\Delta U_{W,R}^{COMP}$ as in Fig. 1. $\Delta U_{W,R}$: correction signal produced by the instrument during sampling, $U_{W,R}^{COMP}$: electrode potential corrected (approximately) with the ohmic voltage drop, T_{PER}: period time of sampling, T_{POL}: polarization time within a period T_I: time of current interruption, T_{SA}: time of sampling, T_M: interval of sampling

In the present work the design of a potentiostat is described, which makes the sampling for automatic compensation of the ohmic voltage drop by periodic interruption of the current. The functioning of the instrument is illustrated by several series of measured data.

Operation of the instrument

Automatic ohmic compensation is based on the principle of current interruption. Interruption occurs in the circuit of the conductive electrode by means of electronic switches (without contacts). The residual leaking current on interruption is less than 20 nA.

The principle of operation can be explained on the equivalent block scheme shown in Fig. 1 as follows: the potential measurable on the reference electrode decreases jump-wise on interruption, as the voltage drop $^{\alpha}\Delta U_{W,R}$ generated on resistance R_1 ceases to exist due to the lack of current. (The schematic potential-time diagram is seen in Fig. 2). The potential on the charged double-layer capacitor is discharged in the moment of interruption, then it decreases exponentially to the rest potential with a time-constant of $\tau = R_F C_F$. (The exponential approximation is correct only in the small interval of the decay time.) If within a short time after interruption of the current (so that the discharge of the double-layer capacitor should not cause significant errors) a sampling is made from the potential $U_{W,R}$ and the control of the potentiostat is designed so that the program potential be identical with this sampling potential, the ohmic voltage drop is automatically compensated. The direct application of this method is not expedient in practice, because it slows down the operation of the potentiostat, as information necessary to the control of the potentiostat is obtained only in the period of sampling. It is much better to generate the $\Delta U_{W,R}$ value by sampling, i.e. the ohmic voltage drop, and to control the potentiostat by the momentary potential $U_{W,R} - \Delta U_{W,R}$. (This means that the $\Delta U_{W,R}$ value is considered to be constant during the polarization time T_{Pol} in a single period.)

In the instrument realized, polarization time T_{Pol} is 25 times larger than the interruption time T_I, thus:

$$T_{PER} = T_I + T_{POL} = 26T_I \tag{1}$$

The time of sampling (T_S) is constant and equal to 20 μs, and it falls always into the last 20 μs period of interruption time (T_I) (Fig. 2). The digital control unit (see in Fig. 6, block DV without the external control K) is designed so that the average time of sampling T_{SA} can be set by a manual multistage switch. For precise automatic compensation, it is expedient to set this time
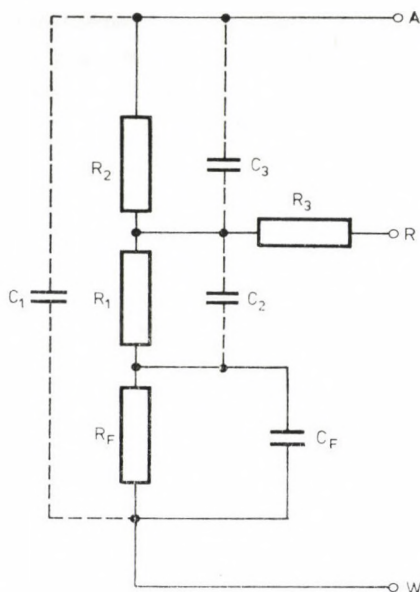
Fig. 3. The schematic equivalent circuit of the electrolyzing cell complemented with stray capacitances,(C_1, C_2, C_3). Others as in Fig. 1

small is order to keep the inaccuracy due to the discharge of the double-layer capacitor negligibly small. However, in practice, this has limits, as the current interruption is not instantaneous. The reason is the restricted speed of electronics, and the distorting effect of stray capacitances of the electrolyzing cell and its wiring (Fig. 3). Correspondingly, the potentials sampled deviate to a small extent from the accurate value. In the instrument built these deviations are the following:

$$\left| \varDelta U_{W,R} - {}^{\alpha}\varDelta U_{W,R} \right| \le 5 \text{ mV} \tag{2}$$

or

$$\left| \varDelta U_{W,R}^{COMP} - {}^{\alpha}\varDelta U_{W,R}^{COMP} \right| \le 5 \text{ mV} \tag{3}$$

Design of the instrument

The block scheme of the instrument is shown in Fig. 4. If we disregard the unit OE and the control units marked by dashed lines, Fig. 4 is the block scheme of a simple, ordinary potentiostat. (The program potential is connected at point *b*, according to the scheme in Fig. 5). With the frequency control unit FC located before the power amplifier T, the upper limiting frequency of the

potentiostat can be varied. The block marked OL is the display unit for blasting. The output and measuring units of the current are placed into the circuit of the working electrode W [9]. From the three output units of current, $I_{W,A\sim}$ is the direct output. $I_{W,A\sim}$ is the output damped with a lowband-pass filter D_2 (e.g. to the connection of the recorder), $I_\sim$ is the low-frequency noise indicator (band-pass filter D_1 is operation at frequencies 10—200 Hz).

The sampling unit generation the ohmic voltage drop (OE) is shown in a block scheme in Fig. 6. Potential $U_{W,R}$ is generated by sampling circuits A_4 and A_6 and by inverter A_5. Electronic switches F_1, F_2 and F_3 (as well as power amplifier T) is operated by the digital control unit DV. In the open position of switch F_3 only the potential signals are generated, whereas auto-
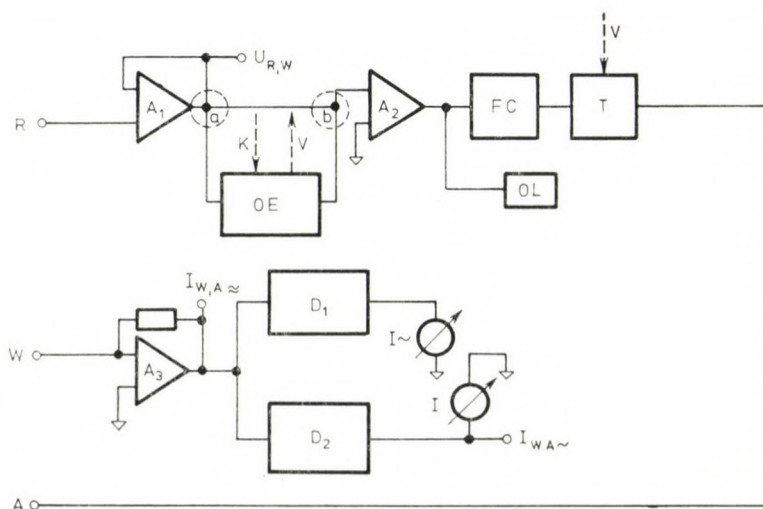
Fig. 4. Block scheme of the potentiostat. W, R, A: electrode connections, A_1, A_2, A_3: amplifiers, FC: circuits setting the upper limiting frequencies of the respons curve, OL: circuits displaying blasting, T: power amplifier, OE: sampling circuit (see Fig. 6), D_1, D_2: amplifiers provided with filters, K: external control, V: control signals (see Fig. 6), $U_{R,W}$: output for measuring the electrode potential, $I_\sim$: low-frequency noise indicator, $I_{W,A\sim}$: direct current output, $I_{W,A\sim}$: current output filtered
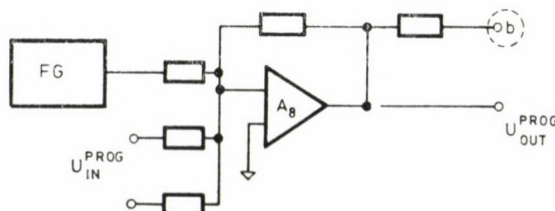
Fig. 5. Circuit generating the program potential. A_8: amplifier, FG: inner function generator, U_{OUT}^{PROG}: output connection of the total (summarized) program potential
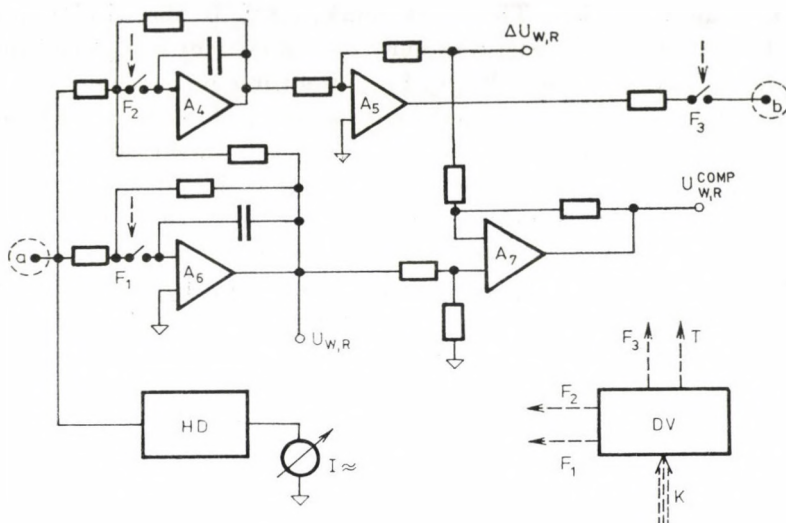
Fig. 6. Block scheme of the sampling and control circuit. A_4, A_5, A_6, A_7: amplifiers, F_1, F_2, F_3: controlled electronic switches, HD: high-frequency amplifier with highband-pass filter, $I_\sim$: high-frequency noise indicator, DV: control unit of sampling circuits, F_1, F_2, F_3, T: control signals to the electronic switches and power amplifier, K: connection of the external (digital) control signal, $\Delta U_{W,R}$, $U_{W,R}^{COMP}$, $U_{W,R}$ output connections of potential signals

matic compensation is made in its closed position. ($I_\sim$ is a high-frequency noise indicator.) Digital control DV can also be fitted to a computer through external switch K.

Checking of the operation of the instrument

Polarization curves taken by the potentiostat built on the above principle serve only for the illustration of the operation and application possibilities of the instrument.

In Fig. 7, anodic polarization curves taken is a 3% aqueous sulfuric acid solution in air at ambient temperature on a molybdenum electrode without ohmic compensation (curve 1) and with ohmic compensation (curve 2) are shown. On comparing the two curves, it is seen that an ohmic voltage drop of several Volts appears in this system, which can be compensated reliably by the instrument corresponding to an accuracy defined by inequality (3). (The Tafel slope of the compensated curve was 13 ± 3 mV.) The maximum ohmic voltage drop which can be compensated by the instrument built by us is ± 3 V or ± 8 V, depending on their design.

As was mentioned in the section discussing the operation of the instrument, the ohmic voltage drop can be displayed during the measurement, thus

from this, and the intensity of the current, the resistance of the system, R_1 can be calculated. The potential dependence of the resistance thus obtained is shown in Fig. 8 (calculated with data given in the previous Figure). The resistance values decreasing with increasing potential can be readily explained in this system: molybdenum oxides with a good coating ability transform fast into "molybdenum blue" having a loose structure [9].
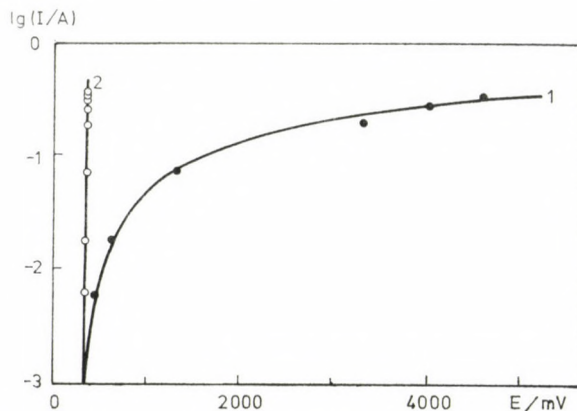
Fig. 7. Anodic polarization curve on molybdenum in an electrolyte containing sulfuric acid
1: without ohmic compensation, 2: with ohmic compensation
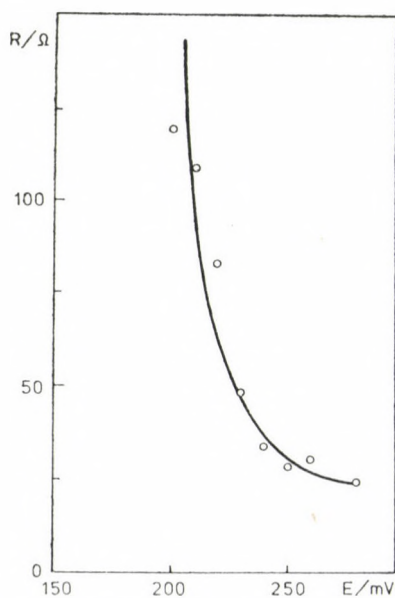
Fig. 8. Variation of the resistance of the coating layer with electrode potential (on molybdenum, in aqueous H_2SO_4)

From the comparison of Figs. 7 and 8, the conclusion can be drawn that in addition to the potential dependence of resistance R_1, its time dependence can also be studied by the instrument, if the change in time is not too fast. (This value may be a maximum of ± 100 V/s in the case of instruments already operating.)

In Fig. 9 the anodic and cathodic polarization curves on a tungsten electrode can be seen without ohmic compensation (curve 1) and with ohmic compensation (curve 2). Measurements were made in an aqueous solution of
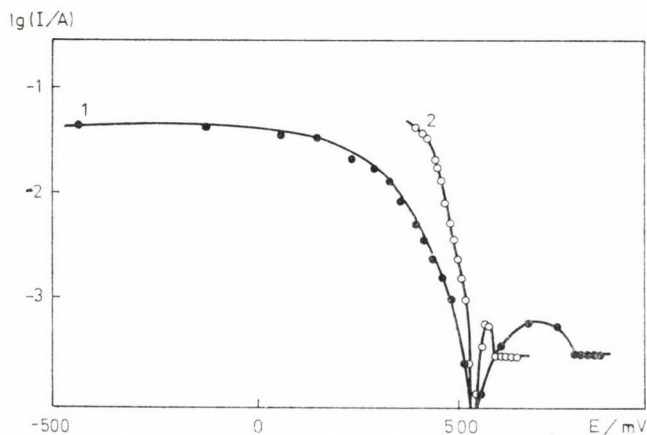
Fig. 9. Anodic and cathodic polarization curves on tungsten electrode, in an electrolyte containing H_2SO_4 and H_2O_2. 1: without ohmic compensation, 2: with ohmic compensation
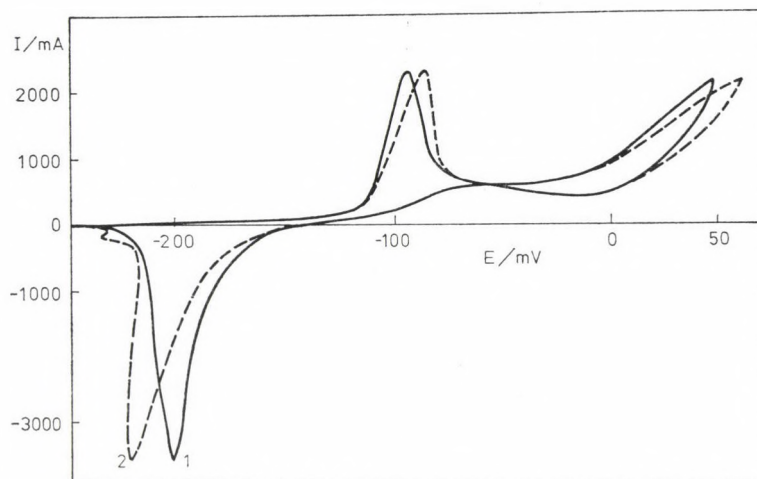
Fig. 10. Cyclic voltammetric curve on a rotating copper disc electrode in a aqueous solution of 2.97 mol/dm³ $HClO_4$ + 0.03 mol/dm³ HCl (rotating electrode: 2150 rpm, rate of potential change: 60 mV/min); 1: $U_{W,R}^{COMP}$ vs. I curve, 2: $(U_{W,R}^{COMP} + \Delta U_{W,R})$ vs. I curve

3% (wt.) H_2SO_4 and 10 wt. $\%$ H_2O_2. As is well seen in the Figure, ohmic compensation brings back the passivation curves on the anode and monotonic polarization curves on the cathod into real, evaluable range [10].

In Fig. 10 cyclic voltammetric curves typical for metal dissolution and metal ion reduction are shown. Curve 1 was taken on a rotating copper disc electrode with ohmic compensation. The starting potential into the anodic direction is —250 mV (with respect to a calomel electrode of 1 mol/dm³). The polarization potential of 60 mV/min controls the electrode potential, which is independent of the ohmic voltage drop. On the anodic branch, at a peak current of —100 mV a salt layer of CuCl is deposited on the surface of the electrode [9]. The increase of current at +50 mV refers to the appearance of Cu^{2+} ions [9]. On the backward, cathodic range, at about —200 mV potential, the CuCl salt layer is reduced with maximum speed.

Curve 2 in Fig. 10 illustrates a special application possibility of the instrument. On recording curve 2, the instrument was operated in a similar way as for drawing curve 1, except that the recorder draws now the anodic and cathodic current as a function of $U_{W,R}^{COMP} + \Delta U_{W,R}$, i.e. the potential containing the ohmic voltage drop too. In the anodic region of the cyclic voltammetric curve thus obtained only the well-known effect is seen: the ohmic voltage drop distorts the polarization curve. The same effect is seen in the cathodic region before the current peak, but at decreasing cathodic current the direction of the potential variation changes sign. The explanation is simple: the rate of the decrease in the ohmic voltage drop is higher than that of the variation in the electrode potential. (The existence of such curves was interpreted so far only by mathematical models [1, 11].) The experimental data in Fig. 10 and their interpretation is in accordance with the results of experiments carried out with rotating disc electrodes and a double potentiostat [9].

REFERENCES

[1] Britz, D.: Electroanal. Chem., **88**, 309 (1978)
[2] Hodgkins, A., Huxley, A., Katz, B.: J. Physiol., **116**, 424 (1952)
[3] Gerischer, H., Staubach, K.: Z. Elektrochem., **61**, 789 (1957)
[4] Dévay, J., Lengyel, B., Mészáros, L.: Acta Chim. Acad. Sci. Hung., **66**, 269 (1970)
[5] Dévay, J., Lengyel, B., Mészáros, L.: Hung. Sci. Instr., **25**, 5 (1972)
[6] Dévay, J., Lengyel, B., Mészáros, L.: Zashch. Met., **9**, 278 (1973)
[7] Dévay, J., Lengyel, B., Mészáros, L., Daróczy, J.: Hung. Sci. Instr., **33**, 1 (1975)
[8] Bezman, R.: Anal. Chem., **44**, 1781 (1972)
[9] Farkas, J., Dobos, L., Kovács, P., Kiss, L.: Acta Chim. Acad. Sci. Hung., **108**, 125 (1981)
[10] Pourbaix, M.: Atlas of Electrochemical Equilibria, Pergamon Press (1966)
[11] Bauer, H. H.: Electroanal. Chem. (Ed.: Bared) Vol. **8**, 1975

COMPENSATION OF OHMIC VOLTAGE DROP ON MODIFIED POLYMER FILM ELECTRODES

György Inzelt[1]*, László Dobos[2] and József Farkas[1]

*([1] L. Eötvös University, Department of Physical Chemistry and Radiology,
H-1088 Budapest, Puskin u. 11—13 and [2] A. József University,
Department of General and Physical Chemistry, H-6701 Szeged, Rerrich B. tér 1)*

TCNQ and PVF polymer film electrodes have been studied by cyclic voltammetry. It has been established that cyclic voltammetric curves become distorted by uncompensated ohmic resistance for medium thick films at scan rates higher than 0.025 V/s. The effect of ohmic voltage drop can be practically eliminated by the use of an Electroflex GMK (Szeged) potentiostat using the interruption technique.

In recent years the study of modified electrodes became one of the most dynamically developing research fields [1—5]. This phenomenon has two basic reasons. One of them is that important new knowledge can be acquired about processes taking place on the surface of electrodes. In the early stage of research, studies were mainly aimed at this purpose. Another reason, which is the driving force of newer research work is the utilization of possibilities in the application of modified electrodes. Most promising results have been achieved in the fields of electrocatalysis, organic and bioelectrochemistry and the preparation of multilayer polymer film electrodes for electrochromic display devices [1—8].

However, when studying electroactive polymer films, not only the general problem of electrochemical measuring technique should be coped with, namely that a certain ohmic voltage drop is to be compensated, but in this case this resistance often changes in time during the measurement. For example, in the case of TCNQ polymer film electrodes, where the basic reaction can be given as follows:

$$TCNQ + e^- + M^+ \rightleftharpoons TCNQ^-M^+$$

the flow of counterions M^+ into the initially neutral film reduces the resistance of the film by orders of magnitudes during reduction [9—10]. In such cases the only applicable method for compensation is the so-called current interruption technique [11, 12]. Commercial potentiostats working on the principle of positive feed-back or alternating current compensation are not suitable for this purpose.

* To whom correspondence should be addressed

We described a potentiostat in a previous publication [13], in which compensation is based on an automatic variant of the interruption technique. In this paper, we study the application of this instrument for the TCNQ polymer film electrode, the electrochemical behaviour of which is well documented in aqueous solutions [9, 10].

In non-aqueous solutions where the ohmic resistance of the solution is larger than that of aqueous electrolyte solutions, we have also carried out experiments with a poly(vinylferrocene) electrode [14,15].

Experimental

The tetracyanoquinodimethane (TCNQ) polymer was prepared by the polycondensation of 2,5-bis(2-hydroxyethoxy)7,7,8,8-tetracyanoquinodimethane with adipoyl chloride [9, 10]. For the preparation of the buffer solution of pH = 7 and concentration of $0.5 \ mol/dm^3$, NaH_2PO_4 and NaOH (Reanal) were used after recrystallization of the analytically pure reagents. As solvent, bidistilled water was used. The polymer was dissolved in tetrahydrofurane. This solution was applied on the surface of a carefully purified Pt electrode, the solvent was evaporated at ambient temperature and the electrode dried at 80 °C for 5 min. As auxiliary electrode, platinum and as reference electrode, a saturated calomel electrode (S.C.E.) were used. The poly(vinylferrocene) (PVF) polymer was prepared by the polymerization of vinylferrocene [16]. Acetonitrile (Reanal) distilled and dried with a 3 Å molecular sieve was used as solvent, recrystallized tetrabutylammonium perchlorate (TBAP, Fluka) served as supporting electrolyte in a concentration of $0.1 \ mol/dm^3$. The method of film preparation was identical with that used for TCNQ, but the solvent of the polymer was CH_2Cl_2. In non-aqueous solution an Ag-wire served as quasi-reference electrode [15]. Before experiments, high purity nitrogen, free of oxygen, was bubbled through the solution, measurements were made in a nitrogen atmosphere. Cyclic voltammetric studies were performed by potentiostat equipped with automatic IR compensation and function generator (Electroflex GMK, Szeged), and by a Hewlett-Packard 7046B XY type recorder. The average sampling time was 40 μs in all experiments [13].

Results and Discussion

In Fig. 1 two cyclic voltammograms obtained on modified Pt-TCNQ electrode are shown. In one case ohmic compensation was applied and in the other it was not. The effect of ohmic compensation is clearly seen, as the decrease of the difference (ΔE_p) in cathodic (E_{pc}) and anodic (E_{pa}) peak potentials and the increase of the anodic (i_{pa}) and cathodic (i_{pc}) peak currents. This is in accordance with the result derived from theory [17, 18]. On the basis of this alone, however, it cannot be determined to what extent the ohmic voltage drop is compensated. Our aim should be the minimization of the rest of ohmic voltage drop (≤ 1 mV), as only so could one differentiate between the effect of the relative slowness of the charge transfer and that of uncompensated ohmic voltage drop, as both effects have practically the same diagnostic criteria [17, 18]. Namely, if we compensate the ohmic voltage drop only partially, our result concerning the rate of charge transfer may be in error by orders of magnitude.
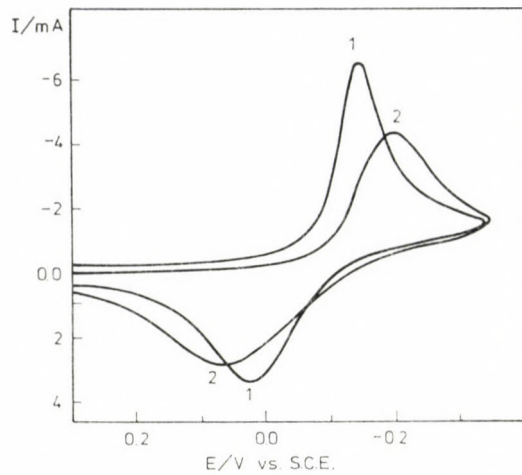
Fig. 1. Cyclic voltammograms of a Pt-TCNQ electrode of a thickness of 85 nm, at a scan rate of 0.6 V/s, in a pH = 7 phosphate buffer with a concentration of 0.5 mol/dm³ at 23 °C; 1 — with compensation, 2 — without compensation
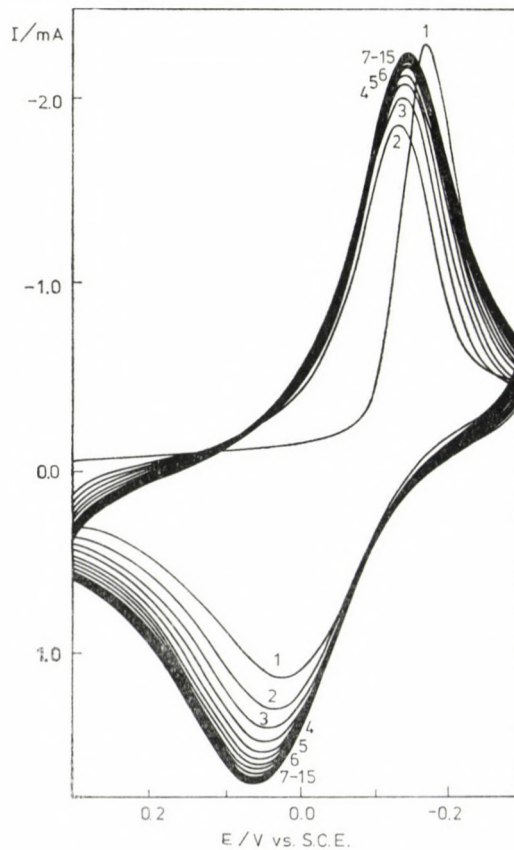
Fig. 2. Series of cyclic voltammograms of a Pt-TCNQ electrode of 50 nm thickness. Conditions as in Fig. 1

On the basis of the experimental results shown above the conclusion can be drawn that the potentiostat applied is capable of compensating the ohmic voltage drop in a system where the resistance changes during the experiment.

In order to determine the extent of compensation, the so-called break-in phenomenon occurring on polymer film electrodes can be utilized. The essence of this phenomenon is that relatively thick ($\bar{d} = 50$—500 nm), freshly prepared films are reduced fully only after several reduction-oxidation cycles, an effect that can be observed mainly at higher scan rates ($v > 0.1$ V/s). In these cases the peak current increases gradually during the repeated cycles, and then reaches a constant, maximum value. The TCNQ electrode shows a somewhat more complicated behaviour, because even in the case of thin films the first cycle differs from the further ones. The reason for this may be a change in the morphology of the polymer film [10, 20].

Thus in the course of the second and further cycles it can be expected that the gradual increase in the peak current causes a rise in the ohmic voltage drop which manifests itself in the gradual shift of peak potentials and thus
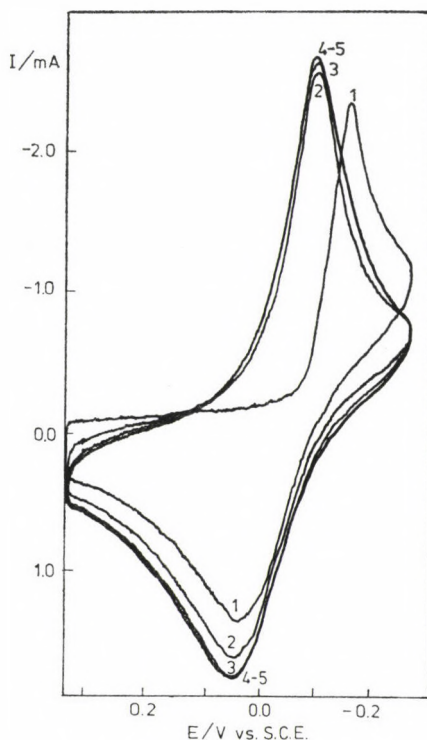
Fig. 3. Series of cyclic voltammograms under identical conditions as in Fig. 1 by applying compensation
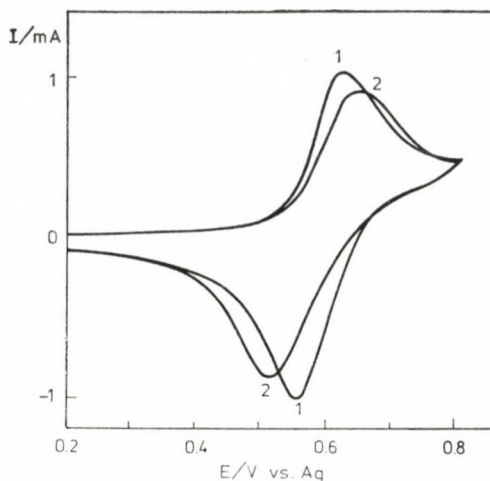
Fig. 4. Cyclic voltammogram of a Pt-PVF electrode ($\Gamma = 4 \times 10^{-8}$ mol/dm²) in a TBAP/ acetonitrile solution with a concentration of 0.1 mol/dm³ at 25 °C and 0.06 V/s; 1 — with compensation, 2 — without compensation

in the increase of ΔE_p. This fact is reflected in the series of curves shown in Fig. 2, where no compensation was applied in the course of the break-in period. In Figure 3 the effect of compensation is illustrated. It can be seen that in this latter case the values of peak potentials do not change from the second cycle on, i.e. ΔE_p remains constant. On comparing the cyclic voltammograms in Figs. 2 and 3, it can also be seen that peak currents are also larger when applying compensation, as we have already seen earlier. From these curves and the potential needed for compensation, which can be drawn separately, the ohmic resistance can be estimated, which was 40 Ω in our case in the range of cathodic peak potential.

Results obtained in non-aqueous solution for a PVF electrode are shown in Fig. 4. The effect of compensation is obvious also in this case. The ohmic voltage drop was proportional to the current also here in the range studied (0.2—5 mA) and it decreased with increasing temperature. The estimated resistance in the range of cathodic peak potential was 50 Ω at 20 °C and 30 Ω at 40 °C.

Based on the above results, it can be established that the compensation of ohmic voltage drop, which is of primary importance for modified polymer film electrodes, can be realized by a potentiostat working on the interruption principle. At the same time, it is proved that the potentiostat Electroflex GMK (Szeged) is suitable for studying polymer film electrodes at the usual rates of potential changes (0.1—1 V/s).

REFERENCES

[1] Snell, K. D., Keenen, A. G.: Chem. Soc. Rev., **8**, 259 (1980)
[2] Murray, R. W.: Acc. Chem. Res., **13**, 135 (1980); in Electroanalytical Chemistry, ed. A. J. Bard, Vol. **13**, pp. 192—368. Marcel Dekker Inc., New York 1984
[3] Albery, W. J., Hillman, A. R.: Royal Chem. Soc., Chem. Ann. Reports C, **78**, 377 (1981)
[4] Johnson, D. C., Ryan, M. D., Wilson, G. S.: Anal. Chem., **56**, 7R (1984)
[5] Inzelt, G.: Kémiai Közlemények, **62**, 163 (1984)
[6] Van de Mark, M. R., Miller, L. L.: J. Am. Chem. Soc., **100**, 3223 (1978)
[7] Merz, A., Bard, A. J.: J. Am. Chem. Soc., **100**, 3222 (1978)
[8] Kaufman, F. B., Engler, E. M.: J. Am. Chem. Soc., **101**, 547 (1979)
[9] Day, R. W., Inzelt, G., Kinstle, J. F., Chambers, J. Q.: J. Am. Chem. Soc., **104**, 6804 (1982)
[10] Inzelt, G., Day, R. W., Kinstle, J. F., Chambers, J. Q.: J. Phys. Chem., **87**, 4592 (1983); J. Electroanal. Chem., **161**, 147 (1984); J. Am. Chem. Soc., **105**, 3396 (1984)
[11] Britz, D.: J. Electroanal. Chem., **88**, 309 (1978)
[12] Schwabe, K.: J. Electroanal. Chem., **100**, 927 (1979)
[13] Farkas, J., Dobos, L., Kovács, P.: Acta Chim. Hung., **120**, 63 (1985)
[14] Daum, P., Lenhard, J. R., Rolison, D., Murray, R. W.: J. Am. Chem. Soc., **102**, 4649 (1980)
[15] Peerce, P. J., Bard, A. J.: Electroanal. Chem., **112**, 98 (1980); **114**, 89 (1980)
[16] Smith, T. W., Kuder, J. E., Wychnik, D.: J. Polym. Sci., Polym. Chem. Ed., **14**, 2433 (1976)
[17] Tacconi, N. R., Calandra, A. J., Arvia, A. J.: Electrochim. Acta, **18**, 571 (1973)
[18] Roullier, L., Laviron, E.: J. Electroanal. Chem., **157**, 193 (1983)
[19] Kaufman, F. B., Schroeder, A. M., Engler, E. M., Kramer, S. R., Chambers, J. Q.: J. Am. Chem. Soc., **102**, 483 (1980)
[20] Chambers, J. Q., Inzelt, G.: Anal. Chem., **57**, 1117 (1985)

MASS-SPECTROMETRIC DETERMINATION OF THE HEAT OF FORMATION OF INDIUM MOLYBDATE

Olivér Kaposi*[1], László Lelik[1], German Aleksandrovich Semenov[2]
and Evgeny Nikolaevich Nikolaev[2]

(*[1] Department of Physical Chemistry, L. Eötvös University H-1088 Budapest,
Puskin u. 11—13. and [2]Zhdanov State University, Leningrad, Srednij pr. 41/43.)*

For the determination of mass spectra in equilibrium vapour over the mixture of $In_2O_{3(s)} + MoO_{2(s)} + MoO_{3(s)}$ the Knudsen effusion mass-spectrometric method has been used.

The appearance potential of positive ions with high intensity and the sublimation enthalpy of Mo_3O_9 and In_2MoO_4 have been measured. The thermodynamic parameters of $In_2MoO_{4(g)}$ were determined by using the Third Law of thermodynamics. The heat of formation of gaseous In_2MoO_4 and the atomization energy for $In_2MoO_{4(g)}$ were found to be -863.0 ± 30 kJ/mol and 2988 ± 40 kJ/mol, respectively.

Introduction

On evaporating metal oxides from a Knudsen cell, significant amounts of $MMoO_4$ ions could be detected by mass spectrometry (M = Mg, Ca, Sr, Sn, Ba, Be, In and Li) [1]. It has been shown that the ions are molecule ions of molybdates. These molybdates are very stable, and this fact calls attention to the possibility that upon the evaporation of certain oxides in the presence of molybdenum their formation should be taken into account also in the interpretation of evaporation experiments based on mass losses. The formation of these molecules in high amounts means also that certain trioxides can transport a significant amount of transition elements at elevated temperatures.

Burns et al. showed [2] first the formation of stable indium molybdate in the gas phase as a reaction product in In_2O_3 and metallic molybdenum at high temperature by mass spectrometry. The structure of the molecule has been studied later by electron diffraction and IR spectroscopy [3, 4].

The aim of the present work is to determine the heat of formation of In_2MoO_4 by using the enthalpy changes in the following reactions:

$$3\ In_2MoO_{4(g)} \rightleftharpoons 3\ In_2O_{(g)} + Mo_3O_{9(g)} \tag{1}$$

* To whom correspondence should be addressed

$$2 \ In_2MoO_{4(g)} \rightleftharpoons 2 \ In_2O_{(g)} + Mo_2O_{6(g)} \qquad (2)$$
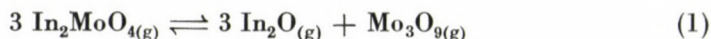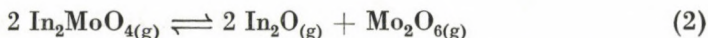
Calculations have been made by using the results of experiments and literature data for the application of the Third Law of thermodynamics.

Results and Discussion

The evaporation properties of metal oxides have been studied by means of the Knudsen effusion mass spectrometric method used earlier for studying metal halides [5, 6].

In the study of the two systems the difference is that the temperature of measurements is by 300—400 K higher for oxides than that for metal halides due to the lower vapour pressure of the oxides.

The appearance potential (AP) of ions formed from the vapour in equilibrium with the solid phase has been measured by a mass spectrometer (MI-1311) equipped with a Knudsen evaporator [7], other evaporation experiments have been carried out by a mass spectrometer of the type MSZ-1301 [8]. Molybdenum Knudsen cells with 0.2 mm slits have been used for evaporation; the temperature has been measured by Pt—PtRh thermocouples.

For measuring the ionization potential (IP), the Knudsen cell was heated up by a temperature programmer of the type Chinoin LP-839, and the temperature was maintained at 1225 K with a stability of ± 1 K during measurements. Ionization efficiency curves were evaluated by linear extrapolation. The electron energy scale has been corrected by the aid of standards given in the literature: $AP_{Ag} = 7.5$ eV [9], and $AP_{Cs^+/CsCl} = 8.7$ eV [10]. The estimated accuracy of the AP values measured is ± 0.3 eV.

The temperature of the evaporator of the mass spectrometer MSZ-1301 was checked by the isothermal evaporation of Ag and CsCl [11] and by the determination of the heat of sublimation of MoO_3 for the thermodynamic measurements. On comparing the literature data for vapour pressures [12, 13], and the ones measured by us, it can be established that the deviation between the fixed point of the thermocouple and the temperature of the sample is 8 K at 850 K and 12 K at 1300 K. Based on this, we corrected the measured temperatures correspondingly.

As we have found in preliminary experiments that the partial pressure of indium oxides in the equilibrium vapour of $1 : 1 \ In_2O_3$ and metallic Mo powder is very low, we applied in our experiments mixtures of In_2O_3 and molybdenum oxides (MoO_2, MoO_3). The data of the mass spectrum of the equilibrium vapour of such a mixture obtained at 1370 K and at an inoization energy of 28 eV are shown in Table I. The mass spectrum was calculated by taking into consideration the mass dependence of the isotopic composition

Table I

Mass spectrum of the equilibrium vapour over the mixture of In_2O_3 *and Mo oxides* ($MoO_2 + MoO_3$)

Ion	In^+	InO^+	In_2O^+	In_2^+	MoO_2^+	MoO_3^+	$In_2MoO_3^+$	$In_2MoO_4^+$
Rel. int.	116	1.2	9.9	2.6	2.5	1.0	1.4	100

Ion	$Mo_2O_4^+$	$Mo_2O_5^+$	$Mo_2O_6^+$	$Mo_2O_7^+$	$Mo_2O_8^+$	$Mo_2O_9^+$
Rel. int.	0.3	1.4	13	0.5	4.9	49.5

and the multiplication factor of the electron multiplier ($\gamma_i = M_i^{-1/2}$ where M_i is the mass number of the i-th ion).

Ions were identified on the basis of mass numbers, isotopic composition and appearance potentials measured.

The ionization efficiency curves of indium-containing molecules of higher intensity are shown in Fig. 1. AP values obtained from the evaluation of
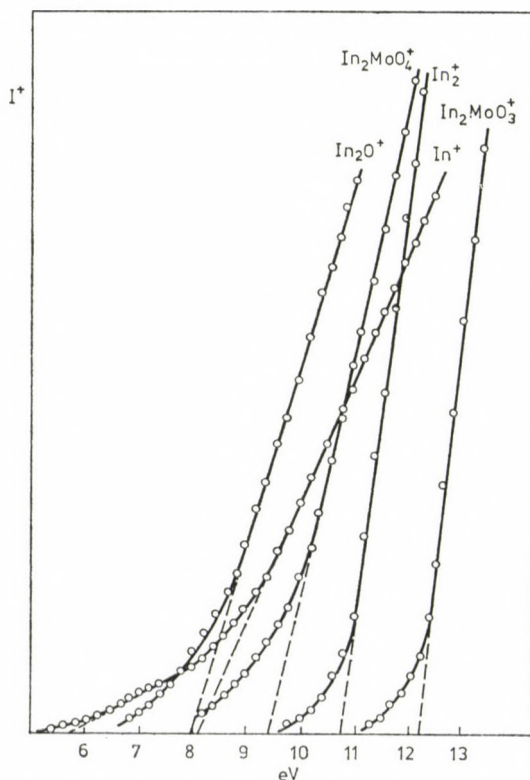
Fig. 1. Ion current intensity of positive ions with higher intensity as a function of corrected electron energy

Table II

Appearance energies of ions of high intensity

Ion	AP (measured) ± 0.3 eV	AP (literature) eV
In^+	5.6; 8.2	5.8 ± 0.3 [9]
In_2O^+	8.0	7.9 ± 0.5 [9]
In_2^+	10.9	—
$In_2MoO_4^+$	9.4	9.5 ± 1 [2, 9]
$In_2MoO_3^+$	12.2	—
$Mo_2O_6^+$	12.1	12.1 ± 0.6 [9]
		11.8 ± 0.6 [14]
$Mo_3O_9^+$	13.2	12.1 ± 1 [9]
		12 ± 1 [14]

ionization efficiency curves are summarized in Table II. The AP values measured agree satisfactorily with literature data.

As is seen from Fig. 1 and Table II, In^+ ions are formed in at least two fragmentation processes. The lower AP value (5.6 eV) agrees exactly with the ionization potential of metallic indium [9]. This fact, together with the high relative intensity of the In^+ ion, proves that In_2O_3 evaporates dissociatively, as was supposed earlier [15]. The AP = 8.2 eV corresponds probably to indium formed in the process

$$In_2O \rightarrow In^+ + InO + e$$
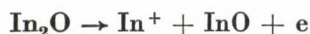
which supports the old hypothesis that in the course of evaporation of In_2O_3 a significant amount of In_2O is also formed [16]. The low intensity InO^+ ions of the spectrum are probably formed in the process

$$In_2O \rightarrow InO^+ + In + e$$

what also supports the previous assumption [2]. To the formation of In_2O, naturally reactions (1) and (2) also contribute. All these facts seem to contradict the assumption [17] that In_2O_3 evaporates congruently and a significant amount of gaseous parent molecules is formed on its evaporation.

The large difference (2.8 eV) between the ionization potential of $In_2MoO_4^+$ and the appeerence potential of the fragment $In_2MoO_3^+$ together with the high relative intensity of In_2MoO_4 (Table I) proves the high stability of the indium molybdate molecule. This stability is due to the strong ionic character of intermolecular forces. The appearance potentials of MoO_2^+ and MoO_3^+ ions could not be measured because of their low intensity, but the fact that on decreasing the ionizing electron energy below 16 eV they disappear from the spectrum, makes their fragment ion nature probable.

The trimers of MoO_2 and MoO_3 and their fragment ions are present in the mass spectrum with a significant intensity (Table I). The temperature

dependence of the ion current intensity of $Mo_3O_9^+$ and its fragment ions was measured and the heat of the process

$$3\ MoO_{3(s)} \rightarrow Mo_3O_{9(g)}$$
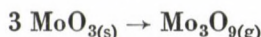
i.e. the sublimation enthalpy of Mo_3O_9 determined from the function $\lg I^+T$ — $- 1/T$ (Fig. 2). The value obtained (ΔH_s at 1160 K $= 354.5 \pm 8$ kJ/mol) agrees well with literature data [18].

From the temperature dependence of ion current intensity of In_2MoO_4 (Fig. 2), the heat of sublimation of In_2MoO_4 has been calculated. The value obtained is $\Delta H_s = 324.4 \pm 9$ kJ/mol at 1160 K.

In the further thermodynamic measurements the ion currents were measured at an ionization potential exceeding the AP by 3 eV, because we supposed that in this case the fragmentation of the molecule was negligible. Calibration for measuring the partial pressures was made with an Ag standard [13], the ionization cross section of molecules was calculated from the Mann cross sections [19] by using the additivity rule. Enthalpy changes in reactions (1) and (2) have been calculated based on the Third Law of termodynamics.

The thermodynamic functions of gaseous In_2O, Mo_2O_6 and Mo_3O_9 were taken from Ref. [20]. These data have been calculated for the In_2MoO_4 molecule by applying the rigid rotor-harmonic oscillator approximation. The molec-
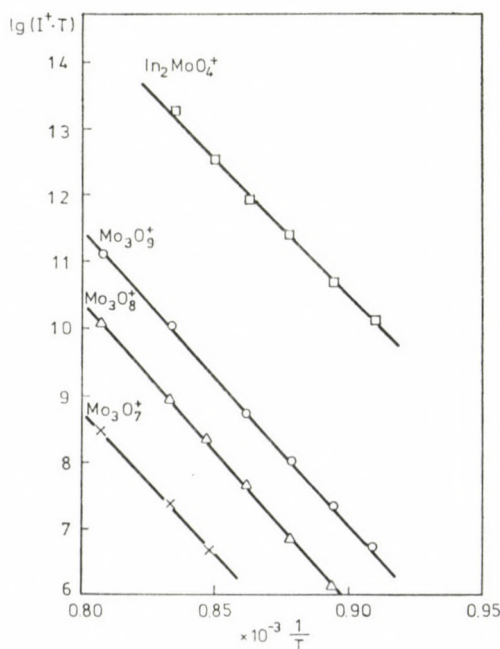
Fig. 2. The Clausius-Clapeyron plots for ions $In_2MoO_4^+$ and $Mo_3O_9^+$ and of the fragments of the latter

ule In_2MoO_4 was supposed to have a bicyclic structure of D_{2d} symmetry. On correcting the In—O distance according to Ref. [21], the distance 2.20 Å given in [3] changed to 2.36 Å. In the calculations, the Mo—O distance was taken as 1.81 Å; bond angles in the ring were taken as O—Mo—O = 85°and O—In—O = 62°. Stretching frequencies originate partly from experimental data in Refs [4, 22], partly from estimates based on similar compounds [20]. Wave numbers used are in cm^{-1}: 930 (A_1), 840 (B_2), 790 (B_2), 402 (A_1), 381 (B_1), 410 (A_1), 300 (B_2), 830 (E), 718 (E), 280 (E) and 80 (E). The thermo- dynamic functions of In_2MoO_4 are summarized in Table III.

The heats of formation needed for the calculation of the heat of forma- tion of In_2MoO_4 were taken from the literature [20]:

$$\Delta H^0_{f,0}(In_2O_{(g)}) = -38.0 \text{ kJ/mol}$$

$$\Delta H^0_{f,0}(Mo_2O_{6(g)}) = -114.0 \text{ kJ/mol}$$

$$\Delta H^0_{f,0}(Mo_3O_{9(g)}) = -1890 \text{ kJ/mol}$$

In Table IV the partial pressures, heats of reaction measured for the components of reactions (1) and (2), as well as the calculated heat of formation for $In_2MoO_{4(g)}$ are shown as a function of temperature.

Table III

Thermodynamic functions of In_2MoO_4

T(K)	C_p(J/mol K)	$S°$(J/mol K)	$-\dfrac{G^0_T - H^0_0}{T}$ (J/mol K)	$H_T - H_0$ (kJ/mol)
298	108.383	374.574	303.070	21.319
1000	150.769	537.072	418.663	118.409
1100	151.958	551.500	430.093	133.548
1200	152.878	564.763	440.770	148.792
1300	153.605	577.030	450.786	164.117
1400	154.180	588.139	459.971	179.435

Table IV

Heat of formation of $In_2MoO_{4(g)}$ as a function of the temperature

Reaction	T(K)	P_{In_2O} (Pa)	$P_{In_2MoO_4}$ (Pa)	$P_{Mo_3O_9}$ or pMo_2O_6 (Pa)	$\Delta H_{r,0}$ (J/mol)	$\Delta H_{f,0}/In_2MoO_{4(g)}$ (kJ/mol)
1	1283	0.20	0.57	0.019	551.9	−851.9
1	1347	0.41	1.85	0.019	595.0	−866.3
1	1474	2.61	16.8	4.05	598.7	−667.8
1	1478	4.91	31.8	7.1	594.5	−886.1
2	1478	4.91	31.8	3.25	510.9	−863.6

As is seen from Table IV, as expected, the heat of reaction does not depend strongly on the temperature. The average value of the heat of formation is:

$\Delta H_{f,0}(In_2MoO_{4(g)}) = -863.1 \pm 4.4 \, kJ/mol$. The error of 4.4 kJ/mol shown does not take into account the error in the estimation of stretching frequencies of In_2MoO_4. On considering this error too, the maximum error in the determination of $\Delta H_{f,0}$ is ± 30 kJ/mol. The heat of atomization of the In_2MoO_4 molecule calculated from the heat of formation measured and the heats of atomization of In, Mo and O taken from the literature [20] is 2988 ± 40 kJ/mol.

REFERENCES

[1] Verhaegen, G., Colin, R., Exsteen, G., Drowart, J.: Trans. Faraday Soc., No. 511, **61**, 1372 (1965)
[2] Burns, R. P., De Maria, G., Drowart, J., Inghram, M. G.: J. Chem. Phys., **38**, 1035 (1963)
[3] Tolmachev, S. M., Rambidi, N. G.: Zh. Strukt. Khim., **12**, 203 (1971)
[4] Shevelkov, V. R., Malttsev, A. A.: Vest. MGU. Ser. Khim. **1969**, 100
[5] Kaposi, O., Lelik, L., Balthazár, K.: High Temp. Sci., **16**, 229 (1983)
[6] Kaposi, O., Lelik, L., Balthazár, K.: High. Temp. Sci., **16**, 311 (1983)
[7] Lelik, L., Balthazár, K., Kaposi, O.: Magy. Kém. Folyóirat, **87**, 481 (1981)
[8] Semenov, G. A., Nikolaev, E. M., Frantseva, N. E.: Primenenie mass specktrometrii v neorganicheskoi khimii, p. 152. Khimia 1976
[9] Gurvich, L. V., Kharachevtsev, G. V., Kondratev, V. N. et al.: Energiya razryva khimicheskikh sviazei. Potentsialy ionizatsii i srodstvo k elektronu. p. 351. Nauka 1974
[10] Gomez, M., Chatillon, Ch., Allibert, M.: J. Chem. Thermodynamics, **14**, 447 (1982)
[11] Sidorov, L. N., Sholts, V. B.: Zh. Fiz. Khim., **41**, 1960 (1967)
[12] Scheer, M. D., Fine, J.: Chem. Phys., **36**, 1647 (1962)
[13] Paule, R. C., Mandel, J.: Pure Appl. Chem., **31**, 371 (1972)
[14] Iveda, Y., Ito, H., Mizuno, T. et al.: High Temp. Sci., **16**, 1 (1983)
[15] Brewer, L.: Chem. Rev., **52**, 38 (1953)
[16] Thiel, A., Luckmann, H.: Z. anorg. Chem., **172**, 353 (1928)
[17] Shukarev, C. A., Semenov, G. A., Ratkovskii, I. A., Perevatshchikov, V. A.: Zh. Obshch. khim., **31**, 2090 (1961)
[18] Kazenas, E. K., Chuzhikov, D. M.: Davlenie i sostav para nad okislami khimicheskii elementov. Nauka, Moskva 1976
[19] Mann, J. B.: Recent Developments in Mass Spectrometry, ed. T. Hayakawa, Univ. Park Press, Baltimore 1970
[20] Termodinamicheskie svoistva individualnykh veshchestv. Ed. Glushko, Nauka 1982
[21] Kulikov, V. A., Ugarov, V. V. Rambidi, N. G.: Zh. Strukt. Khim., **23**, 184 (1982)
[22] Spoliti, M.: Matrix Isolation Spectroscopy, ed. A. J. Barnes, p. 473. D. Reidel Publ. Comp. 1981

COMPUTATION OF THE TIME EVOLUTION
OF CONCENTRATIONS IN REACTIVE SYSTEMS

Sándor Kristyán*

(Department of Chemistry, Box 19065., The University of Texas at Arlington, Arlington, Texas 76019)

A modified version of the power series method is used to solve the system of differential equations of a simple model: formation of oligomers with tetramer being the largest molecule. Besides great accuracy, it has been found that the computational time can be substantially reduced by increasing the time step, as the system approaches equilibrium.

Introduction

Time evolution of the concentrations of the reactive species for an assumed [1] reaction mechanism, with known initial concentrations and measured or approximated rate constants, has been of great interest recently [2—6].

Considering unimolecular and bimolecular elementary steps only a computational procedure developed from the well-known power series method [7] can be used even in the most complicated cases.

Each mechanism is a sequence of elementary steps; the rate is given mathematically by a system of differential equations with the time derivatives of the concentrations on the left side, and polynomials, linear in the rate constants and generally nonlinear in the concentrations, on the right side.

We assume that the solution of the concentration functions [A], [B], ... are in the form of power series:

1.1
$$[A] = \sum_{m=0}^{\infty} a_m \cdot t^m$$

$$[B] = \sum_{m=0}^{\infty} b_m \cdot t^m$$

where [A] and [B] are the concentrations of the substances A and B, respectively, at time $= t$; a_i and b_i are the *constant* coefficients of the two series.

* On leave of absence from the Institute of Isotopes of the Hungarian Academy of Sciences, Budapest

1.1 is differentiated, and the power series of [A] and [B] are added and multiplied by simple rules [8].

A characteristic property of the power series method is the "vanishing of all coefficients" theorem. It states [7], that if a power series has an interval of convergence and a sum which is identically zero throughout this interval, then each series coefficient is zero.

Using the theorem and the expressions of $d[A]/dt$, $d[B]/dt$, $[A] + [B]$ and $[A] \cdot [B]$, we obtain an extremely accurate and simple computational procedure which can be applied to most of the rate process problems.

Discussion

Our model for a sample calculation is the formation of oligomers, with the tetramer being the largest species.

The monomer, dimer, trimer and tetramer are denoted by A, B, C and D, respectively, and their concentrations as [A], [B], [C] and [D].

The mechanism consists of four reversible elementary steps:

2.1
$$2A \underset{k_{-1}}{\overset{k_1}{\rightleftharpoons}} B$$

$$A + B \underset{k_{-2}}{\overset{k_2}{\rightleftharpoons}} C \qquad \begin{aligned} A &= \text{monomer} \\ B &= \text{dimer} \\ C &= \text{trimer} \\ D &= \text{tetramer} \end{aligned}$$

$$A + C \underset{k_{-3}}{\overset{k_3}{\rightleftharpoons}} D$$

$$2B \underset{k_{-4}}{\overset{k_4}{\rightleftharpoons}} D$$
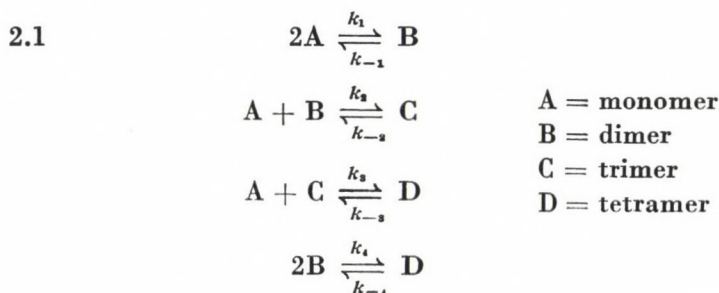
The mechanism defines the following system of differential equations:

2.2
$$d[A]/dt = -2\,k_1[A]^2 + 2\,k_{-1}[B] - k_2[A][B] +$$
$$+ k_{-2}[C] - k_3[A][C] + k_{-3}[D]$$
$$d[B]/dt = k_1[A]^2 - k_{-1}[B] - k_2[A][B] +$$
$$+ k_{-2}[C] - 2\,k_4[B]^2 + 2\,k_{-4}[D]$$
$$d[C]/dt = k_2[A][B] - k_{-2}[C] - k_3[A][C] + k_{-3}[D]$$
$$d[D]/dt = k_3[A][C] - k_{-3}[D] + k_4[B]^2 - k_{-4}[D]$$

The concentrations and their time derivatives are expressed in power series:

2.3
$$[A] = \sum_{m=0}^{\infty} a_m \cdot t^m; \qquad d[A]/dt = \sum_{m=0}^{\infty} (m+1) \cdot a_{m+1} \cdot t^m$$

There are similar equations for [B], [C] and [D].

The above power series are substituted into 2.2, keeping in mind the rule for the multiplication of two series [7, 8].

Now we make use of the "vanishing of all coefficients" theorem and obtain the following recursion formulas:

2.4
$$a_{m+1} = 1/(m+1) \cdot (-2\,k_1 L_m^{A,A} + 2k_{-1}b_m -$$
$$- k_2 L_m^{A,B} + k_{-2}c_m - k_3 L_m^{A,C} + k_{-3}d_m)$$
$$b_{m+1} = 1/(m+1) \cdot (k_1 L_m^{A,A} - k_{-1}\,b_m - k_2\,L_m^{A,B} +$$
$$+ k_{-2}c_m - 2\,k_4 L_m^{B,B} + 2k_{-4}d_m)$$
$$c_{m+1} = 1/(m+1) \cdot (k_2 L_m^{A,B} - k_{-2}\,c_m - k_3\,L_m^{A,C} + k_{-3}\,d_m)$$
$$d_{m+1} = 1/(m+1) \cdot (k_3 L_m^{A,C} - k_{-3}d_m + k_4\,L_m^{B,B} - k_{-4}\,d_m)$$
$$m = 0, 1, 2, 3, \ldots$$

The zero-indexed coefficients are known, since they are equal to the initial concentrations: $a_0 = [A]_0$, $b_0 = [B]_0$, $c_0 = [C]_0$ and $d_0 = [D]_0$. The zero-indexed multiplication terms, L_0, can be calculated: $L_0^{A,C} = a_0 \cdot c_0$, $L_0^{B,B} = b_0^2$, etc.

Using 2.4, first a_1, b_1, c_1 and d_1 are obtained. Now we have the eight series coefficients a_0, a_1, b_0, ..., d_1 necessary to calculate the L_1 multiplication terms: $L_1^{A,B} = a_0 \cdot b_1 + a_1 \cdot b_0$, etc., so a_2, b_2, c_2 and d_2 can be computed, etc.

We recommend that the method be used with the time scale divided into relatively small intervals, and the calculated concentrations of each step become the initial values of the next step. This way only the first few series coefficients have to be determined, since sufficiently short time step, in itself, secures convergence. Otherwise, too many series coefficients might have to be calculated, and the determination whether the necessary convergence criteria are fulfilled could be a very complicated task. Obviously, the series coefficients must be always recalculated since at each step the initial values are different.

Results

A Hewlett—Packard 85 Microcomputer connected to an HP-plotter was used for the calculations. The initial concentration of the monomer is $[A]_0 = 10.0$ mmol, that of the dimer is $[B]_0 = 4.0$ mmol; neither trimer nor tetramer is present at time $= 0$, $[C]_0 = [D]_0 = 0$.

The rate constants are the following:

$$k_1 = 2.5 \cdot 10^{-2} \text{ mmol}^{-1} \cdot \text{sec}^{-1}$$

$$k_{-1} = 2.0 \cdot 10^{-4} \text{ sec}^{-1}$$

$$k_2 = 1.5 \cdot 10^{-2} \text{ mmol}^{-1} \cdot \text{sec}^{-1}$$

$$k_{-2} = 8.0 \cdot 10^{-4} \text{ sec}^{-1}$$

$$k_3 = 1.0 \cdot 10^{-2} \text{ mmol}^{-1} \cdot \text{sec}^{-1}$$

$$k_{-3} = 1.0 \cdot 10^{-4} \text{ sec}^{-1}$$

$$k_4 = 1.5 \cdot 10^{-2} \text{ mmol}^{-1} \cdot \text{sec}^{-1}$$

$$k_{-4} = 1.0 \cdot 10^{-4} \text{ sec}^{-1}$$

The time step, Δt, is 0.05 sec. Figure 1 shows how the concentrations change in time from 0 to 47.5 sec. The calculations and the plotting, together took less than 40 minutes.

A modification, very beneficial to the computer time, could be that the time step, Δt, is gradually increased, since the greatest concentration changes occur always at the beginning, when very short time steps should be used. Later, as the system approaches equilibrium, Δt could be increased substantially without introducing any significant error. Computation of the same system, with Δt increasing from 0.05 to 0.5 sec, needed less than 8 minutes, a great reduction in time demand. In each case eight series coefficients have been calculated. The inherent error of the procedure is proportional to $1/(n+1)!$, that is by an increase of n, the computation can be made as accurate as necessary.
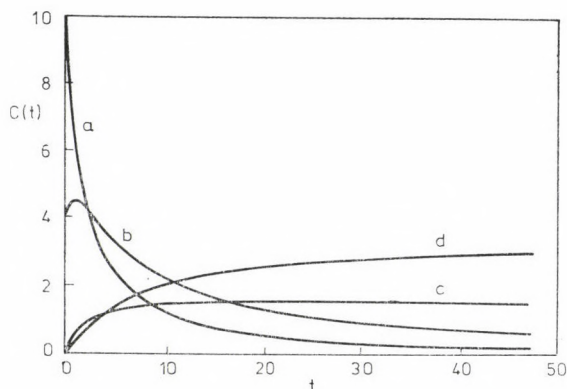
Fig. 1. Time evolution of the concentrations of the monomer (a), the dimer (b), the trimer (c) and the tetramer (d). The concentrations are given in mmol, the time in sec

The applicability of our method is not limited to equilibrating systems; it has been successfully used to solve complex problems, like chemical oscillations [8] and chaotic phenomena [9].

The well-known methods, e.g., the Runge—Kutta, and its modifications have been worked out for the $y' = f(x, y)$ type differential equations, thus their use for systems containing more than two variables could be extremely cumbersome. At the same time, our method [8] is practically insensitive to the number of variables [9].

REFERENCES

[1] Gardiner, W. C.: "Rates and Mechanisms of Chemical Reactions." Chaps. 1—3, 2nd print. W. A. Benjamin, Inc. 1972
[2] Gear, C. W.: Commun. ACM, **14,** 185 (1971)
[3] Edelson, D.: J. Comput. Chem., **1,** 29 (1976)
[4] Stabler, R. N., Chesick, J. P.: Int. J. Chem. Kinet., **10,** 461 (1978)
[5] Carver, M. B., Boyd, A. W.: Int. J. Chem. Kinet., **11,** 1097 (1979)
[6] Deuflhard, P., Bader, G., Nowak, U.: "Larkin . . ." in "Modelling of Chemical Reaction Systems" ed. K. H. Ebert, P. Deuflhard, W. Jager. Chap. 4. Springer-Verlag, Berlin 1981
[7] Kreyszig, E.: "Advanced Engineering Mathematics". Chaps. **4, 16,** 4th ed., Wiley 1978
[8] Szamosi, J., Kristyan, S.: J. Comput. Chem., **5,** 186 (1984)
[9] Szamosi, J., Schelly, Z. A.: in preparation. Correspondence about the applications to chaos should be addressed to Prof. J. Szamosi, Chemistry Department, Western Illinois University, Macomb, Illinois 61455

THE KINETICS OF HYDROQUINONE OXIDATION BY HORSERADISH PEROXIDASE AND HYDROGEN PEROXIDE

Abdulaziz A. Al-Suhybani* and Solaiman H. Al-Khowaiter

(Chemistry Department, College of Science, University of King Saud, P.O.Box 2455, Riyadh-11451, Saudi Arabia)

The kinetics of the horseradish peroxidase (HRP) catalysed reaction between hydroquinone (H_2Q) and hydrogen peroxide has been investigated. The reaction rate (v) was followed via the build up of the absorption of benzoquinone (Q). The reaction conditions were adjusted so that the reaction followed a pseudo first order kinetics. The primary plots of $1/v$ vs $1/[H_2O_2]$ or $1/[H_2Q]$ indicated the operation of a ping-pong mechanism. The secondary plots were used to evaluate the Michaelis constants; $K_m^{H_2O_2} = 5 \times 10^{-6}$ M and $K_m^{H_2Q} = 5 \times 10^{-5}$ M. The effect of pH on the rate revealed the occurrance of two different ionization processes, the first with $pK \simeq 3.7$ and the second with $pK \simeq 8.5$ and both were attributed to the enzyme. From the effect of temperature the activation energy for the catalysed reaction was found to be 26.25 kJ mole^{-1} in comparison with 99.8 kJ mole^{-1} for the uncatalysed reaction. The effect of ionic strength on the reaction rate was found to be small and it did not affect the final yield.

Introduction

Peroxidases are iron-containing enzymes which on the basis of both spectroscopic and magnetic susceptibility data, form definite chemical compounds with their substrate, hydrogen peroxide or organic peroxides. These enzyme substrate compounds cause the very rapid oxidation of oxidizable substances (acceptors), e.g. ascorbic acid [1]. The facility of oxidation and the formation of coloured products are the reason that the reaction of phenols with peroxidase has been known since 1900 [2].

A general scheme by which horseradish peroxidase catalyses the oxidation by H_2O_2 of a variety of organic compounds was suggested by Chance [3] and George [4, 5]:

$$\text{HRP} + \text{H}_2\text{O}_2 \underset{k_{-1}}{\overset{k_1}{\rightleftharpoons}} \text{HRP} - \text{I} \qquad (1)$$

$$\text{HRP} - \text{I} + \text{AH}_2 \underset{k_{-2}}{\overset{k_2}{\rightleftharpoons}} \text{HRP} - \text{II} + \text{AH} \qquad (2)$$

$$\text{HRP} - \text{II} + \text{AH}_2 \underset{k_{-3}}{\overset{k_3}{\rightleftharpoons}} \text{HRP} + \text{AH} \qquad (3)$$

* To whom correspondence should be addressed

$$AH + AH \underset{k_{-4}}{\overset{k_4}{\rightleftharpoons}} \text{Products} \tag{4}$$
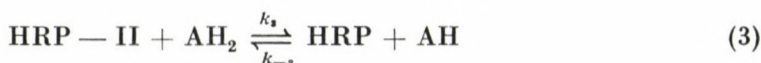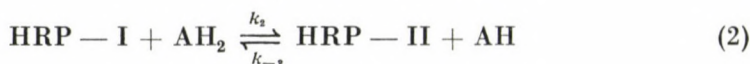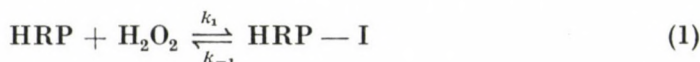
where, HRP-I and HRP-II are the oxidized forms of the enzyme, called compounds I and II, respectively, and AH_2 is the oxidizable substrate. k_2 is usually 40—100 times larger than k_3, both velocity constants being considerably less than k_1[6]. Since HRP has been proposed as an analytical tool [7], it was thought to be important to investigate the kinetics of the overall reaction of the oxidation of H_2Q by H_2O_2 in the presence of the enzyme. This system is hoped to be valuable in analytical studies because of the formation of Q which has a strong absorption and particularly in irradiated systems where the concentration of H_2O_2 or H_2Q is usually very low. It is also suggested to use H_2Q as convenient substrate to measure HRP activity.

Experimental

HRP was a Fluka product (EC 1.11.1.7) and was kept in a refrigerator at 4 °C. When needed, a certain amount was weighed and dissolved in bidistilled water and the solution kept refrigerated until use. These solutions were stable for several months. H_2O_2 was 30% and supplied by Merck and the appropriate concentration was obtained by dilution. The exact concentration was determined using the method of Hochanadel [8]. This method depends on the oxidation of iodide ion to iodine (present as tri-iodide ion) which gives a faint yellow solution ($\lambda_{max} = 350$ nm). H_2Q was a general reagent and was crystallized from hot acidic solution. Q was also a general reagent and was crystallized from hot ethanolic solution. Other chemicals were of Analar grade and were used without further purification.

The reaction rates were followed by following the absorption of Q at its maximum (246 nm), using a Beckman spectrophotometer mode 5270 equipped with repetitive scan system, which is capable of either sereal or overlay scans, and kinetic unit. The recorder has wide range of speeds, i. e. $0.1 - 10$ inch/min. and spans $(0.01 - 3)$. Since the reaction was very fast it was necessary to adjust the experimental conditions and the instrument parameters to suit the rate measurements.

In all experiments, the initial rates were reported and these were the average of at least two runs. 3 mL of sample containing all reactants except one (e.g. HRP) was introduced into a 10 mm cell which was then inserted into position. A small magnet was used to ensure continuous stirring during the reaction. The temperature was kept constant using a thermostat and it was monitored using a small thermocouple. When the temperature became constant, the recorder was allowed to operate at preselected speeds at fixed wavelength and the reaction was initiated by adding a small volume (μLs) of the appropriate concentration of HRP using a Beckman-Pipeter diluter model 273. The pH measurements were carried out using Metrohm pH meter model 632 with a glass electrode.

Results and Discussion

Figure 1 shows repetitive scanning traces for the disappearance of H_2Q absorption and the simultaneous formation of Q absorption. The experimental conditions are indicated in the figure. It was observed that the amount of Q produced is equal to the amount of H_2Q removed and these were calculated taking the extinction coefficient for Q as 2.17×10^4 M^{-1} cm^{-1} at $\lambda = 246$ nm and for H_2Q as 2.44×10^3 M^{-1} cm^{-1} at $\lambda = 288$ nm. The extinction coefficients

were determined experimentally. The agreement is within 3%. The possibility of having products other than Q is ruled out on the ground that the absorption spectrum of the reaction product is identical with an authentic Q as can be seen in Fig. 2. Moreover, the possibility of the product being due to o-quinone is also ruled out since its absorption maximum is at 380 nm [9, 10]. A typical time-optical density curve is shown in Fig. 3.
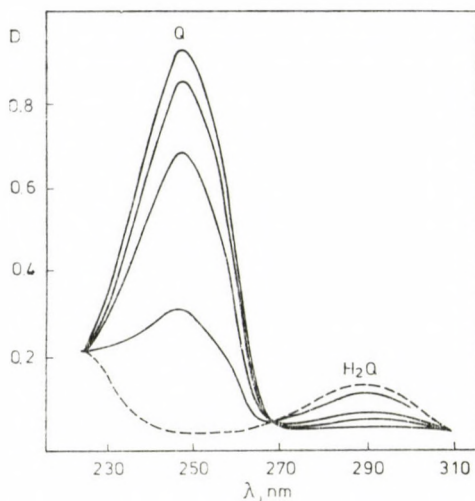
Fig. 1. Repetitive scanning traces for the disappearance of H_2Q absorption and the simultaneous formation of Q absorption. pH = 2.66 [H_2Q] = 5.65×10^{-5} M, [H_2O_2] = 4×10^{-5} M, [HRP] = = 1.4×10^{-8} M, Temp. = 18 °C. Time interval = 1 min; ----- Initial trace
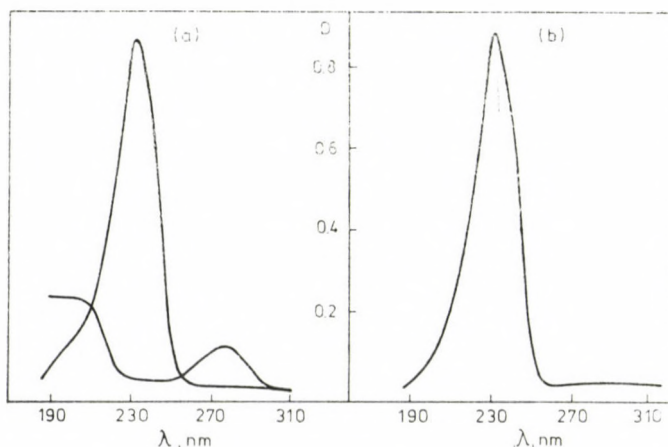
Fig. 2a. The absorption spectrum of Q produced from the catalytic HRP oxidation of H_2Q by H_2O_2, pH = 6.0, [H_2Q] = 4×10^{-5} M, [H_2O_2] = 8×10^{-5} M, [HRP] = 1.36×10^{-8}. Temp. = 18 °C. *Fig. 2b.* The absorption spectrum of an authentic Q; [Q] = 4×10^{-5} M

In all cases the concentration of H_2Q was at least 100 fold that of the enzyme and consequently, the reaction followed first order kinetics. This was shown by plotting $\log v$ versus time and obtaining a straight line at three different pH values.

The mechanism of HRP oxidation as proposed by Chance and later supported by George is as presented in reactions (1—4). The mechanism is of the ping-pong type as demonstrated by plotting the reciprocal of velocity as a function of the reciprocal of either $[H_2O_2]$ or $[H_2Q]$ holding the nonvaried substrate as constant and obtaining parallel lines as can be seen in Fig. 4. This suggests, therefore, that H_2Q behaves similarly as AH_2 in the Chance—George mechanism.
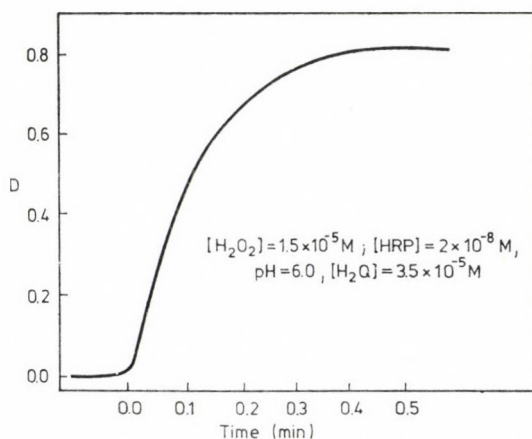
Fig. 3. A typical time-optical density curve for the formation of Q from H_2Q
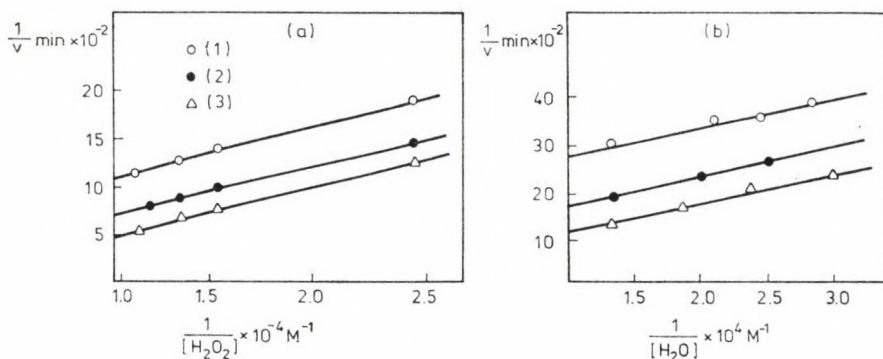
Fig. 4. Double reciprocal plots for HRP catalysed oxidation of H_2Q; pH 6.0; temp = 25 °C; a) Plots of $1/v$ versus $1/[H_2O_2]$ at several constant concentration of H_2Q. (1) = $[H_2Q] = 2 \times 10^{-5}\,M$, (2) = $[H_2Q] = 4 \times 10^{-5}\,M$, (3) = $[H_2O] = 10^{-4}\,M$) Plots of $1/v$ versus $1/H_2Q$ at several constant concentrations of H_2O_2. (1) = $[H_2O_2] = 1.84 \times 10^{-5}\,M$, (2) = $[H_2O_2] = 4.6 \times 10^{-5}\,M$, (3) = $[H_2O_2] = 9.2 \times 10^{-5}\,M$
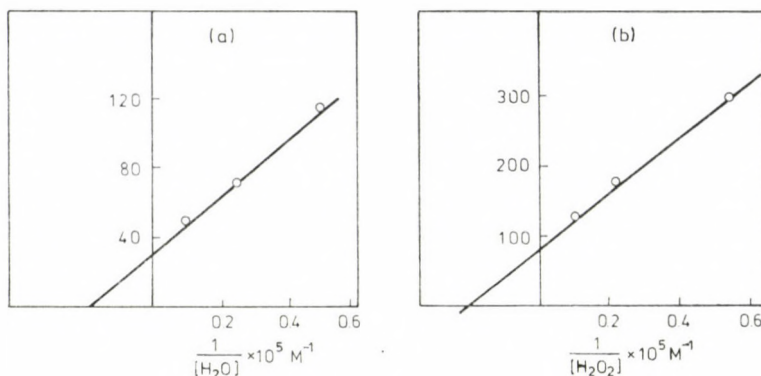
Fig. 5. Secondary plots for HRP-catalysed oxidation of H_2Q by H_2Q_2. (a) Plots of intercepts of Fig. 4(a) versus $1/[H_2Q]$; (b) Plots of intercepts of Fig. 4 (b) versus $1/[H_2O_2]$
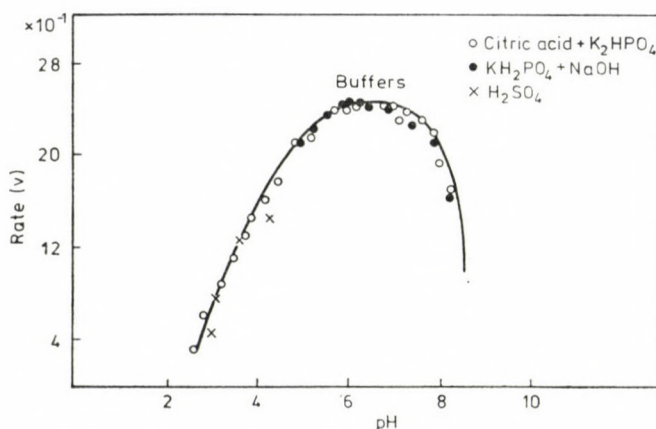
Fig. 6. Rate of HRP catalytic oxidation of H_2Q by H_2O as a function of pH. $[H_2O_2] = 1.5 \times 10^{-5} M$, $[H_2O] = 3.5 \times 10^{-5} M$. Temperature $= 22.5$ °C

For the ping-pong mechanism, the Lineweaver—Burk equation is of the form [11],

$$\frac{1}{v} = \frac{K_m^{H_2O_2}}{V[H_2O_2]} + \frac{K_m^{H_2Q}}{V[H_2Q]} + \frac{1}{V}$$

where v is the observed initial velocity, $K_m^{H_2O_2}$ the Michaelis constant for H_2O_2, $K_m^{H_2Q}$ is the Michaelis constant for H_2Q and V is the maximum velocity. Plots of $1/v$ versus $1/[H_2O_2]$ at different constant $[H_2O]$ yield parallel lines and the slopes of all lines will be the same and equal to $K_m^{H_2O_2}/V$. Similarly, the plots of $1/v$ versus $1/[H_2Q]$ at different constant $[H_2O_2]$ will yield parallel lines with slopes equal to $K_m^{H_2Q}/V$. These results are shown in Fig. 4.

7

Although, the primary plots of $1/v$ versus $1/[H_2O_2]$ or $1/[H_2Q]$ are useful in indicating the operation of a ping-pong mechanism, they can not be used directly to evaluate the kinetics and binding constants, since both slopes and intercepts are complex constants. Therefore, secondary plots of the data must be employed. For the plot shown in Fig. 4a the intercepts of the vertical axis are,

$$\text{Intercept} = \frac{1}{V} + \frac{K_m^{H_2Q}}{V[H_2Q]}$$

A plot of the intercept values versus $1/[H_2Q]$ yields straight line as shown in Fig. 5a, where the slope is $K_m^{H_2Q}/V$. On this plot horizontal intercept is $-1/K_m^{H_2Q}$. Similarly, plotting the intercepts of Fig. 4b against $1/[H_2O_2]$ gives a straight line as can be shown in Fig. 5b, where the horizontal intercept is $-1/K_m^{H_2O_2}$. From Fig. 5a and 5b, $K_m^{H_2Q} = 5 \times 10^{-5}\ M$ and $K_m^{H_2O_2} = 5 \times 10^{-6}\ M$, respectively. These values are considered to be reasonable for this system.

In order to study the possibility of the presence of ionizable hydrogen atoms at the active sites of the enzyme, the rate of H_2Q oxidation was measured as a function of pH and a bell-shaped curve is obtained as can be seen in Fig. 6. It is clear that the maximum catalytic activity is at pH $\sim$6. It was not possible to proceed at pH higher than $\sim$8.5, since the oxidation of H_2Q by air becomes appreciable. However it was obvious that the catalytic oxidation was much slower than the aerobic oxidation. Where it was possible to overlap buffers, similar behaviour was observed, indicating that there was no detectable effect due to buffers.

From the rate-pH profile for the reaction of H_2O_2 with H_2Q in the presence of HRP, it is clear that two different ionization processes are occurring with pK values of 3.7 and 8.5 and both are attributed to the enzyme. Protonation of the former group and ionization of the second causes a decrease in the rate of reaction. The assignment of these pK values to the enzyme is based on the fact that the pK_1 and pK_2 for H_2Q are 9.85 and 11.39 respectively [12] and pK for H_2O_2 is 11.6 [13]; it is clear that these pK values of substrates are out of the range of the pH studied. The pK value of 8.5 could be attributed to HRP-II and it agreed with the results obtained by Dunford et al. [14, 15], using ferrocyanide as a reducing agent. The pK value of 3.7 is close to the value of 4.15 reported by Dunford et al. [14] and attributed to the enzyme, though there are different values in the literature, ranging from less than 4 to more than 5 [14—17]. The pK for the reaction,

$$H\dot{Q} \rightleftharpoons \overset{=}{Q} + H^+ \tag{5}$$

is $\sim$4 [18] and therefore, this reaction may complicate the reaction mechanism, though one might argue that the contribution from reaction (5) is negligible

since reaction (4) is the most rapid reaction in the proposed mechanism and the rate constant for the bimolecular decay of $\bar{Q}$ is $1.7 \times 10^8\ M^{-1}\,s^{-1}$ [19] in comparison with $1.8 \times 10^7\ M^{-1}\,s^{-1}$ for reaction (1) [16] which is the fastest in the proposed mechanism.

The large values of the rates from pH $\sim$6 to $\sim$7 show that H_2Q is readily oxidized. At pH 6, where the rate is maximum, the rate was investigated as a function of temperature and the results are shown in Fig. 7. The activation energy, E_a, was calculated to be 26.25 kJoule/mol from the slope of the Arrhenius plot as can be seen in Fig. 8. For the uncatalysed reaction the corresponding activation energy was determined in a similar manner and
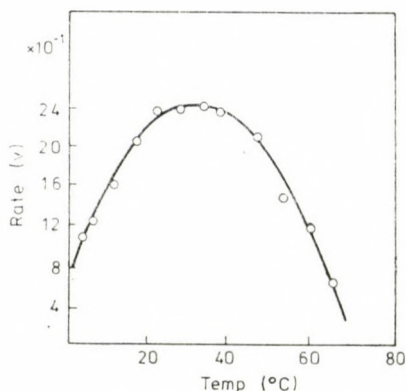
Fig. 7. The rate of HRP catalysed oxidation of H_2Q by H_2O_2 as a function of temperature. $[H_2O_2] = 1.26 \times 10^{-4}\ M$, $[H_2O] = 4.3 \times 10^{-5}\ M$, $[HRP] = 1.36 \times 10^{-8}\ M$. Buffer = Citric acid + K_2HPO_4
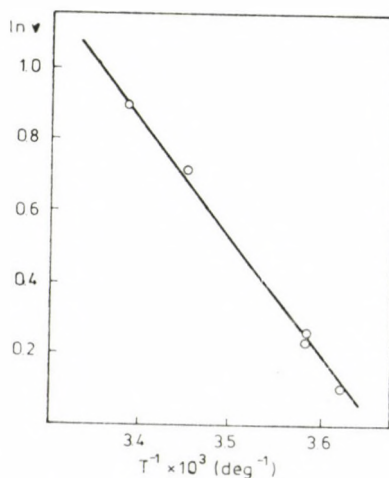
Fig. 8. Arrhenius plot of $\ln v$ vs T^{-1}; all conditions as in Fig. 7

Table I

$I, 10^2 M$	2.75	4.75	6.75	10.8	18.8	34.7	66.7
v, min^{-1}	2.30	2.30	2.27	2.15	1.95	1.90	1.64

was found to be 99.8 kJoule/mol. The activation energy for the catalysed reaction is not much above the activation energy for diffusion in aqueous solutions [20] which means a reaction rate between 10^7 and 10^8 M^{-1} s^{-1} [21], but it has also been pointed out that intermediate complex formation may cause a decrease in activation energy and therefore a low activation energy is necessary but not a sufficient condition for diffusion control [22, 23].

The effect of ionic strength (I) was investigated using KCl as the neutral salt. It was found that salt affected the reaction rate only slightly as can be seen in Table I.

It should be pointed out that yield of Q is not affected by an increase in [KCl].

Since the salt effect is useful in indicating a reaction between charged species, we may conclude that the rate-limiting step is not the reaction:

$$\overline{Q} + \overline{Q} \rightleftharpoons Q + H_2Q \tag{6}$$

This supports our conclusion, mentioned above, that this reaction is faster than any other reactions following the proposed mechanism.

As mentioned earlier, this system seems to be very useful as an analytical tool for the quantitative determination of either H_2O_2 or H_2Q. It is also very clear that H_2Q may be used as a convenient substrate to measure the activity of the enzyme. A further work on this system will be reported later.

*

REFERENCES

[1] Chance, B.: Science, **109**, 204 (1949)
[2] Saunder, B. C., Holmes-Siedle, A. G., Stark, B. P.: Peroxidase, pp. 25—27, Butterworths, London 1964
[3] Chance, B.: Arch. Biochem. Biophys. **41**, 416 (1952)
[4] George, P.: Nature, **169**, 612 (1952)
[5] George, P.: Biochem. J., **54**, 267 (1952)
[6] Marklund, S., Ohlsson, P., Opara, A., Paul, K.: Biochim. Biophys. Acta, **350**, 304 (1979)
[7] Danner, D. J., Brignac, P. J., Arceneaux, D., Patel, V.: Arch. Biochem. Biophys., **156**, 759 (1973)
[8] Hochanadel, C. J.: J. Phys. Chem., **56**, 587 (1952)
[9] Mason, H. S.: J. Biol. Chem., **181**, 803 (1949)
[10] Berger, St., Rieker, A.: in Chemistry of the Quinonoid Compounds (Patai, S., ed) part **1**, chapter **4**, Wiley, New York 1974

[11] Piszkiewkz, D.: in Kinetics of Chemical and Enzyme-Catalyzed Reactions, pp. 124—127, Oxford University Press, New York 1977
[12] Baxendale, J. H., Hardy, H. R.: Trans. Faraday Soc., **49,** 1140 (1953)
[13] Evans, M. G., Uri, N.: Trans. Faraday Soc., **45,** 224 (1949)
[14] Dunford, H. B., Hewson, W. D., Steiner, H.: Can. J. Chem., **56,** 2844 (1978)
[15] Cotton, M. L., Dunford, H. B.: Can. J. Chem., **51,** 582 (1973)
[16] Dolman, D., Newell, G. A., Thulow, M. D.: Can. J. Biochem., **53,** 495 (1975)
[17] Job, D., Ricard, J., Dunford, H. B.: Can. J. Biochem., **56,** 702 (1978)
[18] Patel, K. B., Willson, R. L.: J. Chem. Soc., Faraday Trans. I, **69,** 814 (1973)
[19] Adams, G. E., Michael, B. D.: Trans. Faraday Soc., **63,** 1171 (1967)
[20] Hewson, W. D., Dunford, H. B.: Can. J. Chem., **43,** 1928 (1975)
[21] Schmitz, K. S., Schurr, J. M.: J. Phys. Chem., **76,** 534 (1972)
[22] Dunford, H. B., Hewson, W. D.: Biochemistry, **16,** 2949 (1977)
[23] Jones, P., Dunford, H. B.: J. Theor. Biol., **69,** 457 (1977)

6th International Symposium on Surfactants in Solution

New Delhi, India, August 18-22, 1986
(Sponsored by the Indian Society for Surface Science and Technology)

General Chairman:

DR. K. L. MITTAL
6 David Court
Poughkeepsie, N. Y. 12603
Tele: Office (212) 3091570
        Home (914) 4622326

Program Committee:

DR. K. L. MITTAL, Chairman

DR. D. K. CHATTORAJ, Cochairman
Calcutta, India

DR. A. N. MAITRA, Secretary
Delhi, India

DR. B. LINDMAN, Sweden

DR. P. BOTHOREL, France

International Advisory Committee

DR. D. BALASUBRAMANIAN
India

DR. A. BEN-NAIM
Israel

DR. K. S. BIRDI
Denmark

DR. H. CHAIMOVICH
Brazil

DR. E. CHIFU
Romania

DR. I. DANIELSSON
Finland

DR. H. T. DAVIS
USA

DR. V. DEGIORGIO
Italy

DR. F. C. DE SCHRYVER
Belgium

DR. J. E. DESNOYERS
Canada

DR. R. DESPOTOVIC
Yugoslavia

DR. H. F. EICKE
Switzerland

DR. S. FRIBERG
USA

DR. TIREN GU
Peoples Republic of China

DR. H. HOFFMANN
W. Germany

DR. J. ISRAELACHVILI
Australia

DR. I. B. IVANOV
Bulgaria

DR. C. N. JOO
Korea

DR. J. P. KRATOHVIL
USA

DR. K. KUNITAKE
Japan

DR. J. LYKLEMA
Netherlands

DR. A. J. G. MAROTO
Argentina

DR. K. MEGURO
Japan

DR. B. MOUDGIL
USA

DR. P. MUKERJEE
USA

DR. R. NAGARAJAN
USA

DR. C. J. O'CONNOR
New Zealand

DR. D. O. SHAH
USA

DR. E. D. SHCHUKIN
USSR

DR. P. SOMASUNDARAN
USA

DR. P. STENIUS
Sweden

DR. G. TIDDY
UK

DR. D. VOLLHARDT
E. Germany

DR. D. T. WASAN
USA

DR. E. WOLFRAM
Hungary

Call for Papers

This Symposium is the continuation of the series of symposia dealing with the behavior of surfactants in solution. The first symposium was held in 1976 under the title "Micellization, Solubilization and Microemulsions" in Albany; the second was held under the title "Solution Chemistry of Surfactants" in Knoxville in 1978; the third was held in Potsdam in 1980 and was entitled "International Symposium on Solution Behavior of Surfactants: Theoretical and Applied Aspects." In 1982 it was deemed appropriate to assign a general title to these biennial events and after some deliberations it was decided that a very apropos title would be "Surfactants in Solution" as both the aggregation and adsorption behaviors of surfactants were considered. So the 4th symposium was held in 1982 in Lund, Sweden under this new title, and the most recent (5th) took place in July 1984 in Bordeaux, France. All of these symposia have been very well attended by researchers from many parts of the world, and these have become the premier forums to discuss the latest anent surfactants in solution.

It was in Bordeaux that it was decided to hold the sixth event in this series in New Delhi, as India has old tradition in surface and colloid science, and also it was considered important to hold one of these symposia in the Far East part of the globe. Moreover, the 1986 symposium marks the tenth anniversary (the genesis was in 1976) so it is planned to make this meeting a special event. A special feature of the 1986 symposium is that an International Advisory Committee comprising about 35 prominent researchers representing many parts of the globe has been set up.

As in the past, the program will contain both invited overviews and contributed original research papers. Researchers from practically every part of the globe where there is research activity in the arena of surfactants in solution will be invited to participate, as it is intended to celebrate the 10th anniversary with world-wide representation. In anticipation of an excellent response, we are planning to hold poster sessions in addition to regular oral presentations. Both theoretical and applied aspects of the behavior of surfactants in solution will be covered with emphasis on recent developments. As the theme of the symposium is "Surfactants in Solution" so both their adsorption and aggregation behavior will be accorded due coverage.

Among the topics to be covered are:

1. Surfactant Association: Recent Theoretical and Experimental Developments
2. Thermodynamics and Kinetics of Micellization
3. Surfactant Liquid Crystals: Phase Diagrams and Phase Structure
4. Solubilization
5. Micellar Catalysis
6. Microemulsions: Phase Diagrams, Structure, and Applications (including Reactions in Microemulsions)
7. Biological Amphiphile Systems
8. Adsorption of Surfactants
9. Applications of Surfactants (Tertiary Oil Recovery, Industrial Applications, Applications in Analytical Chemistry, etc.)
10. Biodegradation and Health Aspects of Surfactants.

Papers falling within any of these or allied categories are solicited. Please note that the proceedings will be published (as has been the practice in the past).

If you would like to contribute a paper or desire further information, please contact:

Dr. K. L. Mittal, General Chairman

6 David Court
Poughkeepsie, N. Y. 12603
Telephone: (914) 4622326

Text

The text of the paper should be concise. The description of new compounds (in the Experimental) must include the complete analytical data. Special attention must be paid to structural formulas given within the text. Complicated (non-linear) formulas should be drawn on separate sheets of paper and their position in the text should be clearly marked. The numbering of formulas and equations (in parentheses on the right-hand side) is only needed if they are referred to in the text. Units should conform to the International System of Units (SI). In nomenclature the rules of the I.U.P.A.C. are accepted as standard. Symbols for physical quantities are printed in italic type and should, therefore, be underlined in the manuscript.

References

References should be numbered in order of appearance in the text (where the reference number appears in brackets) and listed at the end of the paper. The reference list, too, should by typed double-spaced. Journal titles are to be abbreviated as defined by the Chemical Abstracts Service Source Index.

Examples:

[1] Brossi, A., Lindlar, H., Walter, M., Schneider, O.: Helv. Chim. Acta, **41**, 119 (1958)
[2] Parr, R. G.: Quantum Theory of Molecular Electronic Structure, Benjamin, New York 1964
[3] Warshel, A.: in Modern Theoretical Chemistry, Vol. 7, Part A (Ed. G. A. Segal), Plenum Press, New York 1977

Tables

Each table should be given a Roman number and a brief informative title. Structural formulas should not be used in column headings or in the body of tables.

Figures

Figures should be numbered consecutively with Arabic numerals. Their approximate place should be indicated in the text on the margin. All figures must be identified on the back by the author's name and the figure number in pencil. Standard symbols (such as circles, triangles, squares) are to be used on line-drawings to denote the points determined experimentally. Line-drawings must not contain structural formulas and comments. Spectra or relevant segments thereof, chromatograms, and X-ray diffraction patterns will be reproduced only if concise numerical summaries are inadequate to replace them. Drawings and graphs should be prepared in black ink on good-quality white or tracing paper. Photographs should be submitted on glossy paper as high-contrast copies. Xerox or similar copies are not suitable for reproduction, but may be used for duplicate copies.

Redrawn illustrations will be sent to the authors for checking. No corrections of figures will, therefore, be accepted in the proofs.

Submission of manuscript

After having completed the corrections suggested by the referees and editors, the final manuscript should be submitted in duplicate, in a form ready for publication. If the corrected manuscript is not returned to the editors *within six weeks*, the intended publication of the paper will be regarded as withdrawn by the authors.

Page charge will not be assessed for the publication, however, authors from overseas countries must contribute to the postage of correspondence by sending, together with the manuscript, international postal coupons to the value of U.S. $ 10.—

Proofs and reprints

A set of proofs will be sent to the submitting author. The proofs must be returned within 48 hours of receipt. Late return may cause a delay in the publication of the paper. 100 reprints will be supplied to the authors free of charge.

Periodicals of the Hungarian Academy of Sciences are obtainable at the following addresses:

Acta Chimica Hungarica

VOLUME 120, NUMBERS 2, OCTOBER 1985

NOTICE TO AUTHORS

Acta Chimica publishes original papers on all aspects of chemistry in English. Before preparing a manuscript for submission to this journal authors are advised to consult recent issues.

Form of manuscript

Manuscripts, tables and illustrations should be submitted in triplicate. Manuscripts should be typewritten double spaced (25 lines, 50 characters per line including spaces). The *title page* should include (1) the title of the paper, (2) the full names of the author(s) in the sequence to be published; apply an asterisk to designate the name of the author to whom correspondence should be addressed, (3) name and address of the institution where the work was done. If the paper is part of a series, reference to the previous communication must be given as a footnote.

Abstract

A summary is printed at the head of each paper. This should not exceed 200 **words** and should state briefly the principal results and major conclusions of the work. It should be suitable for use by abstracting services.

CONTENTS

1

SYNTHESIS OF ALKALOIDS USING REISSERT COMPOUNDS, V*

SYNTHESIS OF 1-(4'-HYDROXY-3'-METHOXYBENZYL)-7--HYDROXY-6-METHOXYISOQUINOLINE (CRISTADINE)

Lajos Kovács** and Péter Kerekes

(Department of Organic Chemistry, Kossuth Lajos University,
H-4010 Debrecen, P.O. Box 20)

Using the appropriate Reissert compound, the total synthesis of a new benzyl-isoquinoline alkaloid, cristadine (1) has been achieved, conclusively proving its structure.

A new 1-benzylisoquinoline alkaloid, cristadine, was isolated by Japanese researchers [2] from the plant *Erythrina crista-galli* Linn. (Leguminosae). The structure determination of cristadine was achieved by spectroscopic methods (UV, IR, NMR, MS) and by some simple chemical transformations. On the basis of these results cristadine proved to be 1-(4'-hydroxy-3'-methoxybenzyl)-7-hydroxy-6-methoxyisoquinoline (1).

Our goal was to prove the structure of cristadine by total synthesis, using the appropriate Reissert compound. Synthesis of the Reissert compound of 7-benzyloxy-6-methoxyisoquinoline (2) has been previously reported [3, 4]. The other component of the synthesis, the suitably substituted benzyl chloride (3) was prepared according to the known procedure [5].

The anion of the Reissert compound, generated by sodium hydride in dimethylformamide at −20 °C under nitrogen, was allowed to react with 4-benzyloxy-3-methoxybenzyl chloride (3) to yield the C-1 substituted Reissert compound (4). Hydrolysis of 4 with base gave dibenzylcristadine (5) in a high yield. The protecting groups were removed either by boiling with alcoholic hydrogen chloride or by catalytic hydrogenation over Pd/C in acetic acid to afford cristadine (1).

The product gave a satisfactory elemental analysis and the data of UV, IR, NMR and mass spectra for synthetic cristadine were in good agreement with those reported for the natural compound. Although the m.p. of our synthetic substance was found to be 80 °C higher than that reported for the natural alkaloid (*lit.* [2] m.p. 128—129 °C), a comparison with an authentic sample, kindly provided by Prof. M. Ju-ichi, showed both compounds to be identical by m.p. and by TLC comparison in different solvent systems.

---

* Part IV, see Ref. [1].
** To whom correspondence should be addressed.

1*

Acta Chim. Hung. 120, 1985
Akadémiai Kiadó, Budapest
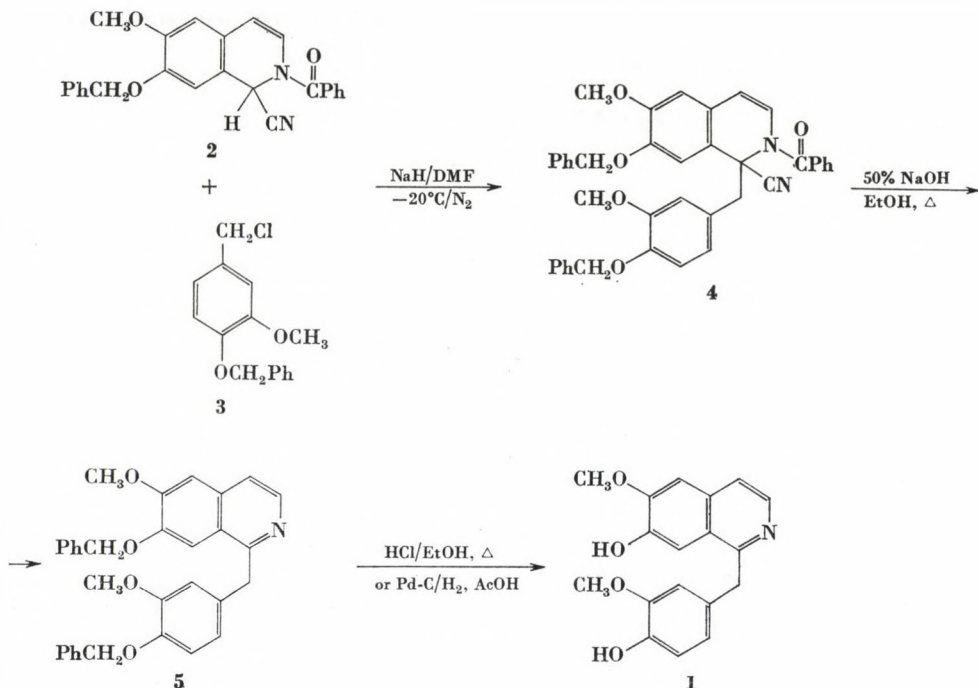
A small sample of synthetic **1**, after treatment with diazomethane, was found to be identical with authentic papaverine on TLC in three different solvent systems.

Experimental

M.p.'s are uncorrected. The IR spectrum was recorded on a Perkin-Elmer 283 B spectrometer. ^{1}H-NMR spectrum was obtained with a Bruker WP 200 SY 200 MHz instrument in DMSO-d_6 solution with TMS as internal standard. The EI mass spectrum was determined by using a VG-7035 (GC-MS-DS) spectrometer (70 eV).

TLC: Kieselgel 60 F 254, Merck. Solvent systems: chloroform : methanol = 9 : 1 (A); benzene : methanol = 8 : 2 (B); ethyl acetate : methanol: *conc.* aqueous NH$_4$OH = 95 : 5 : 5 (C); chloroform : acetone : trimethylamine = 5 : 4 : 1 (D).

C$_1$-Substituted Reissert compound (4)

1.98 g (5 mmol) Reissert compound (**1**) was dissolved in dry DMF (50 mL); the solution was added to a suspension of sodium hydride (0.3 g; 12.5 mmol) in DMF (20 mL) and stirred at −20 °C in N$_2$ atmosphere. After 5 min, 2.88 g (11 mol) of 4-benzyloxy-3-methoxybenzyl chloride, dissolved in 16 mL of DMF, was added dropwise to the reddish-brown solution. Stirring was continued at −20 °C for 1 h, and at room temperature for 12 h. The excess of NaH was decomposed with ethanol. The solvents were evaporated in vacuum. The solid residue was dissolved in benzene (200 mL), washed with water (3×50 mL), and the washings were re-extracted with benzene (50 mL). The combined organic extracts were dried (Na$_2$SO$_4$) and evaporated to yield a crude product, which was triturated with ethanol and filtered (3.83 g; 61.5%; m.p. 160−164 °C). An analytical sample was prepared by crystallization from ethanol; m.p. 172−174 °C.

C$_{40}$H$_{34}$N$_2$O$_5$. Calcd. C 77.15; H 5.50; N 4.50. Found C 77.04; H 5.51; N 4.53%.

Dibenzylcristadine (5)

3.11 g (5 mmol) of crude **4** was refluxed in a mixture of ethanol (250 mL) and water (25 mL) with NaOH (25 g) for 4 h. During this time a crystalline solid precipitated (2.12 g; 86.3%). The crude product was recrystallized from *n*-propanol (115 mL) to yield 1.93 g (78.6%) of **5**, m.p. 171—173 °C.

$C_{32}H_{29}NO_4$. Calcd. C 78.18; H 5.95; N 2.85. Found C 78.20; H 6.02; N 2.87%.

Cristadine (1)

Method A: A solution of 0.492 g (1 mmol) of **5** in 10 mL ethanol and 7.5 mL *conc.* HCl was refluxed for 3 h, then evaporated. The residue was dissolved in water (30 mL) and made alkaline with *conc.* NH_4OH (pH = 10). The precipitate was filtered off, dissolved in a 2 : 1 mixture of chloroform-ethanol (100 mL), washed with water (2×50 mL), dried (Na_2SO_4) and evaporated to give a solid residue (230 mg), which was recrystallized from ethanol (19 mL) to obtain 110 mg (35.3%) of **1**, m.p. 205—209 °C.

Method B: 0.492 g (1 mmol) of **5** was dissolved in acetic acid (10 mL) and hydrogenated in the presence of 0.1 g 10% Pd/C at atmospheric pressure for 3 h. The catalyst was filtered off, and the filtrate evaporated. The residue was dissolved in water (20 mL) and made alkaline (NH_4OH). The precipitate was collected and washed with water. Recrystallization from ethanol (9.5 mL) yielded 105 mg (33.7%) of **1**, m.p. 207—210 °C.

The products obtained by method *A* and *B* were combined and recrystallized from ethanol (13 mL) to give 130 mg of a pale yellow substance, m.p. 210—211 °C.

$C_{18}H_{17}NO_4$. Calcd. C 69.44; H 5.50; N 4.50. Found C 69.34; H 5.52; N 4.48%.

IR: 3400 cm^{-1} (OH).

^{1}H-NMR: the spectral data were completely identical with those of given in the literature [2].

EI MS; *m/e* (*I* %); 311 (M^+; 85); 310 (*M*-1; 100); 296 (*M*-15; 32).

Methylation of cristadine to papaverine

Compound **1** (5 mg) was treated with an ethereal diazomethane solution. The product obtained was identical with papaverine on the basis of TLC comparison in three different solvent systems.

*

REFERENCES

[1] Kerekes, P.: Acta Chim. Acad. Sci. Hung., **106**, 303 (1981)
[2] Ju-ichi, M., Fujitani, Y., Furukawa, H.: Heterocycles, **19**, 849 (1982)
[3] Kerekes, P., Makleit, S., Bognár, R.: Acta Chim. Acad. Sci. Hung., **98**, 491 (1978)
[4] Suess, T. R., Stermitz, F. R.: J. Nat. Prod., **44**, 688 (1981)
[5] Battersby, A. R., Binks, R., Francis, R. J., McCaldin, D. J., Ramuz, M.: J. Chem. Soc., **1964**, 3600

SYNTHESIS AND OXIDATION STUDIES OF SOME FLAVANONE N-SALICYLOYL HYDRAZONES WITH SELENIUM DIOXIDE

Abha Shivhare*, Arun V. Kale and Diwakar D. Berge

(Post Graduate College, Ambah, Morena M.P. 476111, India)

Some newly synthesized flavanone hydrazones have been oxidized with selenium dioxide in dioxane + water system. The structures of the hydrazones and oxidation products have been established by microelemental analyses, m.m.p., co-TLC and spectral data.

We have reported earlier the synthesis of flavanone N-dichlorosalicyloyl hydrazones [1]. In continuation of our previous work on the synthesis and oxidation studies of nitrogeneous flavonoids [2, 3], we report now the interesting reaction of 2'-hydroxychalcones (Ia—f) with salicylic acid hydrazide (II) in alcohol + acetic acid medium, resulting in the formation of flavanone hydrazones IIIa—f. The structures of these compounds have been established by IR spectra: 3260—3300 cm^{-1} (—NH Str.): 3320—3400 cm^{-1} (intra-molecularly hydrogen -bonded OH) and NMR (DMSO): 2.1—3.2 (Ar—H), 6.9—7.2 (CH$_2$— quartet) 4.75—4.95 (CH-quartet [4], due to spin-spin interaction with each other), 7.5—8.2 (—CH$_3$) and 6.0—6.5 τ (OCH$_3$). Microestimation of nitrogen is in accordance with the calculated values. These compounds gave no colour with ethanolic ferric chloride.

In view of the interesting results observed on oxidation of nitrogeneous flavonoids [5, 6]. compounds IIIa—f were also studied separately in oxidation with selenium dioxide (1 : 1.2 mol). After refluxing for four hours on a steam-bath and usual work-up, the reaction mixture afforded an acid (V) in 20—28% yield, and flavones (VIa—f) in 26—39% yield as the major products. These were identified as salicylic acid (m.p. 156 °C) and flavones (VIa—f) by m.p., m.m.p., co-TLC and by recording superimposable IR spectra with authentic samples. From the mother liquor, on chromatography over silica gel as the stationary phase, the flavanones IVa—f (known) and nitrogen-free compounds (VIIb—d, in three cases only) have also been isolated. The flavanones (IVa—f) were characterized by co-TLC and undepressed m.p. on admixture with known samples. The structures of the nitrogen-free products as

---

* To whom correspondence should be addressed.

3,3'-biflavanones are proposed on the basis of the R_f values [7] (half of the monomer) and superimposable IR spectra with the respective flavanones. Interlinking through the 3-position has also been reported [8] as a result of

(Ia-f)   (IIIa-f)

(a)   R=R'=R''=H
(b)   R=R''=H, R'=OCH₃
(c)   R=CH₃, R'=R''=H
(d)   R=CH₃ R'=OCH₃, R''=H
(e)   R=H, R'=R''=OCH₃
(f)   R=CH₃, R'=R''=OCH₃

(IVa-f)   (V)

(VIa-f)   (VIIa-f)
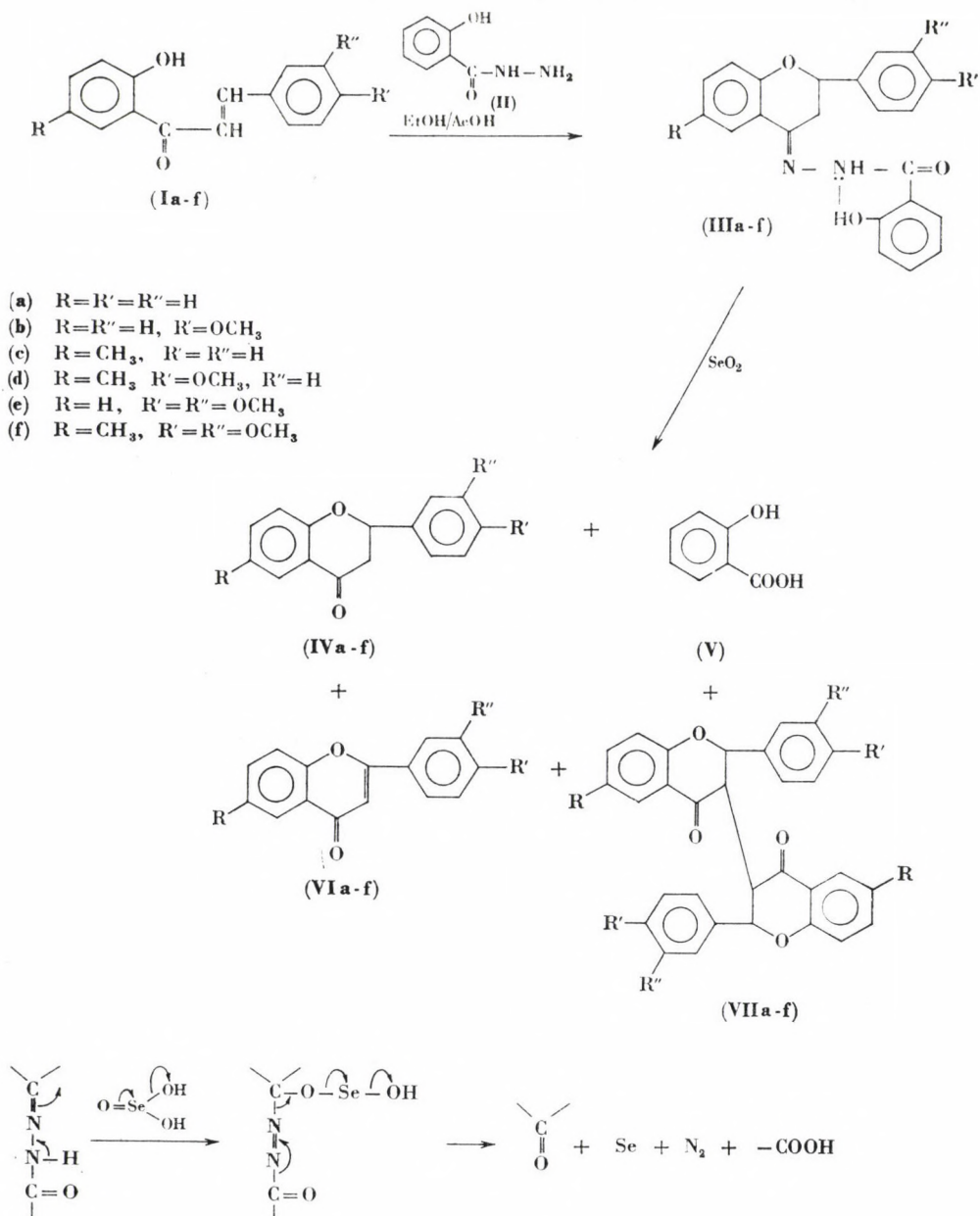
Scheme 1

Table I

Data of the hydrazones **IIIa—f** *and their oxidation products prepared*
with selenium dioxide

Hydrazones III	M.p., °C	Molecular formula	Yield, %	% N		Oxidation products	M.p., °C	Yield, %
				Found	required			
a	224	$C_{22}H_{18}O_3N_2$	55	7.20	7.821	IVa	76	15
						VIa	99	39
						VIIa	detected by TLC	traces
b	212	$C_{23}H_{20}O_4N_2$	51	6.90	7.216	IVb	91	13
						VIb	157	26
						VIIb	182—183	6.5
c	218	$C_{23}H_{20}O_3N_2$	66	7.40	7.526	IVc	105	9
						VIc	120	29
						VIIc	188	7.0
d	209	$C_{24}H_{22}O_4N_2$	64	6.400	6.965	IVd	110	11
						VId	170	30
						VIId	182	6.0
e	195	$C_{24}H_{22}O_5N_2$	59	6.60	6.690	IVe	125	19
						VIe	155	33
						VIIe	detected by TLC	traces
f	193	$C_{25}H_{24}O_5N_2$	57	6.51	6.48	IVf	108	26
						VIf	190	28
						VIIf	detected by TLC	traces

* Salicylic acid (**V**) was isolated in each case (20—28% yield) M.p.'s with authentic samples remained undepressed and are uncorrected.

oxidation with Fenton's reagent [9] and alkaline potassium ferricyanide [10] of the corresponding monomer. The IR spectra of the dimers show carbonyl absorption at 1688—1684 cm^{-1} (characteristic of flavanones).

Experimental

Compound VIIb

M.p. 182—83 °C. Mol. wt. (Rast) 498.2. $C_{32}H_{26}O_6$ (506). Calcd. C 75.88; H 5.138. Found C 71.62; H 5.02%.

Compound VIIc

M.p. 188 °C. Mol. wt. (Rast) 484. $C_{32}H_{26}O_4$ (474). Calcd. C 81.01; H 5.48. Found C 80.2; H 5.60%.

Compound VIId

M.p. 181—82 °C. Mol. wt. (Rast) 524. $C_{34}H_{30}O_6$ (534). Calcd. C 76.40; H 5.61. Found C 74.83; H 5.50%.

Results of the present investigation are recorded in Table I.

*

REFERENCES

[1] Kale, A. V., Shivhare, A., Berge, D. D.: Chem. and Ind., **1984,** 73
[2] Kale, A. V., Berge, D. D.: Indian J. Chem., Sect B, **19,** 409 (1980)
[3] Berge, D. D., Kale, A. V., Sharma, T. C.: Chem. and Ind., **1979,** 282
[4] Harborne, J. B., Mabry, T. J., Mabry, H.: The Flavonoids. Chapman and Hall, London 1975
[5] Barton, D. H. R., Lester, D. J., Ley, S. V.: J. Chem. Soc. Chem. Commun., **1977,** 445
[6] Barton, D. H. R., Lester, D. J., Ley, S. V.: J. Chem. Soc. Chem. Commun., **1978,** 276
[7] Brown, B. R., Sommerfield, G. A.: Tetrahedron Lett., **14,** 905 (1963)
[8] Berge, D. D., Bokadia, M. M.: Tetrahedron Lett., **10,** 1277 (1968)
[9] Mahesh, V. B., Seshadri, T. R.: J. Chem. Soc., **1955,** 2503
[10] Molyneus, R. J., Waiss, A. C., Haddon, W. F.: Tetrahedron, **26,** 1409 (1970)

SIMPLE AND CONDENSED β-LACTAMS, III*

SYNTHESIS OF THREE DIASTEREOMERIC
6-METHYLISOPENAM-3-CARBOXYLIC ACIDS

Ferenc Bertha[1], Károly Lempert[1]** and Mária Kajtár-Peredy[2]

(*[1]Department of Organic Chemistry, Technical University,
H-1521 Budapest, Gellért tér 4. and*

*[2]Central Research Institute for Chemistry of the Hungarian Academy
of Sciences, H-1525 Budapest, Pusztaszeri út 59—67)*

The two epimeric *trans*-6-methylisopenam-3-carboxylic acids **5a** and **6a** and the *cis*-6-methylisopenam-3-carboxylic acid **7a** have been obtained in form of their carboxyl-protected derivatives **5b**, **6b** and **7b** and their sodium salts **5c**, **6c** and **7c**, as outlined in Charts 1 and 2. In addition, the pivaloyloxymethyl ester **5d** and the cyclohexylamide **7e** were prepared. The relative configurations of C-3 of the products have been deduced from the ¹H-NMR spectra and on the basis of considerations concerning the relative thermodynamic stabilities of the 3-epimers.

Almost four decades after the introduction of the penicillins (**1**) and two decades after that of the cephalosporins (**2**) the isolation of thienamycin (**3**), the first member of a fundamentally new class of β-lactam antibiotics, viz. of the carbapenems (**4**) has been announced by Merck's scientists [2]. (For a recent review on carbapenems, see Ref. [3].) The most conspicuous features
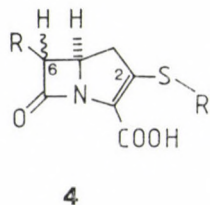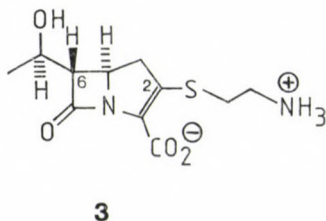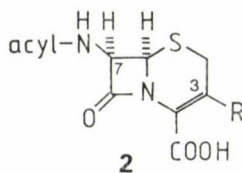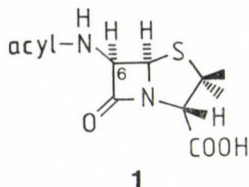
* For Part II. see Ref. [1].
** To whom correspondence should be addressed.

of thienamycin (and the other carbapenems) are (1) the absence of a ring
sulfur atom, (2) the presence of a side chain attached to position 2 of the ring
skeleton through sulfur, and (3) the replacement of the acylamino side chain
of the classical β-lactam antibiotics by a 1-hydroxyethyl side chain (in thiena-
mycin), and by alkyl, hydroxyalkyl or O-sulfated hydroxyalkyl side chains
(in other carbapenem antibiotics).

These unique structural features of thienamycin, together with its out-
standing microbiological properties [4], have stimulated active research not
only into the elaboration of laboratory and practical syntheses of thienamycin
and other natural and non-natural carbapenem antibiotics [3] but also into
the development of synthesis methods for their ring analogs which, in con-
trast to those of the classical β-lactam antibiotics, do not contain an acylamino
side chain.

Here we report on the synthesis of three diastereomeric 6-methyliso-
penam-3-carboxylic acids 5a, 6a and 7a* in the form of their carboxyl-pro-
tected derivatives 5b, 6b and 7b, and their sodium salts 5c, 6c and 7c. In
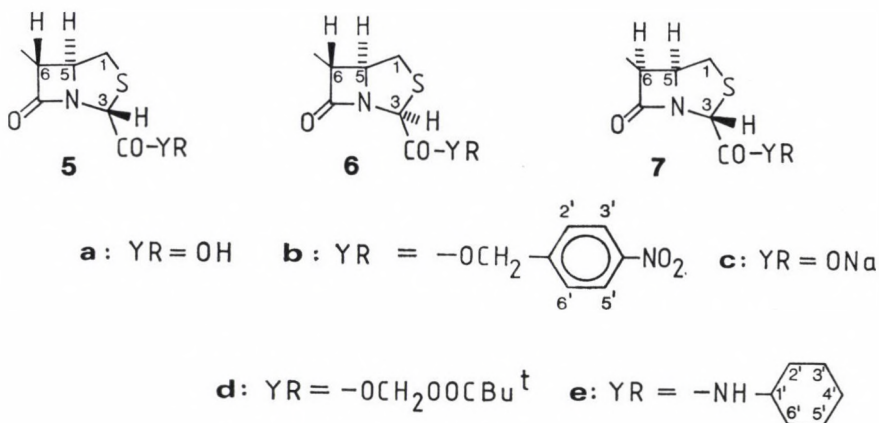
addition, the pivaloyloxymethyl ester 5d and the cyclohexylamide 7e were
prepared. The syntheses are outlined in Charts 1 and 2 and described in detail
in Experimental. It should be pointed out that the diastereomeric esters 12a
and 12b, obtained by partial deethoxycarbonylation of the diester 11, were
not separated but subjected together to sodium borohydride reduction in
methanol at 0 °C. The trans ester 12a was more rapidly reduced than the cis
isomer 12b, and the resulting trans hydroxymethyl derivative 13a was separated
by chromatography from the unchanged cis ester 12b and from a further
fraction consisting of a mixture of the trans (13a) and cis (13b) hydroxymethyl

* All compounds described in the present paper are racemic. For convenience only
one enantiomer is depicted throughout.
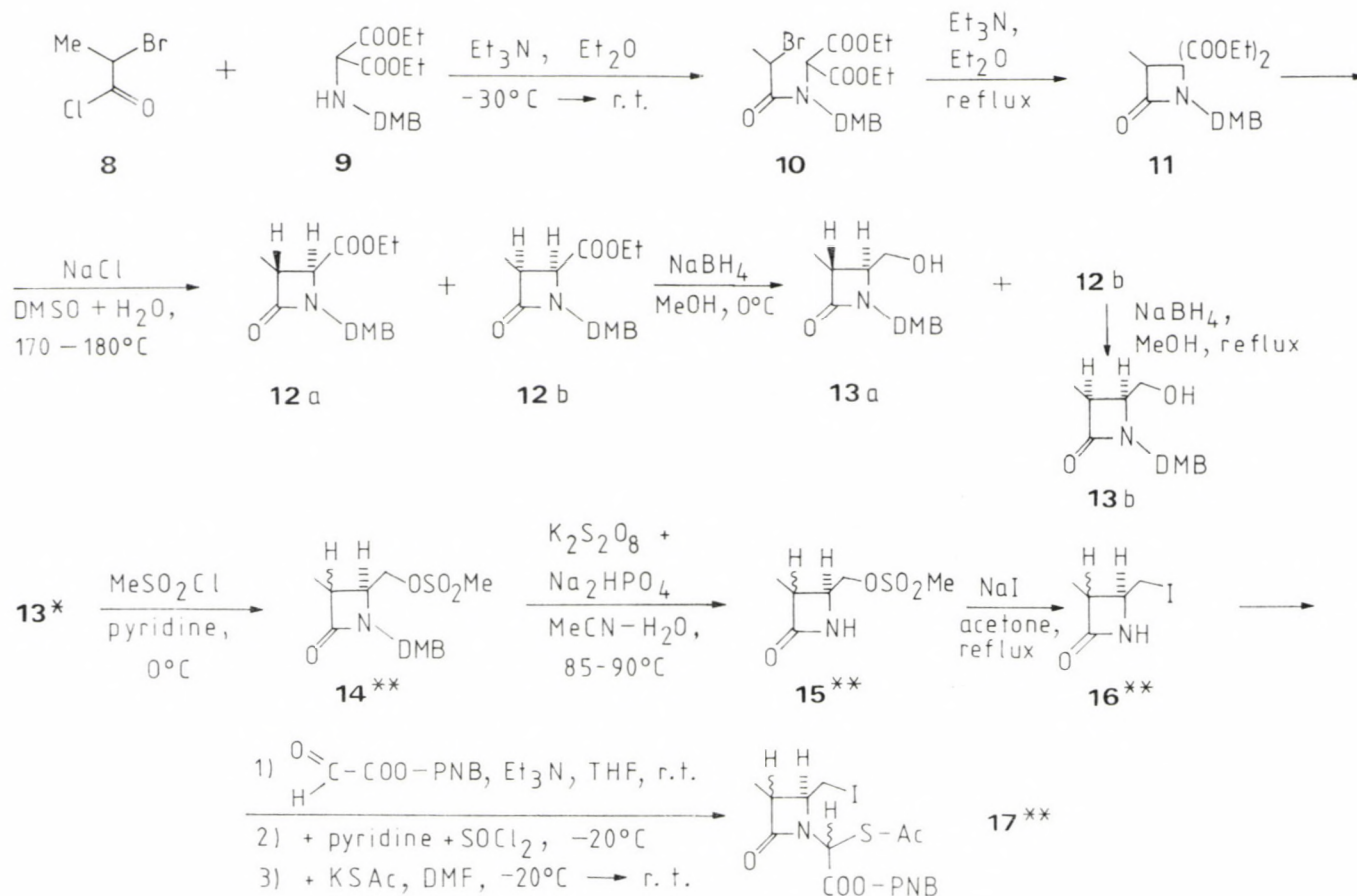
DMB = 2,4-dimethoxybenzyl, PNB = p-nitrobenzyl

* Starting with the pure *trans*- (13a) and *cis*-hydroxymethyl derivatives (13b) the following steps were carried out separately in both series.

** a: *trans*, b: *cis*.

Chart 1

1) $H_2N-\langle\text{cyclohexyl}\rangle$, CH_2Cl_2, r.t.

2) chromatography over silica

5b + **6b**

17a*

5d $\xleftarrow{\text{ClCH}_2\text{OOCBu}^t}{\text{DMF}}$ **5c**   **6c**

1) $H_2N-\langle\text{cyclohexyl}\rangle$, CH_2,Cl_2, r.t.

2) chromatography over silica

7b or **7e**

17b*

7c

PNB = p-nitrobenzyl
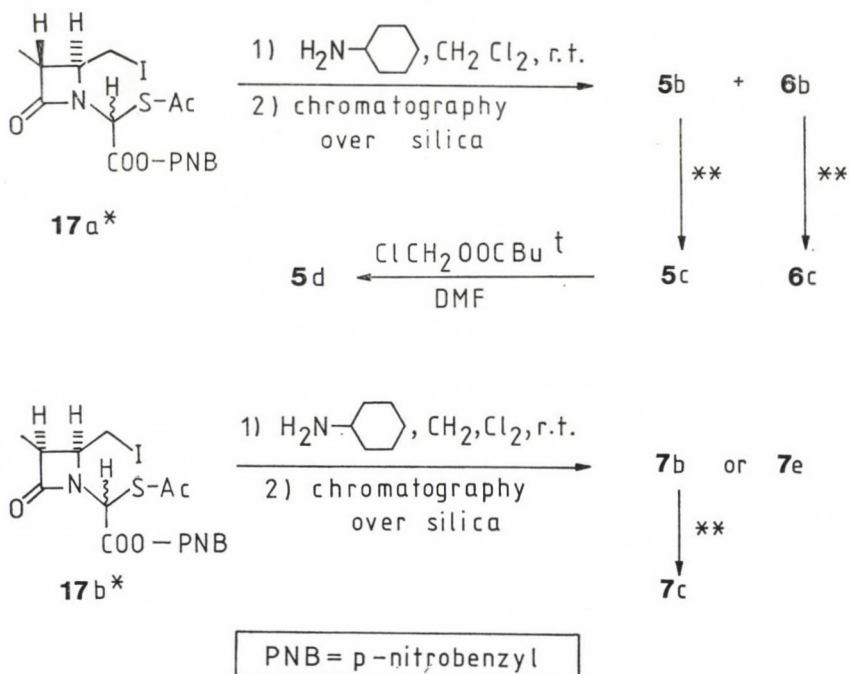
* Diastereomeric mixture.
** H_2Pd-C, dioxane + aq. $NaHCO_3$.

Chart 2

derivatives. The *cis* ester **12b** was reduced under more vigorous conditions to give the *cis* hydroxymethyl derivative **13b**.

Compound **18** was converted into a mixture of the 3-epimers of compound **20** by the same method [5], and a similar method was applied for the synthesis of the 3-epimers of compounds **21a** and **21b** [6]. In contrast to the

18: R=

19: R = H

20: R= , $R' = CH_2Ph$

21a: R = H, $R' = Bu^t$

21b: R = H, $R' = -CH_2-\langle\text{C}_6\text{H}_4\rangle-NO_2$
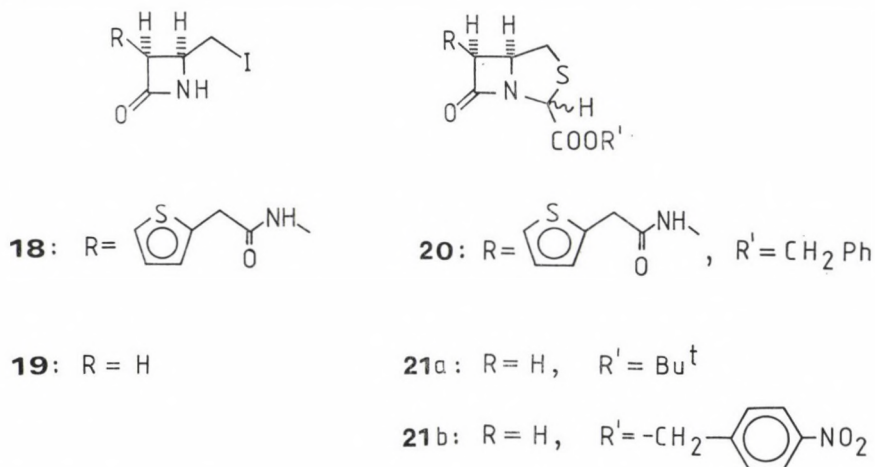
case of compound **20**, we obtained only one 3-epimer (**7b**) in the *cis* series although the precursor **17b** was clearly shown by its ¹H-NMR spectrum to be a mixture of epimers differing in the configurations of the α-carbon atoms of the *N*-substituents. Obviously epimerization has taken place in the course of the ring closure or during work-up and, as a consequence, the isolated bicyclic product is the thermodynamically more stable epimer, i.e. **7b**, having the "natural" relative configurations at C-3 and C-5 (see below).

The relative configurations of C-3 and C-5 in compounds **5—7** were deduced from their ¹H-NMR spectra because the hydrogen atom attached to the α-C atom in compounds of type **22** having the "natural" relative configurations at this atom and C-4 of the β-lactam moiety, i.e. in which the hydrogen atoms attached to these atoms are *trans* relative to each other, and which are the thermodynamically more stable epimers (see e.g. Ref's [6—8]) is known [6, 8—16] to absorb at lower fields than the corresponding hydrogen of the
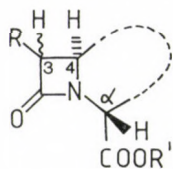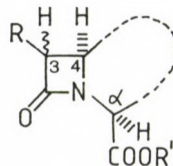
22   **23**

"non-natural" epimers **23**, regardless of whether C-3 of the β-lactam moiety is substituted or not, whether, if C-3 is substituted, 3-H and 4-H are *trans* or *cis* relative to each other, and regardless of the size and nature of the second ring. Therefore, structure **5b** is assigned to the *trans* *p*-nitrobenzyl ester whose hydrogen atom attached to C-3 absorbs at δ 5.58 ppm, and structure **6b** to its 3-epimer whose corresponding hydrogen atom absorbs at δ 4.78 ppm.

The results of the microbiological screenings were disappointing: none of the sodium salts **5b—7b** had any antibacterial or β-lactamase activities.

Experimental

Unless otherwise stated, the ¹H-NMR spectra were obtained at 100 MHz with a Varian XL-100 spectrometer in CDCl₃ solutions, using Me₄Si as the internal reference. The IR spectra were obtained with a Spektromom 2000 instrument (Hungarian Optical Works, Budapest).

Diethyl 1-(2,4-dimethoxybenzyl)-3-methyl-4-oxoazetidine-2.2-dicarboxylate (11)

2-Bromopropionyl chloride (**8**) (70 g; 0.41 mol) was added dropwise with continuous stirring to a mixture of diethyl (2,4-dimethoxybenzylamino)malonate (**9**) [17] (95 g; 0.29 mol), dry ether (350 mL) and triethylamine (34 g; 0.34 mol), the temperature of the reaction mixture

being maintained at -30 °C. Subsequently the mixture was allowed to warm up to ambient temperature, and the crystalline Et$_3$N · HCl was filtered off. The filtrate which contained compound **10** was treated with triethylamine (50 g; 0.50 mol) and refluxed for 6 h. The mixture was allowed to cool, the Et$_3$N·HBr was filtered off, and the filtrate was successively washed with water (150 mL), dil. HCl (water 130 mL + conc. HCl, 20 mL) and water (2×150 mL). The ethereal solution was dried (MgSO$_4$) and evaporated to dryness at reduced pressure. The oily residue was triturated with ether (50 mL) to obtain 66 g (60%) of the crystalline title compound, m.p. 65 °C (from ethyl acetate–light petroleum).

   C$_{19}$H$_{25}$NO$_7$ (379.41). Calcd. C 60.15; H 6.64; N 3.69. Found C 60.24; H 6.46; N 3.98%.

   IR (KBr): 1765—1740 br, 1200, 1035 cm^{-1}.

   ^{1}H-NMR: δ 1.08 t + 1.27 t + 3.91 q + 4.24 q ($J = 7.1$ Hz; $2\times$COOEt), 1.24 d ($J = 7.5$ Hz; 3-Me), 3.78 s ($2\times$OMe), 3.82 q ($J = 7.5$ Hz; 3-H), 4.45 + 4.68 (AB, $J = 15.2$ Hz; N—CH$_2$—Ar), 6.35—6.5 m (3'-H + 5'-H), 7.13 d ($J = 9$ Hz; 6'-H).

Ethyl 1-(2,4-dimethoxybenzyl)-3-methyl-4-oxoazetidine-2-carboxylate, mixture of *trans* and *cis* forms (12a + 12b)

 A mixture of the diester **11** (68.5 g; 0.18 mol), NaCl (12.7 g; 0.22 mol), DMSO (100 mL) and water (6.5 mL, 0.36 mol) was stirred for 30 h at 170—180 °C and, after being allowed to cool, poured into saturated aqueous NaCl solution (500 mL). The solution was extracted with ether ($150 + 4\times100$ mL) to obtain, after conventional work-up, 48.2 g (87%) of the title compound in form of a yellowish oil.

   C$_{16}$H$_{21}$NO$_5$ (307.35). Calcd. C 62.53; H 6.89; N 4.56. Found C 62.70; H 6.90; N 4.51%.

   IR (film): 1760—1740 br, 1205, 1040 cm^{-1}

1-(2,4-Dimethoxybenzyl)-4-hydroxymethyl-3-methyl-2-azetidinone, *trans* form (13a) and ethyl 1-(2.4-dimethoxybenzyl)-3-methyl-4-oxoazetidine-2-carboxylate, *cis* form (12b)

 NaBH$_4$ (35 g; 0.92 mol) was added to a methanolic (700 mL) solution of the above mixture of the *trans* and *cis* esters **12a** + **12b** (142 g; 0.46 mol) with external ice cooling and continuous stirring. The mixture was stirred for an additional 30 min, poured into saturated aqueous NaCl solution (4200 mL) and extracted with ethyl acetate (3×600 mL). The combined organic solutions were dried (MgSO$_4$) and evaporated to dryness at reduced pressure. The oily residue (133 g) was triturated with ether (150 mL) to obtain 51.7 g (42%) of compound **13a**, m.p. 78—79 °C (from 2-propanol–light petroleum).

   C$_{14}$H$_{19}$NO$_4$ (265.31). Calcd. C 63.38; H 7.22; N 5.28. Found C 63.63; H 7.16; N 5.39%.

   IR (KBr): 3300, 1710 cm^{-1}.

   ^{1}H-NMR δ 1.23d ($J = 7.5$ Hz; 3-Me), 2.02 br t (exchangeable, $J = 3$ Hz; CH$_2$OH), 3.00qd ($J = 7.5$ and 2.1 Hz; 3-H), 3.15 td ($J = 4.0$ and 2.1 Hz; 4-H), 3.63m (CH$_2$OH), 3.81s + 3.83s ($2\times$MeO), 4.30 + 4.42 (AB, $J = 14.6$ Hz; N—CH$_2$—Ar), 6.4—6.55 m (3'-H + 5'-H), 7.20d ($J = 9$ Hz; 6'-H).

 The dry residue of the mother liquor was worked up by chromatography (Kieselgel G; CH$_2$Cl$_2$–acetone, 8 : 2) to give the unchanged *cis* ester **12b** (55 g) as an oil, and a mixture of the *trans* and *cis* hydroxymethyl derivatives **13a** and **13b** (24 g) as a crystalline product.

   cis Ester (12b), ^{1}H-NMR: δ 1.17 d ($J = 7.5$ Hz; 3-Me), 1.28 t + 4.22q ($J = 7.1$ Hz; COOEt), 3.37 qd ($J = 7.5$ and 5.8 Hz; 3-H), 3.76s + 3.78s ($2\times$MeO), 3.97 d ($J = 5.8$ Hz; 2-H), 4.18 + 4.59 (AB, $J = 14.4$ Hz; N—CH$_2$—Ar), 6.35—6.5 m (3'—H + 5'—H), 7.12d ($J = 9$ Hz; 6'-H).

1-(2,4-Dimethoxybenzyl)-4-hydroxymethyl-3-methyl-2-azetidinone, *cis* form (13b)

 NaBH$_4$ (25 g; 0.67 mol) was added in small portions to a refluxing solution of the *cis* ester **12b** (46.6 g; 0.15 mol) in dry methanol (250 mL), with continuous stirring. The mixture was refluxed for another 20 min, cooled to room temperature and poured into saturated aqueous NaCl solution (1400 mL). Extraction with ethyl acetate (3×200 mL) and conventional work-up furnished an oil which crystallized when triturated with ether to give 29 g (72%) of the title compound, m.p. 111—112 °C (from 2-propanol–light petroleum).

   C$_{14}$H$_{19}$NO$_4$ (265.31). Calcd. C 63.38; H 7.22; N 5.28. Found C 63.55; H 7.09; N 5.38%.

   IR (KBr): 3370, 1710 cm^{-1}.

¹H-NMR: δ 1.22d (J = 7.5 Hz; 3-Me); 2.16 br s (CH₂OH), 3.22qd (J = 7.5 and 5.0 Hz; 3-H), 3.58 m (4-H), 3.68 m (CH₂OH), 3.80s + 3.82s (2×MeO), 4.28 + 4.43 (AB, J = 14.6 Hz; N—CH₂—Ar), 6.4—6.55m (3'-H + 5'-H), 7.20d (J = 9 Hz; 6'—H).

1-(2,4-Dimethoxybenzyl)-3-methyl-4-(methylsulfonyloxymethyl)-2-azetidinone, trans (14a) and cis forms (14b)

(a) Methanesulfonyl chloride (7.8 g; 68 mmol) was added dropwise to a mixture of the trans hydroxymethyl derivative 13a (15 g; 57 mmol) in dry pyridine (30 mL), with ice-cooling and continuous stirring. The mixture was stirred for further 2 h and poured into water (250 mL). Extraction with CH₂Cl₂ (3×50 mL) and conventional work-up gave an oil. This was taken up in heptane (30 mL) and evaporated to dryness; this operation was repeated once more. The oily residue was triturated with cold ether to give 17.5 g (90%) of the trans compound 14a, m.p. 116—117 °C (from 2-propanol).

C₁₅H₂₁NO₆S (343.39). Calcd. C 52.47, H 6.16, N 4.08. Found C 52.36, H 5.98, N 4.00%.
IR (KBr): 1735, 1350, 1160 cm⁻¹.

¹H-NMR: δ 1.25 d (J = 7.5 Hz; 3-Me), 2.94s (MeSO₂), 2.99qd (J = 7.5 and 2.2 Hz; 3-H), 3.24 td (J = 4.7 and 2.2 Hz; 4-H), 3.80 s + 3.82 s (2×MeO), 4.23 d (J = 4.7 Hz; —CH₂O—), 4.16 + 4.51 (AB, J = 14.5 Hz; N—CH₂—Ar), 6.4—6.55 m (3'-H + 5'-H), 7.18d (J = 9 Hz; 6'-H).

(b) The same method, when applied to the cis hydroxymethyl derivative 13b (28 g; 0.11 mol), furnished 35 g (97%) of the cis compound 14b, m.p. 97—98 °C (from 2-propanol).

C₁₅H₂₁NO₆S (343.39). Calcd. C 52.47; H 6.16; N 4.08. Found C 52.40, H 6.03, N 4.22%.
IR (KBr): 1720, 1350, 1170 cm⁻¹.

¹H-NMR: δ 1.24d (J = 7.5 Hz; 3-Me), 2.94s (MeSO₂) 3.30qd (J = 7.5 and 5.5 Hz; 3-H), 3.73ddd (J = 5.5, 5.8 and 6.0 Hz; 4-H), 3.81 s + 3.84 s (2×MeO), 4.25 + 4.31 (AB part of an ABX spectrum, J_gem = 10.5, J_vic = 5.8 and 6.0 Hz, respectively; —CH₂O—), 4.18 + 4.50 (AB, J = 14.6 Hz; N—CH₂—Ar), 6.4—6.55 m (3'-H + 5'-H), 7.17 d (J = 9 Hz, 6'-H).

3-Methyl-4-(methylsulfonyloxymethyl)-2-azetidinone, trans (15a) and cis forms (15b)

(a) A mixture of the trans 4-(methylsulfonyloxymethyl) derivative 14a (6.85 g; 20 mmol), K₂S₂O₈ (10.8 g; 40 mmol), K₂HPO₄ (13.9 g; 80 mmol), acetonitrile and water (80 mL, each) was vigorously stirred for about 6 h at 85—90 °C under nitrogen, and allowed to cool. The mixture was made slightly alkaline (pH 8) by adding crystalline NaHCO₃. The two phases were separated, and the aqueous phase was extracted with EtOAc (2×50 mL). The combined organic phases were evaporated to dryness under reduced pressure. The residue was taken up in CH₂Cl₂, treated with Norite, dried (MgSO₄) and evaporated to dryness to obtain 6.7 g of an oil which was worked up by chromatography (Kieselgel G; CH₂Cl₂–acetone, 10 : 2) to obtain 2.5 g (65%) of compound 15a, m.p. 84—86 °C (from EtOAc–light petroleum).

C₆H₁₁NO₄S (193.22). Calcd. C 37.30; H 5.74; N 7.25; S 16.59. Found C 37.58; H 5.52; N 7.17; S 16.53%.
IR (KBr): 3200, 1740, 1350, 1160 cm⁻¹.

¹H-NMR: δ 1.36d (J = 7.5 Hz; 3-Me), 3.02 qd (J = 7.5 and 2.3 Hz; 3-H), 3.07s (MeSO₂), 3.59 ddd (J = 2.3, 6.5 and 4.3 Hz; 4-H), 4.28 + 4.41 (AB part of an ABX spectrum, J_gem = 10.9, J_vic = 6.5 and 4.3 Hz, respectively; —CH₂O—), 6.4 br s (NH).

(b) The same method, when applied to the cis (methylsulfonyloxymethyl) derivative 14b (27 g; 79 mmol), furnished 11.4 g (75%) of compound 15b, m.p. 125.5—126.5 °C (from EtOH). [No chromatographic work-up was necessary in this case: the dry residue of the EtOAc solution crystallized when triturated with a small amount of CH₂Cl₂.]

C₆H₁₁NO₄S (193.22). Calcd. C 37.30; H 5.74; N 7.25; S 16.59. Found C 37.35; H 5.51; N 7.36; S 16.30%.
IR (KBr): 3210, 1730, 1355, 1165 cm⁻¹.

¹H-NMR- δ 1.24d (J = 7.5 Hz; 3-Me), 3.10s (MeSO₂), 3.41qdd (J = 7.5, 5.2 and 1.5 Hz; 3-H), 3.94ddd (J = 5.2, 6.5 and 6.0 Hz; 4-H), 4.33 + 4.38 (AB part of an ABX spectrum, J_gem = 10.5, J_vic = 6.5 and 6.0 Hz, respectively; —CH₂O—), 7.4 br s (NH).

4-Iodomethyl-3-methyl-2-azetidinone, trans (16a) and cis forms (16b)

(a) A mixture of the trans methylsulfonyloxymethyl derivative 15a (2.0 g; 10.4 mmol), NaI (6.2 g; 41 mmol) and dry acetone (15 mL) was refluxed for 5 h and evaporated to dryness at reduced pressure. The residue was dissolved in water (20 mL) and the desired product was

2

extracted with CH_2Cl_2 (3×15 mL). Conventional work-up furnished an oil which was crystallized from EtOAc–light petroleum to give 1.65 g (71%) of compound **16a**, m.p. 77–78 °C.

C_5H_8INO (225.03). Calcd. C 26.69; H 3.58; N 6.22. Found C 26.70; H 3.62; N 6.27%.

IR (KBr): 3350, 1730 cm^{-1}.

^{1}H-NMR: δ 1.36d ($J = 7.5$ Hz; 3-Me), 2.90qdd ($J = 7.5$, 2.0 and 0.8 Hz; 3-H), 3.33m (CH_2I), 3.54ddd ($J = 2.0$, 5.5 and 7.5 Hz; 4-H), 6.4 br s (NH).

(b) The same method, when applied to the *cis* (methylsulfonyloxymethyl) derivative **15b** (9.55 g; 49 mmol), gave 8.9 g (80%) of compound **16b**, m.p. 79 °C (from EtOAc–light petroleum).

C_5H_8INO (225.03). Calcd. C 26.69; H 3.58; I 56.39; N 6.22. Found C 26.57; H 3.50; I 56.71; N 6.24%.

^{1}H-NMR: δ 1.24d ($J = 7.5$ Hz; 3-Me), 3.25 m (CH_2I), 3.32qdd ($J = 7.5$, 5.2 and 1.8 Hz; 3-H), 4.07ddd ($J = 5.2$, 6.6 and 8.0 Hz; 4-H), 6.3 br s (NH).

1-(Acetylthio)-(p-nitrobenzyloxycarbonyl)methyl-4-iodomethyl-3-methyl-2-azetidinone, *trans* (17a) and *cis* (17b) forms

(a) A mixture of the *trans* iodomethyl derivative **16a** (1.0 g; 4.4 mmol), p-nitrobenzyl glyoxylate (1.0 g; 4.8 mmol), Et_3N (2–3 drops) and dry tetrahydrofurane (10 mL) was kept for 24 h at ambient temperature. The solution was chilled to -20 °C, and dry pyridine (0.39 mL; 4.8 mmol) and $SOCl_2$ (0.34 mL; 4.6 mmol) were successively added by drops at this temperature. The mixture was stirred at -20 °C for further 40 min. Subsequently a solution of potassium thioacetate (0.55 g; 4.8 mmol) in dry DMF (3 mL) was added at -20 °C by drops. The mixture was stirred for 1 h more at this temperature, allowed to warm up to room temperature and poured into water (20 mL). Extraction with EtOAc (3×10 mL) and conventional work-up furnished an oil which crystallized when triturated with ether to give 1.0 g (50%) of compound **17a** as a 1 : 1 mixture of epimers, m.p. 106–108 °C (from ether).

$C_{17}H_{16}IN_2O_6S$ (492.28). Calcd. C 39.04; H 3.48; N 5.69; S 6.51. Found C 39.07; H 3.68; N 5.73; S 7.02%.

IR (KBr): 1750, 1735, 1685, 1515, 1350, 845 cm^{-1}.

^{1}H-NMR: δ 1.31d + 1.32d ($J = 7.2$ Hz; 3-Me), 2.43s (S-Ac), 2.95qd + 2.98qd ($J = 7.2$ and 2.2 Hz; 3-H), 3.23dd (A part of an ABX spectrum, $J_{gem} = 9.8$, $J_{vic} \approx 9.6$ Hz; CH_AH_BI), 3.53dd + 3.57dd (B part of an ABX spectrum, $J_{gem} = 9.8$, $J_{vic} = 4.0$ and 3.3 Hz, respectively; CH_AH_BI), 3.50ddd + 3.75ddd ($\Sigma J = 2.2 + 3.3 + 10$ and $\Sigma J = 2.2 + 4.0 + 9.2$ Hz, respectively; 4-H), 5.30s + 5.32s ($O-CH_2-Ar$), 5.99s + 6.06s $\left(N-CH{<}{}^C_S \right)$, 7.53 + 8.25 (AA'BB', $J = 8.4$ Hz; $4 \times Ar-H$).

(b) The same method, when applied to the *cis* iodomethyl derivative **16b** (6.7 g; 30 mmol) gave, after chromatographic work-up (Kieselgel G; dry CH_2Cl_2) of the dry residue of the EtOAc extract, 9.1 g (61%) of compound **17b** as a 1 : 1 mixture of epimers in form of a yellow oil.

$C_{16}H_{17}IN_2O_6S$ (492.28). Calcd. C 39.04; H 3.48; N 5.69; S 6.51. Found C 39.12; H 3.40; N 5.65; S 7.00%.

IR (film): 1770–1750, 1710, 1525, 1355, 850 cm^{-1}.

^{1}H-NMR: δ 1.27d + 1.31d ($J = 7.5$ Hz; 3-Me), 2.42 s (S-Ac), 3.10 + 3.52 (AB part of an ABX spectrum, $J_{gem} \approx 10$, $J_{vic} \approx 10$ and ≈ 5 Hz, respectively; CH_2I), 3.35qd ($J = 7.5$ and 5.3 Hz; 3-H), 4.11 ddd + 4.36 ddd ($\Sigma J = 5.3 + \approx 10 + \approx 5$ Hz; 4-H), 5.29 s + 5.32 s ($O-CH_2-Ar$),' 6.04s + 6.11 s $\left(N-CH{<}{}^C_S \right)$, 7.53 + 8.24 AA'BB', $J = 8.6$ Hz; $4 \times Ar-H$).

p-Nitrobenzyl 6-methylisopenam-3-carboxylates, (3RS, 5SR, 6RS) (5b), (3RS, 5RS, 6SR) (6b) and (3RS, 5RS, 6RS) (7b) forms*

(a) Compound **17a** (epimeric mixture; 3.6 g; 7.3 mmol) was stirred with cyclohexylamine (1.45 g; 14.6 mmol) in dry CH_2Cl_2 (36 mL) for 4 h at 0 °C. The crystalline precipitate was filtered off and the filtrate was chromatographed (Kieselgel G; CH_2Cl_2) to obtain 1.27 g (54%) of compound **5b**, m.p. 120 °C (from EtOAc–light petroleum), and 0.83 g (35%) of compound **6b**, m.p. 120 °C (from EtOAc–light petroleum), in the order of decreasing R_f values.

* Systematic names: p-nitrobenzyl 6-methyl-7-oxo-3-thia-1-azabicyclo[3.2.0]heptane-2-carboxylates (2RS, 5SR, 6RS) (5b), (2RS, 5RS, 6SR) (6b) and (2RS, 5SR, 6SR) (7b) forms.

Compound 5b. $C_{14}H_{14}N_2O_5S$ (322.34). Calcd. C 52.17; H 4.38; N 8.69; S 9.95. Found, C 52.10; H 4.42; N 8.80; S 9.82%.

IR (KBr): 1750, 1520, 1350, 850 cm^{-1}.

^{1}H-NMR: δ 1.43d ($J = 7.4$ Hz; 6-Me), 3.00 qd ($J = 7.4$ and 2.4 Hz; 6-H), 3.11 + 3.43 (AB part of an ABX spectrum, $J_{gem} = 11.6$, $J_{vic} = 4.0$ and 7.0 Hz, respectively; 1-H$_2$), 4.15 ddd ($J = 4.0$, 7.0 and 2.4 Hz; 5-H), 5.26s (O—CH$_2$—Ar), 5.60 s (3-H), 7.52 + 8.23 (AA'BB', $J = 8.6$ Hz, 4×Ar—H).

Compound 6b. $C_{14}H_{14}N_2O_5S$ (322.34). Calcd. C 52.17; H 4.38; N 8.69; S 9.95. Found C 52.28; H 4.47; N 8.60; S 9.80%.

IR (KBr): 1760, 1740, 1520, 1355, 850 cm^{-1}.

^{1}H-NMR: δ 1.38d ($J = 7.4$ Hz; 6-Me), 2.95 qd ($J = 7.4$ and 2.0 Hz; 6-H), 3.01 + 3.14 (AB part of an ABX spectrum, $J_{gem} = 11$, $J_{vic} = 9.4$ and 5.4 Hz, respectively; 1-H$_2$), 3.87 ddd ($J = 9.4$, 5.4 and 2.0 Hz; 5-H), 4.79s (3-H), 5.32s (O—CH$_2$—Ar), 7.56 + 8.23 (AA'BB', $J = 8.6$ Hz; 4×Ar—H).

(*b*) The same method, when applied to the epimeric mixture **17b** (7.4 g; 15 mmol) gave 3.5 g (72%) of compound **7b**, m.p. 117 °C (from EtOAc–light petroleum), without of even traces of the 3-epimer being isolated.

$C_{14}H_{14}N_2O_5S$ (322.34). Calcd. C 52.17; H 4.38; N 8.69; S 9.95. Found C 52.20; H 4.30; N 8.87; S 9.97%.

IR (KBr): 1770, 1750, 1525, 1360, 1220, 1025, 865 cm^{-1}.

^{1}H-NMR: δ 1.18d ($J = 7.6$ Hz; 6-Me), 3.10 + 3.31 (AB part of an ABX spectrum, $J_{gem} = 12$, $J_{vic} = 3.8$ and 7.2 Hz, respectively; 1-H$_2$), 3.63 qd ($J = 7.6$ and 5.8 Hz; 6-H), 4.54ddd ($J = 3.8$, 7.2 and 5.8 Hz; 5-H), 5.28s (O—CH$_2$—Ar), 5.57s (3-H), 7.53 + 8.24 (AA'BB', $J = 8.6$ Hz; 4×Ar—H).

N-Cyclohexyl-(3*RS*, 5*SR*, 6*SR*)-6-methylisopenam-3-carboxamide (7e)

Compound **17b** (epimeric mixture; 0.99 g; 2 mmol) was stirred with cyclohexylamine (0.79 g; 8 mmol) in dry CH$_2$Cl$_2$ (10 mL) for 24 h at ambient temperature. The mixture was washed with water, dried (MgSO$_4$) and evaporated to dryness. The residue was chromatographed (Kieselgel G, CH$_2$Cl$_2$) to obtain 0.21 g (70%) of *p*-nitrobenzyl alcohol, identical with an authentic sample, and 0.35 g (65%) of the title compound, m.p. 201—202 °C (from 2-propanol).

$C_{13}H_{19}N_2O_2S$ (267.37). Calcd. C 58.40; H 7.16; N 10.48; S 11.99. Found C 58.35; H 7.20; N 10.51; S 12.07%.

IR (KBr): 3250, 1755, 1635, 1555 cm^{-1}.

^{1}H-NMR: δ 1.18d ($J = 7.6$ Hz; 6-Me), 0.9—2.1 m (cyclohexyl methylenes), 3.04 + 3.22 (AB part of an ABX spectrum, $J_{gem} = 11.8$, $J_{vic} = 5.0$ and 7.0 Hz, respectively; 1-H$_2$), 3.60 qd ($J = 7.6$ and 5.8 Hz; 6-H), 3.7 m (cyclohexyl methine), 4.43ddd ($J = 5.0$, 7.0 and 5.8 Hz; 5-H), 5.40s (3-H), 6.1 br (NH).

Sodium 6-methylisopenam-3-carboxylates, (3*RS*, 5*SR*, 6*RS*) (5c), (3*RS*, 5*RS*, 6*SR*) (6c) and (3*RS*, 5*SR*, 6*SR*) (7c) forms

(*a*) Compound **5b** (322 mg; 1 mmol) was reduced in the presence of NaHCO$_3$ (84 mg; 1 mmol) and a Pd/C catalyst in a mixture of dioxane (6 mL) and water (4 mL) at room temperature and normal pressure. The catalyst was filtered off and washed with a small amount of water. The filtrate and washings were combined, the dioxane was distilled off under reduced pressure. The residual aqueous solution was extracted with CH$_2$Cl$_2$ (3×5 mL) and evaporated to dryness. The residue was taken up in a small amount of ethanol, and the solution was allowed to stand for a few days to give 130 mg (63%) of compound **5c**.

IR (KBr): 1740, 1620, 1590 cm^{-1}.

^{1}H-NMR (D$_2$O): δ 1.44 d ($J = 7.4$; Hz; 6-Me), 3.09qd ($J = 7.4$ and 1.6 Hz; 6-H), 3.12 + 3.44 (AB part of an ABX spectrum, $J_{gem} = 11.4$, $J_{vic} = 6.5$ and 6.4 Hz, respectively; 1-H$_2$), 4.17 ddd ($J = 6.5$, 6.4 and 1.6 Hz; 5-H), 5.42 s (3-H).

The spectrum did not change after the solution had been kept for 1 month at 5 °C showing that compound **5c** is stable under these conditions.

(*b*) The same method (except that the product crystallized from a small amount of a methanol–ether mixture), when applied to compound **6b** (322 mg; 1 mmol), yielded 140 mg (68%) of compound **6c**.

^{1}H-NMR (D$_2$O): δ 1.35d ($J = 7.5$ Hz; 6-Me), 3.10qd ($J = 7.5$ and 1.6 Hz; 6-H), 3.08 + 3.26 (AB part of an ABX spectrum, $J_{gem} = 11$ Hz, $J_{vic} = 8.8$ and 5.5 Hz, respectively; 1-H$_2$), 3.96 ddd ($J = 8.8$, 5.5 and 1.6 Hz; 5-H), 4.70 s (3-H).

2*

The spectrum did not change when the solution was kept for 1 month at 5 °C.

(c) The same method (except that the product crystallized from a small amount of methanol), when applied to compound **7b** (3.22 g; 10 mmol), gave 1.5 g (71%) of compound **7c**.

IR (KBr): 1755, 1620 cm^{-1}.

^{1}H-NMR (D$_2$O): δ 1.20 d (J = 7.6 Hz; 6-Me), 3.17 + 3.30 (AB part of an ABX spectrum, J_{gem} = 11.7, J_{vic} = 5.8 and 6.7 Hz, respectively; 1-H$_2$), 3.70qd (J = 7.6 and 5.4 Hz; 6-H), 4.56ddd (J = 5.8, 6.7 and 5.4 Hz; 5-H), 5.40s (3-H).

The spectrum did not change after storing the solution for 1 month at 5 °C.

Pivaloyloxymethyl (3RS, 5SR, 6RS)-6-methylisopenam-3-carboxylate (5d)

A mixture of the sodium salt **5c** (120 mg; 0.6 mmol), chloromethyl pivalate [18] (120 mg; 0.8 mmol) and anhydrous DMF (6 mL) was stirred for 20 h at ambient temperature and then poured into ethyl acetate (40 mL). The mixture was extracted successively with water (2 × 10 mL) and saturated aqueous NaCl solution (2 × 10 mL), dried (MgSO$_4$) and evaporated to dryness under reduced pressure. The resulting yellowish oil was purified by chromatography (Kieselgel G; light petroleum) to obtain 100 mg (58%) of the title compound as an oil.

C$_{13}$H$_{19}$NO$_5$S (301.36). Calcd. C 51.81; H 6.35; N 4.65; S 10.64. Found C 52.03; H 6.30; N 4.55; S 10.78%.

IR (film) 1780, 1755 cm^{-1}.

^{1}H-NMR: δ 1.23s (t-Bu), 1.43d (J = 7.5 Hz; 6-Me), 3.00qd (J = 7.5 and 2.6 Hz; 6-H), 3.11 + 3.44 (AB part of an ABX spectrum, J_{gem} = 11.5, J_{vic} = 3.7 and 7.1 Hz, respectively; 1-H$_2$), 4.15ddd (J = 3.7, 7.1 and 2.6 Hz; 5-H), 5.53s (3-H), 5.78s (O−CH$_2$−O).

*

REFERENCES

[1] Simig, Gy., Fetter, J., Hornyák, Gy., Zauer, K., Doleschall, G., Lempert, K., Nyitrai, J., Gombos, Zs., Gizur, T., Barta-Szalai, G., Kajtár-Peredy, M.: Acta Chim. Hung. **119**, 17 (1985)

[2] Kahan, J. S., Kahan, F. M., Goegelman, R., Currie, S. A., Jackson, M., Stapley, E. O., Miller, T. W., Miller, A. K., Hendlin, D., Mochales, S., Hernandez, S., Woodruff, H. B.: 16th Intersci. Conf. Antimicrob. Agents Chemother., Chicago, Ill., 1976, Paper No. 227 (Abstr.); Albers-Schönberg, G., Arison, B. H., Kaczka, E. A., Kahan, F. M., Kahan, J. S., Lago, B., Maiese, W. M., Rhodes, R. E., Smith, J. L.: ibid., Paper No. 229 (Abstr.)

[3] Ratcliffe, R. W., Albers-Schönberg, G., in Chemistry and Biology of β-Lactam Antibiotics (Ed. R. B. Morin and M. Gorman), Vol. 2, pp. 227−313. Academic Press, New York etc., 1982

[4] Imipenem (N-Formimidoyl-thienamycin), Merck, Sharp & Dohme Research Laboratories 1983; Salzman, Th. N., Ratcliffe, R. W., Christensen, B. G., Bouffard, F. A., in Natural Products as Medicinal Agents (Ed. J. L. Beal and E. Reinhard) pp. 13−27. Hippokrates Verlag 1981

[5] Huffman, W. F., Hall, R. F., Grant, J. A., Holden, K. G.: J. Med. Chem., **21**, 413 (1978)

[6] Pant, Ch. M., Stoodley, R. J.: J. Chem. Soc., Chem. Commun., **1980**, 928

[7] Ratcliffe, R. W., Salzman, T. N., Christensen, B. G.: Tetrahedron Lett., **21**, 31 (1980)

[8] Nagakura, I.: Heterocycles, **16**, 1495 (1081)

[9] Kamiya, T., Teraji, T., Hashimoto, M., Nakaguchi, O., Oku, T.: J. Am. Chem. Soc., **98**, 2342 (1976)

[10] Osborne, N. F.: J. Chem. Soc., Perkin Trans. 1, **1980**, 150

[11] Smale, T. C.: J. Chem. Soc., Perkin Trans. 1, **1980**, 187

[12] Schmitt, S. M., Johnston, D. B. R., Christensen, B. G.: J. Org. Chem., **45**, 1135 (1980)

[13] Aratani, M., Hagiwara, D., Takeno, H., Hemmi, K., Hashimoto, M.: J. Org. Chem., **45**, 3682 (1980)

[14] Osborne, N. F.: J. Chem. Soc. Perkin Trans. 1, **1982**, 1435

[15] Branch, C. L., Pearson, M. J.: J. Chem. Soc., Perkin Trans. 1, **1982**, 2123

[16] Heck, J. V., Szymonifka, M. J., Christensen, B. G.: Tetrahedron Lett., **23**, 1519 (1982)

[17] Simig, Gy., Doleschall, G., Hornyák, Gy., Lempert, K., Nyitrai, J., Kajtár-Peredy, M., Huszthy, P., Gizur, T.: Tetrahedron, **1985**, in the press

[18] Rasmussen, M., Leonard, N. J.: J. Am. Chem. Soc., **89**, 5439 (1967)

THE ROLE OF THE QUALITY OF CARBON AUXILIARY SUBSTANCES IN THE EMISSION SPECTROSCOPY OF NON CONDUCTING POWDER SAMPLES, I

Zoltán László Szabó[1]* and Enikő Tatár[2]

(*[1]Institute of Inorganic and Analytical Chemistry, L. Eötvös University,
H-1443 Budapest, P.O.B. 123,
[2]Utilizing Enterprise for Raw Materials, H-1475 Budapest, P.O.B. 97*)

The effect of the quality of auxiliary electrodes of graphitic and amorphous carbon basis, and of the quality of graphitic and amorphous carbon powders used as auxiliary substances, on the average temperature of the electrode, on spectral line intensities, on the intensity ratios of spectral line/background, and on the standard deviation of these values was studied, using $CuO + C$ powder mixtures as model substances. Values are decisively determined by the quality of the carrier electrode.

Introduction

The role of the quality of the carbon carrier electrode in the emission spectroscopic methods of analysis of powder samples has been studied already earlier [1, 2]. It was established that amorphous carbon substance of poorer heat conductivity is more advantageous in the investigation of low-volatile samples than graphite. In an earlier work [3], in the investigation of metals, we too, studied counter-electrodes of two kinds, graphitic and amorphous carbon basis, and the electrode surface reactions of carbon electrodes, which proceed between the substance of the electrode and the surrounding active gas atmosphere. These reactions depend on the graphitic or amorphous type of the carbon substances, because their structure and thermal conductivity determine the glowing up of the electrodes, and through this also the reactions with the given gas atmosphere. The role of the material nature of the carbon carrier electrode was observed also in thermochemical reactions, that is in so-called reactions in the substance of the electrode, in indifferent (Ar) atmosphere [4—7], when electrode surface reactions with the original gas atmosphere are absent. Thus, we investigated now in detail the role of the quality of carbon auxiliary substances used most often in chemical emission

* To whom correspondence should be addressed.

spectral analysis, of different kinds of carbon auxiliary electrodes, and of carbon powder additives used in powder mixtures, in the development of spectral line intensities. Here too, flowing Ar gas atmosphere was used, so that reactions with the original gas atmosphere had not to be taken into consideration.

Experiments were carried out with four kinds of carbon electrode materials. These were RW O and RW II, recommended by the German firm Ringsdorff Werke, and SU and SW, manufactured by the Czechoslovakian factory Topolčany. Thus, two graphitic and two amorphous carbon electrode materials were used in our work. Of the carbon powder types generally used in powder mixtures our auxiliary substances SU-601 of Czechoslovakian manufacture and the German carbon powder type RW A were of graphitic character, while the Czechoslovakian SU-602 and a product marked with SW_p (experimental product) were amorphous carbon powders of high electric resistance, manufactured from coke. The characteristics of these products can be found in detail in the catalogues of the manufacturing firms [8, 9]. Our model substance was CuO, as this substance gives because of its high instability, that is because of its high reactivity, reactions easy to investigate. At the same time, the solid residue of these carbon oxide producing reactions is solid metallic copper, the evaporation characteristics of which are different from that of the original sample.

Copper oxide was mixed with the four kinds of carbon powders, and each sample was investigated separately. The carbon powder mixtures were placed into the borings of the given four kinds of carrier electrodes, and thus, results could be compared in 16 variations. Results obtained were doubled by investigating the electrode carrying the sample both in anodic and cathodic connection. Relationships were sought between the nature of the carbon materials, their physical and chemical behaviour, the intensities of the spectral lines produced in the arc and the intensity ratios. The intensity of the selected atomic line of copper was measured, which can be taken on the basis of earlier experiences in first approximation as proportional to the evaporation of the sample. Data on the spectral character ($\Delta Y_{Cu\ II,I}$), formed from the intensity ratio of the ionic and atomic lines selected in the spectrum of copper, which are in connection with the average temperature of the plasma, were also calculated. The amounts of CO_2 and CO, formed in the arc, were measured with our titrimetric gas analytical methods, and their volume ratios were calculated (described in detail in our next paper). These data characterize the oxidation and temperature conditions in the arc. The mass of substance lost from the boring of the electrode by arc excitation and the change in average temperature of the carrier electrode were also measured. Only the first 10 seconds of the burning of the arc were investigated, as according to earlier experiences most of the chemical reactions proceed already during this period,

so that conditions and reaction products determining the intensities of the spectral lines are already present.

Our aim was to find optimal conditions for the methods of analyses. Therefore standard deviation of parallel measurements was also calculated in various cases.

In our present paper relationships between the average temperature of the carrier electrodes, the intensity of the spectra and the carbon auxiliary substances are investigated.

Experimental

CuO + C powder mixtures of 0.3 molar fraction of metal oxide were prepared from the carbon powders of different kind, because we found earlier [3,5] that the greatest changes in thermochemical reactions and spectral line intensities occur at this ratio. The mixtures weighed into the boring of the electrodes (boring diameter 2.7 mm, depth of boring 4 mm, wall thickness of the carrier part with boring 0.75 mm) were investigated with a.c. polarized arc of 10 A average current initiated at maximum voltage, in essence with pulsing direct current. (The instantaneous current strength of this is about twice the above value.) The exciter was a Szakács arc generator, controlled also in the arc circuit [11]. Spectra were taken with an ISZP-22 spectrograph, directly illuminating the slit for 10 s from a distance of 30 cm, on plates of type Agfa-Gevaert 34 B 50. The plates were developed at 20 °C for 5 minutes in Agfa-1 developer. The blackening values of the 282.4 nm atom line of copper were calculated after photometry P_x-transformation and background correction in Y, respectively, in $I = $ num log Y values.

For better evaluation, data characteristic of the average temperature of the electrodes were measured for 15 s with iron-constantan thermocouple, the measuring head of which was sunk laterally to a depth of 2 mm into the auxiliary electrode of 6 mm ∅, 1 mm below the sample, and temperature values were read every 2 s of arc duration. Each of our backening results is generally the mean value of 10 parallel measurements, for which standard deviation is also given. Generally 3—6 parallel temperature measurements were undertaken. For identical moments of arc duration these agreed within 5—25 °C.

Results and discussion

The electrode temperature

Our measuring results were grouped in two ways.

a) On CuO model substance mixed with identical types of carbon powder the effects of different carbon carrier electrodes were compared.

b) It was attempted in carbon carrier electrodes of identical type to clear the role of the quality of various carbon powders.

In both cases the polarity of the carrier electrode containing the sample was also changed.

a) The following two figures show the electrode temperature values measured with the homogenized mixture of copper(II) oxide and four kinds of carbon powder, filled into four kinds of carbon carrier electrodes, as a function of arc duration at anodic (a) and cathodic (b) excitation, with carbon powders of graphitic (Fig. 1) and amorphous (Fig. 2) types. It can be seen that after a flatter initial section curves rise steeply, to attain then a saturate

character. Evidently, the cause of the flatter initial section is that the site of temperature measurement is relatively far, at a distance of about 5 mm from the heat transfer site, i.e. the burning spot of the plasma, and thus, the value used for the characterization of the average electrode temperature is established with delay at the measuring site. The saturation character of the curves arises from the fact that the heat supply rate of the arc is practically constant at the given current, but heat losses in the system increase with increasing electrode temperatures, because of increasing temperature gradients.
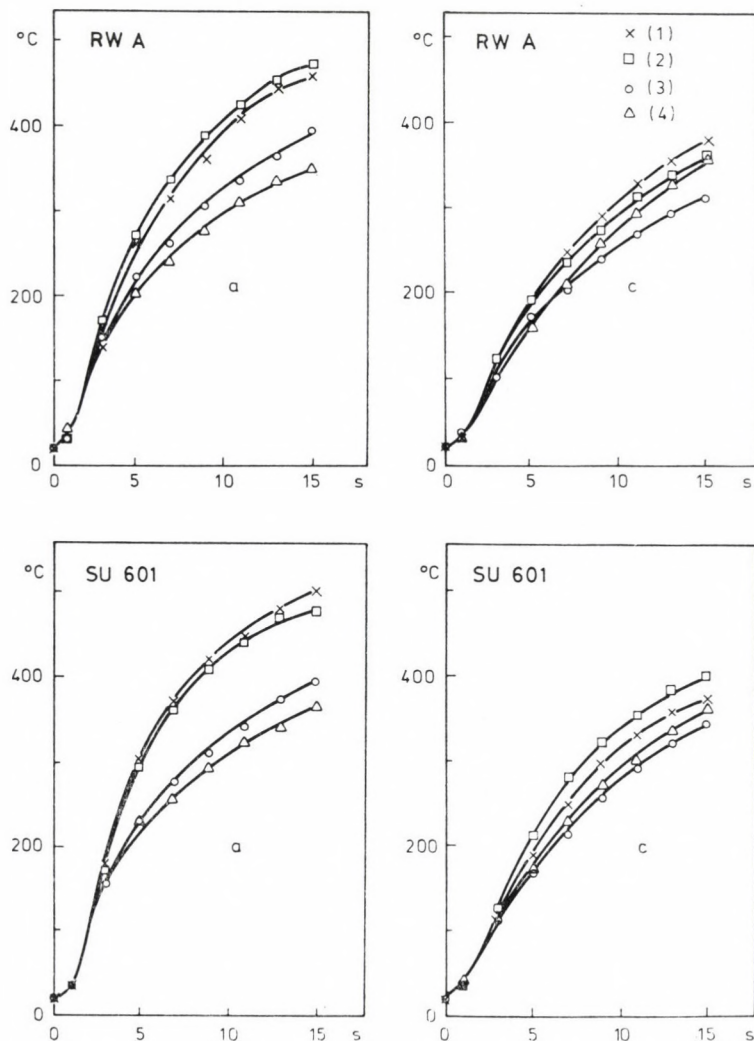
Fig. 1. Electrode temperature in the case of filling prepared with graphitic carbon powder for different kinds of auxiliary electrodes; (1): RW II; (2): SW; (3): SU; (4): RW O

It should be noted that in the case of identical kinds of carbon the temperature of the carrier carbon electrode is always highes after a burning time of 2—3 s at anodic excitation, than at cathodic one. It is an experience often met that though according to certain data in the literature [12] and our own experimental results [13, 14] the temperature of the burning spot of the arc is higher at the cathode, the temperature of the whole mass of the electrode is more increased in anodic connection [15]. (This phenomenon was partly used by Slavin [16], who similarly used anodic d.c. excitation as
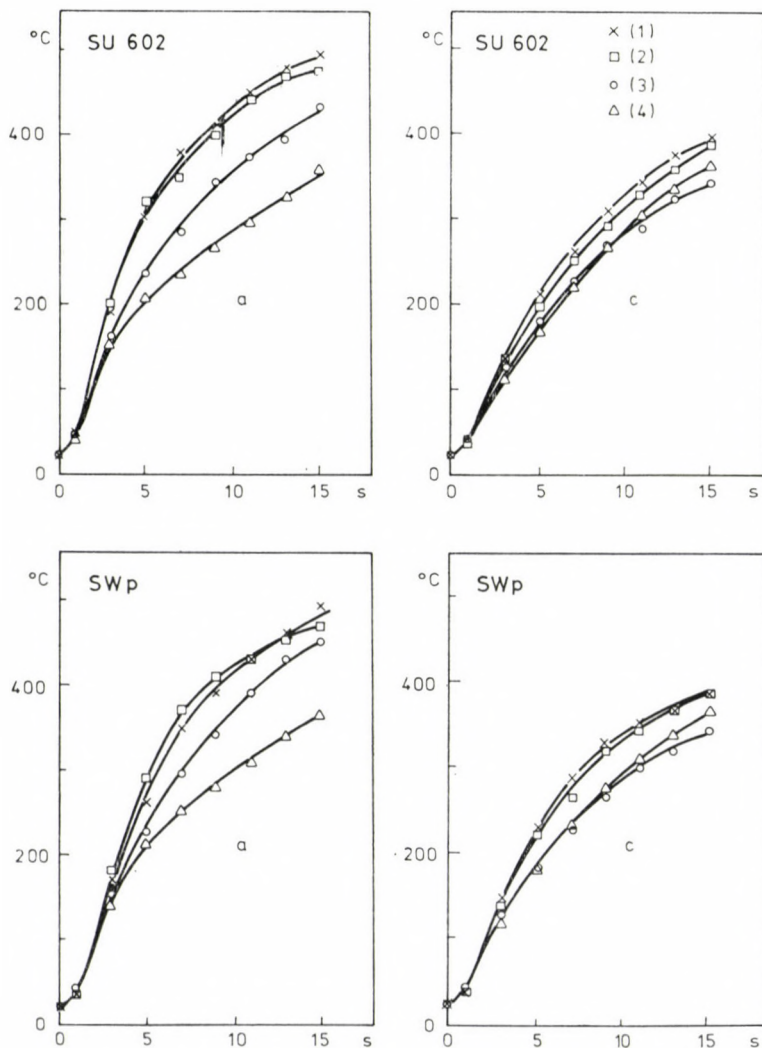
Fig. 2. Electrode temperature in the case of filling prepared with amorphous carbon powder for different kinds of auxiliary electrodes; (1): RW II; (2): SW; (3): SU; (4): RW O

Table I

*Specific electric resistance and thermal conductivity
of carbon electrode substances*

Electrode		$\mu\Omega \cdot cm$	$W/m \cdot K$
Graphitic carbon	RW O	850	146
	SU	1000	140
Amorphous carbon	RW II	6000	25
	SW	6000	20

method of investigation for the total evaporation of powder samples.) However, the least difference between values measured at excitation with the two kinds of polarities was found in the case of the carbon electrode RW O of best thermal conduction.

Moreover, it is to be mentioned that, disregarding the first few seconds of excitation, investigated at identical polarity, the temperature of the better electric and thermal conductor electrodes on graphite basis (RW O, SU) is always lower than that of the electrodes of amorphous carbon type, as heat transmitted by the arc is better conducted by graphitic carbon towards the electrode holders (Table I).

It can be also observed that between temperature values obtained with excitation at the two polarities the differences according to electrode substances are smaller at cathodic than at anodic excitation. The lower electrode temperature of the cathode is less influenced by the thermal conductivity and thermal losses of the electrode substance.

b) It becomes clear from Figs 3 and 4 that in carbon carrier electrodes of identical type (graphitic or amorphous) the average temperature of the carrier electrode is much less influenced by the nature of the carbon powder filling, than by the substance of the carrier electrode. Differences generally are within the error of temperature measurement. Nevertheless, it can be observed in several cases that the temperature of an identical carrier electrode is similarly the lowest, if the mixture was prepared with graphitic type carbon powder RW A of best heat conductivity.

With different carbon powder mixtures electrode temperature values agreeing best were obtained both in anodic and cathodic excitation for the carrier electrode of type RW O. On the other part, the SW electrode of amorphous type, heated up strongest, gave similarly agreeing and well reproducible results at anodic excitation. Thus, the equalizing effect of higher energies is exerted also in this case. However, naturally these effects too, depend on the polarity of the carrier electrode.

It can be established from the aforesaid that the temperature of the whole mass of the electrode is decisively determined by the quality of the carrier electrode itself. Moreover it can be concluded that the carrier electrode, as well as the carbon powder content of the mixture, attempt to dissipate the heat produced by the arc, but depending on its heat conductivity, the mixture containing carbon powder stores also heat in the given case. This is consistent with specific electric resistance data of various carbon powders, which are naturally inversely proportional to heat conduction, and according
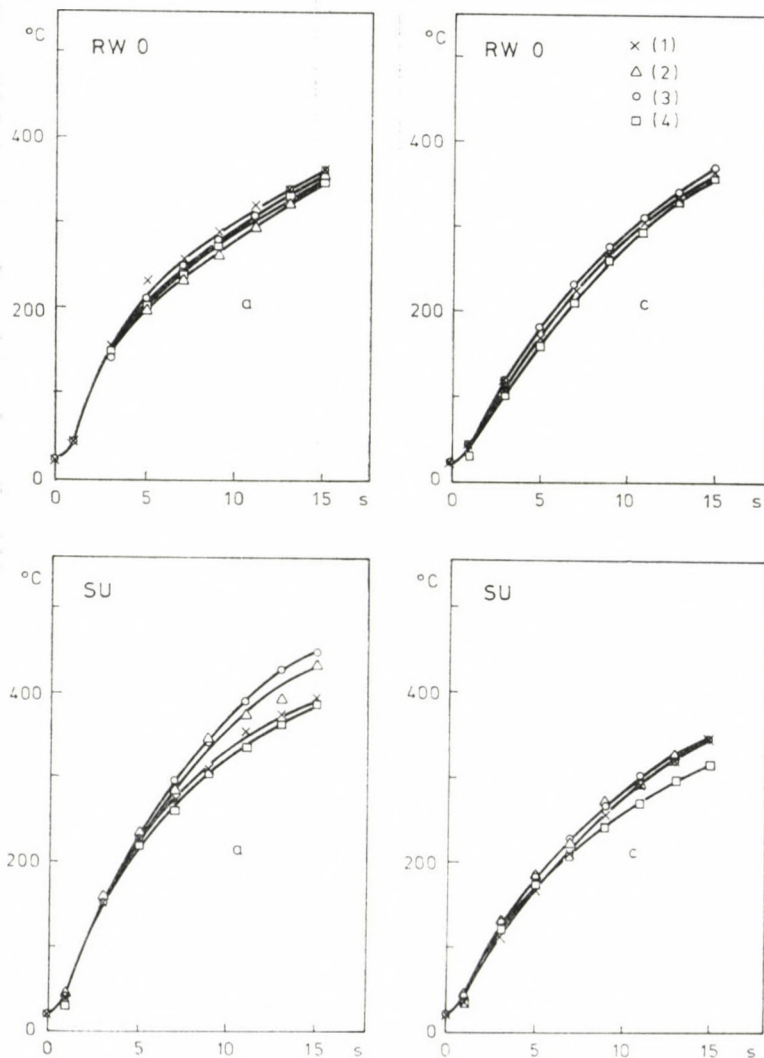
Fig. 3. Electrode temperature in graphitic carbon auxiliary electrodes according to the kinds of carbon powders; (1): SU 601; (2): SU 602; (3): SW_p; (4): RW A
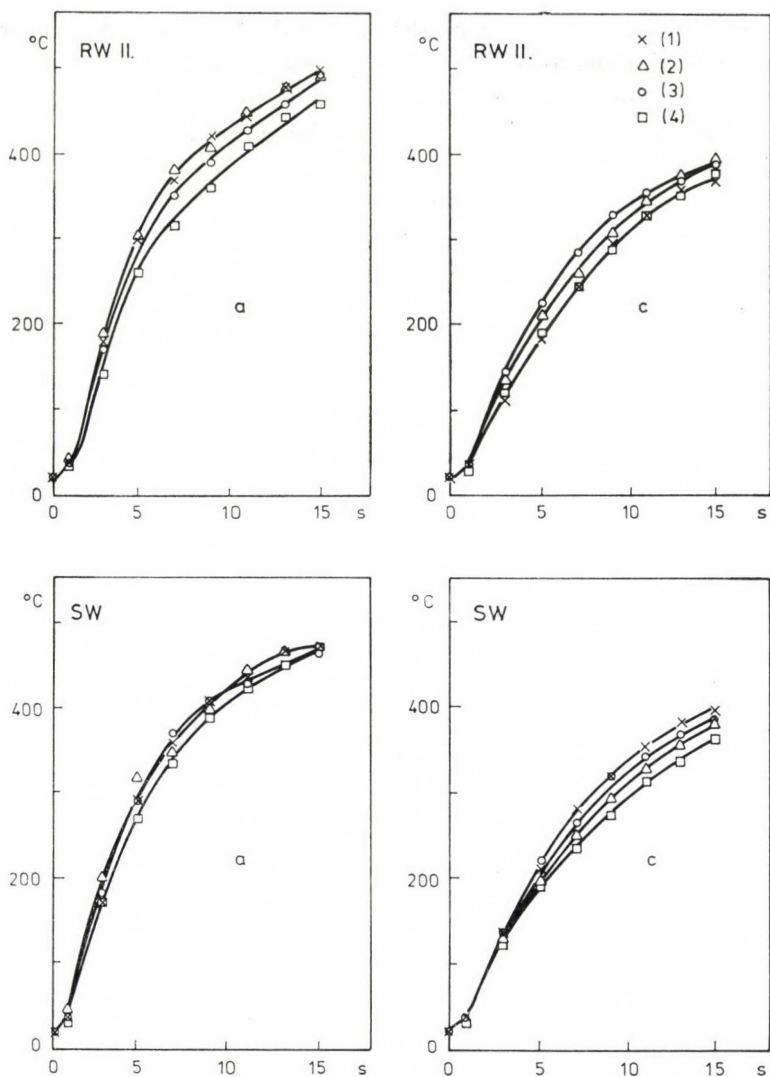
Fig. 4. Electrode temperature in amorphous carbon auxiliary electrodes according to the kinds of carbon powders; (1): SU 601; (2): SU 602; (3): SW_p; (4): RW A

to which the electric conductivities of the 3 directly comparable carbon powders manufactured in Topolčany are at identical sample treatment, compression and other conditions of investigation the following:*

graphite powder	60 $\mu\Omega \cdot$ m
calcined petrol coke	330 $\mu\Omega \cdot$ m
SW_p experimental substance	560 $\mu\Omega \cdot$ m

* Measuring data of the factory Elektrokarbon Topolčany.

However, our measurements took into consideration only the most essential effects, because the temperatures were not measured in the sample itself, but below the sample.

Spectral line intensities

The intensities of the spectral line of Cu raise new problems. In our experiments the intensity of the Cu I 282.4 nm line ($I = \text{num} \log Y_{Cu}$) was considered as proportional to the evaporation of the sample. These values were summarized separately from data obtained in the anodic (Table II) and cathodic (Table III) excitation of the samples.

It was observed already in the investigation of electrode surface reactions [3] that that better heat conducting and therefore colder carbon electrode on graphite basis, having also a more stable crystal structure, is of lower activity. In this case effects arising from the higher temperature of the cathodic burning spot already mentioned are exerted in a larger extent, and the lower temperature of the whole mass of the electrode cannot considerably modify either this, or the extent of chemical reactions.

Table II

Intensity (I) of the Cu I 282.4 nm *line*
10 A, 10 s, *anodic* excitation

| Carrier electrode | | Carbon powder additive to CuO | | | |
| | | graphitic | | amorphous | |
		RW A	SU-601	SU-602	SW_p
Graphitic carbon	RW O	24.4	24.6	15.3	32.1
	SU	42.8	33.5	14.5	54.6
Amorphous carbon	RW II	60.1	51.9	47.4	65.7
	SW	58.6	47.8	46.3	65.2

Table III

Intensity (I) of the Cu I 282.4 nm *line*
10 A, 10 s, *cathodic* excitation

| Carrier electrode | | Carbon powder additive to CuO | | | |
| | | graphitic | | amorphous | |
		RW A	SU-601	SU-602	SW_p
Graphitic carbon	RW O	64.5	58.7	51.2	63.0
	SU	58.0	45.1	36.5	51.1
Amorphous carbon	RW II	42.4	39.8	24.5	67.9
	SW	37.7	24.9	17.0	64.0

It is known from earlier data in the literature [17] and from our own earlier experiments [18, 19] that with increasing electrode temperature evaporation from the electrode increases too, and because of this spectral line intensities are also higher. It can be well seen also in our case that from carbon carrier electrodes, warmed up stronger *as anode* by the action of the arc, that is, from carbons of *amorphous* type, the evaporation of the sample increases too, the intensities of the spectral lines are higher. As contrary to this, in the case of good conductor, and thus colder electrodes of *graphitic* type, *cathodic* excitation results higher spectral line intensities. Here, the burning spot of higher temperature of the arc [13, 14] and the cathodic processes determine decisively the evaporation of the sample. This is now less affected by the temperature of the whole mass of the electrode, because it is lower. However, in the cathodic excitation of the sample the carbon powder SW_p of lowest thermal conductivity mixed to the copper oxide attempts to equalize the cooling effect even of the graphitic auxiliary electrodes of good thermal conductivity. In the colder cathode carrier electrode the own properties of the carbon powder too, assert themselves stronger in the forming of the intensity of spectral lines, since the arc evaporates the sample at the site of the burning spot, and this site is partly the surface of the filling. Therefore, the carbon powder additive plays a greater role in the development of the intensity of the spectral lines, than in that of the average temperature of the electrode.

The standard deviation (s) of the logarithms of spectral line intensities (Y), measured in parallel experiments was also investigated. Results are contained in Tables IV and V. Since the average values ($\overline{Y}$) considerably change according to carbon auxiliary substances, for better comparison standard deviations are given as relative percentage of the mean values:

$$s\% = \frac{s}{\overline{Y}} \cdot 100\%$$

Variation of parallel measurements is partly due to chemical reactions difficult to control. Results permit to conclude that the higher is the electrode temperature, the larger is the extent of interfering chemical reactions. However higher energies partly compensate side effects. Thus, in the anodic excitation of samples the standard deviation of spectral line intensities is lower for carbon carrier electrodes RW II and SW of amorphous type.

In cathodic excitation as mentioned already, the whole mass of the electrode is of lower temperature. The extent of chemical reactions is lower in the electrodes, so that they influence less the evaporation of the sample and the excitation of metal vapours. Here the interfering action of side effects is the lowest in the case of graphitic carbon carrier electrodes of good thermal conductivity.

Table IV

$\overline{Y}_{Cu\ I\ 282.4}$ *values and relative % standard deviations referred to these mean values*
Anodic excitation (10 A, 10 s)

Carrier electrode		Carbon powder additive to CuO							
		graphitic				amorphous			
		RW A		SU-601		SU-602		SW_p	
		$\overline{Y}$	$s\%$	$\overline{Y}$	$s\%$	$\overline{Y}$	$s\%$	$\overline{Y}$	$s\%$
Graphitic	RW O	1.380	6.4	1.370	11.2	1.185	3.0	1.490	7.9
carbon	SU	1.625	5.4	1.515	7.1	1.135	13.0	1.735	3.7
Amorphous	RW II	1.780	1.0	1.715	2.5	1.675	2.4	1.815	2.4
carbon	SW	1.765	1.1	1.680	1.4	1.665	2.4	1.810	3.6

Table V

$\Delta\overline{Y}_{Cu\ I\ 282.4}$ *values and relative % standard deviations, referred to these mean values*
Cathodic excitation (10 A, 10 s)

Carrier electrode		Carbon powder additive to CuO							
		graphitic				amorphous			
		RW A		SU-601		SU-602		SW_p	
		$\Delta\overline{Y}$	$s\%$	$\Delta\overline{Y}$	$s\%$	$\Delta\overline{Y}$	$s\%$	$\Delta\overline{Y}$	$s\%$
Graphitic	RW O	1.810	1.3	1.765	3.6	1.705	2.7	1.795	2.3
carbon	SU	1.760	3.5	1.650	4.4	1.560	4.4	1.705	3.2
Amorphous	RW II	1.620	4.4	1.595	5.1	1.370	10.1	1.830	2.1
carbon	SW	1.570	4.2	1.375	10.8	1.220	9.1	1.800	3.5

Thus, optimal conditions can be selected according to the given purpose. Expectably, in the case of substances of low volatility a sample mixed with graphitic carbon powder will be filled into a carbon carrier electrode of type RW II or SW heated up stronger, and investigated as anode. If the sample is excited as cathode, then, according to experience, a graphitic carbon carrier electrode will be selected.

The change of the logarithm of line/background ratio ($\Delta Y_{Cu,b}$) was also investigated at the Cu I 282.4 atom line as a function of the quality of carbon auxiliary substances. These values are thought to be also suitable for the characterization of the detectability of impurities, as it is known that the behaviour of the main component of the sample decisively determines also that of minor components contained in it (physical and chemical matrix effect). Here the same results were obtained as above. Average $\Delta\overline{Y}_{Cu,b}$ data obtained at anodic and cathodic excitation of the carrier electrode, and the percentage standard deviation of these values, similarly referred to this mean value are summarized in Tables VI and VII:

$$s\% = \frac{s}{\Delta\overline{Y}} \cdot 100\%$$

Table VI

*Average $\Delta\overline{Y}_{Cu,b}$ values at the Cu I 282.4 nm line,
and % standard deviation, referred to the mean value
Anodic excitation*

Carrier electrode		Carbon powder additive to CuO							
		graphitic				amorphous			
		RW A		SU-601		SU-602		SW$_p$	
		$\Delta\overline{Y}$	$s\%$	$\Delta\overline{Y}$	$s\%$	$\Delta\overline{Y}$	$s\%$	$\Delta\overline{Y}$	$s\%$
Graphitic	RW O	1.490	7.0	1.550	8.4	1.370	3.3	1.680	7.7
carbon	SU	1.800	5.8	1.770	8.1	1.325	13.7	1.965	4.7
Amorphous	RW II	1.935	2.8	1.965	6.7	1.935	3.3	1.945	2.4
carbon	SW	1.935	1.9	1.955	3.4	1.920	2.8	1.950	3.5

Table VII

*Average $\Delta\overline{Y}_{Cu,b}$ values measured at the Cu I 282.4 nm line,
and % standard deviation, referred to the mean value
Cathodic excitation*

Carrier electrode		Carbon powder additive to CuO							
		graphitic				amorphous			
		RW A		SU-601		SU-602		SW$_p$	
		$\Delta\overline{Y}$	$s\%$	$\Delta\overline{Y}$	$s\%$	$\Delta\overline{Y}$	$s\%$	$\Delta\overline{Y}$	$s\%$
Graphitic	RW O	1.990	1.4	2.000	2.5	1.945	3.2	2.035	1.3
carbon	SU	1.915	3.7	1.855	5.0	1.770	3.6	1.935	3.9
Amorphous	RW II	1.795	1.8	1.810	5.5	1.620	9.6	1.990	2.3
carbon	SW	1.755	5.0	1.645	6.4	1.475	9.1	1.985	2.8

The highest values, thus expectably also the best detectability of minor components, and the smallest standard deviation of the data above, were obtained at anodic excitation with amorphous carbon carrier electrodes. This too, indicates the advantages of this type of electrode.

In cathodic excitation, the graphitic carbon carrier electrode may be preferred. Naturally, there are exceptions, which call the attention to the fact that in the case of other samples possibly other problems may arise. Thus generalization requires further consideration.

In the investigation of the change of spectral line intensities the extent and effect of chemical reactions was not taken into account. In initially hotter electrodes the extent of thermochemical reactions is of higher. If the sum of energy changes of these reactions is positive, that is, of exothermal character, as in our case the oxidation of carbon(the electrode material and carbon powder mixed to the sample) with oxygen formed in the decomposition of CuO, then

excess thermal energy set free acts with increasing temperature of the electrode in the same direction, and increases parallel with it the evaporation of the sample. On the other hand, evaporation diminishes, if, as in our case, the composition of the sample changes because of the reaction so that a good thermal conductor (in our case metallic copper) is formed, which, owing to its lower evaporation temperature (boiling point) than that of carbon, rapidly decreases the evaporation of the sample [20]. With carbons of amorphous type, this effect seems to be the most essential in cathodic excitation.

The excitation of metal vapours is affected also by the discharge gas atmosphere, by the composition of plasma gases. This changes the spectral line intensities, because plasma parameters are different. Carbon oxides in well measurable amounts are formed in the said thermochemical reactions (see our next communication), the diffusion of which and their departure from the arc gap is relatively slow even in the case of flowing Ar atmosphere [21]. Therefore, though initially pure noble gas atmosphere was used, further discharges proceed already in an atmosphere mixed with carbon oxides. Thus, spectral line intensities fundamentally depending on evaporation are further modified according to the amount of gaseous reaction products, depending on electrode temperature. In our further work these effects were studied, measuring the quantities of gaseous products, and comparing them with spectral line intensities and intensity ratios. This will be reported in the following paper.

Conclusions

In the anodic excitation of mixtures of CuO model substance and carbon powder, suitably carrier electrodes on amorphous carbon basis and possibly carbon powder additives of graphitic type will be used, though results are less influenced by the quality of the carbon powder.

In cathodic excitation a carrier electrode on graphitic carbon basis seems to be more advantageous, because the standard deviation of analytical results is lower and detectability is higher.

REFERENCES

[1] Peter, H.: Silikattechnik, **16,** 23 (1965)
[2] Peter, H.: Silikattechnik, **16,** 53 (1965)
[3] Szabó, Z. L., Fejérdy, H., Buzási, A.: Acta Chim. Acad. Sci. Hung., **80,** 365 (1974)
[4] Szabó, Z. L., Dobolyi-Fejérdy, H.: Acta Chim. Acad. Sci. Hung., **97,** 111 (1978)
[5] Szabó, Z. L., Dobolyi-Fejérdy, H.: Acta Chim. Acad. Sci. Hung., **97,** 125 (1978)
[6] Szabó, Z. L., Dobolyi-Fejérdy, H.: Acta Chim. Acad. Sci. Hung., **98,** 147 (1978)
[7] Szabó, Z. L., Dobolyi-Fejérdy, H.: Acta Chim. Acad. Sci. Hung., **98,** 157 (1978)
[8] Ringsdorff-Spektralkohlen (Catalogue), Ringsdorff Werke GMBH, 5300 Bonn, Bad Godesberg GBR

[9] Spectral Carbon Electrodes (Catalogue), Elektrokarbon Topolčany ČSSR
[10] Szabó, Z. L.: Dissertation for D. Sc., Budapest, 1978, pp. 83
[11] Szakács, O.: 14th Coll. Spectr. Internat., Debrecen, Vol. II, 997 (1967)
[12] Zalesski, A. M.: The Electrical Arc (Hungarian Translation), Technical Ed., Budapest 1968
[13] Szabó, Z. L., Pöppl, L.: Acta Chim. Budapest, **77**, 125 (1973)
[14] Szabó, Z. L.: Acta Chim. Budapest, **85**, 13 (1975)
[15] Pöppl, L., Szabó, Z. L.: Acta Chim. Budapest, **79**, 27 (1973)
[16] Slavin, M. L.: Ind. Eng. Chem. Anal. Ed., **10**, 407 (1938)
[17] Gerlach, W., Rollwagen, W.: Metallwirtsch., **16**, 1083 (1937)
[18] Szabó, Z. L., Szakács, O.: Acta Chim. Budapest, **73**, 143 (1972)
[19] Szabó, Z. L.: Thesis of Dissertation for C. Sc. Budapest 1967, pp. 18.
[20] Szabó, Z. L., Dobolyi-Fejérdy, H.: Acta Chim. Acad. Sci. Hung., **97**, 13 (1978)
[21] Szabó, Z. L., Bertalan, É.: Acta Chim. Hung., **102**, 391 (1979)

THE ROLE OF THE QUALITY OF CARBON AUXILIARY SUBSTANCES IN THE EMISSION SPECTROSCOPY OF NON CONDUCTING POWDER SAMPLES, II

Zoltán László Szabó[1]* and Enikő Tatár[2]

(*[1]Institute of Inorganic and Analytical Chemistry, L. Eötvös University,
H-1443 Budapest, P.O.B. 123,
[2]Utilizing Enterprise for Raw Materials, H-1475 Budapest, P.O.B. 97*)

The quantity of CO_2 and CO produced in the arc was measured for $CuO + C$ powder mixtures, and their volume ratio was calculated. The quality of the carrier electrode and of the carbon powder used in the mixtures was changed. Data measured were compared with the average temperature of the carrier electrodes, and with spectral character data ($\Delta Y_{ionic, atomic lines}$) measured for copper lines. It was found that these values depend on the graphitic or amorphous type of the carbon auxiliary substances, and particularly on the quality and polarity of the carrier electrode.

Introduction

The present paper is the continuation of our preceding work [1]. It was reported there that the average temperature of carrier electrodes filled with non conducting powder samples, in our case carbon powder mixtures of reactive copper(II) oxide, selected as model substance, decisively depends on the structure of graphitic or amorphous carbon. These temperature values are only modified by the properties of carbon powders of different type, used for the powder mixtures of the sample. It was mentioned in our previous paper that gaseous products are often formed in the thermochemical reactions, which change the composition of the discharge gas atmosphere. In this case spectral line intensities are changed, besides by effects depending on energetic conditions and on changed sample composition, also by the change in plasma conditions. In the given case too, even if we used flowing Ar gas atmosphere, in the higher temperature reactions of the $CuO +$ powder mixtures CO and CO_2 were formed in considerable amounts, and exerted their action in the plasma because of their relatively slow exchange by diffusion even in the flowing Ar atmosphere. Our aim was to investigate these phenomena by measuring the amount of the carbon oxides formed in the arc, and attempting two correlate the results with spectral line intensities, complemented by spectral character and electrode temperature data, described in our preceding paper.

* To whom correspondence should be addressed.

3*

*Acta Chim. Hung. 120, 1985
Akadémiai Kiadó, Budapest*

We are convinced that the relatively large fluctuation of spectral line intensities obtained by arc excitation can be mainly attributed to the randomness and incertitude of the side-processes of the arc. One of these problems may be evaporation on uncertain extent and also the sputtering of the mass of the powder mixture filled into the boring of the carrier electrode, caused by the arc. Therefore, the decrease in mass of the sample in the arc was measured and its standard deviation was calculated.

Experimental

In our preceding paper [1] two kinds of graphitic carbon carrier electrodes, RW O of German manufature (Ringsdorff Werke) and the Czechoslovakian carbon SU (Elektrokarbon Topolčany), further carbon carrier electrodes of amorphous type of the two factories (RW and SW), and similarly two graphitic (RW O and SU 601) and two amorphous (SU 602 and SW_p experimental) carbon powders in CuO + C powder mixtures of 0.3 molar fraction of metal oxide were used in the experiments, carried out if flowing Ar atmosphere. Experimental conditions and specification of the carbon types are also to be found in this paper [1]. The amounts of CO and CO_2 formed in the reaction of CuO and C were measured by our titrimetric gas analytical methods [2]: CO_2 was absorbed in $Ba(OH)_2$ standard solution of known volume and titer, and the excess of $Ba(OH)_2$ was determined alkalimetrically. CO was oxidized with $KMnO_4$ in presence fo Ag^+ catalyst, and similarly, the excess of the standard solution was titrated. The volume ratio of the two carbon oxides (CO_2/CO) was also calculated. This ratio depends on oxidation conditions, on the reactivities of the reactants and the gas atmosphere, on the polarity of the electrodes (anodic oxidation, cathodic reduction) and on the temperature of the electrodes [3].

The mass of the samples filled into the electrode boring, their loss in mass (Δg) caused by arc excitation were measured, and the standard deviation of the latter was calculated. In addition to the blackening of the atom line Cu I 282.4 nm, reported in our preceding paper, that of the ion line Cu II 237.0 nm was measured, and from these the so-called spectral character data ($\Delta Y_{Cu\ II,I}$) were calculated, which may characterize changes in the plasma. The correlation of these data was attempted.

Spectra were photographed up to the first 10 s of arc duration on Agfa-Gevaert photographic plates type 34 B 50, and the gas production of the arc was also measured after this period. It was found namely in several of our earlier investigations [4, 5] that predominantly thermochemical reactions proceed already in the first few seconds of arc duration. Reference data of the electrode temperature were also fixed in the 10th second of arc duration. All the gas analytical measuring data given were mean values of 5—8, in loss in mass and spectral line intensity measurements of 10—16 parallel measurements, because CO_2 and CO quantities were measured in separate experimental series, but the simultaneous spectrum photos and weight loss measurements were naturally identical.

Results and Discussion

Tables I and II contain the quantity of carbon oxides in cm³ measured at anodic and cathodic excitation of the carrier electrode. As was to be expected, the total of 64 mean values showed with a few exceptions (not to be considered as characteristic) that in amorphous carbon carrier electrodes, heating up stronger, the decomposition of copper oxide and also the gas producing reactions are of larger extent for a sample mixed with a given type of carbon powder as compared to values obtained with graphitic carrier electrodes. For carbons

Table I

Amount of carbon oxides (cm³) *formed in the arc. Anodic* excitation

Auxiliary electrode		Carbon powder additive to CuO							
		Graphitic				Amorphous			
		RW A		SU 601		SU 602		SW_p	
		CO_2	CO	CO_2	CO	CO_2	CO	CO_2	CO
Graphitic	RW O	0.18	0.59	0.23	0.53	0.03	0.48	0.23	0.72
carbon	SU	0.31	0.75	0.26	0.78	0.26	0.43	0.58	1.23
Amorphous	RW II	1.21	2.36	1.37	2.40	1.25	2.12	1.29	3.00
carbon	SW	1.22	2.47	1.34	2.13	1.32	2.23	1.33	2.89

Table II

Amount of carbon oxides (cm³) *formed in the arc. Cathodic* excitation

Auxiliary electrode		Carbon powder additive to CuO							
		Graphitic				Amorphous			
		RW A		SU 601		SU 602		SW_p	
		CO_2	CO	CO_2	CO	CO_2	CO	CO_2	CO
Graphitic	RW O	0.23	0.92	0.21	0.92	0.26	0.94	0.21	1.10
carbon	SU	0.16	0.86	0.17	0.60	0.12	0.67	0.18	0.74
Amorphous	RW II	0.61	1.33	0.80	1.25	0.55	1.05	0.93	1.81
carbon	SW	0.46	1.17	0.43	0.88	0.38	0.65	0.82	1.76

of different manufacture, but identically of amorphous or graphitic type, differences between the single types are generally small. An exception is the high-resistant carbon powder SW_p manufactured for special experimental purposes, which also increased the CO production of the arc, according to expectation.

It is worth to note that in all the cases the CO production of the arc is higher than that of CO_2. In our case, the following main reactions can be assumed in the arc, one part of which was verified already in our earlier works.

1. CuO $= Cu + O$
2. $CuO + C$ $= Cu + CO$
3. $2 CuO + C = 2Cu + CO_2$
4. $C + O$ $= CO$
5. $C + 2 O$ $= CO_2$
6. $CO_2 + C$ $= 2 CO.$

Though a reaction zone of optimal temperature and a possibility, partly in the electrode filling partly in the plasma, exist for each of the reactions, according to data measured and our earlier experimental results [6, 7] reactions 2, 3 and 6 are the most probable. In the sample remaining in the boring of the

Table III

Decrease in mass of the sample in the arc, and its relative error.
Graphitic carbon powder, *anodic* excitation

Auxiliary electrode		Carbon powder additive to CuO					
		RW A			SU 601		
		Δg calc.	Δg measured	% rel. error	Δg calc.	Δg measured	% rel. error
Graphitic	RW O	0.0011	0.0047	21.3	0.0011	0.0050	28.0
carbon	SU	0.0016	0.0045	22.2	0.0015	0.0036	27.8
Amorphous	RW II	0.0053	0.0178	10.7	0.0057	0.0175	5.1
carbon	SW	0.0055	0.0187	22.5	0.0053	0.0157	5.7

Table IV

Decrease in mass of the sample in the arc, and its relative error.
Graphitic carbon powder, *cathodic* excitation

Auxiliary electrode		Carbon powder additive to CuO					
		RW A			SU 601		
		Δg calc.	Δg measured	% rel. error	Δg calc.	Δg measured	% rel. error
Graphitic	RW O	0.0016	0.0063	7.9	0.0016	0.0064	10.9
carbon	SU	0.0014	0.0046	21.7	0.0011	0.0040	30.0
Amorphous	RW II	0.0029	0.0074	20.3	0.0031	0.0083	18.1
carbon	SW	0.0024	0.0074	48.6	0.0020	0.0037	27.0

electrode after arcing, metallic copper could be identified. The quantity of gaseous products rather fluctuated in the single parallel measurements. We tried to follow this by data in Tables III—VI, where losses of mass directly measured with analytical balance after the anodic and cathodic excitation of the sample in the electrode boring, and losses of mass calculated from gas analytical data, further the standard deviations of directly measured data were compared. The loss in mass of the sample can be attributed to three causes:

1. Loss of carbon oxides formed in the reaction.

2. The amount of substance evaporating into the arc.

3. The spluttering of the substance from the carrier electrode, caused by the pumping (pulsating) action of the a.c. polarized arc.

Differences in loss of mass values measured and calculated from gas analytical results mainly indicate the extent of the spluttering of the substance, because evaporation itself is relatively moderate. This spluttering is also promoted by the degree of fineness of the powder particles of the sample filling and by the flow of carbon oxide gases evolved in the interior of the filling. In our earlier experiments [8, 9] CuO samples of coarse particle size

Table V

Decrease in mass of the sample in the arc, and its relative error.
Amorphous carbon powder, anodic excitation

| Auxiliary electrode | | Carbon powder additive to CuO | | | | | |
| | | SU 602 | | | SW_p | | |
		Δg calc.	Δg measured	% rel. error	Δg calc.	Δg measured	% rel. error
Graphitic	RW O	0.0007	0.0022	18.2	0.0014	0.0049	20.4
carbon	SU	0.0011	0.0020	55.0	0.0027	0.0061	18.0
Amorphous	RW II	0.0051	0.0130	9.2	0.0063	0.0222	11.3
carbon	SW	0.0054	0.0126	15.1	0.0062	0.0195	9.7

Table VI

Decrease in mass of the sample in the arc, and its relative error.
Amorphous carbon powder, cathodic excitation

| Auxiliary electrode | | Carbon powder additive to CuO | | | | | |
| | | SU 602 | | | SW_p | | |
		Δg calc.	Δg measured	% rel. error	Δg calc.	Δg measured	% rel. error
Graphitic	RW O	0.0017	0.0056	26.8	0.0018	0.0069	14.5
carbon	SU	0.0011	0.0025	36.0	0.0013	0.0043	27.9
Amorphous	RW II	0.0024	0.0041	29.3	0.0041	0.0103	21.4
carbon	SW	0.0016	0.0031	74.2	0.0038	0.0101	19.8

were used, and spluttering of lesser extent was observed. However, particle size was not measured. Therefore, an exact evaluation cannot be given here, only the direction of the effects can be indicated.

It will be noted from the tables that numerical data measured directly are always higher than those calculated from the quantity of carbon oxides evolved, while on the other hand losses in mass, caused by the larger extent of chemical reactions and gas evolution increase too, proportionally to the higher temperature of amorphous carbon. From graphitic carbon electrodes generally a larger amount of sample is consumed in cathodic excitation. This is consistent with the behaviour of spectral line intensities reported in our preceding paper [1], which can be traced back to the burning spot of higher temperature of the arc at the cathode [10, 11], and to the larger extent of evaporation following from this. However, the temperature of the whole mass of amorphous carrier electrodes is higher at anodic excitation, because of poorer heat conduction and higher heat capacity values. This increases the extent of reactions, which is reflected also in the mass losses.

The percentage fluctuation of mass losses measured is smaller for amorphous carbon carrier electrodes in anodic excitation, and in cathodic excitation

Table VII

Changes of electrode temperature and plasma conditions according to auxiliary carbon substances.
Anodic excitation

Auxiliary electrode		Carbon powder additive to CuO												
		Graphitic						Amorphous						
		RW A			SU 601			SU 602			SW$_p$			
		T (°C)	CO_2/CO	$\Delta Y_{II,I}$	T (°C)	CO_2/CO	$\Delta Y_{II,I}$	T (°C)	CO_2/CO	$\Delta Y_{II,I}$	T (°C)	CO_2/CO	$\Delta Y_{II,I}$
Graphitic carbon	RW O	292	0.31	−16.0	308	0.43	−14.0	284	0.06	−7.5	297	0.32	−21.0
	SU	318	0.41	−18.5	326	0.33	−21.0	356	0.60	−8.0	367	0.47	−26.0
Amorphous carbon	RW II	385	0.51	−31.0	432	0.57	−37.5	432	0.59	−38.5	413	0.43	−31.5
	SW	408	0.49	−33.5	427	0.63	−34.5	423	0.59	−39.0	425	0.46	−37.5

Table VIII

Changes of electrode temperature and plasme conditions according to auxiliary
carbon substances. Cathodic excitation

Auxiliary electrode		Carbon powder additive to CuO												
		Graphitic						Amorphous						
		RW A			SU 601			SU 602			SW$_p$			
		T (°C)	CO_2/CO	$\Delta Y_{II,I}$	T (°C)	CO_2/CO	$\Delta Y_{II,I}$	T (°C)	CO_2/CO	$\Delta Y_{II,I}$	T (°C)	CO_2/CO	$\Delta Y_{II,I}$
Graphitic carbon	RW O	276	0.25	−12.0	285	0.23	−15.0	284	0.28	−13.5	292	0.19	−17.5
	SU	255	0.19	−13.5	274	0.28	−14.5	282	0.18	−12.5	284	0.24	−15.0
Amorphous carbon	RW II	312	0.46	−34.5	314	0.64	−36.0	329	0.52	−24.5	343	0.51	−41.0
	SW	296	0.39	−31.0	338	0.49	−24.0	312	0.58	−18.0	330	0.47	−41.5

for graphitic electrodes. This too, is in good agreement with the standard deviation of intensities and of relative spectral line intensities referred to background radiation. Data prove again that the spontaneous fluctuation and incertitude of the evaporation of the sample is caused by the difficulty of the control of side reactions discussed.

Tables VII and VIII are given for the characterization of electrode temperature, extent and ratio of the reactions, of changes in the composition of the plasma caused by the evaporation of the sample and the gaseous products, and for the showing of relationships between these characteristics. It can be seen that at higher average electrode temperature the ratio of the two carbon oxides increases too, to the advantage of CO_2, besides their absolute quantities shown in Tables I and II. This is easy to understand, as indeed, if the temperature of the carrier electrode increases, the reaction zones, particularly the zone of CO_2 formation will also increase downwards in the electrode filling. The zone of formation of this is namely the bulk of the electrode filling, while that of CO is the burning spot of higher temperature but of relatively small area of the arc, at the top of the electrode and of the sample, and its immediate surrounding. The temperature and area of the burning spot depend less on the quality of carbon auxiliary substances, than on the average temperature of the electrodes, which is determined and stronger affected by the thermal conductivity and thermal capacity of the carrier electrode.

The dissociation of carbon oxides, particularly that of CO_2, consumes a part of the electric energy of the arc, proportional to its amount formed. At the same time, at higher electrode temperature more sample evaporates. Owing to this, more metal vapour gets into the plasma. Both processes reduce the temperature of the original carbon arc — Ar plasma. This is shown by spectral character data, $\Delta Y_{II, I}$, in Tables VII and VIII, given as the logarithm of the intensity ratio of the spectral lines Cu II 237.0 and Cu I 282.4 nm. These data are correlated with the average temperature of the plasma. It can be observed, that the higher is the temperature of the electrode, that is, the higher is the extent of the chemical reaction and the evaporation of the sample filled in the carrier electrode, the smaller will be this value characterising the average temperature of the arc plasma. This favours at increased evaporation the excitation of atomic lines. Thus, using amorphous carbon carrier electrode in anodic excitation improves the analytical process.

Conclusions

At given excitation conditions the evaporation of the sample and evaporation and excitation conditions are mainly determined by the properties of the electrode carrying the powder sample. At higher carrier electrode tempera-

ture the reaction of the sample contained and also its evaporation are of larger extent. In the initially pure Ar atmosphere carbon oxides produced in the reaction change in the same way the plasma temperature, as the increased amount of metal vapour. In the poorer heat-conductor carbon carrier electrodes of amorphous type these processes are of larger extent in the anodic excitation of the sample. This can be of advantage also from the analytical aspect, because the intensity of atom lines increases, and the reproducibility of experimental conditions is also improved. On the other hand, in cathodic excitation the use of graphitic carrier electrodes of lower temperature is more advantageous.

REFERENCES

[1] Szabó, Z. L., Tatár, E.: Acta Chim. Hung., **120**, 121 (1985)
[2] Szabó, Z. L., Tóth, I.: Acta Chim. Acad. Sci. Hung., **73**, 363 (1972)
[3] Szabó, Z. L., Spectrochim. Acta, **29**, 231 (1974)
[4] Szabó, Z. L., Dobolyi-Fejérdy, H. Acta Chim. Acad. Sci Hung., **97**, 111 (1978)
[5] Szabó, Z. L., Dobolyi-Fejérdy, H.: Acta Chim. Acad. Sci. Hung., **98**, 147 (1978)
[6] Szabó, Z. L.: Acta Chim. Acad. Sci. Hung., **97**, 137 (1978)
[7] Szabó, Z. L., Dobolyi-Fejérdy, H.: Acta Chim. Acad. Sci. Hung., **98**, 147 (1978)
[8] Szabó, Z. L.: Acta Chim. Acad. Sci. Hung., **96**, 201 (1978)
[9] Szabó, Z. L., Dobolyi-Fejérdy, H.: Acta Chim. Acad. Sci. Hung., **97**, 13 (1978)
[10] Szabó, Z. L., Pöppl, L.: Acta Chim. Acad. Sci. Hung., **77**, 125 (1973)
[11] Szabó, Z. L.: Acta Chim. Acad. Sci. Hung., **75**, 13 (1975)

METAL ION COORDINATION IN POLYCRYSTALLINE COPPER(II) COMPLEXES OF α-AMINO ACIDS. VISIBLE AND INFRARED SPECTRAL STUDIES

Terézia Szabó-Plánka

(Department of General and Physical Chemistry, József Attila University, H-6701 Szeged, P.O. Box 105)

Investigation of 30 polycrystalline copper(II) complexes of α-amino acids encountered in proteins was reported. From comparisons of the diffuse reflectance spectra and the carboxylate stretching vibrations of the compounds of known crystal structure with those of complexes of unknown crystal structure, conclusions were drawn on the coordination geometry about the copper(II) ion in the latter group of compounds.

Several attempts have previously been made [1—4] to characterize the coordination geometry about the copper(II) ion in its polycrystalline α-amino acid complexes of unknown crystal structure. Herlinger et al. devised an infrared criterion [1, 2] for the *cis* configuration by comparing the far infrared spectra of complexes of known crystal structure. Misumi et al. [3] attributed the rhombic character of the ESR spectra of some complexes to a rhombic distortion, occurring only in *trans* complexes as a consequence of different Cu—O and Cu—N bond lengths, while, in turn, compounds with *axial* spectra were thought to be of *cis* configuration. However, the character of the ESR spectrum of a pure paramagnetic compound is rather influenced by exchange interactions between crystallographically non-equivalent Cu(II) ions [4, 5]. Yasui and Shimura [6] compared the intensity and shape of the visible diffuse reflectance band with those of *cis*- and *trans*-bis-(glycinato)copper(II) mono-hydrate to draw conclusions on geometric isomers. On the basis of the single--crystal polarized electronic spectra of bis-(*l*-tyrosinato) copper(II) [7], theoretical considerations [4], and of the *axial* character of the ESR spectra of the diluted solid complexes, it is most probable that all the possible d-d bands are below 20 000 cm^{-1} [8]. Thus, in fact, all the effects, which increase the intensity of any d-d band, can be expected to enhance the intensity of the band in the visible region.

In the present work we report an investigation of 30 copper(II) complexes of α-amino acids encountered in proteins. From comparisons of the diffuse reflectance spectra and the carboxylate stretching vibrations of the compounds of known crystal structure with those of complexes of unknown crystal structure, conclusions are drawn on the coordination geometry about the copper(II) ion in the latter group of compounds.

Experimental

The copper(II) complexes of glycine, *l*- and *dl*-alanine, *dl*-valine, *l*-proline, *l*- and *dl*--serine, *l*- and *dl*-threonine, *l*-glutamine, *l*-glutamic acid, *l*-lysine and *l*-arginine (Gly, *l*-Ala, *dl*-Ala, *dl*-Val, *l*-Pro, *l*-Ser, *dl*-Ser, *l*-Thr, *dl*-Thr, *l*-Gln, *l*-Glu, *l*-Lys, *l*-Arg) were prepared by boiling aqueous solutions of ≈ 0.01 mol of the amino acids with excess $CuCO_3 \cdot Cu(OH)_2$ for about half an hour. The deep blue solutions were filtered to remove the excess of basic copper(II) carbonate, and then kept on a water bath to concentrate the solution. In most cases small crystals were obtained when these solutions cooled to room temperature. Complexes of *dl*-Ser and *l*-Arg were precipitated with ethanol and acetone, respectively, during cooling of the solutions on ice. The crystals were filtered, washed with acetone containing a small amount of water, and dried in air.

In the case of Gly the *cis* isomer, and with *l*-Ala the *trans* isomer of the copper(II) complex was obtained. $Trans$-Cu(Gly)$_2$ $\cdot$ H$_2$O was prepared according to [9], and *cis*-Cu(*l*-Ala)$_2$ by ageing an aqueous suspension of the *trans* isomer for two weeks [10].

The copper(II) complexes of *l*-valine, *l*- and *dl*-leucine, *l*- and *dl*-isoleucine, *l*-phenyl-alanine, *dl*-proline, *l*- and *dl*-methionine, *l*- and *dl*-tryptophan, *l*-tyrosine, *l*-asparagine, *l*--glutamine, and *l*- and *dl*-aspartic acid (*l*-Val, *l*-Leu, *dl*-Leu, *dl*-Ileu, *l*-Phe, *dl*-Pro, *l*-Met, *dl*-Met, *l*-Trp, *dl*-Trp, *l*-Tyr, *l*-Asn, *l*-Gln, *l*-Asp, *dl*-Asp) were prepared as follows. 0.01 mol of amino acid was dissolved in 10 cm³ of 1 N NaOH solution, and mixed with 25 cm³ of 0.2 M CuSO$_4$ solution. In most cases crystals of the complexes were obtained at once. The solution of the *l*-Tyr complex was heated before precipitation. The complex of *l*-Val was obtained from this solution a few days later. The copper(II) compound of *dl*-Pro was precipitated with acetone. The crystals were filtered, washed with a 1 : 1 acetone–water mixture, and dried in air. All reagents were REANAL products of analytical grade.

Besides the C, H and N contents*, the Cu(II) contents of the complexes were determined by complexometric titration, and the water contents were determined from their thermogravimetric curves. The derivatograms were recorded on a MOM G425 derivatograph. The experimental and calculated data agreed well.

Diffuse reflectance spectra were recorded on a BECKMAN DU spectrophotometer equipped with a reflectance attachment. The standard was MgO. The samples were powdered until unchanged $\log f(R)$ values were obtained.

Infrared spectra were recorded on a UR 10 (Carl Zeiss, Jena) spectrophotometer, in KBr pellets, in the 400—4000 cm⁻¹ region**.

Results and Discussion

The diffuse reflectance spectra in the visible and near infrared region consist of a single broad band at $(14-17) \cdot 10^3$ cm⁻¹ (Tables I and II), and of a shoulder at lower energies for some compounds. The band intensity is characterized by the $\log f(R)$ value at the maximum, since $f(R)$ is proportional to ε for weakly absorbing compounds if the sample is powdered finely enough [11].

Belford and Yeranos [12] showed that the symmetry-forbidden, vibrationally allowed weak d-d absorption in centric molecules of copper(II) chelates (*trans*-planar complexes) is enhanced by static removal of the central symmetry (*cis*-planar compounds). A lower, further increase in intensity is caused by relatively strong solvent coordination to the fifth coordination position (mono-

* We thank Mrs. M. Bartók for the analyses.
** Thanks are due to Dr. N. Marek for the possibility for infrared measurements.

pyridine adducts) in both groups of complexes, which further increases the non-centricity.

Some structural data on copper(II) complexes of α-amino acids of known crystal structure are listed in Table I. In the 1 : 2 complexes the Cu(II) is coordinated to two carboxylate oxygen and two amino nitrogen atoms, forming approximately square-planar units. The equatorial metal-donor atom distances are about 0.2 nm [10, 13—23]. The *trans*-CuO$_2$N$_2$ units can be regarded as of central symmetry, while molecules with *cis*-CuO$_2$N$_2$ arrangement and the complex Cu(*l*-Glu) · 2H$_2$O with the O$_3$N *equatorial* donor atom set are non-centric. At a distance of 0.23—0.27 nm from the square-planar units, a water molecule, or an *equatorially* non-bonded carboxylate or amide oxygen atom coordinates the Cu(II) *axially*. In the majority of the complexes the second *axial* position is also occupied, with a bond length of 0.25—0.38 nm.

Table I

Geometry, axial bond lengths, diffuse reflectance and infrared spectral data for copper(II) α-amino acid complexes of known crystal structure

Compound[a]	Geometry	Axial bond length[b] shorter[c]	Axial bond length[b] longer[c]	ν_{max}[d]	$\log f(R)_{max}$	Figure	ν_{as}[e]	ν_s[e]
Cu(Gly)$_2$ · H$_2$O[13]	*cis*	0.240 W	0.274 C	15.5	0.02	3A	1610	1394
Cu(*I*-Ileu)$_2$ · H$_2$O[16]	*cis*	0.248 W	0.384 C	16.4	−0.12	3D	1648	1396 1382
Cu(*l*-Ala)$_2$[10]	*cis*	0.237 C	—	16.3	0.18	2B	1652[f] 1624 1605 1587	1388
Cu(*l*-Ser)$_2$[18]	*cis*	0.236 C	0.363 C	16.4	0.15	2D	1673[f] 1637 1612 1606	1401
Cu(*l*-Glu) · 2H$_2$O[23]		0.230 C	0.259 C	13.7	0.08		1629 1608 sh 1576	1409 1394
Cu(*l*-Tyr)$_2$[22]	*trans*	0.234 C	0.307 P	16.9	−0.28	4A	1602[f] 1583 1575 sh	1403
Cu(*l*-Asn)$_2$[19]	*trans*	0.253 A	0.277 A	16.8	−0.33		1631	1414
Cu(*dl*-Pro)$_2$ · 2H$_2$O[17]	*trans*	0.254 W	0.254 W	16.2	−0.34	3G	1636	1359
Cu(*l*-Phe)$_2$[15]	*trans*	0.258 C	0.269 C	15.8	−0.54		1627	1400
Cu(*l*-Met)$_2$[20]	*trans*	0.268 C	0.275 C	16.1	−0.59		1624	1406
Cu)*dl*-Met)$_2$[21]	*trans*	0.271 C	0.271 C	16.6	−0.51		1621	1399
Cu(*l*-Ala)$_2$[14]	*trans*	0.270 C	0.290 C	16.3	−0.09	2A	1621	1399

[a] Upper index refers to the crystal structure reference.

[b] In nm units.

[c] W denotes a water, C a carboxylate, and A an amide oxygen atom as the *axial* donor, while P stands for carbon atoms of the phenolic ring.

[d] In 10^3 cm^{-1} units.

[e] Carboxylate stretching frequencies in cm^{-1} units; sh denotes a shoulder.

[f] One of the two lowest wavenumber bands is assumed to correspond to β_s(NH$_2$).

The variation of the $\log f(R)_{max}$ values in the series is in accordance with the expectations based upon the simple picture [12] shown above. The non--centric molecules have higher $\log f(R)_{max}$ values than centric ones (Table I, Fig. 1), and the tendency can also be observed that, as the shorter *axial* bond length increases, the $\log f(R)_{max}$ decreases (Fig. 1). (It is to be noted that, with the exception of the complex $Cu(dl\text{-Pro})_2 \cdot 2H_2O$, the distance of the sixth donor atom from the Cu(II) is approximately equal to or greater than the bond length of 0.27 nm corresponding to semi-coordination [4], indicating a very weak interaction.) Therefore, the molecules of different complexes appear to have a similar dynamic distortion, which leads to similar effects on the transition moments between d-orbitals. On the other hand, the individual proportionality constants between $f(R)$ and ε [11] should be of similar magnitude for the members of the series.
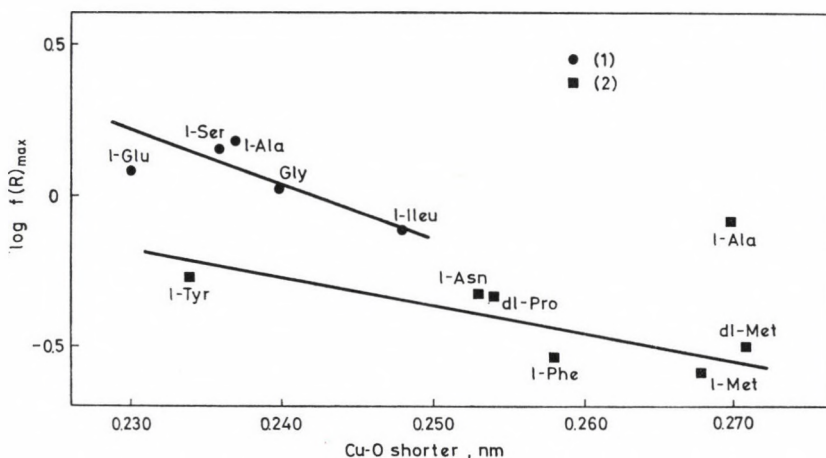
Fig. 1. $\log f(R)_{max}$ vs. length of shorter *axial* Cu—O bond curve for copper(II) α-amino acid complexes of known crystal structure. (1): non-centric molecules, (2): approximately centric molecules

These findings are presumably valid for the compounds of unknown crystal structure, too. We can therefore use the $\log f(R)_{max}$ values to predict whether these compounds are of *cis* or *trans* structure, and whether the interaction with the fifth donor atom is relatively strong or negligible. Suggested copper(II) coordinations are shown in Table II. Naturally, there can be exceptions among the compounds of unknown structure as well as in the group of complexes of known crystal structure. The complex *trans*-$Cu(l\text{-Ala})_2$, with a practically square-planar geometry, has an abnormally high $\log f(R)_{max}$ value (Fig. 1). *Trans*-$Cu(dl\text{-Pro})_2 \cdot 2H_2O$, in which the donor N atoms are members of pyrrolidine rings, has *axial* bonds of equal length (Table I), and hence a lower $\log f(R)_{max}$ would be expected. It seems that those molecular moieties

Table II

Diffuse reflectance and infrared spectral data and probable coordination geometry for copper(II) α-amino acid complexes of unknown crystal structure

Compound	$\overset{\bullet}{\nu}_{max}$ a	$\log f(R)_{max}$	Figure	ν_{as} b	ν_s b	Geometry	Axial interaction c
Cu(l-Asp) · 2H₂O	14.0	0.10		1604e	1314e		rs
Cu(dl-Asp) · 2H₂O	13.6	0.12		1610e	1404e		rs
Cu(l-Pro)₂ · 2H₂O	16.4	0.02	3F	1625	1371	cis d	rs
Cu(dl-Val)₂ · H₂O	16.0	−0.02	3B	1628	1376	cis	rs
Cu(dl-Ala)₂ · H₂O	16.5	−0.15	2C	1667 1628 1593	1396	cis	rs, C
Cu(l-Thr)₂ · H₂O	16.7	−0.25	4D	1624	1396	trans	rs
Cu(dl-Thr)₂	16.4	−0.25	4C	1621 1609	1402	trans	rs, C
Cu(Gly)₂ · H₂O	16.1	−0.26	4B	1614 1594	1392	trans d	rs, C
Cu(l-Lys)₂ · 2H₂O	15.7	−0.32		1619	1395	trans	po
Cu(l-Val)₂	16.0	−0.34	3C	1621	1389	trans	po
Cu(dl-Ileu)₂	16.4	−0.34	3E	1631	1387	trans	po
Cu(dl-Ser)₂	15.9	−0.36	2E	1636	1403	trans	po
Cu(dl-Leu)₂	16.1	−0.44		1632	1403	trans	n
Cu(l-Trp)₂	16.1	−0.52		1629	1390	trans	n
Cu(l-Gln)₂	16.4	−0.54		1621	1403	trans	n
Cu(dl-Trp)₂	16.1	−0.58		1634	1385	trans	n
Cu(l-Arg)₂ · 2H₂O	16.6	−0.59		1608	1399	trans	n
Cu(l-Leu)₂	16.0	−0.65		1633	1405	trans	n

a In 10^3 cm⁻¹ units.

b Carboxylate stretching frequencies in cm⁻¹ units.

c rs — relatively strong, po — probably occurs, n — negligible, C — carboxylate bridge between square-planar units

d Geometry supported by far infrared studies [1, 2, 9].

e Broad, blurred bands.

which do not take part directly in the coordination of copper(II) may have different effects on the transition moments in these complexes from those in other compounds.

In the carboxylate asymmetric stretching region of the infrared spectra, marked differences can be observed, depending on the role of the carboxylate groups in the copper(II) coordination (Tables I and II, Figs 2—4).* Those complexes in which none of the carboxylate groups are involved in relatively short *axial* bonds, have only one $\nu_{as}(CO_2^-)$ (Table I, Figs 2A, 3A, D, G). In *trans*-Cu(l-Tyr)₂ one of the carboxylate groups makes a relatively strong bridge between the square-planar units; the *axial* Cu—O distance is 0.234 nm [22]. The band of the carboxylate asymmetric stretching vibration is split into two bands of approximately equal intensity (Table I, Fig. 4A). In *cis-*

* The medium-intensity or strong band of the scissoring vibration of the amino group $(\beta_s(NH_2))$ can be expected in this region, too. It is generally masked by the strong carboxylate absorption or can be found at lower wavenumbers.
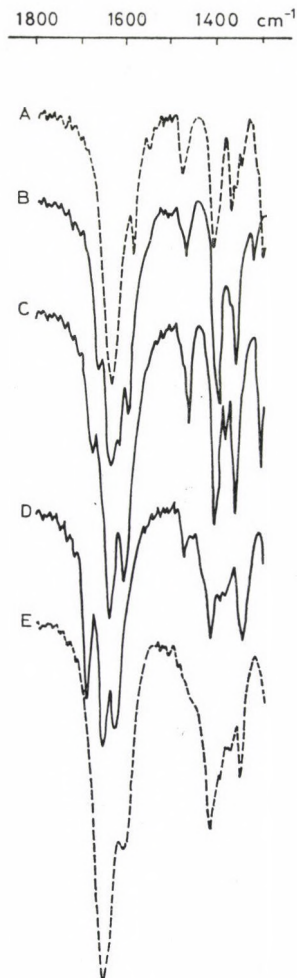
Fig. 2. Carboxylate stretching region of infrared spectra of copper(II) complexes of α-amino acids. A: *trans*-Cu(*l*-Ala)$_2$; B: *cis*-Cu(*l*-Ala)$_2$; C: Cu(*dl*-Ala)$_2$ · H$_2$O; D: *cis*-Cu(*l*-Ser)$_2$; E: Cu(*dl*-Ser)$_2$

-Cu(*l*-Ala)$_2$ and *cis*-Cu(*l*-Ser)$_2$, both the difference between the asymmetric stretching frequencies of the strongly bridging and non-bridging carboxylate groups and the coupling of these vibrations may influence the carboxylate vibrations. A very intense $\nu_{as}(CO_2^-)$ band at 1620—1640 cm^{-1} and bands of lower intensity at both higher and lower frequencies can be observed (Table I, Fig. 2B, D).

On the basis of the $\log f(R)_{max}$ values and the analogies of the infrared spectra to one of the above types, the following modes of copper(II) coordination in the complexes of unknown structure are proposed.
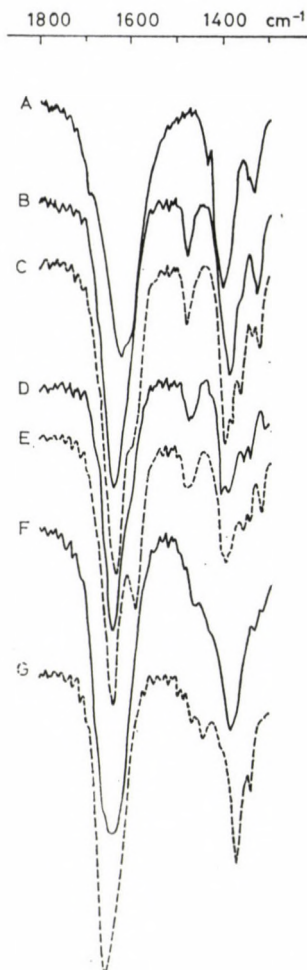
Fig. 3. Carboxylate stretching region of infrared spectra of copper(II) complexes of α-amino acids. A: *cis*-Cu(Gly)$_2$ · H$_2$O; B: Cu(*dl*-Val)$_2$ · H$_2$O; C: Cu(*l*-Val)$_2$; D: *cis*-Cu(*l*-Ileu)$_2$ · H$_2$O; E: Cu(*dl*-Ileu)$_2$; F: Cu(*l*-Pro)$_2$ · 2H$_2$O; G: *trans*-Cu(*dl*-Pro)$_2$ · 2H$_2$O

The complexes Cu(*dl*-Val)$_2$ · H$_2$O and Cu(*l*-Pro)$_2$ · 2H$_2$O have $\log f(R)_{max}$ values corresponding to the *cis* structure with relatively strong *axial* perturbation; however, they have only one $\nu_{as}(CO_2^-)$ (Table II, Fig. 3B, F). There is probably a water molecule at the fifth coordination position. The compound Cu(*dl*-Ala)$_2$ · H$_2$O seems to be of *cis* geometry with a strong carboxylate bridge, since the $\nu_{as}(CO_2^-)$ region of its infrared spectrum is analogous to those of *cis*-Cu(*l*-Ala)$_2$ and *cis*-Cu(*l*-Ser)$_2$ (Fig. 2C).

The $\log f(R)_{max}$ values of the second isomer of Cu(Gly)$_2$ · H$_2$O, Cu(*dl*-Thr$_2$) and Cu(*l*-Thr)$_2$ · H$_2$O correspond to those of *trans* complexes with relatively

strong *axial* interaction (Table II). The $\nu_{as}(CO_2^-)$ bands of the first two of these compounds are split into two bands of approximately equal intensity (Fig. 4B, C), pointing to a strong carboxylate bridge. In the last compound such a bridge is unlikely, since it has only one $\nu_{as}(CO_2^-)$ (Fig. 4D). The strong band at 1582 cm^{-1} is assigned to the $\beta_s(NH_2)$ vibration, since, on one hand, it has a lower intensity than the band at 1624 cm^{-1}. On the other hand, the splitting of 42 cm^{-1} of the $\nu_{as}(CO_2^-)$ band seems to be too high as compared to that of Cu(l-Tyr)$_2$ (<30 cm^{-1}, Table I) with an *axial* bond length of 0.234 nm.

The very low log $f(R)_{max}$ values of Cu(l-Leu)$_2$ and Cu(dl-Leu)$_2$ may be explained by *trans*-planar geometry. An alternative possibility is an elongated octahedral arrangement with relatively strong *axial* bonds. However, the only possible donor atoms for axial coordination are carboxylate oxygens, but the $\nu_{as}(CO_2^-)$ region does not show any carboxylate bridge. Therefore, these two compounds are likely to have practically a *trans*-planar geometry. The assumed geometry of Cu(l-Trp)$_2$, Cu(dl-Trp)$_2$, Cu(l-Gln)$_2$ and Cu(l-Arg)$_2 \cdot 2H_2O$ is the same, though in the last two of these compounds the functional groups of the side-chain may take part in the *axial* coordination, too.
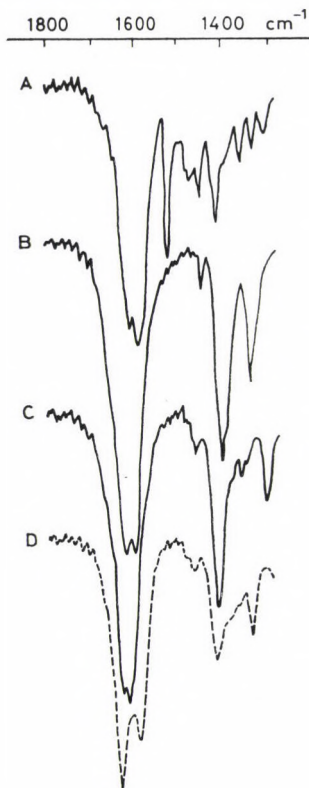
Fig. 4. Carboxylate stretching region of infrared spectra of copper(II) complexes of α-amino acids. A: *trans*-Cu(l-Tyr)$_2$; B: Cu(Gly)$_2 \cdot H_2O$; C: Cu(dl-Thr)$_2$; D: Cu(l-Thr)$_2 \cdot H_2O$

The complexes of aspartic acid are thought to have Cu(II) coordinated similarly to that in Cu(l-Glu) · 2H$_2$O, since their composition and log $f(R)_{max}$ values are the same, though splitting of the broad carboxylate bands cannot be observed.

The complexes Cu(l-Lys)$_2$ · 2H$_2$O, Cu(l-Val)$_2$, Cu(dl-Ileu)$_2$ and Cu(dl-Ser)$_2$ have log $f(R)_{max}$ values corresponding to the *trans* structure. Some kind of *axial* perturbation may occur, though the only $\nu_{as}(CO_2^-)$ band shows no considerable *axial* carboxylate coordination in these compounds.

The *trans* geometry was proposed both by Yasui and Shimura [6] and by us for Cu(l-Thr)$_2$ · H$_2$O and Cu(dl-Thr)$_2$. The complex Cu(dl-Ala)$_2$ · H$_2$O was found of *trans* geometry by the former authors [6], but of *cis* geometry by us. Our finding is supported by the splitting of the carboxylate asymmetric stretching band (see above). In the case of the ligands l-Val, dl-Val and dl-Ileu complexes of different compositions were isolated. Yasui and Shimura [6] prepared the complexes *cis*-Cu(l-Val)$_2$ · H$_2$O, *trans*-Cu(dl-Val)$_2$ and *cis*-Cu(dl-Ileu)$_2$ · H$_2$O, while the compounds *trans*-Cu(l-Val)$_2$, *cis*-Cu(dl-Val)$_2$ · H$_2$O and *trans*-Cu(dl-Ileu)$_2$ were obtained by us. This apparent contradiction may be explained by the fact that in solution a mixture of the *cis* (30—40%) and the *trans* (60—70%) isomers exists [24], and the configuration adopted in the solid state may be determined by kinetic rather than thermodynamic factors, and thus depends strongly on the way of preparation.

<p style="text-align:center">*</p>

REFERENCES

[1] Herlinger, A. W., Wenhold, S. L., Long, II, T. V.: J. Am. Chem. Soc., **92**, 6474 (1970)
[2] Herlinger, A. W., Long, II, T. V.: J. Am. Chem. Soc., **92**, 6481 (1970)
[3] Misumi, S., Isobe, T., Kimoto, S.: Bull. Chem. Soc. Japan, **45**, 2695 (1972)
[4] Hathaway, B. J., Billing, D. E.: Coord. Chem. Rev., **5**, 143 (1970)
[5] Yokoi, H.: Bull. Chem. Soc. Japan, **47**, 639 (1974)
[6] Yasui, T., Shimura, Y.: Bull. Chem. Soc. Japan, **39**, 604 (1966)
[7] Brown, D. H., Mangrio, N. G., Smith, W. E.: Spectrochim. Acta, **35A**, 123 (1979)
[8] Szabó-Plánka, T., Horváth, L. I.: J. Coord. Chem., **13**, 163 (1984)
[9] Delf, B. W., Gillard, R. D., O'Brien, P.: J. Chem. Soc. Dalton, **1979**, 1901
[10] Gillard, R. D., Mason, R., Payne, N. C., Robertson, G. B.: J. Chem. Soc. (A), **1969**, 1864
[11] Kortüm, G., Schreyer, G.: Z. Naturforsch., **11a**, 1018 (1956) and references therein
[12] Belford, R. L., Yeranos, W. A.: Mol. Phys., **6**, 121 (1963)
[13] Freeman, H. C., Snow, M. R., Nitta, I., Tomita, K.: Acta Cryst., **17**, 1463 (1964)
[14] Dijkstra, A.: Acta Cryst., **20**, 588 (1966)
[15] Van der Helm, D., Lawson, M. B., Enwall, E. L.: Acta Cryst., **B27**, 2411 (1971)
[16] Weeks, C. M., Cooper, A., Norton, D. A.: Acta Cryst., **B25**, 443 (1969)
[17] Mathieson, A. McL., Welsh, H. K.: Acta Cryst., **5**, 599 (1952)
[18] Van der Helm, D.: Franks, W. A.: Acta Cryst., **B25**, 451 (1969)
[19] Stephens, F. S., Vagg, R. S., Williams, P. A.: Acta Cryst., **B31**, 841 (1975)
[20] Ou C. C., Powers, D. A., Thich, J. A., Felthouse, T. R., Hendrickson, D. N., Potenza, J. A., Schugar, H. J.: Inorg. Chem., **17**, 34 (1978)
[21] Veidis, M. D., Palenik, G. J.: Chem. Comm., **1969**, 1277
[22] Van der Helm, D., Tatsch, C. E.: Acta Cryst., **B28**, 2307 (1972)
[23] Gramaccioli, C. M., Marsh, R. E.: Acta Cryst., **21**, 594 (1966)
[24] Goodman, B. A., McPhail, D. B., Powell, H. K. J.: J. Chem. Soc. Dalton, **1981**, 822

THEORETICAL STUDY OF THE UV SPECTRA
OF DISILANES

Tamás VESZPRÉMI*, Miklós FEHÉR, Emese ZIMONYI and
József NAGY

*(Department of Inorganic Chemistry, Technical University, Budapest,
H-1521 Budapest, Gellért tér 4.)*

UV spectra of some substituted disilanes were investigated by means of semi-empirical quantum-chemical calculations. The characteristic band of disilanes is of $\sigma^*(Si—Si) \leftarrow \sigma(Si—Si)$ type in case of saturated disilanes, in phenyl derivatives it has $[\sigma^*(Si—Si) - \pi^*] \leftarrow [\sigma(Si—Si) - \pi]$ character. The role of Si 3d orbitals is insignificant.

One of the most striking features of di- and polysilanes is that they absorb in the near ultraviolet and are chromophores when a phenyl group is in a conjugated position. This phenomenon was first reported by Hague and Prince [1] in 1962. Many explanations were published for this fact and some of them are briefly summarized below.

Hague and Prince described the new band in the spectrum of hexaphenyldisilane as the $\pi^* \leftarrow \pi$ band of the phenyl group which has a large bathochromic shift when it is in interaction with the Si—Si bond. Later they altered there view considering Gilman's [2] comment and concluded [3] that the origin of the intense transition was the Ph—Si—Si moiety. Gilman et al. [4] reported that the polysilane skeleton itself has UV absorption. Pitt et al. [5] assumed that an interaction took place between the unoccupied π^* orbitals of the phenyl group and the 3d orbital of silicon and that is the excited state. Sakurai [6, 7] suggested that the ground state is constructed by the conjugation of the silicon atoms of the polysilane chain just like in the case of conjugated alkenes. This σ framework interacts with the aryl or vinyl π system and a new band arises which is as signed as ^1L_a after Platt's [8] classification. Thus the transition is of $[\sigma(3d_{Si}) - \pi^*] \leftarrow [\sigma - \pi]$ type. This was confirmed by the fact that when the $\sigma - \pi$ conjugation is sterically hindered no ^1L_d band arises. That is the case in 1,1,2,2-tetramethyl-3,4-benzo-1,2-disilacyclopentene-3 where the Si—Si and Si—C bonds are in the nodal plane of the π system, thus no $\sigma - \pi$ conjugation is possible. The $\sigma(3d_{Si}) - \pi^*$ conjugation was confirmed by UPS measurements. Benzyltrimethylsilane and pentamethyl-phenyl-disilane have the same HOMO but a very different UV absorption because the excited state of pentamethylphenyldisilane is lower as a conse-

* To whom correspondence should be addressed.

quence of the conjugation. Traven and coworkers [9, 10, 11] concluded from UPS and CT measurements that there might be an interaction between the π^* and $3d_{Si}$ orbitals but ruled out the possibility of interaction or conjugation of the d orbitals. The UV absorption was explained by West et al. [12] in a different way. They considered the ground state as a mixing of σ and π orbitals but the excited state as the π^* orbital of benzene. Ramsey [13] studying the connection between the photochemistry of disilanes and the first UV transition, drew the conclusion from the supposed structure of the transitional complex that the excitation is of $\sigma^* \leftarrow \sigma$ type.

As can be seen the mentioned works give only qualitative models for this phenomenon. The aim of this work is to give a reliable explanation of the spectrum of disilanes based on quantum chemical calculations.

Calculations

A modified version [14] of the CNDO/S method was used for the calculations. The geometry parameters were taken from the literature [15]. The singlet transitions were calculated by the configuration interaction method using the first 42 configurations. The UV spectra were taken from the literature except that of phenylpentamethyldisilane, which was recorded on a SPECORD UV-VIS spectrophotometer in hexane using a 1 cm quartz cell. This compound was prepared by a new method from the reaction of phenyldimethylchlorosilane and trimethylchlorosilane with molten sodium in xylene at boiling temperature, and was purified by distillation. The purity of the compound was checked by gas chromatography.

Results and Discussion

In the course of our work we studied disilanes substituted with unsaturated and saturated groups. After making quantum-chemical calculations on the former ones it can easily be noticed that no mixing of the transitions occurs after the Cl. The longest wavelength band is due to the transition from the HOMO to the LUMO. These levels are of $\sigma(Si-Si)$ and $\sigma^*(Si-Si)$ character, respectively. In case of chlorine and thiomethyl substituents these orbitals also include the lone pair of chlorine and sulfur atoms but the linear coefficients of the Si-Si group are far greater. The bands are polarized in the direction of the Si-Si bond and have medium intensity. Further bands should appear in the far UV but there is no experimental data available for this region. The first transitions of the discussed compounds are summarized in Table I. The calculated oscillator strength (f), the first ionization potentials from UPS measurements (IP) and the calculated energy difference between the HOMO and LUMO (Δ) are also given.

Table I

UV *data of some saturated disilanes* (in eV)

	IP [16]	Δ	E_{sp} calc.	E_{spd} calc.	f	$E_{exp.}$ (ε)
Hexamethyldisilane (I)	8.7	8.64	5.46	5.72	0.229	6.26 (8000) [2]
Chloropentamethyldisilane (II)	8.9	8.54	5.33	5.48	0.193	
1,2-Dichlorotetramethyldisilane (III)	9.2	8.62	5.42	5.59	0.184	6.08 (3200) [19]
1,1,2,2-Tetrachlorodimethyldisilane (IV)	9.9	8.28	5.09	5.50	0.159	
1,2-Difluorotetramethyldisilane (V)	9.3	8.97	5.81	5.83	0.263	6.20 (2300) [20]
1,2-Dimethoxytetramethyldisilane (VI)	8.7	8.42	5.40	5.59	0.266	6.11 (18 000) [21]
1,2-Dimethylthiotetramethyldisilane (VII)	8.5	8.44	5.30	5.48	0.221	5.10 (31 000) [20]

Taking the d orbitals into the calculations (spd) the energies of the UV transitions slightly increase as compared with the calculations without d orbitals. Nevertheless the first transition remains of $\sigma^*(Si-Si) \leftarrow \sigma(Si-Si)$ type. The only anomalous case is the spectrum of **VII** where the great decrease in the energy of the UV transition is not shown by the calculations. As the energy of the HOMO is properly given by the calculation (it can be proved by UPS), the main cause of difference is that the calculations neglect the role of the sulfur lone pair in the first transition. In compounds lacking an Si—Si bond but having an Si—S bond a band arises at about 220 nm (5.64 eV), which is of $\sigma^* \leftarrow n$ type [16]. This band is likely to mix with the Si—Si bond and appears at 243 nm (5.10 eV). In the other compounds the negative inductive effect tends to lower both the energy of the HOMO and the LUMO [17], therefore, the band remains between 198 and 205 nm.

In the UV spectrum of phenyl substituted polysilanes there is a new band at 230—260 nm, which is not present in the spectrum of benzene or trimethylphenylsilane. The only difference between the spectra of benzene and trimethylphenylsilane is that the bonds of the latter occur at longer wavelengths [18]. The main peculiarity of the spectrum of pentamethylphenyldisilane is a new band at 230.5 nm which is of medium intensity, and the other bands are red-shifted. The quantum-chemical calculations predict five sets of bands. The α band has a small intensity and the polarization direction is
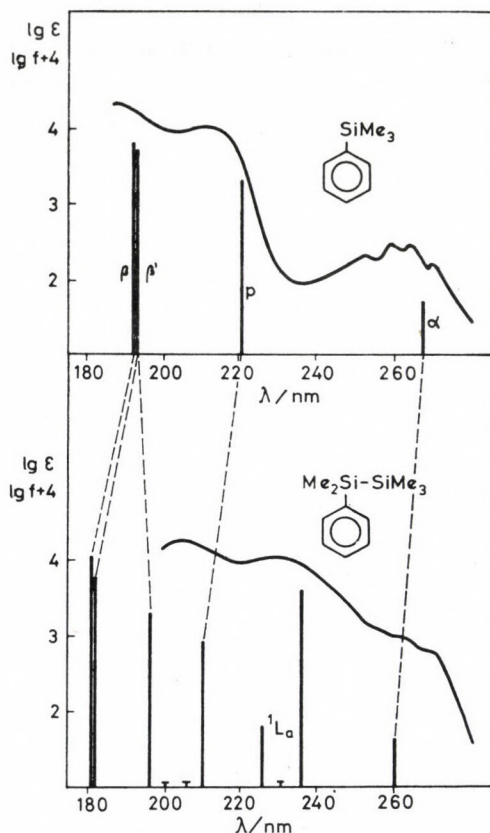
Fig. 1. Calculated and observed UV spectra of trimethylphenylsilane and phenylpentamethyl disilane

perpendicular to the substitution in the plane of the benzene ring. The next ^1L_a band has a medium intensity and is a result of the mixing of the Si—Si bond and the aromatic π system. The bond is made up of three transitions. The first is the transition of $\sigma^*(\text{Si}—\text{Si}) \leftarrow \sigma(\text{Si}—\text{Si})$, the second is $\sigma^*(\text{Si}—\text{Si}) \leftarrow \pi_3$, and the third is the combination of $\pi_5^* \leftarrow \pi_1$ and $\pi_5^* \leftarrow \sigma(\text{Si}—\text{Si})$ transitions where π_3 is the highest occupied π level, π_1^* is the lowest unoccupied one, and the numbering is made accordingly. The p band has medium intensity and is polarized parallel to the substitution in the plane of the benzene ring and contains transitions of the Si—Si bond only for a small extent. The β band has a greater intensity but polarized in the same direction as the p band, and the β' band has the same direction of polarization as the α band and has a very large intensity.

Using orbitals the calculations give the same result. Although the sequence of orbitals is slightly different in these calculations, both give the

Table II

UV data of substituted phenylpentamethyldisilanes

Phenylpentamethyldisilane

		E_{calc}^{*} (eV)	f^{+}	wave function	E_{exp}^{++} (eV)
1.	α	4.78 (4.84)	0.0086 (0.0059)	$0.75\ \Psi_{4-2} + 0.65\ \Psi_{6-1}$	4.77 (790)
2.		5.26 (5.25)	0.3345 (0.0256)	$0.87\ \Psi_{4-1} - 0.42\ \Psi_{5-3}$	
3.	$^{1}L_a$	5.37 (5.37)	0.0007 (0.0254)	Ψ_{4-3}	5.37 (10 900)
4.		5.49 (5.38)	0.0063 (0.0888)	$0.70\ \Psi_{5-1} - 0.59\ \Psi_{7-1}$	
5.	p	5.89 (5.82)	0.0798 (0.3802)	$0.69\ \Psi_{4-1} - 0.42\ \Psi_{6-2}$	5.99 (21 900)
6.		6.08 (6.16)	0 (0.0020)	Ψ_{6-3}	
7.		6.19 (6.18)	0 (0.1567)	$0.74\ \Psi_{5-2} - 0.63\ \Psi_{7-2}$	
8.	β'	6.33 (6.37)	0.3138 (0.0032)	$0.74\ \Psi_{7-3} + 0.64\ \Psi_{6-2}$	
9.		6.81 (6.53)	0.6344 (0.0004)	$0.61\ \Psi_{6-2} - 0.51\ \Psi_{7-3} + 0.47\ \Psi_{4-1}$	
10.	β	6.83 (6.62)	1.1836 (0.4063)	$0.73\ \Psi_{6-1} - 0.64\ \Psi_{4-2}$	

p-Methylphenylpentamethyldisilane

		E_{calc} (eV)	f	wave function	E_{exp}^{++} (eV)
1.	α	4.58	0.0264	$0.82\ \Psi_{4-2} + 0.57\ \Psi_{6-1}$	
2.		5.07	0.0010	Ψ_{4-3}	
3.	$^{1}L_a$	5.17	0.4402	$0.77\ \Psi_{5-3} - 0.58\ \Psi_{4-1}$	5.32 (12 800)
4.		5.59	0.0074	$0.69\ \Psi_{7-1} + 0.59\ \Psi_{5-1}$	
5.	p	5.72	0.0910	$0.65\ \Psi_{4-1} + 0.57\ \Psi_{5-3} - 0.35\ \Psi_{6-2}$	
6.		6.07	0	Ψ_{6-3}	
7.		6.11	0.0004	$0.74\ \Psi_{5-2} + 0.64\ \Psi_{7-2}$	
8.	β'	6.32	0.2628	$0.78\ \Psi_{7-3} - 0.58\ \Psi_{6-2}$	
8.	β	6.72	1.1142	$0.80\ \Psi_{6-1} - 0.56\ \Psi_{4-2}$	
10.	β'	6.74	0.6737	$0.72\ \Psi_{6-2} + 0.48\ \Psi_{7-3} + 0.40\ \Psi_{7-1}$	

p-Chlorophenylpentame thyldisilane

		E_{calc} (eV)	f	wave function	E_{exp}^{++} (eV)
1.	α	4.72	0.0034	$0.75\ \Psi_{4-2} + 0.64\ \Psi_{6-1}$	
2.		5.23	0.3914	$0.83\ \Psi_{5-3} - 0.49\ \Psi_{4-1}$	
3.	$^{1}L_a$	5.41	0.0001	$0.84\ \Psi_{4-3} - 0.36\ \Psi_{7-1}$	5.21 (17 800)
4.		5.42	0.0068	$0.59\ \Psi_{7-1} + 0.51\ \Psi_{5-1} - 0.49\ \Psi_{4-3}$	
5.	p	5.79	0.0942	$0.69\ \Psi_{4-1} + 0.47\ \Psi_{5-3} - 0.39\ \Psi_{6-2}$	
6.		6.11	0	Ψ_{6-3}	
7.		6.14	0	$0.75\ \Psi_{5-2} + 0.61\ \Psi_{7-2}$	
8.	β'	6.35	0.3402	$0.75\ \Psi_{7-3} - 0.61\ \Psi_{6-2}$	
9.	β	6.74	1.1581	$0.74\ \Psi_{6-1} - 0.63\ \Psi_{4-2}$	
10.		6.76	0.0012	$0.77\ \Psi_{5-1} - 0.56\ \Psi_{7-1}$	

* Data from calculations with d orbitals are in parentheses.
** The values in brackets are the molar absorptivities.

same results for UV transitions. The calculations with d orbitals give a somewhat smaller wavelength for α, p, β and β' bands, but the same wavelength for the ^1L_a band.

Introduction of a *para*-methyl group causes a slight bathochromic and hyperchromic effect, the *para*-chlorine substitution has an even smaller influence on the spectrum. The UV transitions of these aromatic compounds can be found in Table II. The calculated wavefunctions are also given, where suffix 3 refers to the LUMO, 4 to the HOMO and the numbering is made accordingly as follows: $1\text{-}\pi_5^*$, $2\text{-}\pi_4^*$, $3\text{-}\sigma^*(\text{Si}-\text{Si})$, $4\text{-}\pi_3$, $5\text{-}\sigma(\text{Si}-\text{Si})$, $6\text{-}\pi_2$, $7\text{-}\pi_1$ in all three compounds. The calculated and observed spectra of phenylpentamethyldisilane and the spectrum of phenyltrimethylsilane for comparison can be seen in Fig. 1. Thus on the basis of quantum-chemical calculations the ground state of the ^1L_a band of aromatic compounds is a mixing of $\sigma(\text{Si}-\text{Si})$ and π orbitals as reported earlier (e.g. [7]), the excited state however is the mixing of $\sigma^*(\text{Si}-\text{Si})$ and π^* orbitals. In saturated compounds $\sigma^*(\text{Si}-\text{Si}) \leftarrow \sigma(\text{Si}-\text{Si})$ transition occurs. The d orbitals of silicon have no considerable effect on the UV spectrum.

REFERENCES

[1] Hague, D. N., Prince, R. H.: Proc. Chem. Soc., **1962**, 300
[2] Gilman, H., Atwell, W. H., Schwebke, G. L.: J. Organomet. Chem., **2**, 369 (1964)
[3] Hague, D. N., Prince, R. H.: J. Chem. Soc., **1965**, 4690
[4] Gilman, H., Harrell, R. L.: J. Organomet. Chem., **5**, 201 (1966)
[5] Pitt, C. G., Jones, L. L., Ramsey, B. G.: J. Am. Chem. Soc., **89**, 5471 (1967)
[6] Sakurai, H., Tasolka, S., Kira, M.: J. Am. Chem. Soc., **94**, 9285 (1972)
[7] Sakurai, J.: J. Organomet. Chem., **200**, 261 (1980)
[8] Platt, J. R.: J. Chem. Phys., **17**, 484 (1949)
[9] Traven, V. F., Piatkina, T. V., Matthews, A., Stepanov, B. I.: Zh. Obshch. Khim., **43**, 685 (1973)
[10] Traven, V. F., West, R., Piatkina, T. V., Stepenov, B. I.: Zh. Obshch. Khim., **45**, 831 (1975)
[11] Traven, V. F., Eismont, M. J., Redchenko, V. V., Stepanov, B. I.: Zh. Obshch. Khim., **50**, 2001 (1980)
[12] West, R., Carberry, E.: Science, **189**, 179 (1975)
[13] Ramsey, B. G.: J. Organomet. Chem., **67**, C67 (1974)
[14] Veszprémi, T.: Chem. Phys. Lett., **88**, 325 (1982)
[15] L. E. Sutton: Tables of Interatomic Distances and Configuration in Molecules and Ions. Burlington House, London 1950
[16] Veszprémi, T., El-Kersh, M., Nagy, J.: J. Organomet. Chem., **184**, 147 (1980)
[17] Veszprémi, T.: Unpublished results
[18] Veszprémi, T., Réffy, J., Karger-Kocsis, J., Nagy, J.: J. Chim. Phys., **75**, 1013 (1978)
[19] Gilman, H., Chapman, D. R.: J. Organomet. Chem., **5**, 392 (1966)
[20] Waldhör, S.: Dissertation, Graz 1973
[21] Hengge, E., Holtschmidt, N.: J. Organomet. Chem., **12**, P5 (1968)

PHOTO-FRIES REARRANGEMENT: REARRANGEMENT OF ACETOXYBENZENE DERIVATIVES

Pavan Kumar SHARMA and Rajinder Nath KHANNA*

(Department of Chemistry, University of Delhi, Delhi-110007, India)

Photo-Fries rearrangement of 1,4-diacetoxybenzene, 1,3,5-triacetoxybenzene, 1,2,3-triacetoxybenzene and 1,2,4-triacetoxybenzene gave the corresponding mono- and di-*C*-acetyl migrated products.

Photo-Fries rearrangement [1—4] is a valuable method for the introduction of an acetyl side chain into *ortho* and *para* positions to a phenolic group. It was observed by us [4] that in the case of diacetoxy- or triacetoxynaphthalene derivatives only one acetyl group migrated to the adjacent *ortho* position over a double bond, while the other acetoxy group(s) remained intact.

All previous studies on photo-Fries migrations in benzene derivatives were carried out mainly with compounds in which only one acetyl or benzoyl group was available for migration. In order to explore the scope of these light-catalyzed reactions and to study the behaviour of diacetoxy- and triacetoxybenzene derivatives during the photo-Fries rearrangement, a study of 1,4-diacetoxybenzene (**1**), 1,3,5-triacetoxybenzene (**2**), 1,2,3-triacetoxybenzene (**3**) and 1,2,4-triacetoxybenzene (**4**) has been undertaken. The phenol esters **1** (m.p. [5] 122 °C), **2** (m.p. [6] 104 °C), and **3** (m.p. [6] 165 °C) were prepared by simple acetylation methods; **4** (m.p. [7] 96—97 °C) was synthesized by Thiele's acetylation of benzoquinone.

Compound **1** on photo-Fries migration gave three products, which were identified as 4-acetoxy-2-acetylphenol (**5**), 2,5-diacetylhydroquinone (**6**) and 2-acetylhydroquinone (**7**). Compound **2** gave 2-acetyl-3,5-diacetoxyphenol (phloroacetophenone diacetate) (**8**) and 5-acetoxy-2,4-diacetyl-1,3-dihydroxybenzene (**9**). Compound **3**, under similar conditions, afforded 6-acetyl-2,3-diacetoxyphenol (**11**) and 2-acetoxy-4,6-diacetyl-1,3-dihydroxybenzene (**12**), and **4** on such rearrangement gave a complex mixture of products from which 2-acetyl-3,6-diacetoxyphenol (**14**) could only be isolated. In any of the reactions no by-products were formed in isolable amounts, and a part of the start-

* To whom correspondence should be addressed.
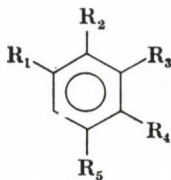
1 $R_1 = R_4 = OCOCH_3$, $R_2 = R_3 = R_5 = H$
2 $R_1 = R_3 = R_5 = OCOCH_3$, $R_2 = R_4 = H$
3 $R_1 = R_3 = R_2 = OCOCH_3$, $R_4 = R_5 = H$
4 $R_1 = R_2 = R_4 = OCOCH_3$, $R_3 = R_5 = H$
5 $R_1 = OH$,· $R_2 = COCH_3$, $R_3 = R_5 = H$, $R_4 = OCOCH_3$
6 $R_1 = R_4 = OH$, $R_2 = R_5 = COCH_3$, $R_3 = H$
7 $R_1 = R_4 = OH$, $R_2 = COCH_3$, $R_3 = R_5 = H$
8 $R_1 = OH$, $R_2 = COCH_3$, $R_3 = R_5 = OCOCH_3$, $R_4 = H$
9 $R_1 = R_3 = OH$, $R_2 = R_4 = COCH_3$, $R_5 = OCOCH_3$
10 $R_1 = R_3 = R_5 = OH$, $R_2 = R_4 = COCH_3$
11 $R_1 = COCH_3$, $R_2 = OH$, $R_3 = R_4 = OCOCH_3$, $R_5 = H$
12 $R_1 = R_5 = COCH_3$, $R_2 = R_4 = OH$, $R_3 = OCOCH_3$
13 $R_1 = R_5 = COCH_3$, $R_2 = R_3 = R_4 = OH$
14 $R_1 = R_4 = OCOCH_3$, $R_2 = OH$, $R_3 = COCH_3$, $R_5 = H$
15 $R_1 = R_2 = R_4 = OH$, $R_3 = COCH_3$, $R_5 = H$

ing esters were recovered on work-up. Though the reactions were found to be time-dependent, the prolongation of the reaction time beyond 12 h did not affect the yields.

All these compounds 5—15 were characterized by spectral studies and their conversions to the corresponding mono- and di-*C*-acetylbenzene derivatives which had previously been synthesized by Friedel-Crafts *C*-acetylation. Interestingly, compound (10) is a naturally occurring product isolated from the bacterium *Pseudomonas feurescens* [8].

Experimental

All m.p.'s are uncorrected. IR spectra were recorded on a Perkin-Elmer IR spectrophotometer Model-621 (ν max in cm^{-1}) in KBr. NMR spectra were obtained on a Perkin-Elmer R-32 (90 MHz) spectrometer using TMS as internal standard. Chemical shifts are recorded in δ ppm. Elemental analyses for all compounds were satisfactory within ±0.04% of the calculated values.

General procedure

Reactant 1—4 (20 mmol) was, dissolved in methanol (600 mL). The solution was divided into three equal portions. Each portion was irradiated under nitrogen atmosphere at a low wavelength, using a 450-W Ace Hanovia UV lamp (Model 6575), for 12 h. The portions were then combined, the solvent removed, and the residue chromatographed on a silica gel column. The column was eluted with petroleum ether and then with increasing amounts of benzene.

Photolysis of 1,4-diacetoxybenzene (1)

Compound 1 on photolysis gave the following three products, in addition to the initial ester (38%):
(a) **4-acetoxy-2-acetylphenol (5)**, colourless needles, m.p. 83—84 °C (yield 15%).
    IR (KBr): 3345 (br, OH), 1715, 1665, 1405, 1355, 1290, 1235, 1195, 1110.
    ^{1}H-NMR (CDCl$_3$): 12.10 (s, 1H, chelated OH), 7.40 (s, 1H, C$_3$—H), 7.15 (d, 1H, $J = 9.5$ Hz, C$_5$—H), 6.90 (d, 1H, $J = 9.5$ Hz, C$_6$—H), 2.60 (s, 3H, OCOCH$_3$), 2.35 (s, 3H, COCH$_3$).
    Acetate, m.p. 70 °C.
(b) **2,5-diacetylhydroquinone (6)**, yellow needles, m.p. 155 °C (yield 10%).
    IR (KBr): 3345 (br, OH), 1665, 1410, 1355, 1310, 1245.
    ^{1}H-NMR (CDCl$_3$): 12.10 (s, 2H, 2 OH, chelated), 7.25 (d, 2H, $J = 3$ Hz, C$_3$ and C$_6$—H), 2.60 (s, 6H, 2 OCH$_3$).
(c) **Quinacetophenone (7)**, greyish needles (yield 35%), m.p. 202 °C (*lit.* [5] m.p. 202—203 °C).
    Acetate, m.p. 70 °C. The recorded data (IR, UV, ^{1}H-NMR spectra) for the product were in complete agreement with those reported for quinacetophenone earlier.

Photolysis of 1,3,5-triacetoxybenzene (2)

Compound 2 on photolysis gave two products along with the initial ester (55%).
(a) **2-acetyl-3,5-diacetoxyphenol (8)**, white needles (yield 15%), m.p. 79—80 °C.
    IR (KBr): 3520 (broad), 1720, 1640, 1410, 1345, 1295, 1240, 1180, 1070 cm^{-1}.
    ^{1}H-NMR (CDCl$_3$): 12.80 (s, 1H, OH, chelated), 6.55 (d, 1H, $J = 3$ Hz, C$_6$—H), 6.45 (d, 1H, $J = 3$ Hz, C$_4$—H), 2.55 and 2.40 (2s, 3H each, 2 OCOCH$_3$), 2.35 (s, 3H, COCH$_3$).
    Compound 8 on deacetylation afforded phloroacetophenone [9].
(b) **5-acetoxy-2,4-diacetyl-1,3-dihydroxybenzene (9)**, white plates, m.p. 150 °C (yield 25%), which on deacetylation gave 2,4-diacetyl-1,3,5-trihydroxybenzene (2,4-diacetyl-phloroglucinol) **(10)**, m.p. 172—73 °C (*lit.* [10] m.p. 169—171 °C). The spectral data recorded were in complete agreement with those reported for the natural product [8].

Photolysis of 1,2,3-triacetoxybenzene (3)

Compound 3 on photolysis gave two products along with the initial ester (60%).
(a) **6-acetyl-2,3-diacetoxyphenol (11)**, white needles (yield 15%), m.p. 110—112 °C.
    IR (KBr): 3115 (br, OH), 1720, 1645, 1365, 1295, 1240.
    ^{1}H-NMR (CDCl$_3$): 12.00 (s, 1H, OH, chelated), 7.55 (d, 1H, $J = 10$ Hz, C$_5$—H), 6.75 (d, 1H, $J = 10$ Hz, C$_4$—H), 2.60 and 2.45 (2s, 3H each, 2 OCOCH$_3$), 2.30 (3H, COCH$_3$).
    Acetate derivative, m.p. 85 °C.
    Compound 11 on deacetylation gave gallacetophenone, m.p. 169—170 °C [11].
(b) **2-acetoxy-4,6-diacetyl-1,3-dihydroxybenzene (12)**, white needles, m.p. 209—210 °C (yield 20%) (*lit.* [12] m.p. 207—209 °C). Deacetylation of 12 afforded 4,6-diacetylpyrogallol **(13)**, m.p. 190 °C (*lit.* [12] m.p. 190—191 °C). The spectral data recorded for both compounds, 12 and 13, were in full agreement with those recorded earlier [12].

Photolysis of 1,2,4-triacetoxybenzene (4)

Photolysis of 1,2,4-triacetoxybenzene (4) gave a complex mixture from which 2-acetyl--3,6-diacetoxyphenol (14) could only be isolated as yellow needles (yield 15%), m.p. 116—118 °C.
    IR (KBr): 3350 (br, OH), 1710, 1645, 1420, 1345, 1240, 1196.
    ^{1}H-NMR (CDCl$_3$): 12.80 (s, 1H, OH, chelated), 6.80 (d, 1H, $J = 10$ Hz, C$_4$—H), 5.85 (d, 1H, $J = 10$ Hz, C$_5$—H), 2.60 (s, 6H, 2 OCOCH$_3$), 2.35 (s, 3H, —COCH$_3$).
    Triacetate, m.p. 100 °C (*lit.* [13] m.p. 95—97 °C), which on deacetylation afforded 3-acetyl-1,2,4-trihydroxybenzene (15), m.p. 160 °C (*lit.* [14] m.p. 157—159 °C).
    Spectral data for 15 were in full agreement with those recorded earlier [14].
    It can be concluded that the normal *ortho* migration constitutes the most vulnerable reaction. Compared with acetoxynaphthalenes, the acetyl migration in acetoxybenzenes takes place more readily and gives higher yields. In di- or triacetoxynaphthalene only one acetyl group migration has been observed due to partial fixation of the double bonds [4], while in di- or triacetoxybenzene migration of one or more than one acetyl groups may take place.

It may be noted that **photo-Fries migration** may be used for the preparation of compounds like **5** and **7—15**, which are difficult to synthesize by other standard methods. In the majority of cases no deacetylation has been observed.

REFERENCES

[1] Anderson, J. C., Reese, C. B.: Proc. R. Soc. London, **1960**, 217
[2] Crouse, D. J., Hurlbut, S. L., Wheeler, D. M. S.: Synth. Commun., **9**, 877 (1979)
[3] Pathak, V. P., Khanna, R. N.: Synthesis, **11**, 882 (1981)
[4] Sharma, P. K., Khanna, R. N.: Indian J. Chem. **23B**, 891 (1984)
[5] Vogel, A. I.: Text book of Practical Organic Chemistry, 3rd Ed., p. 677. Longmans, Green and Co., London—New York—Toronto 1956
[6] Heilbron, I.: Dictionary of Organic Compounds, 4th Ed., pp. 2747 and 2824, London 1965
[7] Govindachari, T. R., Nagrajan, K., Parthasarthy, P. C.: J. Chem. Soc., **1957**, 548
[8] Broadbent, D., Mabalis, R. P., Spencer, H.: Photochemistry, **15**, 1785 (1976)
[9] Gulati, K. C., Sethi, T. R., Venkataraman, K.: Org. Synth., **15**, 70 (1935)
[10] Dean, F. M., Robertson, A.: J. Chem. Soc., **1953**, 1241
[11] Badhwar, I. C., Venkataraman, K.: Org. Synth., **14**, 40 (1934)
[12] Heller, G.: Ber., **45**, 2391 (1912)
[13] Wilgus, H. S., Gates, J. W.: Can. J. Chem., **45**, 1975 (1967)
[14] Nakazawa, K.: J. Pharm. Soc. Japan, **59**, 297 (1939)

SYNTHESIS OF ANTIBACTERIAL QUINONES

Pavan Kumar SHARMA, Bal Kishore ROHATAGI and
Rajinder Nath KHANNA*

(Department of Chemistry, University of Delhi, Delhi-110007, India)

2-Methoxy-6-(1-propyl)-1,4-benzoquinone (**1**), 2,3-dimethoxy-6-(1-propyl)-1,4--benzoquinone (**2**) and 2-methoxy-6-(1-propyl)hydroquinone (**3**) have been synthesized along with their isomers and dipropyl analogues in fair yields by free radical propylation. 2,3-Dimethoxybenzoquinone (**8**) was prepared in yields better than before by a shorter and convenient route.

Volc et al. [1] isolated two pairs of antibiotical metabolites i.e. 2-methoxy--6-(1-propyl)-1,4-benzoquinone (**1**), 2-methoxy-6-(1-propyl)hydroquinone (**3**), 2,3-dimethoxy-6-(1-propyl)-1,4-benzoquinone (**2**), and 2,3-dimethoxy-6-(1--propyl)hydroquinone (**4**) from a culture medium of the fungus *Camrops microspora*. Dean [2] et al. prepared **1** by oxidation of 6-propylguaiacol (**17**) with ferric chloride and potassium persulfate, in poor yields. Compound **2** was also synthesized [3] in low yields by Friedel-Crafts propionylation of pyrogallol trimethyl ether, followed by partial demethylation and Clemmensen reduction, to give 2,3-dimethoxy-6-(1-propyl)phenol. The latter on oxidation with potassium nitrosodisulfonate furnished the quinone (**2**).

Because of the antibacterial activity of the quinone-hydroquinone pairs [1], we became interested in synthesizing these compounds in higher yields. While nitric acid oxidation of **17** gave only 15% of **1**, the action of alkaline hydrogen peroxide on 5-(1-propyl)vanillin (**18**) afforded **3** in 40% yield; the latter, on silver oxide oxidation, gave **1** in quantitative yields. The yields of the *m*-chloroperbenzoic acid oxidation [4] of **18** to give **3** were still higher (80%). Application of the same reaction to 2,3,4-trimethoxybenzaldehyde (**15**) afforded 2,3,4-trimethoxyphenol (**16**) [5]. Oxidation of the latter with aqueous ceric ammonium nitrate gave 2,3-dimethoxybenzoquinone (**8**) [6] in 80% yield. The present route followed for the synthesis of **8** is much shorter and the overall yields are good.

Compound **8** when subjected to free radical propylation using dibutyryl peroxide [7] in acetic acid afforded **2** (65%) and **6** (20%). Compounds (**5, 1**) (**10, 11**) and (**13, 14**) were prepared in similar manner from **7, 9** and **12**, respec-

---

* To whom correspondence should be addressed.
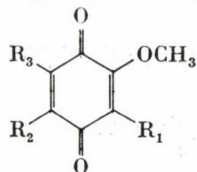
1   $R_1=R_2=H$, $R_3=C_3H_7$
2   $R_1=OCH_3$, $R_2=H$, $R_3=C_3H_7$
5   $R_1=R_3=H$, $R_2=C_3H_7$
6   $R_1=OCH_3$, $R_2=R_3=C_3H_7$
7   $R_1=R_2=R_3=H$
8   $R_1=OCH_3$, $R_2=R_3=H$
9   $R_1=R_3=H$, $R_2=OCH_3$
10   $R_1=C_3H_7$, $R_2=OCH_3$, $R_3=H$
11   $R_1=R_3=C_3H_7$, $R_2=OCH_3$
12   $R_1=R_2=H$, $R_3=OCH_3$
13   $R_1=C_3H_7$, $R_2=H$, $R_3=OCH_3$
14   $R_1=R_2=C_3H_7$, $R_3=OCH_3$
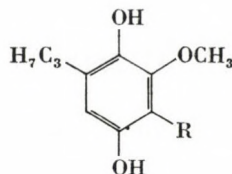
3   R=H
4   $R=OCH_3$
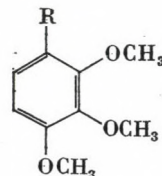
15   R = CHO
16   R = OH
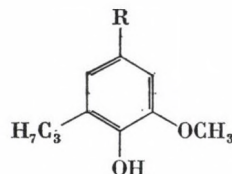
17   R = H
18   R = CHO

tively. ^{1}H-NMR spectra of the dipropyl analogues (i.e. **6, 11** and **14**) were almost identical. Compounds **5, 6, 10, 11, 13, 14** and **18** are new and reported for the first time.

Experimental

All m.p.'s are uncorrected. ^{1}H-NMR spectra (chemical shifts in δ ppm) were recorded in CDCl$_3$ on a Perkin Elmer R-32 (90 MHz) instrument using TMS as internal standard. Column chromatography and TLC were effected on silica gel.

5-(1-Propyl)vanillin (18)

5-Allylvanillin (1.6 g) prepared by allylation of vanillin followed by Claisen migration, gave on reduction in ethyl acetate (60 mL) with Pd/C—H$_2$ (10%; 2g; 4 h) **18** (1.6 g), as a white waxy solid, m.p. 83 °C.

^{1}H-NMR (CDCl$_3$): 0.85 (t, $J = 7$ Hz, 3H, CH$_2$—CH_3), 1.50 (m, 2H, ArCH$_2$—CH_2), 2.60 (t, $J = 9$ Hz; 2H, ArCH_2—CH$_2$—), 3.90 (s, 3H, OCH_3), 6.40 (broad s, Ar—OH), 7.20 (s, 2H, Ar—H), 9.70 (s, 1H, Ar—CHO).

Table I

Reactant	Product	Yield, %	M.p. °C	¹H-NMR data (δ)
7	1	10	78	0.90 (t, 3H, CH_2-CH_3), 1.42 (m, 2H, CH_2CH_3), 2.45 (t, 2H, Ar$-CH_2$), 3.85 (s, 3H, OCH_3), 5.40 and 5.80 (2d, 1H each C_5- and C_3-H)
	5	40	85	0.95 (t, 3H, CH_2CH_3), 1.50 (m, 2H, CH_2CH_3), 2.40 (t, 2H, Ar$-CH_2-$), 3.80 (s, 3H, OCH_3), 5.90 (s, 1H, C_3-H), 6.45 (s, 1H, C_6-H)
8	2	40	viscous oil	0.92 (t, 3H, CH_2-CH_3), 1.44 (m, 2H, CH_2CH_3), 2.45 (t, 2H, Ar$-CH_2-$), 3.95, 3.98 (2s, 3H each, 2 OCH_3), 6.30 (s, 1H, C_5-H).
	6	30	viscous oil	0.92 (t, 6H, $2\times CH_2-CH_3$), 1.45 (m, 4H, $2\times CH_2-CH_3$), 2.45 (t, 4H, $2\times$Ar$-CH_2-$), 3.90 and 3.95 (2s, 3H each, 2 OCH_3).
9	10	35	viscous oil	0.90 (t, 3H, CH_2-CH_3), 1.45 (m, 2H, CH_2-CH_3), 2.45 (t, 2H, Ar$-CH_2-$), 3.90, 3.92 (2s, 3H each, 2 OCH_3), 5.50 (s, 1H, C_6-H).
	11	30	viscous oil	0.90 (t, 6H, $2\times CH_2-CH_3$), 1.45 (m, 4H, $2\times CH_2-CH_3$), 2.46 (t, 4H, $2\times$Ar$-CH_2$), 3.90 and 3.92 (2s, 3H each, 2 OCH_3).
12	13	40	viscous oil	0.95 (t, 3H, CH_2-CH_3), 1.40 (m, 2H, CH_2CH_3), 2.38 (t, 2H, Ar$-CH_2$), 3.80 and 3.92 (2s, 3H each, 2 OCH_3), 5.80 (s, 1H, C_5-H).
	14	30	viscous oil	0.92 (t, 6H, $2\times CH_2-CH_3$), 1.38 (m, 4H, $2\times CH_2-CH_3$), 2.30 (t, 4H, $2\times$Ar$-CH_2-$), 3.85 (s, 6H, 2 OCH_3).

2-Methoxy-6-(1-propyl)hydroquinone (3)

A mixture of 18 (1.5 g) and m-chloroperbenzoic acid (3.5 g) in methylene chloride (35 mL) was stirred for 2 h at room temperature. An aqueous sodium thiosulfate solution (10%, 20 mL) was added and the stirring continued for further 45 min. The reaction mixture was shaken with 10% sodium thiosulfate solution (50 mL) and the two phases were separated. The aqueous phase was extracted with methylene chloride (2×20 mL) and the extract mixed with the organic phase. The organic phase was washed with brine (2×60 mL) followed by water (2×60 mL) and finally dried (MgSO$_4$). The solvent was removed in vacuum and a precooled mixture of freshly distilled THF and methanol (1 : 1, 10 mL) added. An ice-cold solution of 10% KOH in methanol (5 mL) was added in two portions, with shaking. After 15 min, the solution was acidified with 5% HCl and water (100 mL) was added. The solution was extracted with methylene chloride (2×50 mL), the organic phase washed with water (2×50 mL) followed by brine (2×50 mL) and then water, and dried (MgSO$_4$). Evaporation of the solvent left 3 as an oil (1.2 g).

¹H-NMR (CDCl$_3$): 0.9 (t, 3H, CH_2CH_3), 1.50 (m, 2H, ArCH_2-CH_2), 2.40 (t, 2H, ArCH_2CH_2), 3.90 (s, 3H, OCH_3), 5.70 and 6.40 (2d, $J = 2$ Hz 1H each, ArH).

2-Methoxy-6-(1-propyl)benzoquinone (1)

Compound 3 (1.2 g) was dissolved in dry benzene and silver oxide (1.5 g) and sodium sulfate (5 g) were added. The mixture was stirred for 3 h, filtered, and the filtrate evaporated. The residue was crystallized from methanol to obtain orange red crystals of 1 (1.0 g), m.p. 78 °C (lit. [1], m.p. 78—79 °C).

2,3,4-Trimethoxyphenol (16)

2,3,4-Trimethoxybenzaldehyde [8] (15) (2 g) was treated with *m*-chloroperbenzoic acid 45 g) as above to give 16 as a viscous liquid (1.3 g).
^{1}-H-NMR (CDCl$_3$): 3.80, 3.89, 3.95 (3a, 3H each, 3 OCH$_3$), 5.35 (s (broad), 1H, O*H*), 660 (s, 2H, Ar—*H*).

2,3-Dimethoxybenzoquinone (8)

To a solution of 16 (1.2 g) in acetonitrile (80 mL), an aqueous solution of ceric ammonium nitrate (8.1 g in 80 mL of water) was added during a period of 10 min, with shaking in a separating funnel. Water (300 mL) was added, followed by shaking for 5 min. The mixture was extracted with methylene chloride (2 × 100 mL) and the organic phase washed with water (2 × 100 mL), followed by aqueous sodium hydrogen carbonate solution (5%, 2 × 100 mL), and dried (Na$_2$SO$_4$). On concentration a residue was obtained which on chromatographic purification afforded orange coloured crystals (0.8 g) of 2,3-dimethoxybenzoquinone, m.p. 68 °C (*lit.* [6], m.p. 66—67 °C).
^{1}H-NMR (CDCl$_3$): 4.15 (s, 2 × 3H, 2 OCH$_3$), 6.65 (d, 2H, $J = 9$ Hz, C5,6—H).

Reaction of dibutyryl peroxide with 7,8,9 and 12. General Procedure

Benzoquinone (0.001 mol) was dissolved in glacial acetic acid (25 mL) and butyryl peroxide (0.001 mol) was added. The reaction mixture was heated over a free flame till brisk effervescence started. It was transferred to a boiling water bath and heated for 1 h. After cooling, the mixture was poured onto crushed ice and extracted with ether (2 × 50 mL) and dried (Na$_2$SO$_4$). After concentration it was subjected to column chromatography to separate the products. The results are tabulated.

REFERENCES

[1] Volc, J., Sedmera, P., Roy, K., Sasek, V., Vokoun, J.: Collect, Czech. Chem. Commun., 42, 2957 (1977)
[2] Dean, F. M., Osman, A. M., Robertson, A.: J. Chem. Soc., 1955, 11
[3] Mcomie, J. F. W., Robbins, A. I.: Chem. and Ind., 22, 888 (1978)
[4] Hannan, H. L., Barber, R. B., Rapoport, H.: J. Org. Chem., 44, 2153 (1979)
[5] Godfrey, I. M., Sargent, M. V., Elix, J. A.: J. Chem. Soc., Perkin Trans. 1, 1974, 1353
[6] Baker, W., Smith, H. A.: J. Chem. Soc., 1931, 2542
[7] Fieser, L. F., Oxford, R. E.: J. Am. Chem. Soc., 64, 2060 (1974)
[8] Papadakis, P. E., Boand, W.: J. Org. Chem., 26, 2075 (1961)

TRIMETHYLSILYLATED N-ARYL-SUBSTITUTED CARBAMATES

Dezső Knausz[1]*, Zsuzsa Kolos[1], János Rohonczy[1] and
Kálmán Újszászy[2]

(*[1]Department of General and Inorganic Chemistry, Eötvös L. University,
H-1088 Budapest, Múzeum krt. 6—8. and
[2]Central Research Institute for Chemistry, Hungarian Academy of Sciences, H-1025
Budapest, Pusztaszeri út 59—67.)*

Trimethylsilyl N-aryl carbamates were prepared by reaction of the respective aniline derivatives, hexamethyldisilazane and carbon dioxide. Two mol-% of anhydrous $CoCl_2$ was found to act as a catalyst permitting to double the yield during an equal reaction time.

Introduction

In a previous communication a new synthesis for the preparation of trimethylsilylated N-alkyl-substituted carbamates has been reported [1]. By this method the corresponding ammonium carbamates are silylated with chlorotrimethylsilane. A similar method was attempted for the preparation of N-aryl-substituted derivatives. However, the first step of the above synthesis, namely the carbon dioxide addition to aromatic amines did not take place because of the low basicity of latter compounds. Thus methods reported in literature were used for the synthesis of N-aryl derivatives. According to Sheludyakov et al. [2—4], the N-phenyl derivative was prepared by the reaction of aniline and hexamethyldisilazane with the introduction of carbon dioxide at 70 to 75 °C for several hours:

$$RR'NH + (CH_3)_3Si-NH-Si(CH_3)_3 + CO_2 \rightarrow RR'N\overset{\overset{\displaystyle O}{\|}}{C}OSi(CH_3)_3$$
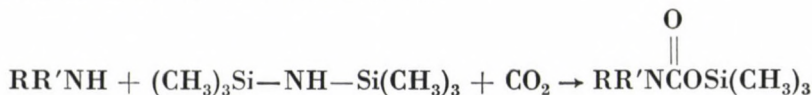
Shiina [5—7] prepared silyl carbamates by the carbon dioxide addition of silylamines using transition metal (Fe, V, Mo and W) chlorides and lithium metal as catalysts. The reaction took place in more than 100 hours, in a low yield. Another drawback of the above method is the fact that the respective silylamine has also to be prepared before the reaction.

---

* To whom correspondence should be addressed.

5*

Acta Chim. Hung. 120, 1985
Akadémiai Kiadó, Budapest
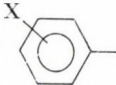
Results

The method of Sheludyakov was employed for the synthesis. First the preparation of the *N*-phenyl derivatives was reproduced, then six new compounds were synthesized. The yields and physical constants of the compounds are summarized in Table I; the characteristic MS, IR and ^{1}H-NMR data are given in Table II.

It is apparent from Table I that part of the compounds can be prepared in low yields and with long reaction times. In order to increase the rate of reaction, relying on the experience of Shiina, transition metal chlorides were employed as catalysts. Anhydrous $CoCl_2$ was found to be efficient.
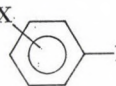
It is noteworthy that even the catalysts were ineffective in the case of aniline derivatives having a pK_a value lower than 2.5 (cf. m-$NO_2C_6H_4NH_2$, p-$NO_2C_6H_4NH_2$ and $(C_6H_5)_2NH$).

Table I

Physical constants and yields of (X—C₆H₄—)NHC(O)OSi(CH₃)₃ *compounds*

	X	Reaction time, h	Yield, %	M.p., °C	GC retention indices	Reference
1	H	6	44.6	129.0—130.0	1485 ± 2	[2]
2	o-CH₃	16	19.4	66.0—67.0	1506 ± 3	
3	p-CH₃	8	42.6	82.5—84.0	1587 ± 2	
4	m-CH₃O	17	41.0	56.0—58.0	1708 ± 3	
5	p-CH₃O	15	60.8	63.0—65.0	1723 ± 3	
6	p-Cl	8.5	51.3	105.0—106.5	1683 ± 3	
7	p-Br	16	34.2	94.0—95.0	1765 ± 4	

Table II

Mass spectra, IR and ^{1}H-NMR *data for* (X—C₆H₄—)NHC(O)OSi(CH₃)₃ *compounds*

	X	Mass spectra M⁺ m/e	Mass spectra M⁺ Int., %	Mass spectra M-15⁺ Int., %	IR (in CCl₄) ν(NH) cm⁻¹	IR (in CCl₄) ν(C=O) cm⁻¹	^{1}H-NMR (δ) in CDCl₃ (TMS standard) NH	^{1}H-NMR (δ) in CDCl₃ (TMS standard) OSi(CH₃)₃
1	H	209	34	17	3440	1719	6.76	0.34
2	o-CH₃	223	45	21	3455	1719	6.45	0.34
3	p-CH₃	223	42	14	3445	1717	7.11	0.31
4	m-CH₃O	239	51	18	3440	1719	7.14	0.33
5	p-CH₃O	239	85	21	3445	1715	7.25	0.33
6	p-Cl	243	43	26	3435	1720	6.98	0.33
7	p-Br	288	50	21	3440	1719	7.00	0.33
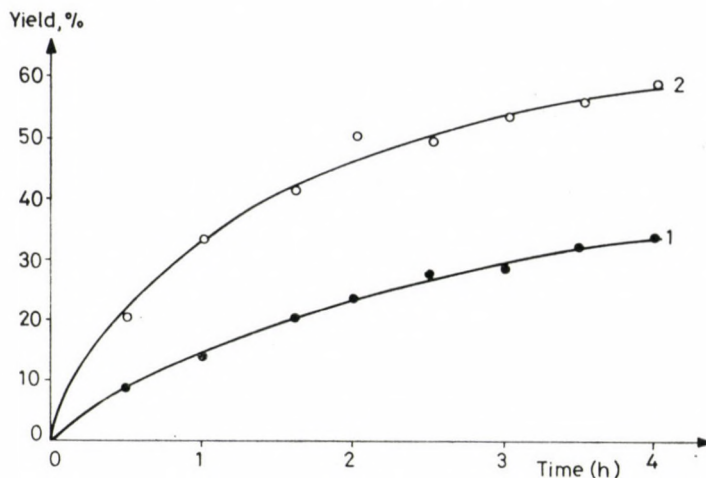
Fig. 1. Relative yields of trimethylsilyl N-p-tolyl carbamate as a function of the reaction time:
(1) non-catalytic reaction, (2) catalytic reaction

Model experiments were performed in order to study and compare the catalyzed and non-catalyzed reactions. p-Toluidine was used as a model compound. Equal amounts of two reaction mixtures of the same composition were placed in two reactors set in the same thermostat. Two mol-% of anhydrous $CoCl_2$ was added to one of the mixtures. Carbon dioxide was introduced at the same rate into the two reactors. The reaction mixtures were analysed in a gas chromatograph using n-hexadecane as internal standard. The results of the experiments revealed that silylated p-toluidine is the primary product in the reaction, followed by the formation of trimethylsilyl-N-p-tolyl carbamate. The quantity of silylated p-toluidine as a function of time exhibits a maximum. This fact suggests that the above compound is an intermediary product in the reaction. The quantity of the product formed in the catalytic and non-catalytic reactions, respectively, is shown in Fig. 1. It is apparent that the yields in the catalyzed reactions are nearly doubled, within the same reaction time. This is also shown in Table III.

Table III

Yields of [structure] — $NHC(O)OSi(CH_3)_3$ compounds in the catalyzed reactions

X	Reaction time, h	Yield %	Yield (cat. react.) / Yield (uncat. react.)
o-CH_3	16	28.7	1.48
p-CH_3	8	79.6	1.87
p-Cl	8.5	86.2	1.68

Experimental

Mass spectra were recorded with an AEI MS 902 spectrometer at 70 eV. IR spectra were obtained with a Specord 75 instrument using CCl_4 as solvent. ^{1}H-NMR data were measured with a 250 WM Brucker 250 MHz instrument. Gas chromatographic retention indices were determined with a 1100 JEOL gas chromatograph on a glass spiral column of 1.5 m × 3 mm i.d., packed with 10% OV-1 on 60—80 mesh Gas-Chrom Q and maintained at 150 °C.

Trimethylsilyl-N-p-tolyl carbamate

p-Toluidine (10.7 g; 0.10 mol) and hexamethyldisilazane (21.1 g; 0.075 mol) were weighed into a three-necked round-bottomed flask equipped with a gas inlet tube, a reflux condenser, a desiccator tube and stirrer. The mixture was heated to 70—75 °C and dry carbon dioxide was introduced at a rate of 40 mL min⁻¹, with vigorous stirring. The formation of the white ammonium carbamate precipitate indicated the start of the reaction. After 8 h the reaction mixture was cooled, and the product which precipitated in crystalline form was separated by filtration and recrystallized from n-hexane. The yield of the gas chromatographically pure product was 9.5 g (42.6%), m.p. 82.5—84.0 °C.

The other compounds listed in Table I were prepared in a similar way.

Trimethylsilyl-N-o-tolyl carbamate

o-Toluidine (10.7 g; 0.1 mol), hexamethyl disilazane (12.1 g; 0.075 mol) and $CoCl_2$ (0.5 g; 0.0036 mol) were weighed into the reaction vessel described above and heated to 70—75 °C, with the introduction of carbon dioxide for 16 h. After cooling, n-hexane (30 mL) was added to the mixture. The product remained in dissolved state and $CoCl_2$ could be filtered off. After evaporation of the solvent, the product was crystallized. The crude product was recrystallized from hexane to yield: 5.6 g (28.7%) of the compound, m.p. 66.0—67.0 °C.

The other compounds listed in Table III were prepared in a similar way.

*

REFERENCES

[1] Knausz, D., Meszticzky, A,. Szakács, L., Csákvári, B., Újszászy, K.: J. Organomet. Chem., **256**, 11 (1983)
[2] Sheludyakov, V. D., Kirilin, A. D., Mironov, V. F.: Zh. Obshch. Khim., **45**, 479 (1975)
[3] Sheludyakov, V. D., Kirilin, A. D., Gusev, A. I., Sharapov, V. A., Mironov, V. F.: Zh. Obshch. Khim., **46**, 2712 (1976)
[4] Kozyukov, V. P., Mironova, N. V., Mironov, V. F.: Zh. Obshch. Khim., **50**, 955 (1980)
[5] Shiina, K.: The VIIIth International Conference on Organometallic Chemistry, 1977, Kyoto, Japan, **5 13**, 207
[6] Shiina, K.: Oshie Jpn. Kokai Tokkyo Koko, **79**, 119418, Chem. Abstr., **92**, 129076 (1980)
[7] Shiina, K.: Oshie Jpn Kokai Tokkyo Koko, **79**, 128552, Chem. Abstr., **92**, 146899 (1980)

CONVERSION OF TOSYL AND MESYL DERIVATIVES OF THE MORPHINE GROUP, XXIV*

REACTIONS OF MORPHINE DERIVATIVES CONTAINING DOUBLE ALLYLIC SYSTEM

Sándor BERÉNYI, Sándor MAKLEIT** and Ferenc RANTAL

(Department of Organic Chemistry, Chemical Institute, Kossuth Lajos University, H-4010 Debrecen, P.O. Box 20)

On the basis of repeated and extended studies of the mechanism of the nucleophilic substitution reactions of 6-O-tosyl-14β-chloro-(bromo) codeine (**Ia** and **Ib**) containing double allylic system (in the pressence of Cl⁻, Br⁻ and N₃⁻ ions and in the absence of an outer nucleophilic partner), it has been found that our former results [Part XIII] are valid only for the reaction of 6-O-tosyl-14β-bromocodeine **Ib**, and that in molecules containing allyl halide and ¦allyl tosylate units the sequence of reactivity is as follows: allyl bromide > allyl tosylate > allyl chloride. Taking this into account, novel combination of mechanism are postulated.

In our previous paper [Part XXIII] nucleophilic substitution reactions of 6-O-tosyl-14β-chlorocodeine (**Ia**) and 6-O-tosyl-14β-bromocodeine (**Ib**), containing double allylic system, with Cl⁻ and Br⁻ ions have been reported. Taking into consideration the structures of the products of azidolysis (N⁻), concerning the mechanism of the multistep reactions it was concluded that in the case of compounds **Ia** and **Ib**, containing both allyl tosylate and allyl halide units, the allyl halide system was more reactive to the nucleophiles investigated.

On the basis of our recent extended studies, however, the above conclusion is true only in the case of **Ib**, and concerning the reactivity of the leaving group in the allylic position of compounds **Ia** and **Ib** the following sequence was found: allyl bromide > allyl tosylate > allyl chloride. Accordingly, starting from compound **Ib**, in dimethylformamide (DMF), the opening step of the reaction is an Sₙ2' reaction of the allyl bromide moiety to afford 7β-substituted neopine tosylate (**IIa—c**). A parallel 1,4-elimination reaction gives 6-tosyloxy-6-demethoxythebaine (**IVc**((Fig. 1).

Further nucleophilic reaction of the isolated intermediates (**IIa—c**) with Cl⁻ or Br⁻ ions yielded 6-chloro- and 6-bromo-6-demethoxythebaine (**IVa** and **IVb**) in an Sₙ2 + 1,2-E type reaction, whereas in the case of N₃⁻ ion 6β,7β-diazidodeoxyneopine (**IIIb**) was obtained as a result of an Sₙ2 reaction.
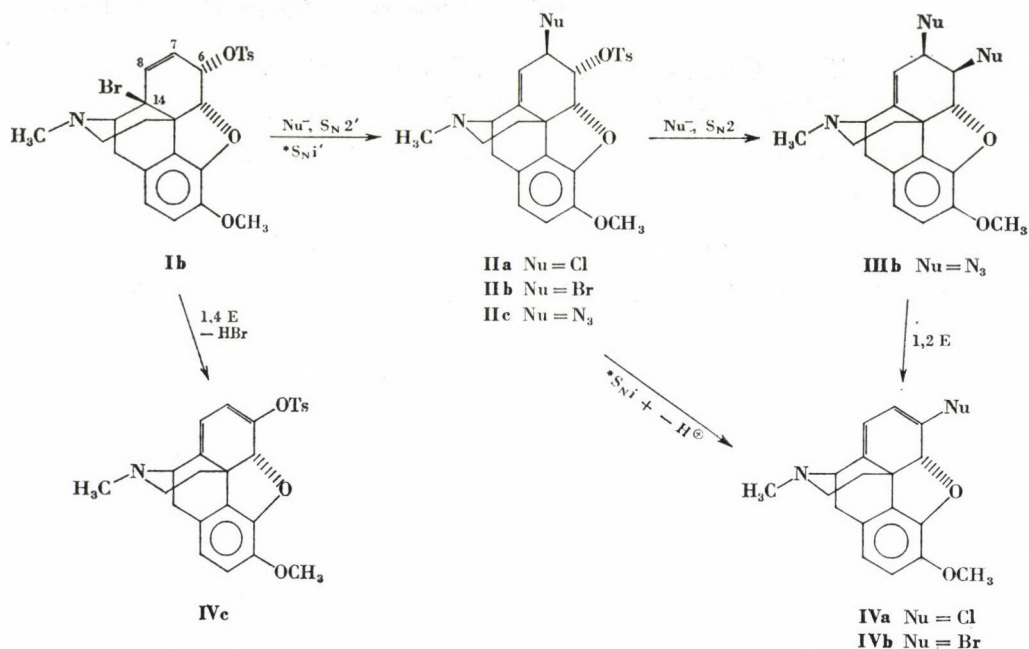
*Absence of outer nucleophilic partner.

Fig. 1

Heating of **Ib** in dimethylformamide for 30 minutes gave **IIb** and **IVc** in approx. 1 : 1 ratio in the absence of a nucleophilic partner. A probable mechanism of the **Ib → IIb** conversion is S_Ni' but the possibility of an S_N2' attack of the Br^- ion liberated in the 1,4-elimination (formation of **IVc**) cannot be excluded. On further heating, **IIb** is converted into **IVb** in a low yield, in an S_Ni type reaction accompanied by loss of proton.

6-*O*-Tosyl-14β-chlorocodeine (**Ia**) with Cl^- and Br^- ions gave **IVa** and **IVb** in excellent yields.

No intermediate (**IIa** and **IIb**) or 1,4-elimination product (**IVc**) could be detected or isolated; from this result we conclude that the first step of the reaction is S_N2 type reaction of the allyl tosylate moiety.

6,14-Disubstituted deoxycodeine (**V**) formed in this way yielded dienes (**IVa** and **IVb**) by S_N2' + 1,2-E mechanism. Compound **V** with N_3^- ion gave **IIIc** as the major product and **IIIb** as a by-product in an S_N1' type reaction. Substance **Ia** afforded **IVc**, too, as a result of 1,4-elimination and **Ia** gave **IIIb** via **IIc**; thus in the case of **Ib** the S_N2' + S_N2 mechanism was exclusive (Fig. 2).

In the absence of an outer nucleophilic partner compound **Ia** have **IIIa** besides **IVc** in dimethylformamide at 150 °C. We suppose that **IIIa** is formed
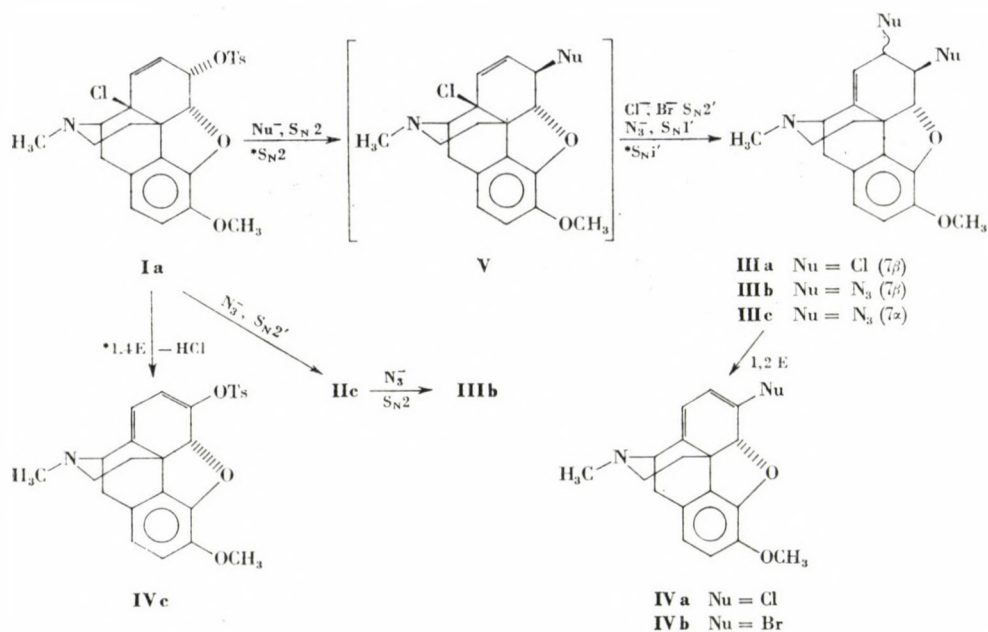
*Absence of outer nucleophilic partner.

Fig. 2

via **Va** according to $S_N2 + S_Ni'$ mechanism. The nucleophilic partner to the first step is provided by hydrogen chloride liberated in the 1,4-elimination. Compound **IIIa** yielded quantitatively **IVa** in a 1,2-E type reaction in dimethylformamide at 100 °C.

Experimental

M.p.'s were measured on a Koffler hot-stage, and are uncorrected. Thin-layer chromatography was performed on Merck 5554 silica gel 60 F_{254} foils using benzene : methanol (8 : 2) developing mixture. The detecting agent was Dragendorff reagent. Column chromatography was effected on Kieselgel 60 H adsorbent using benzene : methanol (9 : 1) eluent. The ^{1}H-NMR spectra were obtained with a Bruker WP 200 SY spectrometer. Mass spectra were measured with a VG-7035 (GC-MS-DS) instrument.

6-*O*-Tosyl-7β-chloroneopine (IIa)

A mixture of **Ib** [Part XXIII] (2.0 g; 3.7 mmol), lithium chloride (0.78 g; 18.5 mmol) and dry dimethylformamide (60 mL) was heated at 100 °C for 50 min, then poured into crushed ice and extracted with ether. The solvent was evaporated to yield an oil, which partly crystallized within 24 h. This substance was then triturated with a small amount of acetone to afford 540 mg of a crystalline product which proved to be a 1 : 1 mixture of **IIa** and **IVc**. From the mother liquor 1.0 g of **IIa**, as a contaminated oily material, was obtained. This product gave 600 mg oil (approx. 33%) on column chromatographic purification. Physical data of the hydrochloride: m.p. 224—225 °C, $[\alpha]_D$ −130 (c = 0.1, water).

Base (oil); ^{1}H-NMR (CDCl$_3$, δ ppm): 2.48 (s, 6H, NCH$_3$, PhCH$_3$); 3.85 (s, 3H, OCH$_3$); 4.7 (t, 1H, 7α-H); 4.93 (t, 1H, 6β-H); 5.08 (d, 1H, 5β-N); 5.8 (d, 1H, 8-H); 6.63 (ABq, 2H, Ar); 7.3 (d, 2H, Ar); 7.6 (d, 2H, Ar).
MS (m/e): 487 (M^+); 452 (M^+-35).

6-O-Tosyl-7β-bromoneopine (IIb)

(a) A mixture of **Ib** (2.0 g; 3.7 mmol), lithium bromide (1.59 g; 18.5 mmol) and dry dimethylformamide (60 mL) was heated at 100 °C for 20 min. The product was worked up as described in the case of **IIa** to obtain 400 mg (approx. 20%) of an oil which, after column chromatographic purification, crystallized from dry ether on standing for several days; m.p. 137—139 °C, [α]$_D$ —340 (c = 0.1, chloroform).
^{1}H-NMR (CDCl$_3$, δ ppm): 2.46 (s, 6H, NCH$_3$, PhCH$_3$); 3.81 (s, 3H, OCH$_3$); 4.80 (q, 1H, 7α-H); 4.94 (t, 1H, 6β-H); 5.18 (t, 1H, 5β-H); 5.8 (d, 1H, 8-H); 6.63 (ABq 2H, Ar); 7.33 (q, 2H, Ar); 7.62 (d, 2H, Ar).
MS (m/e): 531 (M^+); 452 (M^+-79).
(b) Compound **Ib** (0.53 g; 1 : 0 mmol) in dry dimethylformamide (15 mL) was heated at 100 °C for 30 min, then poured into cold water (75 mL) and extracted with ether. The solvent was evaporated after drying, and the residue crystallized from acetone to afford 117 mg of **IVc** [Part XXIII].
85 mg (15.9%) of **IIb** was obtained on column chromatographic purification from the mother liquor.

6β,7β-Dichlorodeoxyneopine (IIIa)

Compound **Ia** (3.0 g; 6.15 mmol) in dry dimethylformamide (90 mL) was heated at 150 °C for 50 min, poured into cold water (500 mL) and extracted with ether. The ethereal solution was washed with water, dried and the solvent evaporated.
The oily residue was triturated with acetone to afford 120 mg (4.3%) of crystalline **IVc**. An oil (600 mg) was obtained from the mother liquor; this gave 350 mg (approx. 16%) of **IIIa** as an oil after column chromatographic purification. This product was crystallized from acetone; m.p. 155—156 °C, [α]$_D$ —366.7 (c = 0.1, chloroform).
^{1}H-NMR (CDCl$_3$, δ ppm); 2.43 (s, 3H, NCH$_3$), 3.9 (s, 3H, OCH$_3$); 4.05 (d, 1H, 6α-H); 4.55 (q, 1H, 7α-H); 4.95 (d, 1H, 5β-H); 5.90 (d, 1H, 8-H); 6.73 (ABq, 2H, Ar).
MS (m/e): 352 (M^+); 317 (M^+-335); 282 (M^+-70).

6-Chloro-6-demethoxythebaine (IVa)

(a) Compound **IIIa** (10 mg; 0.028 mmol) in dry dimethylformamide (1.0 mL) was heated at 100 °C for 24 h, then poured into water (10 mL); the mixture was made alkaline and extracted with ether. The ethereal solution was dried and the solvent evaporated to leave a substance which was homogeneous in TLC; its ^{1}H-NMR and MS data were identical with those published previously [Part XXIII].
(b) A mixture of compound **IIa** (200 mg; 0.41 mmol), lithium chloride (0.1 g; 2.45 mmol) and dry dimethylformamide (6 mL) was heated at 100 °C for 24 h. The solvent was evaporated, 10 mL of water was added and the pH was adjusted to 8 with ammonium hydroxide. The mixture was extracted with chloroform, the solution washed with water, dried and the solvent evaporated. The oily residue gave 105 mg (81%) of a crystalline product on the addition of methanol; this was recrystallized from methanol–chloroform; m.p. 230—233 °C (lit. m. 233—235 °C [Part XXIII]).

6-Bromo-6-demethoxythebaine (IVb)

(a) A mixture of compound **IIb** (217 mg; 0.41 mmol), lithium bromide (0.18 g; 2.0 mmol) and dry dimethylformamide (6 mL) was heated at 100 °C for 24 h and then worked up as described for **IVa** to afford 104 mg (71%) of a crystalline product which was recrystallized from methanol : chloroform (3 : 1) mixture; m.p. 238—241 °C (lit. m.p. 241 °C [Part XXIII]).
(b) 200 mg (0.38 mmol) of **IIb** in dry dimethylformamide (6 mL) was heated at 100 °C for 24 h and worked up as described above to yield 36 mg (26%) of crystalline **IVb**.
*

Text

The text of the paper should be concise. The description of new compounds (in the Experimental) must include the complete analytical data. Special attention must be paid to structural formulas given within the text. Complicated (non-linear) formulas should be drawn on separate sheets of paper and their position in the text should be clearly marked. The numbering of formulas and equations (in parentheses on the right-hand side) is only needed if they are referred to in the text. Units should conform to the International System of Units (SI). In nomenclature the rules of the I.U.P.A.C. are accepted as standard. Symbols for physical quantities are printed in italic type and should, therefore, be underlined in the manuscript.

References

References should be numbered in order of appearance in the text (where the reference number appears in brackets) and listed at the end of the paper. The reference list, too, should by typed double-spaced. Journal titles are to be abbreviated as defined by the Chemical Abstracts Service Source Index.

Examples:

[1] Brossi, A., Lindlar, H., Walter, M., Schneider, O.: Helv. Chim. Acta, **41**, 119 (1958)
[2] Parr, R. G.: Quantum Theory of Molecular Electronic Structure, Benjamin, New York 1964
[3] Warshel, A.: in Modern Theoretical Chemistry, Vol. 7, Part A (Ed. G. A. Segal), Plenum Press, New York 1977

Tables

Each table should be given a Roman number and a brief informative title. Structural formulas should not be used in column headings or in the body of tables.

Figures

Figures should be numbered consecutively with Arabic numerals. Their approximate place should be indicated in the text on the margin. All figures must be identified on the back by the author's name and the figure number in pencil. Standard symbols (such as circles, triangles, squares) are to be used on line-drawings to denote the points determined experimentally. Line-drawings must not contain structural formulas and comments. Spectra or relevant segments thereof, chromatograms, and X-ray diffraction patterns will be reproduced only if concise numerical summaries are inadequate to replace them. Drawings and graphs should be prepared in black ink on good-quality white or tracing paper. Photographs should be submitted on glossy paper as high-contrast copies. Xerox or similar copies are not suitable for reproduction, but may be used for duplicate copies.

Redrawn illustrations will be sent to the authors for checking. No corrections of figures will, therefore, be accepted in the proofs.

Submission of manuscript

After having completed the corrections suggested by the referees and editors, the final manuscript should be submitted in duplicate, in a form ready for publication. If the corrected manuscript is not returned to the editors *within six weeks*, the intended publication of the paper will be regarded as withdrawn by the authors.

Page charge will not be assessed for the publication, however, authors from overseas countries must contribute to the postage of correspondence by sending, together with the manuscript, international postal coupons to the value of U.S. $ 10. —

Proofs and reprints

A set of proofs will be sent to the submitting author. The proofs must be returned within 48 hours of receipt. Late return may cause a delay in the publication of the paper. 100 reprints will be supplied to the authors free of charge.

Periodicals of the Hungarian Academy of Sciences are obtainable at the following addresses:

Acta Chimica Hungarica

VOLUME 120, NUMBER 3, NOVEMBER 1985

NOTICE TO AUTHORS

Acta Chimica publishes original papers on all aspects of chemistry in English. Before preparing a manuscript for submission to this journal authors are advised to consult recent issues.

Form of manuscript

Manuscripts, tables and illustrations should be submitted in triplicate. Manuscripts should be typewritten double spaced (25 lines, 50 characters per line including spaces). The *title page* should include (1) the title of the paper, (2) the full names of the author(s) in the sequence to be published; apply an asterisk to designate the name of the author to whom correspondence should be addressed, (3) name and address of the institution where the work was done. If the paper is part of a series, reference to the previous communication must be given as a footnote.

Abstract

A summary is printed at the head of each paper. This should not exceed 200 words and should state briefly the principal results and major conclusions of the work. It should be suitable for use by abstracting services.

CONTENTS

1

PREPARATION OF NEW TRICYCLIC HETERO SYSTEMS BY CYCLIZATION OF ISOMERIC HYDROXYALKYLAMINOPYRIDOPYRIDAZINONES

Károly KÖRMENDY*, Zsuzsanna SOLTÉSZ**, Ferenc RUFF and István KÖVESDI

(Organic Chemical Department, Eötvös Loránd University, H-1088 Budapest, Múzeum krt. 4/b)

Nine new tricyclic hetero systems (**13—21**) were synthesized by cyclization of 2-hydroxyethylaminopyridopyridazinone and 3-hydroxypropylaminopyridopyridazinone isomers with hydrogen bromide. Compounds **13—16**, **18—21** and **17** contain the imidazopyridopyridazine, the pyrimidopyridopyridazine and the tetraazabenzonaphthene skeleton, respectively. The imidazo and pyrimido rings in compounds **13—16** and **18—21**, respectively, are sensitive to alkali and can be readily cleaved. According to spectral studies, compounds **13—16** and **18—21**, as well as the derivatives **23**, **24** and **26—30**, obtained on alkaline hydrolysis, possess a zwitterionic structure in the base form.

In the course of our earlier work it was observed [1] that 2-hydroxyethylamino- and 3-hydroxypropylaminophthalazinones readily undergo cyclization to give imidazo[2,1-a]phthalazine and pyrimido[2,1-a]phthalazine systems on heating with mineral acids. In the case of analogous reactivities, the preparation of tricyclic hetero systems unknown up to now (**13—16**, **18—21**) is rendered possible starting from isomeric hydroxyalkylaminopyridopyridazinones (**1—8**).

The hydroxyethylaminopyridopyridazinones are known compounds (**1—4**); the four hydroxypropylamino compounds (**5—8**) were obtained by aminolysis of the isomeric monochloropyridopyridazinones with 3-aminopropanol. The starting materials readily undergo cyclization on treatment with 48% hydrobromic acid; for processes **1—4** → **13—16** refluxing for 2 h, and for processes **5—8** → **18—21** refluxing for 30 minutes is suggested. Progress of the reactions can be monitored by the depth of the colour of the hydrobromic acid solution. Compounds **1—8** are dissolved in hydrobromic acid to give an orange or orange-red colour; on the effect of heating, the colour of the solution — except in case of **4** — turns pale yellow (completion of cyclization is indicated by the yellow colour, since the solution of the isolated end-product in hydrobromic acid is yellow). The colour change takes place in 60 minutes in cases **1—3** → **13—15**, while the reaction is significantly faster in processes

---

* To whom correspondence should be addressed.
** Results of the diploma work (Budapest, 1982) of the author are included.

1*

Acta Chim. Hung. 120, 1985
Akadémiai Kiadó, Budapest

$(n=2)$ 1   2   3   4

$(n=3)$ 5   6   7   8

9   10   11   12

Fig. 1

13   14   15

.16   17
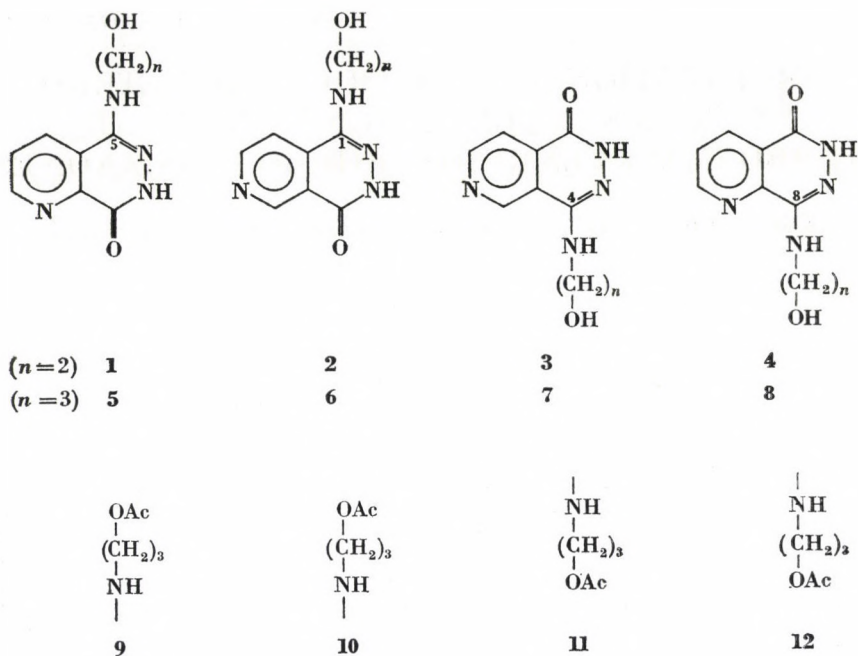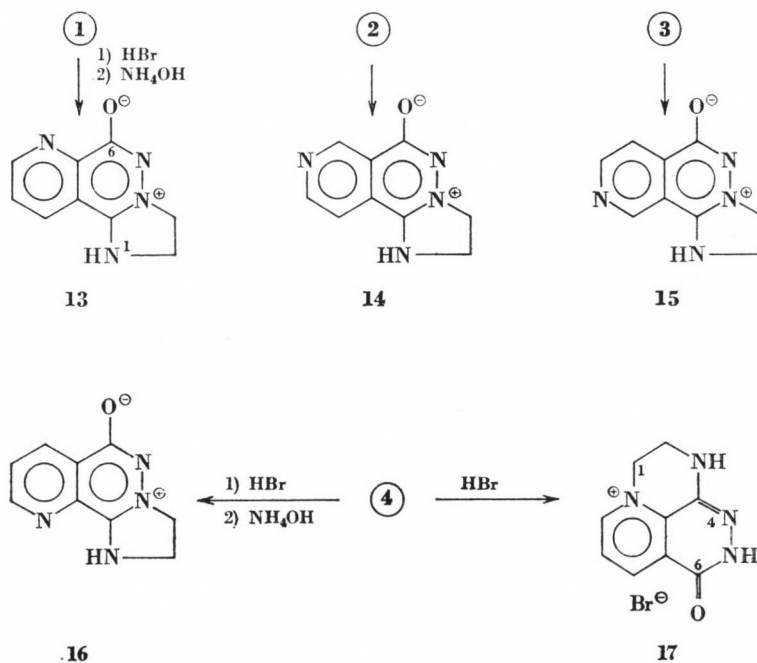
Fig. 2
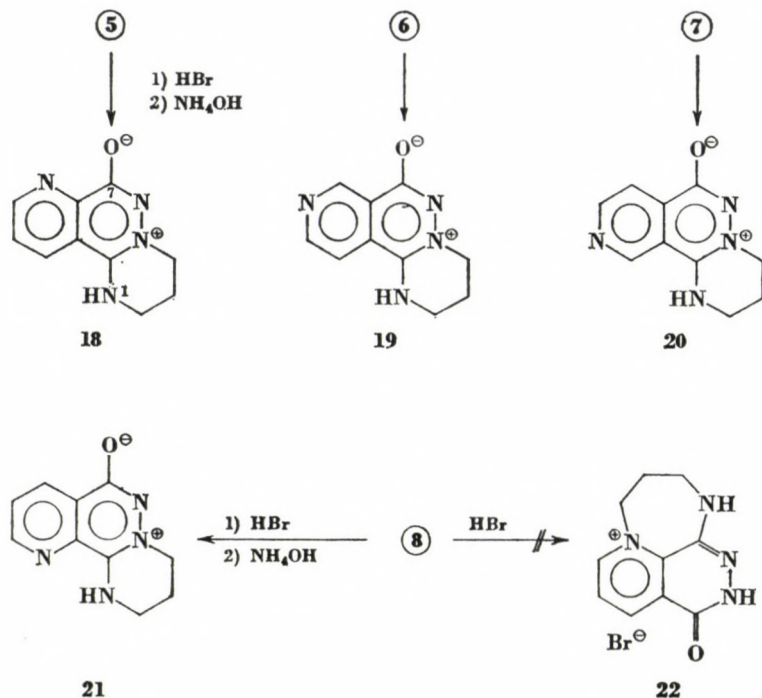
Fig. 3

5—8 → 18—21 (5—10 minutes). The cause of this effect is in accordance with our earlier experience [1] that anellation of the pyrimidine ring to the phthalazinone skeleton is much more favoured than that of the five-membered imidazo ring.

During cyclization, the primary reaction was assumed to be the exchange of OH → Br (transient bromine substitution was rendered probable on the basis of model experiments in our work mentioned [1]); these compounds then undergo cyclization via intramolecular N-alkylation. The end-products separate from the cold acid solution in the form of dibromides with vivid yellow colour, except **16** and **21** which can be isolated as colourless monohydrobromides also from acid media. All dihydrobromides are very unstable; they undergo hydrolysis to give colourless monohydrobromides in water. The aqueous solutions of the monohydrobromides, recrystallized from water or aqueous alcohol, have slightly acid reaction (about pH 4), which indicates a reduced basicity compared with the imidazo[2,1-a] and pyrimido[2,1-a[phthalazinone systems [1]. This is probably due to the electron-withdrawing effect of the nitrogen in pyridine.

In the IR spectra of the salts **13**—**16** and **18**—**21**, and of the bases liberated from them, broad NH bands appear in the range 3300—2000 cm^{-1},

Fig. 4

16   17
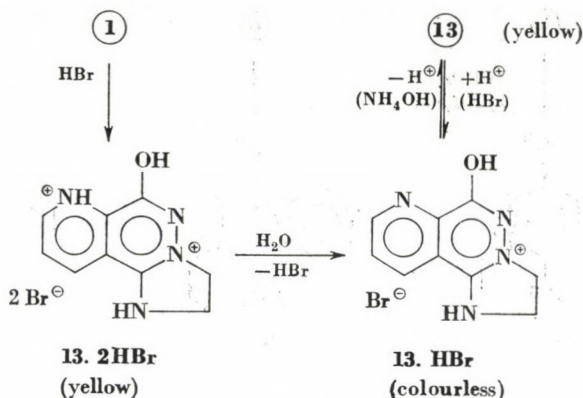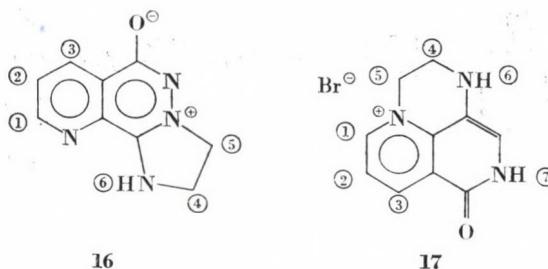
Fig. 5

which are merged also with the OH band in the spectra of the salts. The spectra have no amide carbonyl band, only bands with low intensity can be found above 1600 cm^{-1}, which can be assigned to C=N bonds. The spectra are analogous to the spectra of imidazo[2,1-a]phthalazinone and pyrimido[2,1-a]-phthalazinone with zwitterionic structure, published earlier [4]. Thus a zwitter-ionic structure can also be assumed for these compounds, which is transformed into the enolic form in salts.

Cyclization 4 → 16 takes place in a low yield (about 28%); the main direction of the reaction is the conversion 4 → 17. Since the solution of the hydrogen bromide salt of 17 in hydrobromic acid has a red colour, the colour of the solution turns from orange into red on boiling. This observation indicates that also in the formation of the tetraazabenzonaphthene derivative (17) the difference in ring anellation, depending on the number of ring members, does occur, and it is manifested in the rate of the reaction. In the present case, the coupling in the direction of the N(1) atom accompanied by the formation of a six-membered pyrazino ring takes place faster than the anellation of the five-membered ring into system 16. In process 8 → 21, however, cyclization

In analogous way:

14 - 16 ⟶ 24 - 26

18 - 21 ⟶ 27 - 30
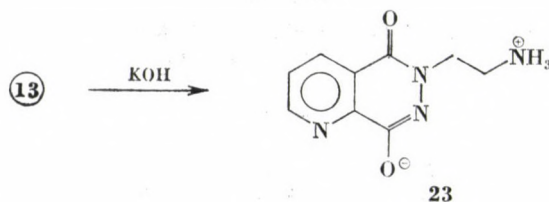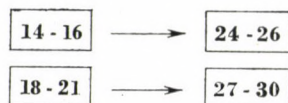
Fig. 6

is favoured in the direction of the N(7) atom, since the pyrimidine ring is formed much faster than the diazepine ring. Such reasons must be responsible for the fact that during the cyclization of **8** with hydrobromic acid, practically no compound **22** is obtained.

In the IR spectrum of **17**, no bands characteristic of charged NH groups are found; the secondary NH group, the amide NH and the carbonyl group bands appear in the ranges expected (3268, $3270-2600$, 1678 cm^{-1}). The positive charge is localized in the pyridine ring, as shown by the IR spectrum.

In compound **16**, the signal of the NH(6) proton overlaps the resonance of the heteroaromatic ring protons, yet it can be distinguished by the integral, and the fine structure of the spectrum. In compound **17**, both NH signals appear distincly in the spectrum. This assignment is confirmed by the higher chemical shift of the heteroaromatic ring protons in **17** as compared with those in **16**, which is probably partly due to the delocalized electron deficit in the heteroaromatic ring.

Table I

Chemical shifts and spin-spin coupling constants of 16 and 17. HBr

Compound	H(1)	H(2)	H(3)	H(4)	H(5)	NH(6)	NH(7)	$J_{H,H}$ Hz
16	9.13 (d.d.)	8.01 (d.d.)	8.62 (d.d.)	3.92 (m.)	4.57 (m.)	8.73 (s.)	—	$J_{1,2}^{ortho} = 4.6$ $J_{2,3}^{ortho} = 7.5$ $J_{1,3}^{meta} = 2.0$
17.HBr	9.59 (d.d.)	8.52 (d.d.)	9.31 (d.d.)	3.72 (m.)	4.97 (m.)	7.68 (s.)	12.70 (s.)	$J_{1,2}^{ortho} = 6.0$ $J_{2,3}^{ortho} = 8.0$ $J_{1,3}^{meta} = 1.0$

Table II

UV *spectral data of N-2-aminoethyl- and N-3-aminopropylpyrido-pyridazine-dione isomers*

Compound	Solvent	λ_max [nm]				(log ε)	
23	EtOH	207 sh 4.45	213 sh 4.16	263 3.80		326 3.65	
	0.1 *N* HCl	227 3.80		255 3.87		303 3.66	
	0.1 *N* NaOH			263 3.85		329 3.65	
24	EtOH	217 sh 4.00		274 3.45		320 3.63	345 sh 3.59
	0.1 *N* HCl	220 sh 3.85		274 3.48		309 3.60	376 3.16
	0.1 *N* NaOH			274 3.43		328 3.64	351 sh 3.61
25	EtOH	220 sh 4.02	226 sh 3.93	264 3.70		305 3.78	
	0.1 *N* HCl	220 sh 3.91	225 sh 3.82	263 sh 3.74	269 3.79	311 3.66	355 sh 3.43
	0.1 *N* NaOH			269 3.52		332 3.79	
26	EtOH	205 sh 4.46	213 sh 4.13	262 3.86		328 3.60	
	0.1 *N* HCl		226 sh 3.84	255 3.96		305 3.61	
	0.1 *N* NaOH			263 3.89		329 3.63	
27	EtOH	207 sh 4.40	213 sh 4.11	263 3.80		327 3.61	
	0.1 *N* HCl	221 3.83		256 3.85		306 3.63	
	0.1 *N* NaOH			263 3.82		331 3.61	
28	EtOH	222 sh 3.95		274 3.44		323 3.63	342 sh 3.60
	0.1 *N* HCl	220 sh 3.86	231 sh 3.42	273 3.49		312 3.62	377 3.17
	0.1 *N* NaOH			273 3.42		326 3.63	345 sh 3.60
29	EtOH	222 sh 3.86		267 3.27		335 3.65	
	0.1 *N* HCl	220 sh 3.77	225 sh 3.69	265 sh 3.57	270 3.58	315 3.50	362 3.33
	0.1 *N* NaOH			268 3.24		337 3.65	
30	EtOH	205 sh 4.48	213 sh 4.17	263 3.88		329 3.60	
	0.1 *N* HCl	227 3.84		256 3.94		305 3.60	
	0.1 *N* NaOH			263 3.88		329 3.61	

The imidazo and pyrimido rings in the new heterocycles (**13—16, 18—21**) can be readily split by aqueous alkali and compounds of *N*-aminoalkyl hydrazid type (**23—30**) are formed. According to the IRs pectra, all derivatives exist in the zwitterionic form, except for **25**. The IR spectra have bands characteristic of $NH_3^{\oplus}$, in the range $3300-2300$ cm^{-1}. The band assigned to the tertiary
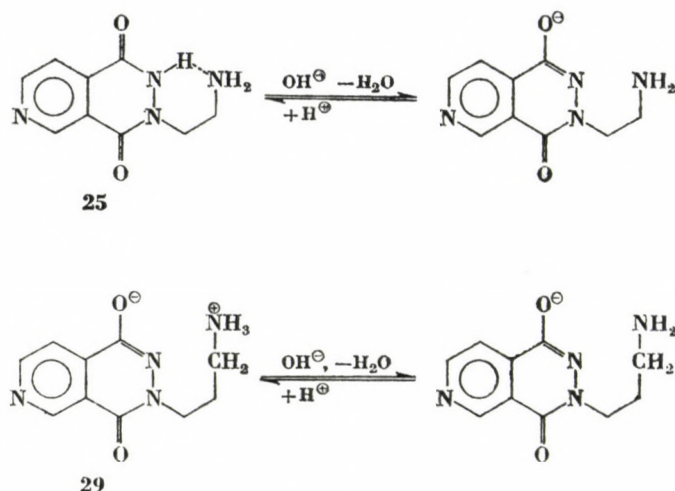
Fig. 7

amide with medium intensity is found at about 1630 cm^{-1}; the intense band of the C=N bond adjacent to the polar carbonyl group appears at 1550 cm^{-1}. In ethanol and in 0.1 N NaOH the UV spectra are practically identical (see Table II), which can be explained only by the fact that they possess a zwitterionic structure also in ethanol.

On the other hand, in solid **25** — as shown by the IR spectrum — there is no $NH_3^{\oplus}$ group; the bands appearing in the range of higher frequencies can be assigned to Amide NH an NH_2 groups. An amide carbonyl group of high intensity appears at 1665 cm^{-1} in the spectrum. The UV spectrum of **25**, recorded in ethanol, resembles neither the spectrum in alkaline solution nor the UV spectrum of **29** in ethanol. The spectrum of **25** recorded in alkaline solution is analogous to the UV spectrum of **29** in alkaline solution. Therefore, **25** must exist in the amide form in solide state and in ethanolic solutions; its formation is stabilized by the electron-withdrawing action of the nitrogen atom in *para* position in the pyridine ring and by the intramolecular hydrogen bond formed. The combined action of the hydrogen bond and the electron-withdrawing activity of the nitrogen atoms in *para* position in the six-membered ring must be responsible for the fact that such an effect has not been observed in other model compounds.

Experimental

M.p.'s were measured with a Boetius apparatus. The IR spectra were recorded with a Zeiss Specord 75 IR instrument in KBr pellets; the UV spectra were obtained with a Zeiss Specord M 40 spectrophotometer in 0.1 N HCl, 0.1 N NaOH and ethanol solutions. The ^{1}H-NMR spectra at 100 MHz were recorded with a Tesla BS 597 instrument in 2 mg/mL DMSO-d_6 solutions at room temperature. The internal standard was DSS.

5-(3-Hydroxypropylamino)pyrido[2,3-d]pyridazin-8(7H)-one (5)

A mixture of 3-aminopropanol (6.0 g; 0.08 mol) and 5-chloropyrido[2,3-d]pyridazin-8(7H)-one (3.62 g; 0.02 mol) [2] was heated at 115 °C for 15 h. The melt was crystallized from water (10 mL) to obtain yellow crystals (2.73 g; 62%). The substance, dried over P$_2$O$_5$ in vacuum at 100 °C, melted at 205—207 °C, then recrystallized on gentle further heating. The prisms formed melted then at 217—218 °C.

C$_{10}$H$_{12}$N$_4$O$_2$ (220.2). Calcd. N 25.4. Found N 25.6%.

IR (KBr): νOH, νNH$_{exo}$ 3430, 3308; νNH$_{Amide}$ 3200—2200; νCO 1655; pyridine ring, νC=N$_{pyridazine}$ 1582, 1470; νC—O 1067 cm^{-1}.

1-(3-Hydroxypropylamino)pyrido[3,4-d]pyridazin-4(3H)-one (6)

A mixture of 1-chloropyrido[3, 4-d]pyridazin-4(3H)-one (3.62 g; 0.02 mol) [3] and 3-aminopropanol (6.0 g; 0.08 mol) was maintained at 115 °C for 15 h. The melt was then recrystallized from water (10 mL) to give yellow crystals (2.98 g; 67.7%), m.p. 231—233 °C.

C$_{10}$H$_{12}$N$_4$O$_2$ (220.2). Calcd. N 25.4. Found N 25.3%.

IR (KBr): νOH, νNH$_{exo}$ 3397, 3330; νNH$_{Amide}$ 3250—2500; νCO 1652; pyridine ring, νC=N$_{pyridazine}$ 1616, 1588, 1470; δNH$_{exo}$ 1555; νC—O 1059 cm^{-1}.

4-(3-Hydroxypropylamino)pyrido[3,4-d]pyridazin-1(2H)-one (7)

A mixture of 4-chloropyrido[3,4-d]pyridazin-1(2H)-one (3.64 g; 0.02 mol) [3] and 3-aminopropanol (6.0 g; 0.08 mol) was heated at 115 °C for 15 h. The mass solidifying on cooling was suspended in some water and filtered. The substance crystallized from water in form of pale yellow needles (3.4 g; 77.3%), m.p. 224—226 °C.

C$_{10}$H$_{12}$N$_4$O$_2$ (220.2). Calcd. N 25.4. Found N 25.5%.

IR (KBr): νOH, νNH$_{exo}$ 3389, 3317; νNH$_{Amide}$ 3200—2400; νCO 1660, pyridine ring, νC=N$_{pyridazine}$ 1612, 1575, 1568, 1459; δNH$_{exo}$ 1551; νC—O 1050 cm^{-1}.

8-(3-Hydroxypropylamino)pyrido]2,3-d]pyridazin-5(6H)-one (8)

A solution of 8-chloropyrido[2,3-d]pyridazin-5(6H)-one (3.64 g; 0.02 mol) [2] in 3-aminopropanol (8 mL) was refluxed for 30 min. After cooling, the cyrstal mass was suspended in water, allowed to stand, then filtered. The halogen-free product was crystallized from water to obtain yellow crystals (3.60 g; 80%), m.p. 197—198 °C.

C$_{10}$H$_{12}$N$_4$O$_2$ (220.2). Calcd. N 25.4. Found N 25.5%.

IR (KBr): νOH, νNH$_{exo}$ 3402, 3328; νNH$_{Amide}$ 3200—2400; νCO 1654; pyridine ring, νC=N$_{pyridazine}$ 1602, 1578, 1478; δNH$_{exo}$ 1534; νC—O 1029 cm^{-1}.

5-(3-Acetoxypropylamino)pyrido[2,3-d]pyridazin-8(7H)-one (9)

The hydroxypropylamino compound 5 (0.220 g; 1 mmol) was dissolved in a mixture of anhydrous pyridine (5 mL) and acetic anhydride (0.5 mL) at room temperature. Next day the mixture was diluted with water, then evaporated to dryness in vacuum and the distillation residue was refluxed with ethanol (10 mL) for 1 h. After the alcoholysis was complete, the dry evaporation residue of the solution was dissolved in some water and saturated with solid NaHCO$_3$ at room temperature. The product which separated was crystallized from ethanol to give yellow crystals (0.200 g; 76.2%), m.p. 198—199 °C; above 230 °C the melt crystallized again.

$C_{12}H_{14}N_4O_3$ (262.3). Calcd. N 21.4. Found N 21.5%.
IR (KBr): νNH 3319, 3264; νCO$_{ester}$ 1719; νCO$_{Amide}$ 1668; pyridine ring 1601, 1586, 1555; δNH 1535; νC—O—C 1265, 1031 cm^{-1}.

1-(3-Acetoxypropylamino)pyrido[3,4-d]pyridazin-4($3H$)-one (10)

The hydroxypropylamino compound **6** (0.220 g; 1 mmol) was acetylated in a mixture of anhydrous pyridine (5 mL) and acetic anhydride (0.5 mL), with mild heating. Next day the solution was diluted with water, evaporated to dryness in vacuum, and the distillation residue was refluxed with ethanol (10 mL) for 1 h. The dry residue of the solution was suspended in water and filtered off. Yellow needles were obtained from ethanol (0.238 g 90.7%), m.p. 201—202 °C.
$C_{12}H_{14}N_4O_3$ (262.3). Calcd. N 21.4. Found N 21.4%.
IR (KBr): νNH 3354, 3336; νCO$_{ester}$ 1743; νCO$_{Amide}$ 1652; pyridine ring 1610, 1585, 1482; δNH 1552; νC—O—C 1227, 1042 cm^{-1}.

4-(3-Acetoxypropylamino)pyrido[3,4-d]pyridazin-1($2H$)-one (11)

Compound **7** (0.220 g; 1 mmol) was dissolved in a mixture of anhydrous pyridine (5 mL) and acetic anhydride (0.5 mL) with mild heating. Next day, water was added to the yellow solution, and it was evaporated to dryness in a rotary evaporator. The *O,O*-diacetyl derivative was decomposed by boiling with ethanol (10 mL) for 1 h, and the product obtained (0.228 g; 86.9%; m.p. 184—186 °C) was crystallized from ethanol to give yellow elongated plates, m.p. 185—186 °C.
$C_{12}H_{14}N_4O_3$ (262.3). Calcd. N 21.4. Found N 21.6%.
IR (KBr): νNH$_{exo}$ 3312; νNH$_{Amide}$ 3250—2600; νCO$_{ester}$ 1744; νCO$_{Amide}$ 1667; νC=N$_{pyridazine}$ 1655; pyridine ring 1624, 1582, 1468; δNH$_{exo}$ 1558; νC—O—O 1243, 1041 cm^{-1}.

8-(3-Acetoxypropylamino)pyrido[2,3-d]pyridazin-5($6H$)-one (12)

Derivative **8** (0.220 g; 1 mmol) was dissolved in a mixture of anhydrous pyridine (10 mL) and acetic anhydride (0.5 mL) with mild heating. Next day the mixture was diluted with water, the solvent was evaporated in vacuum, and the solid residue was refluxed in ethanol (10 mL) for 1 h. The product (0.215 g; 82%; m.p. 126—128 °C) was crystallized from ethanol to obtain yellowish-white needles with unchanged melting point.
$C_{12}H_{14}N_4O_3$ (262.3). Calcd. N 21.4. Found N 21.5%.
IR (KBr): νNH$_{exo}$ 3423; νNH$_{Amide}$ 3350—2600; νCO$_{ester}$ 1749; νCO$_{Amide}$ 1678; νC=N$_{pyridazine}$ 1532; pyridine ring 1603, 1581; δNH$_{exo}$ 1535; νC—O—O 1236, 1047 cm^{-1}.

2,3-Dihydro-1H-imidazo[2,1-a]pyrido[2,3-e]pyridazin-4-ium-6-ol bromide (13.HBr)

A solution of 5-(2-hydroxyethylamino)pyrido[2,3-d]pyridazin-8($7H$)-one (**1**; 2.06 g; 0.01 mol) [2] in 48% hydrobromid acid (10 mL) was refluxed for 2 h; meanwhile the colour of the solution turned from dark orange-red into orange-yellow. The dihydrobromide, with intense yellow colour, precipitated from the cold solution. It decomposed when crystallized from aqueous ethanol to yield the almost colourless monohydrobromide (2.46 g; 91.3%), m.p. 322 °C (decompn.).
$C_9H_9BrN_4O$ (269.1) Calcd. Br 29.7. Found Br 29.9%.
IR (KBr): νOH, νNH 3300—2000; νC=N 1638, 1557; pyridine ring 1608, 1517 cm^{-1}.

2,3-Dihydro-1H-imidazo[2,1-a]pyrido[2,3-e]pyridazin-4-ium-6-olate (13)

This compound was obtained from a hot *conc.* aqueous solution of **13HBr** with *conc.* ammonium hydroxide, as vivid yellow needles; at about 190 °C the powdered substance transformed into needles and above 300 °C it sublimed without melting.
$C_9H_8N_4O$ (188.2). Calcd. N 29.8. Found N 29.9%.
IR (KBr): νNH 3300—2000; νC=N 1662, 1572, 1505; pyridine ring 1620 cm^{-1}.

2,3-Dihydro-1H-imidazo[2,1-a]pyrido[3,4-e]pyridazin-4-ium-6-ol bromide (14. 2HBr)

1-(2-Hydroxyethylamino)pyrido[3,4-d]pyridazin-4(3H)-one (2; 2.06 g; 0.01 mol) [3] was refluxed with 48% hydrobromic acid (10 mL) for 2 h, while the colour of the solution turned from orange-red into orange-yellow. The excess of hydrogen bromide was removed in vacuum, the solid residue suspended in anhydrous ethanol and filtered off (3.27 g; 93.4%) to obtain vivid yellow crystals on recrystallization from a mixture of anhydrous ethanol and ether containing hydrogen bromide; m.p. 254.°C (decompn.).
$C_9H_{10}Br_2N_4O$ (350.0). Calcd. Br 45.7. Found Br 44.8%.
IR (KBr): νOH, νNH$\oplus$ 3300−2100; νC=N 1667, 1653, 1575, 1549; pyridine ring 1612, 1506, 1489 cm^{-1}.

2,3-Dihydro-1H-imidazo[2,1-a]pyrido[3,4-e]pyridazin-4-ium-6-olate (14)

The compound was precipitated from a *conc.* aqueous solution of the hydrobromide by the addition of *conc.* ammonium hydroxide; it was crystallized from some water or ethanol-water to give bright yellow needles, m.p. 238−240 °C.
$C_9H_8N_4O$ (188.2). Calcd. N 29.8. Found N 29.8%.
IR (KBr): νNH 3300−2000; νC=N 1639, 1563; pyridine ring 1608, 1505 cm^{-1}.

2,3-Dihydro-1H-imidazo[2,1-a]pyrido[4,3-e]pyridazin-4-ium-6-ol bromide (15.HBr)

A mixture of 48% hydrobromic acid (10 mL) and 4-(2-hydroxyethylamino)pyrido[3,4-d]-pyridazin-1(2H)-one (2.06 g; 0.01 mol) [3] was refluxed for 2 h. The colour of the solution turned gradually from orange-red into yellow. After evaporation in vacuum, the dibromide (3.10 g; 88.6%) was isolated by means of anhydrous ethanol, and crystallized from a mixture of water and ethanol to obtain the monohydrobromide. The compound undergoes sublimation above 260 °C.
$C_9H_9BrN_4O$ (269.1). Calcd. Br 29.7. Found Br 29.9%.
IR (KBr): νOH, νNH 3300−2200; νC=N 1644, 1570; pyridine ring 1528, 1507 cm^{-1}.

2,3-Dihydro-1H-imidazo[2,1-a]pyrido[4,3-e]pyridazin-4-ium-6-olate (15)

The product precipitated on the addition of *conc.* ammonium hydroxide from a *conc.* aqueous solution of 15.HBr; pale yellow crystals from a mixture of ethanol and water. In the course of m.p. determination, after previous recrystallization, the square plates melted at 332−333 °C with darkening, and then long needles formed from the melt. The latter sublimed on prolanged heating.
$C_9H_8N_4O$ (188.2). Calcd. N 29.8. Found N 29.9%.
IR (KBr): νNH 3600−2200; νC=N 1620, 1542; pyridine ring 1575, 1504 cm^{-1}.

2,3-Dihydro-1H-imidazo[2,1-a]pyrido[3,2-e]pyridazin-4-ium-6-ol bromide (16.HBr)

A solution of 8-(2-hydroxyethylamino)pyrido[2,3-d]pyridazin-5(6H)-one (4; 10.30 g; 0.05 mol) [2] was refluxed in 48% hydrobromic acid (40 mL) for 2 h. The colour of the solution turned dark red during the reaction. On cooling in a refrigerator 16.HBr precipitated from the solution; this was filtered off on a glass filter and washed with some 48% hydrobromic acid. The almost colourless salt (3.80 g; 28.3%) was crystallized from a mixture of ethanol and water to obtain colourless needles; m.p. decomposition started at about 300 °C.
$C_9H_9BrN_4O$ (269.1). Calcd. Br 29.7. Found Br 29.8%.
IR (KBr): νOH, νNH 3185, 3100−2200; νC=N 1636, 1568; pyridine ring 1505 cm^{-1}.

2,3-Dihydro-1H-imidazo[2,1-a]pyrido[3,2-a]pyridazin-4-ium-6-olate (16)

The substance was precipitated from a *conc.* aqueous solution of the salt (16.HBr) and crystallized from water to give yellow plates, m.p. 290−292 °C (decompn.).
$C_9H_8N_4O$ (188.2). Calcd. N 29.8. Found N 30.0%.
IR (KBr): νNH 3300−2400; νC=N 1572, 1545; pyridine ring 1595, 1582, 1474 cm^{-1}.
^{1}H-NMR spectral data are shown in Table I.

2,3-Dihydro-5H-3,4,5,9a-tetraazabenzonaphthen-6-one-9a-ium bromide (17)

The mother liquor of the salt **16.HBr** in hydrobromic acid was evaporated to dryness in vacuum and the solid residue was repeatedly recrystallized from a mixture of water and ethanol. Orange-red crystals (7.71 g; 57.3%) were obtained, which strongly darkened above 300 °C and did not melt up to 370 °C.

$C_9H_9BrN_4O$ (269.1). Calcd. Br 29.7. Found Br 30.0%.

IR (KBr): νNH(3) 3268; νNH$_{Amide}$ 3270−2600; νCO$_{Amide}$ 1678; νC=N$_{pyridazine}$ 1631; pyridine ring 1600, 1576, 1519 cm^{-1}.

^{1}H-NMR spectral data are shown in Table I.

1,2,3,4-Tetrahydropyrimido[2.1-a]pyrido[2,3-e]pyridazin-5-ium-8-ol bromide (18.HBr)

The colour of a solution of the hydroxypropylamino derivative **5** (4.40 g; 0.02 mol) in 48% hydrobromic acid (20 mL) turned from red into orange on boiling for a few minutes. After refluxing for 30 min and concentrating the solution in vacuum, the dihydrobromide with intense yellow colour precipitated. It decomposed to the monohydrobromide on crystallization from ethanol, to yield colourless prisms (5.18 g; 91.5%). M.p.: recrystallization occurred at about 295 °C; above 320 °C the compound decomposed with intense darkening.

$C_{10}H_{11}BrN_4O$ (283.2). Calcd. Br 28.2. Found Br 28.0%.

IR (KBr): νOH, νNH 3300−2300; νC=N 1630, 1572; pyridine ring 1607, 1519 cm^{-1}.

1,2,3,4-Tetrahydropyrimido[2,1-a]pyrido[2,3-e]pyridazin-5-ium-7-olate (18)

The product precipitated from a *conc.* aqueous solution of the salt **18.HBr** on the addition of *conc.* ammonium hydroxide. It was very well soluble in cold water. Yellow needles were obtained by crystallization from ethanol; m.p. 297−299 °C (with the evolution of a gas).

$C_{10}H_{10}N_4O$ (202.2). Calcd. N 27.7. Found N 27.9%.

IR (KBr): νNH 3300−2300; νC=N 1548, 1512; pyridine ring 1620 cm^{-1}.

1,2,3,4-Tetrahydropyrimido[2,1-a]pyrido[3,4-e]pyridazin-5-ium-7-ol bromide (19.HBr) and the dibromide (19.2HBr)

A mixture of 48% hydrobromic acid (10 mL) and the hydroxypropylamino compound **6** (2.20 g; 0.01 mol) was refluxed for 30 min (colour change: orange to yellow). The crude dibromide (3.77 g; about 100%) was isolated by evaporation to dryness in vacuum. It crystallized as a crystalline powder of bright yellow colour from a mixture of anhydrous ethanol and ether; m.p. 273−277 °C (decompn.).

$C_{10}H_{12}Br_2N_4O$ (361.1). Calcd. Br 43.9. Found Br 43.4%.

IR (KBr): νOH, νNH$^{\oplus}$ 3600−2000; νC=N 1642, 1575, 1538; pyridine ring 1600, 1505 cm^{-1}.

When crystallized from a mixture of water and ethanol, the product decomposed into the colourless monohydrobromide (**19.HBr**), m.p. 270−274 °C (decompn.).

$C_{10}H_{11}BrN_4O$ (283.2). Calcd. Br 28.2. Found Br 28.3%.

IR (KBr): νNH 3200−2000; νC=N 1616, 1570, 1554; pyridine ring 1500 cm^{-1}.

1,2,3,4-Tetrahydropyrimido[2,1-a]pyrido[3,4-e]pyridazin-5-ium-7-olate (19)

The compound was precipitated from a *conc.* solution of **19.2HBr** with *conc.* ammonium hydroxide. It crystallized as yellow needles from a small amount of water; m.p.: sublimed at about 340 °C, and did not melt up to 360 °C.

$C_{10}H_{10}N_4O$ (202.2). Calcd. N 27.7. Found N 27.8%.

IR (KBr): νNH 3300−2000; νC=N 1637, 1580, 1543; pyridine ring 1612, 1510, 1500 cm^{-1}.

1,2,3,4-Tetrahydropyrimido[2,1-a]pyrido[4,3-e]pyridazin-5-ium-7-ol bromide (20.HBr)

The hydroxypropylamino compound **7** (2.20 g; 0.01 mol) was refluxed with 48% hydrobromic acid (10 mL) for 30 min (colour change: red to yellow). On evaporation to dryness in vacuum, the crude dibromide (**20.2HBr**) of bright yellow colour was isolated (3.38 g; 92.8%). It crystallized from water as monohydrobromide in colourless needles; m.p.: decomposition with very marked darkening above 330 °C.

$C_{10}H_{11}BrN_4O$ (283.1). Calcd. Br 28.2. Found Br 27.9%.

IR (KBr): νOH, νNH 3325, 3250—2000; νC=N 1630, 1582; pyridine ring 1500 cm^{-1}.

1,2,3,4-Tetrahydropyrimido[2,1-a]pyrido[4,3-e]pyridazin-5-ium-7-olate (20)

The base **20** was liberated from the salt **20.HBr** with *conc.* ammonium hydroxide; the product crystallized from a small amount of water as yellow needles. The compound decomposed above 340 °C and did not melt up to 360 °C.

$C_{10}H_{10}N_4O$ (202.2). Calcd. N 27.7. Found N 27.4%.

IR (KBr): νNH 3300—2000; νC=N 1629, 1574, 1544; pyridine ring 1617, 1510 cm^{-1}.

1,2,3,4-Tetrahydropyrimido[2,1-a]pyrido[3,2-e]pyridazin-5-ium-7-ol bromide (21.HBr)

The hydroxypropylamino compound **8** (2.20 g; 0.01 mol) was dissolved in 48% hydrobromic acid (10 mL). The solution was refluxed for 30 min (colour change: red to yellow). The acid solution was evaporated to dryness in vacuum and the solid residue was dissolved in anhydrous ethanol. The colourless monohydrobromide (2.70 g; 95.4%) was precipitated from the solution with anhydrous ether to obtain a colourless powder; m.p. 320—321 °C (decompn.).

$C_{10}H_{11}BrN_4O$ (283.1). Calcd. Br 28.2. Found Br 28.4%.

IR (KBr): νOH, νNH 3362, 3300, 3178, 3070—2000; νC=N 1641, 1576; pyridine ring 1600, 1513 cm^{-1}.

1,2,3,4-Tetrahydropyrimido[2,1-a]pyrido[3,2-e]pyridazin-5-ium-7-olate (21)

The *conc.* aqueous solution of the salt **21.HBr** was made alkaline (pH 8) with potassium hydroxide solution, then evaporated to dryness in vacuum, on a bath of max. 35 °C temperature. Base **21** was extracted with ethanol from the dry mixture. A yellow powder was obtained on crystallization from a mixture of ethanol and ether; m.p.: melting with decomposition from about 260 °C on.

$C_{10}H_{10}N_4O$ (202.2). Calcd. N 27.7 Found N 27.8%.

IR (KBr): νNH 3265, 3200—2300; νC=N 1633, 1572; pyridine ring 1510 cm^{-1}.

Ring cleavage of imidazo- and pyrimido-pyridopyridazinone derivatives by alkaline hydrolysis

Method: The zwitterion compounds **13—16** and **18—21** or their HBr salts (1 mmol) were refluxed with 5% aqueous potassium hydroxide solution (4 mL) for 30 min. The colour of the solution turned from orange into pale yellow in a few minutes. The crude product, precipitated with hydrochloric acid at pH 8 from the cold solution, was crystallized from water.

6-(2-Ammoniumethyl)pyrido[2,3-d]pyridazin-5-one-8-olate (23)

Alkaline hydrolysis: **13 → 23**; yield: 200 mg (97.0%). Yellow needles were obtained from water. M.p.: the powder of the substance transformed into plates above 230 °C then melted with decomposition at 284—287 °C.

$C_9H_{10}N_4O_2$ (206.2). Calcd. N 27.2. Found N 27.4%.

IR (KBr): νNH$_3^\oplus$ 3200—2300, 2120; νCO, νC=N 1627, 1568; pyridine ring 1590, 1498 cm^{-1}.

UV spectral data are shown in Table II.

2-(2-Ammoniumethyl)pyrido[3,4-d]pyridazin-1-one-4-olate (24)

Alkaline hydrolysis: **14 → 24.** Yield: 192 mg (93.2%), yellow needles from water, m.p. 253—255 °C.

$C_9H_{10}N_4O_2$ (206.2). Calcd. N 27.2. Found N 27.5%.

IR (KBr): $\nu NH_3^{\oplus}$ 3250—2300, 2150; νCO, $\nu C=N$ 1628, 1559; pyridine ring 1601, 1490 cm^{-1}.

UV spectral data are shown in Table II.

3-(2-Aminoethyl)pyrido[3,4-d]pyridazine-2H-1,4-dione (25)

Alkaline hydrolysis: **15 → 25.** Precipitation at pH 5. Yield: 206 mg (100%). A colourless powder was obtained from a dilute solution of water; in m.p. determination the compound sublimed from 297 °C on.

$C_9H_{10}N_4O_2$ (206.2). Calcd. N 27.2. Found N 27.2%.

IR (KBr): νNH 3300—2000; νNH_2 3170, 3035; νCO 1665; pyridine ring 1600, 1565, 1485 cm^{-1}.

UV spectral data are shown in Table II.

7-(2-Ammoniumethyl)pyrido[2,3-d]pyridazin-8-one-5-olate (26)

Alkaline hydrolysis: **16 → 26.** Yield: 200 mg (97%). Yellow needles from water, m.p. 266—268 °C (decompn.).

$C_9H_{10}N_4O_2$ (206.2). Calcd. N 27.2. Found N 27.4%.

IR (KBr): $\nu NH_3^{\oplus}$ 3300—2400, 2050; νCO, $\nu C=N$ 1640, 1570; pyridine ring 1590, 1490 cm^{-1}.

UV spectral data are shown in Table II.

6-(3-Ammoniumpropyl)pyrido[2,3-d]pyridazin-5-one-8-olate (27)

Alkaline hydrolysis: **18 → 27.** Yield: 220 mg (100%). Yellowish-white elongated plates from water, m.p. 261—263 °C.

$C_{10}H_{12}N_4O_2$ (202.2). Calcd. N 25.4. Found N 25.6%.

IR (KBr): $\nu NH_3^{\oplus}$ 3200—2300, 2138; νCO, $\nu C=N$ 1642, 1622, 1570; pyridine ring 1591, 1497 cm^{-1}.

UV spectral data are shown in Table II.

2-(3-Ammoniumpropyl)pyrido[3,4-d]pyridazin-1-one-4-olate (28)

Alkaline hydrolysis: **19 → 28.** Yield: 100 mg (45.4%). The compound is well soluble in water. Yellowish white crystals from ethanol containing a little water, m.p. above 300 °C (decompn.).

$C_{10}H_{12}N_4O_2$ (220.2). Calcd. N 25.4 Found N 25.5%.

IR (KBr): $\nu NH_3^{\oplus}$ 3250—2250, 2130; νCO, $\nu C=N$ 1627, 1553; pyridine ring 1600, 1492 cm^{-1}.

UV spectral data are shown in Table II.

3-(3-Ammoniumpropyl)pyrido[3,4-d]pyridazin-4-one-1-olate (29)

Alkaline hydrolysis: **20 → 29.** The hydrolysate was adjusted to pH 8, and the evaporation residue was crystallized from aqueous ethanol to obtain yellowish white needles. Yield: 210 mg (95.4%), m.p. 237—240 °C.

$C_{10}H_{12}N_4O_2$ (220.2). Calcd. N 25.4. Found N 25.7%.

IR (KBr): $\nu NH_3^{\oplus}$ 3250—2300, 2125; νCO, $\nu C=N$ 1628, 1553; pyridine ring 1598, 1475 cm^{-1}.

UV spectral data are shown in Table II.

7-(3-Ammoniumpropyl)pyrido[2,3-*d*]pyridazin-8-one-5-olate (30)

Alkaline hydrolysis: **21** → **30**. Yield: 188 mg (85.4%). The hydrate separated as colourless needles from water; in vacuum over P_2O_5 at 100 °C it turned yellow on releasing water; m.p. 268—270 °C.

$C_{10}H_{12}N_4O_2$ (220.2). Calcd. N 25.4. Found N 25.4%.

IR (KBr): $\nu NH_3^{\oplus}$ 3270—2400, 2160; νCO, $\nu C{=}N$ 1670, 1637, 1550; pyridine ring 1605, 1497 cm^{-1}.

UV spectral data are shown in Table II.

*

REFERENCES

[1] Körmendy, K., Ruff, F.: Acta Chim. Hung., **112**, 65 (1983)
[2] Körmendy, K., Kovács, T., Szulágyi, J., Ruff, F., Kövesdi, I.: Acta Chim. Acad. Sci. Hung., **108**, 167 (1981)
[3] Körmendy, K., Kovács, T., Ruff, F., Kövesdi, I.: Acta Chim. Hung., **112**, 487 (1983)
[4] Körmendy, K., Ruff. F., Kövesdi, I., Pelczer, I.: Acta Chim. Hung., **117**, 363 (1984)

SIMPLE AND CONDENSED β-LACTAMS, IV*

SYNTHESIS OF SOME 1-(o- AND p-NITROPHENYL)- AND 1-(p-AMINOPHENYL)-2-AZETIDINONES AND DERIVATIVES OF THE 2,2a,3,4-TETRAHYDRO-1H-AZETO[1,2-a]QUINOXALINE RING SYSTEM

Tibor Gizur[1]**, Zsuzsanna Gombos[1], Zoltán Horváth[1]**,
Mária Kajtár-Peredy[2], Károly Lempert[1] and József Nyitrai[1]***

(*[1]Department of Organic Chemistry, Technical University Budapest,
H-1521 Budapest, Gellért tér 4., and
[2]Central Research Institue for Chemistry, Hungarian Academy of Sciences,
H-1025 Budapest, Pusztaszeri út 59—67.*)

The N-phenyl-β-lactams 5—7 (Y=H) were nitrated with acetyl nitrate to give either mixtures of their o- and p-nitro derivatives (Y = o- and p-NO₂, respectively) or the pure o-nitro derivatives, depending on the number and nature of the C-substituents of the starting compounds. Catalytic reduction of all p-nitrophenyl derivatives and of the o-nitrophenylazetidinecarboxylic ester **6m** gave the corresponding amino compounds, while reduction of the o-nitrophenyl derivatives **5b**, **6d**, **6j**, **7b** and **7g** led to derivatives **9—11**, respectively, of 2,2a,3,4-tetrahydro-1H-azeto[1,2-a]quinoxaline. Dimethyl diazomalonate, when thermolyzed in the presence of N-chloroacetyl-p-nitraniline and Rh(II) acetate, furnished the imidate **8** in a low yield, rather than the amide **3c**.

In connection with another research project we were interested in the preparation of 1-(o- and p-nitrophenyl)- (**1**) and 1-(o- and p-aminophenyl)-2-azetidinone derivatives (**2**), and have decided to synthesize these compounds
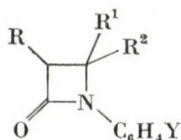
1: Y = o- and p-NO₂

2: Y = o- and p-NH₂

by applying the Sheehan—Bose β-lactam synthesis [2] and subsequent manipulations of the functional groups of the dicarboxylic esters **5** (R=H) (cf. Ref. [3]), the cyclization products of the starting compounds **3**. The related dicarboxylic ester **5e** was obtained starting with the pyrrolidine derivative **4a** as described earlier [4]. The N-substituent in the starting compounds **3** and **4** may be a phenyl group, and the nitro group may be introduced by

---

2

3
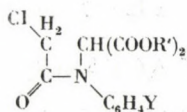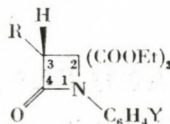
	R'	Y
a	Et	H
b	Et	p-NO$_2$ [5]
c	Me	p-NO$_2$

5*

	R	Y
a		H
b		o-NO$_2$
c	H	p-NO$_2$ [5]
d		p-NH$_2$
e		H
f		o-NO$_2$
g		p-NO$_2$
h		p-NH$_2$
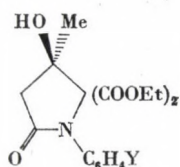
4*

(4a: Y=H)
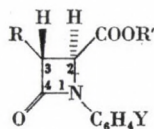
6*
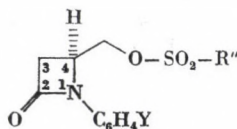
7*

	R	R	Y
a		Et	H
b		Et	p-NO$_2$
c		H	H
d	H	H	o-NO$_2$
e		H	p-NO$_2$
f		H	o-NH$_2$
g		H	p-NH$_2$
h		Et	H
i		H	H
j		H	o-NO$_2$
k		H	o-NH$_2$
l		Me	H
m		Me	o-NO$_2$
n	Me	Me	p-NO$_2$
o		Me	o-NH$_2$
p		Me	p-NH$_2$

	R"	Y
a		H
b		o-NO$_2$
c	Me	p-NO$_2$
d		o-NH$_2$
e		p-NH$_2$
f		H
g		o-NO$_2$
h	p-tolyl	p-NO$_2$
i		o-NH$_2$
j		p-NH$_2$

* Racemic compound(s).   For convenience only one enantiomer is shown

nitration of the compounds **3** (Y=H) or, at a later stage, of the azetidinone derivatives **5—7** (Y=H). The result will be the formation of mixtures consisting mainly of the corresponding 1-(*o*- and *p*-nitrophenyl) derivatives. Alternatively, a particular nitrophenyl, e.g. the *p*-nitrophenyl group may be present in the starting chloroacetyl derivative **3**; starting with compounds **3** (Y = *p*-NO$_2$) the pure 1-(*p*-nitrophenyl) derivatives **5—7** (Y = *p*-NO$_2$) could, in principle, be obtained. However, in contrast to **6a**, **6h** and many related compounds [1, 3, 4], the ester group of compound **6b** could not be reduced to the hydroxymethyl group with NaBH$_4$.

While compound **3a** was nitrated with a mixture of nitric and sulfuric acids, the nitrations of compounds **5—7** (Y=H) were carried out with acetyl nitrate (freshly prepared from fuming nitric acid and acetic anhydride) at low temperatures. The ratio of the resulting *o*- and *p*-isomers was found to depend on the number and nature of the substituents of the saturated carbon atom attached to the lactam nitrogen atom. For details, see Experimental.

Compound **3b** was obtained by allowing *p*-nitraniline to react with diethyl bromomalonate, and chloroacetylation of the resulting diethyl *p*-nitranilinomalonate as described in the literature [5]; the corresponding dimethyl ester **3c** was similarly obtained. Alternatively, diethyl *p*-nitranilinomalonate was synthesized by the reaction of diethyl diazomalonate with *p*-nitraniline in the presence of Cu(acac)$_2$ as catalyst. When, on the other hand, dimethyl diazomalonate was made to react with N-chloroacetyl-*p*-nitraniline in the presence of rhodium(II) acetate, compound **8**, an isomer of the expected
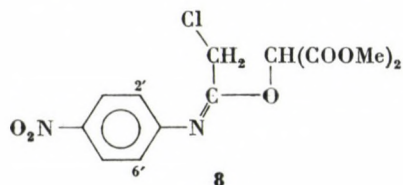
dimethyl N-chloroacetyl-*p*-nitranilinomalonate **3c**, was obtained, because the carbene resulting from the diazomalonate has attacked the oxygen rather than the nitrogen atom of the amide group. The two isomers could be readily differentiated on the basis of their ^{1}H-NMR and mass spectra. Diagnostic for structure **8** are the downfield shift (from δ 5.50 to 5.69 ppm) of the signal of the >C—H proton and the upfield shift (from δ 7.76 to 6.93 ppm) of the doublet of the 2'- and 6'-protons relative to the corresponding signals of compound **3c** in the NMR spectrum, as well as the peaks at *m/z* 197 (^{35}Cl— —CH$_2$—C≡$\overset{+}{N}$—C$_6$H$_4$NO$_2$, by peak matching) and 148 [HOCH(COOMe)$_2^+$·, by peak matching] in the mass spectrum of compound **8**, which are absent from the spectrum of the isomeric **3c**, and the peaks at *m/z* 268 (M—^{35}ClCH$_2$CO + H)

2*

and 77 ($^{35}\text{ClCH}_2\text{C}{\equiv}\overset{+}{\text{O}}$) in the spectrum of the latter compound which, in turn, are absent from the spectrum of compound **8**.

Catalytic reduction of the *p*-nitrophenyl derivatives **5**—**7** (Y=*p*-NO$_2$) (either in pure form or as a mixture with the *o*-isomers) furnished the corresponding *p*-aminophenyl derivatives **5**—**7** (Y=*p*-NH$_2$). However, the *o*-amino-phenyl derivatives **5**—**7** (Y=*o*-NH$_2$), formed in the course of the reduction of the above mixtures, were unstable and cyclized to the corresponding 2,2a,3,4-tetrahydro-1*H*-azeto[1,2-*a*]quinoxaline derivatives **9**—**11**, respec-

a: R = H

b: R =
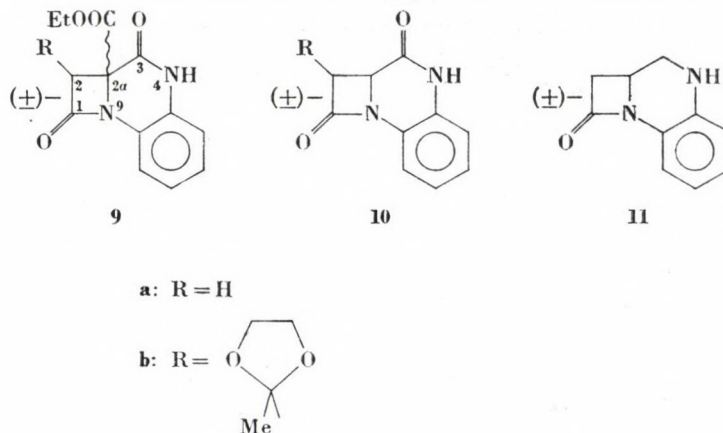
tively. Strikingly, compound **6m** gave, in contrast to the free acid **6j**, the non-cyclized reduction product **6o**. Refluxing of the latter with methanol in the presence of a small amount of acetic acid as catalyst did not give the cyclized product, either.

The relative configurations of C-2 and C-2a in compound **9b** are not known with certainty. Since, however, the ethoxycarbonyl groups of the *trans* ester **6h** and related compounds are known to be more susceptible to nucleo-philic attack (alkaline hydrolysis, sodium borohydride reduction) than those of the diastereomeric *cis* esters ([1, 4]), the ethoxycarbonyl and R groups in compound **9b** may be assumed to be in *cis* relation to each other.

A broad screening of compounds **9a** and **10a**, carried out at the Chemical Works Gedeon Richter, Ltd., Budapest, did not reveal any useful pharma-cological activity.

Experimental

Dimethyl p-nitranilinomalonate

This compound was synthesized by the method described in the literature [5] for the preparation of the homologous diethyl ester. A mixture of p-nitraniline (23.6 g; 171 mmol) and dimethyl bromomalonate (20.3 g; 96 mmol) was maintained for 48 h at 70 °C /27 mbar, and subsequently thoroughly mixed with benzene (20 mL). The unchanged p-nitraniline was filtered off and the filtrate kept for 1 h in a refrigerator to obtain 2.5 g (9.7%) of the title compound,* m.p. 152—154 °C (from i-PrOH).

$C_{11}H_{12}N_2O_6$ (268.23). Calcd. C 49.21; H 4.51; N 10.44. Found C 48.93; H 4.60; N 10.61%.

IR (KBr): 3330, 1740/1720 (d), 1520, 1315, 840 cm^{-1}.

^{1}H-NMR (60 MHz): δ 3.80 s (2×COOMe), 4.80 d (J = 6.6 Hz; —NH—CH$\lessdot$), 5.45 br (NH), 6.58 + 8.02 (AA'BB', J = 9.2 Hz; 4×Ar—H).

Dimethyl N-chloroacetyl-p-nitranilinomalonate (3c)

This compound was prepared by the method described in the literature [5] for the homologous diethyl ester 3b. A mixture of dimethyl p-nitranilinomalonate (0.9 g; 3.3 mmol) and chloroacetyl chloride (1.1 mL; 13.8 mmol) was refluxed for 8 h and allowed to cool. The excess chloroacetyl chloride was decomposed by adding methanol (30 mL). The mixture was evaporated to dryness and the yellow crystalline residue recrystallized from methanol to obtain 0.75 g (66%) of colourless crystals of the title compound, m.p. 98—100 °C.

$C_{13}H_{13}ClN_2O_7$ (344.71). Calcd. C 45.29; H 3.80; Cl 10.29; N 8.13. Found C 45.59; H 4.10; Cl 10.74; N 8.24%.

IR (KBr): 1750/1730 (d), 1695, 1520, 1340, 855, 845 cm^{-1}.

^{1}H-NMR (60 MHz): δ 3.73 s (2×COOMe), 3.86 s (ClCH$_2$CO), 5.50 s ($\gtrdot$C—H), 7.76 + + 8.35 (AA'BB', J = 9.2 Hz; 4×Ar—H).

MS (180 °C), m/z (rel. intensity, %): 344 (20; $M^{+\cdot}$), 313 (3.0), 308 (20; M — HCl), 285 (M — COOMe), 281 (0.9), 280 (2.6), 268 (62; M-[COCH$_2$Cl—H]), 249 (1.6), 236 (0.5; M — [COOMe + CH$_2$Cl]), 221 (46; 280 $\xrightarrow{*}$ 59), 209 (100; 268 $\xrightarrow{*}$ COOMe), 207 (6.0), 192 (4.0; 209 $\xrightarrow{*}$ 17), 163 (8.0), 149 (24; 209 $\xrightarrow{*}$ HCO$_2$Me), 117 (20; 163 $\xrightarrow{*}$ NO$_2$), 103 (12), 77 (10), 76 (13), 59 (21). (Metastable peaks are indicated by $\xrightarrow{*}$.)

Reactions of diazomalonates with p-nitraniline and N-chloroacetyl-p-nitraniline

(a) A mixture of p-nitraniline (5 g; 36 mmol), diethyl diazomalonate (4 g; 22 mmol) dioxane (20 mL) and a small amount of Cu(acac)$_2$ was refluxed for 3 h, and allowed to cool. The unchanged p-nitraniline was filtered off, and the filtrate evaporated to dryness to obtain diethyl p-nitranilinomalonate as an oily product (5.7 g; 89%) which crystallized on scratching; m.p. 123.5 °C (from i-PrOH); lit. m.p. 123—124 °C [5].

IR (KBr): 3400, 1745/1725 (d), 1530, 1330, 840 cm^{-1}.

(b) A mixture of N-chloroacetyl-p-nitraniline (11 g; 52 mmol), dimethyl diazomalonate (8.3 g; 52 mmol), Rh$_2$(OAc)$_4$ (11.4 mg; 0.026 mmol) and dry toluene (100 mL) was refluxed until the evolution of nitrogen ceased (about 1 h); the reaction mixture remained heterogeneous throughout. It was allowed to cool, and the unchanged N-chloroacetyl-p-nitraniline (7 g) was filtered off. The filtrate was evaporated to dryness to leave an oil which, when allowed to stand overnight, partly solidified. The semisolid material was taken up in a small amount of ethanol. The insoluble material was filtered off and recrystallized from ethanol to give 0.5 g (7.7%, based on the non-recovered N-chloroacetyl-p-nitraniline) of compound 8, m.p. 123—124 °C.

$C_{13}H_{13}ClN_2O_7$ (344.71). Calcd. C 45.29; H 3.80; Cl 10.29; N 8.13. Found C 45.23; H 3.84; Cl 10.28; N 8.13%.

IR (KBr): 1750, 1690, 1520, 1320, 870 cm^{-1}.

^{1}H-NMR (60 MHz): δ 3.82 s (2×COOMe), 3.93 s (ClCH$_2$), 5.69 s ($\gtrdot$C—H), 6.93 + 8.20 (AA'BB', J = 9.2 Hz; 4×Ar—H).

MS (180 °C), m/z (rel. intensity, %): 344 (16; $M^{+\cdot}$), 328 (0.6%), 313 (6.5), 308 (0.3; M — HCl), 285 (2.0; M — COOMe), 281 (2.0), 280 (1.0), 249 (0.7), 236 (8.0; M * [COOMe + + CH$_2$Cl]), 207 (1.3), 204 (16; M $\xrightarrow{*}$ MeOH), 197.0119 (by peak matching; 100; M $\xrightarrow{*}$ 147, C$_8$H$_6$N$_2$O$_2$Cl), 163 (5.0), 151 (13; M $\xrightarrow{*}$ NO$_2$), 148.0348 (by peak matching; 4.5; C$_\circ$, 32 (6.2), 103 (5.0), 76 (12), 59 (4.2). (Metastable peaks are indicated by $\xrightarrow{*}$.)

* The diethyl ester was obtained in 40% yield by allowing the reactants to react for 30 days (!) at 70 °C/mbar [5].

Ethyl 1-(p-nitrophenyl)-4-oxo-2-azetidinecarboxylate (6b)

A mixture of compound **5c** [5] (10 g; 29 mmol), NaCl (2.0 g; 34 mmol), dimethyl sulfoxide (16 mL) and water (1.06 mL; 58 mmol) was heated at 170—180 °C, with continuous stirring, until the starting compound **5c** had been consumed (TLC: DC-Alufolien Merck, Kieselgel 60 PF_{254}; benzene–acetone, 9 : 1). The mixture was allowed to cool and poured into brine (80 mL). Conventional work-up by extraction with ether gave an oily product (≈7 g) which crystallized when triturated with i-PrOH. Recrystallization from i-PrOH gave 4 g (52%) of the title compound, m.p. 78 °C.

$C_{12}H_{12}NO_5$ (250.23). Calcd. C 54.54; H 4.57; N 10.60. Found C 54.58; H 4.60; N 10.89%.
IR (KBr): 1770, 1740, 1520, 1335, 855 cm⁻¹.
¹H-NMR (60 MHz): δ 1.27 t + 4.23 q (J = 7.2 Hz; COOEt), 3.05—3.5 m (3-H_2), 4.5—4.65 m (4-H), 7.35 + 8.08 (AA'BB', J = 9.2 Hz; 4×Ar—H).

1-Phenyl-4-tosyloxymethyl-2-azetidinone (7f)

Tosyl chloride (13.5 g; 70.6 mmol) was added at 0 °C, in small portions, to a mixture of 4-hydroxymethyl-1-phenyl-2-azetidinone [3] (10 g; 56.5 mmol) and pyridine (30 mL). When the starting azetidinone was consumed (TLC), the mixture was poured into vigorously stirred ice-water (300 g). The crude crystalline product was recrystallized from ethanol to obtain 16.9 g (90.5%) of the title compound, colourless crystals, m.p. 127 °C.

$C_{17}H_{17}NO_4S$ (331.39). Calcd. C 61.62; H 5.17; N 4.23; S 9.67. Found C 61.86; H 5.37; N 4.01; S 10.01%.
IR (KBr): 1750, 1360, 1180 cm⁻¹.
¹H-NMR (60 MHz): δ 2.34 s (Me, tosyl group), 2.95—3.15 m (3-H_2), 4.2—4.35 m (4-H + —CH_2O—), 7.15 + 7.60 (AA'BB', J = 8.9 Hz; 4×Ar—H, tosyl group), 7.2 m (Ph).

Methyl trans-3-(2-methyl-1,3-dioxolan-2-yl)-1-phenyl-4-oxoazetidine-2-carboxylate (6l)

An ethereal diazomethane solution, freshly prepared from N-methyl-N-nitrosourea (3.15 g; 20 mmol) was added to a solution of compound **6i** [4] (2.77 g; 10 mmol) in CH_2Cl_2 (10 mL) with continuous stirring at room temperature. The mixture was stirred for further 2 h to furnish, after conventional work-up, an oil which crystallized when triturated with ether to give 2.9 g (99%) of the title compound, m.p. 119—120 °C (from EtOH).

$C_{15}H_{17}NO_5$ (291.30). Calcd. C 61.84; H 5.88; N 4.81. Found C 61.98; H 6.13; N 4.60%.
IR (KBr): 1760 cm⁻¹, br.
¹H-NMR (60 MHz): δ 1.5 s (C-Me), 3.55 d (J = 2.6 Hz; 3-H), 3.75 s (COOMe), 3.9—4.1 m (—O—CH_2—CH_2—O—), 4.35 d (J = 2.6 Hz; 2-H), 7.2 s (Ph).

Nitration of compounds 3a, 5a, 5e, 6c, 6i, 6l, 7a and 7f

(a) A mixture of conc. HNO_3 (d = 1.38; 1.3 mL; 18 mmol) and conc. H_2SO_4 (0.8 mL) was added, with ice-salt cooling, dropwise to a vigorously stirred solution of compound **3a** [2a] (5.0 g; 16 mmol) in conc. H_2SO_4 (5 mL); the reaction temperature was maintained throughout the addition between 0—5 °C. The mixture was stirred at this temperature until, according to TLC (DC-Alufolien, Merck, Kieselgel 60 F_{254}; benzene–acetone, 9 : 1), the starting compound had been consumed, and then it was poured into a mixture of crushed ice (200 g) and water (100 mL). The semisolid precipitate was taken up in CH_2Cl_2 (50 mL) and the aqueous layer extracted with CH_2Cl_2 (2×20 mL). Conventional work-up of the combined CH_2Cl_2 solutions furnished an oil which crystallized when triturated with ethanol. Recrystallization from ethanol gave 3.0 g (52%) of diethyl N-chloroacetyl-p-nitranilinomalonate **3b**, m.p. 74—76 °C, lit. m.p. 76—77 °C [5], which was homogeneous according to TLC.

IR (KBr): 1740, 1690, 1520, 1345, 870, 850 cm⁻¹.
¹H-NMR (60 MHz): δ 1.22 t + 4.17 q (J = 7.2 Hz; 2×COOEt), 3.85 s (ClCH₂CO), 5.50 s (>C—H), 7.73 + 8.27 (AA'BB', J = 9 Hz; 4×Ar—H).

(b) A freshly prepared cold mixture of nitric acid (d = 1.5; 10.6 mL; 0.25 mol) and acetic anhydride (26 mL) was added dropwise to a solution of compound **5a** [2a] (27.9 g; 0.1 mol) in acetic anhydride (60 mL), with continuous stirring at −5 °C. The mixture was stirred for 1 h more at this temperature, and poured onto ice (200 g). Conventional work-up by extraction with CH_2Cl_2 (3×40 mL) gave a mixture of diethyl 1-(o-nitrophenyl)- and 1-(p-

-nitrophenyl)-4-oxoazetidine-2,2-dicarboxylates (**5b**, and **5c**, respectively) as an oil (26.9 g), which crystallized when triturated with ether. Recrystallization from ethanol furnished 8.1 g (24%) of the *p*-nitro derivative (**5c**), m.p. 68—69 °C, *lit.* m.p. 66—67 °C [5].
IR (KBr): 1780, 1740, 1520, 1340, 840 cm^{-1}.
^{1}H-NMR (60 MHz): δ 1.3 t + 4.4 q ($J = 7$ Hz; 2×COOEt), 3.63 s (3-H$_2$), 7.7 + 8.1 (AA'BB', $J = 9.2$ Hz; 4×Ar—H).

The dry residue of the mother liquor of the *p*-isomer **5c** was taken up in a small amount of ethanol; a small second crop of this isomer crystallized and was filtered off. The filtrate was evaporated to dryness to obtain 16.1 g (48%) of the almost pure *o*-isomer (**5b**) as the residue. An analytically pure sample, m.p. 98 °C, of the latter was obtained by recrystallization from ethanol.
C$_{15}$H$_{16}$N$_2$O$_7$ (336.30). Calcd. C 53.57; H 4.79; N 8.33. Found C 54.08; H 4.69; N 8.04%.
IR (KBr): 1780, 1740, 1520, 1350, 730 cm^{-1}.
^{1}H-NMR (60 MHz): δ 1.25 t + 4.27 q ($J = 7$ Hz; 2×COOEt), 3.6 s (3-H$_2$), 7.8—8.2 m (4×Ar—H).

(*c*) A freshly prepared cold mixture of nitric acid ($d = 1.5$; 2.2 mL) and acetic anhydride (6 mL) was added dropwise at —5 °C, with continuous stirring, to a solution of compound **5e** [4] (8.4 g; 22 mmol) in acetic anhydride (20 mL). The mixture was stirred for further 30 min at this temperature, and then poured onto ice (50 g). Conventional work-up by extraction with benzene gave a mixture of diethyl 3-(2-methyl-1,3-dioxolan-2-yl)-1-(*o*-nitrophenyl)- and -1-(*p*-nitrophenyl)-4-oxoazetidine-2,2-dicarboxylates (**5f** and **5g**, respectively) which, when triturated with ether, furnished 6.4 g (67%) of **5f**, m.p. 81—82 °C (from ethanol). From the mother liquor 0.3 g (3%) of **5g** m.p. 60—62 °C (from EtOH), was obtained.
C$_{19}$H$_{22}$N$_2$O$_9$ (422.39). Calcd. C 54.03; H 5.25; N 6.63. **5f**: Found C 53.80; H 5.23; N 7.03%. **5g**: Found C 53.71; H 5.53; N 6.81%.
IR (KBr) **5g**: 1780, 1740, 1510, 1340, 840 cm^{-1}.
^{1}H-NMR (60 MHz) **5g**: δ 1.3 t + 4.35 q ($J = 7.3$ Hz; 2×COOEt), 1.55 s (C-Me), 4.0 m (—O—CH$_2$—CH$_2$—O—), 4.4 s (3-H), 7.75 + 8.25 (AA'BB', $J = 9.2$ Hz; 4×Ar—H). **5f**: δ 1.05 t + 1.3 t + 4.25 q + 4.32 q ($J = 7.3$ Hz; 2×COOEt), 1.55 s (C-Me), 4.0 m (—O—CH$_2$—CH$_2$—O—), 4.42 s (3-H), 7.4—8.1 m (4×Ar—H).

(*d*) A freshly prepared cold mixture of nitric acid ($d = 1.5$; 6 mL) and acetic anhydride (15 mL) was added dropwise to a vigorously stirred suspension of compound **6c** [2a] (11.4 g; 60 mmol) in dry CH$_2$Cl$_2$ (50 mL) at 0 °C. The mixture was stirred for further 2 h at this temperature and poured into ice-water (100 g) to obtain a crude crystalline product which was recrystallized from ethanol–ether to give 8.3 g (58%) of a mixture of the 1-(*o*-nitrophenyl)- and 1-(*p*-nitrophenyl-4-oxoazetidine-2-carboxylic acids (**6d** and **6e**, respectively).
C$_{10}$H$_8$N$_2$O$_5$ (236.18). Calcd. C 50.85; H 3.41; N 11.86. Found C 50.85; H 3.52; N 11.84%.
IR (KBr): 3400—2800, 1760—1730 (br), 1520, 1350, 850, 740 cm^{-1}.
This mixture was subjected, without separation into its components, to catalytic reduction (see below).

(*e*) A freshly prepared cold mixture of nitric acid ($d = 1.5$; 2.4 mL) and acetic anhydride (6 mL) was added at —5 °C dropwise to a vigorously stirred solution of compound **6i** [4] (6.9 g; 25 mmol) in dry CH$_2$Cl$_2$ (25 mL). The mixture was stirred for 1 h more at this temperature and poured into ice-water (100 mL). Conventional work-up by extraction with CH$_2$Cl$_2$ furnished an oil which crystallized when triturated with ether to give 5.0 g (63%) of *trans*-3--(2-methyl-1,3-dioxolan-2-yl)-1-(*o*-nitrophenyl)-4-oxoazetidine-2-carboxylic acid (**6j**), m.p. 142—143 °C (from toluene).
C$_{14}$H$_{14}$N$_2$O$_7$ (322.30). Calcd. C 52.17; H 4.38; N 8.69. Found C 52.43; H 4.70; N 8.71%.
IR (KBr): 1770, 1740, 1520, 1340, 730 cm^{-1}.
^{1}H-NMR (60 MHz): δ 1.5 s (C-Me), 3.75 d ($J = 2.6$ Hz; 3-H), 3.9—4.1 m (—O—CH$_2$—CH$_2$—O—), 4.85 d ($J = 2.6$ Hz; 2-H), 6.1 br (COOH), 7.2—8.3 m (4×Ar—H).

(*f*) A freshly prepared cold mixture of nitric acid ($d = 1.5$; 0.53 mL) and acetic anhydride (2 mL) was added dropwise to a solution of compound **6l** (1.7 g; 5.8 mmol) in dry CH$_2$Cl$_2$ (10 mL), with continuous stirring, at 0 °C. The mixture was then stirred for 2 h at this temperature and poured into ice-water (20 mL). Conventional work-up by extraction with CH$_2$Cl$_2$ gave an oil which crystallized when triturated with ether to furnish 1.5 g (77%) of a mixture of the isomeric methyl *trans*-3-(2-methyl-1,3-dioxolan-2-yl)-1-(*o*-nitrophenyl)- and -1-(*p*--nitrophenyl)-4-oxoazetidine-2-carboxylates (**6m**, and **6n**, respectively), m.p. 123 °C (from EtOH).
C$_{15}$H$_{16}$N$_2$O$_7$ (336.30). Calcd. C 53.50; H 4.79; N 8.33. Found C 53.00; H 4.81; N 8.48%.
IR (KBr): 1780, 1750, 1520, 1340, 840, 730 cm^{-1}.
^{1}H-NMR (100 MHz): δ 1.52 s (C-Me), 3.72 d ($J = 3.0$ Hz; 3-H), 3.74 s + 3.85 s (COOMe, *o*- and *p*-isomer, respectively), 4.0—4.2 m (—O—CH$_2$—CH$_2$—O—), 4.52 d + 4.80 d ($J = 3.0$

Hz; 4-H, *p*- and *o*-isomer, respectively), 7.2—8.0 m (Ar—H's, *o*-isomer, and upper-field half of the AA'BB' spectrum of the Ar—H's of the *p*-isomer), 8.24 (lower-field half of the AA'BB' spectrum of the Ar—H's of the *p*-isomer, $J = 9.2$ Hz). Isomer ratio, $o : p \approx 4 : 1$.

(g) A freshly prepared cold mixture of *conc.* HNO_3 ($d = 1.5$; 3 mL; 70 mmol) and acetic anhydride (7.1 mL) was added, with external cooling and vigorous stirring, to a suspenison, precooled to -10 °C, of compound 7a [3] (7.0 g; 27.5 mmol) in acetic anhydride (17 mL) ta such a rate, that the temperature never exceeded -5 °C. The mixture was stirred at this temperature until the starting compound had been consumed according to TLC (DC-Alufolien Merck, Kieselgel 60 PF_{254}; benzene—acetone, 7 : 3) (about 1 h), and then poured onto crushed ice (60 g) to obtain, after conventional work-up and recrystallization from ethanol, 6.2 g (88%) of a mixture of 4-mesyloxymethyl-1-(*o*-nitrophenyl)- and -1-(*p*-nitrophenyl)-2-azetidinones (7b and 7c, respectively).

$C_{11}H_{12}N_2O_6S$ (300.29). Calcd. C 44.00; H 4.03; N 9.33; S 10.68. Found C 44.21, H 4.13, N 9.02, S 10.98%.

IR (KBr): 1750, 1530, 1370, 1350/1340 (d), 1170, 835, 750 cm^{-1}.

^{1}H-NMR (60 MHz): δ 2.82 s + 2.91 (intensity ratio $\approx$2 : 1; mesyl group, two isomers), 2.95—3.3 m (3-CH_2), 4.25—4.6 m (4-H + —CH_2—O—), 7.15—7.85 m (Ph, Ar—H's of the *o*-isomer 7b and upper-field half of the AA'BB' spectrum of the Ar—H's of the *p*-isomer), 8.15 (lower-field half of the AA'BB' spectrum of the Ar—H's of the *p*-isomer 7c, $J = 9.2$ Hz).

The mixture was, without separation into its components, directly subjected to reduction (see below).

(h) Compound 7f (3.3 g; 10 mmol) was similarly nitrated and worked up to obtain 3.6 g (88%) of a non-recrystallized mixture of the 1-(*o*-nitrophenyl)- and 1-(*p*-nitrophenyl)-4--tosyloxymethyl-2-azetidinones (7g and 7h, respectively), a sample of which was recrystallized from *i*-PrOH for analysis, m.p. 178 °C.

$C_{17}H_{16}N_2O_6S$ (376.38). Calcd. C 54.25; H 4.28; N 7.44; S 8.52. Found C 53.98; H 4.06; N 7.68; S 8.22%.

IR (KBr): 1750 (d), 1535, 1360, 1330, 1165, 850, 840, 750 cm^{-1}.

^{1}H-NMR (60 MHz): δ 2.37 + 2.41 (Me of tosyl group, two isomers), 2.70—3.55 m (AB parts of two AB spectra, $J_{gem} = 16$ Hz, $J_{vic} = 2.7$ and 5.4 Hz, respectively; 3-H_2), 4.18—4.65 m (4-H + —CH_2O—), 7.1—8.0 m (Ph, Ar—H's of tosyl and *o*-nitrophenyl groups, upper-field half of the AA'BB' spectrum of the Ar—H's of the *p*-nitrophenyl group), 8.15 (lower-field half of the AA'BB' spectrum of the Ar-H's of the *p*-nitrophenyl group; $J = 9.2$ Hz).

Reduction of compounds 5b, 5c, 5f, 5g and 6j, and of the mixtures of compounds 6d + 6e, 6m + 6n, 7b + 7c and 7g + 7h

The title compounds and mixtures were reduced in methanolic (5c) or ethanolic solution in the presence of 8% Pd—C catalysts at normal pressures and ambient temperatures; owing to the slight solubilities of the isomeric mixtures 7b + 7c and 7g + 7h in ethanol, they were reduced in the form of ethanolic suspensions. The following products were obtained by conventional work-up.

(a) Ethyl 1,3-dioxo-2,2a,3,4-tetrahydro-1*H*-azeto[1,2-*a*]quinoxaline-2a-carboxylate (9a), m.p. 158 °C (from EtOH), in 95% yield from compound 5b. This compound, *lit.* m.p. 153—154 °C (from *i*-PrOH–hexane), had been obtained by a different route before [6].

$C_{13}H_{12}N_2O_4$ (260.24). Calcd. C 60.09; H 4.61; N 10.80. Found C 59.99; H 5.00; N 10.87%.

IR (KBr): 1780, 1720, 1700 cm^{-1} (lit.: 1785, 1690 cm^{-1} [6]).

^{1}H-NMR (100 MHz): δ 1.23 t + 4.24 q ($J = 7.2$ Hz; COOEt), 3.77 + 3.88 (AB, $J = 15.8$ Hz; 2-H_2), 6.9—7.45 m (4×Ar-H), 9.1 br s (NH); *lit.* (DMSO-d_6): δ 3.78 d ($J = 16$ Hz) [6].

(b) Diethyl 1-(*p*-aminophenyl)-4-oxoazetidine-2,2-dicarboxylate (5d), m.p. 103—104 °C (from EtOH), in 96% yield from compound 5c.

$C_{15}H_{28}N_2O_5$ (306.32). Calcd. C 58.76; H 5.92; N 9.14. Found C 59.20; H 5.69; N 9.29%.

IR (KBr): 3500—3100 with local maxima at 3310 and 3200; 1760—1730 br, 810 cm^{-1}.

^{1}H-NMR (60 MHz): δ 1.28 t + 4.25 q ($J = 7$ Hz; 2×COOEt), 2.5—2.8 br (NH_2), 3·48 s (3-H_2), 6.57+7.29 (AA'BB', $J = 9.2$ Hz; 4×Ar—H).

(c) Ethyl 2-(2-methyl-1,3-dioxolan-2-yl)-1,3-dioxo-2,2a,3,4-tetrahydro-1*H*-azeto[1,2-*a*]-quinoxaline-2a-carboxylate (9b), m.p. 156 °C (from EtOH), in 93% yield from compound 5f.

$C_{17}H_{18}N_2O_6$ (346.34). Calcd. C 58.95; H 5.24; N 8.09. Found C 58.60; H 5.42; N 8.19%.

IR (KBr): 1770, 1750, 1690 cm^{-1}.

^{1}H-NMR (100 MHz): δ 1.22 t + 4.22 q ($J = 7.1$ Hz; COOEt), 1.63 s (C-Me), 3.95—4.25 m (—O—CH_2—CH_2—O—), 4.26 s (2-H), 6.85—7.55 m (4×Ar—H), 8.7 br s (NH).

(d) Diethyl 1-(p-aminophenyl)-3-(2-methyl-1,3-dioxolan-2-yl)-4-oxoazetidine-2,2-dicar-boxylate (5h) in 90% yield as an oil from compound 5g.

$C_{19}H_{24}N_2O_7$ (392.41). Calcd. C 58.16; H 6.16; N 7.18. Found C 58.25; H 6.18; N 7.29%.

^{1}H-NMR (60 MHz): δ 1.15 t + 1.27 t + 4.21 q + 4.27 q ($J = 7.2$ Hz; $2 \times$COOEt), 1.52 s (C-Me), 3.4 br (NH$_2$), 3.9—4.0 m (—O—CH$_2$—CH$_2$—O—), 4.25 s (3-H), 6.57 + 7.24 (AA'BB', $J = 9.2$ Hz; $4 \times$Ar-H).

(e) 2,2a-Dihydro-1H-azeto[1,2-a]quinoxaline-1,3(4H)-dione (10a), m.p. 240 °C (from EtOH), in 40% yield, from the mixture of the isomeric compounds 6d + 6e. The highly insoluble compound 6 g formed in the same reaction mixture was filtered off together with the catalyst and discarded.

$C_{10}H_8N_2O_2$ (188.19). Calcd C 63.82; H 4.28; N 14.89. Found C 64.04; H 4.49; N 15.15%.

IR (KBr): 1770, 1670 cm^{-1}.

^{1}H-NMR (100 MHz; CDCl$_3$ + DMSO-d_6): δ 3.45 + 3.58 (AB part of an ABX spectrum, $J_{gem} = 15.6$, $J_{vic} = 3.1$ and 5.1 Hz, respectively; 2-H$_2$), 4.34 dd ($J = 5.1$ and 3.1 Hz; 2a-H), 6.9—7.3 m ($4 \times$Ar—H), 10.5 br s (NH).

(f) 2-(2-Methyl-1,3-dioxolan-2-yl)-2,2a-dihydro-1H-azeto[1,2-a]quinoxaline-1,3(4H)-dione (10b), m.p. 170 °C (from EtOH); in 94% yield from compound 6j.

$C_{14}H_{14}N_2O_4$ (274.28). Calcd. C 61.31; H 5.14; N 10.21. Found C 60.89; H 5.06; N 10.50%.

IR (KBr): 1760 and 1690 cm^{-1}.

^{1}H-NMR (100 MHz; CDCl$_3$ + DMSO-d_6): δ 1.51 s (C-Me), 3.94 d ($J = 2.8$ Hz; 2-H), 3.9—4.3 m (—O—CH$_2$—CH$_2$—O—), 4.21 d ($J = 2.8$ Hz; 2a-H), 6.90—7.35 m ($4 \times$Ar—H), 10.3 br s (NH).

(g) Methyl trans-1-(o-aminophenyl)-3-(2-methyl-1,3-dioxolan-2-yl)-4-oxoazetidine-2-car-boxylate (6o), m.p. 129 °C (from EtOH), in 84% yield from compound 6m, contaminated by the p-nitro isomer (6n).

$C_{15}H_{18}N_2O_5$ (306.30). Calcd. C 58.82; H 6.00; N 9.15. Found C 58.57; H 6.40; N 9.23%.

IR (KBr): 3600—3200, 1760 br, 760 cm^{-1}.

^{1}H-NMR (60 MHz): δ 1.5 s (C-Me), 3.58 d ($J = 2.6$ Hz; 3-H), 3.7 s (COOMe), 3.9—4.1 m (—O—CH$_2$—CH$_2$—O—), 4.2 br (NH$_2$), 4.45 d ($J = 2.6$ Hz; 2-H), 6.6—7.2 m ($4 \times$Ar—H).

(h) 1-(p-Aminophenyl)-4-mesyloxymethyl-2-azetidinone (7e), m.p. 119 °C (from EtOH), in 56% yield, and 2,2a,3,4-tetrahydro-1H-azeto[1,2-a]quinoxalin-1-one (11), m.p. 153 °C (from ethanol, in 24% yield from the isomeric mixture of compounds 7b + 7c.*

The crude reduction product in this case was a mixture of compound 7e, its toluene-sulfonate and compound 11. Because of the slight solubility of the toluenesulfonate, the catalyst had to be thoroughly washed with warm ethanol. Evaporation to dryness of the ethanolic solution gave the above mixture as a gum which solidified when triturated with ether. From this, compound 11 was extracted with CH$_2$Cl$_2$ at room temperature. The insoluble residue was treated with Na$_2$CO$_3$ in an ethyl acetate–water two-phase system at 0 °C, in order to convert the toluenesulfonate into the free base 7e, the final pH being about 9.5.

Compound 7e: $C_{11}H_{14}N_2O_4S$ (270.30). Calcd. C 48.88; H 5.22; N 10.36; S 11.86. Found C 48.99; H 5.42, N 10.37; S 12.23%.

IR (KBr): 3500—3100, with local maxima at 3400, 3350 and 3300; 1720, 1350, 1165, 860, 835 cm^{-1}.

^{1}H-NMR (60 MHz): δ 2.89 s (mesyl group), 2.95—3.4 m (3-H$_2$ + NH$_2$), 4.2—4.6 m (4-H + —CH$_2$O—), 6.61 + 7.16 (AA'BB', $J = 9$ Hz; $4 \times$Ar—H).

Compound 11: $C_{10}H_{10}N_2O$ (174.20). Calcd. C 68.95; H 5.79; N 16.08. Found C 68.69; H 5.93; N 15.80%.

IR (KBr): 3300, 1720 cm^{-1}.

^{1}H-NMR (100 MHz): δ 2.65—3.90 m (2-H$_2$ + 2a-H + 3-H$_2$ + NH), 6.55—7.45 m ($4 \times$Ar—H).

(i) 1-(p-Aminophenyl)-4-tosyloxymethyl-2-azetidinone (7j), m.p. 133—134 °C (from ethanol), in 51% yield, and compound 11, identical (m.p., IR) with the sample described in (c), in 32% yield, from the isomeric mixture of the compounds 7g + 7h by the same procedure as described in (h).

Compound 7j: $C_{17}H_{18}N_2O_4S$ (346.40). Calcd. C 58.95; H 5.24; N 8.09; S 9.26. Found C 59.16; H 5.46; N 7.81; S 8.78%.

IR (KBr): 3420, 3350, 1720, 1360, 1150, 850, 840, 820 cm^{-1}.

^{1}H-NMR (60 MHz): δ 2.4 s (Me, tosyl group), 2.75—3.05 m (3-H$_2$), 3.3 br (exchangeable; NH$_2$), 4.2 br (4-H + —CH$_2$O—), 6.35—7.65 m (two AA'BB' spectra; $8 \times$Ar—H).

---

* In calculating the yields of compounds 7e and 11, the starting mixture was assumed to be the pure isomer 7c and 7b, respectively.

REFERENCES

[1] Bertha, F., Lempert, K., Kajtár-Peredy, M.: Acta Chim. Hung. **120**, 111 (1985)
[2] (a) Sheehan, J. C., Bose, A. K.: J. Am. Chem. Soc., **72**, 5158 (1950); (b) Sheehan, J. C., Bose, A. K.: J. Am. Chem. Soc. **73**, 1761 (1985); see also Ref. [3]
[3] Simig, Gy., Fetter, J., Hornyák, Gy., Zauer, K., Doleschall, G., Lempert, K., Nyitrai, J., Gombos, Zs., Gizur, T., Barta-Szalai, G., Kajtár-Peredy, M.: Acta Chim. Hung., **119**, 17 (1985)
[4] Simig, Gy., Doleschall, G., Hornyák, Gy., Fetter, J., Lempert, K., Nyitrai, J., Gizur, T., Huszthy, P. Kajtár—Peredy, M.: Tetrahedron **41**, 479 (1985)
[5] Chatterjee, B. G., Abdulla, R. F.: Chem. Ber., **102**, 2129 (1969)
[6] Abdulla, R. F.: Tetrahedron Lett., **1974**, 3559; Abdulla, R. F., Fuhr, K. H.: J. Heterocyclic Chem., **13**, 427 (1976)

SYNTHESIS OF NEW *N*-SUBSTITUTED *N*-DEMETHYLAPORPHINE DERIVATIVES

Sándor BERÉNYI, Sándor MAKLEIT* and Ferenc RANTAL

(Department of Organic Chemistry, Chemical Institute, Kossuth Lajos University,
H-4010 Debrecen, P.O.Box 20)

Starting from the 6-chloro and 6-bromo derivatives of 6-demethoxythebaine apocodeine and apomorphine (APO) and new derivatives of *N*-propyl-*N*-demethyl-apocodeine and *N*-propyl-*N*-demethylapomorphine (NPA) containing halogen in position 2 have been synthesized.

In our previous papers [1, 2] we reported the preparation of 6-demethoxy-thebaine (**Ia**) and demethoxyoripavine (**Ib**) which gave apocodeine (**IVe**) and apomorphine (**Ve**) in excellent yields on treatment with methanesulfonic acid. *N*-Demethylation of **Ia** and **Ib** has been achieved with azodicarboxylic acid diethyl ester. The *N*-demethyl derivatives obtained in this way are new starting materials for the preparation of *N*-substituted *N*-demethylapocodeine and -apomorphine derivatives.

In the course of our studies of nucleophilic substitution reactions of 14β-chloro(bromo)codeine tosylate containing double allylic system, 6-chloro-6-demethoxythebaine (**Ic**) and 6-bromo-6-demethoxythebaine(**Id**) were synthesized in good yields [3]. Owing to their structural features, these new compounds can be converted in various ways.

The **aim** of our present work was to synthesize new derivatives of apo-codeine (**IVe**) and apomorphine (**Ve**) possessing halogen in position 2, from compounds **Ic** and **Id**. To our knowledge, by the rearrangement of morphinan-type compounds only morphothebaine containing hydroxyl group in position 2 of the aporphine skeleton, 2,10-dimethoxy-11-hydroxyaporphine possessing methoxy group and their *N*-substituted *N*-demethyl derivatives have hitherto been prepared [4, 5]. On rearrangement with methanesulfonic acid 6-chloro-6-demethoxythebaine (**Ic**) and 6-bromo-6-demethoxythebaine (**Id**) gave 2-chloroapocodeine (94%) (**IVa**) and 2-bromoapocodeine (95%) (**IVb**) in good yields. *O*-Demethylation of **IVa** and **IVb** with 48% hydrobromic acid gave 2-chloroapomorphine (**Va**) in 54% and 2-bromapomorphine (**Vb**) in 63% yield.

Compounds **Ic** and **Id** were *N*-demethylated with azodicarboxylic acid diethyl ester (ADDE). The *N*-demethyl derivatives **IIa, IIb** were alkylated

---

* To whom correspondence should be addressed.

Ia   X=H, R=CH$_3$
Ib   X=H, R=H
Ic   X=Cl, R=CH$_3$
Id   X=Br, R=CH$_3$

IIa   X=Cl
IIb   X=Br

IIIa X=Cl,
       R=CH$_2$—CH$_2$—CH$_3$
IIIb X=Br,
       R=CH$_2$—CH$_2$—CH$_3$

IVa X=Cl, R=CH$_3$
IVb X=Br, R=CH$_3$
IVc X=Cl, R=CH$_2$—CH$_2$—CH$_3$
IVd X=Br, R=CH$_2$—CH$_2$—CH$_3$
IVe X=H,   R=CH$_3$

Va   X=Cl, R=CH$_3$
Vb   X=Br, R=CH$_3$
Vc   X=Cl, R=CH$_2$—CH$_2$—CH$_3$
Vd   X=Br, R=CH$_2$—CH$_2$—CH$_3$
Ve   X=H,   R=CH$_3$
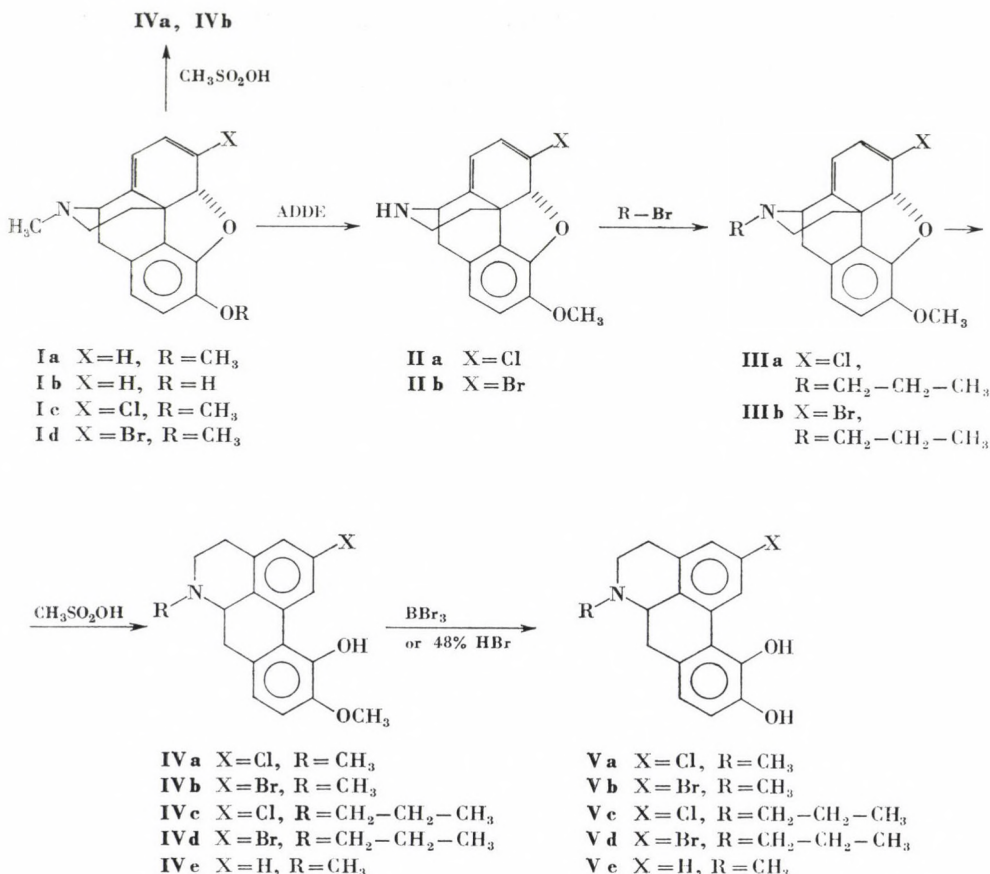
Scheme 1

with propyl bromide, the N-propyl derivatives **IIIa, IIIb** were then rearranged into N-propyl-N-demethylapocodeine 2-chloro- and 2-bromo derivatives (**IVc, IVd**), which were O-demethylated with boron tribromide to afford the apomorphine derivatives **Vc, Vd**.

In this way N-propyl-N-demethyl-2-chloroapomorphine (**Vc**) was obtained in 35.2% yield calculated for **Ic**, and N-propyl-N-demethyl-2-bromoapomorphine (**Vd**) in 9.1% yield calculated for **Id**.

Experimental

M.p.'s were measured with a Koffler apparatus and are uncorrected. Thin-layer chromatography was performed on Merck 5554 silica gel 60 F$_{254}$ foils using benzene : methanol (8 : 2) developing mixture. The spots were visualized with Dragendorff's reagent. Kieselgel 60H was applied for column chromatographic separation using benzene : methanol (9 : 1) eluent. ^{1}H-NMR spectra were measured with a Bruker WP 200 SY spectrometer. Mass spectra were recorded with a VG-7035 (GC-MS-DS) instrument.

N-Demethyl-6-chloro-6-demethoxythebaine (IIa)

A mixture of **Ia** [3] (6.0 g; 19 mmol), ADDE (4.0 g; 22.8 mmol) and dry benzene (60 mL) was refluxed for 15 h. The solvent was then evaporated, the residue dissolved in anhydrous ethanol (120 mL) and ammonium chloride (17 g) in aqueous solution (50 mL) was added. The mixture was allowed to stand at room temperature for 24 h and the ethanol evaporated. The product was isolated as the hydrochloride. The salt was filtered off, dissolved in water and the solution was made alkaline with ammonium hydroxide to obtain 5.04 g (88%) of a crystalline product, m.p. 154—157 °C, $[\alpha]_D$ — 250 ($c = 0.1$, chloroform).

$C_{17}H_{16}O_2NCl$ (301.763). Calcd. N 4.65; Cl 11.78. Found N 4.82; Cl 11.93%.

MS (m/e): 301 (M^+); 226 (M^+—35).

^{1}H-NMR (CDCl$_3$, δppm): 3.90 (s, 3H, OCH$_3$); 5.28 (s, 1H, 5-H), 5.48 (d, 1H, 7-H); 6.10 (d, 1H, 8-H); 6.68 (ABq, 2H, Ar).

N-Demethyl-6-bromo-6-demethoxythabeine (IIb)

According to the procedure described for **IIa** compound **Ib** [3] (4.2 g; 11.6 mmol) gave 2.14 g (52.9%) of a crystalline product, m.p. 174—175 °C, $[\alpha]_D$ — 158.75 ($c = 0.1$, chloroform).

$C_{17}H_{16}O_2NBr$ (346.215). Calcd. N 4.06; Br 23.08. Found N 4.18; Br 22.85%.

MS (m/e): 346 (M^+); 26 (M^+—80).

^{1}H-NMR (CDCl$_3$, δppm): 3.89 (s, 3H, OCH$_3$); 5.35 (d, 1H, 5β-H); 5.43 (d, 1H, 7-H); 6.35 (d, 1H, 8-H); 6.68 (ABq, 2H, Ar).

N-Propyl-N-demethyl-6-chloro-6-demethoxythebaine (IIIa)

A mixture of compound **IIa** (0.9 g; 3.0 mmol), sodium hydrogen carbonate (0.3 g), propyl bromide (0.43 g; 3.5 mmol) and anhydrous ethanol (15 mL) was stirred and refluxed for 20 h. The inorganic salt was filtered off and the solvent evaporated. The residue was triturated with acetone, the inorganic salt filtered off, the solvent evaporated and the residue dissolved in ether. Insoluble unchanged starting material was filtered off, the solvent evaporated and the oily residue was converted into the hydrochloride to yield 0.91 (80%) of a crystalline product, m.p. 237—239 °C, $[\alpha]_D$ — 205 ($c = 0.1$, water).

$C_{20}H_{22}O_2NCl \cdot HCl$ (380.306). Calcd. N 3.68; Cl 18.64. Found N 3.72; Cl 18.64%.

The free base was an oil.

MS (m/e): 343 (M^+); 308 (M^+—35).

^{1}H-NMR (CDCl$_3$, δppm): 0.95 (t, 3H, CH$_3$); 2.75 (m, 4H, CH$_2$CH$_2$); 3.85 (s, 3H, OCH$_3$); 5.28 (s, 1H, 5β-H); 5.53 (d, 1H, 7-H); 6.1 (d, 1H, 8-H); 6.63 (ABq, 2H, Ar).

N-Propyl-N-demethyl-6-bromo-6-demethoxythebaine (IIIb)

Compound **IIb** (2.07 g; 6.0 mmol) was allowed to react with propyl bromide, and treated as described for **IIIa**, to afford 1.78 g (55%) of the hydrochloride of **IIIb**, m.p. 240—243 °C. The crystalline base was prepared from the salt; m.p. 77—79 °C, $[\alpha]_D$ — 168 ($c = 0.1$, chloroform).

$C_{20}H_{22}O_2NBr$ (388.293). Calcd. N 3.6; Br 20.58. Found N 3.9; Br 19.72%.

MS (m/e): 388 (M^+); 308 (M^+—80).

^{1}H-NMR (CDCl$_3$, δppm); 0.95 (t, 3H, CH$_3$); 2.78 (m, 4H, CHCH$_2$); 3.88 (s, 3H, OCH$_3$); 5.35 (s, 1H, 5β-H); 5.48 (d, 1H, 7-H); 6.46 (d, 1H, 8-H); 6.65 (ABq, 2H, Ar).

2-Chloroapocodeine (IVa)

Compound **Ia** (1.0 g; 3.16 mmol) was dissolved in methanesulfonic acid (5 mL) and heated at 96 °C for 1 h. The mixture was cooled and 14 g of potassium hydrogen carbonate in 75 mL of water was added, with stirring. The mixture was stirred for further 1 h and the precipitate filtered off to afford 0.94 g (94%) of the product which was recrystallized from methanol; m.p. 213—215 °C, $[\alpha]_D$ — 55 ($c = 0.1$, chloroform).

$C_{18}H_{18}O_2NCl$ (315.789). Calcd. N 4.43; Cl 11.22. Found N 4.54; Cl 11.89%.

MS (m/e): 315 (M^+).

^{1}H-NMR (CDCl$_3$, δppm): 2.58 (s, 3H, NCH$_3$); 3.93 (s, 3H, OCH$_3$); 6.78 (s, 2H, Ar); 7.08 (d, 1H, Ar); 8.23 (d, 1H, Ar).
Hydrochloride: m.p. 215 °C (decomp.).

2-Bromoapocodeine (IVb)

According to the procedure described for **IVa**, compound **Ib** (1.0 g; 2.77 mmol) gave 0.95 g (95%) material which was crystallized from methanol; m.p. 217—219 °C [α]$_D$ — 116 ($c = 0.5$, chloroform).
C$_{18}$H$_{18}$O$_2$NBr (360.241). Calcd. N 3.88; Br 22.18. Found N 3.92; Br 22.42%.
MS (m/e): 360 (M^+); 280 (M^+—80).
^{1}H-NMR (CDCl$_3$, δppm): 2.55 (s, 3H, NCH$_3$); 3.95 (s, 3H, OCH$_3$); 6.9 (m, 4H, Ar).
Hydrochloride: m.p. 245 °C (decomp.).

N-Propyl-N-demethyl-2-chloroapocodeine (IVc)

Applying the procedure described above, compound **Ic** (1.2 g; 3.15 mmol) gave 1.06 g (88.3%) of the crude product which was converted into the hydrochloride; m.p. 248—249 °C, [α]$_D$ — 104 ($c = 0.1$, water).
C$_{20}$H$_{22}$O$_2$NCl · HCl (385.306). Calcd. N 3.63; Cl 18.40. Found N 3.52; Cl 18.25%.
The free base was an amorphous substance.
MS (m/e): 343 (M^+); 308 (M^+—35).
^{1}H-NMR (CDCl$_3$, δppm): 1.05 (t, 3H, CCH$_3$); 2.4—3.0 (m, 8H, CH$_2$); 6.75 (s, 2H, Ar); 7.1 (s, 1H, Ar); 8.35 (s, 1H, Ar).

N-Propyl-N-demethyl-2-bromoapocodeine (IVd)

Compound **Id** (1.0 g; 2.57 mmol) yielded 0.52 g (52%) of the crude base under the above-mentioned conditions; m.p. of the hydrochloride: 235—237 °C. The free base was a solid, m.p. 75—80 °C, [α]$_D$ — 70 ($c = 0.25$, chloroform).
MS (m/e): 388 (M^+).
^{1}H-NMR (CDCl$_3$, δppm): 1.00 (t, 3H, CCH$_3$), 2.45—3.14 (m, 8H, CH$_2$); 6.75 (s, 2H, Ar); 7.2 (s, 1H, Ar); 8.38 (s, 1H, Ar).

2-Chloroapomorphine (Va)

Compound **IVa** (0.31 g; 1.0 mmol) in 48% hydrobromic acid (12 mL) was refluxed for 12 h; the hydrobromide was filtered off after cooling and recrystallized from methanol to yield 0.203 g (53%) of a crystalline substance m.p.: decomp. above 300 °C; [α]$_D$ — 88.7 ($c = 0.1$, water).
C$_{17}$H$_{16}$O$_2$NCl · HBr (382.689). Calcd. N 3.65. Found N 3.82%.
MS (m/e): 301 (M^+).
^{1}H-NMR (CDCl$_3$, δppm): 3.05 (s, 3H, NCH$_3$); 6.80 (ABq, 2H, Ar); 7.28 (s, 1H, Ar); 8.35 (s, 1H, Ar).

2-Bromoapomorphine (Vb)

Compound **IVb** (0.36 g; 1.0 mmol) in 48% hydrobromic acid (12 mL) was refluxed for 12 h and the reaction mixture was worked up as described for **IVa** to afford 0.27 g (64%) of the crystalline product; m.p. decomp. above 300 °C [α]$_D$ — 78.8 ($c = 0.22$, ethanol).
C$_{17}$H$_{16}$O$_2$NBr · HBr (427.149). Calcd. N 3.27; Br 37.4. Found N 3.38; Br 36.2%.
MS (m/e): 346 (M^+).
^{1}H-NMR (DMSO-d_6, δppm): 3.1 (s, 3H, NCH$_3$); 6.75 (ABq, 2H, Ar); 7.45 (s, 1H, Ar); 8.5 (s, 1H, Ar).

N-Propyl-N-demethyl-2-chloroapomorphine (Vc)

Compound **IVc** (0.34 g; 1 mmol was dissolved in dry chloroform (5.0 mL) and boron tribromide (1.5 g; 6 mmol) in dry chloroform (17 mL) was added during 2 min at room temperature under nitrogen atmosphere, with vigorous stirring. The reaction mixture was stirred

at room temperature for 25 min, then it was poured into a mixture of ice (8 g) and *conc.* ammonium hydroxide (2 mL), stirred for another 30 min, and extracted with chloroform : methanol (3 : 1) mixture. The solution was dried and the solvent evaporated. The residue was triturated with anhydrous ethanol to obtain 0.21 g (65%) of a solid material. Its hydrochloride had m.p. 210—214 °C, $[a]_D$ — 110 ($c = 0.1$, water).

MS (m/e): 329 (M^+); 294 ($M^+ - 35$).

^{1}H-NMR (CDCl$_3$, δppm): 0.99 (t, 3H, CCH$_3$); 1.25 (s, 4H, CH$_2$); 6.67 (ABq, 2H, Ar); 7.05 (s, 1H, Ar); 8.05 (s, 1H, Ar).

N-Propyl-N-demethyl-2-bromoapomorphine (Vd)

According to the procedure described for **Vc** compound **IVd** (0.38 g; 1 mmol) gave 0.22 g (60%) of the product. Its hydrochloride had m.p. 203—206 °C; $[\alpha]_D$ — 103 ($c = 0.1$, water).

MS (m/e): 374 (M^+); 294 ($N^+ - 80$).

^{1}H-NMR (CDCl$_3$, δppm): 1.00 (t, 3H, CH$_3$); 1.55 (s, 4H, CH$_2$); 6.75 (ABq, 2H, Ar); 7.13 (s, 1H, Ar); 8.4 (s, 1H, Ar).

REFERENCES

[1] Berényi, S., Hosztafi, S., Makleit, S., Szeifert, I.: Acta Chim. Acad. Sci. Hung., **110**, 363 (1982); Magy. Kém. Foly., **88**, 170 (1982)
[2] Berényi, S., Hosztafi, S., Makleit, S., Molnár, I.: Acta Chim. Hung., **113**, 51 (1983); Magy. Kém. Foly., **89**, 108 (1983)
[3a] Berényi, S., Makleit, S., Szilágyi, L.: Acta Chim. Hung., **117**, 307 (1984); Magy. Kém. Foly., **90**, 154 (1984)
[3b] Berényi, S., Makleit, S., Rantal, F.: Acta Chim. Hung., **120**, 171 (1985) Magy. Kém. Foly., **91**, 233 (1985)
[4] Schöpf, C., Borkowsky, F.: Justus Liebigs Ann. Chem., **458**, 148 (1927)
[5] Granchelli, F. E., Files, C. N., Soloway, A. H., Neumeyer, J. L.: J. Org. Chem., **45**, 2275 (1980)

DYE-SENSITIZED PHOTO-OXYGENATION OF *SYM*-DIPHENYLTHIOUREA|

(SHORT COMMUNICATION)

Rakesh DUBEY**, Pinki GANDHI*, Shubha JAIN and
Mishri Mal BOKADIA

*(School of Studies in Chemistry, Vikram University,
Ujjain-456.010, M.P. India)*

sym-Diphenylthiourea has been oxidized by singlet oxygen using Methylene blue, Rose Bengal and Eosin-Y sensitizers in methanolic medium. A stable peroxy compound has been isolated as the reaction product (**I**) which has been confirmed by molecular weight determination, elemental analysis and spectral data.

The reaction has been carried out using *sym*-diphenylthiourea (2.0 gm) in methanol (100 mL) and methanolic solution of methylene blue (2 mL $1.0 \times 10^{-4}M$). A tungsten lamp has been used for irradiation purpose (Sylvania, 500 W). (**I**) has been separated by column chromatography using benzene as an eluent. The above reaction has also been carried out in the presence of Rose Bengal and Eosin-Y as sensitizers and same product has been obtained. Participation of singlet oxygen in the reaction has been confirmed by using scavengers which decreased the yield considerably.

I.
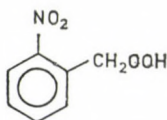
Electronic absorption spectrum of (**I**) shows bands at 206 and 274 nm characteristic of nitro group attached to the benzene nucleus. The infrared spectrum of (**I**) shows important absorption at 3020 cm^{-1} (aromatic), 1535 and

---

* Address for correspondence: Pinki Gandhi, H. No. 115, Shastri Nagar, Ujjain 456.010 (MP) India
** Rakesh Dubey, Environmental Planning & Co-ordination Organization (EPCO), E-5 Sector, Arera Colony, Bhopal 462.016 (MP) India

3

1310 cm^{-1} ($-NO_2$ group) and 890 cm^{-1} (peroxy linkage). The H-NMR spectrum of (I) gives complex multiplet in the range of 2.70—2.90 τ corresponding to the four aromatic protons and a singlet at 5.95 τ corresponding to two protons of $-CH_2$ group. The mass spectrum of (I) gives molecular ion peak at m/e 169.

Calculated C, 49.7; H, 4.1 and N, 8.2 for $C_7H_7NO_4$; Found C, 49.1; H, 4.5 and N, 8.0%.

STOICHIOMETRY, STRUCTURE AND THERMAL STABILITY OF BIS-(SALICYLATO)-DIAQUA COMPLEXES OF BIVALENT METAL IONS

Padmakar V. Khadikar*, Syed Mushtaq Ali,
Mohammod A. Farooqie and Bhagwandas Heda

(Department of Chemistry, Indore University, Khandwa Road, Indore-452001, India)

Reaction of salicylate ion with VO(II), Cu(II), Ni(II), Co(II), Fe(II), Mn(II) and Zn(II) gave bis-(salicylato)-diaqua complexes of these ions. The structure of complexes were predicted from elemental analysis and IR spectra. The decomposition of the complexes was studied by TG, DTG and DTA techniques. The decomposition process consisted of three steps, elimination of two water molecules followed by successive decomposition of dehydrated complex with metal oxide as the end product. The thermal stability of the metal salicylate follows the order: VO(II) > Cu(II) > Zn(II) > Co(II) > Ni(II) > Fe(II) > Mn(II).

Introduction

The versatile chelating ability of salicylic acid with various metals is well established. Structural studies have shown that it can form various types of complexes having different type of bonding, depending on the nature of the metal ion and reaction conditions. Much effort has been devoted to preparation and study of metal chelates of salicylic and nuclear substituted salicylic acids, mainly because of the possibility of their use as antimicrobial agent.

We are much interested in the thermal study of transition metal complexes of salicylic acid, as we have already investigated the antifungal and antibacterial activity of these complexes [1—4]. In view of the importance of the structural activity relationships, it was thought worthy to perform thermogravimetry study of metal complexes of salicyclic acid. Such a study will provide valuable information about dehydration, pyrolysis of the anhydrous complex as well as intermediate products formed during decomposition, which will facilitate and help us in the synthesis of analogous biologically active complexes.

The literature of thermal analysis, so far contains only a few reports dealing with the thermal decomposition of alkali and alkaline earth metal salicylates [5—9]. Little is known about thermal decomposition of Th(V) salicylates [10] and ammonium salicylate [11]. Very recently we have reported

---

* Address for correspondence: 3, Khatipura Road, Indore-452007 (India).

3*

Acta Chim. Hung. 120, 1985
Akadémiai Kiadó, Budapest

TG, DTG and DTA studies of Fe(II), VO(II) and Zn(II) complexes of salicylic acid [12—14]. This report deals with the thermal decomposition of the complexes of VO(II), Cu(II), Ni(II), Co(II), Fe(II), Mn(II) and Zn(II) with salicylic acid studied by TG, DTG and DTA together with the analysis of intermediate products formed during the decomposition process. The stoichiometry and structure of all the complexes along with the dehydrated product is discussed on the basis of analytical and IR studies.

Experimental

Materials and methods

    The complexes were prepared by the method described previously [15]. Equimolar solutions of metal salts and the ligand were prepared and mixed in stoichiometric ratio (M : L = 1 : 2). The solid complexes obtained were washed thoroughly with ethanol, dried and recrystallized from dimethyl formamide. All the reagents used were of BDH AnalaR

Table I

Thermal and analytical data for the bis-(salicylato)-diaqua complexes[a]

Complex	D.P.[b]	Temperature range (°C)	Colour	Composition of the residue	% Weight loss (%W) Cal.	Obs.
(I) $Cu(SA)_2 \cdot 2H_2O$	I	100—240±4	Dark green	$Cu(SA)_2$	9.63	9.5
	II	250—370±2	Blusih green	$CuCO_3$	66.92	66.0
	III	370—560±4	Black	CuO	78.70	78.0
(II) $Ni(SA)_2 \cdot 2H_2O$	I	80—220±2	Green	$Ni(SA)_2$	9.75	9.6
	II	Undiscernible	—	—	—	—
	III	230—520±2	Greenish black	NiO	79.64	79.5
(III) $Co(SA)_2 \cdot 2H_2O$	I	100—220±4	Brown	$Co(SA)_2$	9.75	9.6
	II	230—360±2	Bright red	$CoCO_3$	67.76	67.5
	III	360—520±3	Dark brown	CoO	79.68	79.5
(IV) $Mn(SA)_2 \cdot 2H_2O$	I	80—120±2	Tan	$Mn(SA)_2$	9.86	9.5
	II	Undiscernible	—	—	—	—
	III	220—500±4	Grey green	MnO^c	80.56	79.0
(V) $Fe(SA)_2 \cdot 2H_2O$	I	80—220±2	Dark brown	$Fe(SA)_2$	9.84	9.75
	II	Undiscernible	—	—	—	—
	III	240—620±4	Dark brown	FeO^d	80.36	9.50
(VI) $VO(SA)_2 \cdot 2H_2O$	I	110—260±4	Dirty green	$VO(SA)_2$	9.55	9.50
	II	Undiscernible	—	—	—	—
	III	270—520±3	Dark blue	$O{=}V{=}O^e$	78.0	77.75
(VII) $Zn(SA)_2 \cdot 2H_2O$	I	100—240±4	Dirthy white	$Zn(SA)_2$	9.59	9.50
	II	260—340±2	White	$ZnCO_3$	66.6	66.5
	III	350—450±3	Dirty white	Zn	78.32	77.50

a   = All the experiments were carried out in air at a heating rate of 4 °C/min.
b   = Decomposition Period (Step).
c   = In the final residue, the possibility for formation of Mn_3O_4 cannot be ruled out as the experiments were carried out in air.
d   = FeO was the major end product above 600 °C, however, below this temperature it gets contaminated with Fe_3O_4, as the metal is characterized by its ability to form such oxide.
e   = The end product was expected to be a mixture of vanadium di- and penta-oxides. Formation of V_2O_5 may be due to the oxidation of vanadium dioxide in air.
—   = Indicates that the decomposition product(s) could not be isolated and identified owing to the lack of a clear cut horizontal on the TG curve as the intermediate products are not stable to the required extent.

grade. Metal contents were estimated by conventional gravimetric methods [16]. Elemental analyses (carbon and hydrogen) were carried out in the usual way. The bonding in the complexes was established by IR spectral study.

Elemental analysis

Metal content was determined by the conventional methods [16]. Carbon, hydrogen analyses were carried out using a Colemann CHN analyser-29. The results are recorded in Table I.

IR spectra

IR spectra of all the bis-(salicylato)-diaqua complexes and their dehydrated products were recorded using Perkin-Elmer Grating IR-Spectrophotometer Model-377 by KBr disc technique. The IR-spectrum of salicylic acid was also recorded for comparison. The $4000-400$ cm^{-1} region was scanned in thirteen minutes.

Far infrared spectra were recorded in the region $500-50$ cm^{-1} employing Polytec FIR 30 Fourier Far infrared spectrometer.

Thermogravimetry (TG)

Thermogravimetry was carried out on a Stanton recording thermo balance (HT-Model) of 1 mg sensitivity in static air with a heating rate of 4 °C/min. The chart speed was maintained at 3 inches/hr. All samples ($\approx$100 mg) were of the same particle size and were packed as uniformly as possible in a platinum crucible and the same was used throughout the experiments.

Differential thermal analysis (DTA)

DTA assembly with temperature programmer of F and M Scientific 240 Hewlett Packard and thermocouple platinel-II of Engelhard Ltd., U.S.A. were used. DTA curves for $\approx$35 mg of each sample, were recorded by Rigadenki Kogyo Co. Ltd. recorder in static air at a heating rate 4 °C/min. Alumina was used as a reference standard.

Results and Discussion

Analytical data of the complexes, composition of the residue and decomposition temperature are presented in Table I. TG, DTG and DTA curves are shown in Figs. 1 to 3, while the corresponding transition temperature, TG weight loss data and DTA peak temperature are listed in Table II. The position of the characteristic IR peaks are shown in Table III.

Stoichiometry and structure of the complexes

The analytical data reported in Table I indicates that the stoichiometry of all the complexes is $ML_2 \cdot 2H_2O$, where M stands for VO(II), Cu(II), Ni(II), Co(II), Fe(II), Mn(II), Zn(II) and L the anion of salicylic acid.

The infrared spectrum of the solid salicylic acid is almost identical to that of its complexes in the region $2000-625$ cm^{-1}. The frequencies of most interest with regard to structure are the C—O and O—H vibrations. The ν(C=O) band at 1650 cm^{-1} is shifted to a lower frequency ($\approx$1570 cm^{-1}) in all the complexes showing that complexation has taken place through the carboxyl group [17, 18]. The infrared spectra also shows that the ν(OH) band has shifted from 3240 cm^{-1} in salicylic acid to $\approx$3500 cm^{-1} in the complexes indicating the absence of hydrogen bonding [19]. Appearance of
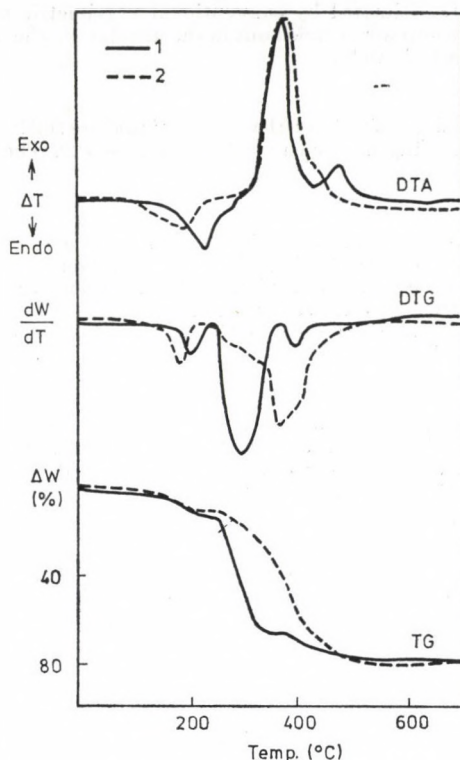
Fig. 1. TG, DTG and DTA curves for bis-(salicylato)-diaqua complexes; (1) Cu(II), (2) Ni(II)

new band in the neighbourhood of 800 cm^{-1} in all the complexes shows that the water molecules are co-ordinated to the metal ion [20—22]. The presence of a band at $\approx$315 cm^{-1} confirms the presence of co-ordinated water [23]. The presence of water as co-ordinated water is further borne out by the thermal decomposition data (Figs. 1 to 3). It may also be noted that the δ O—H (phenolic) bending peak at 1300 cm^{-1} remained almost at the same position for both salicylic acid and its complexes. This shows that there is no loss of proton by the phenolic OH group up on co-ordination.

All the complexes are insoluble in water and common organic solvents suggesting polymeric structure to each of them. Because of their insolubility in common organic solvents extent of polymerization could not be determined. Early reported data on magnetic susceptibility and electronic spectra, except Zn(II), indicated octahedral stereochemistry for all the complexes [24]. The thermal decomposition would appear to be consistent with this type of structure and would suggest that the water molecules are directly bonded to the metal ion along with two salicylate moieties to give a co-ordination number of six for each of the metal(II) ions.
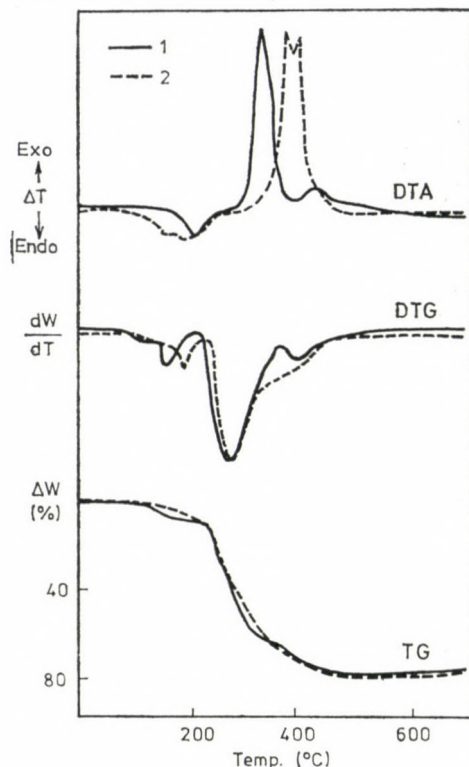
Fig. 2. TG, DTG and DTA curves for bis-(salicylato)-diaqua complexes; (1) Co(II), (2) Mn(II)

The increase in the difference between $\nu COO(asym)$ and $\nu COO(sym)$, (Δ), has been taken as a measure of increasing covalency of the M—O bond [25]. The salicylic acid complexes presented a band at $\approx 1600-1620$ for $\nu COO(asym)$ and at $\approx 1435-1450$ for $\nu COO(sym)$. Thus the covalent character of the M—O bond follows the order: Fe(II) < Mn(II) < Co(II) < Ni(II) < < Cu(II) < Zn(II) < VO(II).

Thermal decomposition

In general TG weight loss data, DTG and DTA curves suggest three steps of the thermal decomposition of the complexes as follows:

Step I

$$[C_6H_4(OH)COO]_2M \cdot 2H_2O \rightarrow [C_6H_4(OH)COO]_2M + 2H_2O$$
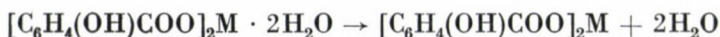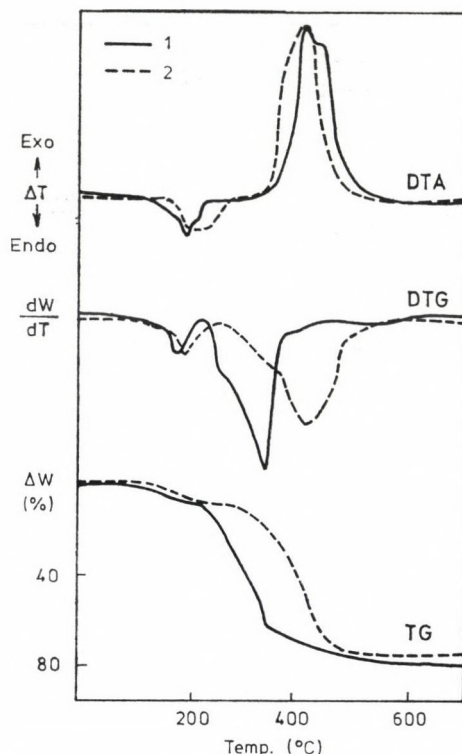
Fig. 3. TG, DTG and DTA curves for bis-(salicylato)-diaqua complexes; (1) Fe(II), (2) VO(II)

Step II

$$[C_6H_4(OH)COO]_2M \rightarrow MCO_3 + \text{combustion (volatile) products; } CO, CO_2, 2H_2O$$

Step III

$$MCO_3 \rightarrow MO + CO_2.$$

At step I, co-ordinated water is lost. This step is characterized by an endothermic effect (DTA curves; Figs. 1 to 3). This is supported by TG curves where the first inflection corresponds to the weight loss of two water molecules (TG curves; Fig. 1 to 3 and Table I).

In steps II and III, pyrolysis of anhydrous complex occurs. In step II, metal carbonate formation and combustion of salicylate moiety takes place; the net effect of step II is exothermic as shown by the DTA curve. The gaseous combustion products of the salicylate moiety are CO, CO_2, H_2O in accordance with those reported for other salicylate systems [7, 9]. In step III, metal carbonate finally decomposes into metal oxide with the evolution of CO_2.

Table II

TG horizontal maximum and range of DTG and DTA peaks of
bis-(salicylato)-diaqua complexes

Complex	D.P.	Range of TG horizontal (°C)	Maxima of the DTG trace (°C)	Range of DTG effect (°C)	Maxima on the DTA trace (°C)		Range of DTA effect
(I) $Cu(SA)_2 \cdot 2H_2O$	I	$100-240\pm4$	200 (m)	$166-219$	210 (s)	*Endo.*	$165-250\pm2$
	II	$250-370\pm2$	300 (s)	$252-333$	350 (s)	*Exo.*	$300-246\pm4$
	III	$370-560\pm4$	392 (m)	$372-419$	480 (s)	*Exo.*	$426-500\pm2$
(II) $Ni(SA)_2 \cdot 2H_2O$	I	$80-220\pm2$	179 (m)	$159-192$	200 (m)	*Endo.*	$100-226\pm2$
	II	Undiscernible	—	—	—		—
	III	$230-520\pm2$	359 (s)	$339-419$	400 (s)	*Exo.*	$226-479\pm4$
(III) $Co(SA)_2 \cdot 2H_2O$	I	$100-220\pm4$	153 (m)	$139-172$	205 (w)	*Endo.*	$166-272\pm4$
	II	$230-360\pm2$	272 (s)	$226-352$	330 (s)	*Exo.*	$300-372\pm2$
	III	$360-520\pm3$	400 (m)	$372-413$	440 (w)	*Exo.*	$400-500\pm4$
(IV) $Mn(SA)_2 \cdot 2H_2O$	I	$80-210\pm2$	186 (w)	$179-192$	205 (w)	*Endo.*	$100-233\pm2$
	II	Undiscernible	—	—	—		—
	III	$220-500\pm4$	272 (s)	$233-313$	390 (m)	*Exo.*	$346-419\pm2$
(V) $Fe(SA)_2 \cdot 2H_2O$	I	$80-220\pm2$	172 (w)	$166-185$	190 (m)	*Endo.*	$110-226\pm2$
	II	Undiscernible	—	—	—		—
	III	$240-620\pm4$	339 (s)	$252-352$	400 (s)	*Exo.*	$372-472\pm4$
(VI) $VO(SA)_2 \cdot 2H_2O$	I	$110-260\pm4$	179 (m)	$172-200$	220 (s)	*Endo.*	$152-266\pm2$
	II	Undiscernible	—	—	—		—
	III	$270-520\pm3$	413 (s)	$379-466$	400 (s)	*Exo.*	$333-459\pm4$
(VII) $Zn(SA)_2 \cdot 2H_2O$	I	$100-240\pm4$	200 (s)	$180-200$	210 (m)	*Endo.*	$200-280\pm4$
	II	$260-340\pm2$	340 (sh)	$320-360$	340 (s)	*Exo.*	$333-400\pm2$
	III	$350-450\pm3$	460 (s)	$440-500$	450 (s)	*Exo.*	$416-526\pm4$

s (sharp), sb (sharp and broad), sh (shoulder), m (medium), mb (medium and broad), w (weak).

This decomposition is endothermic always, the oxidation, however, of a product of cracking from the preceding decomposition process, or that of carbon probably produced an exothermic effect shown on the DTA curve.

At the end of steps I and II, small horizontals occur, whose importance for analytical purposes is rather doubtful. A horizontal corresponding to metal oxide is especially useful for analytical purposes.

The recorded DTA curves (Figs. 1 to 3) are observed to have unusual shapes, however, we have compared them with those reported by earlier workers [5, 7, 9] for other salicylates and observed that they too have obtained unusual shapes of DTA exothermic peaks. Such abnormal shapes are also found in malato-aqua [26] and EDTA [27] complexes of transition metals.

The abnormal shape of exothermic peaks of the DTA curves is probably due to the various gaseous combustion products escaped as a consequence of

Table III

Characteristic I.R. frequencies for bis-(salicylato)-diaqua complexes

	SA	Bis-(Salicylato)-diaqua complexes of		
		Cu(II)	Ni(II)	Co(II)
νCOO^--asy	1660 (s)	1615 (s)	1630 (s)	1620 (s)
νCOO^--sym	1450 (s)	1400 (s)	1420 (s)	1410 (s)
νOH	3600—2600	3660—2700	3670—3000	3650—3000
	(3300) sb	(3380) sb	(3390) sb	(3500) sb
$\delta O-H$	1315 (s)	1315 (s)	1320 (m)	1320 (m)
$\delta\gamma H_2O$	—	870 (m)	860 (s)	860 (s)
$\nu M-O + (C-C)$	—	596 (sh)	585 (sh)	540 (mh)
$\nu M-O +$ ring	—	455 (m)	470 (wb)	425 (m)
ΔCOO^-	—	215	210	210

s (sharp), ss (sharp and broad), m (medium), w (weak), wb (weak and broad), sh (shoulder)

	Bis-(Salicylato)-diaqua complexes of			
	Mn(II)	Fe(II)	VO(II)	Zn(II)
νCOO^--asy	1602 (s)	1630 (s)	1630 (s)	1630 (s)
νCOO^--sym	1400 (s)	1435 (s)	1405 (s)	1410 (s)
νOH	3655—2800	3640—2900	3665—2700	3650—2800
	(3900) sb	(3410) sb	(3340) sb	(3400) sb
$\delta O-H$	1320 (m)	1320 (m)	1310 (w)	1315 (w)
$\delta\gamma H_2O$	850 (s)	855 (s)	860 (s)	855 (s)
$\nu M-O + (C-C)$	580 (w)	565 (sh)	570 (m)	575 (m)
$\nu M-O +$ ring	475 (mb)	450 (w)	430 (w)	435 (w)
ΔCOO^-	202	195	225	220

the decomposition of the organic skeleton, i.e., salicylate moiety of the complex. A large and broad exothermal peak in a wide temperature range on the DTA curve for decomposition of dehydrated complexes indicates beside the decomposition, oxidation and combustion processes too.

Characteristic thermal behaviour of individual complexes

    The persual of Figs. 1—3 indicates that in case of $Cu(SA)_2 \cdot 2H_2O$, $Co(SA)_2 \cdot 2H_2O$ and $Zn(SA)_2 \cdot 2H_2O$ all the three decomposition steps could be distinguished. On the other hand, for $Ni(SA)_2 \cdot 2H_2O$, $Mn(SA)_2 \cdot 2H_2O$, $Fe(SA)_2 \cdot 2H_2O$ and $VO(SA)_2 \cdot 2H_2O$ only two steps could be discernible. In the latter cases the overlapping of steps II and III takes place probably due to almost rapid and continuous decomposition of the dehydrated complexes. In all the cases stoichiometries of the thermal decomposition products are found to be quantitative (Tables I and II).

    It is worthy to note that for $Fe(SA)_2 \cdot 2H_2O$, FeO was the major end product above 575 °C. However, below this temperature it gets contaminated

with Fe_2O_3. As these reactions were carried out in air, there may be possibility of other oxide formation also, but the predominant oxide which might have been formed is Fe_3O_4 as the metal is characterized by its ability to form such oxide. In case of $Mn(SA)_2 \cdot 2H_2O$ the final residue was expected to be a mixture of MnO and Mn_3O_4 (Tables I and II). Similarly for $VO(SA)_2 \cdot 2H_2O$, the end product was found to be a mixture of vanadium di and penta oxides. Formation of V_2O_5 is probably due to the reason that the thermal decomposition takes place in air which causes the oxidation of vanadium dioxide.

Isolation of intermediate products

In order to isolate intermediate products of the thermal decomposition, samples were heated in air to an appropriate temperature in a crucible and the residues were analysed. The decomposition products have also been confirmed by IR and X-ray K-absorption edge studies. However, all the intermediate products of the decomposition steps could not be isolated and identified owing to the lack of a clear cut horizontal on the TG curve, as the intermediate products are not stable to the required extent.

The IR spectra, however, confirm the dehydration (Step I) since the peaks and bands characteristic of the co-ordinated water disappeared in the IR spectra of first decomposition product.

As a result of dehydration the change in stereochemistry of the complexes is observed. It is worthy to note that the colour intensity is increased due to the formation of dehydrated complexes. The composition of the dehydrated complex is checked through elemental analysis, IR spectra and X-ray K-absorption studies.

We have studied the X-ray K-absorption spectra of Cu(II), Ni(II), Co(II) and Zn(II) complexes $(ML_2 - 2H_2O)$ as well as their dehydrated products (ML_2) [28] and have indicated that change in stereochemistry from octahedral to tetrahedral takes place as a consequence of dehydration. Details of the study will be published elsewhere [28].

Thermal stability of the complexes

If the initial decomposition temperature is taken as a measure of the thermal stability of complexes, we can conclude that the stability of the metal complexes increases roughly in the order Mn(II) < Fe(II) < Ni(II) < Co(II) < < Zn(II) < Cu(II) < VO(II).

It is interesting to note that the dehydration temperatures of the complexes increases with the increase in coordinated water frequency. This is also in the order mentioned above.

This finding may also be explained in terms of metal percentage (M% in the complexes (Table I).

Conclusions

Results of this study on thermal decomposition of salicylic acid complexes showed that thermal analysis can be useful for the determination of the number of molecules of water bound, for detecting contamination with starting reagents and for the control of the agreement of declared composition of a compound. It also provides a means for correlating the microbial activity with the change in the stereochemistry of the active species.

The knowledge of heating curves is useful for gravimetric analysis of a compound. For quantitative analysis of the compound studies, a horizontal formed at the first and the last stage of decomposition is only suitable. Particularly the latter is of much quantitative importance.

Increasing heating rates, DTA and DTG peaks as well as horizontal on the TG traces, changed in the manner reported by Schultze [29].

*

REFERENCES

[1] Khadikar, P. V., Pol, B., Heda, B. D.: Indian J. Microbiology, **18,** 175 (1981)
[2] Heda, B. D., Khadikar, P. V.: Indian J. Pharm. Sci., **42,** 174 (1980)
[3] Khadikar, P. V., Heda, B. D.: Indian J. Hospt. Pharm., **17,** 39 (1980)
[4] Khadikar, P. V., Mishra, S., Saxena, C. P.: Curr. Sci., **48,** 20 (1979)
[5] Hora, Y., Osada, H.: Kogyo Kagaku Zasshi, **73,** 1996 (1970)
[6] Hora, Y. Osada, H.: Kyushu Kogyo Diagaku Kenkyu Hokoku Kogaku, **22,** 51 (1971)
[7] Radecki, A., Wesolowski, M.: Thermochim. Acta, **17,** 217 (1976)
[8] Radecki, A., Kobayiczyk, K., Andrzejeczak, B.: Ann. Acad. Med. Gedan, **4,** 127 (1974); Rozpr. Wydz. III. Gdansk. Tow Nauk, **9,** 95 (1972)
[9] Radecki, A., Wesolowski, M.: J. Thermal Anal., **9,** 16 (1976); **9,** 357 (1976); **10,** 233 (1976); **11,** 39 (1977)
[10] Wendlandt, W. W.: Anal. Chim. Acta, **18,** 316 (1958)
[11] Erdey, L., Gal, S., Liptay, G.: Talanta, **11,** 913 (1964)
[12] Khadikar, P. V., Heda, B. D.: Bull. Soc. Chim. Belg., **89,** 1 (1980)
[13] Khadikar, P. V., Gogne, G. R., Heda, B. D.: Bull. Soc. Chim. Belg., **89,** 779 (1980)
[14] Khadikar, P. V., Heda, B. D.: Univ. Indore Res. J. Sci., **1980,** 6
[15] Khadikar, P. V., Ameria, R. L., Kekre, M. G.: J. Inorg. Nucl. Chem., **35,** 4301 (1973)
[16] Vogel, A. I.: Quantitative Inorganic Analysis, Longman 1959
[17] Busch, D. H., Bailar Jr., J. C.: J. Am. Chem. Soc. **75,** 4574 (1953)
[18] Kirschna, S.: J. Am. Chem. Soc., **78,** 2372 (1956)
[19] Green, J. H. S., Kynaston, W., Lindsea, A. S.: Spectrochim. Acta, **17,** 486 (1961)
[20] Fujita, J., Nakamota, K., Kobayashi, M.: J. Am. Chem. Soc., **78,** 3963 (1956)
[21] Sartri, G., Furlani, C., Damiani, A.: J. Inorg. Nucl. Chem., **8,** 119 (1959)
[22] Game, I.: Bull. Soc. Chem. Japan, **34,** 760 (1961)
[23] Goodgame, M., Haywao, A. J.: J. Chem. Soc. (A), **1968,** 1108
[24] Khadikar, P. V., Ameria, R. L.: Ph. D. Thesis, Vikram University 1969
[25] Carillo, A., Vieles, P., Banniol, A.: C. R. Acta Sci., Ser. C, **274,** 912 (1972)
[26] Wendlandt, W. W., Harton, G. R.: Nature, **187,** 769 (1960)
[27] Al-Janabi, M. Y., Ali, N. J., Milad, N. E., Barbooti, M.M .: Thermochimica Acta, **25,** 101 (1978)
[28] Khadikar, P. V., Anikhindi, A. G.: J. Chem. Phys. (to be published)
[29] Schultze, D.: Differential-Thermoanalyse, Berlin, VEB Deutscher Verlag der Wissenschaften 1969

EQUIDENSITOMETRY — A METHOD TO ESTIMATE THE STRUCTURE OF PLASMAS, XIV*

INVESTIGATION OF SPATIAL AND TEMPORAL ELEMENT DISTRIBUTION IN THE D.C.ARC FOR POWDER SPECIMENS AT CATHODIC EVAPORATION

Klaus Dittrich[1]**, Asparuch Petrakiev[2], Todor Oreshkov[3] and Knut Niebergall[1]

(*[1]Karl-Marx-University, Department of Chemistry, 7010 Leipzig, Talstr. 35, GDR,*
[2]Faculty of Physics, Kliment-Okhridsky University, Blv. Anton Ivanov 5,
1126 Sofia, Bulgaria, [3]Chemical Faculty, Technical University, 8010 Burgas, Bulgaria)

By using a combination of spectral photography and photographic equidensitometry the distribution of the elements Li, Al, (Tl), (Sn), Ag, Mg, (Si), Sb, Be and C was investigated in the plasma of the d.c. arc at cathodic evaporation of powder specimens from a crater electrode. The effect of the concentration of the readily ionizable additive Li (Li_2CO_3) on the distribution of the trace elements was studied. A correlation was found between ionization potential of the trace element and additive concentration, on the one hand, and intensity increase, on the other hand. Conclusions were made for optimization of single-element and multielement analyses.

To determine trace elements in pure substances and natural products, analytical methods combined with concentrating techniques are frequently applied. The traces are often bound to carbon powder by adsorption, the latter then being directly subjected to spectral analysis. In order to improve the detection limit, readily ionizable elements like K, Na, Li, Ga, Ba etc. [1—3] are utilized, added in the form of their salts to the carbon powder. Excitation of these specimens is usually performed by d.c. or a.c. arcs. The image of the central part of the discharge is formed on the slit of the spectrograph. When making use of d.c. arcs, some authors [4—7] utilize the intensifying effect of the region close to the cathode and form the image of this region. Improvements of the detection limit attained in this manner may reach one order of magnitude. For this reason it is of particular interest to investigate the temporal-spatial distribution of the elements in the plasma of the d.c. arc. Spatial distribution has been studied so far by radioactive isotopes [8—10], by AAS [11] and by determination of the width and intensity of the spectral lines [12—14]. In this work another method developed by us is described, allowing two-dimensional evaluation of the plasma. The underlying concept is a combination of spectral photography (photography with a stigmatic image-forming spectrograph without slit) and photographic equidensitometry [15]. We applied this method to numerous studies of arc plasmas [16—21]

---

* Part XIII: Spectrochim. Acta, **39B**, 1225 (1985).
** To whom correspondence should be addressed.

and also to studies of inductively coupled plasma [22]. A comprehensive paper is given in [23].

In this paper it will be applied to study the effect of Li (Li_2CO_3) on the distribution of trace elements in the arc plasma. Evaporation of the specimens was performed on the cathode, having a lower temperature as compared to the anode. Owing to this condition, the specimen will evaporate elements.

Experimental

Apparatus

For *spectral arc photograms*: plane-grating spectrograph PGS-2 (Carl-Zeiss-Jena, GDR) without slit. Image formation: direct, reduction 5 : 1 with one lens. Plane grating: 650 lines/mm, blaze wave length 1020 nm. Reciprocal linear dispersion: 3rd order 0.234 nm/mm, 4th order 0.176 nm/mm. Photographic plate: ORWO-WU 3, blue extra hard. Electrodes: cathode (lower electrode) = crater, electrode 6 mm diam. Crater: 4 mm diam, 2 mm depth, anode (upper electrode) = counter electrode, 6 mm diam, conically formed (17 mm length, 2 mm diam). Distance: 5 mm.

For *line spectra*: spectrograph ISP-30 (U.S.S.R.). Slit width: 0.012 mm. Image formation: intermediate with 3 lenses, image of the part of the arc close to the cathode (0 to 2 mm). Exposure: 30 s.

(The reason for using these different instruments was not a matter of principle, but due to the division of work between the institutes participating.)

Materials

Carbon powder, spectral grade.

Li_2CO_3; Li-contents in the carbon powder: 0; 0.25; 0.5; 0.75; 1; 2; 4; 6; 8; 10%, resp. Trace elements: each specimen contained 0.002% Al (Al_2O_3); 0.008% Sn (SnO_2); 0.002% Ag ($AgNO_3$); 0.002% Si (SiO_2); 0.008% Be(Be ($NO_3)_2$); 0.001% Sb (Sb_2O_3); 0.002% Mg (MgO); 0.008% Tl ($TlNO_3$).

Performing of experiments

20 mg carbon powder (mixed with the trace elements and the desired amount of Li_2CO_3) was placed into the crater of the cathode (lower electrode). 10 A d.c. current was used for excitation.

Exposure with the PGS-2 instrument for a spectrogram to be used for equidensitograms was 1 s. Exposure can be performed after differing prefiring times or — also repeatedly —

Table I

Characteristics of the selected spectral transitions ionization potentials and improvements of the total radiation intensity at cathodic evaporation
(anodic evaporation = 100%)

Element and spectral line (nm)	Excitation potential (eV)	Ionisation potential (eV)	Improvement (%)
Li I 323.26	3.83	5.39	—
Al I 308.21	4.02	5.98	310
Tl I 276.79	4.44	6.11	300
Sn I 317.50	4.33	7.34	260
Ag I 328.07	3.78	7.57	260
Mg I 285.21	4.34	7.64	205
Si I 288.16	5.08	8.15	150
Sb I 287.80	5.36	8.64	135
Be I 332.13	6.45	9.32	115
C I 247.86	7.49	11.26	—

during a burn-off. Total intensity with the ISP-30 instrument was determined in the usual manner (exposure 30 s).

The characteristics of the evaluated lines are summarized in Table I. The elements differ above all in their ionization potential.

Spectral photography

The light source, that is, the total d.c. arc was projected with one lens at a reduction of 5 : 1 directly in the slit plane of a stigmatic plane grating spectrograph PGS-2. The entrance slit of this spectrograph had been removed and replaced by a photographic shutter with a circular opening ($r = 0.2 \ldots 0.8$ cm). In this manner one obtains on the photographic plate, instead of the spectral lines, for each transition the total image of the arc. Spectral overlappings may occur, however the resolution of the spectrograph is so good that in not too line-rich spectra very many evaluable spectral plasma images will be obtained.

Photographic equidensitometry

A series of contact copies with different exposure times were made of the spectrograms obtained, on plane film (FU 5 ORWO Wolfen, GDR); these copies, after development, but without fixation were subjected to a second exposure with diffuse light. Due to the Sabattier-effect, after a second development and fixation, a white line will appear on a dark background. This line, the equidensite, connects all points of equal density in the original photogram. A contact copy will then yield a black line against a light background. These individual equidensities were then suitably magnified and mounted together, so that the final result is the total image of the arc as equidensitogram. For calibration of individual equidensities a standard grey wedge was used. Equidensity numbers up to 10 are equal to the density values multiplied by 10; above No. 10, the numbers increase with density values of 0.2 (e.g. No. 10 = density 1.0; No. 15 = density 2.0). For the sake of lucidity only the number of the highest equidensity is marked in the equidensitograms. From this value one can find the values of the other equidensites by counting in the reverse order of succession.

Results and Discussion

Distribution of the matrix elements in the arc

In order to find the distribution of the matrix elements, spectrograms of C I and Li I were taken in the presence of different Li concentrations. Exposures were made at 2 s, 11 s and 20 s after the start of burn-off, so that temporal changes in element distribution could also be observed. Results are represented in Fig. 1. To promote comprehensiveness, the corresponding equidensitograms of C and Li have been combined into one figure each.

Figure 1 shows that in the absence of Li, the distribution of C is close to homogeneous over the whole arc column. Slightly higher enrichments are observable in the vicinity of the cathode. In the presence of 1% Li, Li atoms are present in the cathode space only. This orientation increases with longer burn-off periods. In contrast, the distribution of the C atoms at the beginning of the discharge (after 2 s) is oriented towards the anode. As Li concentration decreases with increasing burn-off time, C distribution becomes homogeneous again. In the presence of high Li concentrations (8%), Li distribution is almost homogeneous at the beginning and subsequently increasingly oriented towards the cathode. C enrichment has its maximum at the anode, and the maximum is slowly shifted towards the centre with increasing burn-off time.
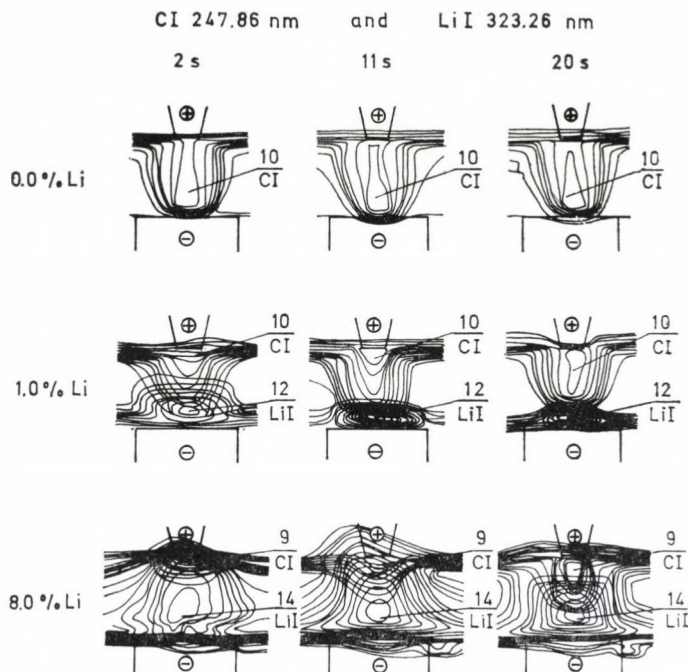
Fig. 1. Dependence of the spatial and temporal distribution of C I and Li I intensity on the Li concentration of the specimen (superimposed equidensitograms)

The reason for these distributions is in the two motion components convection (for all particles) and migration of ions in the electric field, and in the differing ionization degrees in the arc.

The ionization degree of the C atoms difficult to ionize will change with the concentration of the readily ionizable Li, controlling electron pressure. In the absence of Li the ionization degree of C is relatively high at temperatures of 7000 to 8000 °C present in the pure carbon arc, so that the two motion components will result in a homogeneous arc plasma. With increasing Li concentration, arc temperature decreases and electron pressure increases. This results in a reduced ionization degree of C and hence in reduced oriented, field-controlled migration of the C^+ ions. Evaporation decrease from the cathode affects the phenomena. As a result, anode-oriented C distribution will appear. The situation for Li is similar. Arc temperature is lowest at extremely high Li concentration (8%, 2 s). Consequently, the ionization degree of Li will also be lowest, although electron pressure is maximum at these conditions. Hence, Li atoms can move axially by convection (and also by diffusion) toward the centre of the arc. Decreasing Li concentration is equivalent to temperature increase and ionization degree increase for Li, by reason of which oriented

AI I 308.21 nm
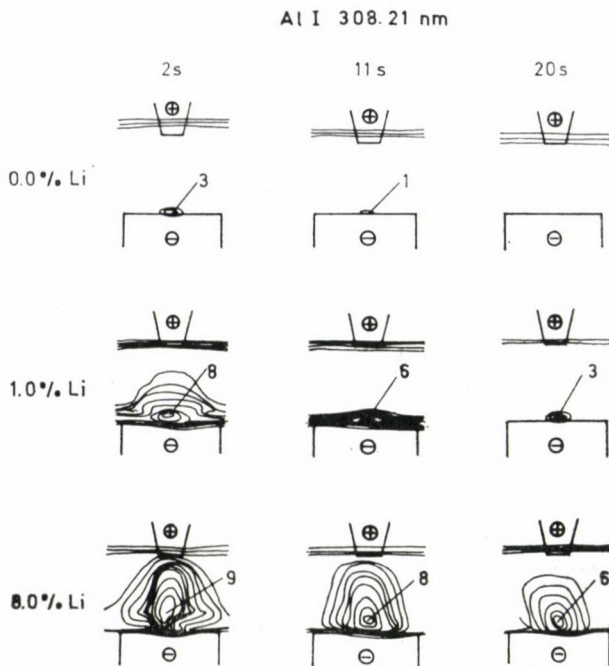
Fig. 2. Dependence of the spatial and temporal distribution of Al I intensity on the Li concentration of the specimen

motion of the Li ions will lead to its enrichment increase in the cathode space, that is, diffusion and convection will be suppressed.

Figure 2—6 demonstrate the results for the trace elements Al I, Ag I, Mg I, Sb I and Be I.

The distribution of the trace elements in the arc plasma is similar to that of Li, that is, at high Li concentrations (8%, 2 s) a more or less pronounced homogeneous distribution of the atoms is observable. At decreasing Li concentrations (gradual evaporation from initial 8%, or lower initial concentration and additional gradual evaporation) the maxima are shifted towards the cathode.

The differences observed between individual trace elements are due to their differing ionization potentials and consequently — under identical external conditions, i.e. electron pressure controlled by C or Li — differing degree of ionization.

Highest Li concentration results, in the case of Al, in homogeneous element distribution. This is similar for Ag I and Mg I too, but in these cases significant homogenization is observed already at an initial Li concentration of 1%. This is even more expressed in the case of the less readily ionizable

4

AgI 328.07 nm
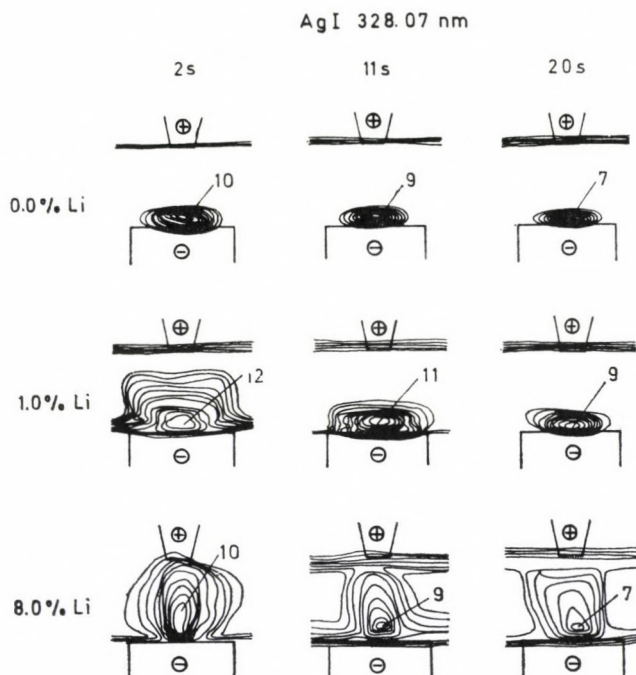
Fig. 3. Dependence of the spatial and temporal distribution of Ag I intensity on the Li concentration of the specimen

MgI 285.21 nm
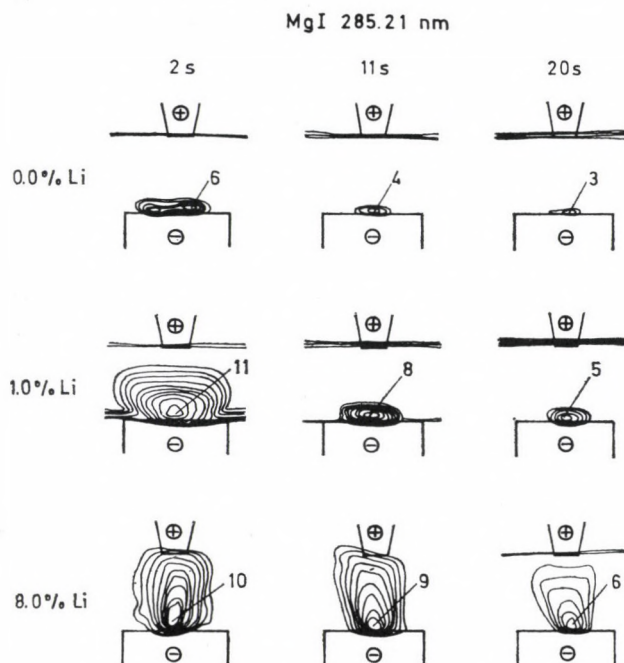
Fig. 4. Dependence of the spatial and temporal distribution of Mg I intensity on the Li concentration of the specimen

Sb I 287.80 nm
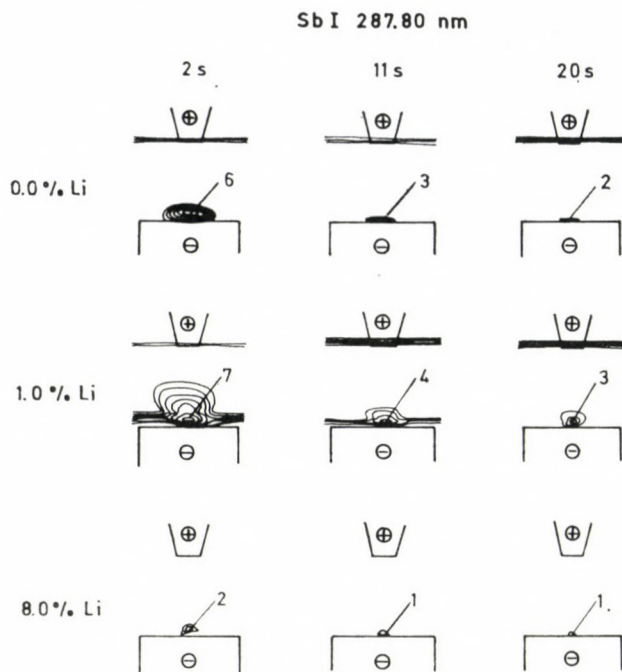
Fig. 5. Dependence of the spatial and temporal distribution of Sb I intensity on the Li concentration of the specimen

Be I 332.13 nm
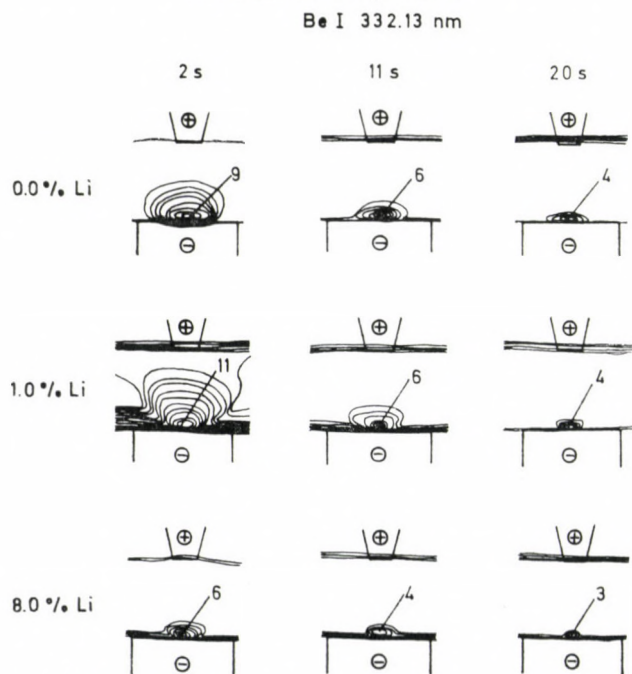
Fig. 6. Dependence of the spatial and temporal distribution of Be I intensity on the Li concentration of the specimen

elements Sb I and Be I. In the Li-free arc only the least ionizable element Be I shows a trend towards homogeneous distribution, all other elements are ionized to such a degree that field-controlled oriented motion of the ions prevents a free distribution of the atoms being in dynamic equilibrium with the ions. All particles are enriched in the cathode space.

Obviously, total intensity of radiation in the respective maxima of the selected atomic lines is also affected by the degree of ionization. This is clearly expressed in the case of Al, where maximum density at 8% Li, 2 s is much higher than at 0% Li, 2 s (cf. equidensities No. 9 and No. 3 in Fig. 2). From the present concept there is no explanation for the substantial intensity decrease of Sb I and Be I lines in the present of 8% Li; other factors must be responsible for the phenomenon. In the case of Sb, the reason might be a very rapid evaporation (<2 s) of the bulk of Sb, caused by the carrier effect of Li_2CO_3. In the case of Be, substantial intensity decrease might presumably be caused by slower evaporation due to increased carbide formation. However, these effects have not been further studied.

The results discussed indicate that for individual elements, differing Li concentrations are required to establish optimum conditions. In multielement analyses, therefore, a compromise must be made. It is also clear that the choice of the arc region close to the cathode for analytical purposes will improve the line to background ratio. We therefore chose the arc section cathode to 2 mm above the cathode to investigate the relationship total intensity during a burn-off versus Li concentration for the individual elements. The results are presented in Fig. 7.

This figure demonstrates that for readily ionizable elements (Al I, Tl I) maximum intensity is reached in the presence of $6-8\%$ Li. For Ag I, Mg I and Sn I whose ionization potential is similar, this value is 2% Li, and for the least readily ionizable Be I around 0.25% Li. For a multielement analysis, a value of $1-2\%$ Li is recommended.

Since already the equidensitograms demonstrated that total intensity is influenced not only by the motion in the arc plasma, but also by evaporation, cathodic and anodic evaporation of the elements was compared, the spectrograms being taken from the arc section close to the cathode (0 to 2 mm) also in the case of anodic evaporation. Also, optimum Li concentration was determined and applied in the case of anodic evaporation. Optimum Li concentration was found to be the same for both evaporation variants.

The improvement by optimum Li concentration is also presented in Table I, clearly manifesting that in the chosen analysis example cathodic evaporation is much preferable. Also, a distinct trend is recognizable that cathodic evaporation is of particular advantage for readily ionizable elements. This trend is attributable to optimum conditions being less clearly defined for more difficultly ionizable elements (cf. Fig. 7).
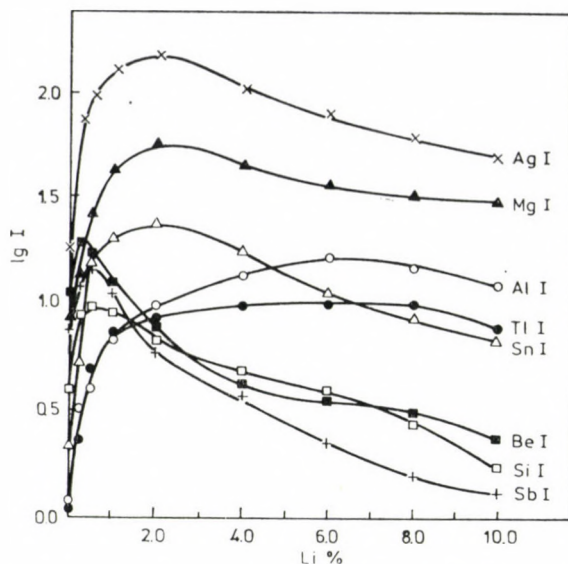
Fig. 7. Total intensity of the special lines Al I 308.21 nm, Tl I 276.79 nm, Sn I 317.50 nm, **Ag I** 328.07 nm, Mg I 285.21 nm, Si I 288.16 nm, Sb I 287.80 nm, Be I 332.13 nm versus Li concentration of the specimen

Conclusions

1. It was stated, by combining spectral photography and photographic equidensitometry, that the distribution of elements in the d.c. arc plasma depends on the concentration of the additive (readily ionizable element), on the ionization potential of the trace element, on the physico-chemical properties (mainly evaporation) of the trace element and on the moment of the burn-off period.

2. The addition of readily ionizable elements (e.g. Li) to the specimen results, at cathodic evaporation of the trace elements and the additive, in a larger excitation zone of the element in the arc. Radiation maxima will be shifted from the space close to the cathode towards the centre of the arc with increasing additive concentration. This shift takes place already at low additive concentrations in the case of difficultly ionizable elements, and only at high additive concentrations in the case of readily ionizable elements.

Since optimum intensity is observed parallel to this shift, a compromise of conditions must be made for multielement analyses; these conditions may, however, be improved for single-element analyses.

3. Best effects in intensity increase are obtained for elements with low ionization potentials by replacing the generally applied anodic evaporation by cathodic evaporation. Also, readily ionizable elements — in cathodic

evaporation — show higher intensity increases with optimum additive concentrations as compared to the results in the absence of additive.

4. It could be confirmed that the plasma-diagnostic method developed allows to improve the detection of trace elements and to elucidate plasma processes. In particular, it could be demonstrated that element distribution in the arc is subjected to a continued temporal change.

REFERENCES

[1] Pinta, M.: Recherche at dosage des éléments traces, Dunod, Paris 1962
[2] Silbershteyn, Kh. I.: Spectral analysis of pure materials (in Russian), Khimiya, Leningrad 1971
[3] Yudelevich, I. G., Buyanova, L. M., Shelpakova, I. R.: Chemical spectral analysis of high-purity materials (in Russian), Nauka, Novosibirsk 1980
[4] Mannkopff, R., Peters, Cl.: Z. f. Phys., **70**, 44 (1931)
[5] Decker, R. J.: Spectrochim. Acta, **28**, 339 (1973)
[6] Larin, N. B., Shishov, V. N., Mishina, E. I.: Handbook of production and analysis of pure materials (in Russian), Gorky 1977
[7] Kurochkina, A. M. Rubinovich, R. S.: Zh. prikl. Spektrosk., **29**, 202 (1978)
[8] Vaynshteyn, E. E., Belyaev, Yu. I.: Zh. anal. khim. **13**, 388 (1958)
[9] Belyaev, Yu. I., Vaynshteyn, E. E., Korolev, V. V.: Zh. anal. khim., **14**, 147 (1959)
[10] Saidel, A. N.: Fundamentals of spectral analysis (in Russian), Nauka, Moscow 1965
[11] Morosov, V. N., Tatarinova, N. A., Shiptsin, S. A.: Zh. prikl. spektrosk., **15**, 984 (1971)
[12] Goldfarb, V. M., Ilina, E. V.: Zh. prikl. spectrosc., **5**, 331 (1966)
[13] Yakhariya, N. F., Shchegolkov, S. V.: Handbook of spectroscopy, methods and applications (in Russian), Nauka, Moscow, Vol. **1**, 1969, p. 258
[14] Avni, R., Boukobza, A.: Spectrochim. Acta, **24B**, 515 (1969)
[15] Dittrich, K., Niebergall, K., Rössler, H.: Spectrochim. Acta, **31B**, 331 (1976)
[16] Dittrich, K., Rössler, H., Niebergall, K.: Acta Chim. Acad. Sci. Hung., **89**, 347 (1976)
[17] Karyakin, A. V., Dittrich, K., Pavlenko, L. I., Babicheva, G. G., Zschocke, R.: Zh. anal. kihm., **34**, 98 (1978)
[18] Oreshkov, T., Petrakiev, A.: XV. Internat. Conf. on Phenomena in Ionized Gases, Minsk, U.S.S.R. Conf. papers, Part II, p. 749, 1981.
[19] Shelpakova, I. R., Dittrich, K., Yudelevich, I. G., Wennrich, R., Shcherbakova, O. I.: Zh. prikl. spektrosk., **34**, 604 (1981)
[20] Dittrich, K., Suleva, A., Niebergall, K.: Spectrochim. Acta, **36B**, 555 (1981)
[21] Oreshkov, T., Petrakiev, A., Dittrich, K.: Spectrochim. Acta, **36B**, 515 (1981)
[22] Niebergall, K., Brauer, H., Dittrich, K.: Spectrochim. Acta, **39B**, 1225 (1984)
[23] Dittrich, K., Niebergall, K.: Progr. anal. atom. spectrosc., **7**, 315 (1984)

PHOTOEVOLUTION OF HYDROGEN FROM WATER ON MODIFIED TiO₂, I

TiO₂ DOPED WITH NiO, Co₃O₄ AND Fe₂O₃

Stanisław Zieliński* and Andrzej Sobczyński

(Laboratory of General Chemistry and Catalyst Synthesis, Faculty of Chemistry, A. Mickiewicz University, 60-780 Poznań, Poland)

Several catalysts composed of TiO₂ and NiO, Co₃O₄ or Fe₂O₃ were prepared. It was found that the admixtures reacted partly with TiO₂ support. PureTiO₂ and the doped catalysts evolved hydrogen from a mixture of water and EDTA under irradiation. The admixture of NiO (1 wt.%) increased the photoactivity of TiO₂ by a factor of 1.4. For all the catalysts the initial step of the photoreaction was the reduction of surface Ti(IV) by photogenerated hydrogen. An explanation of the influence of admixtures on hydrogen evolution is given.

Introduction

Although TiO₂ alone does not decompose water under irradiation [1, 2], some modifications of this oxide are photocatalysts for water splitting. It is well known that platinum-group metals supported on TiO₂ give rise to hydrogen evolution from water over irradiated titania [3, 4, 5]. On the other hand, oxygen and hydrogen evolution from water was observed when TiO₂ was loaded (or mixed) with an oxidation catalyst — RuO₂ [6, 7, 8]. Domen et al. [9, 10] reported that water vapour and liquid water could be photodecomposed on NiO—SrTiO₃ catalyst. They suggested that an admixture of a p-type semiconductor oxide (NiO) played the role of the reduction catalyst, i.e. the conduction band electrons reacted with H⁺-ions through NiO. Thewissen et al. [11] observed a slight enhancement of the photoreduction of $S_2O_8^{2-}$-ion on SrTiO₃— LaCrO₃ powders in comparison with pure SrTiO₃. Moreover, impurity technique has been used to improve the response of TiO₂-based photocatalysts and photoelectrodes, e.g. their n-type conductivity [4, 8] or extending the spectral response of TiO₂ into the visible region [4, 12, 13].

The present paper deals with the influence of NiO, Co₃O₄ and Fe₂O₃ admixtures on hydrogen evolution on irradiated anatase and is a part of our study on the influence of transition metals and their oxides on the photoactivity of titania.

---

* To whom correspondence should be addressed.

Experimental

Catalyst preparation

Pure TiO₂ was obtained by the hydrolysis of TiCl₄. After adjusting the pH to 8.0 with ammonia, the slurry was heated to 353 K, cooled down and filtered. The precipitate was dried overnight at 383 K, annealed at 673 K for 6 h and crushed in an agate mill-mortar. For mixed catalysts the desired amount of $NiCl_2$ ($CoCl_2$ or $FeCl_3$) solution was added to the aqueous slurry of TiO₂, and $Ni(OH)_2$ ($Co(OH)_2$ and $Fe(OH)_3$, respectively) was precipitated with a dilute sodium carbonate solution. The precipitate was filtered, dried and annealed in air at 673 K for 6 h. All chemicals used were of analytical grade, the water was bidistilled in a Pyrex water still.

Characterization of the catalysts

Specific surface area measurements were performed by the static BET method on a Gravimat, Sartorius, Microbalance type 4102 using nitrogen adsorption at 77 K.

X-ray diffraction patterns were taken on a TUR MG 2 diffractometer using CuK_α irradiation.

In order to determine the composition of the catalysts they were treated with boiling concentrated hydrochloric acid for 0.5 h, the slurry was filtered off, and Ni, Co and Fe were measured by atomic absorption spectroscopy (Unicam SP 90).

Reflection spectra of pure TiO₂ and NiO−TiO₂ catalysts were recorded on a Specord M 40 spectrometer using magnesium oxide as a standard. The absorbance were measured in the wavelength range of 200−800 nm.

Hydrogen evolution experiments

0.1 g of the catalyst was placed in a round bottomed Pyrex flask and 100 cm³ of 0.01 M EDTA solution was added. The suspension was magnetically stirred with bubbling oxygen-free argon for 2 h in order to remove traces of oxygen and then illuminated under flowing argon with a medium pressure mercury lamp operated at 180 V. The light passed through the filter which transmitted practically only the 366 nm wavelength. The temperature of the reaction mixture was 298 ± 2 K. Hydrogen evolved under illumination was analysed by gas chromatography using a TCD detector, a column packed with active carbon (413 K) and argon as a carrier gas.

The incident light flux was measured by an oxalate-uranyl actinometer according to the procedure described by Harchard and Parker [14]. The light flux was assumed as 7.2×10^{-2} μmole of quanta per second for the 366 nm wavelength.

Results and Discussion

Three series of doped samples were used for this study: NiO doped TiO₂, Co_3O_4 doped TiO₂ and Fe_2O_3 doped TiO₂. The amounts of dopants are listed in Table I.

As it was mentioned in Experimental, the starting TiO₂ sample was annealed at 673 K. The use of such a low temperature gave pure anatase, what was confirmed by X-ray data. The specific surface area of the pure TiO₂ was $128 \ m^1 \ g^{-1}$.

The doping with NiO, Co_3O_4 and Fe_2O_3 was made on the surface of the above described TiO₂. The intention of the authors was to prepare hetero-geneous samples consisting of islands of dopant oxide on the surface of TiO₂. However, the compositional study of the doped samples showed that only a part of a foreign oxide was dissolved in concentrated HCl. The amounts of dopanst which were dissolved during the treatment with hydrochloric acid

Table I

*Data on the samples investigated and their photoactivity
in hydrogen evolution from water*

Base oxide	Dopant	Amount of dopant wt. %	Solubility of dopant %	Rate of hydrogen evolution		Quantum efficiency %
				$\mu mols^{-1} \times 10^4$	$cm^3 h^{-1} \times 10^3$	
TiO_2	—	—	—	1.8	14.7	0.50
TiO_2	NiO	0.5	x	1.6	13.1	0.45
TiO_2	NiO	1.0	36	2.4	19.3	0.69
TiO_2	NiO	2.0	x	1.3	10.9	0.38
TiO_2	Co_3O_4	1.0	31	traces	traces	—
TiO_2	Co_3O_4	2.0	x	traces	traces	—
TiO_2	Fe_2O_3	0.5	x	1.0	8.4	0.28
TiO_2	Fe_2O_3	1.0	55	1.3	10.9	0.38
TiO_2	Fe_2O_3	2.0	x	traces	traces	—

x — The solubility of dopant was not measured

are given in Table I. The measurements were performed for the samples containing 1 wt.% of dopant oxide. For comparison purposes, pure NiO, Co_3O_4 and Fe_2O_3 were treated with HCl under the same conditions. All three oxides dissolved readily in about ten times shorter period than the doped samples. Titania alone does not dissolve in hydrochloric acid. The annealing of doped TiO_2 at higher temperatures (673—773 K) in hydrogen resulted in the reduction to metals of only a part of the oxide (i.e. NiO, Co_3O_4 and Fe_2O_3). Therefore, it is highly probable that with samples doped with 1 wt.% of NiO, Co_3O_4 or Fe_2O_3, the main part of admixture reacts with anatase and/or migrates into the bulk of TiO_2 crystals. The rest is expected to form some islands on the surface of TiO_2. Our supposition is confirmed by recently published findings of Goldman [15] on the reactions between NiO and TiO_2. According to the above author, the low temperature sintering of a mixture of NiO and TiO_2 leads to the formation of a solid solution of these two oxides. Higher temperatures, above 873 K, cause the formation of a new compound $NiTiO_3$.

X-ray diffraction spectra of the doped samples are similar to the X-ray pattern of pure TiO_2, i.e. show only lines characteristic of anatase and, therefore, they do not provide any information which could contribute to the understanding of the sample structures.

Anatase—TiO_2 is a semiconductor with a band gap of 3.2 eV [16], and any light energy equal to or higher than the band gap is absorbed by TiO_2 and causes the transfer of electron from the valence band into the conduction one. Electrons and holes thus created have sufficient energy to decompose water, i.e. to reduce H^+ and to oxidize O^{2-}. However, both hydrogen and oxygen evolution processes are hindered on pure TiO_2 [16, 17]. The purpose of this study was to introduce some admixtures facilitating hydrogen generation, hence the use of a sacrificial compound (EDTA) which enhances the

oxidation by photogenerated holes. The use of such sacrificial molecules allows us to focus our attention on the cathodic reduction of water (i.e. by photogenerated electrons) which is a slower process. One can see from Figure 1 that the 366 nm light, which was used in all the experiments, was absorbed by TiO_2.

The rates of hydrogen production and quantum efficiencies are listed in Table I. The values given correspond to the stage at which the hydrogen production rates are constant, i.e. after the initial step of the photoreaction (see Fig. 2). One can see from Table I that pure anatase-TiO_2 causes a slow hydrogen generation under illumination. For doped samples, only doping with 1 wt.% of NiO increases the rate of H_2 production under stationary conditions.
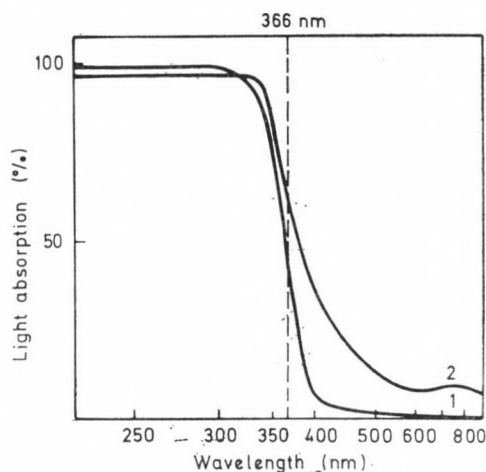
Fig. 1. Visible and UV absorption of the catalysts; 1 — pure TiO_2, 2 — TiO_2 with 2 wt.% NiO
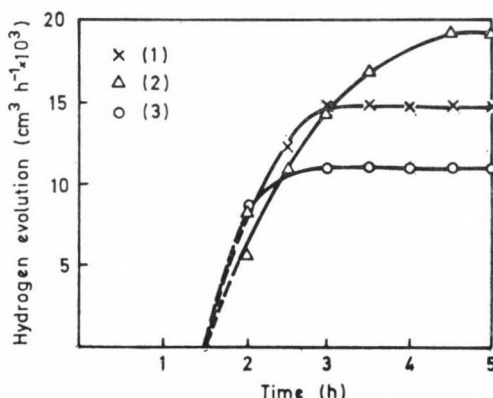
Fig. 2. Light induced water decomposition. Volume of H_2 produced as a function of irradiation time; 1 — pure TiO_2, 2 — TiO_2 with 1 wt.% NiO, 3 — TiO_2 with 1 wt.% Fe_2O_3

The activity of $TiO_2-0.5$ wt.% NiO sample is similar to that of pure TiO_2 and the activity of $TiO_2 - 2$ wt.% NiO catalyst is slightly lower. Among the other samples, only those containing 0.5 and 1.0 wt.% of Fe_2O_3 cause the photogeneration of hydrogen in measurable amounts. The other samples have only traces of hydrogen (<1 cm h$^{-1}\times10^3$).

As it was already mentioned (see Introduction), the admixture of NiO enhanced the photoactivity of $SrTiO_3$ in water splitting. Similarly, the activity of TiO_2-1 wt.% NiO system was by about 40% higher than that of pure TiO_2. For the system of $NiO-SrTiO_3$, however, the increase in hydrogen production was much higher. It seems to be likely that for $SrTiO_3$ with the perovskite structure, NiO does not react with the support and forms only "islands" on its surface. These "islands" act similarly to the "Pt—islands" on $SrTiO_3$ or TiO_2. In the case of the $NiO-TiO_2$ catalysts, there are two factors influencing the activity:

1. the "NiO—islands" on the surface of TiO_2 indeed enhance the hydrogen generation;

2. the formation of solid solution of NiO in TiO_2 or of any new phase distinctly decrease the photocatalytic activity, e.g. $NiTiO_3$ is not active as an anode for water photoelectrolysis [18].

We should add here that the NiO — admixture does not improve much the spectral response of TiO_2 (see Fig. 1).

We can see from Fig. 2 that for the following catalysts: pure TiO_2, TiO_2-1 wt.% NiO and TiO_2-1 wt.% Fe_2O_3, hydrogen started to evolve after more than 1.5 h of illumination. The same phenomenon has been observed for all the catalysts. Moreover, detailed observations of the pure white TiO_2 in the initial step of illumination showed darkening of the catalyst. The blue-black colour was stable as long as there was no contact with oxygen and disappeared when the suspension of the catalyst was exposed to air. This blue-black colour was due to the reduction of some surface Ti(IV) to Ti(III). The above fact has been also observed by Kruczyński et al. [19] for amorphous TiO_2 suspended in 50% KOH and irradiated. The reduction of TiO_2 during irradiation of a RuO_2-TiO_2 mixture in the presence of water vapour was reported recently by one of us [8].

In conclusion, we can say that doping of anatase with 1 wt.% of NiO enhances the hydrogen generation from water under illumination. Unfortunately, the formation of solid solutions (or some compounds) between TiO_2 and dopant oxide lowers the photoactivity of anatase, especially in the case of $Co_3O_4-TiO_2$ and $Fe_2O_3-TiO_2$ systems. NiO seems to act as a mediator in the electron transfer from the conduction band of TiO_2 to the water molecule as it has been reported by Domen et al. [9, 10]. For all the catalysts the initial step of the reaction is the reduction of the surface Ti(IV) by photogenerated hydrogen.

REFERENCES

[1] Van Damme, H., Hall, W. K.: J. Am. Chem. Soc., **101,** 4373 (1979)
[2] Sato, S., White, J. M.: J. Phys. Chem., **85,** 592 (1981)
[3] Sato, S., White, J. M.: Chem. Phys. Lett., **72,** 83 (1980); J. Catal., **69,** 128 (1981)
[4] Borgarello, E., Kiwi, J., Grätzel, M., Pelizzetti, E., Visca, M.: J. Am. Chem. Soc., **104,** 2996 (1982)
[5] Yesodharan, E., Grätzel, M.: Helv. Chim. Acta, **66,** 2145 (1983)
[6] Kawai, T., Sakata, T.: Chem. Phys. Lett., **72,** 87 (1980)
[7] Blondel, G., Harriman, A., Porter, O., Urwin, D., Kiwi, J.: J. Phys. Chem., **87,** 2629 (1983)
[8] Sobczyński, A., White, J. M.: J. Molec. Catal. (in the press)
[9] Domen, K., Naito, S., Onishi, T., Tamaru, K.: Chem. Phys. Lett., **92,** 433 (1982); J. Phys. Chem., **86,** 3657 (1982)
[10] Domen, K. Naito, S., Soma, M., Onishi, T., Tamaru, K.: J. S. C. Chem. Commun., **1980,** 543
[11] Thewissen, D. H. M. W., Eeuwhorst-Reinten, M., Timmer, K., Tinnemans, A. H. A., Mackor, A.: Solar Energy R and D Eur. Comm., VI (Photochem. Photoelectrochem. Photobiol. Proc.) 56, 1981
[12] Matsumoto, Y., Kurimoto, J., Shimizu, T., Sato, E.: J. Electrochem. Soc., **128,** 1040 (1981)
[13] Matsumoto, Y., Kurimoto, J., Amagasaki, Y., Sato, E.: J. Electrochem. Soc., **127,** 2148 (1980)
[14] Murov, S. L.: Handbook of Photochemistry, Marcel Dekker, Inc. New York 1973
[15] Goldman, D. B.: J. Am. Ceram. Soc., **66,** 811 (1983)
[16] Bard, A. J.: J. Photochem., **10,** 50 (1979)
[17] Kiwi, J., Grätzel, M.: J. Phys. Chem., **88,** 1302 (1984)
[18] Salvador, P., Gubienez, C., Goodenough, J. B.: J. Appl. Phys., **53,** 7003 (1982)
[19] Kruczyński, L., Gesser, H. D., Turner, C. W., Speers, E. A.: Nature **291, 399** (1981)

THE APPLICATION OF COLOUR CLASSIFICATION SYSTEMS TO COORDINATION COMPOUNDS

Franz L. WIMMER and Laurence PONCINI*

*(School of Natural Resources, University of the South Pacific,
P.O. Box 1168, Suva, FIJI)*

Two colour order systems (Methuen, Munsell) were used to classify the colours of several metal complexes. This enables, via the ISCC-NBS method, a systematic designation of their colours to be made, thus removing any ambiguities in their colour names.

The colour of a metal complex is an important parameter and should be described accurately. However, the literature abounds with colour descriptions that are vague and meaningless to other workers; for example, orchid, rose, salmon and buff.

This arises for the following reasons. Apart from physiological differences, different observers have differing impressions as to the nature of the colour associated with a particular name. Any one observer assigns a name to the colour of an object by comparing it with his colour memory. It has been shown [1] that what a person imagines to be the colour of a familiar object may be divergent from the actual colour of that object.

The colours of solids can be assessed with either a colorimeter (tinto-meter) or a colour-order system. A number of these systems have been proposed [2, 3]. the most popular being that of Munsell [4]. Three parameters are required to completely describe a particular colour:

hue — that property of visual perception by which different regions of the spectrum are distinguished and named, i.e. red, blue etc.,

saturation — the intensity of a hue or degree of freedom from admixture with white,

lightness — the variation of the visual perception along the continuum between white and black.

In the Munsell system these parameters are referred to as hue, chroma and value respectively.

To our knowledge there has been no extension of colorimetric methods to coordination compounds. We have therefore classified a number of complexes by both the Methuen and Munsell colour systems (see Table I). The

---

* To whom correspondence should be addressed; Department of Chemistry, Purdue University, West Lafayette IN. 47907, U.S.A.

Table I

Colour classification and systematic colour names of some coordination compounds

Compound	Reported colour	Treatment[1]	Colour notation			Colour name	
			Methuen[2]	Munsell[3,4]		Methuen[2]	ISCC-NBS[5]
$Ni(py)_2Cl_2$	pale yellow green[6]	P	28.5A4	6.5GY	8.5/3	pastel green	light yellow green
K_2PdCl_4	yellow greenish brown,[7] red brown	G_3	4D8	4.5Y	5.5/7.5	olive brown	light olive
		G_4	4B5	3.5Y	8/5.5	greyish yellow	moderate yellow
$K_3[Fe(CN)_6]$	red,[7]	P	6.5A>8	3YR	6.5/>15	deep orange	vivid orange
	ruby red[8]	G_2	5A8	7.5YR	7.5/15	deep orange	vivid orange-yellow
		G_3	4A7	3.5Y	8/12	orange yellow	vivid yellow
		G_4	3A6	4.5Y	8.5/8	yellow	light yellow
$[Co(NH_3)_5Cl]Cl_2$	dark red violet[9]	P	13E8	2.5RP	3/9	deep magenta	deep reddish purple
$[Ni(en)_3]Cl_2 \cdot 2H_2O$	orchid[10a]	P	16A7	4.5P	4.5/14.5	reddish violet	vivid purple
$Ni(en)_2Cl_2$	blue[10b]	P	21.5A6	6PB	6/9.5	blue	brilliant blue
$Ni(py)_4Cl_2$	pale blue[11]	G_1	24A3	6.5B	8/2	pale turquoise	very pale blue

[1] P = assessed as prepared/obtained, G_2 = medium ground, G_3 = finely ground, G_4 = very finely ground

[2] Cornerup, A., Wanscher, J. H.: "Methuen Handbook of Colour", 2nd ed., Methuen, London 1967

[3] G = green, Y = Yellow, R = red, P = purple, B = blue

[4] Revised Munsell notations; Newhall, S. M., Nickerson, D., Judd, D. B.: J. Opt. Soc. Am., **33**, 385 (1943). The three symbols indicate hue, value and chroma

[5] Kelly, K. L., Judd, D. B.: "The ISCC-NBS Method of Designating Colours and a Dictionary of Colour Names", Circular 553 National Bureau of Standards, Washington 1955

[6] Goodgame, D. M. L. et al.: J. Chem. Soc., **1964**, 5194

[7] Weast, R. C. (ed.): "CRC Handbook of Chemistry and Physics", 58th ed., CRC Press, West Palm Beach, 1977—78

[8] B.D.H. Chemicals Ltd., Catalogue, 1981—82

[9] Schlessinger, G. C.: Inorg. Synth., **9**, 160 (1967)

[10] State, H. M.: Inorg. Synth. (a) **6**, 200 (1960); (b) **6**, 198 (1960)

[11] Nelson, S. M., Shepherd, T. M.: J. Chem. Soc., **1965**, 3276

complexes, wherever possible, were used in the form in which they were prepared. In the case of very intense colours it was necessary to grind the crystals so that they would fit the available standard colour ranges. From the Munsell notation, a systematic colour name, derived by the National Bureau of Standards [5], that unequivocally describes the colour of the complex can be obtained.

The effect of particle size on the colour for some complexes is also shown in Table I. An estimate of the degree of grinding is tabulated under "treatment". This is necessary for samples with uneven particle sizes (e.g. $K_3[Fe(CN)_6]$ K_2PdCl_4) and for intensely coloured crystals.

Although this method can be employed for any coloured complex, it will be most useful for complexes with non-spectral colours and for those metal ions which form a vast number of complexes with various shades of the same colour (e.g. Cu(II), Rh(III)).

The colours of solution can also be assessed with a colour order system [5]. We have used this method to monitor colour changes in reactions as an alternative to spectrophotometric monitoring. The detection of colour changes is fairly straightforward and the end of a reaction can be easily determined.

Experimental

Potassium ferricyanide was obtained from B.D.H. Ltd and K_2PdCl_4 from Johnson Matthey Ltd. The compounds, $[Ni(py)_2Cl_2]$ [6], $[Ni(py)_2Cl_4]$ [7], $[Ni(en)_2Cl_2]$ [8a], $[Ni(en)_3]Cl_2 \cdot 2 H_2O$ [8b] and $[Co(NH_3)_5Cl]Cl_2$ [9] were prepared by methods reported previously.

The method of colour assessment was similar to that described by Kelly and Judd [5 . Each test sample was prepared by placing a portion of the compound onto a microscope slide to give an area (ca. 2 cm²) of uniform appearance and thickness with a flat matt surface. The bottom of the slide immediately beneath the sample was covered with white paper.

REFERENCES

[1] Kling, J. W., Riggs, L. A.: "Woodworth and Schlosberg's Experimental Psychology", 3rd ed., Holt, Rinehart, Winston, New York, 1971, p. 424; Newhall, S. M., Burnham, R. W., Clark, J. R.: J. Opt. Soc. Amer., 47, 43 (1957;) Bartleson, C. J.: J. Opt. Soc. Amer., 50, 73 (1960)
[2] Wyszecki, G., Stiles, W. S.: "Colour Science", Wiley, New York, 1967, p. 475
[3] Judd, D. B., Wyszecki, G. W.: "Colour in Business, Science and Industry", 2nd ed., Wiley, New York 1967
[4] "Munsell Book of Colour", Munsell Colour Company, Baltimore 1942
[5] Kelly, K. L., Judd, D. B.: "The ISCC-NBS Method of Designating Colours and a Dictionary of Colour Names", Circular 553 National Bureau of Standards, Washington 1955
[6] Goodgame, D. M. L., Goodgame, M., Weeks, M. J.: J. Chem. Soc., 1964, 5194
[7] Nelson, S. M., Shepherd, T. M.: J. Chem. Soc., 1965, 3276
[8] State, H. M.: Inorg. Synth., (a) 6, 198 (1960); (b) 6, 200 (1960)
[9] Schlessinger, G. G.: Inorg. Synth., 9, 160 (1967)

Text

The text of the paper should be concise. The description of new compounds (in the Experimental) must include the complete analytical data. Special attention must be paid to structural formulas given within the text. Complicated (non-linear) formulas should be drawn on separate sheets of paper and their position in the text should be clearly marked. The numbering of formulas and equations (in parentheses on the right-hand side) is only needed if they are referred to in the text. Units should conform to the International System of Units (SI). In nomenclature the rules of the I.U.P.A.C. are accepted as standard. Symbols for physical quantities are printed in italic type and should, therefore, be underlined in the manuscript.

References

References should be numbered in order of appearance in the text (where the reference number appears in brackets) and listed at the end of the paper. The reference list, too, should by typed double-spaced. Journal titles are to be abbreviated as defined by the Chemical Abstracts Service Source Index.

Examples:

[1] Brossi, A., Lindlar, H., Walter, M., Schneider, O.: Helv. Chim. Acta, **41**, 119 (1958)
[2] Parr, R. G.: Quantum Theory of Molecular Electronic Structure, Benjamin, New York 1964
[3] Warshel, A.: in Modern Theoretical Chemistry, Vol. 7, Part A (Ed. G. A. Segal), Plenum Press, New York 1977

Tables

Each table should be given a Roman number and a brief informative title. Structural formulas should not be used in column headings or in the body of tables.

Figures

Figures should be numbered consecutively with Arabic numerals. Their approximate place should be indicated in the text on the margin. All figures must be identified on the back by the author's name and the figure number in pencil. Standard symbols (such as circles, triangles, squares) are to be used on line-drawings to denote the points determined experimentally. Line-drawings must not contain structural formulas and comments. Spectra or relevant segments thereof, chromatograms, and X-ray diffraction patterns will be reproduced only if concise numerical summaries are inadequate to replace them. Drawings and graphs should be prepared in black ink on good-quality white or tracing paper. Photographs should be submitted on glossy paper as high-contrast copies. Xerox or similar copies are not suitable for reproduction, but may be used for duplicate copies.

Redrawn illustrations will be sent to the authors for checking. No corrections of figures will, therefore, be accepted in the proofs.

Submission of manuscript

After having completed the corrections suggested by the referees and editors, the final manuscript should be submitted in duplicate, in a form ready for publication. If the corrected manuscript is not returned to the editors *within six weeks*, the intended publication of the paper will be regarded as withdrawn by the authors.

Page charge will not be assessed for the publication, however, authors from overseas countries must contribute to the postage of correspondence by sending, together with the manuscript, international postal coupons to the value of U.S. $ 10.—

Proofs and reprints

A set of proofs will be sent to the submitting author. The proofs must be returned within 48 hours of receipt. Late return may cause a delay in the publication of the paper. 100 reprints will be supplied to the authors free of charge.

Periodicals of the Hungarian Academy of Sciences are obtainable at the following addresses:

AUSTRALIA
C.B.D. LIBRARY AND SUBSCRIPTION SERVICE
Box 4886, G.P.O., *Sydney N.S.W. 2001*
COSMOS BOOKSHOP, 145 Ackland Street
St. Kilda (Melbourne), Victoria 3182

AUSTRIA
GLOBUS, Höchstädtplatz 3, *1206 Wien XX*

BELGIUM
OFFICE INTERNATIONAL DE LIBRAIRIE
30 Avenue Marnix, *1050 Bruxelles*
LIBRAIRIE DU MONDE ENTIER
162 rue du Midi, *1000 Bruxelles*

BULGARIA
HEMUS, Bulvar Ruszki 6, *Sofia*

CANADA
PANNONIA BOOKS, P.O. Box 1017
Postal Station "B", *Toronto, Ontario M5T 2T8*

CHINA
CNPICOR, Periodical Department, P.O. Box 50
Peking

CZECHOSLOVAKIA
MAD'ARSKÁ KULTURA, Národní třida 22
115 66 Praha
PNS DOVOZ TISKU, Vinohradská 46, *Praha 2*
PNS DOVOZ TLAČE, *Bratislava 2*

DENMARK
EJNAR MUNKSGAARD, Norregade 6
1165 Copenhagen K

FEDERAL REPUBLIC OF GERMANY
KUNST UND WISSEN ERICH BIEBER
Postfach 46, *7000 Stuttgart 1*

FINLAND
AKATEEMINEN KIRJAKAUPPA, P.O. Box 128
SF-00101 Helsinki 10

FRANCE
DAWSON-FRANCE S. A., B. P. 40, *91121 Palaiseau*
EUROPÉRIODIQUES S. A., 31 Avenue de Versailles, *78170 La Celle St. Cloud*
OFFICE INTERNATIONAL DE DOCUMENTATION ET LIBRAIRIE, 48 rue Gay-Lussac
75240 Paris Cedex 05

GERMAN DEMOCRATIC REPUBLIC
HAUS DER UNGARISCHEN KULTUR
Karl Liebknecht-Straße 9, *DDR-102 Berlin*
DEUTSCHE POST ZEITUNGSVERTRIEBSAMT
Sraße der Pariser Kommüne 3–4, *DDR-104 Berlin*

GREAT BRITAIN
BLACKWELL'S PERIODICALS DIVISION
Hythe Bridge Street, *Oxford OX1 2ET*
BUMPUS, HALDANE AND MAXWELL LTD.
Cowper Works, *Olney, Bucks MK46 4BN*
COLLET'S HOLDINGS LTD., Denington Estate
Wellingborough, Northants NN8 2QT
WM. DAWSON AND SONS LTD., Cannon House
Folkstone, Kent CT19 5EE
H. K. LEWIS AND CO., 136 Gower Street
London WC1E 6BS

GREECE
KOSTARAKIS BROTHERS INTERNATIONAL
BOOKSELLERS, 2 Hippokratous Street, *Athens-143*

HOLLAND
MEULENHOFF-BRUNA B.V., Beulingstraat 2,
Amsterdam
MARTINUS NIJHOFF B.V.
Lange Voorhout 9–11, *Den Haag*

SWETS SUBSCRIPTION SERVICE
347b Heereweg, *Lisse*

INDIA
ALLIED PUBLISHING PRIVATE LTD., 13/14
Asaf Ali Road, *New Delhi 110001*
150 B-6 Mount Road, *Madras 600002*
INTERNATIONAL BOOK HOUSE PVT. LTD.
Madame Cama Road, *Bombay 400039*
THE STATE TRADING CORPORATION OF
INDIA LTD., Books Import Division, Chandralok
36 Janpath, *New Delhi 110001*

ITALY
INTERSCIENTIA, Via Mazzé 28, *10149 Torino*
LIBRERIA COMMISSIONARIA SANSONI, Via
Lamarmora 45, *50121 Firenze*
SANTO VANASIA, Via M. Macchi 58
20124 Milano
D. E. A., Via Lima 28, *00198 Roma*

JAPAN
KINOKUNIYA BOOK-STORE CO. LTD.
17-7 Shinjuku 3 chome, Shinjuku-ku, *Tokyo 160-91*
MARUZEN COMPANY LTD., Book Department,
P.O. Box 5050 Tokyo International, *Tokyo 100-31*
NAUKA LTD. IMPORT DEPARTMENT
2-30-19 Minami Ikebukuro, Toshima-ku, *Tokyo 171*

KOREA
CHULPANMUL, *Phenjan*

NORWAY
TANUM-TIDSKRIFT-SENTRALEN A.S., Karl
Johansgatan 41–43, *1000 Oslo*

POLAND
WĘGIERSKI INSTYTUT KULTURY, Marszalkowska 80, *00-517 Warszawa*
CKP I W, ul. Towarowa 28, *00-958 Warszawa*

ROUMANIA
D. E. P., *Bucureşti*
ILEXIM, Calea Grivitei 64–66, *Bucureşti*

SOVIET UNION
SOJUZPECHAT — IMPORT, *Moscow*
and the post offices in each town
MEZHDUNARODNAYA KNIGA, *Moscow G-200*

SPAIN
DIAZ DE SANTOS, Lagasca 95, *Madrid 6*

SWEDEN
ALMQVIST AND WIKSELL, Gamla Brogatan 26
101 20 Stockholm
GUMPERTS UNIVERSITETSBOKHANDEL AB
Box 346, *401 25 Göteborg 1*

SWITZERLAND
KARGER LIBRI AG, Petersgraben 31, *4011 Basel*

USA
EBSCO SUBSCRIPTION SERVICES
P.O. Box 1943, *Birmingham, Alabama 35201*
F. W. FAXON COMPANY, INC.
15 Southwest Park, *Westwood Mass. 02090*
THE MOORE-COTTRELL SUBSCRIPTION
AGENCIES, *North Cohocton, N. Y. 14868*
READ-MORE PUBLICATIONS, INC.
140 Cedar Street, *New York, N. Y. 10006*
STECHERT-MACMILLAN, INC.
7250 Westfield Avenue, *Pennsauken N. J. 08110*

YUGOSLAVIA
JUGOSLOVENSKA KNJIGA, Terazije 27, *Beograd*
FORUM, Vojvode Mišića 1, *21000 Novi Sad*

Acta Chimica Hungarica

VOLUME 120, NUMBER 4, DECEMBER 1985

NOTICE TO AUTHORS

Acta Chimica publishes original papers on all aspects of chemistry in English. Before preparing a manuscript for submission to this journal authors are advised to consult recent issues.

Form of manuscript

Manuscripts, tables and illustrations should be submitted in triplicate. Manuscripts should be typewritten double spaced (25 lines, 50 characters per line including spaces). The *title page* should include (1) the title of the paper, (2) the full names of the author(s) in the sequence to be published; apply an asterisk to designate the name of the author to whom correspondence should be addressed, (3) name and address of the institution where the work was done. If the paper is part of a series, reference to the previous communication must be given as a footnote.

Abstract

A summary is printed at the head of each paper. This should not exceed 200 words and should state briefly the principal results and major conclusions of the work. It should be suitable for use by abstracting services.

CONTENTS

SYNTHESIS OF 6,7-DIAZACHOLESTANE DERIVATIVES[+]

Jacek W. Morzycki and Rafał R. Siciński*

*(Department of Chemistry, The University of Warsaw, 02093 Warszawa, Pasteura 1, Poland**)*

Syntheses of 8β-cyano-6,7-diazacholesterol (**6a**), 6,7-diaza-8(14)-cholesten-3β-ol (**7a**), 6,7-diaza-8(14)-coprosten-3β-ol (**7b**) and some other B-ring hydropyridazine cholestanes are described. All attempts to transform **6a** into the azine **1** failed, and the unusual autooxidation products (**8** and **9**) were isolated.

In connection with studies on the mechanism of vitamin D action [2—4], our attention has been drawn to compounds of potential anti-vitamin activity. One of the most interesting compounds in this respect seemed to be the 6,7--diaza analog of vitamin D_3 and therefore we have undertaken studies on the synthesis of its possible precursor, 6,7-diaza-5,7-cholestadien-3β-ol (**1**). Some nitrogen-containing side chain analogs of vitamin D have been already synthesized [2, 3] and one of them, 25-aza-vitamin D_3 [5], has been found to be an inhibitor of D-activity.

As a possible approach to the azine **1** synthesis, the reaction of the readily available 6,7-dinor-5,8-seco-5,8-cholestadion-3β-ol [6] with hydrazine could be considered. However, recent studies [7] have shown that this reaction does not result in the formation of **1**. An alternative synthetic route to **1**, which was chosen by us, involved the introduction of two nitrogen atoms as a very early stage of the synthesis, followed by the removal of two, superfluous carbons from the ring B. This could be accomplished using the 4-phenyl-1,2,4--triazoline-3,5-dione adduct of 7-dehydrocholesterol **2a** [8] as a source of two nitrogen atoms located at the right place of the steroid molecule and protected against oxidation by a readily removable group. Although the PTAD adduct of ergosterol has often been used for protection of the 5,7-diene during ozonolysis [9] of the double bond in the side chain, it is known that the 6(7)-double bond of the adduct may also be cleaved with an excess of ozone [10]. The ozonolysis of **2b** was carried out in two different solvents: dichloromethane-methanol mixture and in dichloromethane alone.
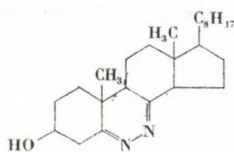
1
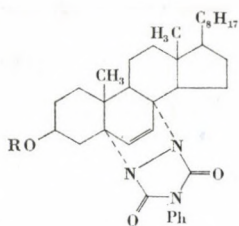
2 a :   R = H
  b :   R = Ac
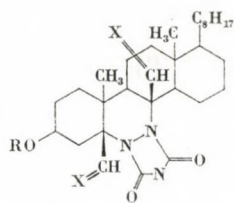
3 a :   R = H;   X = O
  b :   R = Ac;   X = O
  c :   R = Ac;   X = N—OH
  d :   R = Ac;   X = N—OAc
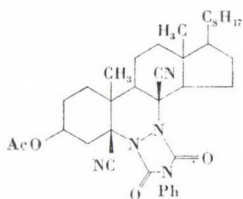
4
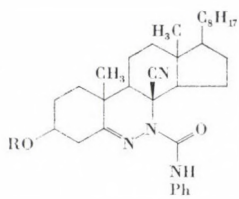
5 a :   R = H
  b :   R = Ac
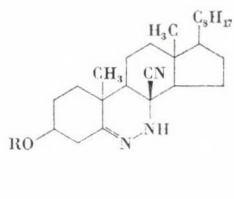
6 a :   R = H
  b :   R = Ac
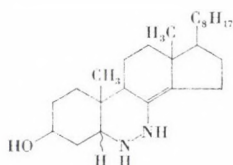
7 a :   5 α
  b :   5 β
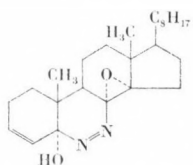
8
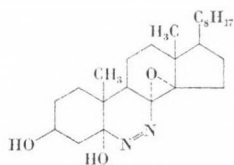
9

In the first case a mixture of at least four compounds (presumably acetals) was formed which, after hydrolysis with hydrochloric acid, afforded the hydroxydialdehyde **3a** in 76% yield. The reaction when performed in the absence of methanol led directly to the dialdehyde **3b**. Our further design was the replacement of both formyl functions in **3b** by good leaving groups, followed by base-catalyzed cleavage of the urazole ring [11] with simultaneous elimination of the substituents at C-5 and C-8. Accordingly, an attempt was made to convert compound **3b** into the 5β,8β-diformate via Baeyer—Villiger oxidation. Unfortunately, both aldehyde groups in **3b** appeared to be resistant towards peracids. As it was found that the dialdehyde **3b** reacted readily with hydroxylamine to give the dioxime **3c**, we decided to replace the formyl groups by cyano, which seemed to be sufficiently easy to remove [12] by hydrolysis. The transformation of the dioxime **3c** into the dinitrile **4** was achieved in highest yields by the thermal elimination of the elements of acetic acid [13] from the acetyl derivative of the dioxime **3d**. Other methods of dinitrile **4** preparation from the dioxime **3c** (see Experimental) were comparatively less efficient, and

direct methods starting from the dialdehyde **3b** (e.g. using hydroxylamine-*O*--sulfonic acid [14]) failed to give **4**. The hydrolysis of the dinitrile **4** was studied in several different solvents (methanol, dioxan, *n*-butanol, diglyme), but the reaction course was essentially the same, the only difference being in the rate of the reaction. The best results were obtained with KOH in refluxing aqueous dioxan. In about 1 hour all starting material disappeared, and the main product (about 85%) was partially hydrolyzed compound **5a**. Further reaction was somewhat slower and led to 8β-cyano-6,7-diazacholesterol (**6a**; 66% yield, in 5 hours). After this phase, the reaction became still slower and much less definite. All attempts to isolate further hydrolysis products were unsuccessful due to their instability and very similar polarity. Since compound **6a** seemed to be a direct precursor of the azine **1**, we tried hydrogen cyanide elimination by many means. It was reasonable to assume that the generation of a negative charge at the neighbouring nitrogen would facilitate cyanide ion abstraction. However, all strong bases tried (NaH, LiH, NaBH$_4$, *t*-BuOK, *n*-BuLi, LDA) failed to give the desired product **1**. Only in the case of lithium aluminium hydride reduction of **6a** did the elimination of HCN occur, with concomitant C—N double bond reduction. Two products, **7a** and **7b**, differing in configuration at C-5, were obtained in a ratio of 5 : 1. Since it was very likely that the easy removal of cyanide during LiAlH$_4$ reduction occurred owing to the proximity of the electron-deficient aluminum atom, and in order to retain the $C_{(5)}$—N double bond, we tried a much milder reducing agent containing aluminum: aluminum isopropoxide. Using this reagent in refluxing benzene, compound **6a** was converted smoothly to the unexpected product **8** in 78% yield. It is obvious from its structure that a molecule of atmospheric oxygen participated in the reaction. The formation of exclusively one product with a $C_{(3)}$—$C_{(4)}$ double bond suggested that the elimination of the 3β-substituent had accompanied the autooxidation process. This was confirmed by the observation that the 3β-acetate derivative **6b** when treated with Al(O-*i*Pr)$_3$ under the same conditions gave also exclusively the same product **8**, although considerably more slowly than the free alcohol **6a**. Presumably, the elimination beginning the whole process, is the rate-determining step.

In separate experiments it was established that compound **8** formed also during the analogous reactions of **5a**, **5b** and even the dinitrile **4**. In the last case the degradation of the 4-phenyl-1,2,4-triazoline-3,5-dione ring*preceded further transformations; TLC control showed the following sequence of reactions: **4** → **5b** → **6b** → **8**. It is noteworthy that no intermediates of the complex transformation **6b** → **8** could by observed. Surprisingly, the same compound **8** was the the main product (45%) also in a next experiment for the removal of HCN from 8β-cyano-6,7-diazacholesterol (**6a**), by pyrolysis at 200 °C. The minor, more polar product (20%) of the reaction appeared to be compound **9** with the 3β-hydroxyl group retained. The structures of both products **8** and

9 unequivocally proved that an oxygen molecule from the air was again involved in the process. The proposed mechanism of the reaction is shown on the scheme.

The key intermediate seems to be the 6,7-diaza-8(14)-dehydro compound *i* which reacts immediately with oxygen in the free-radical chain process [15]

Scheme 1
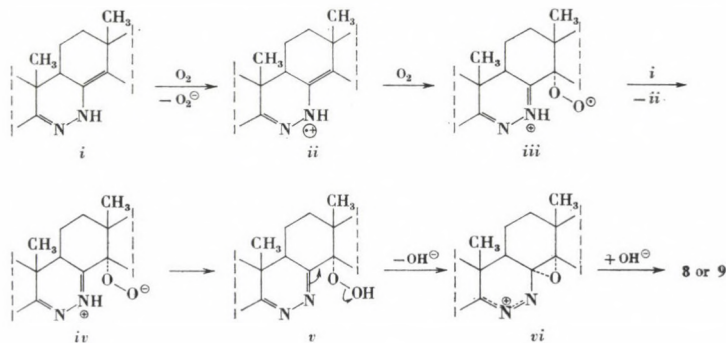
(via *ii*, *iii* and *iv*) to give the 14-hydroxy compound *v*. The most likely primary autooxidation product *v* decomposes to the epoxy-carbocation *vi*. The hydroxyl ion needed to quench this cation at C-5, completing the process, may derive either from the decomposition of the hydroperoxide *v*, or from an external source. The elimination of the 3β-hydroxyl group, largely accompanying the process, may take place at any moment before or during the oxidation. The reactions of **6a** with aluminum isopropoxide and its pyrolysis were also carried out in oxygen-free atmosphere. The experiments failed to afford an intermediate *i*, proving the extreme susceptibility of such a system to oxidation. It cannot be excluded that the autooxidation of *i* occurred during the subsequent work-up of the reaction mixture and/or chromatographic isolation. The reaction of **6a** with Al(O-iPr)₃ effected in the presence of triphenylphosphine gave also **8** in a high yield.

The described synthesis, though it did not afford 6,7-diaza-5,7-cholesta-dien-3β-ol (**1**), represents an efficient and useful approach to 6,7-diazasteroids of potential biological activity. It seems that the above method of transformation of a diene into diaza compounds can be presumably extended to other homocyclic conjugated diene systems.

---

* This observation prompted us to examine the possible application of aluminum iso-propoxide to regenerate the 5,7-diene systems from the corresponding PTAD adducts. However, the reaction of **2b** with Al(O-iPr)₃ was very slow and afforded 7-dehydrocholesterol acetate in a rather poor yield.

Experimental

M.p.'s were determined on a Hoover apparatus and are uncorrected. NMR spectra (^{1}H and ^{13}C) were taken in $CDCl_3$ with Bruker WH-270 FT and Nicolet-200 spectrometers, with TMS as internal standard. IR spectra were recorded on a Nicolet MX-1, in KBr pellets. Mass spectra were obtained at 110—120 °C above ambient temperature, at 70 eV with an AEI MS-9 spectrometer coupled to a DS-50 data system. UV spectra were recorded in absolute ethanol with a Hitachi Model 100—60 recording spectrophotometer. Optical rotations were measured on a Perkin-Elmer Model 41 polarimeter. HPLC was performed on a Waters Associates Model ALC/GPC 204, using a Zorbax-SIL (DuPont) 6.4 mm×25 cm column, monitoring at 250 nm in most cases. Column chromatography was effected on Silica Gel 60, 70—230 mesh, ASTM (Merck).

1,4-Cycloaddition of 4-phenyl-1,2,4-triazoline-3,5-dione to 7-dehydrocholesterol acetate

A solution of 4-phenyl-1,2,4-triazoline-3,5-dione (obtained by oxidation of 12.1 g of 4-phenylurazole with *tert*-butyl hypochlorite) in acetone (190 mL) was added dropwise to a stirred solution of 7-dehydrocholesterol acetate (21.3 g) in benzene (450 mL) and acetone (360 mL) until a faint pink colouration persisted. The reaction mixture was stirred for 1 h and the solvents were removed under reduced pressure to afford a pale yellow foam. Crystallization of the crude material from methanol-acetone (3 : 1) yielded **2b** in pure form (27 g; 90%), m.p. 135 °C, $[\alpha]_D^{25}$ —79° ($c = 0.9$); *lit.* [8] m.p. 133—136 °C, $[\alpha]_D^{21}$ —91.4° ($c = 2.26$).
$C_{37}H_{51}N_3O_4$. Calcd. C 73.85; H 8.54. Found C 73.67; H 8.48%.
IR, ν_{max}: 1760, 1734, 1702 (C=O), 1243 cm^{-1}.
UV (ethanol), λ_{max}: 256 nm ($\varepsilon = 3900$).
^{1}H-NMR, δ: 0.80 (s, 18-H), 0.98 (s, 19-H), 2.00 (s, CH_3COO-), 5.46 (m, w/2 = 25 Hz, 1H, 3α-H), 6.23, 6.42 (ABq, $J = 9$ Hz, 2H, 6-H and 7-H), 7.25—7.50 (m, 5H, aromatic protons).

Ozonolysis of the adduct 2b

(*a*) Compound **2b** (16 g) was dissolved in dichloromethane (600 mL) and treated with an excess of ozone at —70 °C. Dimethyl sulfide (4 mL) was added at —70 °C and the mixture warmed to room temperature. Evaporation of the solvent and filtration through a short silica gel column using benzene-ether mixture (85 : 15) afforded the dialdehyde **3b** (14 g; 83%) as a pale yellow foam, $[\alpha]_D^{25}$ —50° ($c = 0.6$).
IR, ν_{max}: 2740 (aldehyde C—H), 1781, 1739, 1722 (C=O), 1420, 1245 cm^{-1}.
^{1}H-NMR, δ: 0.92 (s, 18-H), 1.17 (s, 19-H), 2.17 (s, 3H, CH_3COO-), 5.08 (m, w/2 = 11.5 Hz, 1H, 3α-H), 7.25—7.50 (m, 5H, aromatic protons), 9.73 (s, 1H, —CHO) 9,97 (s, 1H, —CHO).
(*b*) The adduct **2b** (12 g) in CH_2Cl_2-methanol mixture (2 : 1; 600 mL) was cooled to —70 °C and ozone was passed through the solution until a blue colour appeared. Addition of dimethyl sulfide (4 mL) and evaporation of the solvent gave an oily residue. It was dissolved in acetone (500 mL), diluted hydrochloric acid (1 : 1;, 200 mL) was added, and the mixture was refluxed for 6 h. On cooling, the hydroxydialdehyde **3a**, crystallized in essentially pure state. Yield: 9 g (76%), m.p. 207—208 °C, $[\alpha]_D^{25}$ —28° ($c = 0.9$).
$C_{35}H_{49}N_3O_5$. Calcd. C 71.04; H 8.35. Found C 71.19; H 8.40%.
IR, ν_{max}: 3439 (O—H), 1782, 1726, 1715 cm^{-1} (C=O).
^{1}H-NMR, δ: 0.94 (s, 18-H), 1.13 (s, 19-H), 4.12 (m, w/2 = 21 Hz, 1H, 3α-H), 5.34 (d, $J = 9.5$ Hz, 1H, O—H), 7.30—7.55 (m, 5H, aromatic protons), 9.72 (s, 1H, —CHO), 9.97 (s, 1H, —CHO).
Acetylation of hydroxydialdehyde **3a** (Ac$_2$O, Py, reflux 4 h) afforded the acetoxy compound **3b**, identical in all respects with the product described above under (*a*).

Reaction of the dialdehyde 3b with hydroxylamine

A mixture of **3b** (8 g), hydroxylamine hydrochloride (19.46 g) and sodium acetate (31.36 g) in ethanol (200 mL) was vigorously stirred and heated under reflux for 1 h. The reaction mixture was poured into water and extracted with methylene chloride. The extract was

washed with $NaHCO_3$ solution, water, and then dried and evaporated. The crude product **3c** was purified by filtration through a silica gel column in benzene-ether (4 : 1) solution. Yield: 7 g (83.5%), $[\alpha]_D^{25}$ $-46°$ ($c = 0.5$).

$C_{37}H_{53}N_5O_6$. Calcd. C 66.94; H 8.05. Found C 66.61: H 8.12%.

IR, ν_{max}: 3417 (O—H), 1775, 1722 (C=O), 1417, 1247 cm^{-1}.

^{1}H-NMR, δ: 0.82 (s, 18-H), 1.08 (s, 19-H), 2.02 (s, CH_3COO-), 5.11 (m, w/2 = 11 Hz, 1H, 3α-H), 7.30—7.55 (m, 5H, aromatic protons), 7.59 (s, 1H, —CH=N—), 7.75 (s, 1H, —CH=N—).

MS, m/e: 663 (M^+, 30%), 43 (100%).

Synthesis of the dinitrile 4

(*a*) The dioxime **3c** (7 g) was acetylated overnight with acetic anhydride (15 mL) in pyridine (25 mL). After the usual work-up, the crude, foamy triacetate **3d** was pure enough for use in the next step. Yield: 7.5 g (95%), $[\alpha]_D^{25}$ $-23°$ ($c = 0.8$).

IR, ν_{max}: 1777, 1726 (C=O), 1418, 1246, 1195 cm^{-1}.

^{1}H-NMR, δ: 0.81 (s, 18-H), 1.09 (s, 19-H), 2.07, 2.09, 2.12 (3×s, 3× CH_3COO-), 5.16 (m, w/2 = 12 Hz, 1H, 3α-H), 7.3—7.5 (m, 5H, aromatic protons), 7.93 (s, 1H, —CH=N—), 8.06 (s, 1H, —CH=N—).

The triacetate **3d** (3 g) was refluxed in acetic anhydride (60 mL) for 1 h. After cooling, the reaction mixture was poured onto ice and allowed to stand until all Ac_2O decomposed. The product, dinitrile **4** was extracted with benzene. The extract was washed with water, with saturated sodium hydrogen carbonate solution, then again with water, dried and evaporated. The crude product was filtered through a silica gel column in benzene-ether (95 : 5) solution. Yield: 2.3 g (91%), colourless foam, $[\alpha]_D^{25}$ $-25°$ ($c = 0.7$).

$C_{37}H_{49}N_5O_4$. Calcd. C 70.78; H 7.87. Found C 70.63; H 7.82%.

IR, ν_{max}: 2240 (C≡N), 1777, 1742, 1726 (C=O), 1410, 1240 cm^{-1}.

^{1}H-NMR, δ: 1.10 (s, 18-H), 1.69 (s, 19-H), 2.14 (s, CH_3COO-), 5.18 (m, w/2 = 10 Hz, 1H, 3α-H), 7.35—7.55 (m, 5H, aromatic protons).

^{13}C-NMR, δ: 115.5, 117.0 (—C≡N), 125.8, 128.9, 129.2, 130.1 (aromatic C'-2, C'-4, C'-3, C'-1), 150.5, 152.5 (triazoline-dione C=O), 170.3 (acetate C=O).

MS, m/e: 627 (M^+, 25%), 600 (M^+-HCN, 32%), 585 (M^+-HCN—Me, 14%), 119 (PhNCO, 35%), 43 (100%).

(*b*) The dioxime **3c** (100 mg) was refluxed in acetic anhydride (5 mL) for 1.5 h to yield the dinitrile **4** (70 mg; 74%).

(*c*) The dioxime **3c** (1 g) was dissolved in pyridine (6 mL) and thionyl chloride (1 mL) was added dropwise at 0 °C. The reaction mixture was allowed to stand for 0.5 h to give 710 mg (75%) of **4**.

(*d*) A solution of **3c** (750 mg) and triethylamine (0.67 mL) in methylene chloride (10 mL) was treated dropwise with trifluoromethanolsulfonic anhydride [16] (0.5 mL) in methylene chloride (10 mL) at -70 °C. The reaction was allowed to warm slowly to room temperature (3 h). The yield of **4** was 390 mg (55%).

Hydrolysis of the dinitrile 4

(*a*) To a stirred solution of the dinitrile **4** (950 mg) in dioxan (65 mL) an aqueous solution of KOH (2.6 g in 12.5 mL) was added. The mixture was refluxed for 5 h and poured into water. The products were extracted with benzene, washed with water, dried and evaporated. Silica gel column chromatography of the crude material afforded compounds **5a** (210 mg; 26%; elution with benzene-ether 3 : 1) and **6a** (415 mg; 66% elution with benzene-ether 2 : 3).

Compound **5a**: m.p. 206—209 °C (from acetone-hexane); $[\alpha]_D^{25}$ $+173°$ ($c = 0.6$).

$C_{33}H_{48}N_4O_2$. Calcd. C 74.40; H 9.08. Found C 74.31; H 9.10%.

IR, ν_{max}: 3456 (O—H), 3382 (N—H), 2235 (C≡N), 1714 (C=O), 1519, 1444 cm^{-1}.

UV, λ_{max}: 247 nm ($\varepsilon = 24\,000$).

^{1}H-NMR, δ: 1.12 (s, 18-H), 1.19 (s, 19-H), 3.47 (m, w/2 = 26 Hz, 1H, 3α-H), 6.91 (t, $J = 7$ Hz, 1H, p-ArH), 7.18 (m, 2H, m-ArH), 7.64 (d, $J = 8$ Hz, 2H, o-ArH), 8.58 (s, 1H, N—H).

MS, m/e: 413 (M^+-PhNCO, 56%), 386 (M^+-PhNCO—HCN, 25%), 371 (M^+-PhNCO—HCN—Me), 90%), 353 (M^+-PhNCO—HCN—Me—H_2O, 95%), 119 (PhNCO, 100%).

Compound **6a**: m.p. 103—106 °C (from acetone-hexane); $[\alpha]_D^{25}$ $+224°$ ($c = 0.8$).

$C_{26}H_{43}N_3O$. Calcd. C 75.49; H 10.48. Found C 75.29; H 10.39%.

IR, ν_{max}: 3396, 3315 cm^{-1} (O—H, N—H).

¹H-NMR, δ: 0.91 (s, 18-H), 1.32 (s, 19-H), 3.64 (m, $w/2 = 26$ Hz, 1H, 3α-H), 5.70 (broad s, 1H, N—H).

¹³C-NMR, δ: 128.2 (—C≡N), 153.6 (—C=N—).

MS, m/e: 413 (M^+, 100%), 386 (M^+-HCN, 14%), 371 (M^+-HCN—Me), 60%), 353 (M^+-HCN—Me—H$_2$O, 52%).

(b) The partial hydrolysis of the dinitrile 4 carried out in a similar manner (reaction time 1 h) afforded 5a in 85% yield.

Acetylation of the hydrolysis products 5a and 6a

Compound 5a (100 mg) was acetylated with acetic anhydride (1 mL) in pyridine (2 mL) overnight. The reaction mixture was poured into an aqueous solution of cupric sulfate, and extracted with benzene. The extract was washed successively with CuSO$_4$ solution, water, then dried and evaporated. The crude product was crystallized from aqueous ethanol to afford 5b (82 mg; 76%), m.p. 226—228 °C; $[\alpha]_D^{25} +133°$ ($c = 0.9$).

IR, ν_{max}: 3355 (N—H), 2240 (C≡N), 1728 (acetate C=O), 1706 (C=O), 1518, 1445, 1243 cm⁻¹.

¹H-NMR, δ: 1.16 (s, 18-H), 1.37 (s, 19-H), 2.07 (s, CH$_3$COO—), 4.78 (m, $w/2 = 28$ Hz, 1H, 3α-H), 7.03 (t, $J = 7.5$ Hz, 1H, p-ArH), 7.28 (t, $J = 7.5$ Hz, 2H, m-ArH), 7.50 (d, $J = 7.5$ Hz, 2H, o-ArH).

Analogous acetylation of compound 6a afforded the acetate 6b in 73% yield; m.p. 128—130 °C (from aqueous ethanol); $[\alpha]_D^{25} +198°$ ($c = 1.2$).

IR, ν_{max}: 3338 (N—H), 2230 (C≡N), 1717 (C=O), 1279 cm⁻¹.

¹H-NMR, δ: 1.01 (s, 18-H), 1.40 (s, 19-H), 2.06 (s, CH$_3$COO—), 4.76 (m, $w/2 = 27$ Hz, 1H, 3α-H), 5.53 (s, 1H, N—H).

Lithium aluminum hydride reduction of 6a

(a) 8β-Cyano-6,7-diazacholesterol (6a) (50 mg) dissolved in anhydrous ether (50 mL) was treated with LiAlH$_4$ (50 mg). The reaction mixture was stirred at room temperature for 2 h. The excess of LiAlH$_4$ was decomposed with water, anhydrous Na$_2$SO$_4$ was added, and all inorganic materials were filtered off. The clear filtrate was evaporated and the residue subjected to HPLC separation. Using 10% 2-propanol in hexane, the products 7b (7.0 mg; 15.6%) and 7a (35 mg; 78%) were collected at 50 mL and 60 mL volume, respectively. Compound 7a: m.p. 169—172 °C (from aqueous ethanol); $[\alpha]_D^{25} +21°$ ($c = 1.0$).

C$_{25}$H$_{44}$N$_2$O. Calcd. C 77.26; H 11.41. Found C 77.25; H 11.47%.

IR, ν_{max}: 3355 cm⁻¹ (broad, N—H, O—H).

¹H-NMR, δ: 0.61 (s, 18-H), 0.88 (s, 19-H), 2.71 (dd, $J^1 = 4$ Hz, $J_2 = 12$ Hz, 1H, 5α-H), 3.70 (m, $w/2 = 27$ Hz, 1H, 3α-H).

¹³C-NMR, δ: 119.4 (C-14), 151.8 (C-8).

MS, m/e: 388 (M^+, 100%), 373 (M^+-Me, 13%).

Compound 7b: $[\alpha]_D^{25} +114°$ ($c = 0.6$).

IR, ν_{max}: 3440 (shoulder, O—H), 3358 cm⁻¹ (N—H).

¹H-NMR, δ: 0.64 (s, 18-H), 1.02 (s, 19-H), 3.06 (dd, $J_1 = 3.5$ Hz, $J_2 = 8$ Hz, 1H, 5β-H), 4.19 (m, $w/2 = 18$ Hz, 1H, 3α-H).

MS, m/e: 388 (M^+, 100%), 373 (M^+-Me, 41%).

(b) An analogous reaction was tried at −70 °C (3 h); only unchanged starting material 6a was recovered by HPLC.

Reactions with aluminum isopropoxide

(a) A suspension of Al(O-iPr)$_3$ (250 mg) in the benzene solution of compound 6a (58 mg in 30 mL) was refluxed with vigorous stirring for 3.5 h. After cooling, the reaction mixture was poured into saturated aqueous potassium sodium tartrate solution, washed with water, dried and evaporated. HPLC (3% 2-propanol in hexane) purification of the crude product afforded compound 8, eluting at 20 mL volume, in 78% yield; m.p. 87—89 °C (from hexane-2-propanol); $[\alpha]_D^{25} +10.0°$ ($c = 0.4$).

C$_{25}$H$_{40}$N$_2$O$_2$. Calcd. C 74.96; H 10.06. Found C 75.01; H 10.13%.

IR, ν_{max}: 3350 cm⁻¹ (O—H).

^{1}H-NMR, δ: 0.96 (s, 18-H), 1.12 (s, 19-H), 5.35 (d, $J = 10$ Hz, 1H, 4-H), 5.73 (s, 1H, O—H), 6.07 (m, 1H, 3-H).

^{13}C-NMR, δ: 81.7 (C-5), 118.9 (C-3), 134.6 (C-4).

MS, m/e: 400 (M^+, 7%), 384 (M^+-O, 65%), 372 (M^+-N$_2$, 38%), 369 (M^+-O—Me), 58%), 351 (M^+-O—Me—H$_2$O, 100%).

(b) The reactions of **5a** carried out in an analogous manner gave compound **8** in 76% yield.

The similar reactions of the compounds **4**, **5b** and **6b** with aluminum isopropoxide required longer heating (16 h) and afforded the same product **8** in 57%, 59% and 64% yield, respectively.

Pyrolysis of 8β-cyano-6,7-diazacholesterol (6a)

A sample of **6a** (60 mg), placed in a small tube, was immersed in a hot silicone oil bath (120 °C). After melting of the crystals, the temperature was raised to 200 °C within 10 min. When the temperature exceeded 180 °C evolution of hydrogen cyanide was observed. The tube containing the sample was slowly cooled (in 10 min) to 120 °C and then placed in an ice-bath. The pale yellow, oily product was chromatographed on a HPLC column. Using 8% 2-propanol in hexane, compounds **8** (at 10 mL; 26 mg; 45%), unreacted **6a** (at 46 mL; 3 mg; 5%), and **9** (at 54 mL; 12 mg; 20%) were gradually eluted. Analytically pure **8** was obtained by re-chromatography (2% 2-propanol in hexane); the product was identical in all respects with the compound previously described. Rechromatography (8% 2-propanol in hexane) of **9** afforded an analytically pure sample; m.p. 125—128 °C (dec), $[\alpha]_D^{25}$ +15° ($c = 0.2$).

C$_{25}$H$_{42}$N$_2$O$_3$. Calcd. C 71.73; H 10.11. Found C 71.62; H 10.09%.

IR, ν_{max}: 3380 (O—H), 1040 cm^{-1}.

^{1}H-NMR, δ: 0.98 (s, 18-H), 1.25 (s, 19-H), 3.89 (m, $w/2 = 28$ Hz, 1H, 3α-H), 5.68 (s, 1H, O—H).

MS, m/e: 418 (M^+, 33%), 402 (M^+-O, 11%), 390 (M^+-N$_2$, 37%), 375 (M^+-N$_2$—Me, 46%), 43 (100%).

*

REFERENCES

[1] Part of this work was published in preliminary form: Morzycki, J. W., Siciński, R. R.: Heterocycles, **22**, 2459 (1984)
[2] DeLuca, H. F., Paaren, H. E., Schnoes, H. K.: "Topics in Current Chemistry", Springer-Verlag, Berlin, pp. 1—65 (1979); Ann. Rep. Med. Chem., **15**, 288 (1980)
[3] DeLuca, H. F.: J. Steroid Biochem., **11**, 35 (1979); Biochem. Soc. Trans., **10**, 147 (1982)
[4] Morzycki, J. W., Schnoes, H. K., DeLuca, H. F.: J. Org. Chem., **49**, 2148 (1984)
[5] Onisko, B. L., Schnoes, H. K., DeLuca, H. F.: Tetrahedron Lett., **1977**, 1107; U.S. Pat. 4,217,288
[6] Gumułka, J., Szczepek, W. J., Wielogórski, Z.: Tetrahedron Lett., **1979**, 4847
[7] Szczepek, W. J.: Private communication
[8] Bosworth, N., Emke, A., Midgley, J. M., Moore, C. J., Whalley, W. B., Ferguson, G., Marsh, W. C.: J. Chem. Soc., Perkin Trans. 1, **1977**, 805
[9] Barton, D. H. R., Shioiri, T., Widdowson, D. A.: J. Chem. Soc. (C), **1971**, 1969; Morris, D. S., Williams, D. H., Norris, A. F.: J. Org. Chem., **46**, 3422 (1981)
[10] Euley, S. C., Williams, D. H.: J. Chem. Soc., Perkin Trans. 1, **1976**, 727
[11] Gilani, S. S. H., Triggle, D. J.: J. Org. Chem., **31**, 2397 (1966)
[12] Cacchi, S., Caglioti, L., Paolucci, G.: Chem. Ind., **1972**, 213
[13] Kwok, R., Wolff, M. E.: J. Org. Chem., **28**, 423 (1963)
[14] Streith, J., Fizet, C., Fritz, H.: Helv. Chim. Acta, **59**, 2786 (1976)
[15] Malhotra, S. K., Hostynek, J. J., Lundin, A. F.: J. Am. Chem. Soc., **90**, 6565 (1968)
[16] Hendrickson, J. B., Bair, K. W., Keehn, P. M.: Tetrahedron Lett., **1976**, 603

RING-FORMATION BY METHYLATION OF PHENYLSERINE DERIVATIVES

János R. VARGA[1], Botond PENKE[1]*, Kálmán KOVÁCS[1]
and István PELCZER[2]

(*[1]Institute of Medical Chemistry, University Medical School, H-6720 Szeged, Dóm tér 8.,
[2] EGIS Pharmaceuticals, H-1475 Budapest, POB 100*)

The synthesis of adrenaline-carboxylic acid was attempted by methylation of 3,4-dibenzyloxy-N-carbobenzyloxyphenylserine. The reaction gave two products in non-aqueous medium: N-benzyloxycarbonyl-(3,4-dibenzyloxyphenyl)-*O*-methylserine and 2-oxo-3-methyl-5-(dibenzyloxyphenyl)oxazolidine-4-carboxylic acid. A similar ring-closure reaction had been previously described to occur only in aqueous medium.

Phenylserine [1] and adrenaline-carboxylic acid (*N*-methyl-3,4-dihydroxy-phenylserine) are both well known and stable compounds. However, the latter was synthesized by a very complicated method [2] giving a very poor yield (3.9%). We wanted to find a new, rational synthesis of adrenaline-carboxylic acid and its derivatives suitable for peptide synthesis. Hegedüs [3] worked out a good method for the synthesis of *O*- and *N*-protected dihydroxyphenylserine and the separation of the four stereoisomers. Using 3,4-dibenzyloxyphenyl-serine **1** as starting material, we planned the following route (Fig. 1) for the synthesis for adrenaline-carboxylic acid, on the basis of literary data [3, 4].

The *threo*-3,4-dibenzyloxy-*N*-carbobenzyloxyphenylserine (**2**) was synthesized according to Hegedüs [3]. McDermott's method [4], which is generally used for *N*-methylation of *N*-carbobenzyloxyamino acids, was applied in the synthesis of compound **3**. Unfortunately, the reaction of **2** with methyl iodide and sodium hydride under the described conditions resulted in two main products: *N*-benzyloxycarbonyl-(3,4-dibenzyloxyphenyl)-*O*-methylserine (**4**) and 2-oxo-3-methyl-5-(dibenzyloxyphenyl)oxazolidine-4-carboxylic acid (**5**) (Fig. 2).

The structures of **4** and **5** were proved by NMR spectroscopy using TMS as internal standard. All the ^{1}H-NMR (90 MHz) signals were assignable, but the differences were not remarkably large. Only the integral of aromatic protons differed significantly, indicating the presence of three benzyl (phenyl) groups in **4** and only two in **5**. The methoxy group in **4** gives a singlet at 3.05 ppm, while the *N*-methyl group in **5** resonates at 2.9 ppm. The structure of **5** was confirmed by ^{13}C-NMR (25.2 MHz), showing the signal of the NCH_3 carbon at 31.7 ppm, and two carbonyl lines at 172.2 ppm and 158.0 ppm,

* To whom correspondence should be addressed.
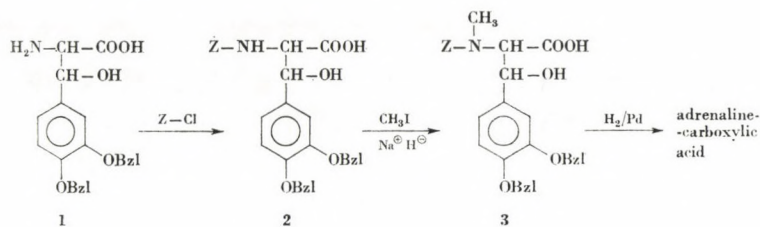
Fig. 1
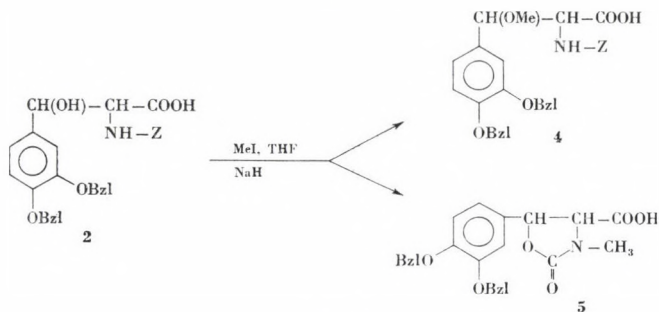
Fig. 2
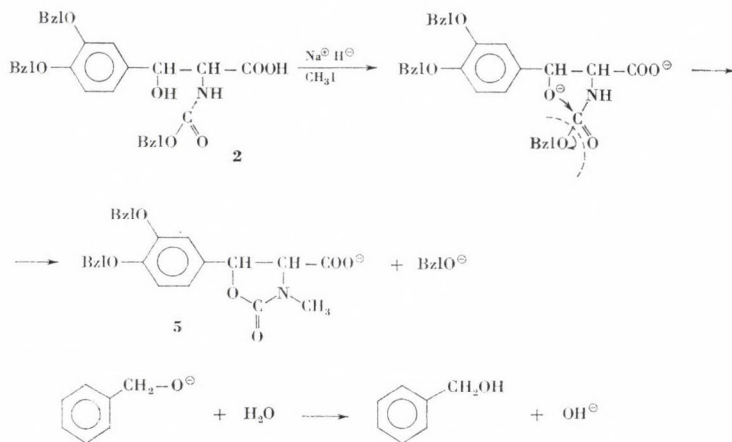
Fig. 3

corresponding to the free acid carbonyl and the CO-carbon of the oxazolidin-
-2-one ring, respectively. It seems that under standard methylation conditions
there are two competitive reactions taking place:

1. methylation of the hydroxyl group resulting in the formation of
   N-benzyloxycarbonyl-(3,4-dibenzyloxyphenyl)-*O*-methylserine (4); and
2. ring closure, catalyzed by the base sodium hydride, and parallel
   N-methylation resulting in 2-oxo-3-methyl-5-(dibenzyloxyphenyl)-
   oxazolidine-4-carboxylic acid (5).

The desired compound **3** — protected adrenaline-carboxylic acid — was formed only in trace amounts.

It is known from the literature [5, 6] that N-carbobenzyloxythreonine and -serine give cyclic products by treatment with aqueous alkali. According to our results, this type of ring closure can also take place in non-aqueous medium; the alcoholic hydroxyl group of **2** attacks the C=O of the N-protecting benzyloxycarbonyl group and benzyl alcohol is liberated (Fig. 3).

As the methoxy compound **4** has no tendency to ring formation, the target compound **3** could be synthesized either by methylation of an O-protected derivative of **2**, or by appropriate hydrolytic cleavage of the cyclic compound **5**.

Experimental

M.p.'s were measured with a Büchi—Tottoli melting point determining apparatus and are uncorrected. The NMR spectra were recorded with VARIAN EM 390 (^{1}H, 90 MHz) and VARIAN XL-100 (^{13}C, 25.2 MHz) spectrometers, respectively.

N-benzyloxycarbonyl-(3,4-dibenzyloxyphenyl)-O-methylserine, 4, and 2-oxo-3-methyl-5-(dibenzyloxyphenyl)-oxazolidine-4-carboxylic acid, 5

3,4-Dibenzyloxy-N-carbobenzyloxyphenylserine (2.1 g) dissolved in 9 mL of dry THF, was reacted at 0 °C with 2.0 mL of methyl iodide in the presence of 0.53 g of sodium hydride (55% suspension in mineral oil). After 24 h stirring at room temperature, 20 mL of ethyl acetate and 10 mL H_2O were added. The N-carbobenzyloxy-3,4-dibenzyloxyphenyl-O-methylserine **4** precipitated as grey crystals. It was purified by repeated extraction of the ethyl acetate solution of **4** with 0.1 M HCl and recrystallized from warm ethyl acetate. Yield: 380 mg (17.5%), m.p. 194—196 °C, $R_f = 0.35$ [EtOAc: (MeOH—AcOH—H_2O, 2 : 1 : 2) 95 : 2 v/v].
$C_{32}H_{31}NO_7$ (541.57). Calcd. C 70.96; H 5.77. Found C 71.3; H 6.04%.

The first mother liquor (THF-ethyl acetate-H_2O) containing **5** was evaporated to dryness; the residue was dissolved in 5% $NaHCO_3$ solution and washed with ether and acidified. The 2-oxo-3-methyl-5-(dibenzyloxyphenyl)oxazolidine-4-carboxylic acid **5** was extracted with ethyl acetate, and crystallized from ethyl acetate-THF. Yield: 880 mg (49.9%), m.p. 125—127 °C, $R_f = 0.42$ [EtOAc: (pyridine-AcOH—H_2O, 20 : 6 : 11) 80 : 20 v/v].
$C_{24}H_{21}NO_6$ (417.44). Calcd. C 68.57; H 5.07. Found C 68.70; H 5.34%.

*

REFERENCES

[1] Erlenmeyer, E., Frühstück, U. E.: Justus Liebigs Ann. Chem., **284**, 36 (1895)
[2] Dalgliesh, C. E., Mann, F. G.: J. Chem. Soc., **1974**, 658
[3] Hegedüs, B., Krassó, A. F., Noack, K., Zeller, P.: Helv. Chim. Acta, **58**, 147 (1975)
[4] McDermott, J. R., Benoiton, N. L.: Can. J. Chem., **51**, 1915 (1973)
[5] Bergel, F., Wade, R.: J. Chem. Soc., **1959**, 941
[6] Stabinsky, Y., Fridkin, M., Zakuth, V., Spirer, Z.: Int. J. Pept, Protein Res., **12**, 130 (1978)

STUDIES ON SOME QUINOLINE DERIVATIVES, II*

FAR INFRARED SPECTRA OF METAL(II) HALIDE AND PSEUDOHALIDE COMPLEXES OF 4-METHYLQUINOLINE

Mohamed Abdel-Rahman Sidahmed Goher** and Afaf Kamal Hafez

(Department of Chemistry, Faculty of Science, Alexandria University, Alexandria, Egypt)

Complexes of the types $M(4\text{-MeQ})_2X_2$ and $M(4\text{-MeQ})X_2$ where 4-MeQ is 4-methylquinoline, M = Co, Ni, Cu, Zn, Cd and Hg and X = Cl, Br, I, SCN, OCN, N_3 and NO_3, have been prepared and characterized. The stereochemistry of these complexes has been deduced from the electronic spectra, magnetic properties and infrared absorption frequencies of the pseudohalide groups. The metal-halogen, and metal-nitrogen stretching vibration frequencies have been assigned and discussed in relation to the structures of the complexes.

Introduction

During the last decades metal(II) complexes of pyridine derivatives have been studied extensively [1]. The corresponding quinoline derivatives, however, have received little attention. Thus while 4-methylpyridine complexes with transition metal halides and pseudohalides have been studied from different viewpoints [2—6], only few complexes of 4-methylquinoline have been reported [7, 8]. In this paper we report on the far infrared spectra of cobalt(II), nickel(II), copper(II), zinc(II), cadmium(II) and mercury(II) halide and pseudohalide complexes of 4-methylquinoline (hereafter abbreviated as: 4-MeQ) otherwise called lepidene. The stereochemistry of these complexes have been deduced from their electronic spectra and magnetic moments.

Experimental

4-MeQ was obtained from Aldrich company.
Physical measurements have been carried out as described previously [9].

Preparation of the complexes

$M(4\text{-MeQ})_2X_2$ (X = Cl, NO_3, M = Co, Cu, Zn, Cd, Hg) complexes were prepared by refluxing the components in 1 : 2 molar ratio dissolved in ethanol for several hours and the final mixture allowed to stand for several days.

$Co(4\text{-MeQ})_2X_2$ (X = Br, I, OCN) and $Co(4\text{-MeQ})(N_3)_2$ complexes were prepared by mixing $Co(NO_3)_2 \cdot 3\,H_2O$ with the ligand in ethanol followed by addition of the aqueous solution of NaX. The final mixture was boiled on a water bath when X was Br, OCN, or N_3,

---

* Part I, Bull. Soc. Chim. France, **1980**, I-278.
** To whom correspondence should be addressed.

until the volume reduced to one half of its original volume. For the iodide complex, NaI dissolved in ethanol was added to a boiling mixture and the final solution allowed to stand for several days.

Ni(4-MeQ)$_2$Cl$_2$: The yellow form was prepared by boiling a mixture of the components until near dryness. The blue form was obtained by the method reported for the quinoline

Table I

Analytical data and some physical properties

Complex	Colour	% Found/calculated					μ_{eff} (BM)
		M	C	H	N	X	
Co(4-MeQ)$_2$Cl$_2$	blue	14.41	56.70	4.50	6.62	19.81	4.41
		14.15	57.73	4.33	6.73	19.81	
Co(4-MeQ)$_2$Br$_2$	blue	11.20	47.30	3.80	5.38	35.35	4.42
		11.60	47.50	3.56	5.54	35.73	
Co(4-MeQ)$_2$I$_2$	green	10.10	40.25	3.04	4.00	46.17	4.50
		9.83	40.05	3.00	4.07	46.72	
Co(4-MeQ)$_2$(NCS)$_2$	blue	12.58	56.80	3.90	12.00		4.26
		12.77	57.30	3.90	12.14		
Co(4-MeQ)$_2$(OCN)$_2$	blue	13.82	61.36	4.01	13.26		4.34
		13.56	61.46	4.22	13.03		
Co(4-MeQ)(N$_3$)$_2$	blue	19.80	40.50	3.34	34.36		4.36
		20.50	41.90	3.14	34.25		
Co(4-MeQ)$_2$(NO$_3$)$_2$	violet	12.35	51.31	3.68	11.68		4.42
		12.55	51.15	3.83	11.93		
Ni(4-MeQ)$_2$Cl$_2$	blue	13.95	57.21	4.08	6.82	17.21	3.42
		14.10	57.67	4.32	6.72	17.02	
Ni(4-MeQ)$_2$Cl$_2$	yellow	14.20	56.82	4.52	6.38	17.12	3.12
		14.10	57.67	4.32	6.72	17.02	
Ni(4-MeQ)Cl$_2$	pinkish red	21.32	44.05	3.49	5.27	25.36	3.32
		21.15	43.97	3.29	5.13	25.96	
Ni(4-MeQ)$_2$(NCS)$_2$	pale green	12.42	56.88	4.04	12.30		3.01
		12.73	57.25	3.90	12.14		
Ni(4-MeQ)$_2$(NO$_3$)$_2$	green	12.62	51.24	3.90	12.02		0.00
		12.52	51.16	3.84	11.94		
Cu(4-MeQ)$_2$Cl$_2$	green	15.25	57.07	4.37	6.55		1.86
		15.09	57.09	4.28	6.65		
Cu(4-MeQ)Cl$_2$	brown	23.20	43.10	3.40	5.15		1.95
		22.86	43.23	3.25	5.04		
Cu(4-MeQ)$_2$Br$_2$	greenish yellow	12.19	46.85	3.60	5.58		1.84
		12.46	47.15	3.53	5.48		
Cu(4-MeQ)$_2$(NCS)$_2$	green	14.00	57.00	3.64	12.00		1.92
		13.60	56.59	3.88	11.99		
Cu(4-MeQ)$_2$(NCO)$_2$	blue	15.30	58.10	4.25	12.70		1.90
		15.03	57.82	4.25	12.80		
Cu(4-MeQ)(N$_3$)$_2$	brown	22.05	41.10	3.32	33.30		1.94
		21.85	41.32	3.12	33.70		
Zn(4-MeQ)$_2$Cl$_2$	white	15.66	56.78	4.08	6.80		0.00
		15.46	56.78	4.25	6.60		
Zn(4-MeQ)$_2$Br$_2$	white	12.83	46.66	3.72	5.50		0.00
		12.76	46.86	3.54	5.46		
Zn(4-MeQ)(N$_3$)$_2$	white	22.75	41.35	3.24	33.30		0.00
		22.35	41.05	3.10	33.49		
Cd(4-MeQ)Cl$_2$	white	34.56	36.30	2.70	4.12		0.00
		34.41	36.74	2.75	4.28		
Hg(4-MeQ)Cl$_2$	white	48.52	29.00	2.20	3.40		0.00
		48.36	28.93	2.17	3.30		
Hg(4-MeQ)(N$_3$)$_2$	white	47.21	28.27	2.20	23.12		0.00
		46.87	28.05	2.10	22.90		

complex [10]. The 1 : 1 nickel(II) chloride complex was obtained from the yellow 1 : 2 complex by heating at 120° to a constant weight.

Cu(4-MeQ)(N₃)₂ complex was prepared by the method reported for the preparation of the 3-picoline complex [11]. Cu(4-MeQ)(NCS)₂ complex was prepared adding an aqueous Cu(NO₃)₂ solution to the ligand in 1 : 1 molar ratio, stirring the boiled mixture and then adding a KSCN solution. The green 1 : 2 complex was formed immediately and then it changed to the brown 1:1 complex

M(4-MeQ)₂(NCS)₂ complexes were prepared according to the method recommended by Vogel [12] for the preparation of pyridine complexes.

Zinc(II) and mercury(II) azide complexes were prepared by the methods given for the corresponding azides of pyridine [13, 14].

The metal contents were determined by standardized methods.

Result and Discusion

The elemental analyses of the isolated complexes together with their colours and some physical properties are collected in Table I.

This work consists of two parts. In the first part the stereochemistry of the isolated complexes is deduced from their electronic spectra and the magnetic moments. The second part is concerned with the assignments and discussion of the metal-halogen and metal-pseudohalide and metal-ligand stretching modes.

Cobalt(II) complexes

The electronic spectra of the solid blue complexes are indicative of tetrahedral geometry [15], exhibiting the $^4T_1(P) \leftarrow \, ^4A_2$, ν_3, transition as a multiple band. The similarity of the spectra of the solid state and in solution, except for Co(4-MeQ)(N₃)₂, together with the intensity of the absorption bands, indicate that the tetrahedral geometry is maintained in solution too. Figure 1, shows that the spectra of the complexes are very similar except that the bands are shifted to higher frequencies in the sequences I < Br < Cl < OCN < < NCS < N₃. This order agrees well with that found [16] for CoX₄²⁻ complex anions, except that azide is between chloride and cyanate. This may be due to the fact that the azide complex, is bridged through the azide groups. The tetrahedral structures of these complexes are confirmed by their room-temperature magnetic moments (Table I). which indicate high spin cobalt(II) ion [17]. The spectrum of the hygroscopic violet cobalt(II) nitrate complex differs a little from those of the other cobalt complexes. However, its spectrum is very similar to that observed for the tetrahedral Co(NO₃)₄²⁻ complex ion [18]. Its magnetic moment (4.42 *BM*) strongly implies tetrahedral geometry.

Nickel(II) complexes

The electronic spectrum of the solid blue Ni(4-MeQ)₂Cl₂ complex exhibits a strong multiple band (Figure 2 and Table II) in the 18,500—15,000 cm⁻¹ range which is consistent with tetrahedral nickel(II) ion [19] and assigned
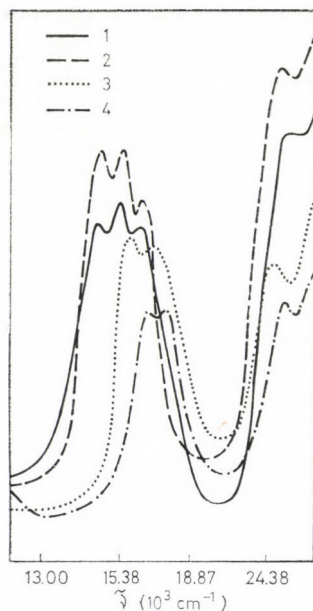
Fig. 1. Electronic spectra of: (1) $Co(4\text{-}MeQ)_2I_2$, (2) $Co(4\text{-}MeQ)_2Br_2$, (3) $Co(4\text{-}MeQ)_2Cl_2$, (4) $Co(4\text{-}MeQ)_2(NCS)_2$
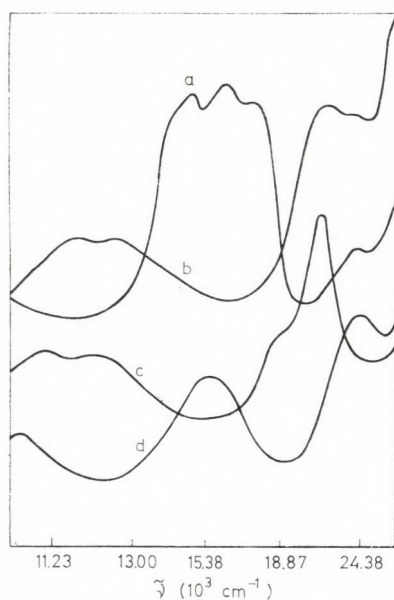
Fig. 2. Electronic spectra of solid complexes: (a) $Ni(4\text{-}MeQ)_2Cl_2$ (blue), (b) $Ni(4\text{-}MeQ)_2Cl_2$ (yellow), (c) $Ni(4\text{-}MeQ)Cl_2$, (d) $Ni(4\text{-}MeQ)_2(NO_3)_2$

to the $^3T_1(P) \leftarrow {}^3T_1$, ν_3, transition. The spectrum of the yellow 1 : 2 isomer is very similar to that reported [20] for the corresponding quinoline complex. The splitting of the low frequency band may suggest a distorted octahedral geometry. The observed bands may be assigned to $^3A_{2g} \leftarrow {}^3B_{1g}$ (11,764 cm^{-1} ,

Table II

Electronic spectral data for the complexes

Complex	Solvent	Maximum absorption (cm^{-1})
Co(4-MeQ)$_2$Cl$_2$	NM	16806, 15625
	Acetone	17241 (300), 16873 (460)
Co(4-MeQ)$_2$Br$_2$	NM	16129, 15151, 14493
	Acetone	16666 (250), 15151 (480)
Co(4-MeQ)$_2$I$_2$	NM	16000, 15037, 14388
	Acetone	15151 (140,) 14388 (180), 13513 (230)
Co(4-MeQ)$_2$(NCS)$_2$	NM	17699, 16393
	Acetone	17699 (300), 15873 (750)
Co(4-MeQ)$_2$(OCN)$_2$	NM	17857, 16949, 16129
Co(4-MeQ)$_2$(N$_3$)$_2$	NM	18691, 16529
Co(4-MeQ)$_2$(NO$_3$)$_2$	NM	19230, 18182
	Acetone	18691 (94)
Ni(4-MeQ)$_2$Cl$_2$[a]	NM	24390, 18518, 16529, 15037
Ni(4-MeQ)$_2$Cl$_2$[b]	NM	24900, 21739, 12500, 11764
Ni(4-MeQ)$_2$(NCS)$_2$	NM	24390, 20920, 14285
Ni(4-MeQ)$_2$(NO$_3$)$_2$	NM	24390, 15748, 10952
Cu(4-MeQ)$_2$Cl$_2$	NM	25641, 15151
Cu(4-MeQ)Cl$_2$	NM	19608, 13513
Cu(4-MeQ)$_2$Br$_2$	NM	12988, 16129
	Acetone	23585 (870), 15151 (200)
Cu(4-MeQ)$_2$(NCS)$_2$	NM	22727, 15384
Cu(4-MeQ)$_2$(NCO)$_2$	NM	16260
Cu(4-MeQ)(N$_3$)$_2$	NM	22727, 18518, 14084

NM = nujol mull spectra, ε is given between parentheses

$^3E_g \leftarrow {}^3B_{1g}$ (12,500 cm^{-1}), $^3A_{2g} \leftarrow {}^3B_{1g}$ (21,739 cm^{-1}) and $^3E_g(^3P) \leftarrow {}^3B_{1g}$ (24,900 cm^{-1}) in D_{4h} symmetry [20]. The latter band may be mixed with a charge-transfer transition. The spectrum of the 1 : 2 thiocyanate complex exhibiting a band at 20,920 cm^{-1} assigned to the $^3T_{1g}(P) \leftarrow {}^3A_{2g}$, ν_3, transition and at 14,285 cm^{-1} to the $^3T_{1g} \leftarrow {}^3A_{2g}$, ν_2 transition [19] suggesting octahedral structure.

While the spectrum of the 1 : 1 chloride complex suggests a five coordinate nickel(II) ion [19], but octahedral structure may not be ruled out. It may be attained through a sixth longer bond to a chloride opposite the ligand making a weaker contribution to the ligand field. The spectrum of Ni(4-MeQ)$_2$(NO$_3$)$_2$ complex together with its diamagnetism suggests square planar structure [21].

Copper(II) complexes

The position of the d—d bands observed in the spectra of the solid $Cu(4\text{-MeQ})_2X_2$ (X = Cl, Br, NCS or OCN) complexes suggests six coordinate pseudooctahedral structures [22]. On the other hand the spectra of the 1 : 1 complexes exhibit a relatively strong band around 19,000 cm^{-1} together with a moderate d—d band around 13,500 cm^{-1}. The position of this latter band suggests [23] five coordinate structure for these complexes. The spectrum of the azide complex closely resembles that reported for the $Cu(3\text{-picoline})(N_3)_2$ complex whose polymeric trigonal bipyramidal structure has been proved by X-ray analysis [11]. The higher frequency band may be assigned to a charge-transfer transition from the bridging group to the copper(II) atom. As the spectra of these 1 : 1 complexes resemble one another, one may suggest trigonal bipyramidal stereochemistry for them.

The room temperature magnetic moments (Table I) given for the 1 : 2 complexes are consistent with that of a copper(II) ion being in an orbitally non-degenerate ground state [17].

Infrared spectra

Anion vibration

The vibration frequencies of the thiocyanate, cyanate and azide groups are given in Table III.

The results indicate bridging thiocyanate groups [24] in the 1 : 1 and 1 : 2 complexes except for $Co(4\text{-MeQ})_2(NCS)_2$ which possesses terminal N--bonded thiocyanate groups.

Table III

Pseudohalide stretching vibration frequencies (cm^{-1})

Complex	ν_{as}	ν_s	δ
$Co(4\text{-MeQ})_2(NCS)_2$	2095 vs, 2080 vs	780 m	440 w
$Ni(4\text{-MeQ})_2(NCS)_2$	2115 vs, 2080 vs	812 w, 770 m	472 m, 445 w
$Cu(4\text{-MeQ})_2(NCS)_2$	2105 vs, 2085 s	808 w, 770 m	477 m, 440 w
$Co(4\text{-MeQ})_2(NCO)_2$	2220 vs, 2190 s	1340 m	618 w, 603 m
$Cu(4\text{-MeQ})_2(NCO)_2$	2240 vs, 2220 vs	1338 m, 1325 m	610 m, 600 m
$Co(4\text{-MeQ})(N_3)_2$	2120 vs, 2100— 2080 vs, 2060 vs	1340 m, 1290 s	670 m, 630 w, 595 m
$Cu(4\text{-MeQ})(N_3)_2$	2090 vs, 2075 vs 2055 vs	1338 w, 1285 m	665 w, 602 w
$Zn(4\text{-MeQ})(N_3)_2$	2130 s, 2090 vs 2065 vs	1350 m, 1290 s	665 wm, 608 m, 600 m
$Hg(4\text{-MeQ})(N_3)_2$	2045 vs, 2020 s	1355 m, 1300 m	645 w, 685 m

The frequencies of the cyanate groups for the 1 : 2 cobalt complex resemble those reported [24] for the anionic complexes $Co(NCO)_4^{2-}$, indicating terminal N-cyanate groups for this tetrahedral complex. Those of the 1 : 2 copper complex indicate bridging cyanate ligands [7].

The spectra of the 1 : 1 azide complexes exhibit split ν_{as} N_3 band. Split ν_{as} N_3 vibration mode has been frequently observed [11, 25, 26] for copper(II) azide complexes containing terminal and bridging azide groups. The appearance of the ν_s N_3 bands in the spectra of 1 : 1 complexes suggests asymmetric azide groups.

The spectra of the nitrato complexes show NO bands at 1440 and 1315 cm^{-1} for cobalt and at 1415 and 1305 cm^{-1} for nickel complex, which indicate unidentate nitrate groups [24]. These results confirm the structures suggested from the electronic spectra of these complexes i.e. that they exhibit terminal $O-NO_2$ groups.

Far infrared spectra

(a) Ring vibrations of 4-methylquinoline

Table IV summarizes the observed vibration frequencies below 650 cm^{-1}. The general feature of the ligand vibrations above 650 cm^{-1} is the slight shift

Table IV

Infrared absorption frequencies (cm^{-1}) *of metal-halide and metal-pseudohalide complexes of 4-methylquinoline (4-MeQ)*

Compound	Quinoline ring vibrations	νM—X	νM—$N(L)$
4-MeQ	595 m, 575 wm, 400 m		
$Co(4\text{-}MeQ)_2Cl_2$	632 wm, 590 w, 415 m	340 s, 313 s	220 s
$Co(4\text{-}MeQ)_2Br_2$	620 m, 590 w, 412 m	255 sh, 245 vs	220 ms
$Co(4\text{-}MeQ)_2I_2$	618 m, 592 w, 415 m	230 s	225 sh
$Co(4\text{-}MeQ)_2(NCS)_2$	620 m, 590 w, 415 m	330 s, 305 s	230 s
$Co(4\text{-}MeQ)_2(NCO)_2$	630 m, 590 w, 410 m	385 s, 348 s	230 s
$Co(4\text{-}MeQ)_2(NO_3)_2$	625 wm, 590 w, 410 m	265 m	235 ms
$Co(4\text{-}MeQ)(N_3)_2$	630 w, 590 sh, 418 m	370 s	265, 245 s
$Zn(4\text{-}MeQ)_2Cl_2$	625 wm, 590 m, 412 m	320 m, 295 ms	235 s
$Zn(4\text{-}MeQ)_2Br_2$	620 w, 588 m, 415 m	250 ms, 220 m	235 ms
$Zn(4\text{-}MeQ)(N_3)_2$	620 w, 590 m, 410 m	340 m	238 ms
$Ni(4\text{-}MeQ)_2Cl_2{}^a$	640 w, 590 m, 415 m	320 s, 305 s	240 s
$Ni(4\text{-}MeQ)_2Cl_2{}^b$	632 m, 582 w, 418 m	— —	235 s
$Ni(4\text{-}MeQ)Cl_2$	628 m, 580 w, 420 m	— —	245 s
$Cu(4\text{-}MeQ)_2Cl_2$	628 m, 582 w, 420 m	290 s, 265 wm	250 s
$Cu(4\text{-}MeQ)Cl_2$	632 w, 580 m, 418 m	290 sh, 268 s	250 s
$Cu(4\text{-}MeQ)_2Br_2$	630 w, 580 w, 420 m	250 s	250 s
$Cu(4\text{-}MeQ)_2(NCS)_2$	630 w, 582 m, 418 m	320 ms	255 s
$Cu(4\text{-}MeQ)_2(NCO)_2$	630 m, 580 w, 420 m	390 ms	245 s
$Cu(4\text{-}MeQ)(N_3)_2$	630 vw, 490 w, 422 m	387 m	260, 247 s
$Cd(4\text{-}MeQ)Cl_2$	635 w, 582 m, 420 m	— —	<200
$Hg(4\text{-}MeQ)(N_3)_2$	644 m, 580 sh, 415 m	— —	<200

[a] Blue tetrahedral form.
[b] Yellow polymeric octahedral form.

to higher frequencies upon complexation of 4-MeQ. However, two bands below 650 cm^{-1} experience significant shifts to higher frequencies. These two bands: 595 and 400 cm^{-1} are ring deformation modes. In addition, the 570 cm^{-1} band in the free ligand appears around 590 cm^{-1} and 580 cm^{-1} for tetrahedral and polymeric octahedral complexes, respectively. The 595 cm^{-1} band is the more sensitive to the stereochemistry of the complexes of a given metal e.g. Ni(4-MeQ)$_2$Cl$_2$ (tetrahedral) 640, 415 cm^{-1} and Ni(4-MeQ)$_2$Cl$_2$ (polymeric octahedral) 632, 418 cm^{-1}. While these two bands shift upon complexation, the relationships between such shifts and the stereochemistry of the complexes are not so significant as those found [1a, 1b] for corresponding vibrations of coordinated pyridine.

(b) *Metal-halogen and metal-nitrogen stretching vibrations*

The νM—X stretching vibrations are identified by their shifts to lower frequencies when X is progressively changed from chloride to iodide. The νM—N(L) and other metal-ligand (anion) are assigned on the assumption that for a series of complexes, MX$_2$L$_n$, of the same stereochemistry, the νM—N (L) vibrations occur at approximately the same frequencies for a given metal. The metal-halogen and metal-nitrogen frequencies assigned to these bases are given in Table IV.

Tetrahedral ML$_2$X$_2$(C$_{2v}$) complexes are expected to show two νM—X vibrations ($A_1 + B_1$) and two νM—N(L) vibrations ($A_1 + B_2$) which are IR-active. The spectra of the tetrahedral chloro complexes of Ni and Co are characterized by two strong bands and one medium to strong band in the 200—400 cm^{-1} region. The former two bands are νM—X vibrations, because they shift down to $\approx$0.77 of their values in analogous bromo derivatives, and lower still in iodo derivatives. The frequency of the third band is almost independent of halogen and is accordingly assigned to a νM—N(L) vibration. The spectrum of Zn(4-MeQ)$_2$Cl$_2$ exhibits two bands, associated with the νZn—Cl vibrations, which are absent from the analogous bromo complex, and therefore both possess tetrahedral structures. The νM—X vibrations of cobalt complexes lie 10—25 cm^{-1} above those of comparable zinc or nickel complexes. This trend was observed in the case of corresponding pyridine complexes [1a, 1b].

Table V compares the νM—X and νM—N(L) vibrations of some 4-MeQ complexes with corresponding complexes of pyridine and quinoline. While the νM—X vibrations of 4-MeQ, like the pyridine complexes, lie $\approx$10 cm^{-1} higher than those of quinoline, the νM—N(L) vibrations of pyridine complexes lie $\approx$30 cm^{-1} above those of both quinoline and 4-methylquinoline. In the case of the polymeric distorted octahedral Cu(4-MeQ)$_2$Cl$_2$ complex the νCu—Cl vibrations are lower by $\approx$30 cm^{-1} (Tables IV and V) than those of the analo-

Table V

Comparison of νM—X and νM—L in some ML_2X_2 complexes

Complex	νM—X	νM—L	Ref.
$Co(py)_2Cl_2$	344, 304	252	[1a]
$Co(Q)_2Cl_2$	333, 312	226	[1a]
$Co(4\text{-}MeQ)_2Cl_2$	340, 313	220	
$Co(py)_2Br_2$	274, 242	250	[1a]
$Co(4\text{-}MeQ)_2Br_2$	255, 245	225	
$Cu(py)_2Cl_2$	294, 235	268	[1a]
$Cu(Q)_2Cl_2$	332	259	[1e]
$Cu(4\text{-}MeQ)_2Cl_2$	290, 265	250	
$Cu(py)_2Br_2$	255, 202	269	[1a]
$Cu(Q)_2Br_2$	266	256	[1e]
$Cu(4\text{-}MeQ)_2Br_2$	250	250	
$Zn(py)_2Cl_2$	329, 296	220	[1a]
$Zn(Q)_2Cl_2$	316, 300	205	[1b]
$Zn(4\text{-}MeQ)_2Cl_2$	320, 295	235	

py = pyridine, Q = quinoline

gous quinoline complex. The position of νM—X vibrations reflects the influence of the electron-releasing methyl group which increases the base strength of 4-methylquinoline compared with quinoline.

The spectra of tetrahedral $Co(4\text{-}MeQ)_2(NCX)_2(X = O$ or S) complexes exhibit two bands associated with the νCo—NCX vibrations which reveal N-bonded cyanate or thiocyanate groups. The appearance of a single band associated with the νM—N_3 vibration in the spectra of the 1 : 1 azide complexes suggests that one of the azide groups is terminal and the other acts as a bridging group leading to polymeric tetrahedral for cobalt and zinc complexes and polymeric five coordinate structure for the copper complex.

The polymeric octahedral 1 : 2 as well as five coordinate 1 : 1 chloro complexes of nickel do not show the νNi—Cl vibration bands, as they are expected to be below 200 cm^{-1} [1e] for bridging chloro complexes.

REFERENCES

[1] e.g. (a) Gill, N. S., Nuttall, R. H., Scaife, D. E., Sharp, D. W. A.: J. Inorg. Nucl. Chem., **18**, 79 (1961); (b) Clark, R. J., Williams, C. S.: Inorg. Chem., **4**, 350 (1965); (c) Frank, C. W., Rogers, L. B.: Inorg. Chem., **5**, 615 (1966); (d) McWhinnie, W. R.: J. Inorg. Nucl. Chem., **27**, 2573 (1965); (e) Goldstein, M., Mooney, E. F., Anderson, A., Gebbie, H. A.: Spectrochim. Acta, **21**, 105 (1965)
[2] Allan, J. R., Brown, D. H., Nuttall, R. H., Sharp, D. W. A.: J. Inorg. Nucl. Chem., **27**, 1305 (1965)
[3] Gill, N. S., Kingdon, H. J.: Austral. J. Chem., **19**, 2197 (1966)
[4] Buffagni, S., Vallarino, L. M., Quagliano, J. V.: Inorg. Chem., **3**, 480 (1964)
[5] Brewer, D. G., Wong, P. T. T., Sears, M. C.: Can. J. Chem., **46**, 3177 (1968)
[6] Burgess, J.: Spectrochim. Acta, **24A**, 277 (1968)
[7] Kohout, J., Kabešova, M., Hvastijova, M., Gažo, M.: Coll. Czech. Chem. Commun., **43**, 379 (1978); Durčanska, E., Jarovicky, M., Jane, E., Sram, R. O. T.: Proc. Conf. Coord. Chem., **1976**, 51; C. A., **90**, 47678a

[8] Rao, C. D., Mohapatra, B. K., Guru, S.: Indian J. Chem. Sec., A., **18A,** 186 (1979); Dawn, A. W., Ongley, P. A.: Chem. Ind. (London), **1963,** 493
[9] Goher, M. A. S., Hasanein, A. A., El-Subruiti, G. M.: Bull. Soc. Chim. France, **1982,** I-221
[10] Goodgame, D. M. L., Goodgame, M.: J. Chem. Soc., **1963,** 207
[11] Goher, M. A. S., Mak, T. C. W.: Inorg. Chim. Acta, **89,** 119 (1984)
[12] Vogel, A.: A textbook of Quantitative Inorganic Analyses, 3rd. Edition, Longman, London 1972
[13] Agrell, I.: Acta Chem. Scand., **25,** 1630 (1971)
[14] Agrell, I.: Acta Chem. Scand., **24,** 3575 (1970)
[15] Lever, A. B. P., Nelson, S. M.: J. Chem. Soc., **1966,** 859
[16] Cotton, F. A., Goodgame, D. M. L., Goodgame, M.: J. Amer. Chem. Soc., **83,** 4890 (1961)
[17] Figgis, B. N., Lewis, J.: Progr. Inorg. Chem., **6,** 37 (1964)
[18] Cotton, F. A., Dunne, T. G.: J. Amer. Chem. Soc., **84,** 5194 (1964)
[19] Lever, A. B. P.: Inorganic Electronic Spectroscopy, Elsevier, Amsterdam 1968
[20] Goodgame, D. M. L., Goodgame, M., Weeks, M. J.: J. Chem. Soc., **1964,** 5194
[21] Lever, A. B. P., Lewis, J., Nyholm, R. S.: J. Chem. Soc., **1963,** 5042
[22] Ereday, R. J.: J. Chem. Soc., A., **1971,** 3035
[23] Bew, M. J., Dudley, R. J., Feredy, R. J., Hathaway, B. J.: J. Chem. Soc., A **1971,** 1437
[24] Nakamoto, K.: Infrared Spectra of Inorganic and Coordination Compounds, 2nd. Edition, Wiley, Interscience, New York, London 1963
[25] Goher, M. A. S., Mak, T. C. W.: Inorg. Chim. Acta, **85,** 117 (1984)
[26] Goher, M. A. S., Mak, T. C. W. (to be published)

MOLECULAR COMPOUNDS OF HYDROXY ARYL SCHIFF'S BASES WITH AROMATIC TRI- AND DINITRO COMPOUNDS

Yousry Moustafa Issa[1]*, Ahmed Mahmoud Hindawy[2],
Aida Lofty El-Ansary[1] and Raafat Moustafa Issa[3]

(*[1]Chemistry Department, Faculty of Science, Cairo University,
[2] Alexandria University, [3] Tanta University, Cairo, Egypt*)

The charge-transfer interaction between hydroxy aryl Schiff's bases and aromatic tri- and dinitrobenzenes is investigated using IR, UV and ^{1}H-NMR spectroscopy. The results reveal that complex formation takes place through π-electron transfer only in case of non-acidic and weak acidic acceptors, while with strong acidic acceptors the reaction takes place through both electron and proton transfer. The results show that the aniline ring is the moiety involved in the charge-transfer interaction.

Introduction

Charge-transfer (CT) complexes of aromatic nitro compounds with π-donor systems were the subject of several interesting investigations [1—6]. Numerous studies considered the CT complexes of aromatic amines, aromatic hydrocarbons with condensed ring system, however, few investigators dealt with the CT complexes of Schiff's bases [7—9].

Complex formation between some benzylidene aniline and *p*-nitrophenol was demonstrated by the change in the intensity of the ν_{OH} band of *p*-nitrophenol at 3610 cm^{-1}, it was reported that the intensity of the ν_{OH} band is a more or less linear function of the Hammett σ constant of the substituent on the benzylidene aniline molecule [7]. It was also suggested that complex formation between *p*-nitrophenol and benzylidene aniline derivatives would take place through intermolecular hydrogen bonding involving the OH group of *p*-nitrophenol and the C=N linkage of benzylidene aniline [8]. From a detailed IR spectroscopic study of CT complexes, formed by the interaction of a series of dinitro- or trinitrobenzenes with some *p*-CH$_3$ or OCH$_3$ substituted benzylidene aniline, it was concluded that complex formation involves $\pi—\pi^*$ or $\pi—\pi^*$ and proton transfer from the acceptor to the C=N linkage [9].

In the present investigation the CT complexes of some hydroxy derivatives of benzylidene aniline as donors with some aromatic dinitro- and trinitrobenzenes are studied using UV, IR, and ^{1}HNMR spectroscopy.

* To whom correspondence should be addressed.

Table I

Important bands in the IR *spectra of* CT *complexes with nonacidic
or weak acidic acceptors*

Donor	colour	M.P. (°C)	νOH	NO$_2$ asym	NO$_2$ sym	γCH
Complexes with picryl chloride (1)						
Bands of free acceptor				1553, 1540	1348	788
a	brown	204		1550, 1530	1342	—
b	brown	178		1545, 1537	1340	770
c	orange brown	178		1550, 1540, 1530	1342, 1335	771
d	orange	178		1548, 1540, 1535	1330	—
e	orange	188		1550, 1540, 1535	1335	780
f	orange	186		1545, 1535	1330	—
g	brown	202		1540, 1535	1335	—
h	reddish brown	107		1548, 1540, 1535	1342, 1335	
i	orange	182		1548, 1540, 1530	1340, 1330 sh	770
j	dark brown	112		1555, 1540, 1535	1342, 1335	782
k	brown	205		1550, 1542, 1535	1340, 1335	780
l	orange	177		1550, 1540, 1530	1340, 1333	770
n	brown	213		1550, 1545, 1535	1345, 1336	772
o	orange	170		1550, 1540, 1528	1345, 1335	775
Complexes with trinitrotoluene (2)						
Bands of free acceptor				1550, 1520	1360	800
a	brown	68		1550, 1540, 1515	1355, 1345	—
b	brown	184		1550, 1542, 1520	1350 b	792
c	pale brown	141		1545, 1540, 1510	1350, 1340 sh	795
d	pale brown	79		1550, 1542, 1518	1355, 1348	—
e	brown	83		1545, 1530, 1518	1350 b	—
f	pale brown	163		1545 b, 1520	1350 b	793
g	pale brown	80		1548, 1540, 1520	1350 b	790
h	pale brown	84		1550, 1542, 1515	1348	795
i	yellow brown	74		1545, 1540, 1510	1350, 1340	792
j	brown	79		1550, 1540, 1520	1350 b	790
k	pale brown	80		1550, 1543, 1520	1348 b	792
l	pale brown	81		1550, 1540, 1520	1350	792
m	brown	72		1548, 1542, 1518	1353	795
n	pale brown	77		1550, 1542, 1520	1352	793
o	brown	76		1550, 1540, 1510	1350 b	790
Complexes with 2,4-dinitrophenol (3)						
Bands of free acceptor			3270	1540, 1520	1350	928, 825
a	dark brown	93	3260	1530, 1515	1345	925, 820
b	dark brown	119	3260	1535, 1515	1343	923, 820
c	pale buff	115	3260	1535, 1510	1343	925, 818
d	pale buff	112	3250	1530, 1515	1342	922, 818
e	yellow	118	3260	1535, 1515	1345	918, 820
g	brown	128	3250	1525, 1515	1335	920, 818
h	pale brown	114	3260	1530, 1515	1340	918, 820
i	pale brown	103	3260	1525, 1515	1340, 1335	918, 820
j	brown	113	3260	1530, 1515	1342	920, 820
k	dark brown	177	3250	1535, 1515	1340	919, 821
l	brown	138	3260	1530, 1515	1345	917, 820
m	brown	107	3260	1535, 1515	1343	915, 820

Table 1 (continued)

Donor colour		M.P. (°C)	νOH	NO$_2$ asym	NO$_2$ sym	γCH
Complexes with 2,5-dinitrophenol (**4**)						
Bands of free acceptor				1552, 1535	1355	850, 837, 818
a	dark brown	oil	3280	1550, 1530	1352	
b	dark brown	154	3270	1550, 1530	1350	
c	grey	155		1535	1355	845, 833, 815
d	brown	83	3270	1545, 1535	1352	832
e	pale brown	104	3280	1548, 1530	1350	840, 825
f	green	175		1540	1348	843, 825
g	brown	97	3280	1545, 1530	1350	848, 835, 810
h	brown	99	3290	1548, 1530	1351	845, 830, 815
i	brown	86	3285	1545, 1528	1350	845, 830
j	dark brown	89	3270	1542, 1528	1350	848, 833, 815
k	brown	189		1540, 1528	1345	845, 835, 815
l	grey	156	3260	1540, 1528	1350	848, 830
m	brown	98	3290	1545, 1530	1350	848, 833, 815

sh: shoulder, b: broad

Experimental

All compounds used in the present investigation were pure BDH chemicals. The preparation of complexes and the working procedures are the same as described previously [3]. The donors used have the general structural formula:
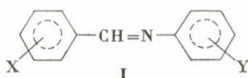
in which X and Y are: (H, *o*-OH), **a**, (H, *m*-OH) **b**, (H, *p*-OH) **c**, (*o*-OH, H), **d**, (*m*-OH, H) **e**, (*p*-OH, H) **f**, (*o*-OH, *o*-OH) **g**, (*o*-OH, *m*-OH) **h**, (*o*-OH, *p*-OH) **i**, (*m*-OH, *o*-OH) **j**, (*m*-OH, *m*-OH) **k**, (*m*-OH, *p*-OH) **l**, (*p*-OH, *o*-OH) **m**, (*p*-OH, *m*-OH) **n** and (*p*-OH, *p*-OH) **o**.

The acceptors used are non-acidic acceptors such as picryl chloride (**1**), trinitrotoluene (**2**); acceptors with weak acidic properties as 2,4-dinitrophenol (**3**), 2,5-dinitrophenol (**4**) or acceptors with strong acidic character as picric acid (**5**), 3,5-dinitrosalicylic acid (**6**) and 3,5--dinitrobenzoic acid (**7**).

The IR spectra were recorded on a UNICAM SP 1000 infrared spectometer in KBr discs, whereas the NMR spectra on a Perkin Elmer R 34-220 Hz NMR spectrometer (the NMR measurements were done at UMIST- Manchester- England during a scientific visit of R.M. Issa). The electronic absorption spectra were recorded on a PYE UNICAM SP 1750 recording spectrophotometer applying the nujol mull technique.

Results and Discussion

The intermolecular interaction between the donors and accepto rs used in the present investigation, as gathered from the results of IR and NMR spectra depends to a large extent on the nature of the acceptor. The various types of interaction are discussed in the following:

Interaction involving electron transfer

This type of CT interaction is observed when the **donors react with non-acidic acceptors (1) and (2)** or the weak acidic ones **(3)** and **(4)**. The spectral characteristics of these compounds are as follows.

IR spectra (Table I)

The γ_{CH} bands of the donor part of the CT complex (benzylidene aniline derivatives) are shifted to higher wavenumbers whereas those of the acceptors are shifted to lower values. This shift is observed with CT complexes involving $\pi-\pi^*$ interaction in which a π-electron is transferred from the HOMO on the donor to the LUMO of the acceptor. The shift of the γ_{CH} bands of the anilino ring is greater than the shift of those of the benzal, this behaviour reveals that the electron transfer to the acceptor would originate from the anilino ring. Such CT interaction leads to obvious shifts in the NO_2-bands of the acceptors to lower wavenumbers. The asym. and sym. NO_2-bands of **(1)** and **(2)** display in many cases a higher splitting in the spectra of the CT complexes indicating increased differentiation in the energy of the NO_2-groups. For compounds formed with donors containing the OH-group in *p*-position of the anilino ring the highest shifts to lower values are observed as a result of the possible hydrogen bonding between the *p*-OH and the *p*-NO_2 groups.

The OH bands of the donor parts of the CT complex show varied behaviour depending on the position of the OH group. The shifts are not regular for compounds containing two OH groups due to difficulties concerning the differentiation between the two bands, for those with one group only a general trend would be pointed out. The ν_{OH} for donors (a) and (b) are shifted to higher wavenumbers as a result of the decrease in the strength of the intramolecular hydrogen bond and the π-electron density on the donor part. The shift in the ν_{OH} bands of (b), (c), (e) and (f) to higher wavenumbers is much obvious due to the destruction of the intermolecular hydrogen bonding liable to exist in the solid lattice of the donor. The shift with (b), (c) and (f) is higher than (e) since the OH-group in the latter compound is probably involved in an intermolecular hydrogen bond with the facing NO_2 group on the acceptor molecule.

NMR spectra

The ^{1}H NMR spectra of the donors in $CDCl_3$ show a group of signals within the 6.7—7.8 ppm range due to the aromatic protons of the two rings. The OH signals are observed downfields at 9.8—10.9 ppm. The acceptors

chosen in this investigation are (1) and (2) since they have their signals at much higher δ-values (8.9—9.3 ppm) compared to the aromatic protons of the donors.

A comparison between the NMR spectra of the CT complexes and those of the components reveals that the signals of the acceptors are shifted to lower δ-values while those of the donors are displaced to higher ones. The magnitude of the shift varies according to the donor and acceptor used; also the shift is higher with the signals due to anilino protons which is in accordance with the results of the IR spectra.

Based on the information obtained from the IR and NMR spectra, the CT interaction can be formulated as in (II).

II
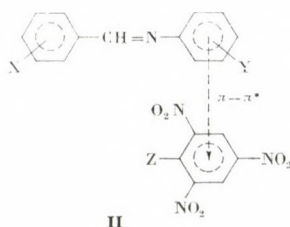
Electronic absorption spectra

The electronic absorption spectra of the CT complexes of this group display a single CT band within the 450—570 nm range corresponding to the $\pi - \pi^*$ intermolecular charge-transfer interaction with $E_{CT} = 2.18—2.25$ eV. This assumption is supported by calculating the energy of the CT interaction for the complexes with acceptor (3) using the relation given by Briegleb [1]:

$$E_{CT} = I_p - E_A + C$$

where I_p is the ionization potential of the donor, its value can be determined from the electronic absorption spectra [10] (8.8—9.1 eV); E_A is the electron affinity of the acceptor, it is -0.7 eV [11] for trinitrotoluene; C is the coulombic force between the electron transferred and the positive hole left behind, it is -5.6 eV.

The values of E_{CT} thus obtained amount to 2.5—2.8 eV which coincide well with that determined from λ_{max} (2.18—2.25 eV). The plots of E_{CT} as a function of I_p are more or less linear relations with almost identical slopes but varied intercepts. From the intercepts the electron affinities of the acceptors under investigation are determined and 0.86, 0.69, 0.58 and 0.54 eV for acceptors 1—4 are obtained. The values are comparable to those evaluated from the electronic absorption spectra [10] and also with the literature values in case of acceptor (2) [11].

The existence of only one absorption band in the electronic absorption spectra reveals that the CT complex formation between the benzylidene aniline derivatives and the trinitro or dinitrobenzenes under investigation takes place through $\pi - \pi^*$ bonding. The contribution of $n - \pi^*$ type interaction to complex formation is low or absent.

Interaction involving electron and proton transfer

This type of interaction occurs when the donors used are allowed to react with acceptors of strong acidic property, namely acceptors (5), (6) and (7). The IR and NMR spectra of these complexes differ considerably from those of their components.

IR spectra

The IR spectra of the CT complexes compared to those of the free components exhibit a new group of broad intense bands within the $3000-2400$ cm^{-1} range which can be assigned to the stretching mode of the $=N^+-H$ structure formed through the transfer of a proton from the phenolic groups of (6) and (7) or the carboxyl group of (8) [3]. This is supported by the disappearance of the OH bands corresponding to these groups and the shift of the $C=N$ band to lower values in the spectra of the CT complexes. The γ_{CH} bands of the donors shift to higher wavenumbers while those of the acceptors are shifted to lower ones, a behaviour which is characteristic of the $\pi - \pi^*$ CT interaction. The shift in the γ_{CH} bands of the anilino part are higher than those of the benzal part which is identical with the case of CT complexes involving electron transfer only.

The proton transfer from the acceptor to the donor and the formation of the CT complex leads to the destruction of the intramolecular or the intermolecular hydrogen bonding involving one NO_2-group of the acceptor molecule. This leads to a decreased difference in the energy states of the NO_2-groups hence the number of the asym. NO_2-bands becomes less than in the free acceptor. The asym. NO_2-bands shift to higher or lower wavenumbers a behaviour which is common for CT complexes of the acceptors under study involving proton transfer [3]. The sym. NO_2-bands are mostly shifted to lower values as a result of the increased π-electron density on the ring of the acceptor part of the CT complex. The ν_{OH} bands of the donor part display a shift to higher values. For complexes of donors with the OH group in o-position, the shift reflects the destruction of the intramolecular hydrogen band as a result of the protonation of the azomethine nitrogen. For donors with the OH-group in m- or p-positions the shift is brought about by the decreased π-electron density on the donor ring and elimination of the intermolecular hydrogen bond existing in the solid lattice of the free donor.

Table II

Important bands in the IR *spectra of* CT *complexes with strong acidic acceptors*

	Donor colour	M.P. (°C)	=N⁺—H	νOH	C=O	NO₂ sym	NO₂ asym	δ_CH
			$=N^+-H$	νOH	$C=O$	NO_2 sym	NO_2 asym	δ_{CH}
Complexes with picric acid (5)								
Bands of free acceptor				3110		1555, 1540, 1530	1350	784
a	olive green	175	2900—2400			1560, 1538	1339	779
b	brown	162	2900—2400			1560, 1540	1340	781
c	brownish yellow	175	2900—2400			1550, 1545	1342, 1335	—
d	yellow	161	2900—2400			1555, 1541	1343	781
e	yellow	180	2900—2400			1550,1540	1342	778
f	yellow	211	2900—2400			1547	1335	780
g	olive green	174	2900—2400			1550, 1540	1330	—
h	brown	126	2900—2400			1560, 1542	1335	—
i	yellow	193	2900—2400			1550, 1540	1340, 1332	775
j	dark brown	164	2900—2400			1550, 1542	1340	779
k	dark brown	146	2900—2400			1555, 1540	1340	—
l	yellow	185	2900—2400			1548, 1535	1335 b	—
m	dark brown	152	2900—2400			1548, 1540	1340	781 sh
n	dark brown	141	2900—2400			1555, 1538	1340	780 sh
o	brownish yellow	264	2900—2400			1555, 1537	1345, 1335	780 sh
Complexes with 3,5-dinitrosalicylic acid (6)								
Bands of free acceptor				3570 3460 3100	1700 1675	1540, 1530	1349	925, 825
a	grey	210	2900—2300	3170	1645	1533	1345	920, 818
b	brown	129	2900—2300	3210	1685	1530	1342	922, 815
c	pale brown	212	2900—2300	3130	1660	1533, 1525	1345, 1330	912, 810
d	orange brown	173	2900—2300	3160	1685	1528	1345	913, 812
e	buff	203	2900—2300	3180	1675	1530	1343	—, 815
f	pale yellow	240	2900—2300	3130	1655	1515	1320	915, 812
g	dark brown	174	2900—2300	3160	1640	1528	1342	920, 812
h	buff	124	2900—2300	3200	1675	1530	1335	922, 815
i	dark brown	204	2900—2300	3150	1645	1535, 1515	1345, 1335	920, 813
j	dark brown	176	2900—2300	3170	1650	1530	1342	920, 813
k	brown	120	2900—2300	3200	1680	1535	1340	918, 812
l	greenish yellow	206	2900—2300	3200	1660	1535, 1520	1350,1335	922, 815
m	dark brown	110	2900—2300	3190	1675	1530	1344	920, 817
n	dark brown	127	2900—2300	3200	1680	1535	1342	918, 813
o	pale brown	242	2900—2300	3160	1650	1530, 1520	1340 b	920, 812
Complexes with 3,5-dinitrobenzoic acid (7)								
Bands of free acceptor				3190		1550, 1540	1350	823, 808, 727
a	brown	164	3000—2300			1540	1342	—, 800, 722
b	brown	156	3000—2300			1540	1345	820, 800, 720
c	yellow	164	3000—2300			1535	1342	—, 795, 723
d	orange	113	3000—2300			1535	1340	820, —, 718
e	dark brown	117	3000—2300			1540	1340	—, 800, 720
f	buff	192	3000—2300			1537	1335	818, —, 722
g	dark brown	123	3000—2300			1545	1345	—, 790, 722
h	brown	118	3000—2300			1545	1341	—, 800, 722
i	yellow	205	3000—2300			1540	1336	818, 795, 718
j	dark brown	119	3000—2300			1543	1345	—, 801, 722
k	dark brown	126	3000—2300			1540	1343	—, 800, 720
l	yellow	208	3000—2300			1538	1340	815, 800, 720
m	brown	190	3000—2300			1542	1340	—, 800, 725
n	dark brown	137	3000—2300			1545	1345	—, 800, 723
o	pale brown	245	3000—2300			1540	1342	815, 795, 720

b: broad, sh: shoulder

NMR spectra

The NMR spectra of the complexes in comparison to those of the free components reveal a shift of the signals due to the donor part to higher fields whereas those of the acceptor are shifted to lower fields. This result from the $\pi - \pi^*$ interaction leading to the increased π-electron density on the acceptor and its decrease on the donor. The shift in the signals of the donor part in this class of complexes is of higher magnitude than in case of CT complexes involving electron transfer only. This can be ascribed to the positively charged azomethine linkage $(C=N^+-H)$ which exerts a higher deshielding effect on the aromatic protons than the azomethine bond $(CH=N)$.

The NMR spectra of the CT complexes involving proton transfer exhibit a broad signal within the 5.6—9.8 ppm range which is absent in the NMR spectra of electron-transfer complexes. This signal can be attributed to the proton of the protonated azomethine nitrogen $(=N^+-H)$. The position of the signal depends on the nature of both donor and acceptor.

Table III

Signals in the NMR spectra of CT complexes with 3.5-dinitrobenzoic acid

Acceptor	Donor c		Donor f		Donor i		Donor o		Proton
	donor	compl.	donor	compl.	donor	compl.	donor	compl.	
Signals of acceptor part of the complex									
7.67	—		—		—		—		OH
8.80		8.62		8.37		8.65		8.38	H^2
8.97		8.93		9.03		8.95		9.03	H^4
8.70		9.00		9.08		9.03		9.08	H^6
Signals of the anilino part									
	7.05	7.20	7.10	8.18	7.30	7.40	7.65	7.20	H^2
	6.75	6.85	6.80	6.88	6.83	6.90	6.75	6.80	H^3
			7.10	7.15					H^4
	6.75	6.85	6.80	6.88	6.83	6.90	6.75	6.80	H^5
	7.05	7.20	7.10	7.18	7.30	7.40	7.65	7.70	H^6
		4.85		8.65		9.40		6.50	$C=N^+-H$
	8.80	8.98			9.10	9.18	8.10	8.38	OH
							8.4		
Signals of the benzal part									
	7.75	7.81	7.70	7.75			7.00	7.07	H^2
	7.40	7.45	7.30	7.37	6.90	6.95	6.85	6.90	H^3
	7.55	7.54			7.15	7.18			H^4
	7.40	7.45	7.30	7.37	7.18	7.22	6.85	6.90	H^5
	7.75	7.81	7.70	7.75	7.30	7.30	7.00	7.07	H^6
	10.00		10.00	d.f.	10.00	d.f.	9.00	9.12	OH
	6.65	6.75	6.60	6.65	6.77	6.85	6.72	6.77	$=C-H$

d.f.: Downfields above 10 ppm

Electronic absorption spectra

The visible electronic absorption spectra of the CT complexes belonging to this class exhibit also one CT band within the 430—470 nm range. The band is situated at higher energies compared to that of CT complexes not involving the proton transfer. This is due to the higher ionization potential of the protonated azomethine molecule and the lower electron affinity of the anion of the acceptor compared to the neutral molecule. A quantitative treatment for this class of CT complexes is difficult because the protonation energy changes by the different acidity of the acceptor and basicity of the donor.

From the results of the IR-, NMR- and electronic spectra of the present investigation, the bonding in the CT complexes of benzylidene anilines and picric acid can be formulated as follows:

III
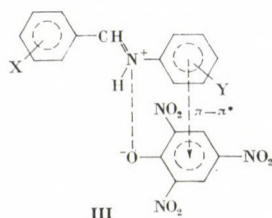
REFERENCES

[1] Briegleb, G., Della, H.: Angew. Chem., **72**, 401 (1960); **76**, 326 (1964); Z. Elektrochem., **63**, 6 (1959); **64**, 347 (1960); Z. physik. Chem. (Frankfurt), **24**, 359 (1960)
[2] Kross, R. D., Fassel, V. A.: J. Am. Chem. Soc., **79**, 38 (1957); Spectrochim. Acta, **8**, 142 (1952)
[3] Issa, R. M., Hindawey, A. M., Issa, Y. M.: Z. physik. Chem. (Leipzig), **253**, 96 (1973); Acta Chim. Acad. Sci. Hung., **88**, 341 (1975); **92**, 263 (1976(; Rev. Roum. Chim., **25**, 1355 (1980); **26**, 667 (1981); Ind. J. Chem., **19A**, 615 (1979); Monatsh. Chem., **111**, 27 (1980); Gazz. Chim. Ital., **111**, 27 (1981)
[4] Foster, R., Hammick, D. L., Placito, P. J.: J. Chem. Soc. **1954**, 3986; **1956**, 3881; Trans. Faraday Soc., **59**, 2287 (1963); **61**, 1620 (1965)
[5] Ross, S. D., Labes, M. M.: J. Am. Chem. Soc., **76**, 74, 3000, 4176 (1954); **77**, 4916 (1955); **78**, 343 (1956)
[6] Homer, J.: J. Chem. Soc., (A), **1969**, 277, 773, 777, 1984, 2862; (**1970**), 931
[7] Wienstein, J., McIninch, E.: J. Am. Chem. Soc., **82**, 6064 (1960)
[8] Kovavic, J. E.: Spectrochim. Acta, **23A**, 183 (1977)
[9] Hindawey, A. M., Issa, Y. M., Issa, R. M., Rizk, H. F.: Acta Chim. Hung., **112**, 415 (1983)
[10] Issa, Y. M.: Spectrochim. Acta, **40A**, 137 (1984)
[11] Herbstein, F. H.: "Perspective of structural chemistry", Vol. **4**, Eds. I. D. Dunitz and J. A. Ibers, John Wiley. N. Y. (1971)

DIELS-ALDER REACTIONS OF
3(2H)-ISOQUINOLINONES, V*

REACTION WITH DIMETHYL ACETYLENEDICARBOXYLATE
(SHORT COMMUNICATION)

László Hazai[1], Antal Schnitta[1], Gyula Deák[1]** and
József Tamás[2]

(*[1]Institute of Experimental Medicine, Hungarian Academy of Sciences,
H-1450 Budapest, P.O.B. 67, and [2]Central Research Institute for Chemistry,
Hungarian Academy of Sciences, H-1525 Budapest, P.O.B. 17)*

In earlier papers [1—4] we have reported the Diels-Alder reactions of
3(2H)-isoquinolinones with dienophiles in which the component effecting the
addition reaction contained a $C=C$ double bond. In the present paper investi-
gations are described in which dienophiles containing the $C\equiv C$ triple bond
were used; the best known and most widely employed representative of these
dienophiles is dimethyl acetylenedicarboxylate. Although in the analogous
reactions reported in the literature [5] (e.g., the reaction of 2-pyridone with
dimethyl acetylenedicarboxylate) primarily a Michael addition takes place in
similar compounds or, in the case of other derivatives, the occurrence of the
addition reaction can only be assumed by the presence of the decomposition
products of the adduct expected but not isolable even as an intermediary
product, in some cases, under mild conditions dimethyl acetylenedicarboxylate
(in the following, DMAD) can favourably be used as a dienophilic agent.

In the knowledge of these results, the reaction of 1-phenyl-4-methyl-
-3(2H)-isoquinolinone (**1**) and DMAD was examined at different temperatures
(Scheme 1). In benzene solution, no reaction took place either at room tem-
perature or at the boiling point; in xylene solution, after refluxing at 110 °C
for several hours, the product of Michael addition (**3**) was isolated from the
reaction mixture, instead of the adduct expected (**2**), after separating it from
several unidentifiable by-products; the formation of the Diels-Alder adduct
(**2**) could not be detected. The structure of **3** was confirmed by both the IR
(amide 1625 cm^{-1}, ester: 1725, 1270 and 1210 cm^{-1}) and the ^{1}H- and ^{13}C-NMR
spectra (see Experimental); however, a product with satisfactory analysis
could not be obtained; the substance could not be purified by the column
chromatographic technique, either. For this reason, **3** was identified in the

---

* Part IV: see Ref. [4]

** To whom correspondence should be addressed

3*

Acta Chim. Hung. 120, 1985
Akadémiai Kiadó, Budapest
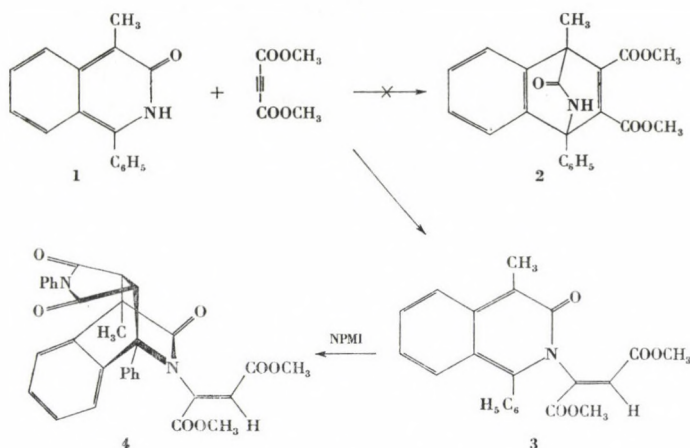
Scheme 1

form of its adduct with *N*-phenylmaleimide; **3** was refluxed with NPMI in xylene to obtain the adduct **4** with satisfactory analysis. Compound **4** was assumed to have the conformation shown in Scheme 1; the maleimide part has probably *endo* position (see Ref. [4]), and the geometry of the olefinic side-chain — on the basis of literature analogues [6] — is shown to be *E*. The NMR spectra, owing to the poor solubility of the compound, cannot be used for confirming the structure; therefore, in addition to the satisfactory elemental analysis data and the consistent IR spectrum, the structure of **4** was supported by its characteristic mass spectrum, which allowed to draw the following important conclusions:

(1) the mass number (m/z 550) of the molecular ion with low intensity corresponds to the molecular mass of the adduct expected;

(2) the mass spectrometric *retro*-synthetic reaction path could be observed: this is the formation of the m/z 377 and 173 ions. Their ratio was nearly constant in time, at the same time they correspond to the molecular ions of the starting compounds (*A* and *B*; see Experimental);

(3) the appearance of the ion with m/z 365 has an outstanding diagnostic value; this can be regarded as the product of the other possible RDA (*retro*-Diels-Alder) process occurring under electron bombardment; on the basis of its mass number, this ion can be formed by fission releasing the following $C_7H_7NO_5$ unit:

$$O{=}C{=}N{-}C{=}CH{-}COOCH_3$$
$$\overset{|}{C}OOCH_3$$
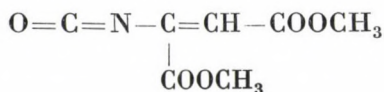
from the molecular ion, that is, the probable structure of the fragment ion is:

m/z 365
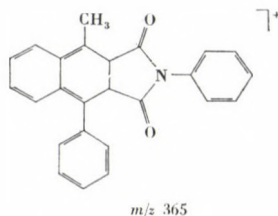
This latter mass spectrometric statement is all the more interesting and important here, since Acheson and Tasker [6] described a reaction accompanied by the loss of isocyanate in the reaction of 2-pyridones, without the isolation of the adduct (Scheme 2). The authors, although they failed in isolating dimethyl
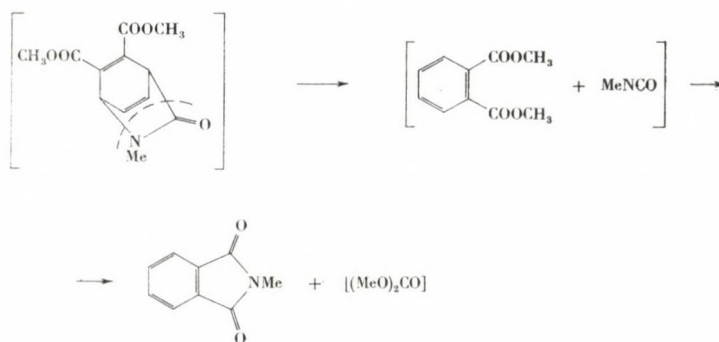
Scheme 2

carbonate, assumed completion of the adduct formation on the basis of N--methylphthalimide isolated.

The conversion of compound **3** into adduct **4** is an additional example that compounds, which can be hardly or not at all purified, may be identified by adduct formation in a Diels-Alder reaction.

Experimental

M.p.'s were measured with a Büchi—Tottoli melting point determining apparatus and are uncorrected. The IR spectra were recorded with a Perkin-Elmer 457 spectrophotometer in KBr pellets, the NMR spectra with WM-250 (^{1}H) and WP-80SY (^{13}C) Bruker instruments in CDCl$_3$ solution at 250 (^{1}H) and 20 MHz (^{13}C) in 5 mm tubes at room temperature, using the deuterium signal of the solvent as the lock and TMS as internal reference. The mass spectra were obtained with an AEI MS-902 type double focussing mass spectrometer; operating conditions: 70 eV, 8 kV, 100 μA, direct insertion with a temperature of the ion chamber of 200 °C.

Preparation of the Michael adduct and its reaction with NPMI

1-Phenyl-4-methyl-3(2H)-isoquinolinone [7] (1.177 g; 5 mmol) and DMAD (1.35 g; 9.5 mmol) were refluxed in xylene (60 mL) for 23 h. After evaporating the reaction mixture to dryness, the oil obtained was subjected to chromatographic separation on a column packed

with Al_2O_3 and, after combining the appropriate fractions, by evaporation of the solvent and rubbing the residual oil with ether, compound **3** (0,35 g; 18.5%) was obtained; m.p. 180—182 °C.

IR (KBr): $\nu C=O$ Amide 1625, ester bands 1730, 1270 and 1210 cm^{-1}.

^{1}H-NMR (ppm, $CDCl_3$): CCH_3 2.50 s (3H), OCH_3 3.63 and 3.83, $2 \times$ s (2×3H), $=CH$ 6.85, s (1H), ArH 6.80, t (7), 7.02, d (5), $\sim$7.3 m (3', 4', 5'), $\sim$7.45 (6, 2', 6'), 7.55 d (8).

^{13}C-NMR (ppm, $CDCl_3$): CCH_3 11.6, OCH_3 52.1, 53.3, $=CH$ 117.2, 117.9*, $=CHN$ 140.4, 140.9*, C-4a, 8a 121.8, 122.9, C-2',6' and C-3',5' 128.3, 128.6**, C-4,5,6,7,8,4' 126.8, 128.6**, 129.3, 129.9, 130.5, 131.0, C-1' 132.5, C-1 146.9, $C=O$ 160.0, 162.7, 163.0.

As the analysis of the product was not satisfactory, it was refluxed with NPMI (0.076 g; 0.44 mmol) in xylene (15 mL) for 12 h. The solid product was filtered off, washed with ether and dried to obtain **4** (0.1 g; 45.5%), m.p. 287—289 °C.

$C_{32}H_{26}N_2O_7$. Calcd. C 71.10; H 4.85; N 5.9. Found 71.04; H 4.93; N 5.10%.

IR (KBr): $\nu C=C$ 1640 cm^{-1}, $\nu C=O$ 1700, 1715, 1730, 1775 cm^{-1} (shoulders).

MS, m/z ($I\%$): 550 (1) M; 519 (5) M-OCH_3; 491 (5) M-$COOCH_3$; 377 (100) A; 365 (11); 363 (5); 349 (8); 318 (23) (377 $\underline{\quad \times \quad} COOCH_3$); 286 (4); 235 (6); 218 (30); 203 (6); 202 (6); 173 (10) B; 91 (5); 77 (4).

<div align="center">*</div>

REFERENCES

[1] Hazai, L., Deák, Gy., Tóth, G., Schnitta, A., Szőllősy, A., Tamás, J.: Acta Chim. Hung., **113**, 237 (1983)

[2] Hazai, L., Deák, Gy., Schnitta, A., Haskó-Breuer, J., Horváth, E.: Acta Chim. Hung., **116**, 303 (1984)

[3] Hazai, L., Schnitta, A., Deák, Gy., Tóth, G., Szőllősy, Á.: Acta Chim. Hung., **117**, 99 (1984)

[4] Tóth, G., Almásy, A., Hazai, L., Schnitta, A., Deák, Gy.: Can. J. Chem., **63**, 1001 (1985)

[5] Advances in Heterocyclic Chemistry (Eds A. R. Katritzky and A. J. Boulton), Vol. **23**, p. 265. Academic Press, New York—San Francisco—London 1978

[6] Acheson, R. M., Tasker, P. A.: J. Chem. Soc. (C), **1967**, 1542

[7] Hazai, L., Deák, Gy., Tóth, G., Volford, J., Tamás, J.: J. Heterocycl. Chem., **19**, 49 (1982)

---

* Double signal due to hindered rotation about the amide C—N bond
** Two overlapping lines

SYNTHESIS AND SPECTRAL STUDIES OF SOME
(E)-α-[(ARYL)SULFONYL]CHALCONES

Moole Venkataramana REDDY *and Sirigireddy REDDY

(Chemical Laboratories, KSRM College of Engineering, Cuddapah-516 003, A.P., India)

Fourteen new α-[(aryl)sulfonyl]chalcones have been prepared by condensing phenacyl-4-nitrophenacyl-aryl sulfones with aromatic aldehydes. The (E)-configuration for these compounds has been assigned on the basis of infrared and proton magnetic resonance spectral data.

Introduction

Active methylene compounds such as arylsulfonylacetic acids, benzyl-sulfonylacetic acids, ethyl phenylsulfonylacetate, phenacylphenyl sulfones condense [1—4] with aromatic aldehydes in the presence of catalytic amounts of ammonia or a primary amine in glacial acetic acid affording α, β-unsaturated sulfones. The condensation yields in each case exclusively a single geometrical isomer, presumably the (E)-isomer, which is the more stable one. In an attempt to prepare a series of new α-[(aryl)sulfonyl]chalcones, which are intermediates for the synthesis of 2-pyrazolines and cyclopropanes, the preparation of new phenacyl- and p-nitrophenacyl-arylsulfones seemed to be of interest to us.

Results and Discussion

New phenacyl- and 4-nitrophenacyl-aryl sulfones have been prepared in fairly high yields following the procedure of Tröger [5]. Fluorobenzene, bromobenzene, methoxybenzene have been converted into the appropriate p-substituted benzenesulfonyl chlorides by chlorosulfonylation [6]. The corresponding arylsulfinate [7] has been condensed with phenacyl or 4-nitrophenacyl bromide in ethanol to give phenacyl- and 4-nitrophenacyl-aryl sulfones.

The infrared spectra of these sulfones (1) have strong bands around 1680 cm^{-1} characteristic of the carbonyl stretching frequency. The characteristic absorptions of the sulfonyl groups at 1330—1300 and 1145—1120 cm^{-1} are also displayed by these sulfones. The NMR spectra show a singlet around 4.75 ppm due to the active methylene (CH$_2$) group.

A number of new α-[(aryl)sulfonyl]chalcones have been prepared by the condensation of phenacyl- and 4-nitrophenacyl-aryl sulfones with aromatic

* To whom correspondence should be addressed

Table I

Physical data of (E)-α-[(aryl)sulfonyl]chalcones, $Ar - \overset{\overset{\displaystyle O}{\|}}{C}(Ar'\ SO_2)C = CH - Ar''$

No.	Ar	Ar'	Ar''	Yield, %	M.p., °C	Found, %		Calcd., %	
						C	H	C	H
1	C_6H_5	C_6H_5	$4\text{-}FC_6H_4$	62a	142—143	68.54	4.21	68.83	4.12
2	C_6H_5	C_6H_5	$4\text{-}C_2H_5O, 3\text{-}CH_3OC_6H_3$	58b	162—163	68.03	5.17	68.22	5.24
3	$C_6H_5^+$	$4\text{-}FC_6H_4$	$4\text{-}FC_6H_4$	63a	125—126	65.48	3.62	65.61	3.67
4	C_6H_5	$4\text{-}FC_6H_4$	$2\text{-}ClC_6H_4$	69b	120—121	63.15	3.67	62.92	3.52
5	C_6H_5	$4\text{-}FC_6H_4$	$4\text{-}ClC_6H_4$	65a	128—129	63.07	3.70	62.92	3.52
6	C_6H_5	$4\text{-}BrC_6H_4$	$4\text{-}CH_3C_6H_4$	58a	109—110	59.62	3.68	59.87	3.88
7	C_6H_5	$4\text{-}BrC_6H_4$	$4\text{-}FC_6H_4$	56a	105—106	56.48	3.28	56.64	3.16
8	C_6H_5	$4\text{-}BrC_6H_4$	$2\text{-}ClC_6H_4$	68c	160—161	54.46	3.24	54.62	3.05
9	C_6H_5	$4\text{-}BrC_6H_4$	$2\text{-}NO_2C_6H_4$	72c	159—160	53.64	3.12	53.40	2.98
10	C_6H_5	$4\text{-}CH_3OC_6H_4$	$4\text{-}C_2H_5O, 3\text{-}CH_3OC_6H_3$	57a	130—131	66.58	5.17	66.30	5.34
11	C_6H_5	$4\text{-}CH_3OC_6H_4$	$4\text{-}ClC_6H_4$	61a	119—120	63.74	4.28	63.99	4.15
12	C_6H_5	$4\text{-}CH_3OC_6H_4$	$2\text{-}NO_2C_6H_4$	69c	135—136	62.17	4.22	62.40	4.04
13	$4\text{-}NO_2C_6H_4$	C_6H_5	$2\text{-}ClC_6H_4$	60a	141—142	59.16	3.38	58.95	3.29
14	$4\text{-}NO_2C_6H_4$	C_6H_5	$2\text{-}NO_2C_6H_4$	64c	200—201	57.28	3.34	57.52	3.21

+ Present Chem. Abstr. index name: (E)-2-[(4-Fluorophenyl)sulfonyl]-1-phenyl-3-(4-fluorophenyl)-2-propen-1-one. Products recrystallized from (a) ethanol (b) 2-propanol (c) glacial acetic acid

aldehydes in glacial acetic acid solution in the presence of catalytic amounts of benzylamine (Table I).

In α-[(aryl)sulfonyl]chalcones (2), the arylsulfonyl and benzoyl groups, which bear some structural resemblance to each other and which are both

$$Ar-\overset{\overset{O}{\|}}{C}-CH_2SO_2Ar' \;+\; Ar''-CHO \;\xrightarrow[\text{AcOH}]{C_6H_5CH_2NH_2}\; Ar-\overset{\overset{O}{\|}}{C}-\underset{\underset{CH-Ar''}{\|}}{C}-SO_2Ar'$$

<div align="center">1   2</div>
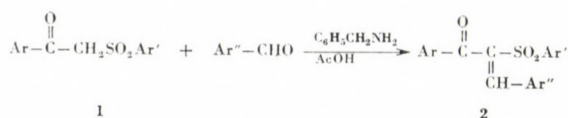
bulky, are cross-conjugated with the $-C{=}CHAr''$ group. It would be of interest to know which of them is in *(E)* and which is in *(Z)* position to the aryl group. Keeping this in view, a number of new α-[(aryl)sulfonyl]chalcones have been prepared to study their geometrical configuration.

The two isomeric forms possible for α-[(aryl)sulfonyl] chalcones are **3** and **4**. Since the chalcones are of the type $R^1R^2C{=}CHR^3$, their configurations

<div align="center">3   4</div>
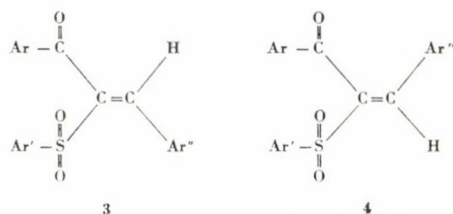
Table II

IR *and NMR spectra of (E)-α-[(aryl)sulfonyl]chalcones*

No.	IR, cm^{-1} (KBr)				NMR, δ ppm (CDCl$_3$)	
	νC=C out-of-plane	δCH	νC=O	νSO$_2$	δ(C=CH)	substituent in aromatic rings
1	1618	820	1654	1315, 1140	8.04	—
2	1612	800	1655	1310, 1140	8.02	4.04 (q) (CH$_2$CH$_3$), 3.50 (s) (OCH$_3$), 1.38 (t) (CH$_2$CH$_3$)
3	1620	805	1654	1320, 1145	8.06	—
4	1621	810	1655	1320, 1146	8.48	—
5	1616	814	1652	1318, 1142	8.05	—
6	1610	805	1650	1312, 1142	8.08	2.20 (s) (CH$_3$)
7	1618	812	1650	1315, 1140	8.05	—
8	1620	818	1650	1318, 1142	8.47	—
9	1618	815	1652	1315, 1140	8.57	—
10	1610	800	1650	1310, 1135	8.03	4.04 (q) (CH$_2$CH$_3$), 3.85 (s) (CH$_3$), 3.51 (s) (CH$_3$), 1.39 (t) (CH$_2$CH$_3$)
11	1615	810	1652	1320, 1145	8.02	3.85 (s) (CH$_3$)
12	1620	812	1654	1315, 1140	8.50	3.85 (s) (CH$_3$)
13	1618	818	1666	1318, 1144	8.55	—
14	1620	820	1664	1320, 1146	8.58	—

cannot be determined from the C—H stretching and deformation vibrations. However, a qualitative structural diagnosis is possible by examining the characteristic vibrational frequencies of the C=C and C=O bonds and the influence of substituents on them. The stretching vibrational frequencies of the C=C and C=O bonds in these compounds are given in Table II.

An examination of the infrared spectral data in Table II reveals that in α-[(aryl)sulfonyl]chalcones the substituents in the aromatic ring =CH—Ar″ do not have any significant effect on the frequency of the C=O stretching vibration. It may be noted that the carbonyl band appears almost at the same frequency (around 1650 cm^{-1}), whether the substituent is an electron-withdrawing group like —NO$_2$, or an electron-releasing group such as —CH$_3$ or —OCH$_3$. If the benzoyl group is situated *trans* to ring A as in the simple known chalcone 5, there will be conjugative interaction of the carbonyl and phenyl (ring A) groups through —CH=CH. In such a case a substituent in ring A will increase or decrease the carbonyl stretching frequency depending upon its ability to withdraw or release electrons. An electron-releasing group

5
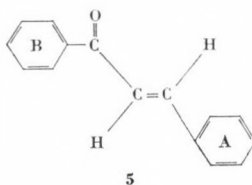
in the *para* position of ring A will lower the C=O stretching frequency due to the decreasing of the force constant of the carbon-oxygen bond; and an electron-attracting group in the *para* position will increase the carbonyl stretching frequency. The data in Table II thus indicate that there is no appreciable conjugative interaction between the *para*-substituted styryl group and the carbonyl group. A situation like this can arise on steric grounds if the benzoyl group is situated *cis* to the benzene ring carrying the substituent R (see 6). The increase in the carbonyl stretching frequency in compounds No. 13, 14 is due to the presence of the nitro substituent in *para* position of the benzoyl group.

The infrared spectra of these α[(aryl)sulfonyl]chalcones also exhibit strong bands in the region 815—800 cm^{-1} confirming that they are all tri-

6
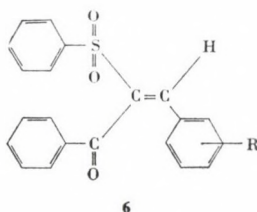
substituted ethylenic compounds [8]. The spectra also have strong bands in the region $1620-1610$ cm^{-1} [9] due to the C=C vibration and very strong peaks in the regions $1320-1310$ and $1146-1136$ cm^{-1}, characteristic of sulfonyl groups [10].

Proton magnetic resonance spectral data are considered to give most reliable physical evidence for the configurational assignment of (E) and (Z) isomers. However, application of NMR to α, β-unsaturated ketosulfones seems to be very limited. The NMR spectra of the α-[(aryl)sulfonyl]chalcones analyzed are presented in Table II. Since these compounds are trisubstituted ethylenes of the type C_6H_5C=CH. chemical shifts have been used to assign the geometrical configuration.

By applying the additive rule of Matter [11], the chemical shifts for the vinylic protons of (E)-α-[(aryl)sulfonyl] chalcones have been calculated. The calculated value for the vinylic proton is found to be 8.53 ppm and the observed values varied from 8.02 to 8.58 ppm for (E)-α-[(aryl)sulfonyl]chalcones. Further it is found that if the aromatic ring *gem* to the vinylic proton contains a nitro or a chloro group in the *ortho* position, the chemical shift for the vinylic proton appears around 8.50 ppm. This is in agreement with the value 8.49 ppm reported earlier [12] for the compound in which the vinylic hydrogen and aromatic ring are in *gem* position. Hence the method of preparation and also the infrared and proton magnetic resonance spectral data confirm that all the α-[(aryl)sulfonyl]chalcones investigated in this work are (E)isomers.

Experimental

All m.p.'s were determined on a Toshniwal apparatus and are uncorrected. IR spectra were obtained on a Perkin-Elmer 257 instrument in KBr pellets. NMR spectra were recorded in CDCl$_3$ using a Perkin-Elmer R-32 spectrometer (90 MHz) with TMS as internal standard.

Bromobenzene, fluorobenzene, anisole, acetophenone, 4-nitroacetophenone and the arylaldehydes were commercial products and purified when necessary.

The substituted benzenes were converted into the corresponding sulfonyl chlorides by chlorosulfonylation[6], and then into sodium arylsulfinates[7].

General procedure for the preparation of phenacyl-aryl sulfones (1)

To a solution of phenacyl bromide (α-bromoacetophenone) (0.05 mol) in ethanol (200 mL), the appropriate sodium arylsulfinate (0.05 mol) was added and the reaction mixture was refluxed for $6-8$ h. The product which separated on cooling was filtered off and washed several times with water to remove sodium bromide. The product was then recrystallized from ethanol. Phenacyl-phenyl sulfone, m.p. $90-91$ °C (*lit.* [3] m.p. $91-92$ °C); phenacyl-*p*--fluorophenyl sulfone, m.p. $148-149$ °C; phenacyl-*p*-bromophenyl sulfone, m.p. $121-122$ °C; phenacyl-*p*-methoxyphenyl sulfone, m.p. $104-105$ °C; *p*-nitrophenacyl-phenyl sulfone, m.p. $136-137$ °C).

General method for the synthesis of (E)-α-[(aryl)sulfonyl]chalcones (6)

A solution of phenacyl-aryl sulfone (0.01 mol) in acetic acid (10 mL) was mixed with an aryl aldehyde (0.01 mol) and benzylamine (0.5 mL), and refluxed for 3 h. The solution was cooled and ether (50 mL) was added. In some cases partial precipitation of the product occurred.

This was filtered off and the ethereal solution was washed successively with dilute hydrochloric acid, aqueous 10% NaOH, saturated $NaHSO_3$ solution and water. Evaporation of the dried ethereal layer gave usually a solid product. In some cases when the residue was a syrup, it was triturated with a little methanol, the resulting solid was filtered off and recrystallized from a suitable solvent. Relevant data of the compounds synthesized are given in Tables I and II.

*

REFERENCES

[1] Reddy, M. V. R., Reddy, S.: Synthesis, **1984,** 322 and preceding papers cited therein
[2] Reddy, M. V. R., Reddy, S.: Acta Chim. Hung., **115,** 269 (1984)
[3] Balasubramanian, M., Baliah, V.: J. Indian Chem. Soc., **32,** 493 (1955)
[4] Balasubramanian, M., Baliah, V.: J. Chem. Soc., **1954,** 1844
[5] Troger, J., Beck, W.: J. Prakt. Chem., **87,** 295 (1913)
[6] Huntress, E. H., Carten, F. H.: J. Am. Chem. Soc., **62,** 511 (1940)
[7] Fielf, L., Clark, R. D.: Organic Synthesis, Coll. Vol. **IV,** p. 674. John Wiley, New York 1963
[8] Rao, C. N. R.: Chemical Applications of Infrared Spectroscopy, p. 147. Academic Press, London 1963
[9] Colthup, N. B., Daly, L. H., Wiberely, S. E.: Introduction to Infrared and Raman Spectroscopy, p. 225. Academic Press, New York 1964
[10] Bellamy, L. J.: The Infrared Spectra of Complex Molecules, Methuen, London, 1959
[11] Matter, U. E., Pascual, C., Pretsch, E., Pross, A., Simon, W. J., Sternhell, S.: Tetrahedron, **25,** 691 (1969)
[12] Chamberlain, N. F.: The Practice of NMR Spectroscopy with Spectra-Structure Correlations for Hydrogen-1, p. 157. Plenum Press, New York, 1974

BIOLOGICALLY POTENT ANALOGUES OF PROSTACYCLIN, III

SYNTHESIS OF THE NITRILO-ANALOGUE OF 13-OXAPROSTACYCLIN*

Lajos Novák[1], Péter Kovács[1], János Rohály[1], István Stadler[3],
Péter Körmöczy[3] and Csaba Szántay[1,2]**

(*[1]Institute for Organic Chemistry, Technical University, H-1521 Budapest, Gellért tér 4,
[2] Central Research Institute for Chemistry, H-1525, Budapest, P.O.B. 17, and
[3] Chinoin Pharmaceutical and Chemical Works Ltd., H-1045 Budapest, Tó u. 1—5.*)

The synthesis and antiaggregant activity of the nitrilo analogue (5) of 13-oxa-prostacyclin are described. The synthetic sequence begins with the epoxy-alcohol 6 and proceeds via the 13-oxaprostaglanding $F_{2\alpha}$ and $F_{2\beta}$ derivatives (9 and 16). The oxaprostaglandin was converted into the azido derivative 19, which was cyclized to the desired imine 5. Compound 5 had lower biological activity than prostacyclin.

Prostacyclin (1), a recently discovered unstable metabolite of prosta-glandin-endoperoxide [2—4], has an important role in the inhibition of blood platelet aggregation and causes relaxation of arterial smooth muscle [5—10]. Prostacyclin can induce significant improvement in several vascular diseases, and is generally considered a potential antithrombotic agent. Unfortunately, the therapeutical utility of prostacyclin is severely limited by the great hydro-lytic lability of the molecule [11] and its fast metabolism [12—14]. Therefore various analogues of prostacyclin have been synthesized with the aim of developing chemically and metabolically stabilized analogues [6, 15—19].

In an effort to overcome the inherent metabolic instability problem of prostacyclin, we have recently synthesized a series of 13-thia- and 13-oxa-
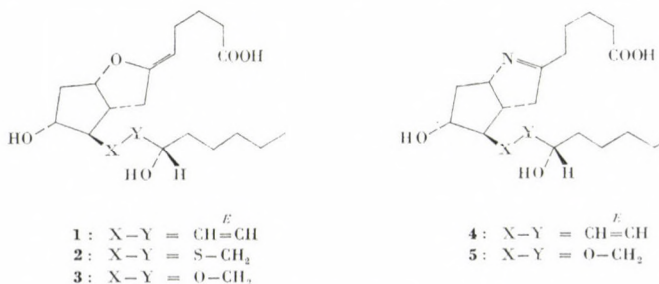
1 : X—Y = CH=CH
2 : X—Y = S—CH₂
3 : X—Y = O—CH₂

4 : X—Y = CH=CH
5 : X—Y = O—CH₂

prostacyclin derivatives (types 2 and 3) and evaluated them for in vitro anti-aggregant activity on human platelet-rich plasma [20—23]. Of all these new prostacyclin analogues, the most potent inhibitor of ADP-induced aggregation was 13,14-dihydro-13-oxaprostacyclin (3). Its sodium salt exhibited a tenfold weaker antiaggregant activity (IC_{50}: 0.02 μg/mL) than prostacyclin.

However, the 13-oxaprostacyclin (3) is also an unstable molecule; because of the presence of the labile enol-ether functional group, being susceptible to rapid hydrolysis and thus leading to inactivation, it had a half-life of about 5 min under physiological conditions.

An approach to stabilize chemically the prostacyclin nucleus is the substitution of the enol-ether function with an isosterical group. 9-Deoxy--9α,6-nitrilo-PGF$_1$ (4, nitrilo-prostacyclin) is one of the most stable prostacyclin analogues reported, possessing an antiplatelet activity comparable to that of prostacyclin [24, 25]. This result prompted us to synthesize the nitrilo analogue of 13-oxaprostacyclin (5).

The initial steps of the synthetic approach to the target compound 5 are outlined in Scheme 1. The optically active epoxy-alcohol (6), which can be synthesized stereoselectively from Corey's lactone [26], was converted into the corresponding mesylate (7) in the usual manner. Treatment of this mesylate with 2(S)-hydroxy-1-heptanol (8) [27] in the presence of a catalytic amount of $BF_3 \cdot Et_2O$ resulted in a mixture of three compounds. Separation of this mixture by repeated column chromatography afforded the desired 9-O--mesylate of 13-oxaprostaglandin F$_{2\alpha}$ (9), its positional isomer (10), and the 11-O-mesylate of 13-oxaprostaglandin F$_{2\alpha}$ (11) (ratio of 9 : 10 : 11, ca. 3 : 6 : 1)*. Compound 11 was formed by the migration of the mesyl group in 9, probably through a cyclic intermediate (12).

A variety of procedures were investigated for the inversion of configuration at position C-9 from S into R. This was necessary, because in the second part of the synthesis we planned to introduce an azido group by an S_N-2--reaction, which would inverse the configuration (Scheme 2).

Reaction of the mesylate 9 with tetrabutylammonium acetate in boiling acetone readily furnished the 9-O-acetate of the prostaglandin F$_{2\beta}$ derivative (13). Unfortunately, this acetate was not reactive enough; it was recovered virtually unchanged after exposure to sodium azide.

Reaction of the mesylate 9 with tetrabutylammonium chloride afforded a mixture of the 9-epimeric chloro compounds (14 and 9-epi-14) in a ratio of ca. 3 : 1, probably due to the partial S_N1 character of this displacement reaction.

---

* The structural assignments for isomers 9, 10 and 11 are supported by standard spectral methods (see Experimental). Further, from the ring opening reaction of epoxycyclopentanol the more polar compound proved to be the 13-oxyprostaglandin derivative and the less polar major compound had the position-isomeric structure [23].

The reaction with potassium superoxide gave a better result. In this approach the mesylate **9** was protected by reaction with dihydropyran and phosphoryl chloride, and the resulting 11,15-bis(tetrahydropyranyl ether) of **9** was treated with potassium superoxide in dimethyl sulfoxide and 1,2-

6 : R = H
7 : R = Ms

8

9

10

12

11
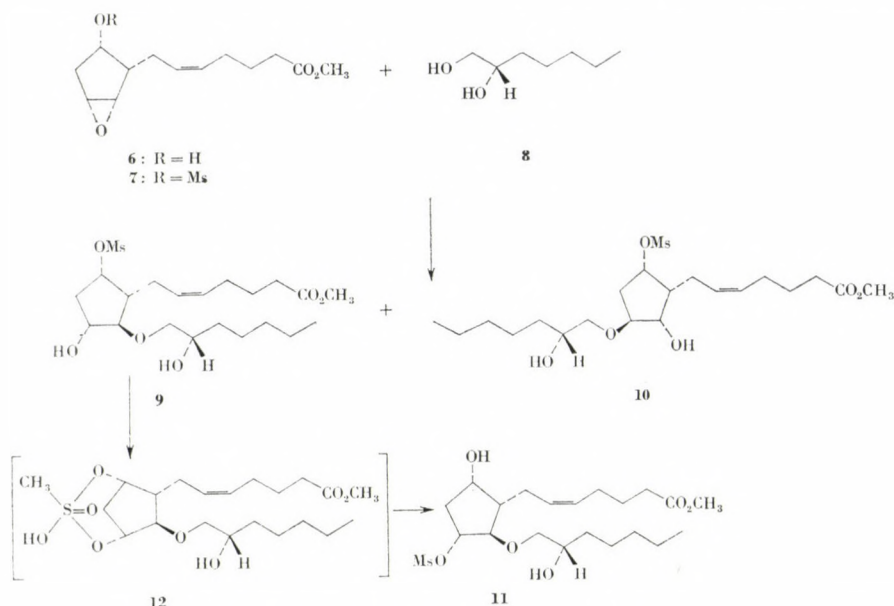
Scheme 1. Synthesis of 13-oxaprostaglandin

	X	R
13 :	OAc	H
14 :	Cl	H
15 :	I	H
16 :	OH	THP
17 :	OTs	THP

18 :   R = THP
19 :   R = H

20 :   R = THP
21 :   R = H
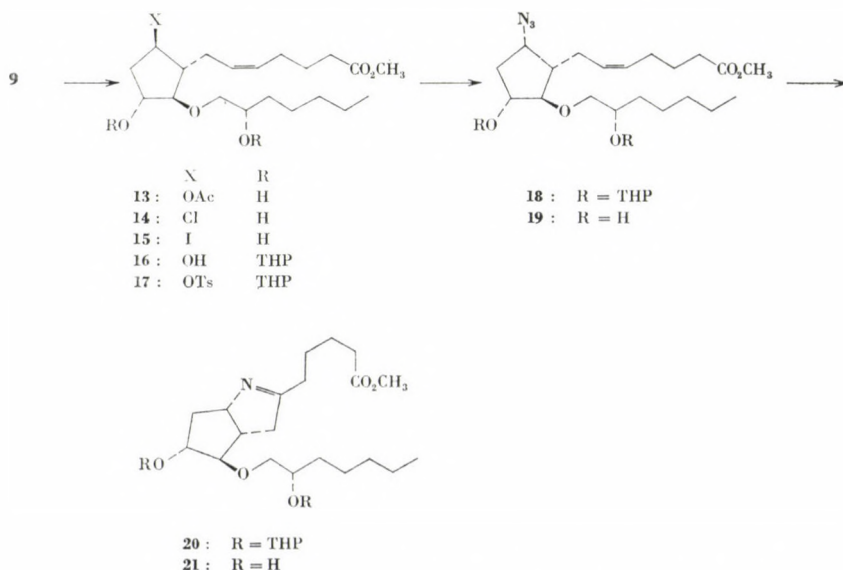
Scheme 2. Synthesis of the nitrile analogue of 13-oxaprostacyclin

·dimethoxyethane containing dicyclohexyl-18-crown-6. The reaction proceeded satisfactorily, yet the desired product (16) was obtained in only a modest yield (48%).

In the next step of Scheme 2, the prostaglandin $F_{2\beta}$ derivative 16 was converted into the corresponding tosylate (17) by reaction with tosyl chloride in pyridine, and then this tosylate was made to react with sodium azide in hexamethylphosphoramide. The azide 18 obtained was subjected to thermal cyclization and the resulting imine 20 was converted into the methyl ester of the target compound 21 by deprotection. The sodium salt of 5 was prepared by base-catalyzed hydrolysis of the methyl ester 21.

Finally, the required inversion of configuration at C-9 in 9 was accomplished without the protection of the hydroxyl groups. To do this, we allowed the mesylate 9 to react with tetrabutylammonium iodide. The stereochemically pure iodo compound 15 was immediately converted into the azide 19 by reaction with freshly prepared silver azide in methylene chloride. Thermolysis of this azide furnished the desired nitrilo-prostacyclin analogue (21).

As expected, the nitrilo analogue of 13-oxaprostacyclin was quite stable even in a pH 1 solution at room temperature for several hours and it formed a hygroscopic hydrochloride salt.

The nitrilo analogues of 13-oxaprostacyclin was evaluated for inhibition of ADP-induced aggregation of rabbit platelet-rich plasma using the procedure of Born [28]. Contrary to expectations, the sodium salt of 5 had only weak inhibitory activity. The ID_{50} value was $4 \cdot 10^3$ times higher than that of prostacyclin. It did not show blood pressure lowering activity in cat, in the $0.001-1$ mg/kg concentration range.

Experimental

IR spectra were obtained with a Spectromom 2000 spectrometer. ^{1}H-NMR spectra were recorded at 100 MHz using a JEOL FX-100 FT instrument. All signals are expressed in ppm downfield from Me$_4$Si ($\delta = 0.0$) used as internal standard. The following abbreviations are used: singlet (s), doublet (d), triplet (t), quartet (q), multiplet center (mc), broad (br). Mass spectra were determined on a JEOL-20K and JMS-01SG-2 combined GC/MS system: ionizing energy 74 eV, acc. voltage 10 kV, ionizing current 200 μA. The spectroscopic data for all new compounds were consistent with the assigned structures.

Homogeneity of the products was determined by ascending thin-layer chromatography (TLC) on precoated sheets (silica gel 60 F 254 Merck). Column chromatography was carried out on 40—63 nm silica gel at 2—3 bar pressure; eluant flow rate 5—10 mL/min. All reactions were made in purified solvents. The solvents were dried by storage over molecular sieves (type 4 Å), with the exception of methanol, which was stored over type 3 Å molecular sieves. Organic extracts were always dried over MgSO$_4$ before filtration and evaporation in vacuum.

(—)-Methyl [7-(5-hydroxy-2,3-α-epoxycyclopentyl)]heptanoate 5'-mesylate (7)

To a cooled (—10 °C) and stirred mixture of 4.0 g (17 mmol) of (—)-methyl [7(5--hydroxy-2,3α-epoxycyclopentenyl)]-heptanoate (6) and 6.72 g (66 mmol) of triethylamine in 50 mL of dry methylene chloride there was added dropwise 5.72 g (50 mmol) of methanesul-

fonyl chloride, and the resulting mixture was stirred at -10 °C for 2 h. The reaction mixture was poured into ice-water (150 mL) and the layers were separated. The aqueous phase was extracted twice with methylene chloride (100 mL each), and the combined organic layers were washed with 5% HCl and with H_2O, and then dried over $MgSO_4$. After filtration and concentration, the crude product (5.3 g) was purified by column chromatography to afford 4.88 g (92%) of 7; TLC (hexane-acetone, 3 : 2) Rf 0.6.

IR (liquid film): 1730 (CO), 1460, 1360, 1340, 1220, 1165, 1040, 1010, 970, 920 cm^{-1}.

^{1}H-NMR(CDCl$_3$): δ 2.25 (11H, mc, 5CH$_2$, CH), 2.88 (3H, s, CH$_3$—SO$_2$), 3.32 (2H, mc, 2CH—O), 3.58 (3H, s, OCH$_3$), 4.95 (1H, m, CH—O), 5.42 (2H, m, CH=CH).

MS m/e (relative intensity): 318 ($<$1) [M^+], 288 (1) [M-CH$_3$OH], 222 (5), 204 (6), 191 (11), 173 (6), 162 (7), 148 (11), 140 (100), 135 (12), 130 (20), 98 (19), 91 (26), 80 (55), 67 (33), 55 (17).

13,14-Dihydro-13-oxaprostaglandin-$F_{2\alpha}$ 9-mesylate methyl ester (9)

To a stirred solution of 3.75 g (12 mmol) of 7 in 10 mL of dry ether was added 1.8 g (13.6 mmol) of 2(S)-hydroxy-1-heptanol (8). The mixture was cooled in an ice-bath to 5 °C and treated portionwise during 1 min with 1 mL of BF$_3$ · Et$_2$O. The reaction mixture was allowed to warm to room temperature over 6 h. The solvent was evaporated under reduced pressure, the residue dissolved in methylene chloride, and then filtered through a short column. Concentration in vacuum gave a mixture of three compounds; separation was effected by column chromatography to give products 9 (faster moving, 0.85 g; 17.2%), 11 (0.27 g; 5.5%), and 10 (slower moving, 1.68 g; 34%).

9: TLC (CHCl$_3$-acetone, 7 : 3) R_f 0.31.

IR (liquid film): 3350 (OH), 1730 (CO), 1460, 1430, 1380, 1360, 1345, 1250, 1170, 1130, 1090, 1060, 980, 910 cm^{-1}.

^{1}H-NMR (CDCl$_3$): δ 0.89 (3H, t, J = 7 Hz, CH$_3$), 1.3 (8H, bs, 4CH$_2$), 1.6—2.1 (4H, m, 2CH$_2$), 2.15—2.5 (7H, m, 3CH$_2$, CH), 2.98 (3H, s, CH$_3$SO$_2$), 3.3—4.0 (3H, m, OCH$_2$, O—CH), 3.68 (3H, s, OCH$_3$), 4.12 (2H, m, 2 O—CH), 4.95 (1H, m, O—CH), 5.45 (2H, m, CH=CH).

MS m/e (relative intensity): 450 ($<$1) [M^+], 354 (2) [M-CH$_3$SO$_3$H], 336 (5) [M-H$_2$O—CH$_3$SO$_3$H], 222 (13), 191 (13), 162 (4), 149 (7), 148 (6), 143 (19), 135 (9), 101 (26), 96 (32), 83 (56), 79 (31), 67 (18), 55 (100), 44 (36), 42 (48).

10: TLC (CHCl$_3$-acetone, 7 : 3) R_f 0.39.

IR (liquid film): 3400 (OH), 1735 (CO), 1455, 1380, 1360, 1340, 1250, 1185, 1115, 1100, 1050, 985, 910 cm^{-1}.

^{1}H-NMR (CDCl$_3$): δ 0.89 (3H, t, J = 7 Hz, CH$_3$), 1.3 (8H, bs, 4CH$_2$), 1.55—2.0 (4H, m, 2CH$_2$), 2.1—2.55 (7H, m, 3CH$_2$, CH), 3.02 (3H, s, CH$_3$SO$_2$), 3.3 (2H, mc, O—CH$_2$), 3.55 (1H, m, O—CH), 3.66 (3H, s, OCH$_3$), 4.1 (2H, mc, 2 O—CH), 4.9 (1H, m, O—CH), 5.4 (2H, CH=CH).

MS m/e (relative intensity): 450 ($<$1) [M^+], 354 (2) [M-CH$_3$SO$_3$H], 336 (12) [M-H$_2$O—CH$_3$SO$_3$H], 222 (18), 204 (11), 195 (18), 191 (10), 173 (5), 162 (5), 149 (8), 148 (9), 143 (7), 135 (10), 101 (35), 96 (26), 83 (62), 79 (22), 67 (19), 55 (100), 44 (28), 42 (54).

11: TLC (CHCl$_3$-acetone, 7 : 3) R_f 0.33.

IR (liquid film): 3340 (OH), 1725 (CO), 1460, 1440, 1380, 1365, 1345, 1250, 1180, 1120, 1090, 1040, 980, 910 cm^{-1}.

^{1}H-NMR (CDCl$_3$): δ 0.89 (3H, t, J = 7 Hz, CH$_3$), 1.3 (8H, bs, 4CH$_2$), 1.5—2.0 (4H, m, 2CH$_2$), 2.2—2.5 (7H, m, 3CH$_2$, CH), 2.99 (3H, s, CH$_3$SO$_2$), 3.3 (2H, m, O—CH$_2$), 3.67 (3H, s, OCH$_3$), 3.8—4.15 (3H, 3 O—CH), 4.8 (1H, m, O—CH), 5.45 (2H, m, CH=CH).

MS m/e (relative intensity): 450 ($<$1) [M^+], 354 (4) [M-CH$_3$SO$_3$H], 336 (7) [M-H$_2$O—CH$_3$SO$_3$H], 222 (11), 204 (5), 191 (11), 173 (5), 162 (5), 149 (9), 148 (7), 143 (21), 135 (7), 101 (26), 96 (30), 83 (59), 79 (35), 67 (14), 55 (100), 43 (36), 42 (48).

13,14-Dihydro-13-oxaprostaglandin-$F_{2\beta}$ 9-acetate methyl ester (13)

To a stirred solution of 9 (0.25 g; 0.55 mmol) in dry acetone (10 mL) was added tetra-butylammonium acetate (0.66 g, 2.2 mmol), and the resulting solution was refluxed for 20 h. The solvent was evaporated and the residue dissolved in ether. The ethereal solution was washed with brine, dried, and then concentrated. The oily residue was purified by column chromatography to give 13 (0.16 g; 70%), TLC (CHCl$_3$-acetone, 7 : 3) R_f 0.75.

IR (liquid film): 3300 (OH), 1730 (CO), 1460, 1445, 1360, 1240, 1165, 1105, 1080, 1040 cm^{-1}.

4

^{1}H-NMR (CCl$_4$): δ 0.85 (3H, t, $J = 6$ Hz, CH$_3$), 1.1—2.5 (19H, m, 9CH$_2$, CH), 2.0 (3H, s, CH$_3$CO), 3.5 (5H, m, CH$_2$—O, 3 CH—O), 3.6 (3H, s, OCH$_3$), 4.65 (1H, m, CH—O), 5.4 (2H, mc, CH=CH).

9β-Chloro-9-deoxy-13,14-dihydro-13-oxaprostaglandin-F_2 methyl ester (14) and 9α-chloro-9-deoxy-13,14-dihydro-13-oxaprostaglandin-F_2 methyl ester (9-epi-14)

To a stirred solution of 9 (0.5 g; 1.1 mmol) in dry acetone (15 mL) was added tetra-butylammonium chloride (1.2 g; 4.4 mmol) and the resulting mixture was refluxed for 24 h. After evaporation in vacuum, the residue was taken up in ether, filtered, and the solvent was evaporated under reduced pressure. The residue was purified by column chromatography to yield a mixture of 14 and its epimer (0.32 g; 75%); TLC (CHCl$_3$-acetone, 7 : 3) R_f 0.83 and 0.79.

IR (liquid film): 3350 (OH), 1730 (CO), 1460, 1440, 1380, 1360, 1245, 1100, 1040 cm^{-1}.

MS m/e (relative intensity): 392 (3) and 390 (6) [M^+], 361 (3), 359 (8) [M-OCH$_3$], 354 (10) [M-HCl], 336 (10) [M-HCl—H$_2$O], 305 (5), 261 (9), 259 (24), 223 (33), 205 (35), 191 (45), 188 (62), 157 (22), 140 (29), 55 (100).

13,14-Dihydro-13-oxaprostaglandin-$F_{2\alpha}$ 9-mesylate methyl ester 11,15-bis(tetrahydropyran-2-yl ether)

To a stirred mixture of 1.32 g (2.9 mmol) of 9 and 0.97 g (12 mmol) of dihydropyran in 30 mL of dry benzene was added 5 drops of phosphoryl chloride, and the resulting mixture was stirred at room temperature for 2 h. Triethylamine was added to neutralize the mixture, then it was poured into brine (30 mL). The layers were separated, and the aqueous phase extracted with benzene (3 × 20 mL). The combined organic layers were washed with brine, dried over MgSO$_4$, and concentrated. The residue was chromatographed to give 1.65 g (91%) of the 11,15-bis(tetrahydropyran-2-yl ether) of 9; TLC (benzene-acetone, 10 : 1) R_f 0.3.

IR (liquid film): 1740 (CO), 1460, 1440, 1380, 1360, 1320, 1280, 1260, 1200, 1120, 1080, 1040 cm^{-1}.

^{1}H-NMR (CCl$_4$): δ 0.88 (3H, t $J = 6$ Hz, CH$_3$), 1.0—2.4 (31H, m, 15CH$_2$, CH), 2.98 (3H, s, CH$_3$—SO$_2$), 3.3—4.15 (8H, m, 3CH$_2$—O, 2-CH—O), 4.65 (2H, m, 2 O—CH—O), 5.03 (1H, m, CH—O), 5.44 (2H, m, CH=CH).

13,14-Dihydro-13-oxaprostaglandin-$F_{2\beta}$ methyl ester 11,15-bis(tetrahydropyran-2-yl ether) (16)

A cooled (0 °C) mixture of 11,15-bis(tetrahydropyran-2-yl) ether of 9 (0.3 g; 0.5 mmol) and 18-Crown-6 (0.54 g; 1.4 mmol) in dimethyl sulfoxide and 1,2-dimethoxyethane (4 mL each) was mixed with potassium superoxide (0.27 g, 3.8 mmol), and the resulting solution was stirred at room temperature for 4 h. The reaction mixture was poured into ice-water (15 mL), acidified with 5% HCl, and then the organic layer was separated. The aqueous portion was extracted with there portions of ether (20 mL each). The combined organic extracts were dried over MgSO$_4$ and evaporated. The oily residue was treated with ethereal diazomethane solution, and then purified by column chromatography to afford 0.12 g (48%) of 16; TLC (hexane-acetone, 7 : 3) R_f 0.75.

IR (liquid film): 3400 (OH), 1735 (CO), 1460, 1450, 1380, 1360, 1305, 1250, 1200, 1140, 1080, 1030, 960 cm^{-1}.

MS m/e (relative intensity): 540 (<1) [M^+], 455 (6) [M-THP], 438 (7) [M-HOTHP]. 356 (31), 354 (29), 338 (30), 283 (53), 239 (44), 222 (68), 185 (25), 143 (66), 140 (50), 99 (100).

13,14-Dihydro-13-oxaprostaglandin-$F_{2\beta}$ methyl ester 9-tosylate 11,15-bis(tetrahydropyran-2-yl ether) (17)

To a stirred solution of 16 (0.47 g; 0.85 mmol) in dry pyridine (10 mL) was added p--toluenesulfonyl chloride (0.34 g; 1.8 mmol) and the resulting solution was stirred at room temperature for 2 h. The reaction mixture was poured into ice-water (30 mL) and the layers were separated. The aqueous phase was extracted with three portions of benzene (20 mL each), and the combined organic layers were washed with H$_2$O, brine, dried (MgSO$_4$), and

concentrated. The oily residue was purified by column chromatography to give 0.32 g (53%) of **17**; TLC (benzene-EtOAc 6 : 4) R_f 0.9.

IR (liquid film): 1735 (CO), 1600, 1460, 1450, 1380, 1360, 1275, 1250, 1170, 1120, 1080, 1030, 970 cm^{-1}.

MS m/e (relative intensity): 577 (1), 279 (18), 155 (11), 149 (100), 97 (21), 91 (35), 85 (33), 78 (51), 69 (34), 57 (69), 55 (49).

9-Azido-9-deoxy-13,14-dihydro-13-oxaprostaglandin-$F_{2\alpha}$ methyl ester 11,15-bis(tetrahydropyran-2-yl) ether) (18)

To a stirred solution of 0.49 g (0.7 mmol) of **17** in 15 mL of hexamethylphosphoramide was added 0.06 g (0.85 mmol) of sodium azide, and the resulting solution was stirred at 40 °C for 24 h. The reaction mixture was poured into ice-water (20 mL), the organic layer was separated and the aqueous phase extracted with ether (3 × 30 mL). The combined organic extracts were dried (MgSO$_4$), filtered, and concentrated under reduced pressure. The residue was chromatographed to give **18** (0.17 g; 42%); TLC (hexane-acetone, 7 : 3) R_f 0.8.

IR (liquid film): 2180 (N$_3$), 1740 (CO), 1460, 1380, 1360, 1270, 1255, 1190, 1120, 1080, 1030, 980 cm^{-1}.

^{1}H-NMR (CDCl$_3$): δ 0.88 (3H, t, $J = 6$ Hz, CH$_3$), 1.0—2.6 (31H, m, 15CH$_2$, CH), 3.5 (9H, mc, 3CH$_2$O, 3CH—O), 3.65 (3H, s, OCH$_3$), 4.25 (1H, m, CH—N$_3$), 4.75 (2H, m, O—CH—O) 5.4 (2H, m, CH=CH).

9-Deoxy-9α,6-nitrilo-13,14-dihydro-13-oxaprostaglandin-$F_{1\alpha}$ 11,15-bis(tetryhydropyran-2-yl ether) (20)

Compound **18** (0.24 g; 0.42 mmol) was dissolved in 10 mL of 1,2-dimethoxyethane and the solution was refluxed for 24 h. The solvent was evaporated under reduced pressure and the residue purified by column chromatography to yield **20** (0.11 g; 50%); TLC (hexane-acetone, 7 : 3), R_f 0.2.

IR (liquid film): 1735 (CO), 1635 (C=N), 1460, 1435, 1380, 1350, 1250, 1195, 1110, 1070, 1020, 985, 900 cm^{-1}.

MS m/e (relative intensity): 537 (4) [M^+], 506 (4) [M-OCH$_3$], 452 (3), 437 (21), 422 (20), 368 (36), 352 (14), 338 (16), 254 (42), 238 (32), 222 (20), 85 (100), 58 (18).

9β-Iodo-9-deoxy-13,14-dihydro-13-oxaprostaglandin-$F_{2\alpha}$ methyl ester (15)

To a stirred solution of **9** (0.5 g; 1.1 mmol) in dry acetone (15 mL) was added tetrabutyl-ammonium iodide (1.62 g; 4.4 mmol) and the solution was refluxed for 16 h. After evaporation of the solvent in vacuum the oily residue was taken up in ether, filtered, and evaporated. The residue was purified by column chromatography to yield **15** (0.42 g; 80%); TLC (CHCl$_3$-acetone, 7 : 3) R_f 0.8.

IR (liquid film): 3300 (OH), 1730 (CO), 1460, 1440, 1380, 1360, 1245, 1180, 1100, 1040, 960 cm^{-1}.

^{1}H-NMR (CDCl$_3$): δ 0.88 (3H, t, $J = 6$ Hz, CH$_3$), 1.3 (8H, bs, 4CH$_2$), 1.6—2.0 (4H, m, 2CH$_2$), 2.1—2.55 (7H, m, 3CH$_2$, CH), 3.5 (4H, mc, CH$_2$—O, CH—O, CH—I), 3.68 (3H, s, OCH$_3$), 4.15 (2H, mc, 2CH—O), 5.45 (2H, m, CH=CH).

MS m/e (relative intensity): 482 (<1) [M^+], 354 (4) [M-HI], 336 (13) [M-HI—H$_2$O], 305 (6) [M-HI—H$_2$O—OCH$_3$], 223 (23), 222 (40), 191 (28), 173 (10), 135 (37), 83 (51), 55 (100).

9-Azido-9-deoxy-13,14-dihydro-13-oxaprostaglandin-$F_{2\alpha}$ methyl ester (19)

To a stirred solution of silver nitrate (0.5 g; 2.9 mmol) in H$_2$O (10 mL) was added a solution of sodium azide (0.2 g; 3 mmol). The resulting suspension was filtered and the solid residue successively washed with H$_2$O, EtOH, ether and methylene chloride (20 mL each), and then covered with methylene chloride (10 mL). To this stirred suspension was added a solution of **15** (0.42 g; 0.9 mmol) in methylene chloride (2 mL) and the resulting mixture was refluxed for 24 h, under argon. After cooling, the precipitate was filtered off and the solvent evaporated in vacuum. The oily residue was purified by column chromatography to afford **19** (0.3 g; 88%); TLC (CHCl$_3$-acetone, 7 : 3) R_f 0.78.

IR (liquid film): 3340 (OH), 2180 (N$_3$), 1730 (CO), 1640 (C=C), 1460, 1445, 1380, 1360, 1250, 1190, 1180, 1110, 1060 cm^{-1}.

MS m/e (relative intensity): 397 ($<$1) [M^+], 354 (2) [M-HN$_3$], 336 (10) [M-NH$_3$—H$_2$O], 305 (3), 223 (18), 222 (23), 205 (9), 191 (23), 173 (11), 135 (25), 67 (37), 55 (100).

9-Deoxy 9α,6-nitrilo-13,14-dihydro-13-oxaprostaglandin-$F_{1\alpha}$ methyl ester (21)

Method A: Compound **19** (0.5 g; 0.95 mmol) was dissolved in 20 mL of dry 1,2-dimethoxy-ethane and the resulting solution was refluxed for 24 h. The solvent was evaporated under reduced pressure and the residue purified by column chromatography to give **21** (0.24 g; 56%); TLC (benzene-CH$_3$OH, 5 : 1) R_f 0.65.

IR (liquid film): 3320 (OH), 1735 (CO), 1640 (C=N), 1460, 1380, 1360, 1250, 1220, 1160, 1080, 1060 cm^{-1}.

^{1}H-NMR (CCl$_4$): δ 0.9 (3H, t, J = 6 Hz, CH$_3$), 1.3 (6H, mc, 3CH$_2$), 1.55 (6H, mc, 3CH$_2$), 1.95—2.6 (9H, m, 4CH$_2$, CH), 3.4 (4H, mc, CH$_2$—O, CH—O, CH—N), 3.6 (3H, s, OCH$_3$), 4.2 (2H, mc, 2CH—O).

MS m/e (relative intensity): 369 ($<$1) [M^+], 320 (3) [M-H$_2$O—OCH$_3$], 239 (6), 221 (5), 220 (9), 208 (11), 191 (10), 184 (8), 143 (16), 142 (56), 101 (18), 97 (22), 83 (44), 69 (13), 57 (44), 55 (100).

Method B: To a cooled (0 °C) solution of **20** (0.22 g; 0.42 mmol) in dry methanol (5 mL) was added saturated methanolic HCl solution (1 mL) and the resulting mixture was allowed to warm to room temperature (3 h) The solvent was then evaporated under reduced pressure and the oily residue treated with dry ether to give the hydrochloride of **21** (hygroscopic semi-solid; 0.17 g; 85%).

IR (KBr). 3250 (b, OH), 1730 (CO), 1670 (C=$\overset{+}{N}$H), 1460, 1435, 1380, 1360, 1320, 1240, 1190, 1160, 1080, 960 cm^{-1}.

9-Deoxy-9α,6-nitrilo-13,14-dihydro-13-oxaprostaglandin-F$_{1\alpha}$ (5) sodium salt

A solution of **21** (0.41 mmol) in 1 mL of MeOH was mixed with 6 mL of 0.1 N NaOH and the resulting mixture was stirred at room temperature for 24 h. MeOH was removed in vacuum and the solution diluted to 20 mL with H$_2$O. Samples containing 1.0 mg of the sodium salt of **5** were prepared by lyophilizing 0.1 mL aliquots of the above solution.

<center>*</center>

REFERENCES

[1] Part II of this series: Novák, L., Aszódi, J., Kolonits, P., Szabó, É., Stadler, I., Simoni-desz, V., Szántay, Cs.: Acta Chim. Hung., **113**, 355 (1983)
[2] Moncada, S., Gryglewski, R., Bunting, S., Vane, J. R.: Nature, **263,** 663 (1976)
[3] Gryglewski, R., Bunting, S., Moncada, S., Flower, R. J., Vane, J. R.: Prostaglandins, **12**, 685 (1976)
[4] Johnson, R. A., Morton, D. R., Kinner, J. H., Gorman, R. R., McGuire, J. C., Sun, F. F., Whittaker, W., Bunting, S., Salmon, J., Moncada, S., Vane, J. R.: Prostaglandins, **12,** 915 (1976)
[5] Moncada, S., Higgs, E. A., Vane, J. R.: Lancet, **1**, 18 (1977)
[6] Nicolaou, K. C., Gasic, G. P., Barnette, W. E.: Angew. Chem., Int. Ed. Engl., **17**, 293 (1978)
[7] Whittle, B. J. R., Boughton-Smith, N. K., Moncada, S., Vane, J. R.: Prostaglandins, **15**, 955 (1978)
[8] Moncada, S., Vane, J. R.: in Prostacyclin, pp. 5—16. (Eds J. R. Vane and S. Bergstrom), Raven Press, New York 1979
[9] Moncada, S., Vane, J. R.: in Advances in Prostaglandin and Thromboxane Research, Vol. **7**, pp. 43—60. (Eds B. Samuelsson, P. W., Ramwell, and R. Paoletti), Raven Press, New York 1980
[10] Moncada, S., Vane, J. R.: Philos Trans. R. Soc. London, **294**, 305 (1981)

[11] Chiang, Y., Kresge, A. J., Cho, M. J.: J. Chem. Soc. Chem. Commun., **1979,** 129, and references cited therein
[12] Sun, F. F., Taylor, B. M.: Biochemistry, **17,** 4096 (1978)
[13] McGuire, J. C., Sun, F. F.: Arch. Biochem. Biophys., **189,** 92 (1978)
[14] Sun, F. F., Taylor, B. M.: Prostaglandins, **21,** 307 (1981)
[15] Bartmann, W., Beck, G., Knolle, J., Rupp, H.: Angew. Chem., **92,** 850 (1980)
[16] Skuballa, W., Vorbrüggen, H.: Angew. Chem., Int. Ed. Engl., **20,** 1046 (1981), and references cited therein
[17] Bartmann, W., Beck, G.: Angew. Chem., Int. Ed. Engl., **21,** 751 (1982), and references cited therein
[18] Flohé, L., Böhlke, H., Frankus, E., Kim, S.-M. A., Lintz, W., Loschen, G., Michel, G., Müller, B., Schneider, J., Seipp, U., Vollenberg, W., Wilsmann, K.: Arzneim.-Forsch. (Drug Res.), **33,** (II), 1240 (1983)
[19] Shibasaki, M., Torisawa, J., Ikegami, Sh.: Tetrahedron Lett., **1983,** 3493
[20] Novák, L., Aszódi, J., Szántay, Cs.: Tetrahedron Lett., **1982,** 2135
[21] Novák, L., Aszódi, J., Stadler, I., Simonidesz, V., Szántay, Cs.: in Advances in Prostaglandin, Thromboxane, and Leukotriene Research, Vol. **11,** pp. 275—280 (Eds B. Samuelsson, R. Paoletti, and P. Ramwell), Raven Press, New York 1983
[22] Novák, L., Aszódi, J., Rohály, J., Stadler, I., Körmöczy, P., Simonidesz, V., Szántay, Cs.: Acta Chim. Hung., **113,** 111 (1983)
[23] Novák, L. Aszódi, J., Kolonits, P., Szabó, É. Stadler, I., Simonidesz, V., Szántay, Cs.: Acta Chim. Hung., **113,** 355 (1983)
[24] Bundy, G. L., Baldwin, J. M.: Tetrahedron Lett., **1978,** 1371
[25] Lock, J. E., Coceani, F., Hamilton, F., Greenaway-Coates, A., Olley, P.: J. Pharmacol. Exp. Ther., **215,** 156 (1980)
[26] Novák, L., Rohály, J., Kajtár, M., Szántay, Cs.: Acta Chim. Acad. Sci. Hung., **102,** 91 (1979)
[27] Novák, L., Aszódi, J., Kolonits, P., Kajtár, M., Szántay, Cs.: Tetrahedron, **38,** 153 (1982)
[28] Born, G. V. R.: Nature, **194,** 927 (1962)

EVALUATION OF APPLICABILITY OF AAS 1 N ATOMIC ABSORPTION SPECTROMETER, FLAPHO 4 FLAME PHOTOMETER, P 100 AUTOMATIC SAMPLE CHANGER AND K 201 RECORDER OF VEB CARL ZEISS JENA FOR FLAME DISCRETE NEBULIZATION*

Henryk Matusiewicz

(Technical University of Poznań, Department of Analytical Chemistry, 60-965 Poznań, Poland)

In this paper the flame discrete sample nebulization, a procedure for sample introduction in flame emission and atomic absorption spectrometry is examined using the VEB Carl Zeiss Jena commercial apparatus. The delivery of small volumes of solution, 100 μL may be accomplished manually with modified Teflon microsampling cup, or automatically by a suitable sample changing system. The parameters pertinent to the operation of this commercial system, including injected volume, damping, carry-over, length of plastic tubing, type of burner head are considered, and the optimal operating conditions were established. The utility of the method and apparatus is demonstrated by the direct determination of copper, iron and zinc in rock salt and brine.

Introduction

The ability to perform trace level metal analysis on small volumes of solution, especially in the geochemical, biological and clinical field, has grown increasingly important in recent years. The possibility of working in flame photometry with small amounts of sample was first demonstrated in 1963 when Lang and Hermann [1] were able to reduce the volume needed to as low as 10 μL by using a direct nebulizer-flame assembly and an oscilloscope. In 1973, Sebastiani, Ohls and Riemer [2] described a method wherein they introduced a defined volume of solution 50—200 μL into the nebulizer of an atomic absorption instrument using a microliter pipet.

In conventional atomic absorption (AAS) or emission spectrometry (AES) the sample is continuously aspirated into the flame, and the reading is taken when a signal plateau is reached. Sample material is aspirated continuously so that typically between 0.5 and 2 mL of sample solution is consumed. In comparison, less than one tenth of this volume is needed for the discrete

---

* Presented at the VIth Polish Spectroanalytical Conference, Białowieża, 25—29 May, 1981, Poland.

sample nebulization. The prime advantage of this technique lies in the ex-
tremely small sample quantity required, typically $\sim 50-100 \ \mu L$, it also allows
the nebulization of solutions with a very high dissolved solids content through
the burner-nebulizer without clogging, or of organic solvents which may not
normally be regarded as suitable for flame spectrometry. Finally, the tech-
nique has the potential for extremely rapid sample throughout, and the presence
of substantially fewer interferences.

One disadvantage of this technique is that because the sample is added
as a short burst over a fraction of a second, the precision with the technique
is not as high as with the regular macrosampling technique. Another disadvan-
tage is that the short time given to the detector-recorder system to respond
to the signal may necessitate the use of a special recorder or peak recording
device to measure the response. Finally, this method involves a micropipetting
step that is generally not required in standard aspiration.

In view of the above statements, it seemed worth-while to evaluate the
applicability of the discrete nebulization AAS and AES using particular
instruments made by Carl Zeiss Jena, as well as parameters pertinent to the
design and operation of such system: sample size, damping, carryover, and
reproducibility for a fixed set of conditions. One other observation which
might be take into account is that theoretically, this technique should be
adaptable to different models and makes of instruments, but this has not
always proven to be the case. Thus this method can not be considered routine,
as documented by Cresser [3], who reviewed discrete sample nebulization in
atomic spectroscopy. The application of this approach in an emission and
absorption measurement have been described recently [4—8]. An improved
Teflon cup [9] for microsampling technique is presented which facilitates
sample changing. In addition, an automatic sampler the Carl Zeiss Jena P 100
has been adapted to automate the discrete nebulization for use in flame AAS
or AES. This is an important accessory for trace metal determinations in a
large number of applications, for example in the clinical and biochemical
sectors. Finally, the sequential determination of trace metals such as copper,
iron and zinc in 10% solution of rock salt and brine provides an illustration
of how this microvolume sampling technique can be used by using equipment
made by VEB Carl Zeiss Jena, DDR.

Preliminary studies

Instrumentation

The basic instruments used were a classical single beam atomic absorp-
tion spectrometer Carl Zeiss Jena AAS 1 N and a filter flame photometer
FLAPHO 4 connected to a fast-response strip chart potentiometric recorder

K 201 with a time constant of 0.04 sec/cm. Normal hollow cathode lamps of the same manufacture and flame atomization were used for atomic absorption and flame emission analyses, respectively. Lamp currents and slit widths were as recommended by the manufacture. The standard burner heads were used. Optimum gas flow rates and burner positions were determined while aspirating continuously standard solutions of the given elements. The peak heights were measured as signals proportional to the concentration. Recorder paper speed was also adjusted to achieve the best sharp profile peak. The P 100 automatic sample changer was adapted for automated discrete nebulization. When using the AAS 1 N or FLAPHO 4 in conjunction with the P 100 in this technique, the latter has to be equipped with the holder gib for 1.5 mL plastic sample tubes.

Sample introduction system

The manual dipping technique was used for the flame discrete nebulization. The sample introduction system is schematically shown in Figures and Photographs [9]. A drop of sample solution was transferred with a micropipette into a newly designed Teflon sampling cup. The cup was one of a series of small holes with one center bigger hole, made by drilling the plane surface of a Teflon rod. The capillary tube was removed from the blank solution, placed quickly on the sample drop until the latter had completely disappeared from the cup; the capillary tube was then immediately returned to the blank solution. Transfer of the capillary tube between the blank and micro-volume of sample solutions must be very quick, because the blank solution must be continuously nebulized between nebulization of the sample solution to prevent blockage of the nebulizer-burner system. It is important to inject reproducibly the sample drop into nebulizer of the apparatus. The yielded transient signals are transient peaks. Peak heights are measured.

Sampling device for the Teflon microsampling cup

Analysis using the discrete nebulization technique which can be carried out manually by dipping a capillary tube into a small hole in the surface of a Teflon rod, depends on the transfer of the sample drop into the nebulizer of the spectrometer. This is accomplished by using one of a variety of sampling devices such as micropipettes, dispensers or syringes. The analyst should evaluate as many different types of these devices as he can; techniques vary from operator to operator and are related to different aspects. Consequently, reproducibility is significantly dependent upon the sample introduction technique. In spite of that the following have been evaluated: ultramicro dispenser with Eppendorf tip, Hamilton syringe without disposable tip, Finnpette

device, and glass micropipette. In all cases the injected volume was 100 μL. The reproducibility of the signals for FLAPHO 4 and AAS 1 N in emission and absorption modes, respectively, was measured by using 25 replicate 1 ppm Ca standard water solution. The relative standard deviation of each series was calculated from the peak height of the emission or absorption signals. The best precision was obtained by using a glass micropipette giving a reproducibility of 1.4—1.5%.

Determination of optimum conditions

Before a discrete nebulization can be used for practical analysis and for a particular instrument a number of parameters must be investigated. For convenience, experiments designed to determine the optimum conditions are discussed individually below.

Effect of injection volume

In flame AAS or AES 0.5 to 2.0 mL of sample solution is generally used for the determination of a single element. A recorded signal, such as that shown in Fig. 1A, is obtained. When a high chart speed is used for the recording of these signals, a preliminary investigation clearly indicated that after a solution consumption of only approximately 100 μL for AAS 1 N and 150 μL for FLAPHO 4 the almost final height, that is, a stationary signal is achieved
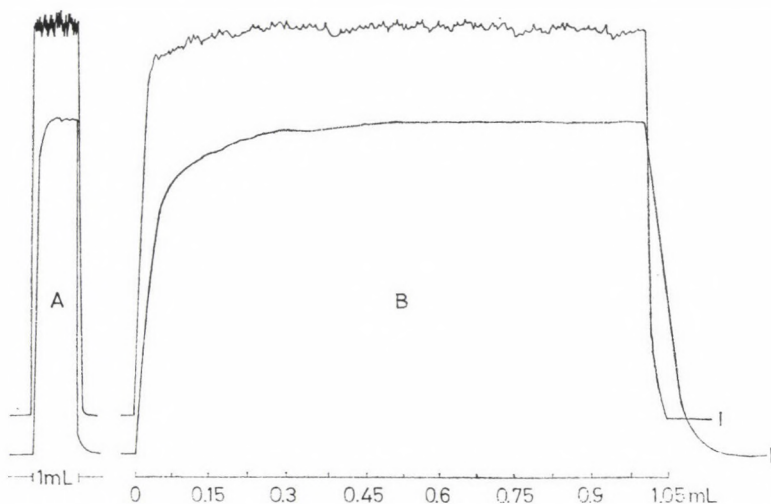

Fig. 1. Recorder tracings obtained aspirating 1 mL of sample into air-C_2H_2 flame, 1 ppm Ca by AAS 1N (curve 1), and 1 ppm Na by FLAPHO 4 (curve II). A: chart speed 1 min/cm, B: same signal expanded using a chart speed of 5 s/cm
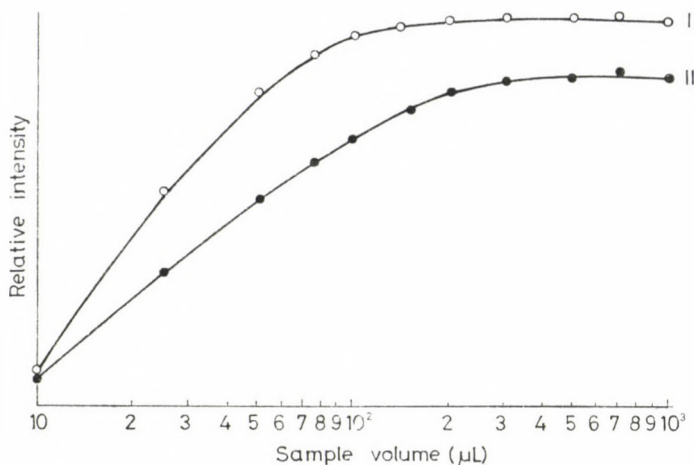
Fig. 2. Effect of injected sample volume on absorption signal for 1 ppm Ca (curve I), and on emission intensity for 1 ppm Na (curve II), demonstrating that absorption and emission intensity reaches a plateau at approximately 100 μL and 150 μL, respectively

This amount of liquid is sufficient to utilize fully the concentration sensitivity of flame AAS or AES.

The influence of the volume of the injected sample on the absorption or emission intensity was determined. Such an effect can be seen in Fig. 2 where several volumes 10—1000 μL of 1 ppm Ca or 1 ppm Na standard water solution were injected into the flame through standard nebulizers. Increasing the amount of sample increases the absorption or emission intensity until a plateau at approximately 100 μL or 150 μL is reached; additional sample merely results in the peak becoming wider. This means that samples 100 μL (e.g. of 1 ppm Ca) or 150 μL (e.g. of 1 ppm Na) give approximately the same concentration sensitivity achieved with larger samples (e.g. 1 mL) for AAS or AES. The absolute sensitivity (weight basis) is however about 10 times improved for a 100 μL sample. Aliquots of 100 μL of 1 ppm Ca and 150 μL of 1 ppm Na, respectively, produced transient absorption or emission signals equivalent to about 95% or 90% of the corresponding value attained using continuous nebulization of larger sample volumes. Based on the evidence here, a 100 μL or 150 μL sample size, respectively is used for further discussion. These results for the manual discrete nebulization technique are in good agreement with atomic absorption results described elsewhere [2, 10—12].

Effect of damping

Berndt and Jackwerth [10] showed that the reduction in signal caused by discrete sample nebulization, in contrast to continuous nebulization, could be explained in part at least, in terms of instrument response time. The sensitivity

of determination drops rapidly with increasing damping. Figure 3 shows the record of the Mg signals with different damping settings of the instrument AAS 1 N used. At a nebulization rate of 4 mL/min ($\sim$67 μL/sec) for example, a 100 μL sample is nebulized in 300 msec. With a detector/recorder time constant of 500 msec (the lowest setting of the AAS 1 N instrument) instrument response time might be expected to be the limiting factor. However, the time taken for the sample to pass through the flame, after dilution with the N_2O- $-C_2H_2$ flame mixture, might be well above 300 msec, making the 500 msec time constant less significant. If, on the other hand, a 100 μL pulse is nebulized more slowly over 400 msec (e.g. at 3 mL/min for more viscous solutions), damping effect would be less pronounced.

The results do show a reduction of discrete nebulization signal compared to continuous nebulization. However, this could be explained using the theory that the sample does not remain in the flame long enough in order to have the amplifier of this particular instruments gain a representative quick and full signal. This is caused by the fact that the amplifier has a minimum damping that is contained within the instruments. This did not present a problem since all results would be correct if the conditions of the instruments remained the same. The damping of AA instrument must be at the lowest setting since the impulse signals rapidly become smaller with increased time constant and for AAS 1 N this response time should be about 0.1 sec.

The determination using FLAPHO 4 can be done only with one selectable time constant 1.0 sec.

Carryover

The great source of error in a flame discrete nebulization with a dipping technique is carryover (memory effect). Carryover is the residue present in the capillary tubing and in the nebulizer/burner system from the previous sample. Carryover has its greatest effect when changing from a concentrated solution to a dilute solution. It is also dependent on the nebulizer uptake, the sample volume injected, and is markedly reduced by an intermediate rinse. Carryover can easily be determined for a particular solution as shown in Fig. 4A, which is an example of carryover test for Na aqueous solution. Contamination rates were measured amounting up to about 21% of the last signal. Carryover is greatest at low uptake rates because the aspirating air through the capillary is not as effective in flushing as it at higher rates. Moreover, at higher uptake rates more sample is aspirated into the flame thus reducing the effect of the quantity present in the capillary. This observation is well documented in the next Figure 4B (contamination rate about 7%). An intermediate rinse between sample can reduce carryover by a factor of 3—5. Ideally, a rinse should consist of the solution being determined. This reduces carryover
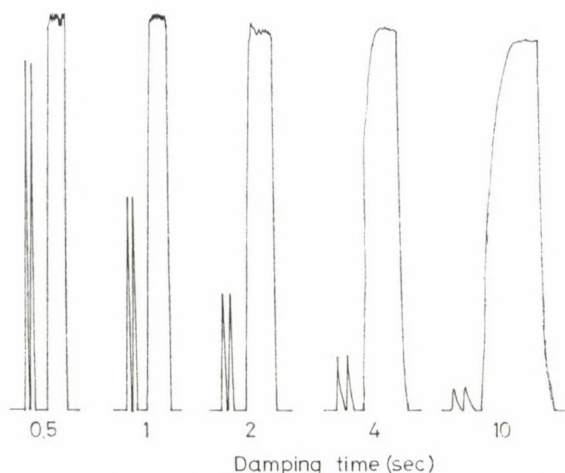
Fig. 3. Effect of damping time on absorption signal for 2 ppm Mg for 100 μL aliquots and for continuous nebulization ($\sim$1 mL), for AAS 1 N as recorded on a K 201 recorder
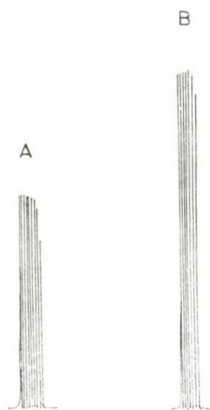

Fig. 4. Carryover test, 1 ppm Na aqueous solution, sample volume 150 μL, A: carryover — 21.2%, nebulizer aspiration rate — 2.7 mL/min (FLAPHO 4), B: carryover — 6.7% nebulizer aspiration rate — 4.0 mL/min (AAS 1 N)

to a minimum as the residue is matched to that of sample. However, a rinse with the sample is not always possible (e.g. high solids or biological fluids) and a distilled water or solvent rinse may be required. A specially designed Teflon sampling cup [9] with possibility for an intermediate very convenient rinse between samples well met this above mentioned requirements.

It should be noted, that the baseline drift in both cases was not observed.

Effect of length of plastic tubing

The peak height would be expected to vary according to the length of plastic tubing. The length of plastic tubing (i.d. 0.9 mm) from the sample
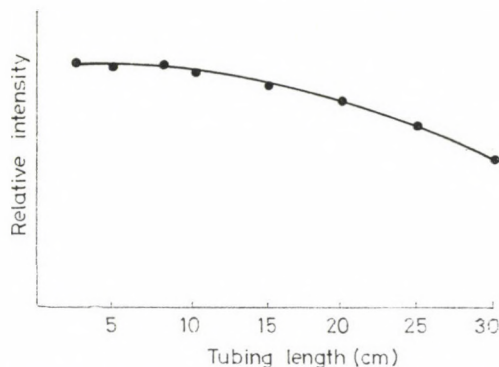
Fig. 5. Effect of the tubing length on the peak height for 100 μL injected volume. Concentration — 2 ppm Zn (AAS 1 N)

drop to the needle of the nebulizer of AAS 1 N was varied. As shown in Fig. 5, in the case of water solution, variation of the length of tubing between 3 and 30 cm did effect the peak height in a small degree only. The peak heights were unchanged up to 8 cm; the subsequent decrease with longer tubing was due to introduce dilution. Small sample size solutions were introducing by plastic tubing of 6 cm for both instruments.

Type of burner head

By direct comparison using a 5 cm one-slot burner for a nitrous oxide-acetylene flame, a 5 cm three-slot burner for an air-acetylene flame, and one other conventional emission-type burner, giving cylindrical flame shape (Meker burner, 58 holes) line-emission/absorption intensities were found to be directly proportional to flame length. Multipass optical systems (3 times in the case of AAS 1 N) were also shown to effect emission and absorption in the same way.

It appears that the 5 cm one-slot burner provides nearly optimum sensitivity and versatility in most flame emission and absorption work. As was expected, self-absorption in the long flame in discrete nebulization is not a serious problem. To analyse solutions at higher concentrations, which would show strong self-absorption and pronounced flattening of the calibration curves, it is a simple matter to turn the burner head crosswise to the optical path, just as recommended for reducing sensitivity in classical continuous nebulization atomic absorption [13] or emission [14] spectrometry.

Automated discrete nebulization technique

Automation is desirable in AAS or AES primarily because it reduces operator time and improves precision in analytical chemistry. The first automated discrete nebulization for dispensing small volume samples in flame

AAS was introduced in 1976 by Berndt and Jackwerth [15]. The Carl Zeiss Jena P 100 automatic samples accessory was adapted to automate the discrete nebulization method for use in flame AAS and AES.

The dipping technique of the flame discrete nebulization utilizing the Carl Zeiss Jena P 100 automatic samples was used equipped with an AAS 1 N and K 201. The P 100 must be equipped with polyethylene sample vessels 1.5 mL capacity and the holder gibs for these cups especially constructed by this same firm. The peak heights were measured as signals proportional to the concentration. Determinations were made with the fastest damping (damping factor 0.5 sec) and with an initial sample flush and a dip of 2 sec (the lowest possible adjusted cycling time on time unit 3 in P 100 which corresponds to a sample volume of about 100 μL with nebulizer uptake rate of 3 mL/min for air-acetylene flame, and 134 μL with nebulizer uptake rate of 4 mL/min for nitrous oxide-acetylene flame. After each sample insertion a distilled water rinse, which eliminates the effects of carryover, with simultaneous automatic zero setting was employed. The method and the AAS and AES instrument parameters are identical for both manual and automated injections.

By comparing the RSD, results obtained using manual dipping technique were compared to those obtained using the P 100. A 100 μL aliquots of the sample solution were injected manually 25 times using a microliter glass pipette and also automatically by the P 100 (100 μL for nebulizer uptake
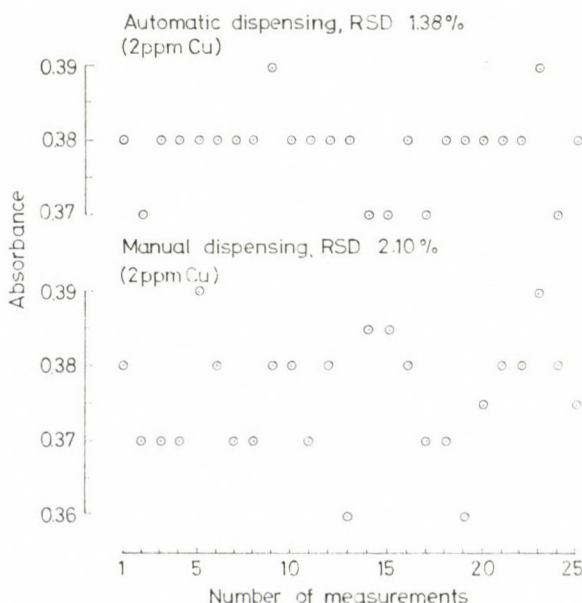

Fig. 6. A comparison of automatic and manual sample injection for 100 μL

rate of 3 mL/min). The RSD of each series was calculated from the peak heights of the AA signals. Results are illustrated in Fig. 6. The length of a complete measuring cycle is 9 sec. Although in some cases the same RSD are found by manual as well as by mechanical sample injection, the superiority of the auto sampler can be sometimes confirmed.

Analytical application

The determination of traces such as Cu, Fe and Zn in 10% solution of rock salt and brine was used an example of a high dissolved solids sample solution and provides an illustration of how this discrete nebulization technique, using equipment of Carl Zeiss Jena, can be used.

Preliminary studies were performed using a 100 μL aliquots of 5% (w/v) solutions. However, subsequent work showed that there were no burner clogging problem with 100 μL aliquots of 10% solution of salts if rinse of distilled water is carried out between each sample. Furthermore, the latter were utilized in all further work. When continuous aspiration of this solution was attempted, the nebulizer become clogged within a few minutes. Each sample was run twice and the average peak was compared with the calibration curves to give the concentration of Cu, Fe and Zn. The metals matched working standards were prepared in the 10% NaCl solution (Merck, Suprapur). To guarantee the accuracy of the results of the analysis, then, a separate calibration using the addition methods must be carried out for each sample type, so that rapid, on-the-spot microstandard additions were made directly in the Teflon microsampling cone by using a procedure described elsewhere [11].

Table I

Analytical results of trace elements in 10% *(w/v) rock salt and brine**

Element	Sample 1		Sample 2		Sample 3		Sample 4		Sample 5	
	A	B	A	B	A	B	A	B	A	B
Cu	150	120	120	100	2.0	2.7	9.2	10.9	130	100
Fe	830	701	720	805	81	71	421	411	202	221
Zn	130	151	80	70	15	12	290	300	110	105

* Concentration expressed as ng of metals per gram of salt and based on a single analysis average of two determinations
    A: Discrete nebulization, 100 μL
    B: Hanging mercury drop electrodeposition-emission spectrographic technique [18]
    Sample 1: Wieliczka salt mine, Poland
    Sample 2: Kłodawa salt mine, Poland
    Sample 3: Inowrocław salt mine, Poland
    Sample 4: Karlowe Vary salt, Czechoslovakia
    Sample 5: Ciechocinek brine, Poland

This technique was applied to the analysis of the samples listed in Table I. The analytical results for samples obtained by the discrete nebulization and by the another method [16] are in good agreement. The precision of this method was measured in the present studies for atomic absorption (2 ppm Cu, Fe, Zn) to be about 4% RSD at a 100 μL sample volume.

Conclusions

The work described above clearly shows that a conventional Carl Zeiss Jena nebulizer in conjunction with a typical burner heads and spectrometric equipment has an important place in multielement trace analysis on microliter samples. Evidence is available that the type of nebulizer described here. together with the suggested method of sample transfer, is applicable to conventional Carl Zeiss atomic absorption and flame photometer equipment.

There is not significant difference in accuracy and precision between nebulization of small volumes and continuous nebulization, and the discrete nebulization is a complement to, rather than a replacement for, any present sampling method.

REFERENCES

[1] Lang, W., Hermann, R.: Mikrochim. Acta, **1963,** 872
[2] Sebastiani, E., Ohls, K., Riemer, G.: Fresenius Z. Anal. Chem., **264,** 105 (1973)
[3] Cresser, M. S.: Prog. Anal. Atom. Spectrosc., **4,** 219 (1981)
[4] Matusiewicz, H.: Anal. Chim. Acta, **136,** 215 (1982)
[5] Boyko, W. J., Keliher, P. N.: Can. J. Spectrosc., **27,** 51 (1982)
[6] Sobel, C. B.: Appl. Spectrosc., **38,** 444 (1984)
[7] Robertson, F. A., Edwards, A. C., Cresser, M. S.: Analyst, **109,** 1265 (1984)
[8] Brown, A. A., Taylor, A.: Analyst, **109,** 1455 (1984)
[9] Matusiewicz, H.: Intern. Lab. **13,** 24 (1983)
[10] Berndt, H., Jackwerth, E.: Spectrochim. Acta, **30B,** 169 (1975)
[11] Fry, R. C. Nortway, S. J., Denton, M. B.: Anal. Chem. **50,** 1719 (1978)
[12] Kojima J., Iida, C.: Analyst, **107,** 1000 (1982)
[13] Epstein, M. S., Winefordner, J. D.: Talanta, **27,** 177 (1980)
[14] Pickett, E. E., Koirtyohann, S. R.: Anal. Chem., **41,** 28A (1969)
[15] Berndt, H.; Jackwerth, E.: At. Absorpt. Newsl., **15,** 109 (1976)
[16] Matusiewicz, H.: Analyst (in press)

BOOK REVIEWS

Holló, J. (ed.): *Food Industries and the Environment*

International Symposium,Budapest, Hungary 9—11 September, 1982. Akadémiai Kiadó, Budapest, 1984. 565 p.

This book, a joint edition with Elsevier Science Publishers as the 9th volume of the series Developments in Food Science, contains the papers on the international symposium held in Budapest, dealing with environmental protection problems in the food industries:
— water pollution
— air pollution (dust, stench)
— soil pollution
— energy
— wastes
— microbiology and hygiene
— vibration
— noise.

The symposium was organized by CIIA (Commission Internationale des Industries Agricoles et Alimentaires), by the Hungarian Scientific Society for Food Industry and by the Committee of Chemical Technology of the Hungarian Academy of Sciences.

The volume contains the three plenary lectures delivered by Holló, Kovács and Nay Khtun, the closing address held by Dardenne, and 64 papers grouped as follows:
1. General topics, 14 papers
2. Canning industry, 7 papers
3. Dairy industry, 8 papers
4. Meat industry, 18 papers
5. Other industrial branches, 7 papers
6. Noise — stench, 6 papers

The papers dealt with environmental pollution problems of the food industries (meat, dairy, canning, sugar, starch, spirits, beer, bakery, fodder). Development of low-waste technologies and application of membrane filtration in the food industries were subjects particularly emphasized.

The major part of the papers was directed towards the solution of waste-water problems. Numerous novel processes were treated: physico-chemical methods, flotation using chemicals, electroflocculation processes ultilizing activated biological sludge, aerobic and anaerobic fermentation processes. Utilization of material recovered from waste-water was also discussed wastes as a possible source of energy (anaerobic fermentation to methane). One paper deals with the utilization of waste-water for irrigation purposes.

The volume presents a list of the authors' addresses. A subject index facilitates finding literature references.

The book is of interest to governmental libraries, libraries of Academic and industrial research institutions; engineers engaged in the food industries; chemists working in laboratories of foodstuff research, or responsible for environmental protection.

Péter Biacs

Central Food Research Institute,
Budapest

5*

Acta Chim. Hung. 120, 1985
Akadémiai Kiadó, Budapest

E. Upor, M. Mohai, Gy. Novák: *Photometric Methods in Inorganic Trace Analysis*

Akadémiai Kiadó, Budapest 1985

The English, revised version of the book appeared as joint edition published by Akadémiai Kiadó, The Publishing House of the Hungarian Academy of Sciences, Budapest, Hungary and Elsevier Science Publishers B. V., Amsterdam, The Netherlands. At the same time, the Elsevier's edition of this monograph is the 20th Volume in the series of "Comprehensive Analytical Chemistry" and connects with Volume XIX, in which the theoretical and general aspects of spectrometry were described.

The first part of the book reviews the main steps in the photometric methods. Chapter 1 deals (rather shortly) with the position and further possibilities of photometric methods in trace analysis. The next four chapters summarize the most important problems influencing the choice and result of individual analyses, as the planning, elaboration and control of analytical methods; methods suitable for separation of interferences, and concentration possibilities (including precipitation, ion-exchange, extraction and distillation or electrochemical methods); preparation of samples for analysis (including sampling, storage of samples, sample processing and phase analysis); and the error sources influencing the accuracy of determination. All chapters have their separate references.

It follows that the main Chapter of the monograph is the 6th one, entitled "Determination of the individual elements" (more than 200 pages of a total of 403), starting from its first subtitle: "Alkali metals" to the 44th one: "Zirconium". Of course, the volumes of these parts are different depending on the importance and usual concentration of given element(s) or even on the difficulties of its determination.

The general structure of discussion is as follows:

(i) A brief account is given of the analytical (complex chemical) properties of the ions of the element in question;

(ii) When a fair number of well-proved reagents are known for the determination, their fundamental properties are tabulated;

(iii) If one reagent is outstandingly applicable for the determination in the authors' experience, procedures based on other reagents are not given;

(iv) An attempt is made to mention the variants suitable for analysis of the most important types of samples;

(v) A detailed description is given primarily of those determinations that have been elaborated in the authors' laboratory or in the application of which they have had experience;

(vi) If the element in question can be determined advantageously by some other method too, this is referred to.

The book is complete with a subject index and an Appendix, summarizing in alphabetical order the common names, structural formules and chemical names of the most important (organic) reagents referring to the elements to be determined.

The practical usefulness is the main point of the monograph, based first of all upon the experiences, which have been gained by the authors' well-known research in this area: in developing and improving methods for the determination of trace elements in ores, rocks and other natural materials. The large number of analytical procedures cover more than 44 elements and illustrate basic theoretical points.

The book, as invaluable practical guide may be recommended to research and analytical chemists and advanced students alike.

Lajos Barcza

Institute of Inorganic and
Analytical Chemistry,
Eötvös Loránd University, Budapest

P. W. J. M. Boumans: *Line Coincidence Tables for Inductively Coupled Plasma Atomic Emission Spectrometry*

2nd Edition, Pergamon Press, Oxford, 1984,
Volumes **1** and **2**: 929 pages

The second edition of Boumans' Line Coincidence Tables for inductively coupled plasma atomic emission spectrometry (ICP-AES) followed the first edition after four years, which reflects both the importance and the success of the work. Indeed, the development of the ICP-AES methods requires knowledge of spectral interferences, in particular line coincidences. Clearly, ICP-AES methods are ever more applied in analytical chemistry.

It is interesting to compare atomic absorption and atomic emission spectroscopic (AAS and AES) methods from the point of view of interference effects. The interference effects relevant to both AAS and AES are classified into two groups: "spectral interferences" and "non-spectral interferences". Considering the problem of line interferences one can conclude that AAS methods generally have an advantage over AES methods. This stems from the fact that in AAS only the coincidence of the resonance lines within the spectral window can cause analytical errors, which happens in a few cases (about 30 line overlaps are known). On the other hand, in AES coincidences with any lines can occur and may result in analytical error if disregarded. The number of coincidences is rather large in the often line-rich atomic and ionic spectra emitted by the ICP.

It has been documented that the ICP-AES methods have an advantage over the AAS methods as to non-spectral interferences. This manifests in the reduced level of volatilization and ionization interferences, well-known in flame AAS, and of gas phase dissociation interferences often found in graphite furnace AAS. In addition, the capability of multi-element analysis, the higher detection power for a group of elements and the large linear range of the analytical curves are interesting positive aspects of ICP-AES. The multi-element capability has the disadvantage that many spectral interferences can occur. However, it also provides a broad choice of analysis lines with good **detection** limits.

In AES methods using other excitation sources (e.g. arc, spark, glow-discharge) the knowledge of line coincidences is important as well. Spectral data (wavelengths and intensities of lines) determined with the use of these excitation sources became first available in 1939 in the comprehensive form of the M.I.T. Wavelength Tables (200—1000 nm, 190 000 lines). Further tabulations have been published so as to cover vacuum ultraviolet range or for special excitation conditions. The applicability of the line intensity data taken from the classical tabulations is limited, however, because the relative intensities change with the character of the excitation source and even for one and the same type of source large differences may occur.

Argon ICPs form a favourable exception. If the same type of nebulizer (e.g. a pneumatic nebulizer) is used, the relative sensitivities (= intensities per unit of concentration) do not differ widely from source to source, if the ICP is operated under compromise conditions for multi-element analysis. This favourable property was exploited in setting up the Line Coincidence Tables. Boumans tabulated the so-called "critical concentration ratio" (CCR), defined as the ratio of the concentration of interferent to analyze at which the ratio of the intensities of interfering line to analysis line in the spectral window of the latter is unity (50% of line interference). It follows from this definition that the higher the CCR value for a certain combination of an interfering and analysis line, the smaller the magnitude of the interference. The value of the CCR depends on the sensitivities (S_l and S_a), the difference in wavelengths ($\Delta\lambda$) and the effective line profiles, thus on the spectral band width (ΔW) of the spectrometer applied.

The main body of tables comprises the CCR tables for 892 prominent lines i.e. "most sensitive lines" of 67 elements. A separate CCR table is given for each prominent lines. Interfering lines within an interval of ±0.25 nm about the analysis lines are taken into account. The CCRs are tabulated for spectral bandwidths of 0.010, 0.015, . . ., 0.035, 0.040 nm, so the user can read the data that apply to the spectral bandwidth of his own apparatus. The CCR tables contain also the sensitivity data (S_l, S_a), the detection limit (c_L) and the rank number of the analysis line (order of increasing detection limit). The "finding lists" in the 1st volume facilitates access to the CCR tables. The general rules for consulting the CCR tables are illustrated by several examples, such as the selection of "interference free" lines for Nb, W and Zr as minor constituents in the spectrum of a stainless steel (Fe, Ni and Cr major elements) An example of even greater complexity is of a mixture of rare earths and associated elements

Sc, Y, Hf. Zr. A separate "finding list" summarizes the prominent lines suitable for ICP emission spectrography (638 lines in the 230—440 nm range).

The "introduction" (Volume 1) gives an adequate explanation and discussion of the principles, the computations underlying the tables and testing methods, which have played role in the determination of the CCR values. It is noted here that the exploitation of the line intensities of the arc spectra (National Bureau of Standards) made it possible to set up the CCR tables at the present stage of development of the ICP-AES. The relative intensities of the arc spectra were converted to the ICP scale with the aid of experimental conversion factors. Testing has been continued in the author's laboratory (Philips Research Laboratories, Eindhoven) after the appearance of the 1st edition. "Fortunately the paving of the bumpy roads leading to a definite solution of the spectral interference problem in the ICP-AES is not left as a tasks for a single laboratory" — Boumans says [(Spectrochim. Acta, **38B**, 747 (1983)]. The results of these recent works appear in the 2nd edition, which contains 172 revised or added CCR tables. According to the author's intention the "modification, adaptation and extension" are not finished either at the present stage and "regular updating of the present tables can be envisaged". This is certainly necessary, as Boumans clearly recognizes: the number of tabulated possible interfering lines is by far not yet large enough. Therefore the tables will give certainly only about rejection of lines as being unsuited for an analysis. Acceptance as being "free from interference" does require further experimental checks. The user should be well aware of this limitation.

On the whole, Boumans' Line Coincidence Tables may be classed among the indispensable "laboratory tools". The two volumes cost about the half price of a quartz ICP torch. The use of the tables may save time and argon, and thus may also the life of torches in that the number of experimental checks on interferences can be substantially reduced by a judicious a priori line selection.
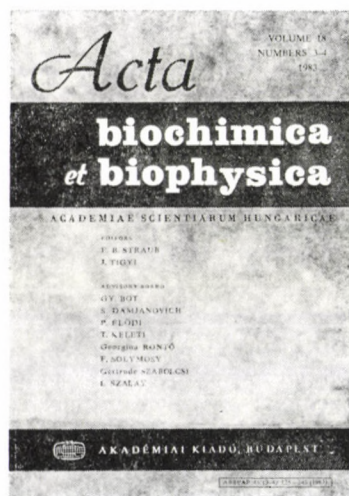
Tibor KÁNTOR

Institute for General and Analytical
Chemistry, Technical University of
Budapest

The journal publishes original papers on biochemistry and biophysics. Its main topics are: proteins (structure and synthesis), enzymes, nucleic acids, regulatory and transport processes, bioenergetics, excitation, muscular contraction, radiobiology, biocybernetics, functional structure and ultrastructure. Book reviews are also presented.

Order form
to be returned to
KULTURA
Hungarian Foreign Trading Company
P.O. Box 149, H-1389 Budapest, Hungary
□ Please enter my/our subscription for
  ACTA BIOCHIMICA ET BIOPHYSICA for one year
□ Please enter my/our standing order for
  ACTA BIOCHIMICA ET BIOPHYSICA starting with

Name: _____

Address: _____

Date and signature: _____

Contents of Volume 17. Numbers 3–4

BOOK REVIEWS

Text

The text of the paper should be concise. The description of new compounds (in the Experimental) must include the complete analytical data. Special attention must be paid to structural formulas given within the text. Complicated (non-linear) formulas should be drawn on separate sheets of paper and their position in the text should be clearly marked. The numbering of formulas and equations (in parentheses on the right-hand side) is only needed if they are referred to in the text. Units should conform to the International System of Units (SI). In nomenclature the rules of the I.U.P.A.C. are accepted as standard. Symbols for physical quantities are printed in italic type and should, therefore, be underlined in the manuscript.

References

References should be numbered in order of appearance in the text (where the reference number appears in brackets) and listed at the end of the paper. The reference list, too, should by typed double-spaced. Journal titles are to be abbreviated as defined by the Chemical Abstracts Service Source Index.

Examples:

[1] Brossi, A., Lindlar, H., Walter, M., Schneider, O.: Helv. Chim. Acta, **41**, 119 (1958)
[2] Parr, R. G.: Quantum Theory of Molecular Electronic Structure, Benjamin, New York 1964
[3] Warshel, A.: in Modern Theoretical Chemistry, Vol. 7, Part A (Ed. G. A. Segal), Plenum Press, New York 1977

Tables

Each table should be given a Roman number and a brief informative title. Structural formulas should not be used in column headings or in the body of tables.

Figures

Figures should be numbered consecutively with Arabic numerals. Their approximate place should be indicated in the text on the margin. All figures must be identified on the back by the author's name and the figure number in pencil. Standard symbols (such as circles, triangles, squares) are to be used on line-drawings to denote the points determined experimentally. Line-drawings must not contain structural formulas and comments. Spectra or relevant segments thereof, chromatograms, and X-ray diffraction patterns will be reproduced only if concise numerical summaries are inadequate to replace them. Drawings and graphs should be prepared in black ink on good-quality white or tracing paper. Photographs should be submitted on glossy paper as high-contrast copies. Xerox or similar copies are not suitable for reproduction, but may be used for duplicate copies.

Redrawn illustrations will be sent to the authors for checking. No corrections of figures will, therefore, be accepted in the proofs.

Submission of manuscript

After having completed the corrections suggested by the referees and editors, the final manuscript should be submitted in duplicate, in a form ready for publication. If the corrected manuscript is not returned to the editors *within six weeks*, the intended publication of the paper will be regarded as withdrawn by the authors.

Page charge will not be assessed for the publication, however, authors from overseas countries must contribute to the postage of correspondence by sending, together with the manuscript, international postal coupons to the value of U.S. $ 10.—

Proofs and reprints

A set of proofs will be sent to the submitting author. The proofs must be returned within 48 hours of receipt. Late return may cause a delay in the publication of the paper. 100 reprints will be supplied to the authors free of charge.

Periodicals of the Hungarian Academy of Sciences are obtainable at the following addresses:

AUSTRALIA
C.B.D. LIBRARY AND SUBSCRIPTION SERVICE
Box 4886, G.P.O., *Sydney N.S.W. 2001*
COSMOS BOOKSHOP, 145 Ackland Street
St. Kilda (Melbourne), Victoria 3182

AUSTRIA
GLOBUS, Höchstädtplatz 3, *1206 Wien XX*

BELGIUM
OFFICE INTERNATIONAL DE LIBRAIRIE
30 Avenue Marnix, *1050 Bruxelles*
LIBRAIRIE DU MONDE ENTIER
162 rue du Midi, *1000 Bruxelles*

BULGARIA
HEMUS, Bulvar Ruszki 6, *Sofia*

CANADA
PANNONIA BOOKS, P.O. Box 1017
Postal Station "B", *Toronto, Ontario M5T 2T8*

CHINA
CNPICOR, Periodical Department, P.O. Box 50
Peking

CZECHOSLOVAKIA
MAD'ARSKÁ KULTURA, Národní třída 22
115 66 Praha
PNS DOVOZ TISKU, Vinohradská 46, *Praha 2*
PNS DOVOZ TLAČE, *Bratislava 2*

DENMARK
EJNAR MUNKSGAARD, Norregade 6
1165 Copenhagen K

FEDERAL REPUBLIC OF GERMANY
KUNST UND WISSEN ERICH BIEBER
Postfach 46, *7000 Stuttgart 1*

FINLAND
AKATEEMINEN KIRJAKAUPPA, P.O. Box 128
SF-00101 Helsinki 10

FRANCE
DAWSON-FRANCE S. A., B. P. 40, *91121 Palaiseau*
EUROPÉRIODIQUES S. A., 31 Avenue de Versailles, *78170 La Celle St. Cloud*
OFFICE INTERNATIONAL DE DOCUMENTATION ET LIBRAIRIE, 48 rue Gay-Lussac
75240 Paris Cedex 05

GERMAN DEMOCRATIC REPUBLIC
HAUS DER UNGARISCHEN KULTUR
Karl Liebknecht-Straße 9, *DDR-102 Berlin*
DEUTSCHE POST ZEITUNGSVERTRIEBSAMT
Sraße der Pariser Kommüne 3–4, *DDR-104 Berlin*

GREAT BRITAIN
BLACKWELL'S PERIODICALS DIVISION
Hythe Bridge Street, *Oxford OX1 2ET*
BUMPUS, HALDANE AND MAXWELL LTD.
Cowper Works, *Olney, Bucks MK46 4BN*
COLLET'S HOLDINGS LTD., Denington Estate
Wellingborough, Northants NN8 2QT
WM. DAWSON AND SONS LTD., Cannon House
Folkstone, Kent CT19 5EE
H. K. LEWIS AND CO., 136 Gower Street
London WC1E 6BS

GREECE
KOSTARAKIS BROTHERS INTERNATIONAL
BOOKSELLERS, 2 Hippokratous Street, *Athens-143*

HOLLAND
MEULENHOFF-BRUNA B.V., Beulingstraat 2,
Amsterdam
MARTINUS NIJHOFF B.V.
Lange Voorhout 9–11, *Den Haag*

SWETS SUBSCRIPTION SERVICE
347b Heereweg, *Lisse*

INDIA
ALLIED PUBLISHING PRIVATE LTD., 13/14
Asaf Ali Road, *New Delhi 110001*
150 B-6 Mount Road, *Madras 600002*
INTERNATIONAL BOOK HOUSE PVT. LTD.
Madame Cama Road, *Bombay 400039*
THE STATE TRADING CORPORATION OF
INDIA LTD., Books Import Division, Chandralok
36 Janpath, *New Delhi 110001*

ITALY
INTERSCIENTIA, Via Mazzé 28, *10149 Torino*
LIBRERIA COMMISSIONARIA SANSONI, Via
Lamarmora 45, *50121 Firenze*
SANTO VANASIA, Via M. Macchi 58
20124 Milano
D. E. A., Via Lima 28, *00198 Roma*

JAPAN
KINOKUNIYA BOOK-STORE CO. LTD.
17-7 Shinjuku 3 chome, Shinjuku-ku, *Tokyo 160-91*
MARUZEN COMPANY LTD., Book Department,
P.O. Box 5050 Tokyo International, *Tokyo 100-31*
NAUKA LTD. IMPORT DEPARTMENT
2-30-19 Minami Ikebukuro, Toshima-ku, *Tokyo 171*

KOREA
CHULPANMUL, *Phenjan*

NORWAY
TANUM-TIDSKRIFT-SENTRALEN A.S., Karl
Johansgatan 41–43, *1000 Oslo*

POLAND
WĘGIERSKI INSTYTUT KULTURY, Marszalkowska 80, *00-517 Warszawa*
CKP I W, ul. Towarowa 28, *00-958 Warszawa*

ROUMANIA
D. E. P., *Bucureşti*
ILEXIM, Calea Grivitei 64–66, *Bucureşti*

SOVIET UNION
SOJUZPECHAT — IMPORT, *Moscow*
and the post offices in each town
MEZHDUNARODNAYA KNIGA, *Moscow G-200*

SPAIN
DIAZ DE SANTOS, Lagasca 95, *Madrid 6*

SWEDEN
ALMQVIST AND WIKSELL, Gamla Brogatan 26
101 20 Stockholm
GUMPERTS UNIVERSITETSBOKHANDEL AB
Box 346, *401 25 Göteborg 1*

SWITZERLAND
KARGER LIBRI AG, Petersgraben 31, *4011 Basel*

USA
EBSCO SUBSCRIPTION SERVICES
P.O. Box 1943, *Birmingham, Alabama 35201*
F. W. FAXON COMPANY, INC.
15 Southwest Park, *Westwood Mass. 02090*
THE MOORE-COTTRELL SUBSCRIPTION
AGENCIES, *North Cohocton, N. Y. 14868*
READ-MORE PUBLICATIONS, INC.
140 Cedar Street, *New York, N. Y. 10006*
STECHERT-MACMILLAN, INC.
7250 Westfield Avenue, *Pennsauken N. J. 08110*

YUGOSLAVIA
JUGOSLOVENSKA KNJIGA, Terazije 27, *Beograd*
FORUM, Vojvode Mišića 1, *21000 Novi Sad*